Siliconoids with Pending Silylenes as Platform for Mono– and Bimetallic Homogeneous Catalysts

Dissertation

zur Erlangung des Grades
des Doktors der Naturwissenschaften
der Naturwissenschaftlich-Technischen Fakultät
der Universität des Saarlandes

von

M. Sc. Luisa Giarrana

Saarbrücken 2026

Tag des Kolloquiums:	10.04.2026
Dekan:	Prof. Dr.-Ing. Dirk Bähre
Berichterstatter:	Prof. Dr. David Scheschkewitz
	Priv.-Doz. Dr. André Schäfer
Vorsitz:	Prof. Dr. Andreas Speicher
Akad. Mitglied:	Dr. Bernd Morgenstern

The present dissertation was prepared in the time between April 2021 and February 2026 at the chair for General and Inorganic Chemistry at the Faculty of Natural Science and Engineering of Saarland University under the supervision of Prof. Dr. David Scheschkewitz.

Die vorliegende Dissertation wurde in der Zeit zwischen April 2021 und Februar 2026 am Lehrstuhl für Allgemeine und Anorganische Chemie der Naturwissenschaftlich-Technischen Fakultät an der Universität des Saarlandes unter der Aufsicht von Prof. Dr. David Scheschkewitz angefertigt.

Zusammenfassung

Übergangsmetallkomplexe mit Liganden, die auf niedervalenten Hauptgruppenelementen basieren, stellen eine vielseitige neue Plattform für die homogene Katalyse dar. Die vorliegende Arbeit erweitert den Umfang der Silicoide, Siliciumcluster mit teilweise unsubstituierten Siliciumzentren, durch Funktionalisierung mit kleinen σ-Donor-/π-Akzeptor-Bausteinen und Übergangsmetallen, wodurch neue strukturelle Motive und Reaktivitäten mit katalytischem Potenzial erschlossen werden. Die Herstellung eines heterobimetallischen Clusters mit vollständiger Eingliederung des Übergangsmetallzentrums in das Clustergerüst sowie einer seltenen Iridium-Lithium-Wechselwirkung gelang durch reduktive Halogenideliminierung ausgehend von dem kürzlich beschriebenen Iridium-Si_6/Silylen-Komplex. Die weitere Funktionalisierung des heterobimetallischen Iridasilicoids mit Gruppe 4 Übergangsmetallen liefert multimetallische Clusterverbindungen mit großem Potenzial für katalytische Anwendungen.

Das geringe Gerüstatom/Ligand-Verhältnis in den Si_6-Hybridclustern schränkt den Zugang zu den reaktiven Siliciumzentren ein. Verbesserte Zugänglichkeit wurde durch Verwendung des erweiterten Si_7-Kerns bei unveränderter Substituentenanzahl erreicht, wodurch Geometrie und elektronische Struktur modifiziert werden. In der vorliegenden Arbeit wurde die externe Addition von Tetrylenen an das Si_7-Gerüst untersucht, die zu den gewünschten Hybridclustern führte. Basierend auf diesen Systemen wurden $Fe(CO)_4$– sowie bislang unzugängliche Nickel–Silicoid/Silylen-Komplexe erhalten. Der cod-Hilfsligand am Nickelzentrum ist leicht durch PPh_3 oder CO substituierbar. Zudem erwies sich der Ni(cod)-Si_7/Silylen-Komplex als leistungsfähiger Katalysator für die Hydrosilylierung terminaler Alkene.

Abstract

Transition metal complexes employing ligands derived from low-valent main group elements constitute a versatile new platform for homogenous catalysis. This thesis expands the scope of siliconoids, silicon clusters with partially unsubstituted silicon vertices, through functionalization with σ-donor/π-acceptor building blocks and transition metals, yielding novel structural motifs and reactivities with catalytic potential. The formation of a heterobimetallic cluster with full transition metal incorporation into the cluster scaffold and a rare iridium-lithium interaction is obtained by reductive halide elimination of the previously reported iridium-Si_6/silylene complex. Further functionalization with Group 4 metals affords multimetallic clusters with great potential for catalytic applications.

The low vertex-to-ligand ratio in Si_6 hybrid clusters limits access to the reactive silicon sites. Improved accessibility was achieved using the expanded Si_7 core with a retained number of substituents, introducing modified geometry and electronics. In this work, the exohedral addition of tetrylenes to the Si_7 framework was explored, yielding the intended hybrid clusters. Based on these systems, $Fe(CO)_4$ and previously inaccessible nickel siliconoid/silylene complexes were obtained. The auxiliary cod ligand at the nickel center is readily exchanged by PPh_3 or CO, respectively, and the Ni(cod)–Si_7/silylene complex proved as a potent catalyst in the hydrosilylation of terminal alkenes.

List of Publications

As part of this cumulative dissertation:

- Luisa Giarrana, Michael Zimmer, Bernd Morgenstern, David Scheschkewitz, Tetrylene-Functionalized Si_7–Siliconoids. *Inorg. Chem.* **2024**, *63*, 20083–20087. https://doi.org/10.1021/acs.inorgchem.4c00474
- Luisa Giarrana, Nadine E. Poitiers, Alida Stürmer, Volker Huch, Bernd Morgenstern, Michael Zimmer, David Scheschkewitz, Heterobimetallic unsaturated silicon clusters (siliconoids) with transition metal-expanded scaffolds. *Dalton Trans.* **2025**, *54*, 10441–10447. https://doi.org/10.1039/D5DT01135C
- Luisa Giarrana, Dennis Welterlich, Michael Zimmer, Bernd Morgenstern, David Scheschkewitz, Stable Nickel Complexes of a Siliconoid/Silylene Hybrid: Competent Hydrosilylation Catalysts for Terminal Olefins. *Inorg. Chem. Front.* **2026**, Advance Article. https://doi.org/10.1039/D6QI00025H

Others:

- Taiki Imagawa, Luisa Giarrana, Diego M. Andrada, Bernd Morgenstern, Masaaki Nakamoto, David Scheschkewitz, Stable Silapyramidanes. *J. Am. Chem. Soc.* **2023**, *145*, 4757–4764. https://doi.org/10.1021/jacs.2c13530
- Philipp Dabringhaus, Silja Zedlitz, Luisa Giarrana, David Scheschkewitz, Ingo Krossing, Low-Valent M_xAl_3 Cluster Salts with Tetrahedral $[SiAl_3]^+$ and Trigonal-Bipyramidal $[M_2Al_3]^{2+}$ Cores (M=Si/Ge). *Angew. Chem. Int. Ed.* **2023**, *62*, e202215170.
  English Version: https://doi.org/10.1002/anie.202215170
  German Version: https://doi.org/10.1002/ange.202215170

Acknowledgements/Danksagung

An erster Stelle möchte ich mich recht herzlich bei **Prof. Dr. David Scheschkewitz** für die Möglichkeit bedanken, meine Doktorarbeit in seiner Gruppe durchzuführen. Vielen Dank für die immerwährende Unterstützung und die stetige Verfügbarkeit für Fragen und Diskussionen. Darüber hinaus möchte ich mich für die Ermöglichung der Teilnahme an zahlreichen (inter)nationalen Konferenzen bedanken.

Ein großer Dank gilt **Dr. André Schäfer** für die Anfertigung des Zweitgutachtens sowie für die wertvollen Gespräche und Ratschläge über die letzten Jahre hinweg.

Vielen Dank an meinen wissenschaftlichen Begleiter **Prof. Dr. Andreas Speicher** für die Übernahme des Amtes.

Ein großes Dankeschön an **Dr. Carsten Präsang** für den unermüdlichen Einsatz im Laborbetrieb, die stete Auskunftsbereitschaft bei jeglichen Fragen und für die zahlreichen fachlichen Impulse im Laufe der Jahre.

Ein besonders großer Dank gilt **Dr. Bernd Morgenstern** für die Kristallstrukturanalysen und die ausdauernden Bemühungen, bei Problemen unzählige Lösungsversuche zu unternehmen, sowie die angenehmen Unterhaltungen.

Dr. Michael Zimmer danke ich für die Durchführung von VT-Experimenten und Festkörper-NMR Studien.

Bei **Dr. Diego Andrada** möchte ich mich bedanken für anregende Diskussionen und der gelegentlichen Hilfestellung bei meiner Einarbeitung in die theoretischen Berechnungen.

Ich möchte einen ganz herzlichen Dank an **Andreas Adolf, Britta Schreiber, Sylvia Beetz, Henrike Waller**, **Vanessa Grabowski**, **Leonie Wirtz**, **Bianca Iannuzzi**, **Dominika Posse**, **Emily Elisa Klein**, **Susanne Harling**, **Dana Barghoud**, **Dr. Andreas Rammo** richten, für Organisation, Messungen, technischen und handwerklichen Beistand, sowie allgemein für eine angenehme Zusammenarbeit.

Vielen Dank an alle aktuellen und ehemaligen Mitglieder des Arbeitskreises, insbesondere **Michel Bollmann, Tim Wiesmeier, Ankur UrPils, Liane H. Müller, Kashish, Peter A. M. Spies, Satyabrata Das, Nimisha Gautam**, **Suman Das**, **Daniel Mühlhausen, Dr. Nadine E. Poitiers, Dr. Marc C. Hunsicker**, **Thomas Büttner, Dr. Anna-Lena Thömmes, Dr. Philipp F. Grewelinger** und **Dr. Nasrina Parvin**, sowie auch **Simon Petrus Muhm** vom AK Munz, für den inspirierenden Austausch, die gute Zusammenarbeit und die Freundschaften, die sich über die Arbeit hinaus entwickelt haben.

Ein spezieller Dank gilt **Daniel Mühlhausen**, für die unzähligen gemeinsamen Momente innerhalb und außerhalb der Uni seit dem ersten Tag unseres Bachelorstudiums. Vielen Dank für die kontinuierliche Hilfsbereitschaft und den Rückhalt in allen Phasen der Studienzeit.

Ich danke **Dr. Nadine Poitiers** von ganzem Herzen für die vertrauensvolle und geduldige Zusammenarbeit, die sich als richtungsweisend für meine Entwicklung als Chemikerin erwiesen hat. Danke für die stetige Unterstützung und Freundschaft über die Jahre hinweg.

Ich danke **Hannah Theis**, **Wilma Isabel Koblé**, **Alexander Bohdjalian**, **Dennis Welterlich** und **Cedric Kloos**. Die Betreuung ihrer Bachelorarbeiten und Vertiefungen war für mich eine bereichernde Erfahrung. Ein besonderer Dank gilt **Dennis** und **Cedric**, die über die Zusammenarbeit hinaus zu guten Freunden wurden.

Meinem Partner **Dr. Philipp Frank Grewelinger** danke ich von Herzen für fünf Jahre voller Unterstützung, sowohl in wissenschaftlichen Belangen als auch im privaten Bereich. Danke für alles.

Vielen Dank an meine Freunde für den Beistand während der Zeit meiner Promotion. Ein besonderer Dank gilt **Jannik**, **Hoffi**, **Schurich**, **Elena**, **Doreen**, **Kathi**, **Valentin** und **Giulia** die mich über die Jahre hinweg in allen Lebenslagen begleitet haben und mir immer wieder geholfen haben, einen Ausgleich zum wissenschaftlichen Alltag zu finden.

Ein herzlicher Dank gilt auch meiner Familie, insbesondere meinen Eltern, **Barbara** und **Vito Giarrana**. Danke für den unerschütterlichen Rückhalt, die bedingungslose Unterstützung und die vermittelten Werte, die maßgeblich zu meinem bisherigen Weg beigetragen haben. Ich liebe euch.

Table of Contents

List of Abbreviations

[2.2.2]-crypt	4,7,13,16,21,24-Heoxaoxa-1,10-diaza-bicyclo[8.8.8]hexacosane
A	**A**mpere
Å	**Å**ngström
Ar	**Ar**yl substituent
B3LYP	**B**ecke hybrid-**3**-parameter functional and the correlation functional of **L**ee, **Y**ang and **P**arr
C	**C**elsius
cal	**Cal**ories
CGMT	**C**arter-**G**oddard-**M**alrieu-**T**rinquier
Cp*	Pentamethyl**c**yclo**p**entadienyl ($C_5Me_5^-$)
CPCM	**C**onductor-like **P**olarizable **C**ontinuum **M**odel
CVD	**C**hemical **V**apor **D**eposition
Cy	**Cy**clohexyl
DFT	**D**ensityl **F**unctional **T**heory
Dip	2,6-**Di**isopropyl**p**henyl
eV	**E**lectron**v**olt
e.g.	latin ***e**xempli **g**ratia*: “for example”
E_{hyb}	**Hybrid**ization **E**nergy
eq	**Eq**uivalent
en	**E**thylenediami**n**e
$E_{S,T}$	**E**nergy of the **S**inglet **T**riplet Gap
Et	**Et**hyl ($-C_2H_5$)
et al.	latin ***et al**ii:* “and others”
h	**Ho**ur
HOMO	**H**ighest **O**ccupied **M**olecular **O**rbital
Hz	**H**ert**z**
IBO	**I**ntrinsic **B**ond **O**rbitals
i. e.	latin ***id est***: „that is”
*i*Pr	***i**so*-**Pr**opyl ($-C_3H_7$)
*i*Bu	***iso*-Bu**tyl ($-C_4H_9$)
IR	**I**nfra**r**ed (spectroscopy)
K	**K**elvin
LUMO	**L**owest **U**noccupied **M**olecular **O**rbital
M	**M**olar (mol L^{-1})
MAS	**M**agic **A**ngle **S**pinning

Me	**Me**thyl (-CH_3)
Mes	**Mes**ityl (2,4,6-Trimethylphenyl)
min	**min**ute
MHz	**M**ega **H**ert**z**
MO	**M**olecular **O**rbital
*n*BuLi	***n*-Bu**tyl**li**thium
Naph	**Naph**thalene
NHC	***N*-H**eterocyclic **C**arbene
NMR	**N**uclear **M**agnetic **R**esonance
Ph	**Ph**enyl
ppm	**P**arts **P**er **M**illion
QTAIM	**Q**uantum **T**heory of **A**toms in **M**olecules
RT	**R**oom **T**emperature
*t*Bu	***tert*-Bu**tyl (-C_4H_9)
TD	**T**ime **D**ependent
thf	**T**etra**h**ydro**f**urane
Tip	2,4,6-**T**ri**i**sopropyl**p**henyl (2,4,6-*i*$Pr_3C_6H_2$)
TMS	**T**ri**m**ethyl**s**ilyl ($SiMe_3$)
TOF	**T**urn**o**ver **F**requency
TON	**T**urn**o**ver **N**umber
UV	**U**ltra**v**iolet
Vis	**Vis**ible
VT	**V**ariable **T**emperature
XRD	**X**-**r**ay **d**iffraction

Preface

Due to the societal revolutions enabled by the semiconducting properties of silicon, the late 20th and early 21st century are often referred to as the "silicon age".[1] Indeed, silicon has become the key element for modern life and the associated technologies. While in English the term "silicon" prevailed, introduced by Thomson due to the similarity to boron and carbon,[2] Davy initially coined the name "silicium", derived from the word "*silex*" (*lat.* for "flint" or "pebble") with the ending -ium referring to the metalloid character.[3] He established a technique for the isolation of metallic and semimetallic elements based on melt flow electrolysis of molten compounds. While this approach enabled the first isolation of elemental sodium, potassium, calcium and related elements, elemental silicon could not be obtained in pure form.[3–5] Early mentions in literature point towards the discovery of elemental silicon by Lavoisier in the late 18th century, who, however, mistook it for a compound containing an oxide of a yet unknown element rather than the element itself.[6,7] In 1824, Berzelius finally isolated silicon for the first time in its elemental, albeit amorphous form by reduction of SiF_4 with potassium metal.[8] Another 30 years later, the production of crystalline silicon by electrolysis of a mixture of NaCl and $AlCl_3$, containing small traces of $SiCl_4$, was reported by Deville,[9] marking an important step towards the use of silicon in applications. A milestone of these developments was achieved in the 1950s: the purification of metallurgical silicon by conversion to chlorosilanes, distillation and finally chemical vapor deposition (CVD), now known as the Siemens process, affording polycrystalline, high purity silicon.[10]

As silicon is a predominantly tetravalent non-metal with partial metallic character (= metalloid) and a significant band gap of 1.12 eV,[11] the highest impact of silicon in the digital age arguably originates from its prototypical semiconductor properties. Semiconductor-grade silicon is indispensable in modern society due to its essential role in the technology of solar cells and integrated circuits. These devices are commonly fabricated from single-crystal silicon, for example grown by the Czochralski method,[12] a melt-based crystal growth technique initially developed in 1915.[13–15] Another important purification technique is the zone melting or also called "floating-zone technique" invented by Bernal and further elaborated by Pfann.[16,17]

Even though elemental silicon occurs extremely rarely in nature (if at all), it is the second most abundant element in the earth's crust in the form of minerals, with an abundance of 27.7% by weight,[18,19] only surpassed by oxygen (46.6% by weight). In nature, silicon typically exists in form of silica or silicates (silicon dioxide), which are used in the production of widely applied materials such as ceramics,[20–22] glass[21] or concrete.[23,24] Although carbon, the "element of life", as compared to its heavier congener silicon, constitutes only a minor fraction of the earth's crust (0.2%), its unmatched ability to form stable and diverse compounds make it the chemical basis of all known life and a dominant subject of chemical research.[25–27] Two major differences

distinguish these two Group 14 elements from each other, namely their size and electronegativity.[18,28,29] Owing to its larger atomic radius and lower electronegativity (Si 1.90, C 2.55 on the Pauling scale),[30,31] silicon forms weaker and more polar Si–H (hydridic) and Si–C bonds than carbon (C–H protic), which accounts for the pronounced reactivity of organosilanes.[32–35] The synthesis of Et_4Si by Friedel and Crafts in 1863,[36] along with the isolation of the first silicone polymers in 1940, following Kipping's pioneering work on polysiloxanes,[37] paved the way for modern organosilicon chemistry. Nowadays, siloxane polymers (silicones) are essential materials in everyday life owing to their widespread use as rubbers, insulators, seals, heat-transfer media, paint binders, lubricants, or medicinal implants.[38,39] Their large-scale availability became possible with the independent invention of the "direct process" by Rochow and Müller in 1941-1942, which enabled the industrial production of organosilanes.[40–44] This process involves the copper-catalyzed reaction of elemental silicon with alkyl halides in a fluidized-bed reactor to afford the corresponding organosilanes.

Molecular organosilicon chemistry experienced major breakthroughs with the discovery of the first isolable silene by Brook and co-workers in 1981[45] and the long-sought disilene by West *et al.*,[46] together with the subsequently reported low-valent decamethylsilicocene by the group of Jutzi.[47] In recent years, unsaturated and low-valent silicon species have attracted considerable attention owing to their versatility, *e.g.* as ligand systems in the activation of small molecules.[48,49] In addition, they find application in catalysis, either as catalytically active species or as ligand frameworks that modulate the performance of catalytic metal centers.[48–51] Beyond this, low-valent silicon compounds are applied in the extension of polymeric systems,[52] but they also play an important role as intermediates in deposition processes, such as the deposition of amorphous silicon (a–Si) thin films by CVD.[53–56]

Regarding the activation of inert and nonpolar bonds in catalytic processes, transition metals occupied a unique role for almost a century.[57] Although the exploration of main group compounds capable of mimicking transition metal properties has gained considerable attention in recent years,[58,59] transition metals remain dominant. A major advantage of transition metals over organocatalysts is their unique ability to "shuttle between different oxidation states",[57,60] enabling a wide range of redox-mediated transformations. This is supported by the corresponding ligand system. Among others, low-valent silicon-based ligand systems turned out to be valuable ligands for transition metal complexes, with applications in homogeneous catalysis.[61,62] Historically, the majority of transition metal catalysts have relied on precious transition metals, which are of low natural abundance and often high toxicity. Consequently, increasing interest is being directed towards employing more sustainable catalytic systems based on early 3d transition metals, which are generally more abundant and less toxic.[58,59]

1. Introduction

1.1 Low valent Group 14 compounds

Compared to transition metal complexes, molecular main group species usually offer a limited range of accessible oxidation states, because of the smaller number of available valence electrons.[63] This constraint becomes apparent in the reactivity and catalytic abilities of main group element compounds. Changes in their oxidation states often result in electronically less favorable states with low thermodynamic stability. The associated high reactivity frequently leads to oligomerization or disproportionation to more stable oxidation states. For the lighter Group 14 elements, carbon and silicon, the most stable oxidation state in molecules is +IV.[64,65] Nonetheless, lower oxidation states can be stabilized kinetically and/or thermodynamically. In the last half century, the isolation of R_2E-type compounds (E = Group 14 element) with the central atom E in the oxidation state +II was enabled by the use of appropriate substituents or ligands. Heavier low-valent silicon compounds, much like their carbon analogues, serve for instance as crucial precursors in the formation of larger molecules and as versatile ligands for transition metal complexes, with significant relevance in catalysis and small-molecule activation.

1.1.1 Theoretical background

Tetrylenes, Group 14 metallylenes, are defined by a central tetrel atom in oxidation state +II and are generally described by the formula R_2E (E = C, Si, Ge, Sn, Pb). In contrast to heavier germylenes, stannylenes and plumbylenes, stable examples of the lighter homologues, carbenes and silylenes, remained elusive for a long time due to their tendency for oligomerization and disproportionation reactions as well as their instability under ambient conditions, *i. e.* exposure to air, moisture and room temperature.[66] Regarding the energetic ground state, tetrylenes strongly favor a singlet state (S = 0) with a doubly occupied non-bonding orbital and a vacant, energetically higher, perpendicular p_z orbital.[67] In contrast, carbenes of the type R_2C^{II} (R = hydrogen, sterically encumbering alkyl or aryl groups),[68] possess a small to vanishing σ-pπ gap and therefore a much more accessible triplet state (S = 1).[69] The energy gap between the non-bonding σ- and π-type orbitals, which is $\Delta E_{S,T}$ = −14 kcal mol^{-1} for $:CH_2$,[70] becomes small enough for the electron spins to align in parallel according to Hund's rule, resulting in one electron occupying a π-type p_z orbital and the second residing in an sp^2-type orbital (Figure 1).[69,71] The tetrylenes exhibit a decreasing tendency towards hybridization with increasing atomic number, accompanied by an increase in the s orbital character of the lone pair located at the tetrel atom E (E = C, Si, Ge, Sn, Pb). Consequently, an $(ns)^2(np)^2$ valence electron configuration is favored for the heavier Group 14 metallylenes. The geometry of the tetrylenes is influenced by the electron-orbital-distribution,

leading to a comparatively broad R–C–R angle, illustrated by θ = 134° for :CH_2,[72,73] vs. acute angles for H_2E^{II} species (H_2Si^{II} (92.7°) > H_2Ge^{II} (91.5°) > H_2Sn^{II} (91.1°) > H_2Pb^{II} (90.5°)).[71,74,75] This trend is consistent with the inert-pair effect, which asserts that the non-bonding HOMO (highest occupied molecular orbital) is lowered in energy with increasing atomic number due to increasing s-character. Consequently, a decrease in the H-M-H bond angle is expected down the group.

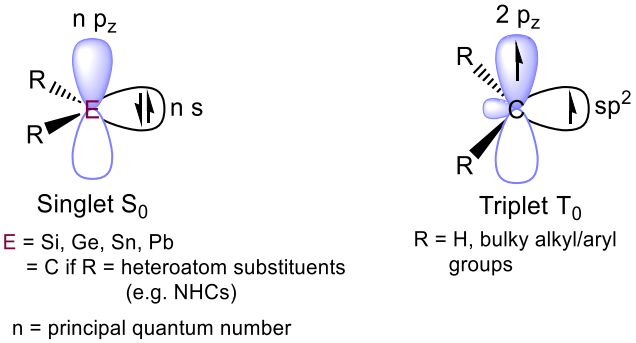

Figure 1. Energetic ground state of tetrylenes.

The formal dimerization of two tetrylene fragments results in the formation of multiple bonds between the central tetrel atoms. Simple carbenes, such as methylene, favor a triplet ground state as described in the previous section. The combination of two triplet fragments leads to a classical C=C double bond with a rigid, planar geometry arising from the low energy required for hybridization (E_{hyb}). In contrast, a direct interaction between two singlet fragments is generally energetically unfavorable due to Pauli repulsion. This is consistent with the increase in hybridization energies down the group.[66,71,74–79] These considerations led to the so-called “double bond” rule, a long-held assumption stating that heavier main group elements, including those of Group 14, are incapable of forming multiple bonds.[80–82] With the report of the first distannene in 1976 by Lappert and co-workers followed by the corresponding digermene in 1982,[83–86] this rule was invalidated for Group 14 elements, marking the advent of heavier alkene analogues. Around the same time, in 1981, Brook *et al.* reported a mixed C=Si silene[45] and the group of West succeeded in isolating the first stable disilene, further discussed in chapter 1.1.3.[46] In parallel, the pioneering work of Power demonstrated that main group element double bonds can be formed by exploiting the lone pair effect,[87] that is the decreasing participation of the s-electrons in the bonding along the group. During this period, in the 1980s, the Carter-Goddard-Malrieu-Trinquier (CGMT) model was developed.[88,89] The CGMT model provides a rationale for the formation of multiple bonds based on the mutual donation between a sp^2-type lone pair orbital of one fragment and a vacant p orbital at the tetrel center of another molecule. The increasing deviation from planarity arises from the minimization of steric repulsion between the bulky substituents and from donor-acceptor interactions involving the vacant p_z orbital, with the singlet-triplet energy of the tetrylene fragments largely dictating the interaction and degree of *trans*-bending.[87,90] Hence, an increased $\Delta E_{S,T}$ of the tetrylene

fragments is generally associated with a reduced *trans*-bending of the double bond, whereas smaller gaps tend to correlate with more pronounced bending, which can be qualified by the *trans*-bent angle θ or, in the corresponding syn-arrangement, the *cis*-bent angle θ'.[87] The *trans*-bent angle θ is defined by the angle between the R_2E planes and the E=E vector, reflecting the degree of pyramidalization at the tetrel atoms (Figure 2). The magnitude of θ is strongly influenced by the nature of substituents and solvent.[91–94] Another useful structural parameter for characterizing E=E double bonds is the twist angle τ, which corresponds to the angle between the planes defined by the two tetrel atoms and their substituents (Figure 2). The twist angle τ is tunable through the selection of appropriate ligands/substituents.[87,95]

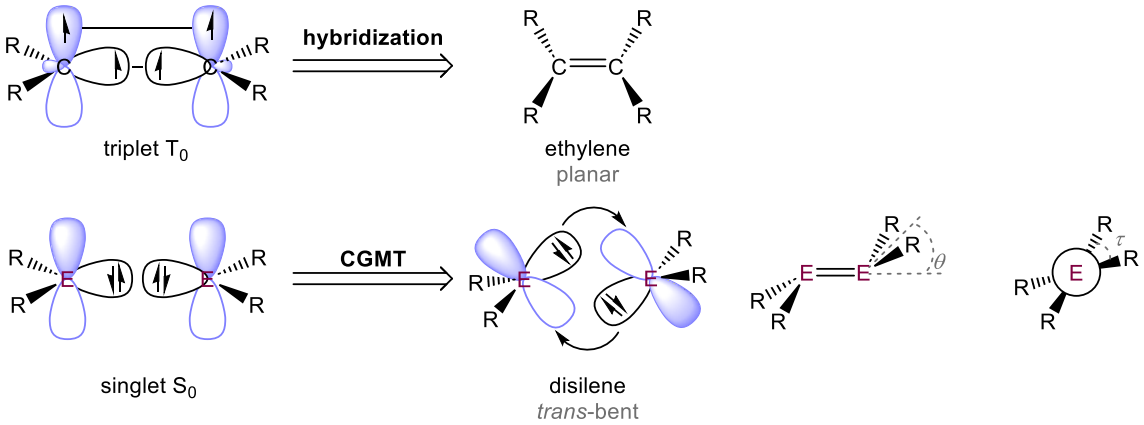

Figure 2. Bonding models of Group 14 orbital interactions.

A different strategy was pursued to enable the isolation of low valent E^{II} species by preventing dimerization and thus element-element bond formation. The first example of a monomeric compound featuring an Si^{II}-tetrel center was the iconic decamethyl silicocene **I-1** (Figure 3, left) reported by Jutzi *et al.* in 1986, which employed two bulky pentamethyl-cyclopentadienyl ligands in η^5-coordination to silicon.[47,96] Following the pioneering work of Bertrand *et al.* on the isolation of persistent carbenes,[69,97] Arduengo and co-workers reported the first isolable, room temperature stable *N*-heterocylic carbene **I-2** (Figure 3, left).[98] The successful isolation of **I-2** was enabled by a twofold stabilization strategy, involving both thermodynamic and kinetic contributions. Thermodynamic stabilization arises from mesomeric effects through intramolecular donation of the lone pair π-electrons of the nitrogen atoms into the formally vacant p_z orbital of the central tetrel atom. Steric stabilization is achieved using bulky substituents, with adamantly groups (Ad) effectively shielding the tetrel center against dimerization (Figure 3).

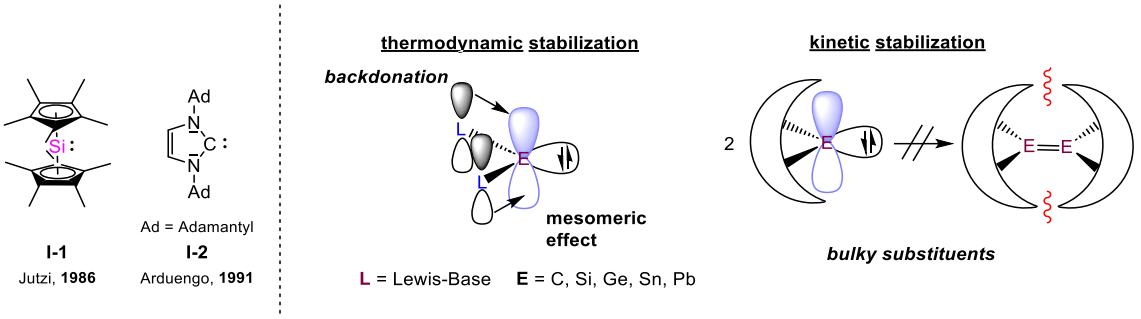

Figure 3. Left: Decamethylsilicocene **I-1** by Jutzi[47,96] and first isolated *N*-heterocyclic carbene **I-2** by Arduengo.[98] Right: General stabilization methods of tetrylenes.

Applying this concept of double stabilization to carbon's heavier congener silicon led to the first stable and genuine silylene **I-3** (see Chapter 1.1.2, Figure 4), reported by the groups of West and Denk in 1994.[99] Since then, the number of stable silylenes has steadily increased and continues to grow. Key developments will be summarized and organized in the following sub-chapters.

1.1.2 Stable Silylenes and their Reactivity

Silylenes, as detailed in the previous sub-chapter, are low-valent Group 14 species that possess a singlet ground state, which made their experimental stabilization and isolation elusive for a long time. First experimental indications for the existence of silylenes were reported by Goldstein and co-workers in 1964,[100] when pentamethyldisilane was obtained from the reduction of dimethyldichlorosilane at 260 °C with sodium-potassium vapor in the presence of trimethylsilane. This finding provided indirect evidence for the presence of Me_2Si^{II}, which was proposed to insert into the Si–H bond of $Me_3Si–H$.[101] The isolation of the first stable silylene was, however, not achieved until two decades later, with the report of Jutzi's decamethylsilicocene **I-1** (Chapter 1.1.1, Figure 3).[47] Building on the concept of thermodynamic and kinetic stabilization established for Arduengo's *N*-heterocyclic carbene **I-2** (Chapter 1.1.1, Figure 3),[98] the first stable *N*-heterocyclic silylene **I-3a** (Figure 4) was reported in 1994 by the groups of West and Denk.[99] **I-3a** features a central silicon atom embedded in a five-membered *N*-heterocyclic ring with a saturated backbone. Shortly afterwards, derivatives with an unsaturated backbone **I-3b**,[102] a benzene ring in the backbone **I-4** by Gehrhus *et al.*[103] (Figure 4) or modified substituents at the nitrogen atoms were disclosed. Soon, the concept was extended to an entire family of silylenes:[104–114] Driess and co-workers prepared zwitterionic silylene **I-6** in 2006 (Figure 4).[106] Around the same time, base-stabilized chloro-silylenes **I-7** and **I-8** were reported by the groups of Roesky[107,115] and Baceiredo.[108] Of relevance for this thesis, **I-7** has been proven to be an excellent electrophile for the transfer of the intact silylene moiety to anionic nucleophilic substrates.[61] **I-10a,b** represent stable silylenes with a system that employs only one nitrogen atom together with an

additional B/C–P donor,[108–110] while **I-5**[104] entirely lacks N or P donors and is instead stabilized by bulky silyl substituents at the α-C atoms. The related structure **I-9** combines an adjacent nitrogen atom and bulky substituents on the opposite side.[111] More recently, novel silylenes have been reported including *e.g.* Siemeling's example featuring a 1,1'-ferrocendiyl backbone.[112]

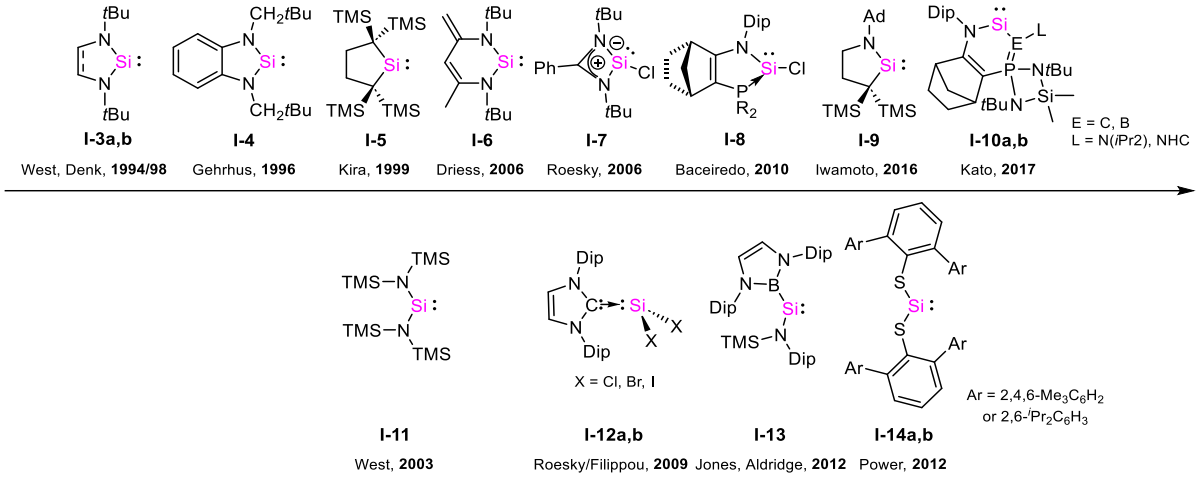

Figure 4. Selected examples of cyclic (top) and acyclic (bottom) silylenes over time (Dip = 2,6-diisopropylphenyl).[99,102–104,106–111,116–121]

A further accomplishment in the history of tetrylenes was the isolation of stable acyclic silylenes. Owing to the smaller singlet-triplet gap ($\Delta E_{S,T}$) and larger bite angles of acyclic silylenes compared to cyclic silylenes,[120–124] acyclic silylenes exhibit higher reactivity. Nearly 15 years elapsed between the first reports of the cyclic silylenes **I-3a/b** by West and co-workers[125,126] and the isolation of the first stable acyclic silylene. Although the group of West had already laid the groundwork for the synthesis of acyclic silylenes in 2003 with the preparation of **I-11** (Figure 4, bottom), it was only semi-stable and could be handled exclusively at low temperatures.[117] In 2009 and 2011, the groups of Roesky and Filippou reported on halogen substituted silylenes **I-12a,b**, which, however, required external stabilization by an *N*-heterocyclic carbene.[118,119,127] In 2012, the first room temperature stable, two-coordinate acyclic silylenes were reported by Jones and Aldrige *et al.* (**I-13**) [120] and almost simultaneously yet independently by Power and co-workers (**I-14a,b**).[121] The increased conformational flexibility of acyclic silylenes, compared to their cyclic counterparts constrained within a rigid framework, promotes oxidative processes and facilitates selective bond activation.[128] The geometry, together with the comparatively small singlet-triplet gap ($\Delta E_{S,T}$) enables the acyclic silylenes to mimic transition metal reactivity and to engage in the activation of inert small molecules such as H_2, CO and ethylene (*e.g.* **I-15** – **I-19**, Scheme 1).[113,129] In rare cases, such as the coordination of CO to the tetrel center of the acyclic gallanediyl silylene in **I-18** (Scheme 1), reported by Schulz *et al.* in 2020, the silylene framework remains intact and the lone pair at the tetrel central atom is preserved.[130] Notably, certain cyclic silylenes also engage in small

molecule activation and catalysis, for example in dehydrogenation reactions or C–F and C–H bond activation.[111,113,131,132]

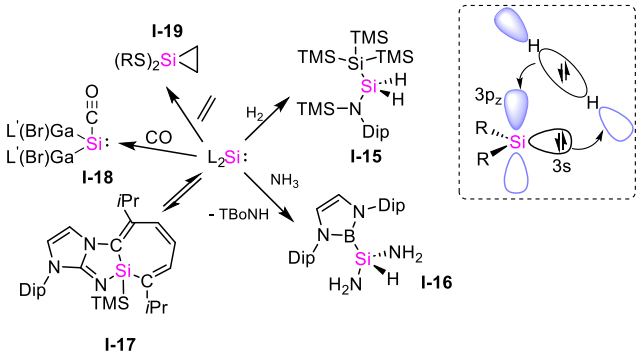

Scheme 1. Selected examples for the reactivity of acyclic silylenes towards small molecules (Dip = 2,6-$iPr_2C_6H_4$, TBoN = –N($SiMe_3$){B(DAB′)}, DAB′ = (XylNCH)$_2$).[113,129,130]

The presence of two reactive, low valent Si^{II} centers within a single molecule defines the class of bis(silylenes). The first reported bis(silylene) **I-20** (Figure 5) was described by Gehrhus and Lappert *et al.* in 2005[133] and revealed two non-interacting silylene fragments oriented away from each other. Conversely, in Roesky's bis(silylene) **I-21**[134] and in the N/P stabilized **I-22** reported by the groups of Baceiredo and Kato,[135] the two Si^{II} centers are connected through a σ-bond. In the following years, various derivatives including backbone modified species **I-23a-f** were disclosed giving rise to a range of distinct properties.[132,136,137] The pincer-type geometry of many bis(silylenes) enables the cooperative activation of small molecules like H_2, CS_2, ethylene, NH_3 or CO with subsequent formation of a ketene (*e.g.* **I-24** – **I-27**, Figure 5).[137]

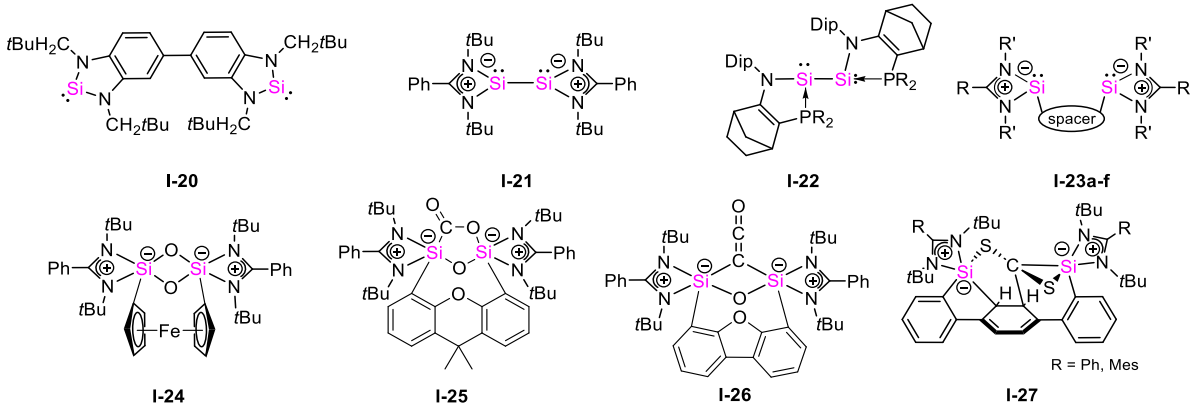

Figure 5. Examples of bis(silylenes) and products of the activation of small molecules.[132–137]

The high s-character of the lone pairs located at the tetrel centers and the resulting ambiphilicity of silylenes and bis(silylenes) make them valuable ligands for transition metals.[61,138–140] Numerous acyclic and cyclic silylenes have demonstrated to coordinate to first, second and third row transition metals (selected examples **I-28** – **I-30**, Figure 6).[61,136,137,140–143] The coordination chemistry of silylenes and bis(silylenes) also extends to late 4d and 5d transition metals, as demonstrated by complexes such as **I-31**[141] and **I-32**,[144] which exhibit remarkable catalytic activity.[145–147] Current trends increasingly favor the coordination

of the more abundant first row transition metals or even applications that avoid the use of transition metals altogether.[148–153]

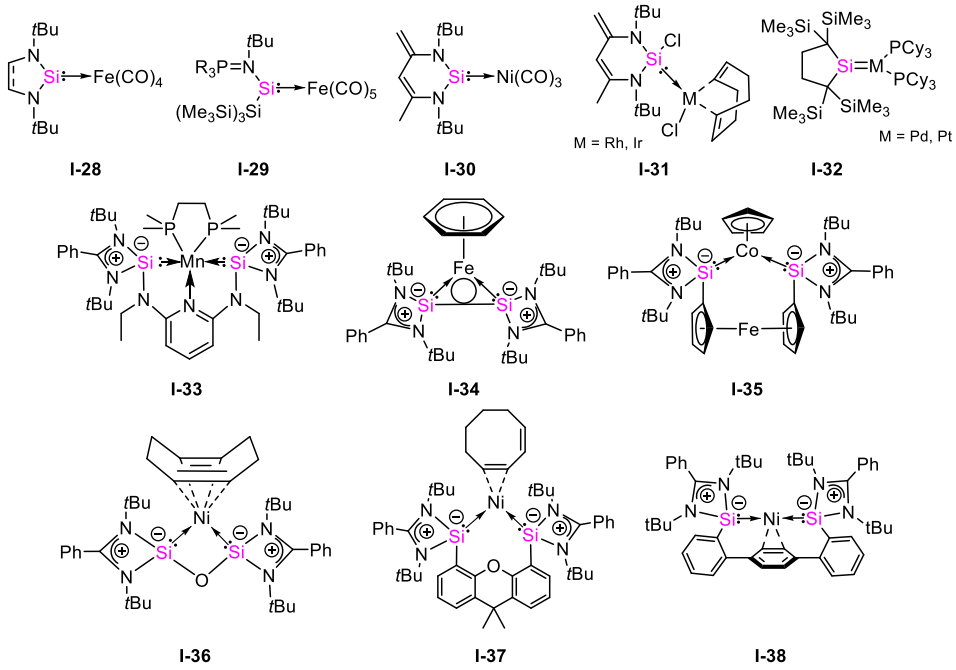

Figure 6. Selected examples of transition metal silylene complexes.[61,136,137,140–144,148–153]

In addition to the bidentate coordination of 3d transition metals such as Mn, Fe, Co or Ni by the two Si^{II} centers of bis(silylenes) (*e.g.* **I-34** – **I-37**),[149–152] their pincer-type geometry also enables cooperative binding of transition metal complexes. This mode of interaction gives rise to pronounced metal-ligand cooperativity as shown in **I-33**[148] (Figure 6).[61,125,148–150,154,155] Remarkably, depending on the electronic and steric properties of the bis(silylene) backbone, the coordination of the central metal atom by an external ligand can proceed in a classical fashion as in **I-36**,[151] in a non-classical manner as in **I-37**[152] or even without the need of an external ligand as demonstrated by **I-38**.[153] Silylene or bis(silylene) transition metal complexes have been shown to act as highly active catalysts in homogeneous reactions including C-C or C-N cross coupling, olefin hydrogenation, cycloaddition, hydroborylation and hydrosilylation.[61,125,154]

1.1.3 Disilenes and Disilenides

Double bonds of heavier main group elements had long been regarded as unattainable according to the double bond rule (see Chapter 1.1.1).[80–82] The rule was overturned in the second half of the 20th century with reports of both homonuclear and heteronuclear multiple bonds among main group elements. As early as 1976, the formation of the first heavier Group 14 compounds with a homonuclear heavier double bond, namely distannene **I-39** and digermene **I-40** (Figure 7), was described by Lappert and co-workers.[83–86] Although Gusel'nikov and Flowers had already reported on the observation of intermediate silaethylenes

(silenes) in 1967,[156,157] the first heteroatomic double-bonded species containing two Group 14 elements, silene **I-41**, was isolated and characterized by Brook *et al.* in 1981/1982.[45,158] This compound was obtained through a photochemical reaction of tris(trimethylsilyl)acylsilane. Using this method, as well as the sila-Peterson reaction,[159] salt elimination reactions from (alkyl)halotetrylanes[160] or thermal/photochemical addition reactions,[161] additional silene derivatives were disclosed in the following years (*e.g.* **I-42**, **I-43**, Figure 7).[161–163]

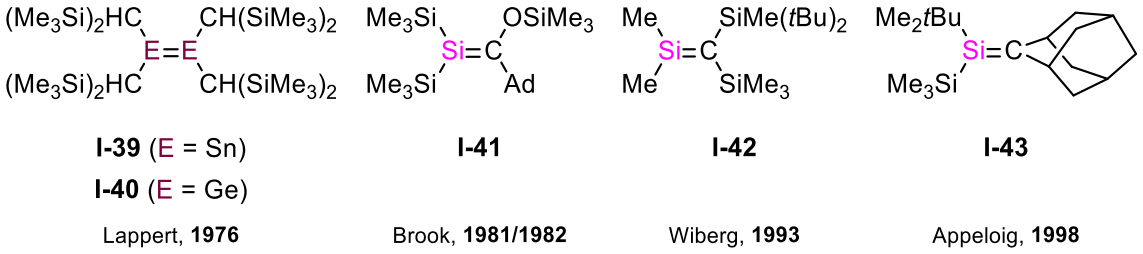

I-39 (E = Sn)
I-40 (E = Ge)
Lappert, **1976**

I-41
Brook, **1981/1982**

I-42
Wiberg, **1993**

I-43
Appeloig, **1998**

Figure 7. Selected examples of the first heavier double bonded species.[45,83–85,158,161,162]

Around the same time as the isolation of the heteronuclear silene **I-41**,[45] the first disilene **I-46** containing two silicon atoms in the oxidation state +II was reported by West and co-workers (Scheme 2).[46] The possibility of disilenes acting as transient intermediates had already been discussed in 1973 by Roark and Peddle.[164] Numerous synthetic attempts to access an isolable disilene, including those by Kipping *et al.*,[37,165] were unsuccessful. Starting from mesityl-substituted trisilane **I-44** (Mes = 2,4,6-trimethylphenyl), photolytic elimination of hexamethyldisilane finally allowed West and co-workers to obtain disilene **I-46** (Scheme 2).[46] The mechanistic proposal invokes a silylene intermediate **I-45**, whose isolation, however, remains elusive to this day.

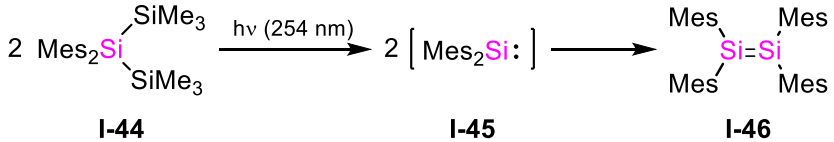

I-44

I-45

I-46
West, **1981**

Scheme 2. Synthesis of first stable disilene **I-46** reported by West *et al.* in 1981 (Mes = 2,4,6-trimethylphenyl).[46]

Following the pioneering work of West *et al.*, further disilene derivatives were reported using related synthetic approaches.[79,166–168] In 1988, Tip_4-substituted disilene was reported by Watanabe and co-workers.[169] Reduction of the twofold-chlorinated silane precursor Tip_2SiCl_2 with a lithium/ naphthalene solution led to the formation of disilene **I-48** (Scheme 3),[169] providing a novel synthetic approach toward the formation of disilenes. In a related manner, disilene $(SiMe_3)_2HC)_2Si=Si(CH(SiMe_3)_2)_2$ was synthesized by Masamune *et al.* in the same year.[170] In this case as well, the formation of a transient silylene species was proposed, although direct experimental evidence remains elusive. The synthesis of disilenes using the more common reducing agent KC_8 was subsequently investigated and revealed efficient

dehalogenation of 1,2-dihalodisilanes. This method further provides access to unsymmetrical disilenes.[168,171–174]

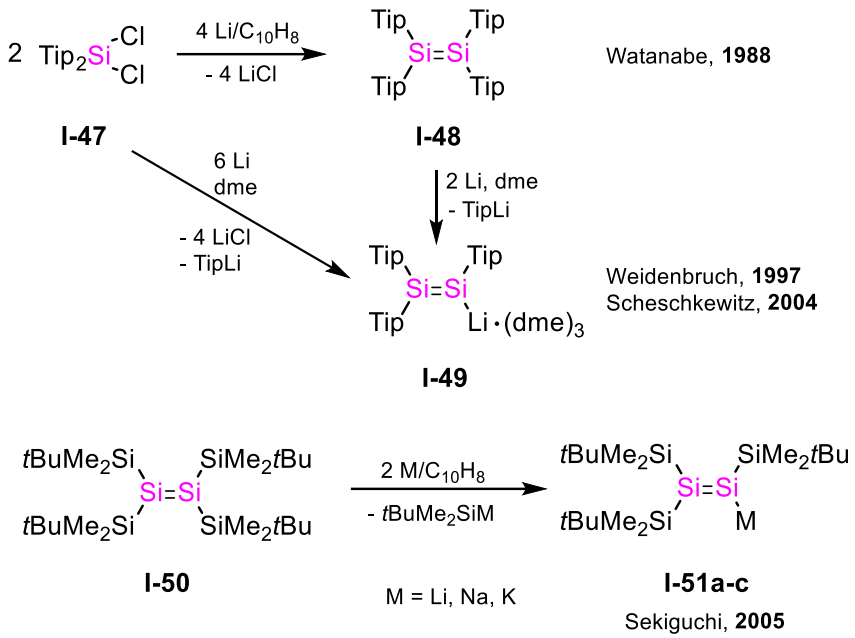

Scheme 3. Top: Formation of Tip_4-disilene and its lithium disilenide derivative; Bottom: Reduction of *t*$BuMe_2Si$-disilene.[169,175–177]

Regarding the reactivity of disilenes, typical double bond transformations such as addition reactions have been investigated.[178] The addition of polar compounds like water, alcohols, ammonia, and related substrates to disilenes afforded the isolation of numerous silanes.[168,178] Furthermore, cycloaddition reactions with alkenes, chalcogenes or isonitriles yielded a variety of disilacycles.[179,180] In parallel, efforts were directed toward preserving the double bond character, inspired by strategies used in the generation of larger macro- or supramolecular systems featuring heavier unsaturated units.[167,181]

Another important aspect of olefin reactivity in synthetic organic chemistry, particularly in total syntheses, involves nucleophilic and electrophilic substitution at unsaturated carbon atoms.[182–184] Building on this concept, the functionalization of heavier double bonds was examined with respect to their nucleophilic and electrophilic behavior. Subsequently, several nucleophilic and electrophilic disilene derivatives have been reported over the past two decades demonstrating their value in synthetic low-valent main group chemistry.[168,181,185–188] Reduction of disilenes to anionic disilavinyl analgoues of tetrasubstiuted disilenes is predominantly achieved by treating the corresponding disilene with alkali metals. For Tip_4Si_2, initial attempts to reduce disilene **I-48** with elemental lithium as a strong reducing agent were undertaken by Weidenbruch *et al.* in 1997 aiming to access the corresponding lithium disilenide **I-49**.[175] It was only in 2004 that Scheschkewitz finally succeeded in isolating disilenide **I-49** (Scheme 3).[176] Around the same time, Sekiguchi and co-workers obtained disilenide derivatives **I-51a-c** in a related manner, starting from the disilene (*t*$BuMe_2)_3Si_2$ **I-50**,

using the corresponding alkali metal (M = Li, Na, K)/ naphthalene solution (Scheme 3, bottom).[177,189]

Owing to their nucleophilic nature, disilenides have been employed in a variety of salt metathesis reactions, transferring the Si=Si moiety to numerous substrates.[168,181,185,186,188,190–192] For instance, disilenide **I-49** reacts with aryl halides, providing an alternative route to unsymmetrically substituted disilenes.[191,192] With regard to macromolecular chemistry, **I-49** was applied in regiospecific [2+2] cycloadditions of alkynes with the Si=Si fragments, affording σ-π-conjugated organosilicon hybrid polymers.[193] Furthermore, **I-49** proved to be a key compound in the formation of small tricyclic rings that can subsequently serve as precursors for silicon clusters (see Chapter 1.2.3).[194]

In addition to transmetallation reactions of lithium disilenide **I-49** with alkali or alkaline earth metals,[195] a few examples of its direct complexation with transition metals have also been reported. Remarkably, only very few stable, monomeric η^1-coordinated disilenide transition metal complexes have been obtained directly from disilenide precursors, such as the chloro zirconocene disilene **I-52** (Scheme 4).[196] Addition of half an equivalent of a zinc or copper halide precursor affords the dimeric, transition metal bridged zinc complex **I-53** or the cuprate **I-54**, respectively (Scheme 4).[195]

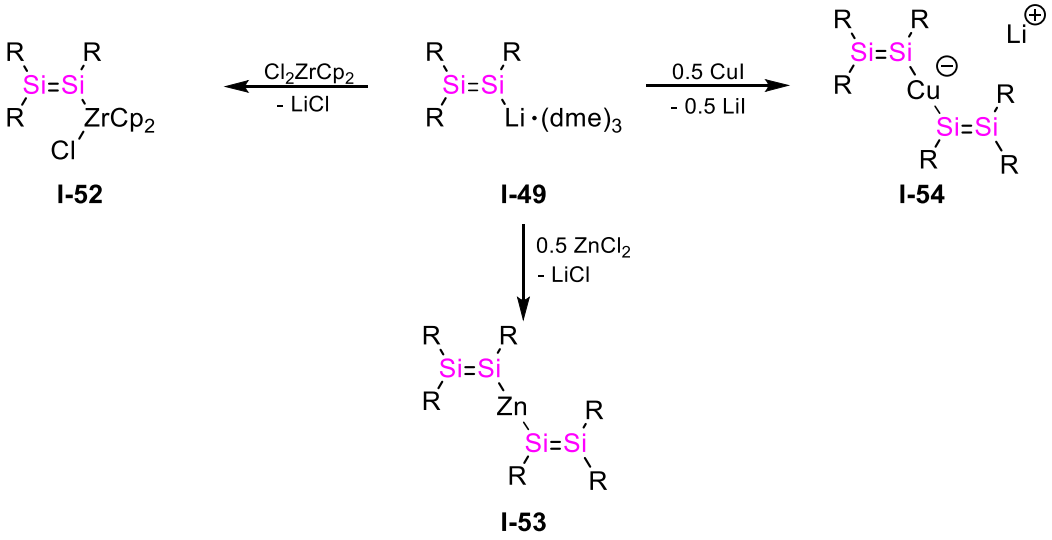

Scheme 4. Reactivity of lithium disilenide **I-49** towards transition metal precursors (R = 2,4,6-triisopropylphenyl).[195,196]

Beyond their nucleophilic reactivity, various η^2-disilene transition metal complexes retaining the Si=Si double bond have been reported, particularly with late transition metals such as Pt, Pd and Hg.[168,197] Similar η^2-complexes have also been obtained from disilyne, disilane or silylene precursors, which undergo reduction or dimerization to furnish the corresponding disilene transition metal complexes.[197]

1.2 Silicon Clusters

The significance of silicon clusters arises primarily from their use as model systems for bulk and surfaces of silicon on the nanoscale, as well as from their potential in the development of molecularly precise device structures.[198–204] In the silicon deposition process, silicon clusters play an important role as proposed intermediates.[54,56,205–208] Silicon clusters consist of a small, well-defined number of silicon atoms arranged in a framework composed solely of Si–Si bonds, forming a three-dimensional scaffold. Distinguished by their inherent connectivity, charge and substitution pattern, silicon clusters are typically divided into three principal categories: saturated silicon cage clusters,[209–211] Zintl ions[212–219] and siliconoids.[220–222] In the following sub-chapters, the saturated silicon cages and Zintl ions will be outlined briefly, whereas the siliconoids, as the main focus of the present work, will be discussed in greater detail.

1.2.1 Saturated Silicon Cages

Saturated silicon cages consist exclusively of saturated, tetracoordinate silicon vertices and carry at least one substituent that is not part of the cluster core itself. They follow the general formula Si_nR_m ($n \leq m$).[221] Three common synthetic routes are applied to access such saturated silicon clusters: (a) Wurtz-type coupling of suitable halogenated silane precursors with reducing metals, (b) salt elimination reactions between halogenated and metalated (cyclo-) silanes, and (c) aluminium chloride or photolytically induced rearrangement or contraction of (poly)cyclic oligosilanes. Given the large number of known saturated silicon cage compounds and the extensive studies on their properties and reactivity,[209–211,221] the following section provides an overview of selected, representative examples (Figure 8) together with their synthesis and characteristic properties.

The first saturated silicon cluster was reported in 1970 by West and co-workers with bicyclo[2.2.2]octasilane Si_8Me_{14} (type **A**, Figure 8) obtained from of a mixture of Me_2SiCl_2 and $MeSiCl_3$ (2.75:1) by reduction with sodium/ potassium alloy in the presence of naphthalene.[223] Refinement of this synthetic protocol subsequently enabled the isolation of additional polycyclic polysilanes containing six to thirteen silicon vertices in the central cluster scaffold.[224] Later, Masamune *et al.* reported the type **B** saturated silicon cage (Figure 8) prepared through a combination of strategies (a) and (b), and further derivatization by quenching with the corresponding dichlorosilanes.[225] In 2012, the Iwamoto group described the formation of a related type **B** silicon cluster, initiating with a four-membered cyclotetrasilane and proceeding *via* a dianionic Si_4-ring as an intermediate. Owing to the larger size of the precursor, this route provided higher yields than those obtained for Masamunes clusters.[226] By changing the reducing agent from Na/ K alloy to finely dispersed lithium, Hengge and Jenker obtained a bicyclco[3.2.1]silane in 1991.[227] An improved isolated yield was later reported by Kira *et al.* in

2004, employing branched tris(chlorodimethylsilyl)(methyl)silane in a reductive dimerization.[228]

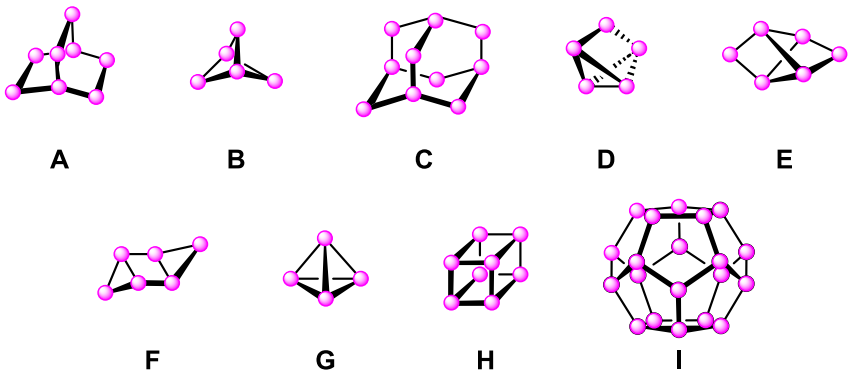

Figure 8. Selected examples of saturated silicon clusters (○ = SiR_n, n = 0,1,2).

Applying method (c), the photolytical or $AlCl_3$ induced contraction or rearrangement, to Masamune's type **A** silicon cluster yields bicyclo[2.2.1]heptasilanes.[224,229] An $AlCl_3$ induced rearrangement of a cyclohexasilanyl-substituted bicyclo[3.3.1]heptasilane afforded the first and only all-silicon adamantane tricyclclo[3.3.1.1]decasilane (type **C**, Figure 8), reported by Marschner and co-workers in 2005.[230] Decasila-adamantane is of particular significance, as it provides a representation of a stable, molecular fragment derived from the diamond-type lattice of crystalline silicon.

Expanding the family of multicyclic saturated silicon cages, in 2009 Sekiguchi *et al.* reported the first example of tricyclo[2.1.0.$0^{2,5}$]pentasilane (type **D**, Figure 8).[231] This compound is obtained from the reaction of the calcium salt of 1,2,3,4-tetrakis(di-*tert*-butylmethylsilyl) tetrasilabicyclo[1.1.0]butan-2,4-diide with trichlorophenylsilane.[245] Owing to the presence of a remaining chloride substituent, reductive cleavage can be applied to generate an anionic derivative, enabling further use in salt metathesis reactions. Shortly thereafter, Scheschkewitz *et al.* reported a structurally comparable cluster of type **D**.[232] In 1988, Masamune described the reductive homocoupling of 1,2-di-*tert*-butyl-1,1,2,2-tetrachlorodisilane with 2.5 equivalents of lithium/ naphthalene in dimethoxyethane to afford the tricyclic [2.2.0.0]hexasilane (type **E**, Figure 8) together with additional products such as cyclotetrasilane and tetracyclo[3.3.0.0.0]octasilane.[233] It was not until 2007 that Kira and Iwamoto reported the isolation of tricyclo[3.1.0.$0^{2,4}$]hexasilane with a chair-like scaffold (type **F**, Figure 8), synthesized by reducing 2,2-dibromotrisilane and 2,2,3,3,-tetrabromotetrasilane with elemental sodium metal.[234] Irradiation of the hexasilane led to the rearrangement into a [2.2.0.0]tricyclic scaffold, which is structurally comparable to Masamunes tricyclic [2.2.0.0]hexasilane[233] (type **E**, Figure 8).

The exploration of polyhedral silicon frameworks initiated with the isolation of the smallest conceivable tetrahedron, tetrasilahedrane, reported by Wiberg in 1993.[162] The first tetrasilatetrahedrane (type **G**, Figure 8) was synthesized from 2,2,3,3-tetrabrominated

tetrasilane with supersilyl sodium (*t*Bu_3SiNa). A decade later, a related derivative was obtained employing $MeDis_2$ groups (Dis = $CH(SiMe_3)_2$) as sterically demanding substituents, which induced increased shielding and resulted in shorter endocyclic Si–Si bond lengths. Meanwhile, it was shown that Wiberg's tetrasilahedrane could also be accessed in higher yields through one-pot-reactions of $HSiCl_3$, $Cl_3Si–SiCl_3$ or $Cl_3Si–SiCl_2–SiCl_3$ with supersilyl sodium.[235] At approximately the same time, Sekiguchi and co-workers reported on the reduction of 1,1,2,2-tetrachlorinated disilane or $DipSiCl_3$ with $Mg/MgBr_2$ yielding the iconic hexasilaprismane.[236] A similar hexasilaprismane was isolated later on under reductive coupling of a 1,2,3-trichlorocyclotrisilane with magnesium by the Scheschkewitz group.[232]

Moving further into polyhedral octasilanes, cubic structures were first described and isolated in 1988 by Matsumoto *et al.* with the synthesis of the octasilacubane (type **H**, Figure 8).[237] Reduction of 2,2,3,3-tetrabrominated tetrasilane or the corresponding tribrominated disilane *t*$BuMe_2Si–SiBr_3$ with sodium metal affords the anticipated octasilacubane. Shortly thereafter, in 1992, H. Matsumoto, N. Matsumoto and Sekiguchi independently reported on three persilacubanes obtained through similar synthetic strategies.[237–240] Reduction with sodium metal or $Mg/MgBr_2$ of the corresponding alkyl- or aryl-substituted trichlorosilanes furnishes the cubic Si_8 cluster. Most recently, Lips and co-workers described the isolation of an anionic derivative.[241]

An even larger silicon cluster system was reported by the groups of Wagner and Holthausen in 2014 with the largest saturated silicon cage compound known to date, the twenty-atomic silafullerane (type **I**, Figure 8).[242] It features twelve exohedral $SiCl_3$ substituents, eight peripheral chloro-substituents and an encapsulated chloride ion that imparts to an overall negative charge.[242] A one-step reaction of hexachlorodisilane with [*n*Bu_4N]Cl and *n*Bu_3N in a 20:2:1 ratio affords the [20]silafullerane in reasonably high yields.

Compared to their linear and ladder-type oligo-/polysilane congeners, applications of saturated silicon cage compounds remain limited to date. While chain-type silanes find use as photoinitiators, in electroluminescent diodes and microlithography due to their characteristic photochemical and optical properties with $\sigma–\sigma^*$ transitions of oligo- and polysilanes with UV/Vis-absorptions at λ = 250 – 400 nm,[243–246] studies on the utilization of cage oligosilanes in materials science have not been reported hitherto. Nevertheless, preliminary investigations into their functionalization could enable the construction of more versatile extended systems and the incorporation of such clusters into functional materials. In addition to halogenation reactions (*e.g.* BCl_3, I_2, Br_2, CCl_4, PCl_5)[228,247–249] and subsequent reduction steps to generate anionic clusters suitable for further nucleophilic functionalization,[221,231,249] only a few reports have addressed the reactivity of saturated silicon cages towards transition metal precursors.[249] Treatment of dianionic [2.2.0.$0^{2,5}$]hexasilane **I-55** with $Cp^*_2TiCl_2$ or

$(PPh_3)_2PdCl_2$ does not afford a transition metal complex but instead the oxidation product, hexasilaprismane **I-56** (Scheme 5), highlighting the role of **I-55** as a potent two-electron reductant.[249] Notably, the hexasilaprismane framework is also obtained upon reduction of trichlorinated cyclotrsilane with lithium/ naphthalene or upon treatment of tetrachlorodisilane, $DipSiCl_3$ or trichlorocyclotrisilane with magnesium and magnesium bromide.[232,236,249]

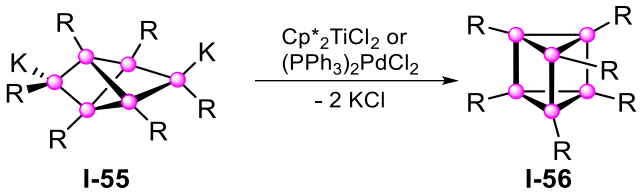

I-55 **I-56**

Scheme 5. Oxidation of dianionic [2.2.0.0^{2,5}] hexasilane **I-55** with transition metal complexes to hexasilaprismane **I-56** (= Si, R = 2,4,6-trimethylphenyl).[249]

1.2.2 Zintl Ions

In contrast to saturated silicon cages, Zintl ions are completely ligand-free, “naked” polyanionic clusters of p-block elements.[221,250] In the late 1800s, Joannis first described the reaction of elemental lead with sodium in liquid ammonia, which produced a deep green solution.[251] It was not until 1931 that Eduard Zintl, the namesake of the Zintl ions, conducted comprehensive studies in which solutions of sodium in liquid ammonia were reacted with a wide range of main group elements.[252] According to Zintl’s proposal, an idealized complete transfer of electrons from the electropositive alkali metal to the more electronegative p-block element leads to the formation of polyanionic species composed of multiple atoms. A decade later, Laves introduced the term “Zintl-border” to describe the division between groups 11-13 and 14-17, and the salt-like phases of alkali metals associated with this boundary were subsequently termed “Zintl phases”.[253] Zintl ions of Group 14 serve as important building blocks for the synthesis of large nanoclusters due to their diverse chemical properties and reactivity. Today, the scope of Zintl ions encompasses intermetalloid clusters with transition metals incorporated into main-group cages, organometallic or intermetallic derivatives, functionalized organo-Zintl ions, as well as oligomeric species.[250] Although numerous Zintl ions have been reported, the tetrahedral $[E_4]^{4-}$ **I-57** and the tricapped trigonal $[E_9]^{4-}$ **I-59** (Figure 9), are the most prevalent species, accompanied by two isolated examples of pentaatomic $[E_5]^{2-}$ ion **I-58**.[254,255] Beyond these common motifs, several noteworthy exceptions exist, including the eight-atomic $[Sn_8]^{6-}$ cluster described by Sevov *et al.*,[256] butterfly shaped $[E_4]^{6-}$ in Ba_3E_4 (E = Si, Ge),[257,258] Y-shaped $[Si_4]^{12-}$ stars,[259,260] five-membered $[E_5]^{6-}$ rings (E = Si, Pb)[259–264] and the six-membered $[E_6]^{10-}$ species.[265,266] Given the extent of Zintl ion chemistry,[212–219,221,250,267] the present work focusses on a selected subset of polyhedral silicon-based Zintl ions relevant to the overarching topic of this thesis.[261–264]

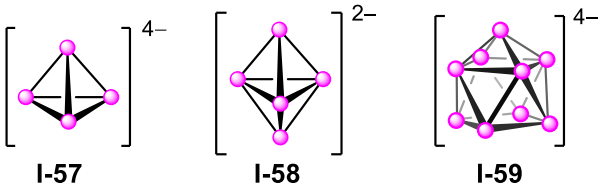

Figure 9. Reported geometries of common silicon-based Zintl ion motifs (○ = Si).[254,255]

Owing to the pronounced polarity resulting from effective charge separation, solid Zintl phases are insoluble in common organic solvents. For a long time, their solubility was limited to liquid ammonia at low temperatures.[268] In general, clusters of the type A_4E_9 and $A_{12}E_{17}$, which carry lower charges per atom, exhibit better solubility than A_4E_4. Over the past 50 years, alternative solvents such as ethylenediamine together with stabilizing agents like cryptands[269,270] or crown ethers,[271] have enabled the isolation and structural characterization of Zintl anions by X-ray diffraction analysis.[272] Nevertheless, the silicon-based Zintl anions $[Si_4]^{4-}$ and $[Si_9]^{4-}$ remained elusive in solution for a long time. Although solution stable $[E_9]^{4-}$ species of the heavier Group 14 elements (E = Ge[273], Sn[274]) have been known since the 1970s to 1990s,[291] it was only in 2009 and 2010 that the first examples of the corresponding tetraanionic nonasilicide were reported by Korber and co-workers in the ammoniates $Rb_4Si_9 \cdot (NH_3)_x$ (x = 4.75 and 5).[254,275]

The group of Fässler recently succeeded in isolating $[Si_4]^{4-}$ and $[Si_9]^{4-}$ and separating them by fractional crystallization from a solution of the binary phase $K_{12}Si_{17}$.[276] Prior to this breakthrough, NMR spectroscopic evidence had already indicated the presence of both $[Si_4]^{4-}$ and $[Si_9]^{4-}$ in solution and several isolation attempts had been undertaken, including the preparation of corresponding transition metal complexes.[277,278]

The functionalization of Zintl ions (**I-60**, Scheme 6) with suitable electrophiles has been proposed by Wiberg to afford partially substituted, lower charged species such as **I-61,** which upon complete substitution could yield a neutral tetrahedrane **I-62**, thereby conceptually linking Zintl anions to saturated silicon cage compounds.[162,279] Yet, the experimental realization of this concept remained an insurmountable challenge for a long time due to the limited solubility of highly charged Zintl anions in common organic solvents and their intrinsic instability arising from their high reduction potentials.

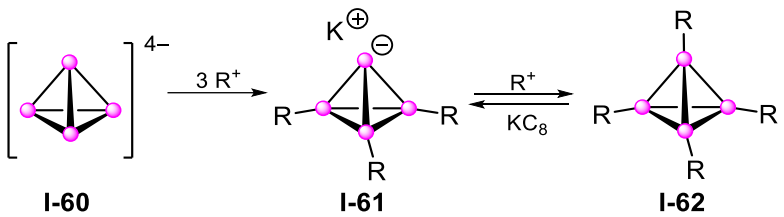

Scheme 6. Conceptual substitution of $[Si_4]^{4-}$ Zintl ion **I-60** to afford saturated silicon cage **I-62** (○ = Si).[162]

Only a few examples are known for the reactivity of silicon-based Zintl ions with transition metals. To date, $[(MesCu)_2Si_4]^{4-}$ **I-63** (Figure 10) remains the only structurally characterized $[Si_4]^{4-}$ transition metal complex.[280] Complex **I-63** is obtained by reacting $K_6Rb_6Si_{17}$ with mesityl copper in liquid ammonia, with the two η^3-coordinated CuMes fragments capping the central Si_4 tetrahedron, preserving the tetraanionic charge. This structural motif also provided the first evidence of $[Si_4]^{4-}$ in the solid state prior to its isolation and subsequent crystallographic characterization by the groups of Fässler and Korber.[277,278]

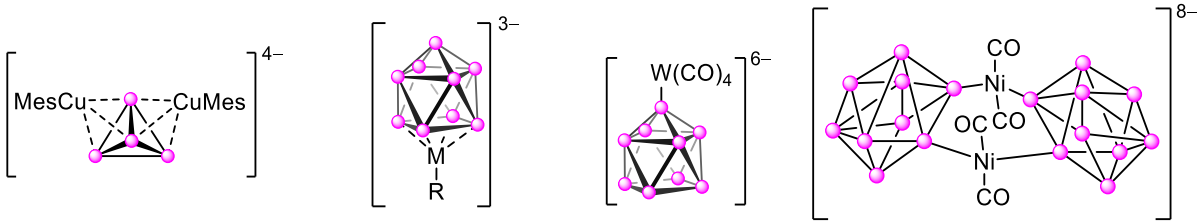

I-63 **I-64** (M = Zn, R =Ph) **I-65** (M = Cu, R = NHC^{Dip}) **I-66** **I-67**

Figure 10. Transition metal complexes with silicon-based Zintl ions as stabilizing ligands (● = Si, Mes = 2,4,6-trimethylphenyl, NHC^{Dip} = bis(2,4,6-diisopropylphenyl) *N*-heterocyclic carbene).[280–285]

$[Si_9]^{4-}$ Zintl ion **I-59** carries a lower charge per atom as opposed to $[Si_4]^{4-}$, which translates into higher stability in solution and thus better control over its reactivity, ultimately enabling a broader range of transition metal complexes. For example, reaction of $K_{12}Si_{17}$ with $ZnPh_2$[281] or $NHC^{Dip}CuCl$[282,283] affords the η^4-coordinated transition metal complexes $[Si_9Zn–Ph]^{3-}$ **I-64** and $[Si_9Cu–NHC^{Dip}]^{3-}$ **I-65**, respectively (Figure 10). A further example is the tungsten tetracarbonyl Si_9 Zintl complex **I-66** (Figure 10), recently reported by Korber and co-workers.[284] For the preparation of **I-66**, $K_6Rb_6Si_{17}$ was treated with $W(CO)_4$(tmeda) in the presence of [2.2.2]-cryptand in liquid ammonia. The coordination of the $W(CO)_4$ fragment resembles that of a silylene ligand, coordinating through a single silicon vertex while four alkali metal cations occupy the immediate coordination sphere and two additional cations reside within the cryptand cavities. In 2009, the same group reported on the conversion of $K_6Rb_6Si_{17}$ with $[Ni(CO)_2(PPh_3)_2]$ in liquid ammonia, affording the binuclear complex $[Si_9Ni(CO)_2]_2^{8-}$ **I-67** (Figure 10), in which the nickel centers bridge a pair of $[Si_9]^{4-}$ moieties through a central six-membered Si_4Ni_2 ring.[285] To date, no catalytic applications of transition metal complexes with silicon-based Zintl clusters have been reported.

1.2.3 Siliconoids

Owing to their partially unsubstituted silicon cluster scaffolds, siliconoids serve as a conceptual link between saturated silicon cage compounds and Zintl ions. Siliconoids are considered key intermediates in gas-phase-deposition processes (CVD) leading to amorphous silicon (a–Si) which is used in various semiconducting devices.[220,221,286,287] The partially unsubstituted cluster scaffold of siliconoids resembles that of silicon surface materials on a molecular scale.

In particular, the hemispheroidally coordinated vertices resemble the dangling bonds of silicon surfaces, thereby establishing siliconoids as molecular model systems for these materials. A deeper understanding of the reactivity of such surfaces requires the exploration of siliconoids.

The term “siliconoid” derives from the parent term “metalloid” or “metalloid cluster”, originally introduced by Schnöckel for molecular clusters of Group 13 that feature more metal-metal than metal-ligand bonds and possess exposed cluster atoms entirely free of peripheral bonds.[288–290] Metalloids are typically prepared by treating metastable solutions of metal monohalides with nucleophilic scavenging reagents, affording clusters containing up to 84 metal atoms and reaching diameters of up to 2 nm. The oxidation state of the atoms in the cluster scaffold is restricted to either 0, as in the elemental form, or +I, as found in the low-valent precursors. In 2007, Schnepf and coworkers expanded this concept to Group 14 metalloid clusters with the general formula E_nR_m (E = Ge, Sn; n>m), in which naked and substituted tetrel atoms coexist within the same scaffold.[291] The average oxidation state is between 0 and +I, even though Group 14 elements generally favor the +II oxidation state. Subsequently, Scheschkewitz coined the term “siliconoids” for unsaturated, molecular silicon clusters that feature at least one unsubstituted cluster vertex, irrespective of the average oxidation state.[232] The sole criterion for the “naked” silicon atom is a hemispheroidal coordination environment, corresponding to that of surface atoms in spherical particles and thereby supporting the use of siliconoids as model systems. The hemispheroidality is quantified by the parameter Φ, which is defined using a reference plane formed by four atoms. The atom under consideration is bonded to three cluster vertices with the sum of the three angles being closest to 360°. By convention, the deviation of the fourth atom from the plane is assigned a negative value. If the deviation of the scrutinized atom from the plane is negative, the atom adopts a (distorted) tetrahedral coordination environment, whereas a positive value indicates hemispheroidal coordination (Figure 11).[221]

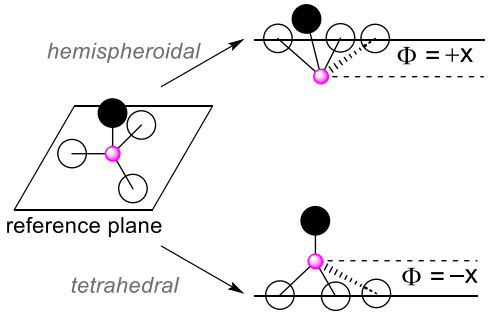

Figure 11. Visual explanation of the difference between a tetrahedral and a hemispheroidal coordination (○ = Si, ○ = substituent in plane, ● = substituent out of plane).

Four general synthetic approaches are employed for the synthesis of siliconoid clusters: (a) the use of disilenides as low-valent Si sources; (b) the reductive coupling of two or more halogenated Si^{IV} precursors, analogous to the formation of saturated silicon cage clusters; (c) thermally induced conversions such as isomerization, cluster contraction, dimerization; and (d)

the partial derivatization of silicon-based Zintl Ions.[221] The absence of silylenes as low-valent silicon sources in method (a) for many years is largely attributed to the comparatively late discovery of stable silylenes.[99] Only recently have examples been reported in which asymmetrical disilenes are generated from silylene precursors.[292–294]

In 2005, application of method (a) to Tip_3-lithium disilenide enabled Scheschkewitz to isolate the first stable siliconoid **I-68a** featuring a hemispheroidal coordination vertex (Scheme 7). At the time, this species was described as "a molecular silicon cluster with a 'naked' vertex atom".[295] Treatment of four equivalents of disilenide **I-49** with silicon tetrachloride affords **I-68a** together with a systematic oxidative byproduct, a peraryl-substituted tetrasilabutadiene. A related approach was later applied by Iwamoto and co-workers.[296] Starting from potassium-disilenide **I-69**[297] and 0.5 equivalents of tetrachloro silane, a differently substituted siliconoid **I-68b** was obtained (Scheme 7). The hemispheroidality parameters for **I-68a** and **I-68b** were determined to be very similar with Φ = 0.192 Å (**I-68a**) and Φ = 0.183 Å (**I-68b**), with both structures being highly distorted due to transannular interactions.[221]

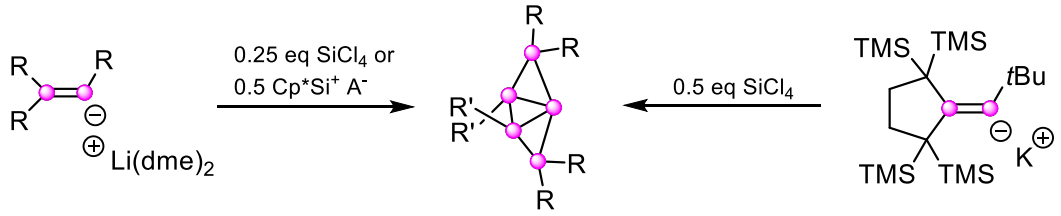

I-49 **I-68a,b** **I-69**

Scheme 7. Synthesis of siliconoid **I-68a,b** from disilenides **I-49** or **I-69** (○ = Si, **I-68a**: R = R' = 2,4,6-triisopropylphenyl; **I-68b**: R = $C((SiMe_3)_2CH_2)_2$, R' = *t*Bu).[295,296]

In 2010, the groups of Breher and Schnöckel reported on the isolation of pentasila[1.1.1]propellane **I-70** (Scheme 8),[298] a species already proposed by Masamune *et al.* in 1991.[299] Pentasila[1.1.1]propellane **I-70** was obtained from the reductive reaction of Mes_2SiCl_2 and Si_2Cl_6 in a 3:1 ratio in presence of lithium/ naphthalene, albeit in rather low yield.[298] The unsubstituted silicon vertices display a Si–Si distance of 2.636 Å and the hemispheroidality parameter Φ indicates that both "naked" silicon atoms are hemispheroidally coordinated with Φ = +1.323 Å and Φ = +1.313 Å, thereby fulfilling the criteria for the classification as a siliconoid.

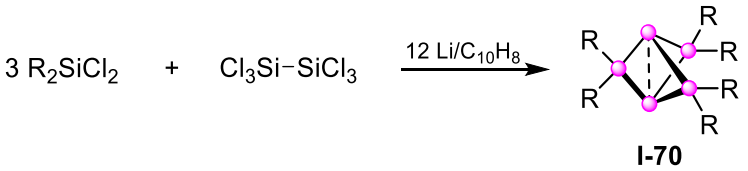

I-70

Scheme 8. Reductive coupling of silane and disilane precursors to form **I-70** (○ = Si, R = 2,4,6-trimethylphenyl).[298]

Although an all-silicon analogon of Hückel-aromatic benzene remains hypothetical, several hexasila isomers have been reported over the years.[194,234,236,249] While Sakurai and Sekiguchi's hexasilaprismane is rather electron-precise,[236] the tricyclic Si_6R_6 isomer **I-72**

(Scheme 9) reported by Scheschkewitz *et al.* exhibits a strongly delocalized, dismutational substitution pattern.[194,300] Reductive dimerization of trichloro cyclotrisilane **I-71** or pentamethylcyclopentadienyl-substituted cyclotrisilene affords the hexasilabenzpolarene **I-72** (Scheme 9).[301,302] In **I-72**, the oxidation states range from +II for the SiR_2 moieties to +I for SiR, and 0 for the unsubstituted vertices. This reflects a twofold dismutation, yielding a central Si_4 plane featuring a rhomboidal coordination environment, composed of two unsubstituted and two monosubstituted silicon atoms, connected by two opposing saturated SiR_2 fragments. The structure adopts a chair-like Si_6-ring with a dismutated arrangement of the substituents, resulting in cyclic electron delocalization across the central four-membered ring. Consequently, **I-72** is referred to as the "dismutational isomer of hexasilabenzene".[194,300] Notably, the "naked" silicon atoms display an unusually elongated Si–Si bond distance of 2.729 Å. Together with the electron density distribution in the solid state, this points to a pseudo-tricoordinate environment and is reflected in the high hemispheroidality value of Φ = +1.115 Å (Si_{11} Φ = +1.054 Å/ +0.311 Å, Si–Si 2.498 Å).

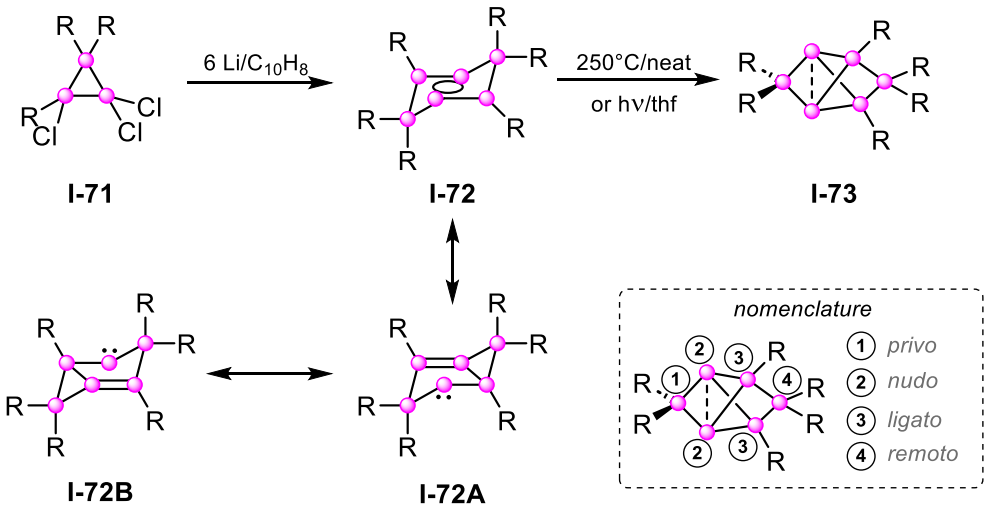

Scheme 9. Reductive dimerization of cyclotrisilane **I-71** to hexasilabenzpolarene **I-72** and photolytical/thermal rearrangement to global minimum isomer **I-73** (○ = Si, R = 2,4,6-triisopropylphenyl).[194,301]

Thermal or photolytical treatment of **I-72** leads to the rearranged **I-73** (Scheme 9)[301] which consists of a propellane motif not unlike that of Breher's propellane scaffold **I-70** (Scheme 8),[298] with a $SiTip_2$ silylene unit bridging the two propeller blades. As a side product, a Si_{11} siliconoid is formed, representing the largest fully characterized silicon cluster core reported to date.[301] Since the parent species represents the energetically deepest point on the Si_6H_6 potential energy surface, **I-73** can be considered as the global minimum isomer of hexasilabenzene.[301] Akin to the dismutational isomer **I-72**, **I-73** exhibits an unusually long Si–Si distance of 2.708 Å between the unsubstituted silicon vertices, which is roughly 13% longer than a typical Si–Si single bond (2.3 – 2.4 Å). This elongation is a consequence of the lack of significant direct bonding interaction and is reflected in the calculated reaction energy towards dihydrogen that is weaker than in common disilanes.[298] In experimental charge density

investigations of **I-72** and **I-73** by Stalke and Scheschkewitz,[303] the bonding situation between the bridgehead silicon atoms was further elucidated. The absence of a bond path in the executed theoretical calculations is indicative of a considerable biradical character; however, this feature is highly sensitive to subtle variations in the electron density of the systems. The "naked" silicon atoms in **I-73** show a pronounced hemispheroidal coordination environment with Φ = +1.354 Å.[301] The UV/Vis spectrum of **I-73** shows a longest wavelength absorption of λ_{max} = 473 nm,[301] which is significantly blue-shifted compared to that of the unbridged propellane **I-70** at λ_{max} = 546 nm.[298] In the ^{29}Si NMR spectra, the hemispheroidally coordinated silicon vertices of the hexasilabenzene isomers **I-72** and **I-73** give rise to distinct upfield-shifted signals, comparable to those observed for many Zintl ions.[258,276,304–310] In contrast to $[Si_4]^{4-}$ **I-57** and $[Si_9]^{4-}$ **I-59** but similar to $[Si_5]^{2-}$ **I-58** however, the siliconoids **I-72** and **I-73** also show signals in the very low field region resulting in an overall distribution of the chemical shifts across approximately 450 ppm.[311] The broad range of NMR chemical shifts reflects the characteristic magnetic anisotropy of siliconoids. For the "naked" bridgehead atoms, a diatropic current vortex is calculated, leading to pronounced magnetic shielding, whereas the mono- and disubstituted vertices experience a paratropic current loop.[300,312–315] The overall induced molecular current in **I-72** and **I-73** is of diamagnetic character with a magnitude of approximately 10 nAT^{-1}. This value closely matches the one typically associated with classical 6π Hückel-aromatic benzene. In planar Hückel-aromatic systems, however, a central paramagnetic vortex coexists with the overall diamagnetic ring current.[300] The central diatropic current loop in **I-72** and **I-73** rather resembles the spherical aromaticity in P_4. With the delocalization of the six electrons in **I-72** confined to the central, planar four-membered ring,[316] which consists of two π,σ- and two non-bonding electrons in contrast to six π-electrons in Hückel-aromatic benzene, it displays dismutational aromaticity accompanied by a remarkable kinetic stability.[300] In comparison, the thermodynamically favored hexasilabenzpolarene **I-73** decomposes rapidly upon exposure to air but shows outstanding thermal stability under intert conditions, which even allows for gas-phase transfer with only very minor decomposition.[301] In order to distinguish the four distinct positions in **I-73** and inspired by the *ortho*, *meta* and *para* positions in benzene derivatives, Scheschkewitz *et al.* coined the terms *privo*, *nudo*, *ligato* and *remoto* (Scheme 9).[317]

In 2020, Lips and co-workers reported the conversion of their butterfly shaped Si_4 precursor **I-74** at 400°C into the highly unsaturated Si_6R_4 siliconoid **I-75** (Scheme 10, left), the first example of a siliconoid with amino-substituents instead of sterically encumbering alkyl, aryl or silyl groups.[318] Although the reaction mechanism has not been fully elucidated, the proposed elimination of a bis(amino)silylene as an initial step, analogous to the formation of Iwamoto's Si_8 and Si_7 siliconoids, is plausible.[222,296,318,319] The molecular structure of **I-75** can be described as a distorted trigonal prism, with each triangular face composed of two SiR moieties

and one “naked” vertex. The unsubstituted silicon vertices show a Si–Si distance of 2.636 Å and exhibit a distinctly hemispheroidal coordination environment of Φ = +1.45/ +1.48 Å, which clearly identifies **I-75** as a siliconoid. Quantum mechanical calculations support the absence of a direct bonding interaction between the “naked” silicon vertices: no bond critical point is found between the two bridgehead silicon atoms by Bader’s quantum theory of atoms in molecules (QTAIM)[320] and no intrinsic bond orbital (IBO)[321,322] is present for a corresponding σ-bond. The central butterfly shaped Si_4R_2 ring features only two σ-bonds, which accounts for the pronounced differences in the Si–Si bond lengths within the ring: two of the bonds are significantly elongated, while the two shorter ones approach typical Si=Si double bond lengths. This bonding pattern points toward the presence of multicenter bonding.[318] Moreover, each of the unsubstituted silicon vertices carries a lone pair, which enables the formulation of two resonance structures that resemble a C_6H_4 butalene-type isomer.[323] Two years later, in 2022, the same group reported on the isolation of another unexpected isomer of hexasilabenzene **I-77** (Scheme 10, right).[324] Owing to its twisted *cis*-bent geometry, **I-77** was described as comparable to the buckled dimer due to its alleged structural resemblance to the Si(100) surface. Unlike **I-72** and **I-73**, **I-77** contains only one unsubstituted silicon vertex, which shows a pronounced hemispheroidal coordination environment with Φ = 1.70 Å. The reactivity of **I-77** toward elemental iodine or methyl iodide results in a twofold substitution, yielding either the iodinated product or the methylated derivative at the anionic “naked” silicon vertex, accompanied by iodination of the former positively charged silicon vertex.[324] Reduction of **I-77** with KC_8 leads to an anionic cluster that retains the Si_6 framework, and was further functionalized using electrophiles such as methyl iodide, SiX_4 (X = Cl, Br) and $BH_3{\cdot}SMe_2$.[325]

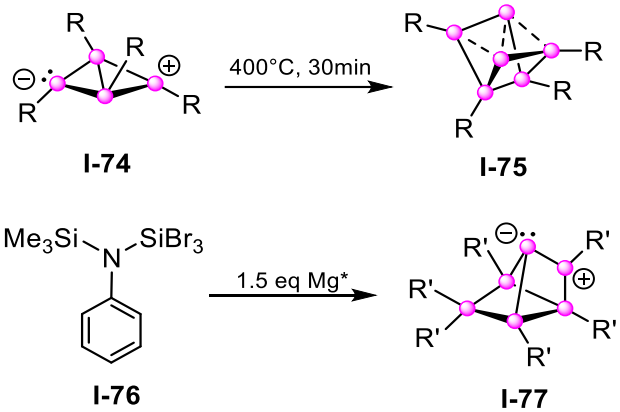

Scheme 10. Synthesis of Si_6 siliconoids **I-75** (top) and **I-77** (bottom) by Lips (○ = Si, R = N(SiMe$_3$)Dip [Dip = 2,6-diisopropylphenyl], R’ = N(SiMe$_3$)Ph).[318,324]

Recently, the Fässler group successfully applied method (d) to synthesize a novel siliconoid by using soluble Zintl anions as precursors to access anionic siliconoids.[326] Addition of six equivalents of Si(*t*Bu)$_2$HCl to the activated Zintl phase $K_{12}Si_{17}$/[2.2.2]-cryptand in thf affords the trisubstituted, monoanionic Si_9 siliconoid **I-78** (Scheme 11). During crystallization, partial loss of a silyl substituent was observed as a result of disproportionation, giving rise to the

disubstituted dianionic species **I-79**.[326] All seven exposed cluster atoms show a distinctly hemispheroidal coordination environment with values between Φ = +1.268 and Φ = +1.585 Å. The Si–Si bond lengths are shorter than in the bare tetraanionic $[Si_9]^{4-}$ **I-59**, which reflects the reduced Coulomb repulsion associated with the remaining two negative charges.[275,277]

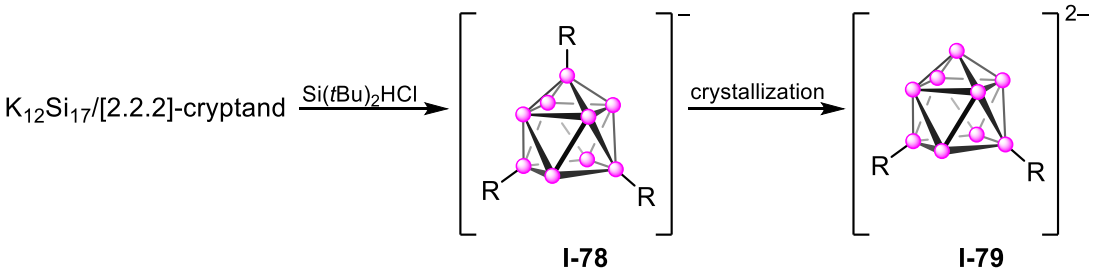

Scheme 11. Formation of anionic Si_9 siliconoid **I-78** and subsequent derivatization to dianionic **I-79** (○ = Si, R = $SiHtBu_2$, $Si(TMS)_3$, $SnCy_3$).[326]

Further anionic siliconoids, derived from the dismutational hexasilabenzene isomer **I-72**, were obtained by Scheschkewitz *et al.* starting in 2016. Reductive cleavage of one Tip substituent from **I-72** with a lithium/ naphthalene solution led to the *ligato*-lithiated siliconoid **I-80**, which features a bridged propellane scaffold (Scheme 12), similar to that of the global minimum isomer of hexasilabenzene **I-73**.[327] The two ”naked” Si atoms remain unaffected by the reduction, while a negatively charged silicon center is generated. These anionic silicon clusters provide a conceptual bridge between neutral siliconoids and bare, polyanionic Zintl clusters. **I-80** can also be prepared through an extended reduction of **I-71** by adding an additional equivalent of reducing agent lithium/ naphthalene, thereby circumventing the isolation of **I-72**.[327]

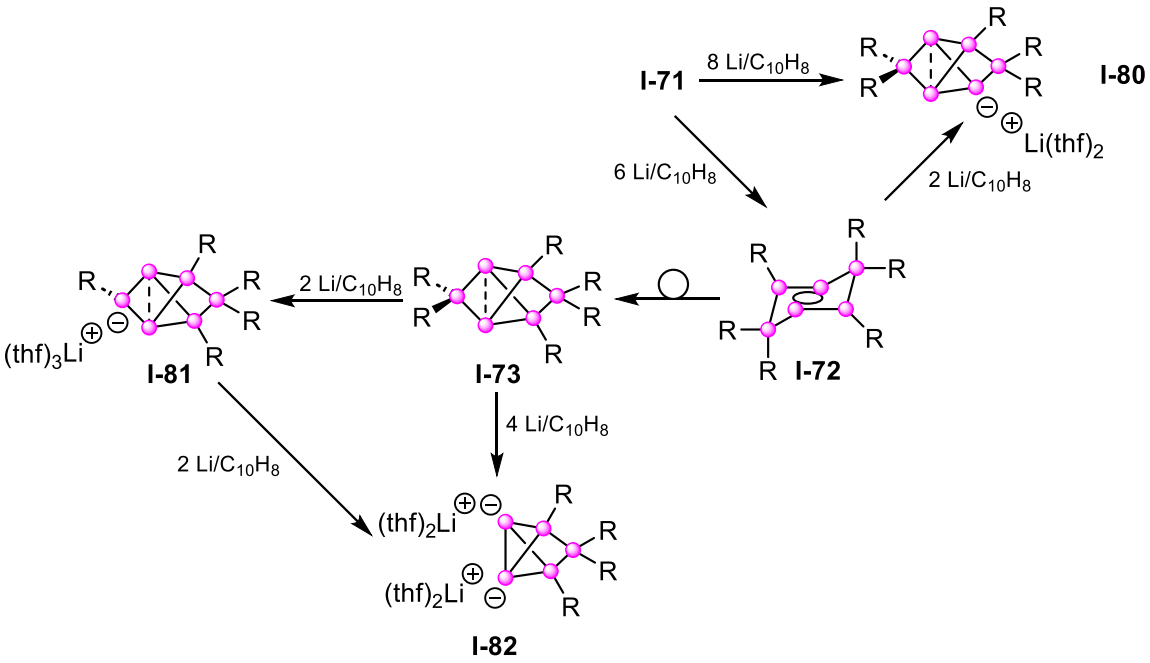

Scheme 12. Transformation between various siliconoids and silicon clusters (○ = Si, R = 2,4,6-triisopropylphenyl).[327–329]

Notably, the reduction of the global minimum isomer **I-73** itself by two equivalents of lithium/ naphthalene results in the cleavage of a different Si–C bond affording the regioisomeric *privo*-lithiated Si_6 siliconoid **I-81** (Scheme 12).[328] The position of the anionic functionality within the propellane motif gives rise to a distinctly different inherent electronic character, which directly affects the ^{29}Si NMR chemical shifts, depending on whether the negative charge resides at the *privo*-position or elsewhere. Substitution at these positions leads to a substituent-dependet shift of the signal assigned to the corresponding silicon vertex, which can be rationalized using the Hammett parameter σ_m, that quantifies the electronic nature of the substituent. The effect is reversed depending on whether the same substituent is attached at the *privo*- or the *ligato*-position. When an electronegative substituent occupies the *ligato*-position, the *privo*-vertex becomes deshielded, whereas attachment of the corresponding substituent at the *privo*-position leads to a shielding effect. Reaction with Group 13-15 electrophiles proved the anionic Si_6 siliconoids **I-80** and **I-81** as versatile synthons enabling the transfer of an intact benzpolarene framework.[328]

Further reduction of **I-81** or direct treatment of **I-73** with two additional equivalents (four in total) of the reducing agent, affords the dianionic silicon cluster **I-82** through cleavage of the *privo*-$SiTip_2$ unit (Scheme 12).[329] The molecular structure of **I-82** features a five-atomic scaffold composed of a $Si_4Tip_2^{2-}$ tetrahedron edge-bridged by the remaining $SiTip_2$ unit, which reveals a close structural relationship to the edge-on protonated Zintl ion $[\mu\text{-}HSi_4]^{3-}$ described by Fässler.[311] Owing to its symmetry, three signals appear in the ^{29}Si NMR spectrum, including a distinct high field resonance at −298 ppm for the two anionic, unsubstituted vertices, which is in the characteristic region for bare silicides.[275,277,278] Treatment of **I-82** with dichlorides of boron or phosphorous restores the six-atomic benzpolarene framework yielding **I-83a,b**, albeit with an amino-substituted B or P heteroatom in the *privo*-position (Scheme 13).[329] These examples further reinforce the analogy to silicon surfaces in technological doping processes of bulk silicon materials.

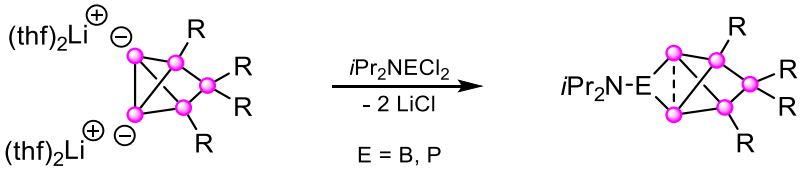

I-82 **I-83a,b**

Scheme 13. Doping of dianionic **I-82** with heteroatoms (E = B, P) in *privo*-position (○ = Si, E = B (**a**), P (**b**), R = 2,4,6-triisopropylphenyl).[329]

The functionalization of the *ligato*-lithiated Si_6 siliconoid can be affected either exohedrally or endohedrally. Exohedral attachment of functional groups to the cluster is achieved by reaction with electrophiles such as benzoylchloride, chlorotrimethylsilane[317] or metallocene precursors giving transition metal complexes (**I-84a,b** M = Zr, Hf, Scheme 14).[330] In this way, it is also

possible to link the siliconoid motif to other cluster systems such as silsesquioxanes, which serve as model systems for silicon monoxide.[331] Treatment of **I-80** with chloro stabilized amidinato tetrylenes **I-7a-c**[107,115,332,333] gives rise to siliconoid/tetrylene hybrid species **I-85a-c** (Scheme 14) under retention of the structural motif characteristic of siliconoids.[330] With the pending auxiliary tetrylene ligand, **I-85a-c** are potent precursors for the formation of transition metal complexes featuring siliconoid clusters.

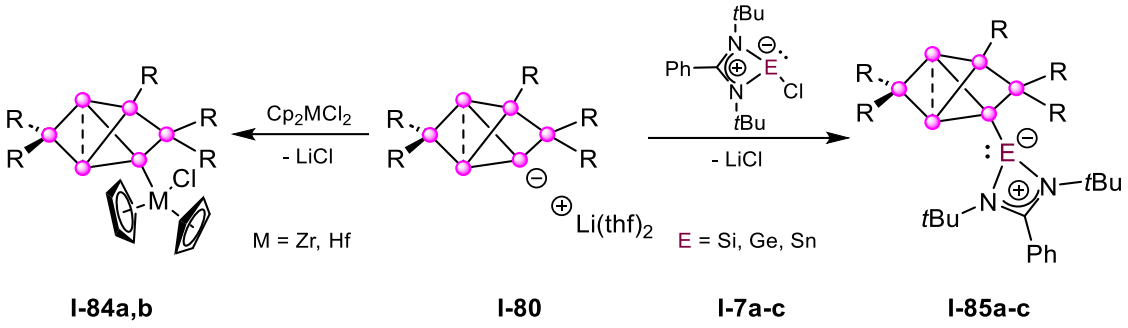

Scheme 14. Functionalization of *ligato*-Si_6Li **I-80** with metallocenes to complexes **I-84a,b** and tetrylenes to hybrids **I-85a-c** (○ = Si, E = Si (**a**), Ge (**b**), Sn (**c**), M = Zr (**a**), Hf (**b**), R = 2,4,6-triisopropylphenyl).[330]

The lone pairs of Si_6/tetrylene hybrids **I-85a-c** (Scheme 14) enable versatile reactivity toward transition metal centers. In analogy to the previously discussed silylene-transition metal clusters (see Chapter 1.1.2), reaction of **I-85a-c** with $Fe_2(CO)_9$ leads to the coordination of the tetrylene unit to the iron center in the $Fe(CO)_4$–siliconoid/tetrylene complexes **I-86a-c** (Scheme 15).[330] In this case, an interaction of the transition metal with the siliconoid cluster scaffold is not apparent. In contrast, reaction of **I-85a** with $[Rh(CO)_2Cl]_2$ affords a Si_7Rh heterosiliconoid **I-88**, in which the rhodium center is fully incorporated into the cluster core.[334] In the reaction mixture, **I-88** unexpectedly rearranges to the rhodium-substituted Si_6 siliconoid **I-89** at room temperature, restoring the intact benzpolarene framework and shifting the rhodium center into the periphery (Scheme 15). This transformation requires the presence of an unidentified intermediate as source of an activated CO equivalent: **I-88** is stable after isolation but can be prompted to still undergo the reaction by addition of 0.1 equivalents of siliconoid/tetrylene **I-85a-c** and 0.4 equivalents of $[Rh(CO_2)Cl]_2$.[334] In a similar manner, reaction of **I-85a-c** with $[IrcodCl]_2$ affords the Ir–Si_6/tetrylene complexes **I-87a-c** *via* oxidative addition to the Si–Si bond between the *privo*- and *nudo*-Si atom (Scheme 15).[334] The iridium center in **I-87a-c** is coordinated not only by the tetrylene fragment but also by the former *nudo*-silicon vertex. **I-87a-c** was shown to be an efficient catalyst for alkene isomerization with exceptionally high TOF and TON values.[334] In addition, the presence of a residual chloride renders **I-87a-c** amenable to further functionalization.

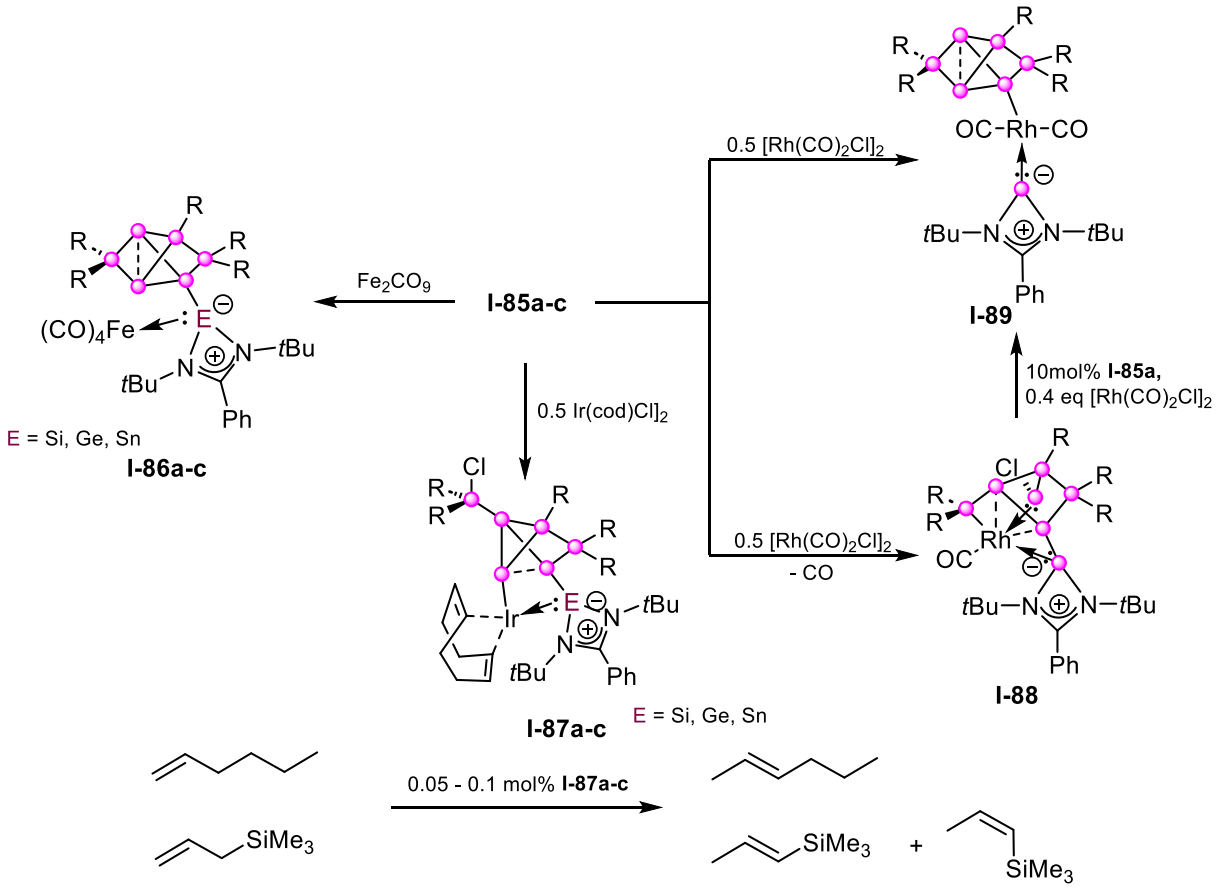

Scheme 15. Transition metal complexes of **I-86 – I-89** and **I-87a-c** as a catalyst for alkene isomerization (○ = Si, E = Si (**a**), Ge (**b**), Sn (**c**), R = 2,4,6-triisopropylphenyl).[330,334]

Returning to the more accessible first row transition metals, attempts to complex nickel with the siliconoid/tetrylene ligand **I-85a-c** were investigated, but no reaction was observed. Interestingly, when the reaction was performed under a CO atmosphere, the C–O-insertion product **I-90** was formed, featuring a silene bond and a Si–O–Si bridge between the tetrylene moiety and the *privo*-vertex (Scheme 16).[335]

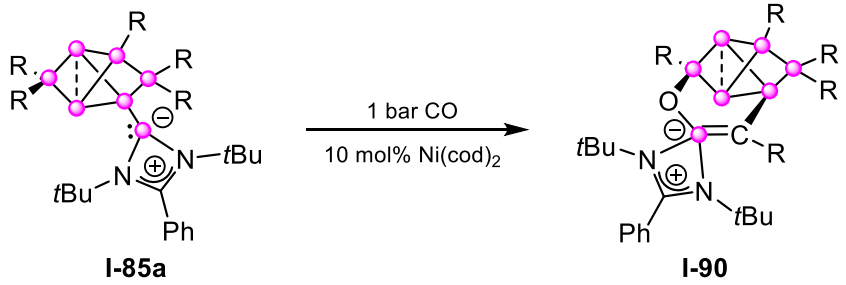

Scheme 16. Reactivity of **I-85a** towards CO in presence of $Ni(cod)_2$ (○ = Si, R = 2,4,6-triisopropylphenyl).[335]

In contrast to the exohedral functionalization with an additional tetrylene moiety, endohedral cluster expansion was observed when the *ligato*-lithiated Si_6 siliconoid **I-80** was reacted with Jutzi's decamethylsilicocene **I-1**.[336] In this transformation, a transient silylene-functionalized Si_6 cluster is proposed, ultimately yielding the atomically precise expanded, neutral Si_7 siliconoid cluster **I-91** (Scheme 17). The central unit of **I-91** consists of three unsubstituted

silicon vertices arranged in an isosceles triangle. The two basal silicon atoms display pronounced hemispheroidal coordination with values of Φ = +1.341 and +1.308 Å, whereas the apical silicon atom shows negligible hemispheroidality with a value of Φ = +0.039 Å. The geometry can alternatively be described as a persila[1.1.1]propellane with twofold bridging of the propeller blades.[221] Similar to the Si_6-siliconoids **I-72** and **I-73**, **I-91** shows a wide dispersion of chemical shifts in the ^{29}Si NMR spectrum. A slight downfield-shift is observed for the apical Si atom (δ = −138.4 ppm) compared with the basal Si atoms (δ = −241.9 and −229.6 ppm), though these values are still within the chemical shift range typical for "naked" cluster atoms.[194,301,327,328,330] In contrast, pronounced deshielding is observed for the monosubstituted silicon atoms, appearing at δ = 156.0 and 181.9 ppm. As in the case of **I-73**, the Si_7H_6 parent compound corresponding to **I-91** also represents the global minimum on the potential energy surface.[337] It is noteworthy that the structure of **I-91** may correspond to the Si_7Tip_6 species detected by EI-MS in the spectroscopic investigation of Si_5Tip_6 siliconoid **I-68b**.[295]

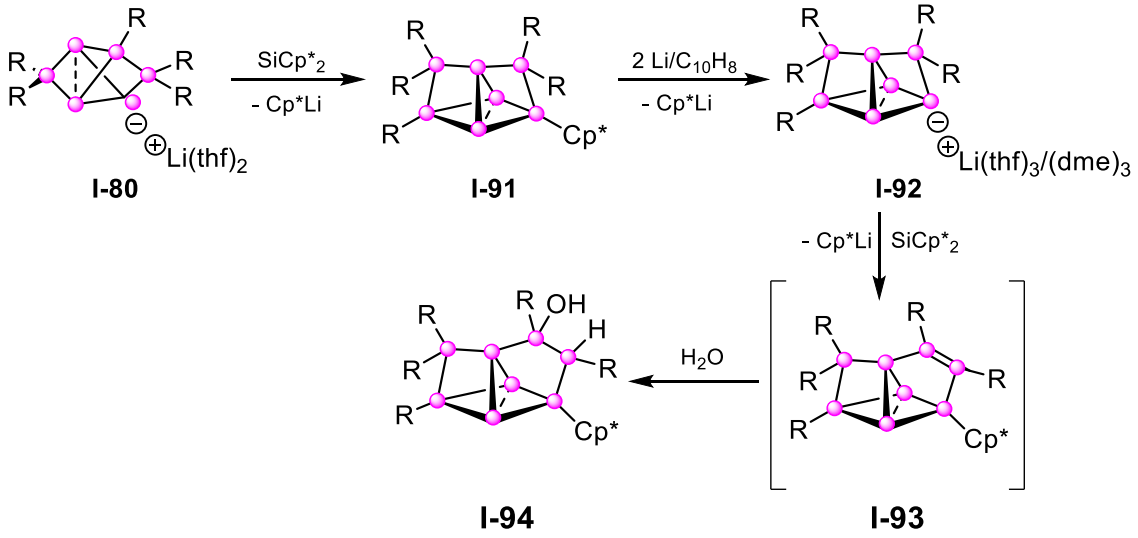

Scheme 17. Atomically precise expansion of Si_6 siliconoid to Si_7 and Si_8 siliconoids (○ = Si, R = 2,4,6-triisopropylphenyl).[336]

Reductive cleavage of the Cp* moiety in **I-91** affords lithiated Si_7 siliconoid **I-92**, which upon subsequent treatment with $SiCp^*_2$ leads to the formation of the further expanded Si_8 siliconoid **I-93** (Scheme 17), featuring a proposed exohedrally bridging Si=Si double bond.[336] Although Si_8 **I-93** itself could not be isolated, the hydrolysis product, the structurally analogous Si_8OH species **I-94** (Scheme 17), is isolable, thereby confirming the Si=Si double bond reactivity of **I-93**. In the anionic Si_7 siliconoid **I-92**, the structural parameters remain essentially unchanged compared with **I-91** (base: Φ = +1.287 and +1.273 Å, apex: Φ = +0.085 Å). In contrast, the structural environment of Si_8OH **I-94** and thus presumably also that of Si_8 **I-93,** shows a distortion of the apical silicon atom, resulting in a more tetrahedral coordination with a negative hemispheroidality parameter Φ. Hence, only the two basal, "naked", hemispheroidal Si atoms

are retained and can be considered decisive for classifying the Si_8 compounds as siliconoid clusters with Φ = +1.336 and +1.302 Å.

Table 1. Overview and comparison of the essential structural and electronic features of representative siliconoids reported by the Scheschkewitz group.[194,301,327,328,330,336]

	Si_6 **I-72**	Si_6 **I-73**	*ligato*-Si_6Li **I-80**	*privo*-Si_6Li **I-81**	Si_6NHSi **I-85a**	Si_7Cp^* **I-91**	Si_7Li **I-92**
d(Si–Si) [Å]	2.7287	2.7076	2.551	2.556	2.604	2.648	2.560
largest Φ [Å]	+1.115	+1.354	+1.281	+1.308	+1.314	+1.341	+1.287
$\delta(^{29}Si_{unsubst})$	−89.3	−274.2	−237.29/ −238.15	−222.2/ −231.4	−244.6/ −260.7	−229.6/ −241.9	−191.9/ −195.7
λ_{max} [nm]	623	473	364	468	472	326	450

A similar insertion into the cluster scaffold was observed by addition of NHC-stabilized dichloro germylene to **I-85a**. The reaction proceeds initially *via* a dangling side arm followed by rearrangement to the germanium-inserted species. Subsequent reduction affords the heterosiliconoids **I-95a-c** (Scheme 18)[338] with structures closely resembling the Si_7 cluster scaffolds **I-91** and **I-92** (Scheme 17). Further examples of the endohedral cluster expansion were reported for chalcogen-insertion into the siliconoid/tetrylene hybrid **I-85a** yielding the heterosiliconoids **I-96a-c** (E = S, Se, Te) (Scheme 18),[339] which adopt geometries similar to those of the Si_8 clusters **I-93** and **I-94** (Scheme 17).[336]

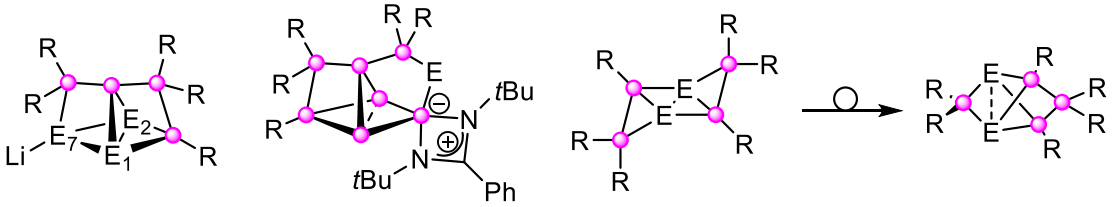

E = Si or Ge **I-95a-c** | E = S, Se, Te **I-96a-c** | E = Ge, Sn **I-97a,b** | E = Ge, Sn **I-98a,b**

Scheme 18. Synthesis of heterosiliconoids **I-95-I-98** (○ = Si, R = 2,4,6-triisopropyphenyl).[338–341]

It should be noted that treatment of disilenide **I-49** with $GeCl_2$·dioxane or $SnCl_2$ in the presence of lithium/ naphthalene leads to the digerma- and distannatetrasila analogues **I-98a,b** of the hexasilabenzene isomer (Scheme 18).[340–342] In the case of **I-98a**, the digerma-substituted dismutational isomer can be isolated and a slow isomerization to the global minimum isomer **I-97a** is observed at room temperature. Acceleration is achieved by heating to 65°C for 12 hours. For the tin analogue, however, the corresponding dismutational isomer **I-97b** was not detectable even at −80°C, indicating extremely low thermal stability.[342] Although **I-97a,b** and **I-98a,b** cannot be considered true siliconoids due to their lack of a hemispheroidal silicon vertex, their structures closely resemble those of the Si_6 siliconoids **I-72** and **I-73**, hence they can still be designated as heterosiliconoids. In a similar fashion, mixed clusters were reported by the groups of Breher[343] and Lips.[344]

A recent example for an anionic Si_7 siliconoid with a different core structure and only three substituents was reported by Lips and co-workers. Reduction of their bicyclic Si_4 ring (**I-74**, Scheme 10) with potassium graphite in presence of crown ether affords the Si_7 siliconoid **I-100**[345] *via* formation of a homocyclic, isolable silylene.[346] To date, no reactivity has been reported for this Si_7 siliconoid.

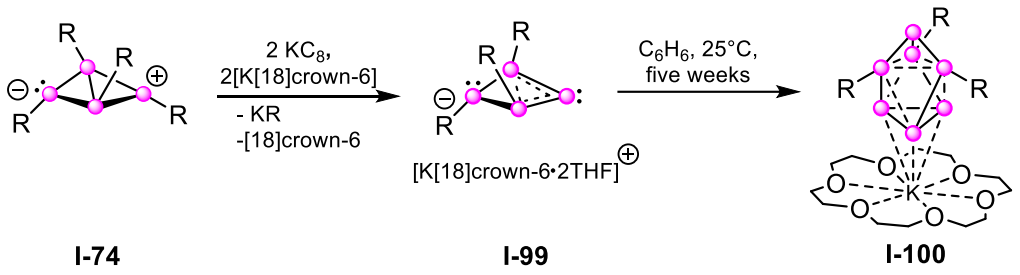

I-74 **I-99** **I-100**

Scheme 19. Synthesis of anionic Si_7 siliconoid **I-100** by Lips *et al*. *via* silylene **I-99**.[346]

2. Aims and Scope

As siliconoids serve as versatile model systems for bulk silicon, owing to their proposed role as intermediates in the gas phase deposition process of elemental silicon, the investigation of their formation mechanisms, the functionalization pathways and modelled “surface-chemistry” is of fundamental research interest. In this context, our group has examined both endohedral and exohedral expansions of siliconoids using Group 14 precursors as well as heteroatom doping (see Chapter 1.2.3). Due to the unprecedented electronical behavior arising from the partially unsubstituted and therefore highly reactive silicon atoms, siliconoids have recently attracted attention as ligand systems. Though only a limited number of transition metal complexes featuring siliconoids as ligands has been realized to date, and their application – particularly in catalysis – remains scarcely explored.

One of the rare examples is the iridium siliconoid/silylene catalyst **I-87a** (Chapter 1.2.3, Scheme 15,) previously reported in our group. Reaction of Si_6-siliconoid/silylene **I-85a** with bis[(1,5-cyclooctadiene)iridium(I) chloride] affords **I-87a** through opening of the silicon cluster core accompanied by chlorination of the pendant silicon side arm.[334] The presence of the chloride substituent in **I-87a** motivated a subsequent reduction step aimed at inducing a rearrangement that may fully incorporate the iridium center into the cluster core (Scheme 20).

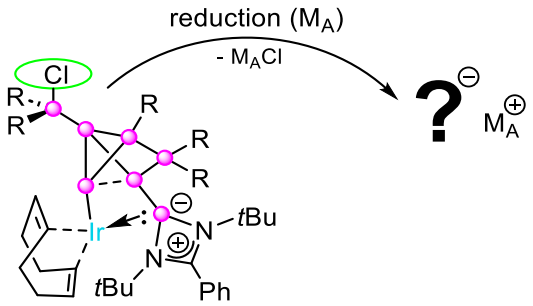

I-87a **A-1**

Scheme 20. Proposed reduction of iridium complex **I-87a** to **A-1** (○ = Si, M_A = alkali metal, R = 2,4,6-triisopropyphenyl).

A rearranged, supposedly heterobimetallic cluster **A-1** would provide access to potential transmetallation pathways toward heteromultimetallic transition metal complexes, a class of compounds currently of considerable interest because of their catalytic performance, for example as enzyme surrogates,[347–349] in the production of dihydrogen for energy storage applications[350] or as homogeneous catalysts supported by main group ligand systems.[351,352] Although the controlled introduction of an additional transition metal center into an existing transition metal complex is often considered the most challenging step, several reports have demonstrated successful transmetallation processes initiated by alkali metals.[353] Building on this knowledge, the reactivity of a proposed heterobimetallic siliconoid **A-1** toward early

transition metal precursors should be explored in order to provide access to multimetallic clusters for which significant potential as homogenous catalyst can be anticipated.

As noted earlier, the steric encumbrance imposed by the Tip substituents in Si_6Tip_5 derivatives limits the range of isolable siliconoid-based transition metal complexes. With the exception of iron carbonyl **I-86a** (Chapter 1.2.3, Scheme 15), the isolation of first row transition metal complexes employing Si_6-siliconoid/tetrylene hybrids as directing ligands remained elusive prior to the present work. This highlighted the need of further investigation into the chemistry of the Si_7 siliconoids, which possess an extended silicon scaffold relative to their Si_6 analogues while retaining the number of Tip substituents. The thus improved accessibility of the unsubstituted silicon vertices is expected to influence both the kinetic and electronic properties of the clusters. To enhance the σ-donating properties, as demonstrated for the of Si_6-siliconoid/tetrylene hybrids **I-85a-c**, the functionalization of the lithiated Si_7 core **I-92** with *N*-heterocyclic tetrylenes was a central goal of this thesis (Scheme 21).

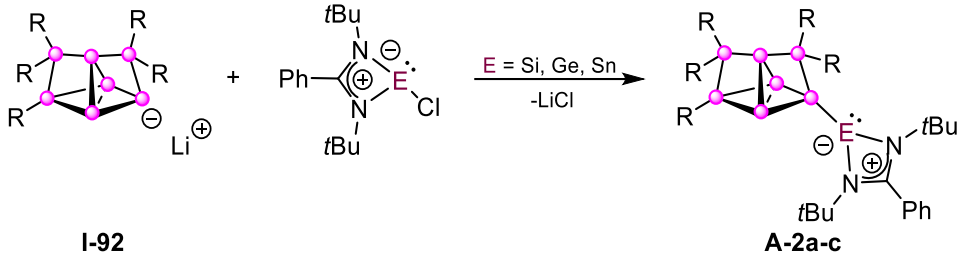

I-92 **A-2a-c**

Scheme 21. Proposed formation of tetrylene-functionalized Si_7 cluster **A-2a-c** (○ = Si, E = Si (**a**), Ge (**b**), Sn (**c**), R = 2,4,6-triisopropyphenyl.)

With the proposed Si_7-siliconoid/tetrylene species **A-2a-c**, investigations into their reactivity toward first row transition metals should be performed and compared with corresponding results for the Si_6-siliconoid/tetrylene hybrids. In this context, another target of this thesis was the incorporation of first row transition metals into the cluster scaffold: complexes of the type **A-3**, which interact directly with the siliconoid cluster core, were anticipated (Scheme 22).

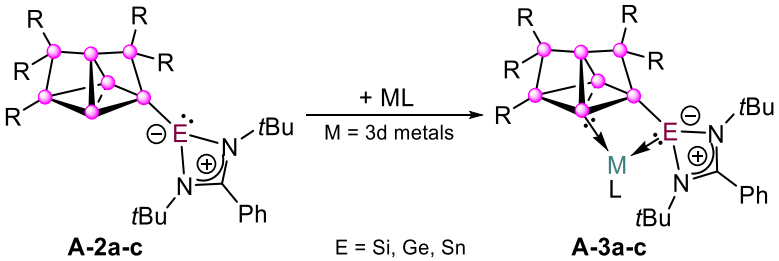

A-2a-c E = Si, Ge, Sn **A-3a-c**

Scheme 22. Complexation of transition metal precursors by proposed siliconoid/tetrylene hybrids **A-2a-c** (○ = Si, E = Si (**a**), Ge (**b**), Sn (**c**), M = 3d transition metal, L = ligand, R = 2,4,6-triisopropyphenyl).

The targeted transition metal siliconoid/tetrylene complexes **A-3a-c** should subsequently be evaluated for their reactivity toward small molecules. Given that transition metal silylene compounds have demonstrated pronounced activity in small molecule activation, enabled by the free coordination sites at the metal centers which also render them as valuable catalysts,[113,129] the potential of **A-3a-c** in homogeneous catalysis should further be explored.

3. Results and Discussion

3.1 Heterobimetallic unsaturated silicon clusters (siliconoids) with transition metal-expanded scaffolds

Reproduced from Luisa Giarrana, Nadine E. Poitiers, Alida Stürmer, Michael Zimmer, Volker Huch, Bernd Morgenstern, David Scheschkewitz, *Dalton Trans.* **2025**, *54*, 10441–10447. https://doi.org/10.1039/D5DT01135C with permission from the Royal Society of Chemistry and all authors.

The results are additionally concluded and put into context in Chapter 4.

Author Contributions

Luisa Giarrana
Lead: Data curation, Formal analysis, investigation, writing (original draft)
Equal: Conceptualization

Nadine E. Poitiers
Equal: Conceptualization
Supporting: Conceptualization, data curation, formal analysis, investigation

Alida Stürmer
Supporting: Data curation, formal analysis, investigation

Michael Zimmer
Lead: Data curation (solid-state NMR)
Supporting: Formal analysis, methodology, validation

Volker Huch
Lead: Data curation
Supporting: Formal analysis, methodology, visualization

Bernd Morgenstern
Lead: Data curation
Supporting: Formal analysis, methodology, visualization

David Scheschkewitz
Lead: Funding acquisition, project administration, resources, supervision, writing (review & editing)
Equal: Conceptualization
Supporting: Formal analysis, investigation, methodology

Dalton Transactions

ROYAL SOCIETY OF CHEMISTRY

PAPER

View Article Online
View Journal | View Issue

Cite this: *Dalton Trans.*, 2025, **54**, 10441

Heterobimetallic unsaturated silicon clusters (siliconoids) with transition metal-expanded scaffolds†

Luisa Giarrana,[a] Nadine E. Poitiers,[a] Alida Stürmer,[a] Michael Zimmer,[a] Volker Huch,[a] Bernd Morgenstern[b] and David Scheschkewitz *[a]

Received 14th May 2025,
Accepted 12th June 2025

DOI: 10.1039/d5dt01135c

rsc.li/dalton

We report a heterobimetallical unsaturated silicon cluster (siliconoid) with a formally anionic group 9 metal vertex (Ir) in close contact to the lithium counter-cation, thus constituting a rare example of transition metal–lithium interactions. The anionic cluster is obtained by reductive chloride elimination from the corresponding neutral siliconoid complex of iridium(I) chloride with lithium/naphthalene. The previously exohedral transition metal center is fully incorporated into the siliconoid cluster scaffold giving rise to an irida-heterosiliconoid reminiscent of the corresponding homonuclear Si_7 species. Despite the formal negative charge at the iridium center, the nucleophilic site is on one of the adjacent silicon vertices judging from the reactivity toward group 4 metallocene dichlorides, Cp_2MCl_2 (M = Zr, Hf). Under elimination of LiCl, the Cp_2MCl moieties in the heterobimetallic products are installed as pending functionalities under retention of the literally uncompromised iridasiliconoid core.

Introduction

Heterobimetallic species have been receiving growing attention over the last decades due to their unique electronic and catalytic properties. Mixed metallic compounds are frequently used as catalysts, for instance in the production of H_2 in the context of energy storage,[1a] as enzyme surrogates in water oxidation[1b] or in (m)ethanol fuel cells.[1c,d] In Fischer–Tropsch chemistry, bimetallic phases[1e] and – increasingly – heterobimetallic nanoparticles are competent heterogenous catalysts.[1f] Numerous bimetallic main group-transition metal complexes have been reported for their activity in homogenous catalysis,[2] among them neutral compounds such as **I**[3a] (N_2 reduction) and anionic derivatives such as **II** (CO_2 derivatization).[3b] Late first and second row transition metals readily form metal-element bonds to E_n ligands (*e.g.* E = group 13 to 15 atom), but the controlled implementation of a second or third transition metal center remains a challenge, especially if different to the first.[4]

Due to the low electronegativity of the constituting elements, main group metalloid clusters, such as Zintl anions,[5] represent competent ligand systems for late transition metals and thus considerable potential in homogenous catalysis.[5] Especially germanium and tin-based Zintl anions[6] and – more recently – their silicon congeners have been employed as extraordinarily electron-rich ligands towards transition metal centers.[7] More specifically, Zintl clusters with either metal vertices (*e.g.* **III**, Fig. 1)[8] or endohedral metal centers (*e.g.* **IV**)[9] have been described, along with dimeric clusters such as **V**.[7a] Even multimetallic cluster species have been reported by the groups of Goicoechea and Sevov: the straightforward addition of a second transition metal to a rhodium-germanium cluster **VI** leads to the formation of **VII**[10] (Fig. 1) or a Rh–Ir intermetallic cluster **VIII**.[11] With the neutral rhodium species **VI**, the first example of a homogeneous catalyst derived from Zintl anions was disclosed with considerable activity in alkene hydrogenation and H/D exchange.[10]

As we proposed based on the isolation of lithiated derivatives, unsaturated silicon clusters (siliconoids)[12] as otherwise neutral molecular species are conceptually related to Zintl anions through the formal replacement of negative charges by covalently bonded substituents.[13] Accordingly, the availability of nucleophilic anionic siliconoids provided access to the first transition metal-substituted derivatives: a *ligato*-lithiated Si_6 siliconoid served as a precursor for X-type ligation toward $M(Cp)_2Cl$ (M = Zr, Hf).[12g] In contrast, the realization of L-type coordination required the grafting of a tetrylene

[a]*Krupp-Chair in Inorganic and General Chemistry, Saarland University, Campus C4.1 Saarbrücken, 66123 Saarbrücken, Germany.*
E-mail: david.scheschkewitz@uni-saarland.de
[b]*Service Center X-Ray Diffraction, Saarland University Campus Saarbrücken C4.1, 66123 Saarbrücken, Germany*

† Electronic supplementary information (ESI) available. CCDC 2447272, 2447286 and 2447266. For ESI and crystallographic data in CIF or other electronic format see DOI: https://doi.org/10.1039/d5dt01135c

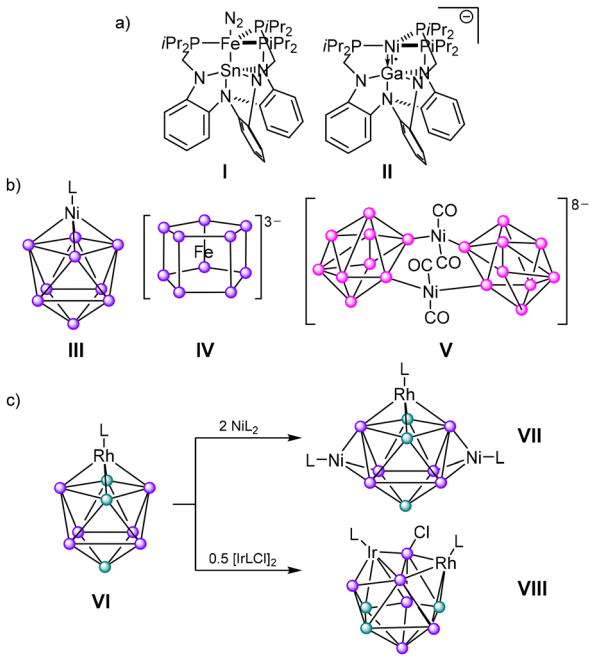

Fig. 1 (a) Selected examples of heterobimetallic complexes with main group elements and (b) transition metal-incorporating Zintl anions of the main group elements (c) heteromultimetallic Zintl-type complexes (● = Ge, ● = Ge-Hyp, ● = Si; L = cyclooctadienyl, Hyp = tris(trimethylsilyl)silyl).

side-arm in the *ligato* position. The resulting globally neutral metallasiliconoid **1** (Scheme 1),[13g,h] however, exhibits only partial incorporation of the group 9 metal into the cluster scaffold due to the cage-opening chlorine transfer from the transition metal. Nonetheless, **1** proved to be competitively active and selective as the catalyst of the isomerization of 1-hexene to 2-hexene.

Herein, we report the first complete inclusion reactions of any transition metal as hetero-vertices of siliconoids using a reductive elimination approach. The reaction of **1** gives rise to a 7-vertex iridasiliconoid reminiscent of the neutral Si_7 derivative. The product shows close contacts between the transition metal centers and the lithium counter-cation, further highlighting the conceptual relationship between siliconoids and Zintl anions. Finally, we demonstrate that heterobimetallic complexes with group 4 metals are readily obtained by reaction

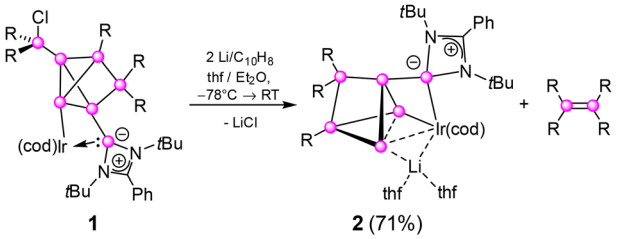

Scheme 1 Synthesis of Si_6Ir-Li **2** by reduction of **1**[12h] with $Li/C_{10}H_8$ (● = Si; R = 2,4,6-triisopropylphenyl, cod = 1,5-cyclooctadiene).

of the anionic clusters with the appropriate metallocene dichlorides.

Results and discussion

We anticipated that the reductive elimination of chloride from the incompletely metal-incorporated siliconoid **1** may either prompt the reintegration of its pending chlorosilyl group into the cluster framework or its complete cleavage. Both eventualities could in principle result in additional metal-cluster interactions and hence prompt the desired complete incorporation of the metal center into the cluster core. Indeed, reaction of **1** with lithium/naphthalene in thf led to the complete cleavage of the exohedral Tip_2SiCl-group to yield a new product **2** in 71% isolated yield (Scheme 1). The lithium salt **2** was fully characterized by X-ray diffraction on single crystals, UV/vis spectroscopy and multinuclear NMR spectroscopy.

The product mixture shows the characteristic ^{29}Si NMR signal of tetrakis(2,4,6-triisopropylphenyl)disilene at 52.8 ppm,[14] which is apparently formed as a systematic by-product that can however be separated by crystallization. The distribution of the remaining ^{29}Si NMR chemical shifts of **2** is akin to that of Si_6- and Si_7 siliconoids.[12a,c,e,g] According to the 2D $^{29}Si/^{1}H$ correlation of the isolated product, the deshielded signal at 152.8 ppm is assigned to the $SiTip_2$ unit and the most shielded resonances at −184.0 and −226.3 ppm to the Ir-bonded unsubstituted silicon vertices. One further highfield signal at −103.2 ppm can be attributed to the vertex carrying the amidinato silylene, which in turn gives rise to a signal at 36.0 ppm, slightly downfield-shifted compared to the precursor (**1**: $\delta^{29}Si$ 32.9 ppm).[12h] The SiTip vertex resonates at 108.2 ppm and thus at unusually low field. Most notably, the major ^{7}Li NMR signal of **2** is significantly downfield-shifted to 5.99 ppm. A minor broad signal at 1.12 ppm likely belongs to a different coordination mode of the Li counter-ion that however, does not affect the coordination and the chemical shifts of the remaining nuclei.

Single crystals of **2** were obtained from hexane in 71% yield and the molecular structure in the solid state was confirmed by X-ray diffraction (Fig. 2a). The unit cell contains two molecules of **2** in the asymmetric unit with slightly differing bonding values. In the following, the arithmetic mean values will be discussed (see ESI Table S2† for exact values). The cleavage of the exohedral silyl group in **1** indeed resulted in the full incorporation of the Ir(cod) center into a distorted benzpolarene motif in **2**. The term benzpolarene was recently introduced by our group to refer to the highly polarized, tetracyclic global minimum isomer of benzene, in analogy to benzvalene as another prominent isomer of benzene.[12e] The amidinato silylene sidearm in **2** completes the coordination sphere at Ir1, while Li1 assumes a bridging position across the Si2–Ir1 bond.

The anionic iridasiliconoid **2** is therefore best described as a heteroanalogue of the doubly bridged propellane motif of the Si_7 scaffolds **IX** and **X**, although with some noteworthy differences (Fig. 2b).[12d] While in **IX** and **X**, the "upper" three

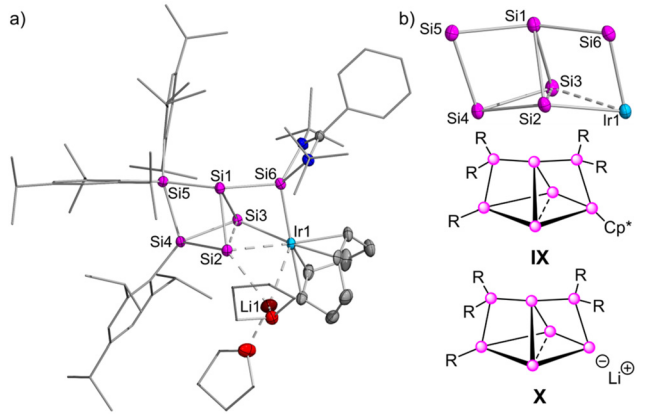

Fig. 2 (a) Molecular structure of iridasiliconoid as contact ion pair **2** in the solid state. The inverted structure (1 − *x*, 1 − *y*, 1 − *z*) is displayed for consistent visualization. Hydrogen atoms omitted for clarity. Thermal ellipsoids at 50% probability. Arithmetic mean values of selected bond lengths [Å] and angles [°]: Ir1–Li1 2.880(8), Si2–Li1 2.611(8), Ir1–Si2 2.641 (1), Ir1–Si6 2.344(1), Ir1–Si3 2.411(1), Si2–Si3 2.475(2), Si1–Si6 2.285(2), Si1–Si5 2.321(2), Si1–Si2 2.327(2), Si1–Si3 2.423(2), Si2–Si4 2.388(2), Si3–Si4 2.331(2), Si4–Si5 2.402(2); Si6–Ir1–Li1 122.7(2), Si3–Ir1–Li1 107.1(2), Si3–Si2–Li1 113.9(2), Si2–Ir1–Li1 56.3(2), Si6–Ir1–Si3 69.2(4), Si5–Si1–Si6 149.9(7); (b) Central cluster motif in comparison with 7-vertex clusters **IX** and **X** (● = Si, R = 2,4,6-triisopropylphenyl, Cp* = C_5Me_5).

silicon atoms are almost linear (**IX:** 173.8°, **X:** 174.0°) giving rise for a seesaw coordination environment, the apical silicon atom Si1 of the central triangular motif of **2** is canted away from the Si5–Si6 vector towards Si2, the basal silicon atom connected to the lithium counter-cation (Si5–Si1–Si6 149.9 (7)°). This is presumably a consequence of the tetravalency of this vertex (whereas Si3 is formally trivalent), which implies a more electron-precise bonding situation with considerably shorter bonds. Concomitantly, Si1 acquires a much more pronounced hemispheroidal coordination environment (**2:** ϕ = 0.5542, **IX:** ϕ = −0.0390, **X:** ϕ = −0.0994).[13k] For a tetracoordinate atom, the hemispheroidality parameter ϕ describes the deviation of the "naked" silicon vertex from a reference plane, defined by the three bonded atoms, for which the sum of bond angles is closest to 360°, in comparison to a fourth substituent, which is set to be a negative value as per convention.[13k] If ϕ results in a negative value, a tetrahedral coordination is suggested, whereas a positive value indicates a hemispheroidal coordination environment of the vertex in question.

The distance between the unsubstituted vertices in **2** (Si2–Si3 2.475(2) Å) is remarkably shortened compared to homonuclear Si_6 and Si_7 siliconoids.[12a,c,e,g] The metal-silicon bond due to the L-type coordination by the silylene side arm (Si6–Ir1 2.344(1) Å) is significantly shorter than the X-type interaction with the *nudo*-vertex Si3 (Si3–Ir1 2.411(1) Å). These values are in line with previously reported silicon-iridium single bonds (2.245 Å–2.574 Å).[15] The pronounced lengthening of the third silicon-iridium contact (Ir1–Si2 2.641(1) Å) can be attributed to the bridging by the lithium counteraction in the sense of an unprecedented agostic 3c2e Ir–Si–Li interaction. In fact, only very few Ir–M (M = alkali metal) contact ion pairs have been crystallographically characterized.[16] Despite its bridging nature, the Ir1–Li1 distance of 2.880(8) Å in **2** is in good agreement with the reported Ir···Li distances in a diphenyliridate (2.882/2.886 Å).[17] The distance between Si2···Li1 (2.611(8) Å) in **2** is well within the range of further reported Si···Li siliconoid distances (2.56–2.77 Å).[12c–e]

The longest wavelength absorption in the UV/vis spectrum of **2** at λ_{max} = 543 nm is slightly blue-shifted compared to the starting material **1** (λ_{max} = 576 nm) but red-shifted in contrast to previously reported *ligato*-substituted siliconoids (λ_{max} = 364 to 521 nm).[12c,e,g] The TD-DFT calculated value at $\lambda_{max,calc}$ = 528 nm (PBE0/DEF2-TZVPP level of theory)[18] confirms the assignment to the HOMO → LUMO transition (78% contribution, see ESI† for further details). Besides, an additional intense absorption band at λ = 425 nm agrees well with calculated transitions at 418 nm (HOMO−3 → LUMO 35%, HOMO−2 → LUMO 39%) and 430 nm (HOMO → LUMO + 3 78%) (ESI Table S7†).

We probed the reactivity of Si_6Ir-Li **2** towards Me_3SiCl and Me_3SnCl, as representative common electrophiles. The components of the reaction mixture, however, could not be isolated nor identified with certainty. To explore the application of anionic Si_6Ir-Li **2** as a precursor for the grafting of a second transition metal center, we then investigated the reaction with group 4 metallocene dichlorides as electrophilic substrates (Scheme 2) since $ZrCp_2Cl_2$ and $HfCp_2Cl_2$ were shown to readily undergo clean salt metathesis reactions in the case of homonuclear siliconoids and as well as electron-precise silicon species.[12g,20] The reactions of **2** with Cp_2MCl_2 (M = Zr, Hf) in benzene at room temperature yielded the corresponding substituted siliconoids **3a,b** in isolated yields of 14% and 32%, respectively. Interestingly, **3a** proved to be much less stable than **3b** leading to as yet unidentified decomposition products during work-up. The yields are furthermore compromised by the competing formation of an unidentified side product, which could be due to the elimination of CpLi according to residual ^{1}H and ^{13}C NMR signals in the spectra of **3a**/**3b** at 5.869/5.810 ppm and 114.32/112.85 ppm, respectively (ESI†).[19] Attempts to detect CpLi by ^{7}Li NMR, however, remained unsuccessful.

The NMR spectra of **3a,b** show very similar signal patterns. The ^{29}Si NMR signals were assigned based on 2D ^{29}Si/^{1}H NMR

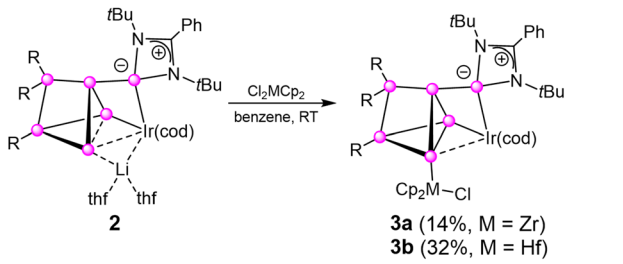

Scheme 2 Synthesis of group 4 metallocenyl-substituted iridasiliconoids **3a,b** from **2** and Cl_2MCp_2 (M = Zr (**3a**), Hf (**3b**); ● = Si; R = 2,4,6-triisopropylphenyl; cod = 1,5-cyclooctadiene).

correlation spectra. The signals of the $SiTip_2$ unit (**3a**: 73.8 ppm, **3b**: 75.9 ppm) are significantly upfield-shifted with a $\Delta\delta$ of about 75 ppm compared to the starting material (**2**: 149.3 ppm). Similar highfield-shifts are observed for the SiTip units, assigned based on the cross-peaks in the aromatic region (**2**: 108.2 ppm, **3a**: 73.5 ppm, **3b**: 68.1 ppm). The resonance attributed to the Si atom of the pending N-heterocyclic silylene (**3a**: 30.5 ppm, **3b**: 29.9 ppm) is found in the same range as the corresponding signals of the precursors (**1**: 32.9 ppm, **2**: 36.0 ppm) suggesting that the environment of the coordinated Ir-cod moiety is mostly preserved. The most downfield-shifted resonance compared to **2** is the signal assigned to the Si–M atom (**2**: −226.3 ppm, **3a**: −40.9 ppm, **3b**: −36.6 ppm). The two remaining highfield signals (**3a**: −77.9/−131.9 ppm, **3b**: −90.4/−131.1 ppm) correlate to the unsubstituted silicon atoms (Si1, Si3) but are somewhat more deshielded than in the starting material (**2**: −103.2/−184.0 ppm).

Compared to the starting material **2**, the longest wavelength absorptions in the UV/vis spectra of **3a**,**b** are considerably red-shifted from λ_{max} = 551 nm (**2**) to 601 nm (**3a**, Zr) and 647 nm (**3b**, Hf) indicating a significantly smaller HOMO–LUMO gap.

Single crystals of both **3a** (14%) and **3b** (32%) were obtained overnight from concentrated hexane solutions at −26 °C (**3a**) and room temperature (**3b**) (Fig. 3). X-ray diffraction analysis confirmed the molecular structures in the solid state with formation of bonds between the group 4 metal M (M = Zr, Hf) and Si2 rather than Ir1, possibly because of the higher stability of Si–M bonds[21] compared to bimetallic transition metal bonds as well as the larger differences in electronegativity (Pauling values Si 1.90, Zr 1.33, Hf 1.3, Ir 2.20).[22] The elongated distance between Si2 and Ir1 (Fig. 3, **3a**: 2.726(1) Å, **3b**: 2.748(1) Å) compared to **2** (2. 641(1) Å) suggests a somewhat weaker interaction in line with the presence of the additional Si2–M bond. Consequently, the Si2–Si3 bond (**2**: 2.475(2) Å) is shortened to the length of a typical Si–Si single bond (2.30–2.40 Å, **3a**: 2.388(1) Å, **3b**: 2.390(2) Å).[21b] The Si2–M bond lengths (**3a**: 2.744(9) Å, **3b**: 2.723(1) Å) are on the shorter end of reported Si-M (M = Zr, Hf) single bonds (Si–Zr = 2.7429–2.924 Å, Si–Hf = 2.729–2.939 Å).[12g,21] Comparable bond distances were reported for tris(trimethylsilyl) hafnium derivatives by Rheingold, Geib and Tilley, (d_{Si-Hf} = 2.729 Å/ 2.748 Å)[21a,b] and for a zirconocenecyclosilane by Marschner and coworkers (2.743 Å).[21c] Table 1 compares pertinent structural and spectroscopic data of heterobimetallic siliconoids **2**, **3a** and **3b**.

As in the case of **2**, the seesaw coordination at Si1 is strongly distorted to a hemispheroidal environment (**3a**: ϕ = 0.7148, **3b**: ϕ = 0.7206). The more covalent bonding of the Si–M bond in **3a** and **3b** gives rise to even more acute Si5–Si1–Si6

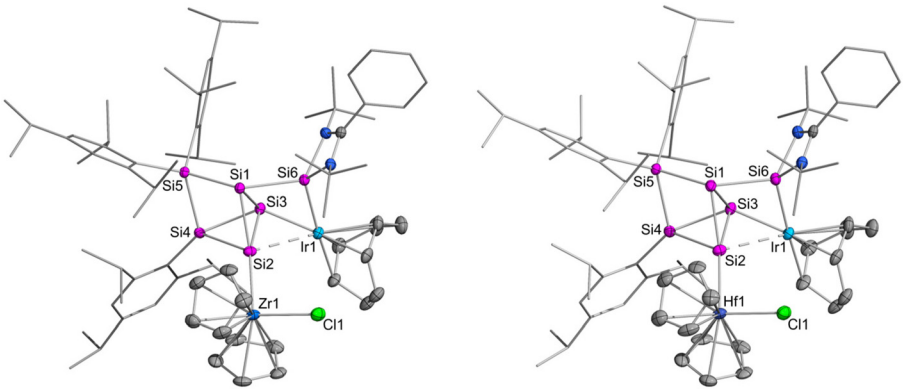

Fig. 3 Molecular structures of heterobimetallic siliconoids **3a** (left) and **3b** (right) in the solid state. The inverted structure (1 − *x*, 1 − *y*, 1 − *z*) is displayed for consistent visualization. Hydrogen atoms are omitted for clarity. Thermal ellipsoids are set at 50% probability. Selected bond lengths [Å] and angles [°]: (a) Ir1–Si2 2.726(1), Ir1–Si3 2.345(9), Ir1–Si6 2.319(9), Zr1–Si2 2.744(9), Zr1–Cl1 2.452(9), Si2–Si3 2.388(1), Si1–Si3 2.495(1), Si1–Si2 2.336(1); Si6–Ir1–Si3 71.0(3), Si6–Ir1–Si2 78.3(3), Si3–Ir1–Si2 55.6(3), Ir1–Si2–Zr1 112.4(3), Cl1–Zr1–Si2 103.0(3), Si3–Si4–Si2 60.2(4), Si5–Si4–Si2 101.0(4) Si5–Si1–Si6 136.4(2); (b) Ir1–Si2 2.748(1), Ir1–Si3 2.345(1), Ir1–Si6 2.318(2), Hf1–Si2 2.723(1), Hf1–Cl1 2.420(1), Si2–Si3 2.390(2), Si1–Si3 2.492(2), Si1–Si2 2.338(2); Si6–Ir1–Si3 70.9(5), Si6–Ir1–Si2 78.1(4), Si3–Ir1–Si2 55.3(4), Ir1–Si2–Hf1 113.9(5), Cl1–Hf1–Si2 100.8(4), Si3–Si4–Si2 57.5 (5), Si5–Si4–Si2 101.1(6), Si5–Si1–Si6 135.9(7).

Table 1 Selected analytical data of **2** and **3a**,**b**. Literature data of precursor **1** for comparison[12h]

Compound	δ^{29}Si NH*Si* [ppm]	δ^{29}Si unsubstituted *Si* [ppm]	*d* (Si–Si, unsubstituted) [Å]	*d*(Si2–M) [Å]	∢ Si5–Si1–Si6 [°]
Si_7Ir **1**	32.9	−125.6/−128.8	2.305(2)/2.548(2)	2.305(2)	—
Si_6Ir-Li **2**	36.0	−184.0/−226.3	2.475(2)	2.658(1)	149.9(7)
Si_6Ir-Zr **3a**	73.5	−77.9/−131.9	2.388(12)/2.495(1)	Si2···Ir1 2.726(1)/Si2–Zr1 2.744(9)	136.4(2)
Si_6Ir-Hf **3b**	68.1	−90.4/−131.1	2.390(2)/2.494(2)	Si2···Ir1 2.748(1)/Si2–Hf1 2.723(1)	135.9(7)

angles than in **2** (**3a**: 136.4(2)°, **3b**: 135.9(7)°, **2**: 149.9(7)°) and the Si_7 siliconoids **IX** and **X** (Fig. 2, **IX**: 173.8°, **X**: 174.0°).[12a] Although the Cl1–M1–Si2 angle (**3a**: 103.0(3), **3b**: 100.8(4)°) is more acute than expected, an initially suspected Ir–Cl interaction is unlikely given the rather long distances (Ir···Cl: 4.5206(9) Å (**3a**), 4.478(2) Å (**3b**)).

Conclusions

In conclusion, we report on the isolation and full characterization of the first heterobimetallic siliconoid with fully incorporated transition metal vertex. The contact ion pair **2** comprising the anionic iridasiliconoid and the lithium countercation resembles the corresponding Si_7 siliconoid species. Reactions of **2** with Cp_2MCl_2 (M = Zr and Hf) results in the heterobimetallic siliconoids **3a** and **3b** in which the group 4 metal moiety is exohedrally attached to the silicon vertex in α-position to iridium while the irida-incorporated heterosiliconoid scaffold is preserved in principle.

Author contributions

L. Giarrana, N. E. Poitiers and A. Stürmer performed the synthetic work and data analysis, L. Giarrana, N. E. Poitiers and D. Scheschkewitz designed the study, D. Scheschkewitz acquired the funding; V. Huch and B. Morgenstern carried out the X-ray diffraction studies, M. Zimmer did the solid state and VT NMR measurements, L. Giarrana performed the DFT calculations, L. Giarrana and D. Scheschkewitz wrote the manuscript.

Conflicts of interest

There are no conflicts of interest to declare.

Data availability

All data associated with this manuscript are available in the ESI.† Crystallographic data for **2**, **3a** and **3b** have been deposited at the CCDC (2447272, 2447286 and 2447266†) and can be obtained from **https://www.ccdc.cam.ac.uk/structures**.

Acknowledgements

Funding by the Deutsche Forschungsgemeinschaft (DFG SCHE 906/4-4) is gratefully acknowledged. Instrumentation and technical assistance for this work were provided by the Service Center X-ray Diffraction, with financial support from Saarland University and German Science Foundation (project number INST 256/506-1). The authors thank Dr. Diego Andrada and Prof. Stella Stopkowicz for access to their computational clusters.

References

1 (*a*) M. R. DuBois and D. L. DuBois, The roles of the first and second coordination spheres in the design of molecular catalysts for H_2 production and oxidation, *Chem. Soc. Rev.*, 2009, **38**, 62; (*b*) R. Brimblecombe, G. F. Swiegers, G. C. Dismukes and L. Spiccia, Sustained water oxidation photocatalysis by a bioinspired manganese cluster, *Angew. Chem., Int. Ed.*, 2008, **47**, 7335; (*c*) E. Antolini, Catalysts for direct ethanol fuel cells, *J. Power Sources*, 2007, **170**, 1; (*d*) S. Song, W. Zhou, Z. Liang, R. Cai, G. Sun, Q. Xin, V. Stergiopoulos and P. Tsiakaras, The effect of methanol and ethanol cross-over on the performance of PtRu/C-based anode DAFCs, *Appl. Catal., B*, 2005, **55**, 65; (*e*) B. H. Davis, Fischer–Tropsch synthesis: Overview of reactor development and future potentialities, *Top. Catal.*, 2005, **32**, 143; (*f*) U. Pal, J. F. Sanchez Ramirez, H. B. Liu, A. Medina and J. A. Ascencio, Synthesis and structure determination of bimetallic Au/Cu nanoparticles, *Appl. Phys. A*, 2004, **79**, 79.

2 Selection of reviews on heterometallic complexes in homogeneous catalysis: (*a*) P. Buchwalter, J. Rosé and P. Braunstein, Multimetallic catalysis based on heterometallic complexes and clusters, *Chem. Rev.*, 2015, **115**, 28; (*b*) W. Xu, M. Li, L. Qiao and J. Xie, Recent advances of dinuclear nickel-and palladium-complexes in homogeneous catalysis, *Chem. Commun.*, 2020, **56**, 8524; (*c*) S. A. Laneman and G. G. Stanley, Homogeneous Bimetallic Hydroformylation Catalysis - Two Metals Are Better Than One, in *Adv. in Chem*, Amercian Chemical Society, 1992, ch. 24, vol. 230, pp. 349–366; (*d*) R. G. Fernando, C. D. Gasery, M. D. Moulis, G. G. Stanley, M. Iglesias, E. Sola, L. A. Oro, I. Dutta, G. Sengupta, J. K. Bera, M. J. Page, D. B. Walker, B. A. Messerle, E. Bodio, M. Picquet, P. Le Gendre, M. Garland, L. Gan, D. Jennings, J. Laureanti and A. K. Jones, in *Homo- and heterobimetallic complexes in catalysis*, ed. P. Kalck, Springer International Publishing, Switzerland, 1st edn, 2016; (*e*) R. M. Haak, S. J. Wezenberg and A. W. Kleij, Cooperative multimetallic catalysis using metallosalens, *Chem. Commun.*, 2010, **46**, 2713.

3 (*a*) M. J. Dorantes, J. T. Moore, E. Bill, B. Mienert and C. C. Lu, Bimetallic iron–tin catalyst for N_2 to NH_3 and a silyldiazenido model intermediate, *Chem. Commun.*, 2020, **56**, 11030; (*b*) M. V. Vollmer, R. C. Cammarota and C. C. Lu, Reductive Disproportionation of CO2 Mediated by Bimetallic Nickelate(–I)/Group 13 Complexes, *Eur. J. Inorg. Chem.*, 2019, 2140.

4 (*a*) E. Zintl and A. Harder, Polyplumbide, Polystannide und ihr Übergang in Metallphasen, *Z. Phys. Chem. Abt. A*, 1931, **154a**, 47; (*b*) T. F. Fässler, in *Zintl Ions: Principles and Recent Developments*, Struct. Bonding, Springer-Verlag, Berlin, Heidelberg, 2011; (*c*) S. Scharfe, F. Kraus, S. Stegmeier, A. Schier and T. F. Fässler, Zintl ions, cage compounds, and intermetalloid clusters of group 14 and group 15 elements, *Angew. Chem., Int. Ed.*, 2011, **50**, 3630;

(*d*) R. J. Wilson, D. Weinert and S. Dehnen, Recent developments in Zintl cluster chemistry, *Dalton Trans.*, 2018, **47**, 14861.

5 (*a*) M. T. Whited, Pincer-supported metal/main-group bonds as platforms for cooperative transformations, *Dalton Trans.*, 2021, **50**, 16443; (*b*) M. T. Whited, Metal–ligand multiple bonds as frustrated Lewis pairs for C–H functionalization, *Beilstein J. Org. Chem.*, 2012, **8**, 1554; (*c*) M. T. Whited and B. L. H. Taylor, Metal/organosilicon complexes: structure, reactivity, and considerations for catalysis, *Comments Inorg. Chem.*, 2020, **40**, 217.

6 (*a*) W. T. Pennington, R. C. Haushalter and B. W. Eichhorn, Synthesis and structure of closo-$Sn_9Cr(CO)_3^{4-}$: The first member in a new class of polyhedral clusters, *J. Am. Chem. Soc.*, 1988, **110**, 8704; (*b*) J. M. Goicoechea and S. C. Sevov, Organozinc Derivatives of Deltahedral Zintl Ions: Synthesis and Characterization of *closo*-$[E_9Zn(C_6H_5)]^{3-}$ (E = Si, Ge, Sn, Pb), *Organometallics*, 2006, **25**, 4530; (*c*) E. N. Esenturk, J. Fettinger and B. Eichhorn, Synthesis and characterization of the $[Ni_6Ge_{13}(CO)_5]^{4-}$ and $[Ge_9Ni_2(PPh_3)]^{2-}$ Zintl ion clusters, *Polyhedron*, 2006, **25**, 521; (*d*) S. Scharfe, T. F. Fässler, S. Stegmaier, S. D. Hoffmann and K. Ruhland, $[Cu@Sn_9]^{3-}$ and $[Cu@Pb_9]^{3-}$: Intermetalloid Clusters with Endohedral Cu Atoms in Spherical Environments, *Chem. – Eur. J.*, 2008, **14**, 4479; (*e*) N. S. Willeit, V. Hlukhyy and T. F. Fässler, Synthesis, Structure and Catalytic Properties of $Hyp_3[Ge_9Rh]PPh_3$, *Z. Anorg. Allg. Chem.*, 2024, **24**, e202400171.

7 (*a*) S. Joseph, M. Hamberger, F. Mutzbaurer, O. Härtl, M. Meier and N. Korber, Chemistry with Bare Silicon Clusters in Solution: A Transition–Metal Complex of a Polysilicide Anion, *Angew. Chem., Int. Ed.*, 2009, **48**, 8770; (*b*) M. Waibel, F. Kraus, S. Scharfe, B. Wahl and T. F. Fässler, $[(MesCu)_2(\eta^3\text{-}Si_4)]^4$: A mesitylcopper-stabilized tetrasilicide tetraanion, *Angew. Chem., Int. Ed.*, 2010, **49**, 6611; (*c*) D. O. Downing, P. Zavalij and B. W. Eichhorn, The *closo*–$[Sn_9Ir(cod)]^{3-}$ and $[Pb_9Ir(cod)]^{3-}$ Zintl Ions: Isostructural IrI Derivatives of the *nido*,–E_9^{4-} Anions (E = Sn, Pb), *Eur. J. Inorg. Chem.*, 2010, 890; (*d*) F. S. Geitner and T. F. Fässler, Low oxidation state silicon clusters–synthesis and structure of $[NHC\ Dipp\ Cu\ (\eta^4\text{-}Si_9)]^{3-}$, *Chem. Commun.*, 2017, **53**, 12974.

8 J. M. Goicoechea and S. C. Sevov, Deltahedral germanium clusters: insertion of transition-metal atoms and addition of organometallic fragments, *J. Am. Chem. Soc.*, 2006, **128**, 4155.

9 B. Zhou, M. S. Denning, D. L. Kays and J. M. Goicoechea, Synthesis and Isolation of $[Fe@Ge_{10}]^{3-}$: A Pentagonal Prismatic Zintl Ion Cage Encapsulating an Interstitial Iron Atom, *J. Am. Chem. Soc.*, 2009, **131**, 2802.

10 O. P. E. Townrow, C. Chung, S. A. Macgregor, A. S. Weller and J. M. Goicoechea, A neutral heteroatomic zintl cluster for the catalytic hydrogenation of cyclic alkenes, *J. Am. Chem. Soc.*, 2020, **142**, 18330.

11 O. P. E. Townrow, A. S. Weller and J. M. Goicoechea, Controlled cluster expansion at a Zintl cluster surface, *Angew. Chem., Int. Ed.*, 2024, **63**, e202316120.

12 (*a*) K. Abersfelder, A. J. P. White, R. J. F. Berger, H. S. Rzepa and D. Scheschkewitz, A Stable Derivative of the Global Minimum on the Si_6H_6 Potential Energy Surface, *Angew. Chem., Int. Ed.*, 2011, **50**, 7936; (*b*) A. Jana, V. Huch, M. Repisky, R. J. F. Berger and D. Scheschkewitz, Dismutational and global–minimum isomers of heavier 1,4–dimetallatetrasilabenzenes of group 14, *Angew. Chem., Int. Ed.*, 2014, **53**, 3514; (*c*) P. Willmes, K. I. Leszczyńska, Y. Heider, K. Abersfelder, M. Zimmer, V. Huch and D. Scheschkewitz, Isolation and versatile derivatization of an unsaturated anionic silicon cluster (siliconoid), *Angew. Chem., Int. Ed.*, 2016, **55**, 2907; (*d*) K. I. Leszczyńska, V. Huch, C. Präsang, J. Schwabedissen, R. J. F. Berger and D. Scheschkewitz, Atomically precise expansion of unsaturated silicon clusters, *Angew. Chem., Int. Ed.*, 2019, **58**, 5124; (*e*) Y. Heider, N. E. Poitiers, P. Willmes, K. I. Leszczyńska, V. Huch and D. Scheschkewitz, Site-selective functionalization of Si_6R_6 siliconoids, *Chem. Sci.*, 2019, **10**, 4523; (*f*) L. Klemmer, V. Huch, A. Jana and D. Scheschkewitz, An anionic heterosiliconoid with two germanium vertices, *Chem. Commun.*, 2019, **55**, 10100; (*g*) N. E. Poitiers, L. Giarrana, K. I. Leszczyńska, V. Huch, M. Zimmer and D. Scheschkewitz, Indirect and Direct Grafting of Transition Metals to Siliconoids, *Angew. Chem., Int. Ed.*, 2020, **59**, 8532; (*h*) N. E. Poitiers, L. Giarrana, V. Huch, M. Zimmer and D. Scheschkewitz, Exohedral functionalization vs. core expansion of siliconoids with Group 9 metals: catalytic activity in alkene isomerization, *Chem. Sci.*, 2020, **11**, 7782; (*i*) N. E. Poitiers, V. Huch, M. Zimmer and D. Scheschkewitz, Chalcogen-Expanded Unsaturated Silicon Clusters: Thia-, Selena-, and Tellurasiliconoids, *Chem. – Eur. J.*, 2020, **26**, 16599; (*j*) N. E. Poitiers, V. Huch, M. Zimmer and D. Scheschkewitz, Siliconoid Expansion by a Single Germanium Atom through Isolated Intermediates, *Angew. Chem., Int. Ed.*, 2022, **61**, e202205399; (*k*) Y. Heider, P. Willmes, V. Huch, M. Zimmer and D. Scheschkewitz, Boron and phosphorus containing heterosiliconoids: stable p-and n-doped unsaturated silicon clusters, *J. Am. Chem. Soc.*, 2019, **141**, 19498.

13 (*a*) D. Scheschkewitz, A molecular silicon cluster with a "naked" vertex atom, *Angew. Chem., Int. Ed.*, 2005, **44**, 2954; (*b*) M. Moteki, S. Maeda and K. Ohno, Systematic search for isomerization pathways of hexasilabenzene for finding its kinetic stability, *Organometallics*, 2009, **28**, 2218; (*c*) D. Nied, R. Köppe, W. Klopper, H. Schnöckel and F. Breher, *J. Am. Chem. Soc.*, 2010, **132**, 10264; (*d*) K. Abersfelder, A. J. P. White, H. S. Rzepa and D. Scheschkewitz, Synthesis of a Pentasilapropellane. Exploring the Nature of a Stretched Silicon– Silicon Bond in a Nonclassical Molecule, *Science*, 2010, **327**, 564; (*e*) S. Ishida, K. Otsuka, Y. Toma and S. Kyushin, An organosilicon cluster with an octasilacuneane core: a missing silicon cage motif, *Angew. Chem., Int. Ed.*, 2013, **52**, 2507; (*f*) A. Tshurusaki, C. Iizuka, K. Otsuka and S. Kyushin, Cyclopentasilane-fused hexasilabenzvalene, *J. Am. Chem.*

Soc., 2013, **135**, 16340; (*g*) A. Tsurusaki, K. Kamiyama and S. Kyushin, Tetrasilane-Bridged Bicyclo [4.1. 0] heptasil-1 (6)-ene, *J. Am. Chem. Soc.*, 2014, **136**, 12896; (*h*) F. Breher, Stretching bonds in main group element compounds—Borderlines between biradicals and closed-shell species, *Coord. Chem. Rev.*, 2007, **251**, 1007; (*i*) T. Iwamoto and S. Ishida, Silicon compounds with inverted geometry around silicon atoms, *Chem. Lett.*, 2014, **43**, 164; (*j*) S. Kyushin, in *Organosilicon Compounds: Theory and Experiment (Synthesis)*, ed. V. Y. Lee, Academic Press (Elsevier), 2017, vol. 1, ch. 3, pp. 69–144; (*k*) Y. Heider and D. Scheschkewitz, Stable unsaturated silicon clusters (siliconoids), *Dalton Trans.*, 2018, **47**, 7104; (*l*) Y. Heider and D. Scheschkewitz, Molecular silicon clusters, *Chem. Rev.*, 2021, **121**, 9674.

14 (*a*) H. Watanabe, K. Takeuchi, N. Fukawa, M. Kato, M. Goto and Y. Nagai, Air-stable tetrakis (2, 4, 6-triisopropylphenyl) disilene. Direct synthesis of disilene from dihalomonosilane, *Chem. Lett.*, 1987, **16**, 1341; (*b*) H. Watanabe, K. Takeuchi, K. Nakajima, Y. Nagai and M. Goto, The First Preparation of Disilene via Reductive DehaIogenation of 1,2-DichIorodisiIane. The Formation of an Unusual Air-Oxidation Product, 1-Oxa-2-silacyclopent-3-ene Derivative, *Chem. Lett.*, 1988, **17**, 1343.

15 (*a*) S. Kaufmann, S. Schäfer, M. T. Gamer and P. W. Roesky, Reactivity studies of silylene $[PhC(NtBu)_2](C_5Me_5)$ Si–reactions with $[M\ (COD)\ Cl]_2$ (M= Rh (i), Ir (i)), S, Se, Te, and BH_3, *Dalton Trans.*, 2017, **46**, 8861; (*b*) M. Stoelzel, C. Präsang, B. Blom and M. Driess, N-heterocyclic silylene (NHSi) rhodium and iridium complexes: synthesis, structure, reactivity, and catalytic ability, *Aust. J. Chem.*, 2013, **66**, 1163; (*c*) M. Aizenberg, J. Ott, C. J. Elsevier and D. Milstein, Rh(I) and Rh(III) silyl PMe3 complexes. Syntheses, reactions and ^{103}Rh NMR spectroscopy, *J. Organomet. Chem.*, 1998, **551**, 81.

16 (*a*) M. Karni, J. Kapp, P. von Ragué Schleyer, Y. Apeloig and Z. Rappoport, in *The Chemistry of Organic Silicon Compounds*, ed. Z. Rappoport and Y. Apeloig, John Wiley & Sons, Chichester, 2001, ch. 1, vol. 3, pp. 1–183; M. Weidenbruch, Chapter 3, pp. 391–428; (*b*) M. Kraftory, M. Kapon and M. Botoshansky, *The Chemistry of Organic Silicon Compounds*, ed. Z. Rappoport and Y. Apeloig, John Wiley & Sons, Chichester, 1998, ch. 5, vol. 2, pp. 181–264.

17 T. Iwasaki, T. Akaiwa, Y. Hirooka, S. Pal, K. Nozaki and N. Kambe, Synthesis of and structural insights into contact ion pair and solvent-separated ion pair diphenyliridate complexes, *Organometallics*, 2020, **39**, 3077.

18 PBE0: (*a*) J. P. Perdew, M. Ernzerhof and K. Burke, Rationale for mixing exact exchange with density functional approximations, *J. Chem. Phys.*, 1996, **105**, 9982; (*b*) C. Adamo and V. Barone, Toward reliable density functional methods without adjustable parameters: The PBE0 model, *J. Chem. Phys.*, 1999, **110**, 6158; (*c*) J. P. Perdew, K. Burke and M. Ernzerhof, Generalized gradient approximation made simple, *Phys. Rev. Lett.*, 1996, **77**, 3865.

19 S. Bachmann, B. Gernert and D. Stalke, Solution structures of alkali metal cyclopentadienides in THF estimated by ECC-DOSY NMR-spectroscopy (incl. software), *Chem. Commun.*, 2016, **52**, 12861.

20 T.-L. Nguyen and D. Scheschkewitz, Activation of a Si=Si Bond by η1-Coordination to a Transition Metal, *J. Am. Chem. Soc.*, 2005, **127**, 10174.

21 (*a*) H.-G. Woo, R. H. Heyn and T. D. Tilley, σ-Bond metathesis reactions for d0 metal-silicon bonds that produce zirconocene and hafnocene hydrosilyl complexes, *J. Am. Chem. Soc.*, 1992, **114**, 5698; (*b*) J. Arnold, D. M. Roddick, T. D. Tilley, A. L. Rheingold and S. J. Geib, Preparation and characterization of tris (trimethylsilyl) silyl and tris (trimethylsilyl) germyl derivatives of zirconium and hafnium. X-ray crystal structures of $(\eta^5\text{-}C_5Me_5)Cl_2HfSi(SiMe_3)_3$ and $(\eta^5\text{-}C_5Me_5)Cl_2HfGe(SiMe_3)_3$, *Inorg. Chem.*, 1988, **27**, 3510; (*c*) R. Fischer, D. Frank, W. Gaderbauer, C. Kayser, C. Mechtler, J. Baumgartner and C. Marschner, α, ω-Oligosilyl Dianions and Their Application in the Synthesis of Homo- and Heterocyclosilanes, *Organometallics*, 2003, **22**, 3723; (*d*) C. Kayser, D. Frank, J. Baumgartner and C. Marschner, Reactions of oligosilyl potassium compounds with Group 4 metallocene dichlorides, *J. Organomet. Chem.*, 2003, **667**, 149; (*e*) Z. Dong, C. R. W. Reinhold, M. Schmidtmann and T. Müller, A Stable Silylene with a σ^2, π- Butadiene Ligand, *J. Am. Chem. Soc.*, 2017, **139**, 7117; (*f*) T.-I. Nguyen and D. Scheschkewitz, Activation of a Si Si Bond by η-Coordination to a Transition Metal, *J. Am. Chem. Soc.*, 2005, **127**, 10174; (*g*) Z. Wu, J. B. Diminnie and Z. Xue, Synthesis and Characterization of Group 4 Amido Silyl Complexes Free of Anionic π-Ligands, *Inorg. Chem.*, 1998, **37**, 6366; (*h*) A. Sauermoser, T. Lainer, G. Glotz, F. Czerny, B. Schweda, R. C. Fischer and M. Haas, Synthesis and Characterization of Methoxylated Oligosilyl Group 4 Metallocenes, *Inorg. Chem.*, 2022, **61**, 14742; (*i*) B. L. L. Reant, D. De Alwis Jayasinghe, A. J. Wooles, S. T. Liddle and D. P. Mills, Comparison of group 4 and thorium M(IV) substituted cyclopentadienyl silanide complexes, *Dalton Trans.*, 2023, **52**, 7635.

22 L. Pauling, *J. Am. Chem. Soc.*, 1947, **69**, 542.

3.2 Tetrylene-Functionalized Si_7–Siliconoids

Reproduced from Luisa Giarrana, Michael Zimmer, Bernd Morgenstern, David Scheschkewitz, Tetrylene-Functionalized Si_7–Siliconoids. *Inorg. Chem.* **2024**, *63*, 20083–20087. https://doi.org/10.1021/acs.inorgchem.4c00474 with permission from all authors and ACS (https://pubs.acs.org/articlesonrequest/AOR-MBZBMJ34PWKDBXPETSXG).

The results are additionally concluded and put into context in Chapter 4.

Author Contributions

Luisa Giarrana

Lead: Data curation, formal analysis, investigation, writing (original draft)

Equal (D.S.): Conceptualization

Michael Zimmer

Lead: Data curation (solid-state NMR)

Supporting: Data curation, formal analysis, methodology, validation

Bernd Morgenstern

Lead: Data curration

Supporting: Formal analysis, methodology, visualization

David Scheschkewitz

Lead: Funding acquisition, project administration, resources, supervision, writing (review & editing)

Equal (L.G.): Conceptualization

Supporting: Formal analysis, investigation, methodology

Inorganic Chemistry

pubs.acs.org/IC

Communication

Tetrylene-Functionalized Si_7−Siliconoids

Luisa Giarrana, Michael Zimmer, Bernd Morgenstern, and David Scheschkewitz*

Cite This: *Inorg. Chem.* 2024, 63, 20083−20087

Read Online

ACCESS | Metrics & More | Article Recommendations | Supporting Information

ABSTRACT: The core expansion of metallic or metalloid clusters by the addition of further homo- or heteronuclear vertices is pivotal to the nucleation and growth of particles. The exohedral grafting of a low-valent functionality followed by endohedral incorporation have been identified as key steps. Following previous work on the Si_6 series, we now report the synthesis and full characterization of the amidinatotetrylene-functionalized seven-vertex siliconoids $Si_7R_5[E(N^tBu)_2CPh]$ (E = Si, Ge, Sn). In the case of the silylene derivative, the solid-state structure was determined by single crystal X-ray diffraction.

The growth processes of nanoparticles have attracted considerable interest in past decades, which will likely further increase with the recent award of the Nobel prize in chemistry for the discovery and development of quantum dots.[1] Unsaturated silicon clusters (siliconoids) serve as isolable molecular model systems for intermediates during the deposition of elemental silicon in bulk and nanoscalar form.[2] A variety of siliconoids has been isolated since the first report by one of us in 2005,[3a] for example by Wiberg et al.,[4] Kyushin et al.,[3c,e−g] Iwamoto et al.,[5] Breher et al.,[3c] Fässler et al.,[6] Lips et al.,[7] and our group.[8]

Anionically functionalized siliconoids undergo atomically precise core expansion through a repeatable two-step process: nucleophilic substitution of one of the Cp* groups of Jutzi's $SiCp^*_2$ silicon(II) reagent followed by reductive cleavage of the residual second Cp* moiety, in both cases as Cp^{*-},[8d] reiterates the oxidative addition/reductive elimination events during nanoparticle growth. The use of Roesky's amidinatochlorosilylene $[PhC(^tBuN)_2]SiCl$ as an alternative electrophile allowed for the isolation of a plausible yet unobserved intermediate of the siliconoid expansion, a silylene-substituted Si_6 siliconoid.[8g] While cluster expansions with transition metals are well-established for substituent-free Zintl anions of germanium and tin,[9] the pending silylene functionality was shown to be a prerequisite as an auxiliary ligand for the incorporation of transition metals to neutral siliconoids.[8g] We also demonstrated that substitution/reduction sequences applied to heavier tetrylenes EX_2 (E = Ge, Sn) lead to the endohedral and exohedral incorporation of the corresponding tetrel atom or moiety to the siliconoid cluster.[8d,i,j]

In a similar vein, the reduction of the neutral Si_7 siliconoid **I** with lithium/naphthalene affords the lithiated siliconoid Si_7R_5Li **II**, which was reported to directly afford $Si_8R_5Cp^*$ **III** with an exohedral Si═Si double bond upon treatment with $SiCp^*_2$ (Figure 1).[8d] Plausibly, this reaction as well proceeds via the initial occurrence of an Si_7 cluster with exohedral Cp*-silylene functionality, which could not be observed experimentally either, as in the case of the corresponding $Si_6 \rightarrow Si_7$ expansion.[8d] We therefore became interested in the preparation of tetrylene-substituted Si_7 siliconoids in order to check whether its unique core structure with seesaw-type coordination of the central silicon atom is similarly persistent as the hexasilabenzpolarene[3d,8a] motif of the Si_6 siliconoids.

We here report the straightforward and essentially quantitative reactions of the lithiated siliconoid **II** with amidinatochlorotetrylenes of the Roesky-type leading to tetrylene-substituted Si_7 siliconoids, as shown by multinuclear NMR analysis and confirmed by a representative X-ray diffraction study on single crystals of the silylene case.

Amidinatochlorotetrylenes readily undergo salt metathesis reactions.[8d,g,10] The resulting substitution products are considerably less prone to rearrangements than Cp*-substituted silylenes[11] due to the electron donation by the nitrogen lone pairs to the silicon center. Moreover, we have shown previously that the *ligato*-lithiated hexasilabenzpolarene **I** can be readily functionalized with pending amidinatotetrylene groups under retention of the uncompromised hexasilabenzpolarene cluster core. We therefore anticipated a similar behavior for the corresponding Si_7 motif. Indeed, the treatment of lithiated Si_7 siliconoid **II** with the appropriate amidinatochlorotetrylene (E = Si, Ge, Sn) **1a−1c**[10] results in an instantaneous color change of the reaction mixture from orange to dark red/brown accompanied by precipitation of a colorless solid, presumably LiCl. The rapid and uniform conversion of the starting materials was confirmed by ^1H NMR monitoring of the reaction mixtures (Scheme 1). The similarity of the ^{29}Si NMR spectra to that of **II** suggested the formation of the desired tetrylene-siliconoid hybrids **2a−2c** and thus the complete preservation of Si_7 core structure.[8d] The assumed products **2b** and **2c** were isolated as red-brown solids after filtration from hexane in 67−71% yield, while **2a** was isolated as brown crystals from a concentrated pentane solution. Compounds **2a−2c** were characterized by multinuclear NMR,

Special Issue: Dialogue on Zintl Chemistry

Received: February 2, 2024
Revised: March 11, 2024
Accepted: March 14, 2024
Published: March 19, 2024

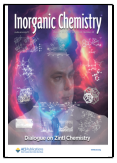

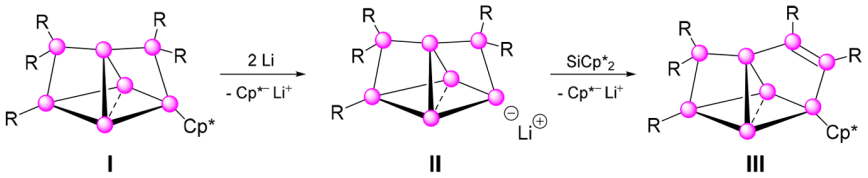

Figure 1. Previously reported Si_7 siliconoid motifs and extension to Si_8 with $SiCp^*_2$ (magenta ball = Si; R = 2,4,6-triisopropylphenyl).

Scheme 1. Grafting of Group 14 Tetrylenes1a−1c to the Si_7 Cluster Scaffold of II Resulting in Tetrylene/Siliconoid Hybrids2a−2c (Magenta Ball = Si; E = Si, Ge, Sn; R = 2,4,6-Triisopropylphenyl)

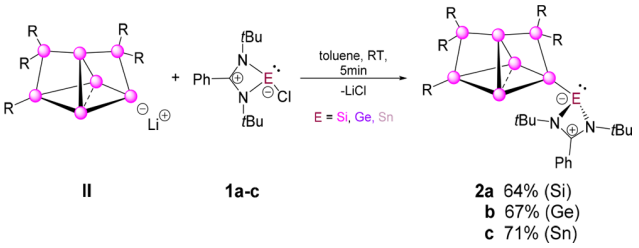

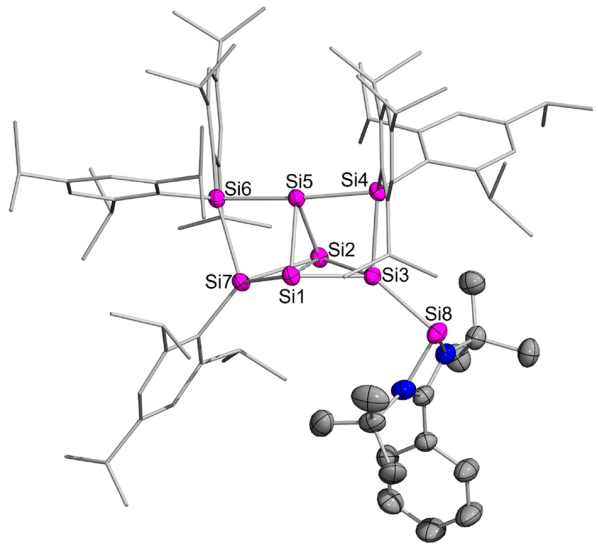

Figure 2. Molecular structure of silylene-substituted siliconoid **2a** in the solid state. Hydrogen atoms have been omitted for the sake of clarity. Thermal ellipsoids are set at the 50% probability level. Selected bond lengths (Å) and angles [°]: Si3−Si8 2.4066(8), Si1−Si2 2.6199(7), Si1−Si5 2.3507(8), Si2−Si5 2.3259(8), Si1−Si3 2.3392(8), Si2−Si3 2.3542(8), Si3−Si4 2.4027(8), Si1−Si7 2.3333(7), Si2−Si7 2.3389(8), Si4−Si5 2.3658(8), Si5−Si6 2.3663(8), Si6−Si7 2.4131(8); Si4−Si5−Si6 174.83(3), Si1−Si3−Si8 135.87(3), Si2−Si3−Si8 131.57(3), Si4−Si3−Si8 123.93(3), Si5−Si2−Si1 56.38(2), Si2−Si5−Si1 68.14(2), Si5−Si1−Si2 55.48(2), Si7−Si1−Si3 109.54(3).

elemental analysis, UV/vis and IR spectroscopy. Moreover, the representative molecular structure of **2a** was confirmed by an X-ray diffraction analysis on single crystals.

Single crystals suitable for X-ray analysis of silylene/siliconoid hybrid **2a** were obtained from a concentrated pentane solution at −26 °C in 64% isolated yield (Figure 2). The compound crystallizes in triclinic space group $P\bar{1}$ with two molecules of **2a** and one molecule of pentane in the asymmetric unit. The silylene-functionalized siliconoid **2a** exhibits an analogous geometrical arrangement of the Si_7 vertex as the neutral $Si_7Tip_5Cp^*$ **I** and lithiated **II**, which is also manifest in the ^{29}Si NMR shifts. The cluster core can be described as [1.1.1]-pentasilapropellane in which two of three propeller blades (Si3, Si7) are bridged to the third (Si5) by the disubstituted silicon atoms Si4 and Si6, resulting in the aforementioned seemingly strained bonding situation with seesaw-type tetracoordination at Si5. The distance of the unsubstituted Si1 and Si2 atoms is with 2.6199(7) Å just in between those of the lithiated Si_7Li **II** (2.5596(8) Å) and the neutral Si_7Cp^* **I** (2.648(1) Å).[8d] The Si3−Si8 bond length in **2a** is 2.4066(8) Å and hence in the range of the other Si−Si single bonds within the cluster scaffold (2.259(8)−2.4131(8) Å), which is reminiscent of the reported distances in lithiated Si_7 **II**.[8d] As previously found for the tetrylene-substituted Si_6, the cluster core is hardly affected by the nature of the silylene.[8g] Compared to the corresponding Si_6−Si bond of 2.4294(9) Å,[8g] the bond Si3−Si8 distance in **2a** is slightly shortened, indicating a stronger interaction between the cluster and the tetrylene moiety.

Similar to the reported data of the lithiated Si_7 **II** (174.00°),[8d] the Si4−Si5−Si6 bond angle is almost linear with 174.83(3)°. According to our previously published formalism for discrimination between a distorted tetrahedral and hemispheroidal coordination,[2a] the hemispheroidality parameter ϕ was determined. For this purpose, a reference plane is required, defined by those three bonded atoms (Si2, Si4, and Si6 in the case of Si5 as unsubstituted vertex) that exhibit a sum of bond angles closest to 360° ($\sum_{Si5}$ = 359.88°). The deviation of the fourth atom of the coordination sphere (Si1) from this plane is set to a negative value as per convention. The hemispheroidality parameter ϕ is given by the sign of the deviation of the unsubstituted vertex (Si5) from the reference plane in comparison to the aforementioned fourth substituent (Si1). A positive value indicates a hemispheroidal coordinated vertex and a negative value, a (distorted) tetrahedral coordination.[2a] The resulting hemispheroidality parameter ϕ = −0.0220 Å for Si5 is only marginally negative, in line with a strongly distorted tetrahedral environment, as already apparent from visual inspection.

The ^{29}Si NMR spectra of **2a−2c** reveal the diagnostic wide dispersion for siliconoids.[2a,3a,d,8] All signals were assigned based on 2D $^1H/^{29}Si$ correlation NMR spectra (Table 1). Furthermore, we supported the trends of the observed ^{29}Si NMR shifts with theoretical calculations at the OLYP/def2-TZVP[12] level of the B3LYP/def2-TZVP[13]-optimized structure of **2a** (Table 1, the OLYP functional is ideal for unsaturated silicon clusters as we have shown previously,[8d] see the Supporting Information for further details). The unique yet unsurprising feature of the silylene-substituted siliconoid **2a** is a signal at 24.1 ppm due to the pending silylene center. The chemical shift of the remote monosubstituted SiTip vertex Si7 at approximately 160 ppm remains close to invariant in **2a−2c** irrespective of the nature of the tetrel element. The same

https://doi.org/10.1021/acs.inorgchem.4c00474
Inorg. Chem. 2024, 63, 20083−20087

Table 1. Experimental and Calculated[29]Si NMR Shifts (ppm) of SiliconoidsI and II and Siliconoid-Tetrylene Hybrids2a−2c[a]

	Si_7Cp^* I[8d]	Si_7Li II[8d]	Si_7NHSi 2a	Si_7NHGe 2b	Si_7NHSn 2c
Si1	−229.6 [−237.6]	−191.9 [−197.0]	−211.6 [−217.5]	−209.6 [−217.9]	−198.3 [−215.1]
Si2	−241.9 [−255.5]	−195.7 [−204.8]	−219.0 [−222.1]	−217.6 [−222.1]	−210.9 [−222.3]
Si3	181.9 [180.3]	284.3 [292.1]	211.7 [216.4]	220.2 [221.7]	237.8 [220.6]
Si4	2.6 [10.6]	10.8 [18.1]	0.3 [6.2]	−0.1 [4.5]	5.7 [4.3]
Si5	−138.4 [−139.4]	−66.1 [−73.1]	−101.2 [−108.8]	−100.7 [−109.3]	−85.8 [−104.6]
Si6	15.0 [20.2]	60.1 [78.4]	32.4 [37.7]	32.4 [39.3]	37.9 [43.7]
Si7	156.0 [154.6]	148.0 [150.7]	159.6 [158.8]	160.4 [159.4]	163.3 [161.0]
Si8			24.1 [25.2]		

[a]Calculated shifts at the OLYP/def2-TZVP[12] level of theory in brackets.

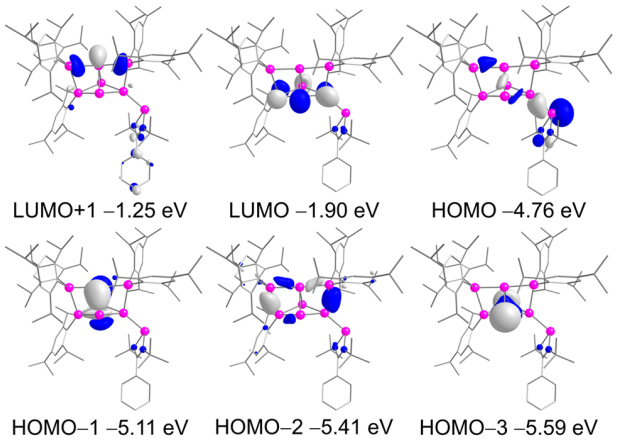

Figure 3. Canonical orbitals of 2a at the B3LYP/def2-TZVP level of theory (contour value = 0.05).

applies to the two $SiTip_2$ moieties with unremarkable resonances at about 0 and 35 ppm. Conversely, the signals of the tetrylene-carrying Si3 are progressively deshielded from 2a (E = Si, 211.6 ppm) via 2b (E = Ge, 220.2 ppm) to 2c (E = Sn, 237.8 ppm). The same effect, although less pronounced, applies to the seesaw-coordinated Si5. The ^{1}H NMR spectra exhibit strictly analogous splitting patterns for 2a and 2b, while 2c shows a slightly different splitting (see the Supporting Information for details) although the relative intensities are still in line with the structurally corresponding stannylene-siliconoid 2c. The ^{119}Sn NMR spectrum of 2c shows one singlet at 196.6 ppm obviously originating from the stannylene center. Although it is considerably downfield shifted compared to the Cl-substituted amidinato precursor 1c (29.6 ppm),[10d] the effect is much less pronounced than in the case of the Si_6-stannylene (267.8 ppm (major)/336.5 ppm (minor)).[8g] Furthermore, only one set of signals was observed in the ^{29}Si and the ^{119}Sn NMR spectra for 2b and 2c, confirming the presence of just a single rotational isomer in solution.[8g] In the CP-MAS ^{29}Si NMR spectra, 2b and 2c show broadened signals due to the amorphous character of the samples. The observation of an additional signal not present in solution (2b E = Ge, −59.4 ppm, 2c E = Sn, −60.1 ppm) is tentatively attributed to contamination with air and/or moisture during measurement due to the less than perfectly closing sample rotors (see the Supporting Information for details).

To investigate the electronic properties of the novel structures, we optimized the tetrylene−siliconoid hybrid 2a−c at the B3LYP/def2-TZVP[13] level of theory (see Supporting Information for details). The optimized geometry of 2a nicely reproduces the one determined experimentally in the solid state, albeit with slightly elongated bonds. The diagnostic ^{29}Si NMR shifts for 2a−2c calculated by the GIAO method at the OLYP/def2-TZVP[12] level of theory are an excellent match with the experimental values (Table 1). The HOMO predominantly represents the tetrel lone pair, while the HOMO−1 primarily consists of cluster-bonding orbitals (Figure 3). The LUMO+1 is situated at the seesaw-coordinated Si5 as well as the Si4 and Si6 atoms, and the LUMO is located at the basal Si atoms of the siliconoid moiety (Si1, Si2, Si3, Si7), which is reminiscent of the corresponding

Table 2. Comparison of Wavelengths λ_{max}, Oscillator Strengths f, and Excitation Energy E from Experimental and TD-DFT[12] Calculations for Siliconoid-Tetrylene Hybrids2a−2c

	experimental		DFT			
	λ_{max} (nm)	excitation energy E (eV)	λ_{max} (nm)	excitation energy E (eV)	oscillator strength f	transitions (% contribution)
2a	532	2.3308	589	2.1138	0.0124	HOMO→LUMO (99)
			514	2.4115	0.0052	HOMO−1→LUMO (98)
	371	3.3418	424	2.9232	0.0568	HOMO→LUMO+1 (96)
2b	514	2.4125	556	2.2286	0.0085	HOMO→LUMO (99)
			513	2.4150	0.0056	HOMO−1→LUMO (98)
	407	3.0463	408	3.0415	0.0605	HOMO→LUMO+1 (76)
						HOMO−1→LUMO+1 (16)
2c	520	2.3843	562	2.2077	0.0088	HOMO→LUMO (99)
			515	2.4055	0.0067	HOMO−1→LUMO (97)
	417	2.9732	413	3.0002	0.0596	HOMO−1→LUMO (4)
						HOMO−1→LUMO+1 (3)
						HOMO→LUMO+1 (60)
						HOMO→LUMO+2 (4)

https://doi.org/10.1021/acs.inorgchem.4c00474
Inorg. Chem. 2024, 63, 20083−20087

orbitals in the unfunctionalized hexasilabenzpolarene Si_6Tip_6[8a,j] as well as Breher et al.'s Si_5Mes_6 propellane.[3c] Likewise, the HOMO−3 suggests a weak bonding interaction between the *nudo*-atoms (Si1, Si2) and strongly resembles the HOMO−1 in Si_5Mes_6 as well as the HOMO−2 in hexasilabenzpolarene Si_6Tip_6.

The longest wavelength absorptions in the experimental UV/vis spectra (see Supporting Information) are observed as very broad bands at λ_{max} = 532 nm (ε = 704 M^{-1} cm^{-1}, **2a**), 514 nm (ε = 580 M^{-1} cm^{-1}, **2b**), and 520 nm (ε = 870 M^{-1} cm^{-1}, **2c**). These values are strongly red-shifted compared to the corresponding Si_6-tetrylene hybrids (Si_6NHSi 472 nm, Si_6NHGe 436 nm, Si_6NHSn 436 nm).[8g] Although TD-DFT calculations somewhat overestimate these red shifts, the trends within the series are nicely reproduced, in particular when considering the very broad nature of absorption bands and the associated large uncertainty in the determination of the maxima (Table 2, Figures S31 and S32). The calculated HOMO−LUMO gaps are in the range of the reported values for siliconoids.[3c,8a,j] Additional absorption bands at around 371−417 nm (Table 2) and 324−345 nm (Supporting Information Table S8) are observed and are in agreement with the calculated values. According to TD-DFT, they arise from a combination of several transitions (see Supporting Information for details).

In conclusion, we successfully grafted heavier group 14 amidinato tetrylenes to the Si_7 cluster of **II**, thus providing access to tetrylene-functionalized Si_7 siliconoids **2a**−**2c**. In contrast to the cluster expansion previously observed upon reaction of **II** with Jutzi's decamethyl silicocene to **III**,[8d] the Si_7 cluster core remains unperturbed, reiterating our observations for the reactions of the heavier group 14 tetrylenes with the *ligato*-lithiated Si_6 siliconoid. We are currently investigating the properties of **2a**−**2c** as ligands toward various transition metals.

■ ASSOCIATED CONTENT

Supporting Information

The Supporting Information is available free of charge at https://pubs.acs.org/doi/10.1021/acs.inorgchem.4c00474.

Experimental procedures and analytical data, plots of NMR spectra, and crystallographic and computational details (PDF)

Accession Codes

CCDC 2308133 contains the supplementary crystallographic data for this paper. These data can be obtained free of charge via www.ccdc.cam.ac.uk/data_request/cif, or by emailing data_request@ccdc.cam.ac.uk, or by contacting The Cambridge Crystallographic Data Centre, 12 Union Road, Cambridge CB21EZ, UK; fax: + 441223336033.

■ AUTHOR INFORMATION

Corresponding Author

David Scheschkewitz − *Krupp-Chair for General and Inorganic Chemistry, Saarland University, 66123 Saarbrücken, Germany;* orcid.org/0000-0001-5600-8034; Email: scheschkewitz@mx.uni-saarland.de

Authors

Luisa Giarrana − *Krupp-Chair for General and Inorganic Chemistry, Saarland University, 66123 Saarbrücken, Germany*

Michael Zimmer − *Krupp-Chair for General and Inorganic Chemistry, Saarland University, 66123 Saarbrücken, Germany*

Bernd Morgenstern − *Service Center X-ray Diffraction, Saarland University, 66123 Saarbrücken, Germany*

Complete contact information is available at: https://pubs.acs.org/10.1021/acs.inorgchem.4c00474

Notes

The authors declare no competing financial interest.

■ ACKNOWLEDGMENTS

Funding by the Deutsche Forschungsgemeinschaft (DFG SCHE 906/4-4) is gratefully acknowledged. We thank Prof. Stella Stopkowicz and Dr. Diego Andrada for access to their computational clusters as well as helpful discussions.

■ REFERENCES

(1) (a) Ekimov, A. I. Optical Properties of Semiconductor Quantum Dots in Glass Matrix. *Phys. Scr.* **1991**, *T39*, 217−222. (b) Efros, A. L.; Brus, L. E. Nanocrystal Quantum Dots: From Discovery to Modern Development. *ACS Nano* **2021**, *15*, 6192−6210.

(2) (a) Heider, Y.; Scheschkewitz, D. Stable unsaturated silicon clusters (siliconoids). *Dalton Trans.* **2018**, *47*, 7104−7112. (b) Iwamoto, T.; Ishida, S. Silicon Compounds with Inverted Geometry around Silicon Atoms. *Chem. Lett.* **2014**, *43*, 164−170. (c) Kyushin, S. In *Organosilicon Compounds: Theory and Experiment (Synthesis)*; Lee, V. Y., Ed.; Academic Press, 2017; Chapter 3, Vol. 1.

(3) (a) Scheschkewitz, D. A Molecular Silicon Cluster with a "Naked" Vertex Atom. *Angew. Chem., Int. Ed.* **2005**, *44*, 2954−2956. (b) Moteki, M.; Maeda, S.; Ohno, K. Systematic Search for Isomerization Pathways of Hexasilabenzene for Finding Its Kinetic Stability. *Organometallics* **2009**, *28*, 2218−2224. (c) Nied, D.; Köppe, R.; Klopper, W.; Schnöckel, H.; Breher, F. Synthesis of a Pentasilapropellane. Exploring the Nature of a Stretched Silicon−Silicon Bond in a Nonclassical Molecule. *J. Am. Chem. Soc.* **2010**, *132*, 10264−10265. (d) Abersfelder, K.; White, A. J. P.; Rzepa, H. S.; Scheschkewitz, D. A Tricyclic Aromatic Isomer of Hexasilabenzene. *Science* **2010**, *327*, 564−566. (e) Ishida, S.; Otsuka, K.; Toma, Y.; Kyushin, S. An Organosilicon An Organosilicon Cluster with an Octasilacuneane Core: A Missing Silicon Cage Motif. *Angew. Chem., Int. Ed.* **2013**, *52*, 2507−2510. (f) Tsurusaki, A.; Iizuka, C.; Otsuka, K.; Kyushin, S. Cyclopentasilane-Fused Hexasilabenzvalene. *J. Am. Chem. Soc.* **2013**, *135*, 16340−16343. (g) Tsurusaki, A.; Kamiyama, K.; Kyushin, S. Tetrasilane-Bridged Bicyclo[4.1.0]heptasil-1(6)-ene. *J. Am. Chem. Soc.* **2014**, *136*, 12896−12898.

(4) Fischer, G.; Huch, V.; Mayer, P.; Vasisht, S. K.; Veith, M.; Wiberg, N. $Si_8(SitBu_3)_6$: A Hitherto Unknown Cluster Structure in Silicon Chemistry. *Angew. Chem., Int. Ed.* **2005**, *44*, 7884−7887.

(5) Iwamoto, T.; Akasaka, N.; Ishida, S. A heavy analogue of the smallest bridgehead alkene stabilized by a base. *Nat. Commun.* **2014**, *5*, 5353−5359.

(6) Schiegerl, L. J.; Karttunen, A. J.; Klein, W.; Fässler, T. F. Anionic Siliconoids from Zintl Phases: $R_3Si_9^-$ with Six and $R_2Si_9^{2-}$ with Seven Unsubstituted Exposed Silicon Cluster Atoms (R = Si(*t*Bu)$_2$H). *Chem.—Eur. J.* **2018**, *24*, 19171−19174.

(7) Keuter, J.; Schwedtmann, K.; Hepp, A.; Bergander, K.; Janka, O.; Doerenkamp, C.; Eckert, H.; Mück-Lichtenfeld, C.; Lips, F. Diradicaloid or Zwitterionic Character: The Non-Tetrahedral Unsaturated Compound $[Si_4\{N(SiMe_3)Dipp\}_4]$ with a Butterfly-type Si_4 Substructure. *Angew. Chem., Int. Ed.* **2017**, *56*, 13866−13871.

(8) (a) Abersfelder, K.; White, A. J. P.; Berger, R. J. F.; Rzepa, H. S.; Scheschkewitz, D. A Stable Derivative of the Global Minimum on the Si_6H_6 Potential Energy Surface. *Angew. Chem., Int. Ed.* **2011**, *50*, 7936−7939. (b) Jana, A.; Huch, V.; Repisky, M.; Berger, R. J. F.; Scheschkewitz, D. Dismutational and Global-Minimum Isomers of Heavier 1,4-Dimetallatetrasilabenzenes of Group 14. *Angew. Chem.,*

Int. Ed. **2014**, *53*, 3514−3518. (c) Willmes, P.; Leszczyńska, K. I.; Heider, Y.; Abersfelder, K.; Zimmer, M.; Huch, V.; Scheschkewitz, D. Isolation and Versatile Derivatization of an Unsaturated Anionic Silicon Cluster (Siliconoid). *Angew. Chem., Int. Ed.* **2016**, *55*, 2907−2910. (d) Leszczyńska, K. I.; Huch, V.; Präsang, C.; Schwabedissen, J.; Berger, R. J. F.; Scheschkewitz, D. Atomically Precise Expansion of Unsaturated Silicon Clusters. *Angew. Chem., Int. Ed.* **2019**, *58*, 5124−5128. (e) Heider, Y.; Poitiers, N. E.; Willmes, P.; Leszczyńska, K. I.; Huch, V.; Scheschkewitz, D. Site-selective functionalization of Si_6R_6 siliconoids. *Chem. Sci.* **2019**, *10*, 4523−4530. (f) Klemmer, L.; Huch, V.; Jana, A.; Scheschkewitz, D. An anionic heterosiliconoid with two germanium vertices. *Chem. Commun.* **2019**, *55*, 10100−10103. (g) Poitiers, N. E.; Giarrana, L.; Leszczyńska, K. I.; Huch, V.; Zimmer, M.; Scheschkewitz, D. Indirect and Direct Grafting of Transition Metals to Siliconoids. *Angew. Chem., Int. Ed.* **2020**, *59*, 8532−8536. (h) Poitiers, N. E.; Giarrana, L.; Huch, V.; Zimmer, M.; Scheschkewitz, D. Exohedral functionalization *vs.* core expansion of siliconoids with Group 9 metals: catalytic activity in alkene isomerization. *Chem. Sci.* **2020**, *11*, 7782−7788. (i) Poitiers, N. E.; Huch, V.; Zimmer, M.; Scheschkewitz, D. Chalcogen-Expanded Unsaturated Silicon Clusters: Thia-, Selena-, and Tellurasiliconoids. *Chem.—Eur. J.* **2020**, *26*, 16599−16602. (j) Poitiers, N. E.; Huch, V.; Morgenstern, B.; Zimmer, M.; Scheschkewitz, D. Siliconoid Expansion by a Single Germanium Atom through Isolated Intermediates. *Angew. Chem., Int. Ed.* **2022**, *61*, No. e202205399.

(9) (a) Sevov, S. C.; Goicoechea, J. M. Chemistry of Deltahedral Zintl Ions. *Organometallics* **2006**, *25*, 5678−5692. (b) Scharfe, S.; Kraus, F.; Stegmaier, S.; Schier, A.; Fässler, T. F. Zintl Ions, Cage Compounds, and Intermetalloid Clusters of Group 14 and Group 15 Elements. *Angew. Chem., Int. Ed.* **2011**, *50*, 3630−3670. (c) Li, F.; Muñoz-Castro, A.; Sevov, S. C. $[Ge_9\{Si(SiMe_3)_3\}_3\{SnPh_3\}]$: A Tetrasubstituted and Neutral Deltahedral Nine-Atom Cluster. *Angew. Chem., Int. Ed.* **2012**, *51*, 8581−8584. (d) Li, F.; Sevov, S. C. Synthesis, Structures, and Solution Dynamics of Tetrasubstituted Nine-Atom Germanium Deltahedral Clusters. *J. Am. Chem. Soc.* **2014**, *136*, 12056−12063. (e) Kysliak, O.; Schrenk, C.; Schnepf, A. $\{Ge_9[Si(SiMe_3)_2(SiPh_3)]_3\}^-$: Ligand Modification in Metalloid Germanium Cluster Chemistry. *Inorg. Chem.* **2015**, *54*, 7083−7088. (f) Kysliak, O.; Schnepf, A. $\{Ge_9[Si(SiMe_3)_3]_2\}^{2-}$: a starting point for mixed substituted metalloid germanium clusters. *Dalton Trans.* **2016**, *45*, 2404−2408. (g) Geitner, F. S.; Dums, J. V.; Fässler, T. F. Derivatization of Phosphine Ligands with Bulky Deltahedral *Zintl* Clusters—Synthesis of Charge Neutral Zwitterionic Tetrel Cluster Compounds $[(Ge_9\{Si(TMS)_3\}_2)^tBu_2P]M(NHC^{Dipp})$ (M: Cu, Ag, Au). *J. Am. Chem. Soc.* **2017**, *139*, 11933−11940. (h) Geitner, F. S.; Klein, W.; Fässler, T. F. Synthesis and Reactivity of Multiple Phosphine-Functionalized Nonagermanide Clusters. *Angew. Chem., Int. Ed.* **2018**, *57*, 14509−14513. (i) Frischhut, S.; Klein, W.; Drees, M.; Fässler, T. F. Acylation of Homoatomic Ge_9 Cages and Subsequent Decarbonylation. *Chem.—Eur. J.* **2018**, *24*, 9009−9014. (j) Geitner, F. S.; Klein, W.; Storcheva, O.; Tilley, T. D.; Fässler, T. F. Early-Transition-Metal Complexes of Functionalized Nonagermanide Clusters: Synthesis and Characterization of $[Cp_2(MeCN)Ti(\eta^1\text{-}Ge_9\{Si(TMS)_3\}_3)]$ and $K_3[Cp_2Ti(\eta^1\text{-}Ge_9\{Si(TMS)_3\}_2)_2]$. *Inorg. Chem.* **2019**, *58*, 13293−13298. (k) Boyko, M.; Hlukhyy, V.; Jin, H.; Dums, J. V.; Fässler, T. F. Extracting $[Pd@Sn_9]^{4-}$ and $[Rh@Pb_9]^{4-}$ Clusters from their Binary Alloys Using "Metal Scissors. *Z. Anorg. Allg. Chem.* **2020**, *646*, 1575−1582. (l) Geitner, F. S.; Fässler, T. F. Cluster Expansion versus Complex Formation: Coinage Metal Coordination to Silylated $[Ge_9]$ Cages. *Inorg. Chem.* **2020**, *59*, 15218−15227. (m) Townrow, O. P. E.; Chung, C.; Macgregor, S. A.; Weller, A. S.; Goicoechea, J. M. A Neutral Heteroatomic Zintl Cluster for the Catalytic Hydrogenation of Cyclic Alkenes. *J. Am. Chem. Soc.* **2020**, *142*, 18330−18335. (n) Wallach, C.; Selic, Y.; Witzel, B. J. L.; Klein, W.; Fässler, T. F. Filled trivacant icosahedra as building fragments in 17-atom endohedral germanides $[TM_2@Ge_{17}]^{n-}$ (TM = Co, Ni). *Dalton Trans.* **2021**, *50*, 13671−13675. (o) Gienger, C.; Schnepf, A. Neutral $R_3PAuGe_9(Hyp)_3$ (R = Et,nPr,iPr,nBu,tBu, Cy) (Hyp = $Si(SiMe_3)$ Clusters give new insights into the ligand strength of the metalloid $[Ge_9(Hyp)_3]^-$ cluster. *Z. Anorg. Allg. Chem.* **2021**, *647*, 1695−1701. (p) Townrow, O. P. E.; Duckett, S. B.; Weller, A. S.; Goicoechea, J. M. Zintl Cluster Supported Low Coordinate Rh(i) Centers for Catalytic H/D Exchange Between H2 and D2. *Chem. Sci.* **2022**, *13*, 7626−7633. (q) Gienger, C.; Schynowski, L.; Schaefer, J.; Schrenk, C.; Schnepf, A. New Intermetalloid Ge_9-clusters with Copper and Gold: Filling Vacancies in the Cluster Chemistry of $[Ge_9(Hyp)_3]^-$ (Hyp = $Si(SiMe_3)_3$). *Eur. J. Inorg. Chem.* **2023**, *26*, No. e202200738.

(10) (a) So, C.-W.; Roesky, H. W.; Magull, J.; Oswald, R. B. Synthesis and Characterization of $[PhC(NtBu)_2]SiCl$: A Stable Monomeric Chlorosilylene. *Angew. Chem., Int. Ed.* **2006**, *45*, 3948−3950. (b) Sen, S. S.; Roesky, H. W.; Stern, D.; Henn, J.; Stalke, D. High Yield Access to Silylene RSiCl (R = $PhC(NtBu)_2$) and Its Reactivity toward Alkyne: Synthesis of Stable Disilacyclobutene. *J. Am. Chem. Soc.* **2010**, *132*, 1123−1126. (c) Nagendran, S.; Sen, S. S.; Roesky, H. W.; Koley, D.; Grubmüller, H.; Pal, A.; Herbst-Irmer, R. RGe(I)Ge(I)R Compound (R = $PhC(NtBu)_2$) with a Ge−Ge Single Bond and a Comparison with the Gauche Conformation of Hydrazine. *Organometallics* **2008**, *27*, 5459−5463. (d) Sen, S. S.; Kritzler-Kosch, M. P.; Nagendran, S.; Roesky, H. W.; Beck, T.; Pal, A.; Herbst-Irmer, R. Synthesis of Monomeric Divalent Tin(II) Compounds with Terminal Chloride, Amide, and Triflate Substituents. *Eur. J. Inorg. Chem.* **2010**, *2010*, 5304−5311.

(11) (a) Inoue, S.; Leszczyńska, K. An Acyclic Imino-Substituted Silylene: Synthesis, Isolation, and its Facile Conversion into a Zwitterionic Silaimine. *Angew. Chem., Int. Ed.* **2012**, *51*, 8589−8593. (b) Leszczyńska, K. I.; Deglmann, P.; Präsang, C.; Huch, V.; Zimmer, M.; Schweinfurth, D.; Scheschkewitz, D. Pentamethylcyclopentadienyl-substituted hypersilylsilylene: reversible and irreversible activation of C═C double bonds and dihydrogen. *Dalton Trans.* **2020**, *49*, 13218−13225.

(12) (a) Perdew, J. P. Density-functional approximation for the correlation energy of the inhomogeneous electron gas. *Phys. Rev. B* **1986**, *33*, 8822−8824. (b) Becke, A. D. Density-functional exchange-energy approximation with correct asymptotic behavior. *Phys. Rev. A* **1988**, *38*, 3098−3100. (c) Lee, C.; Yang, W.; Parr, R. G. Development of the Colle-Salvetti correlation-energy formula into a functional of the electron density. *Phys. Rev. B* **1988**, *37*, 785−789.

(13) (a) Schäfer, A.; Horn, H.; Ahlrichs, R. Fully optimized contracted Gaussian basis sets for atoms Li to Kr. *J. Chem. Phys.* **1992**, *97*, 2571−2577. (b) Schäfer, A.; Huber, C.; Ahlrichs, R. Fully optimized contracted Gaussian basis sets of triple zeta valence quality for atoms Li to Kr. *J. Chem. Phys.* **1994**, *100*, 5829−5835. (c) Weigend, F.; Ahlrichs, R. Balanced basis sets of split valence, triple zeta valence and quadruple zeta valence quality for H to Rn: Design and assessment of accuracy. *Phys. Chem. Chem. Phys.* **2005**, *7*, 3297−3305. (d) Weigend, F. Accurate Coulomb-fitting basis sets for H to Rn. *Phys. Chem. Chem. Phys.* **2006**, *8*, 1057−1065.

https://doi.org/10.1021/acs.inorgchem.4c00474
Inorg. Chem. 2024, 63, 20083−20087

3.3 Stable Nickel Complexes of a Siliconoid/Silylene Hybrid Ligand: Competent Hydrosilylation Catalysts for Terminal Olefins

Reproduced from Luisa Giarrana, Dennis Welterlich, Michael Zimmer, Bernd Morgenstern, David Scheschkewitz, *Inorg. Chem. Front.* **2026**, Advance Article. https://doi.org/10.1039/D6QI00025H with permission from all authors, the Chinese Chemical Society (CCS), Peking University (PKU), and the Royal Society of Chemistry.

The results are additionally concluded and put into context in Chapter 4.

Author Contributions

Luisa Giarrana

Lead: Data curation, formal analysis, investigation, writing (original draft)

Equal (D.S.): Conceptualization

Dennis Welterlich

Supporting: Data curation, formal analysis, investigation

Michael Zimmer

Lead: Data curation (VT- and solid-state NMR)

Supporting: Formal analysis, methodology, validation

Bernd Morgenstern

Lead: Data curation

Supporting: Formal analysis, methodology, visualization

David Scheschkewitz

Lead: Funding acquisition, project administration, resources, supervision, writing (review & editing)

Equal (L.G.): Conceptualization

Supporting: Formal analysis, investigation, methodology

INORGANIC CHEMISTRY FRONTIERS

RESEARCH ARTICLE

View Article Online
View Journal

Cite this: DOI: 10.1039/d6qi00025h

Stable nickel complexes of a siliconoid/silylene hybrid ligand: competent hydrosilylation catalysts for terminal olefins

Luisa Giarrana,[a] Dennis Welterlich,[a] Michael Zimmer,[a] Bernd Morgenstern[b] and David Scheschkewitz *[a]

Received 5th January 2026,
Accepted 11th February 2026

DOI: 10.1039/d6qi00025h

rsc.li/frontiers-inorganic

The use of abundant, first row transition metals instead of platinum group metals is a contemporary goal in homogenous catalysis research. Electron-rich silylenes are increasingly established as viable alternatives to carbene-based ligand systems. Here we report that – depending on the first row transition metal fragment employed – a silylene hybridized with a Si_7-siliconoid (Tip_5Si_7NHSi **1**) either coordinates to the metal centre *via* the silylene side-arm exclusively ($Fe(CO)_4$ complex) and thus retains an unperturbed metalloid core or coordinates in a chelating manner involving the donation by unsubstituted vertices (Ni(cod)-fragment, cod = 1,5-cyclooctadiene). The siliconoid/silylene ligand **1** is bonded more strongly than cod so that the latter is readily replaced by PPh_3 or CO ligands. The cod derivative is catalytically active in the hydrosilylation of terminal olefins with the secondary silane Ph_2SiH_2.

Introduction

Transition metal complexes are still the benchmark in homogenous catalysis. Especially the precious late 4d and 5d transition metals show outstanding catalytic activity in the value-added transformations of small molecules such as CO, CO_2, NH_3 or H_2.[1,2] The toxicity, low abundance and high price of these metals moved 3d transition metals into focus over the last years.[3] Their lower propensity for $2e^-$ redox steps, however, requires the use of non-innocent ligands and hence metal–ligand cooperativity in many cases.[4,5] More recently, the incorporation of heavier elements of the p-block into the ligand system has proven to induce chemical non-innocence.[6–10] In particular, low-valent motifs such as silylenes, germylenes and stannylenes have been employed as ligands towards base metals in order to improve their performance in homogenous catalysis.[11–19]

Even with chemically innocent coordination environment, nickel is an outstanding catalyst in many homogenous transformations, for instance, in alkene hydrogenation and cross-coupling reactions.[20,21] The nickel complexes with amidinato-stabilized silicon(II) **I**[22] and with dialkylsilylene ligand **II** (Fig. 1)[23] paved the way for a broad variety of stable Ni(0) complexes with low-valent group 14 ligands.[11,24–28] A mixed NHC/NHSi-stabilized Ni complex **III** reported by Driess *et al.* activates dihydrogen and thus reductively transforms HBcat into a Ni^{II} borylene complex.[24] Subsequently, various bis(silylenes) with different bridging backbones such as **IV**,[25] **V**[26] or **VI**[27]

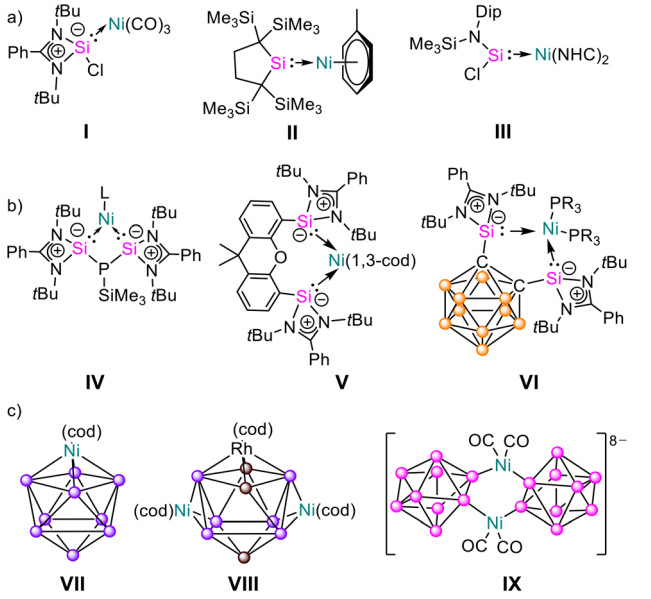

Fig. 1 Selected examples of low-valent group 14 ligands with nickel (a, b and c) (○ = BH, ○ = Ge, ○ = Ge-Hyp (Hyp = $Si(SiMe_3)_3$), ○ = Si, Dip = 2,6-diisopropylphenyl, 1,3-cod = 1,3-cyclooctadienyl, cod = 1,5-cyclooctadienyl, NHC = *N*,*N*′-diisopropyl-3,4-dimethylimidazol-2-ylidene).

[a]*Krupp-Chair for General and Inorganic Chemistry, Saarland University, 66123 Saarbrücken, Germany. E-mail: scheschkewitz@mx.uni-saarland.de*
[b]*Service Center X-ray Diffraction, Saarland University, 66123 Saarbrücken, Germany*

were employed as bidentate ligands for nickel to result in the activation of H_2, CO, or NH_3 and other small molecules.[11–19,28]

Group 14-based cluster systems[29–31] have recently come to the fore as potentially redox-active ligands, but examples of their coordination to nickel are scarce and studies on catalytic activity even rarer. The Goicoechea group reported on the capping of a Ni(II) centre onto the dianionic Ge_9 Zintl cluster **VII**[32] (Fig. 1). The corresponding rhodium derivative can be converted to the heterodimetallic Ni_2-Rh-Ge_9 cluster **VIII**.[33] Although the Rh-Ge_9-cluster is an active catalyst in the hydrogenation of cyclooctadiene (cod), in case of **VII** no information on catalytic activity is available. The only silicon-cluster based nickel complex thus far was isolated by Korber *et al.* as the eightfold negative charged, dimeric Si_9–$(Ni(CO)_2)_2$–Si_9 cluster **IX**[34] with no reported catalytic activity. Siliconoids (unsaturated silicon clusters)[29,30,35–40] have been employed as ligands to various transition metals.[36,37] The incorporation of an amidinato silicon(II) side arm proved a useful strategy to enable coordination to electroneutral transition metal fragments, for instance to $Fe(CO)_4$ with Si_6 siliconoid/silylene hybrid ligand **X**,[36] yet nickel complexes of siliconoids remain elusive.

In view of the catalytic activity of an iridium complex derived from **X** in alkene isomerization,[37] we had previously attempted to coordinate it to a nickel carbonyl fragment (*in situ*-generated from $Ni(cod)_2$ under CO atmosphere) but isolated nickel-free **XI** instead (Scheme 1) as the product of complete CO cleavage. DFT calculations regarding the mechanism of CO splitting, however, suggested cooperativity between the siliconoid core and the nickel centre in experimentally undetected intermediates.[38] Plausibly, the lack of space at the Si_6 core of **X** prevents the observation, let alone isolation of any involved nickel complex.

We therefore anticipated that an expansion to a Si_7 core could increase the available space for metal coordination. Indeed, we now report the isolation and full characterization of siliconoid-transition metal complexes employing a core-expanded Si_7 cluster with pending amidinato-silylene as a ligand.[40] While the $Fe(CO)_4$ fragment is only coordinated by the silylene sidearm, the reaction with $Ni(cod)_2$ results in a product with distinct interactions of the Si_7 core with the nickel centre. Straightforward ligand exchange of cod yields the corresponding PPh_3 and CO complexes. Competent catalytic activity in hydrosilylation of terminal alkenes is demonstrated. During benchmark reactions with $Ni(cod)_2$, we unexpectedly found that this simple Ni(0) precursor exhibits remarkable activity in these alkene hydrosilylations as well, which once more illustrates the importance of appropriate control experiments in homogenous catalysis.

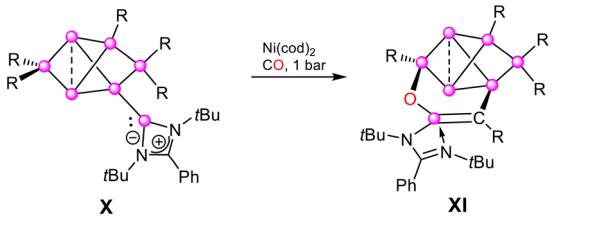

Scheme 1 Reported reaction of Si_6 siliconoid/silylene hybrid with CO in the presence of $Ni(cod)_2$ (○ = Si, R = 2,4,6-triisopropylphenyl).[38]

Results and discussion

In order to quantify our assumption regarding the reduced steric demand of the Si_7 system, we initially investigated the complexation of the Si_7 siliconoid/silylene hybrid **1**[40] to an $Fe(CO)_4$ fragment, aiming for a direct comparison with the Si_6 system **X**-$Fe(CO)_4$.[36] Reaction of **1** with one equivalent of $Fe_2(CO)_9$ at 60 °C (aluminium heating block temperature) in benzene overnight indeed leads to quantitative conversion. The desired iron tetracarbonyl complex **2** crystallizes in 46% yield from pentane (Fig. 2, top). Notably, the corresponding products could not be obtained with the corresponding germylene or stannylene-Si_7-hybrids.[40]

The molecular structure of **2** in the solid state as determined by single crystal X-ray diffraction (Fig. 2, bottom)

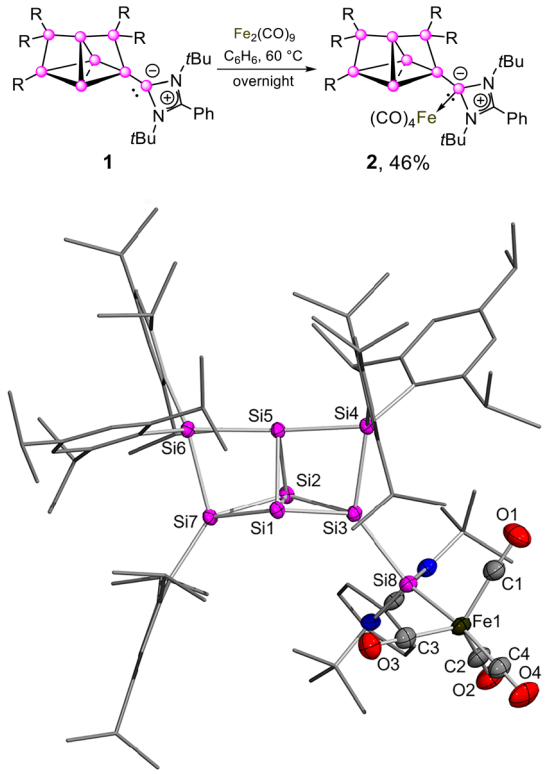

Fig. 2 Top: Reactivity of Tip_5Si_7NHSi **1** towards $Fe_2(CO)_9$ (○ = Si, R = 2,4,6-triisopropylphenyl). Bottom: Molecular structure of iron tetracarbonyl siliconoid/silylene hybrid **2** in the solid state. Hydrogen atoms are omitted for clarity. Thermal ellipsoids at 50% probability. Selected bond lengths [Å] and angles [°]: Fe–Si8 2.253(6), Si3–Si8 2.391(8), Si1–Si2 2.618(8), Si1–Si3 2.315(8), Si1–Si5 2.332(8), Si1–Si7 2.323(7), Si2–Si3 2.366(7), Si2–Si5 2.346(8), Si2–Si7 2.356(8), Si3–Si42.428(8) , Si4–Si5 2.388(7), Si5–Si6 2.381(7); Fe1–Si8–Si3 129.0(3), Si4–Si5–Si6 171.0(3), Si8–Fe1–C4 171.7(9).

reveals a silylene-coordinated Fe1 centre with a Fe–Si8 bond length of 2.253(6) Å, considerably shortened compared to **X**-Fe(CO)$_4$ (2.384 Å)[37] but well within the range of reported sterically unencumbered Si–Fe(CO)$_4$ species (2.196–2.405 Å).[41–44] The short Fe–Si bond length is a first indication for the validity of our working hypothesis that the expanded cluster core may ease the steric strain in the envisaged complexes. For a more quantitative description, we calculated the percent buried volume %V_{bur} [45,46] of **2** *vs.* that of **X**-Fe(CO)$_4$ using the SambVca open-source application.[47] As expected, **X** shows a somewhat larger buried volume of 64.9%V_{bur} in comparison with **1** (55.3%V_{bur}) at the iron centre of the Fe(CO)$_4$ fragment.[36] The assumption of a better accessibility of **1** compared to **X** is thus confirmed in principle; both values are at the upper end of the range found for typical bulky ligands. For context, common ligands for transition metals exhibit %V_{bur} values of around 30–60%.[48] Sterically more demanding ligands exceed these values: the carbazole ligand by Hinz with 74.8%,[49] the triazene by Masuda (80.1%)[50] or a tetradentate combination of N,N and P,P ligands by Constable and Housecroft (88.0%).[51]

As in **X**-Fe(CO)$_4$,[36] the Si$_7$ system **2** shows no interactions between the cluster core and the iron moiety. The Si1–Si2 distance is at 2.618(8) Å almost identical with that in the free ligand **1** (2.620 Å).[40] The CO ligands complete the trigonal–bipyramidal coordination sphere of the iron centre with C–O bond lengths (1.144–1.152 Å) and Fe1–C distances (1.769–1.794 Å) in the range of reported Fe(CO)$_4$ complexes.[41–44,52] The most notable distortion from the cluster bonding situation in the free ligand **1** is the Si4–Si5–Si6 seesaw angle of 171.0(3)° in **2**, which is slightly smaller than in **1** (174.8°).[40]

The ^{29}Si NMR spectrum of **2** shows the familiar wide signal distribution of siliconoids with eight signals in the range of 172.7 to −209.0 ppm. The signal at 172.7 ppm, assigned to Si3 based on ^{1}H/^{29}Si 2D NMR spectra, is significantly upfield-shifted compared to the free ligand **1** (211.7 ppm).[40] In contrast, the signal of the silylene moiety (Si8) is strongly downfield-shifted from 24.1 ppm (**1**)[40] to 100.5 ppm (**2**), which is very similar to the reported shift differences between **X** and its iron complex.[36] Owing to Berry pseudorotation, the ^{13}C NMR spectrum of **2** reveals only one single signal for the four characteristic CO ligands at high field at 216.79 ppm.[53]

FT-IR spectroscopy reveals four CO stretching vibrations ($\tilde{V}_{CO,exp}$ = 2026, 1953, 1923, 1907 cm^{-1}), in line with the absence of symmetry in **2**. The carbonyl stretching frequency at $\tilde{V}_{CO,exp}$ = 2026 cm^{-1} is in accordance with that of the silylene complex of Fe(CO)$_4$ ($\tilde{V}_{CO,exp}$ = 2026 cm^{-1}) reported by Jana and Roesky,[41] suggesting a similar ligand-to-metal σ-donation but a slightly higher donation than in the Si$_6$-analogue ($\tilde{V}_{CO,exp}$ = 2022 cm^{-1}). Theoretical support is provided by calculations at the B3LYP/def2-TZVPP[54–57] level of theory with stretching frequencies at $\tilde{V}_{CO,calc}$ = 2009 and 1901 cm^{-1}. The longest wavelength UV-Vis absorption of **2** occurs at $\lambda_{max,exp}$ = 525 nm (ε = 380 M^{-1} cm^{-1}) with a bathochromic shift compared to that of the Si$_6$-analogue ($\lambda_{max,exp}$ = 470 nm, ε = 1890 M^{-1} cm^{-1})[36] but a marginally hypsochromic shift compared to the starting material **1** ($\lambda_{max,exp}$ = 532 nm, ε = 704 M^{-1} cm^{-1}).[40] The experimental values for **2** are in good agreement with the TD-DFT results ($\lambda_{max,calc}$ = 528 nm; see SI for details).

For the envisaged coordination to a nickel centre, we opted for bis(cyclooctadiene) nickel(0) Ni(cod)$_2$ as precursor, given that Ni(CO)$_4$ is highly volatile and toxic (and not commercially available). Addition of 1 eq. of solid Ni(cod)$_2$ to a solution of **1** in toluene at ambient temperature caused a colour change of the mixture from brown to blackberry red. After work-up (see SI), the desired Ni-siliconoid complex **3a** was isolated as dark red, block-shaped crystals in 46% yield (Scheme 2). The residual cod ligand in **3a** can be readily replaced by adding 1 eq. of solid PPh$_3$ to the reaction mixture of **1** and Ni(cod)$_2$ affording the triphenylphosphine-derivative **3b** in 49% yield.

Single crystals were obtained from a concentrated pentane solution of **3a,b** at −26 °C. X-ray diffraction analysis confirmed the solid-state structure of **3a** in the triclinic space group *P*$\bar{1}$ and **3b** in the monoclinic space group *I*2/*a* (Fig. 3). In contrast to the previously discussed iron complex **2**, an interaction of the transition metal atom with the Si1 and Si3 atom is observed for **3a**/**3b**. The overall decreased congestion at the unsubstituted silicon vertices given their increased number in the Si$_7$/silylene scaffold **1** compared to the Si$_6$-hybrid **X** not only allows stable nickel coordination in the first place but also gives rise to significant interactions with the cluster core. In **3a**,**b**, the Ni1 atom is not only coordinated by the central Si8 atom of the silylene unit (Si3–Si8 **3a:** 2.183(8) Å/**3b:** 2.212(5) Å), as in the case for iron in **2**, but also by the Si1 and Si3 atoms. With bond distances of 2.302(5) Å (**3a**)/2.216(8) Å (**3b**) the Si1–Ni1 bond lengths are well within the common range (2.075–2.499 Å),[19,22–28,34,58–61] while the distances between Si3 and Ni1 are with 2.428(5) Å (**3a**)/2.379(8) Å (**3b**) slightly elongated. In **3a**, a longer Si1–Ni1 bond accompanied by a shorter Si1–Si3 bond (2.429(6) Å) is observed while the reduced donor strength of PPh$_3$ leads to a contraction of the Si1–Ni1 bond and thus a slight elongation of the Si1–Si3 bond in **3b** (**3a:** 2.429(6) Å; **3b:** 2.468(1) Å). These structural parameters reflect the stronger σ-donor character of the cod ligand com-

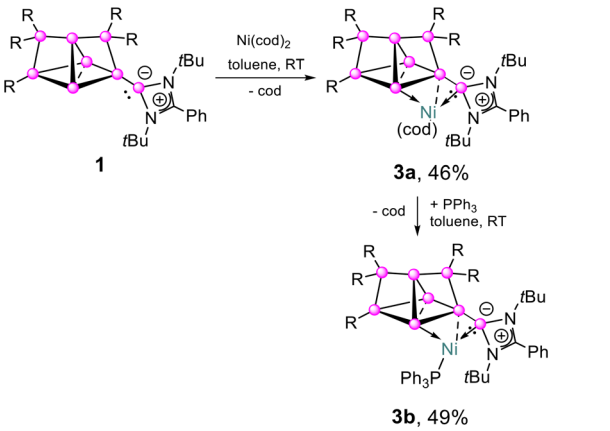

Scheme 2 Synthesis of nickel siliconoid/silylene complexes **3a** and **3b** (○ = Si, R = 2,4,6-triisopropylphenyl).

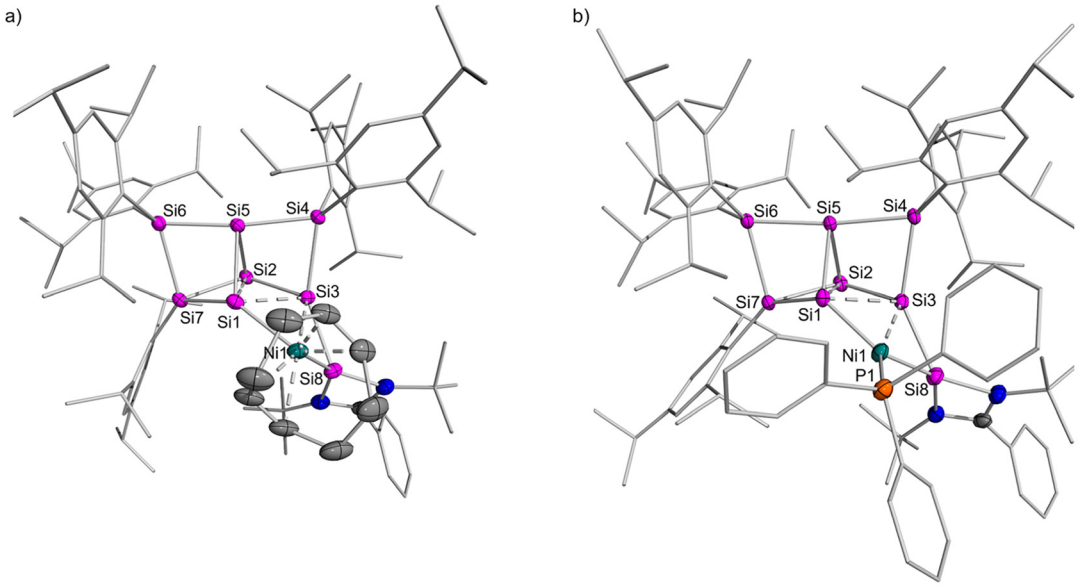

Fig. 3 Molecular structure of Ni(cod)-**3a** (left) and Ni(PPh_3)-siliconoid/silylene complex **3b** (right) in the solid state. Hydrogen atoms are omitted for clarity. Thermal ellipsoids at 50% probability. Selected bond lengths [Å] and angles [°]: (a) Ni1–Si1 2.302(5), Ni1–Si3 2.428(5), Ni1–Si8 2.212(5), Si1–Si2 2.674(6), Si1–Si3 2.429(6), Si1–Si5 2.362(6), Si1–Si7 2.324(6), Si2–Si5 2.335(6), Si2–Si7 2.352(6), Si2–Si3 2.392(1), Si3–Si8 2.291(6), Si3–Si4 2.424(6), Si4–Si5 2.371(6), Si5–Si6 2.362(6), Si6–Si7 2.425(6); Si8–Ni1–Si1 108.6(2), Si1–Ni1–Si3 61.7(2), Si8–Ni1–Si3 59.0(2), Si4–Si5–Si6 171.7(2); (b) Ni1–P1 2.200(7), Ni1–Si1 2.216(8), Ni1–Si3 2.378(8), Ni1–Si8 2.183(8), Si1–Si2 2.782(1), Si1–Si3 2.468(1), Si1–Si5 2.366(1), Si1–Si7 2.294(1), Si2–Si5 2.336(1), Si2–Si7 2.384(1), Si2–Si3 2.400(1), Si3–Si8 2.293(1), Si3–Si4 2.422(1), Si4–Si5 2.373(9), Si5–Si62.378(1), Si6–Si7 2.409(1); Si8–Ni1–Si1 120.2(3), Si1–Ni1–Si3 64.9(3), Si8–Ni1–Si3 60.2(3), Si4–Si5–Si6 173.1(4).

pared to PPh_3, while also highlighting the influence of the appreciable π-acceptor ability of PPh_3 on the electronic structure at the nickel centre. In agreement with lowered electron density in the Si_7 scaffold due to tighter bonding of the Ni1 centre in **3b** compared to **3a**, the distance between the Si1 and Si2 atom of 2.782 (1) Å in **3b** exceeds the distances between the unsubstituted vertices of so far reported propellane-like siliconoids (2.551 to 2.728 Å), while for **3a** it is with 2.674(6) Å in the reported range.[29,30,34–40] The concomitant upfield-shift of the Si2 atom in the ^{29}Si NMR spectrum of **3b** (**3a:** −340.7, **3b:** −287.6 ppm) is in line with the above mentioned shift of cluster electron density towards the perimeter of the Si2 atom. The seesaw Si4–Si5–Si6 angle in **3a** of 171.74(2)° is similar to that in **2** (171.0(3)°) and hence, slightly smaller than for **3b** (173.10(4)°) and the previously reported Si_7 cluster scaffolds ($Si_7Tip_5Cp^*$: 173.8°, Si_7Tip_5Li: 174.0°, Tip_5Si_7NHSi **1:** 174.8°).[39,40] The geometry around the Ni centre in **3a** is approximately tetrahedral with the coordinating silicon vertices (Si1 and Si8) and the two geometrical centres of the η^2-coordinated C=C double bonds of the cod ligand, which is comparable to the case of NHSi(Cl)–Ni$(CO)_3$ **I**.[22] In stark contrast, the substitution of the cod ligand by PPh_3 leads to a trigonal planar coordination environment around Ni1 in **3b** (largest deviation from Si1–Si8–Ni1–P1 plane for Ni1 = −0.018 Å), similar to the situation in **V**.[26]

Interestingly, in case of **V**, a substitution of the cod moiety by two PMe_3 units was shown to lead to a more symmetric tetrahedral geometry, a scenario likely prevented in case of **3b** by insufficient space to accommodate two PPh_3 ligands. Although the smaller $\%V_{bur}$[45,46] of **1** compared to **X** in the context of Fe$(CO)_4$ coordination indicates better accessibility as noted above, the tighter coordination under participation of the siliconoid core results in a much higher value of $\%V_{bur}$ = 69.9 at the nickel centre in **3b**.

The ^{29}Si NMR spectra of **3a** and **3b** retain the typical wide distribution observed for siliconoids,[29,30,36–40] albeit less pronounced than in **2**. The range of the chemical shifts covered in **3b** is with $\Delta\delta$ = 360.8 ppm considerably smaller in comparison to **1** but also to **3a** (Table 1), (**1**: $\Delta\delta$ = 430.7;[40] **3a** $\Delta\delta$ = 429.8 ppm). The former low-field signal of the SiTip group Si7 (**1**: 211.7 ppm, **2**: 172.7 ppm) is upfield-shifted by no less than $\Delta\delta \geq 122$ ppm for **3a** (δ = 50.0 ppm) and **3b** (δ = 63.9 ppm, d, $^4J_{P,Si}$ = 8.80 Hz). We suggest that this pronounced shielding of Si7 is a consequence of the perturbation of the cluster current,

Table 1 Experimental and calculated ^{29}Si NMR shifts (ppm) of siliconoid complexes **3a–c** at ambient temperature in C_6D_6. Calculated shifts at the TPSSh-D3(BJ)/def2-TVP[56,57,62,63] level of theory in brackets

	3a (L = cod)	**3b** (L = PPh_3)	**3c** (L = $(CO)_2$)
Si1	−154.0 [−148.1]	−87.3 (d) [−68.5]	−160.5 [−160.9]
Si2	−340.7 [−354.9]	−287.6 (d) [−291.0]	−342.2 [−354.4]
Si3	−10.2 [−9.0]	0.4 [−6.5]	−4.0 [−7.7]
Si4	−13.3 [−18.7]	−41.4 [−45.2]	−10.1 [−11.6]
Si5	−83.1 [−81.1]	−60.0 (d) [−68.2]	−81.9 [−78.5]
Si6	39.0 [35.1]	39.7 [30.6]	44.6 [37.1]
Si7	50.0 [56.5]	63.9 [65.4]	70.9 [80.1]
Si8	89.1 [90.4]	73.5 [84.6]	96.5 [93.1]

characteristic of siliconoids,[29,30,36–40] by coordination of Ni to the Si_7 core. The basal unsubstituted vertex without nickel contact Si2 is strongly shielded in both **3a** and **3b** compared to the free ligand (**3a**: −341 ppm; **3b**: −287.6 ppm (d, $^3J_{P,Si}$ = 28.5 Hz); *cf.* **1**: −219 ppm). The most downfield-shifted signals are now due to the amidinato-substituted silicon(II) centre Si1 coordinated to nickel (**3a**: 89.1 ppm; **3b**: 73.6 ppm, *cf.* **1**: 24.1 ppm (ref. 40)). The apical, substituent-free cluster vertex Si5 resonates at comparatively lower field (**3a**: −154.0 ppm; **3b**: −87.3 (d, $^3J_{P,Si}$ = 8.50 Hz) ppm; *cf.* **1**: −211.6 ppm). The $^{31}P\{^1H\}$ NMR spectrum of **3b** shows a single signal at −26.4 ppm. The shifts are in good agreement with the GIAO calculated values for the optimized structures **3a** and **3b** (B3LYP-D3(BJ)/def2-TZVP level of theory[54–57,62]) at TPSSh/def2-TZVP level of theory (Table 1).[62,63]

In case of the siliconoid/silylene hybrid ligand **X** with the Si_6 core, the addition of $Ni(cod)_2$ in a CO atmosphere had been shown to give rise to the incorporation of a completely cleaved CO moiety into the periphery of the cluster scaffold. This led to the formation of a formal Si=C double bond to the amidinato-substituted silicon(II) centre in **XI** (Scheme 1).[38] We therefore probed the behaviour of **3a,b** towards carbon monoxide. Stirring of **3a,b** under CO (1 bar) led to a colour change from blackberry red to blood red (Scheme 3). To avoid secondary decomposition reactions, the reaction was stopped immediately after disappearance of the last violet tint by removal of all volatiles under reduced pressure. The product **3c** crystallizes from pentane in 44% yield. Due to the facile decomposition in reaction mixtures and under reduced pressure, the complete work-up needed to be carried out at slightly reduced temperatures (<10 °C) until isolation of **3c** in the form of a crystalline solid, which is then stable even when redissolved.

The ^{13}C NMR spectrum of isolated **3c** shows two additional signals at low field, δ = 196.3 and 204.9 ppm, which are assigned to the carbonyl ligands based on their similarity with those of comparable Ni-carbonyl complexes (δ = 199.3 and 202.5 ppm for Roesky's amidinato silylene-$Ni(CO)_3$ **I**[22] and δ = 198.8 and 206.2 ppm for the mixed silylene–carbene coordinated $Ni(CO)_2$ complex reported by Driess[64]). The ^{29}Si NMR signals of isolated **3c** are similar to the Ni(cod) complex **3a**: a lowfield signal at 96.6 ppm for the remote silicon atom and three highfield signals at −81.9, −160.4 and −342.0 ppm for the unsubstituted Si atoms. This supports a structurally and electronically similar geometry to that of **3a**.

The longest wavelength absorption in the UV-Vis spectrum of **3a** at $\lambda_{max,exp}$ = 538 nm (ε= 8190 M^{-1} cm^{-1}) is reproduced well by TD-DFT calculations on the optimised minimum structure of **3a**. It is assigned to a combination of three transitions at $\lambda_{max,calc}$ = 546 nm (HOMO → LUMO 52.6%), 520 nm (HOMO−1 → LUMO 72.6%) and 516 nm (HOMO → LUMO+1 65.4%) at the TPSSh/def2-TZVP level of theory[56,57,62,63] (for details see SI). The different coordination geometry of the central nickel atom in **3b** is manifest in a strong red-shift of the experimental longest wavelength UV-Vis absorption of approximately $\Delta\lambda$ = 56 nm. It is observed as a broad band at $\lambda_{max,exp}$ = 596 nm (624 M^{-1} cm^{-1}) tailing to about 700 nm. Notably, the extinction coefficient is one order of magnitude smaller than in case of **3a**, which suggests considerable effect of the ligand exchange on the electronic structure (*vide infra*).

TD-DFT calculations at the TPSSh/def2-TZVP level of theory assign the observed bands to a weak transition at $\lambda_{max,calc}$ = 740 nm (HOMO → LUMO 89.6%) and slightly stronger transitions at $\lambda_{max,calc}$ = 572 nm (HOMO → LUMO+1 76.8%) and 555 nm (HOMO → LUMO+2 92.3%). A second absorption in the experimental UV-Vis spectrum of **3b** at $\lambda_{max,exp}$ = 519 nm (ε = 1127 M^{-1} cm^{-1}) is assigned to the calculated transition at 472 nm for the (HOMO−4 → LUMO 31.0%). The colour change in the reaction to **3c** to a lighter red becomes apparent in the blue-shifted absorption in the UV-Vis spectrum ($\lambda_{max,exp}$ = 525 nm, ε = 9630 M^{-1} cm^{-1}), compared to the precursors **3a** and **3b** (**3a**: $\lambda_{max,exp}$ = 538 nm, ε = 8190 M^{-} cm^{-1}, **3b**: $\lambda_{max,exp}$ = 596 nm, ε = 624 M^{-1} cm^{-1}), but in reasonable agreement with the calculated value at $\lambda_{max,calc}$ = 506 nm, (HOMO → LUMO + 2 99.6%). The calculated transitions correspond to HOMO–LUMO gaps of ΔE = 3.00 eV (**3c**)/2.88 eV (**3a**)/2.39 eV (**3b**), which reproduces the experimentally observed trend (**3c** (2.37 eV) > **3a** (2.31 eV) > **3b** (2.08 eV)). Owing to the geometry of **3b**, featuring the trigonal planar-coordinated Ni centre, DFT calculations suggest an amidinato-centred LUMO in contrast to **3a** and **3c**, where the LUMO is mostly localized at the unsubstituted Si vertices of the siliconoid ligand, resulting in a smaller HOMO–LUMO gap in **3b** (Fig. 4). The lack of spatial coincidence of HOMO and LUMO results in the smaller extinction coefficient of **3b** compared to **3a** and **3c**.

The molecular structure of **3c** in the solid state was confirmed by X-ray diffraction analysis on single crystals grown from a pentane solution at −26 °C (Fig. 5). Just as **3b**, the CO complex **3c** crystallizes in the monoclinic space group *I*2/*a*. The central geometry around the nickel centre (Si1–Ni1–Si8 108.6(4)°/C1–Ni1–C2 111.1(2)°) is like in **3a** approximately tetrahedral. The seesaw angle Si4–Si5–Si6 (173.6(5)°) is in good agreement with **3b** and the free ligand.[39,40] Ni1–Si bond distances in **3c** (Ni1–Si1 2.335(9) Å, Ni1–Si3 2.501(1) Å, Ni1–Si8 2.236(1) Å) are slightly elongated compared to **3a,b** (**3a** Ni1–Si1 2.302(5) Å, Ni1–Si3 2.428(5) Å, Ni1–Si8 2.212(5) Å; **3b** Ni1–Si1 2.216(8) Å, Ni1–Si3 2.378(8) Å, Ni1–Si8 2.183(8) Å), which can be attributed to the strong π-acceptor character of CO, leading to increased competition for metal-based backdonation and an associated weakening of the Ni–Si interaction.[22,34,64,65] The Ni1–C1/C2 (Ni1–C1 1.807(4) Å, Ni1–C2 1.799(4) Å) as well as the C–O (C1–O1 1.135(4) Å, C2–O2 1.130(5) Å) bond lengths are in the expected range.[22,34,64,65]

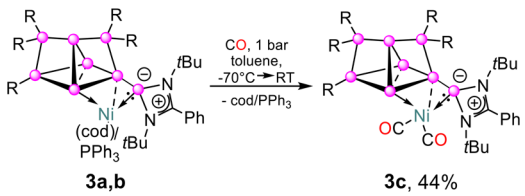

3a,b **3c**, 44%

Scheme 3 Reactivity of nickel siliconoid/silylene hybrids **3a,b** towards CO (● = Si, R = 2,4,6-triisopropylphenyl).

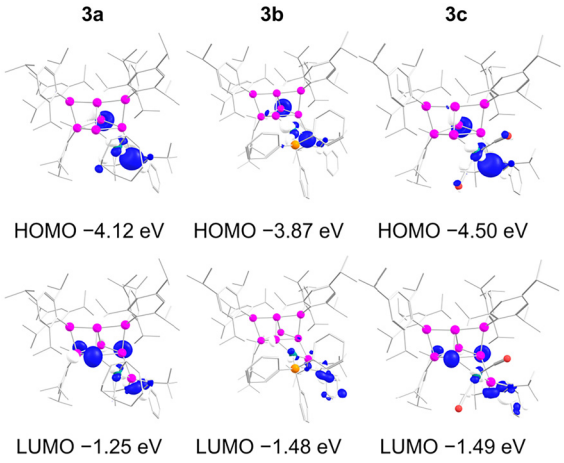

Fig. 4 Selected frontier orbitals of nickel complexes **3a–c** at the B3LYP/def2-TZVP level of theory[54–57] (contour value = 0.05).

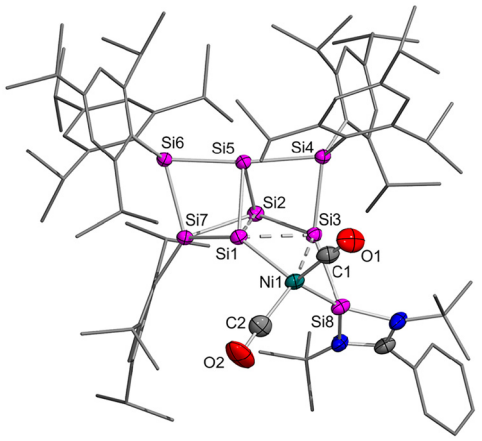

Fig. 5 Molecular structure of $Ni(CO)_2$-siliconoid/silylene complex **3c** in the solid state. Hydrogen atoms are omitted for clarity. Thermal ellipsoids at 50% probability. Selected bond lengths [Å] and angles [°]: Ni1–Si1 2.335(9), Ni1–Si3 2.501(1), Ni1–Si8 2.236(1), Ni1–C1 1.807(4), Ni1–C2 1.799(4), C1–O1 1.135(4), C2–O2 1.130(5), Si1–Si2 2.667(1), Si1–Si3 2.444(1), Si3–Si8 2.310(1); C1–Ni1–C2 111.1(2), Ni1–C1–O1 175.4(4), Ni1–C2–O2 177.3(4), Si1–Ni1–Si8 108.6(4), Si1–Si3–Ni1 56.3(3), Si8–Si3–Ni1 55.2(3), Si1–Si3–Si8 102.6(5), Si4–Si5–Si6 173.6(5).

The FT-IR spectrum of **3c** exhibits significant CO-stretching bands at 2015 and 1976 cm^{-1}. The bands in the IR spectrum of **3c** are more red-shifted in comparison with other reported Si–Ni$(CO)_n$ silylene-ligands, comparable to the NHSi–NHC–Ni$(CO)_2$ compound by Driess *et al.* ($\tilde{V}_{CO}$ = 1952 and 1887 cm^{-1}),[64] the bis(NHSi)–Ni$(CO)_2$ by Radius ($\tilde{V}_{CO}$ = 2039 and 2006 cm^{-1})[65] and the dimeric Si_9 cluster by Korber *et al.* **IX** ($\tilde{V}_{CO}$ 1999 and 1937 cm^{-1}).[34] This observation implies a similarly strong σ-donating ability of the siliconoid/silylene ligand **1** as the above mentioned low-valent silicon species, which is due to the enhanced Ni → CO π-backdonation of the electron-rich ligands.

In view of the relevance of hydrosilylation, especially in industrial scale,[66,67] precious transition metals such as platinum remain the gold standard.[68] The application of the lighter congeners, like nickel, has attracted increasing attention in recent years owing to the higher abundancy,[69–71] however most complexes only show moderate reactivity under harsh conditions.[72,73] In a preliminary test, we added a catalytic quantity of **3a** to $PhSiH_3$ to test its activity towards primary silanes. Vigorous gas evolution indicated the formation of H_2 and indeed oligo- and polysilanes are detected in the reaction mixture as major products. Apparently dehydrocoupling is the favourable reaction pathway for sterically undemanding silanes. In contrast, the tertiary silane Et_3SiH did not show any reactivity at all towards styrene in the presence of **3a**. As a compromise in terms of steric congestion, we chose the secondary silane Ph_2SiH_2, and indeed, the addition of catalytic quantities of **3a** to Ph_2SiH_2 led to the desired conversion of alkene substrates with minor formation of disilanes and higher oligomers as by-products and was therefore selected for more detailed investigations regarding the scope of alkene substrates. Reaction of cyclohexene with Ph_2SiH_2 did not show any sign for the conversion to the hydrosilylation product even after 72 h, instead exhibiting signals assigned to the formation of tetraphenyldisilane and the according hydrogenation product cyclohexane. We concluded that the steric hindrance is limiting the accessibility of the catalyst and hence, only the de-hydrocoupling side-reaction followed by hydrogenation is observed in case of internal alkenes (see NMR spectra in the SI), and we thus turned our attention to terminal alkenes.

To identify optimal reaction conditions, we performed a more detailed pre-screening for the hydrosilylation of vinyltrimethylsilane with Ph_2SiH_2 in the presence of variable catalyst loadings of **3a–c** (Table 2). With 0.5 mol% of catalyst **3a** in C_6D_6 at ambient temperatures, we observed full conversion of vinyltrimethylsilane after two hours under formation of the anti-Markovnikov product **A** in 46% spectroscopic yield (entry

Table 2 Screening of the reaction conditions for the hydrosilylation catalysis of vinyltrimethylsilane (mesitylene as internal standard)

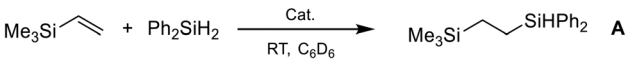

Entry	Cat.	Cat. loading [mol%]	Conversion [%]	Spectr. yield **A** [%]	Time [h]
1	None	0	0	0	>48
2	**3a**	0.5	>99	46	2[a]
3	**3a**	0.05	>99	45	8
4	**3a**	0.05	>99	23	72[b]
5	**3b**	0.5	29	24	48[a]
6	**3b**	0.05	8	0	48
7	**3c**	0.5	8	0	48[a]
8	**3c**	0.05	4	0	48
9	Ni(cod)$_2$	0.5	>99	43	<1
10	Ni(cod)$_2$	0.05	>99	42	5.5
11	Ni(cod)$_2$	0.05	>99	31	5.5[b]

[a] 0.6 mmol substrate, 1.1 eq. diphenylsilane. [b] In the presence of Hg.

2). Lowering the catalyst loading to 0.05 mol%, required a longer reaction time of 8 h (**A** 45%, entry 3), yet the selectivity for **A** over by-products such as oligosilanes and presumably the twofold-substituted silylation product remains virtually unaffected. There are no indications for the formation of the Markovnikov product **M** in these cases. A mercury drop test revealed a slower reaction to **A** with an overall lower spectroscopic yield, however exhibiting a higher ratio of **A** compared to the twofold-substituted silylation product (23 : 6) than in the reaction without the presence of Hg (9 : 5).(entry 4), indicating that the catalyst is partially decomposed to nickel particles in the course of the reaction, which are known to be highly active but unselective in heterogenous catalysis.[74,75] A blank run without any catalyst gave no conversion at all after more than 48 h (entry 1). Employing phosphine and carbonyl derivatives **3b** and **3c** as catalysts resulted in incomplete conversions at 0.5 mol% and a negligible conversion at 0.05% (entries 5 to 7). Their lack of catalytic activity can be attributed to the tighter coordination of the phosphine and carbonyl ligands in **3b** and **3c** compared to the cod ligand in **3a**, blocking the binding site for the alkene and silane substrates more effectively. Intended as another control experiment with regard to the precatalytic activity, we probed the catalysis with 0.5 mol% of $Ni(cod)_2$ under the same conditions as for **3a**. Surprisingly, an even faster conversion of vinyltrimethylsilane (50 minutes, entry 9) was observed. With reduced catalyst loading 0.05 mol% of $Ni(cod)_2$ full conversion is achieved after 5.5 h, with the anti-Markovnikov species **A** as the major product (42.5%, entry 10). Although there are many examples reported for the hydrosilylation with $Ni(cod)_2$ in combination with a stabilizing ligand, *e.g.* phosphines or NHCs,[76,77] there are only very few reports on catalysis using $Ni(cod)_2$ itself on substrates such as styrene,[78] α-(trifluormethyl)styrene[79] and imines.[80] To the best of our knowledge, the $Ni(cod)_2$-catalysed hydrosilylation of unactivated terminal alkenes has never been reported. While **3a** is thus somewhat less active than $Ni(cod)_2$ itself, it can still be considered a competent catalyst for the anti-Markovnikov hydrosilylation of vinyltrimethylsilane.

After the preliminary optimization of the reaction parameters with the vinyltrimethylsilane benchmark, we sought to expand the substrate scope to other terminal alkenes. Additional electron-rich examples, namely 1-hexene, vinyl- and allyl cyclohexane, and allyltrimethylsilane were investigated but also comparatively electron-poor styrene and allylbenzene included for comparison. Reactions were carried out at ambient temperature in C_6D_6 with the catalyst load kept constant at 0.05 mol% of **3a** (Table 3). As above, control experiments employing $Ni(cod)_2$ as the catalyst were performed under the same conditions for comparison (see SI, Table S1). While the anti-Markovnikov product **A** is obtained without any sign for the formation of the Markovnikov product **M** in the electron rich cases (entries 1 to 5), electron-poor styrene and allylbenzene unexpectedly gave rise to the branched product in an almost 1 : 1 ratio (entries 6 and 7).[68,81–83] Note that Markovnikov hydrosilylation – formerly considered an undesired outcome – has been moving into focus in recent years.[67]

Concerning the hydrosilylation with catalyst **3a**, a general trend becomes apparent. While all cases investigated react to full conversion resulting in turn-over numbers (TONs) of approximately 2000, higher turnover frequencies (TOFs) up to

Table 3 Catalytic hydrosilylation of terminal olefins with Ph_2SiH_2 using nickel complex **3a** as a homogeneous catalyst

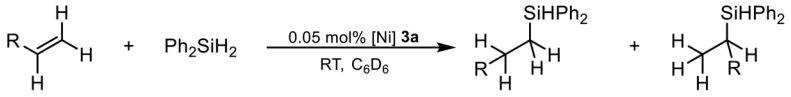

anti-Markovnikov (**A**) Markovnikov (**M**)

Entry	Substrate	Time [h]	Conversion [%]	Product	Spectr. yield [%]	TOF [h^{-1}]
1	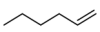	0.25	>99	**A**	39	8000
2A	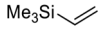	1	30	**A**	24	640
2B		4	79	**A**	40	400
2C		8	>99	**A**	45	250
3A	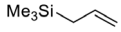	8	27	**A**	20	67
3B		192	83	**A**	45	9
3C		408	>99	**A**	48	5
4A		0.08	60	**A**	33	14 300
4B		72	97	**A**	37	27
4C		168	>99	**A**	59	12
5A		0.5	34	**A**	13	1350
5B		192	85	**A**	38	9
5C		408	>99	**A**	40	5
6A		2	33	**A : M**	9 : 16	530
6B		24	90	**A : M**	23 : 29	75
6C		54	>99	**A : M**	27 : 31	37
7A		0.5	30	**A : M**	18 : 13	1190
7B		24	88	**A : M**	33 : 32	73
7C		54	>99	**A : M**	38 : 34	37

8000 h^{-1} are observed for the open chain substrates such as 1-hexene (entry 1) and the vinyl-substituted alkenes (entries 2, 4 and 6). Spectroscopic yields of **A** up to 59% (entries 1, 2C and 4C) are obtained without any evidence for the formation of the Markovnikov product (**M**). On the other hand, the allyl-substituted substrates (entries 3 and 5) show rather slow conversions with TOFs down to 5 h^{-1} and spectroscopic yields of **A** around 40–48% (entry 3C and 5C). In contrast, the electron-poor substrates styrene and allylbenzene (entry 6 and 7) produce an almost equimolar spectroscopic ratio of **M** to **A** with TOFs of around 37 h^{-1} at full conversion. Presumably due to catalyst degradation, the TOFs are decreasing during the progress of the reactions (entries 2–7 A *vs.* B *vs.* C). Moreover, the formation of unidentifiable/volatile byproducts reduces the (spectroscopic) yield of the **A**/**M** hydrosilylation products.

To put the obtained results into perspective: Tilley *et al.* reported a dimeric, halogenated Ni catalyst reaching TONs of up to 970 (0.1 mol%, 17 h at 23 °C) with a selectivity ratio of 3 : 1 in favour of terminal hydrosilylation,[84] while a nickel pincer complex reported by the group of Hu on the other hand, gives even higher TONs and TOFs (up to 100 000 h^{-1} at 0.01 mol%/83 000 h^{-1} at 0.025 mol%).[85] Employing $Ni(cod)_2$ as the catalyst results in instant conversion of 1-hexene reiterating the result with vinyltrimethylsilane as a substrate (see SI, Table S1). Allylcyclohexane and allyltrimethylsilane were not fully converted in the presence of $Ni(cod)_2$ even after 21 days likely because of catalyst degradation (see SI, Table S1). In contrast, **3a** resulted in full conversion of both substrates, albeit slowly (TOF 5 h^{-1} each, entries 3C and 5C, Table 3).

Conclusions

In summary, we reported the preparation and full characterization of a terminal $Fe(CO)_4$ complex of a Si_7/silylene hybrid ligand. Unlike in the case of the corresponding Si_6/silylene system, the lower steric demand of the organic residues per silicon cluster vertex also allowed for the preparation of a series of the first stable nickel complexes of a siliconoid/silylene with 1,5-cyclooctadiene, triphenylphosphine and carbon monoxide acting as auxiliary ligands. The coordination environment of the PPh_3 derivative stands out with a trigonal planar nickel centre while the cod and CO complexes show distorted tetrahedral nickel coordination spheres. The cod-coordinated nickel complex turned out to be active in the hydrosilylation of terminal alkenes with an interesting preference for anti-Markovnikov regioselectivity in case of electron-richer substrates and unselective formation of both regiomers for electron-poor alkenes.

Author contributions

L. Giarrana performed the synthetic work and data analysis with partial support by D. Welterlich; L. Giarrana. and D. Scheschkewitz designed the study. D. Scheschkewitz acquired the funding; B. Morgenstern performed the X-ray diffraction studies. M. Zimmer performed the solid state and variable temperature NMR measurements. L. Giarrana performed the DFT calculations. L. Giarrana wrote the initial manuscript draft. L. Giarrana and D. Scheschkewitz reviewed and edited the manuscript.

Conflicts of interest

There are no conflicts of interest to declare.

Data availability

All data associated with this manuscript are available in the supplementary information (SI). Supplementary information is available. See DOI: **https://doi.org/10.1039/d6qi00025h**.

CCDC 2504459 (**2**), 2504461 (**3a**), 2504467 (**3b**) and 2504470 (**3c**) contain the supplementary crystallographic data for this paper.[86a–d]

Acknowledgements

Funding by the Deutsche Forschungsgemeinschaft (DFG SCHE 906/4-4) is gratefully acknowledged. Instrumentation and technical assistance for this work were provided by the Service Center X-ray Diffraction, with financial support from Saarland University and German Science Foundation (project number INST 256/506-1). The authors thank Prof. Stella Stopkowicz for access to her computational cluster.

References

1 R. H. Crabtree, *The Organometallic Chemistry of the Transition Metals*, John Wiley & Sons, Hoboken, NJ, 2009.
2 K. S. Egorova and V. P. Ananikov, Which metals are green for catalysis? Comparison of the toxicities of Ni, Cu, Fe, Pd, Pt, Rh, and Au salts, *Angew. Chem., Int. Ed.*, 2016, **55**, 12150.
3 T. J. Hadlington, Heavier tetrylene-and tetrylyne-transition metal chemistry: it's no carbon copy, *Chem. Soc. Rev.*, 2024, **53**, 9738.
4 W. I. Dzik, X. P. Zhang and B. de Bruin, Redox noninnocence of carbene ligands: carbene radicals in (catalytic) C–C bond formation, *Inorg. Chem.*, 2011, **50**, 9896.
5 K.-S. Feichtner and V. H. Gessner, Cooperative bond activation reactions with carbene complexes, *Chem. Commun.*, 2018, **54**, 6540.
6 R. C. Cammarota, L. J. Clouston and C. C. Lu, Leveraging molecular metal–support interactions for H_2 and N_2 activation, *Chem. Rev.*, 2017, **334**, 100.
7 R. C. Cammarota, J. Xie, S. A. Burgess, M. V. Vollmer, K. D. Vogiatzis, J. Ye, J. C. Linehan, A. M. Appel, C. Hoffmann, X. Wang, V. G. Young and C. C. Lu,

Thermodynamic and kinetic studies of H_2 and N_2 binding to bimetallic nickel-group 13 complexes and neutron structure of a Ni(η^2-H_2) adduct, *Chem. Sci.*, 2019, **10**, 7029.

8 M. J. Dorantes, J. T. Moore, E. Bill, B. Mienert and C. C. Lu, Bimetallic iron–tin catalyst for N_2 to NH_3 and a silyldiazenido model intermediate, *Chem. Commun.*, 2020, **56**, 11030.

9 B. J. Graziano, M. V. Vollmer and C. C. Lu, Cooperative bond activation and facile intramolecular aryl transfer of nickel–aluminum pincer–type complexes, *Angew. Chem., Int. Ed.*, 2021, **60**, 15087.

10 J. T. Moore, M. J. Dorantes, Z. Pengmei, T. M. Schwartz, J. Schaffner, S. L. Apps, C. A. Gaggioli, U. Das, L. Gagliardi, D. A. Blank and C. C. Lu, Light–Driven Hydrodefluorination of Electron–Rich Aryl Fluorides by an Anionic Rhodium–Gallium Photoredox Catalyst, *Angew. Chem., Int. Ed.*, 2022, **61**, e202205575.

11 B. Blom, D. Gallego and M. Driess, N-heterocyclic silylene complexes in catalysis: new frontiers in an emerging field, *Inorg. Chem. Front.*, 2014, **1**, 134.

12 R. Waterman, P. G. Hayes and T. D. Tilley, Synthetic development and chemical reactivity of transition-metal silylene complexes, *Acc. Chem. Res.*, 2007, **40**, 712.

13 A. V. Protchenko, J. I. Bates, L. M. A. Saleh, M. P. Blake, A. D. Schwarz, E. L. Kolychev, A. L. Thompson, C. Jones, P. Mountford and S. Aldridge, Enabling and probing oxidative addition and reductive elimination at a group 14 metal center: cleavage and functionalization of E–H bonds by a bis (boryl) stannylene, *J. Am. Chem. Soc.*, 2016, **138**, 4555.

14 T. J. Hadlington, J. A. B. Abdalla, R. Tirfoin, S. Aldridge and C. Jones, Stabilization of a two-coordinate, acyclic diaminosilylene (ADASi): completion of the series of isolable diaminotetrylenes: E (NR 2) 2 (E= group 14 element), *Chem. Commun.*, 2016, **52**, 1717.

15 D. C. H. Do, A. V. Protchenko, M.Á Fuentes, J. Hicks, P. Vasko and S. Aldridge, N–H cleavage vs. Werner complex formation: reactivity of cationic group 14 tetrelenes towards amines, *Chem. Commun.*, 2020, **56**, 4684.

16 Z. Mo, T. Szilvási, Y. Zhou, S. Yao and M. Driess, An Intramolecular Silylene Borane Capable of Facile Activation of Small Molecules, Including Metal–Free Dehydrogenation of Water, *Angew. Chem., Int. Ed.*, 2017, **56**, 3699.

17 D. Wendel, A. Porzelt, F. A. D. Herz, D. Sarkar, C. Jandl, S. Inoue and B. Rieger, From Si(II) to Si(IV) and back: reversible intramolecular carbon–carbon bond activation by an acyclic iminosilylene, *J. Am. Chem. Soc.*, 2017, **139**, 8134.

18 S. Takahashi, E. Bellan, A. Baceiredo, N. Saffon-Merceron, S. Massou, N. Nakata, D. Hashizume, V. Branchadell and T. Kato, A Stable N–Hetero–*Rh*–Metallacyclic Silylene, *Angew. Chem., Int. Ed.*, 2019, **58**, 10310.

19 A. Meltzer, C. Präsang and M. Driess, Diketiminate silicon (II) and related NHSi ligands generated in the coordination sphere of nickel (0), *J. Am. Chem. Soc.*, 2009, **131**, 7232.

20 S. Z. Tasker, E. A. Standley and T. F. Jamison, Recent advances in homogeneous nickel catalysis, *Nature*, 2014, **509**, 299.

21 V. Vermaak, H. C. M. Vosloo and A. J. Swarts, The development and application of homogeneous nickel catalysts for transfer hydrogenation and related reactions, *Coord. Chem. Rev.*, 2024, **507**, 215716.

22 G. Tavčar, S. S. Sen, R. Azhakar, A. Thorn and H. W. Roesky, Facile syntheses of silylene nickel carbonyl complexes from Lewis base stabilized chlorosilylenes, *Inorg. Chem.*, 2010, **49**, 10199.

23 C. Watanabe, Y. Inagawa, T. Iwamoto and M. Kira, Synthesis and structures of (dialkylsilylene) bis (phosphine)-nickel, palladium, and platinum complexes and (η^6-arene)(dialkylsilylene) nickel complexes, *Dalton Trans.*, 2010, **39**, 9414.

24 T. J. Hadlington, T. Szilvási and M. Driess, Silylene–Nickel Promoted Cleavage of B—O Bonds: From Catechol Borane to the Hydroborylene Ligand, *Angew. Chem., Int. Ed.*, 2017, **56**, 7470.

25 N. C. Breit, T. Szilvási, T. Suzuki, D. Gallego and S. Inoue, From a zwitterionic phosphasilene to base stabilized silyliumylidene-phosphide and bis (silylene) complexes, *J. Am. Chem. Soc.*, 2013, **135**, 17958.

26 Y. Wang, A. Kostenko, S. Yao and M. Driess, Divalent silicon-assisted activation of dihydrogen in a bis (N-heterocyclic silylene) xanthene nickel (0) complex for efficient catalytic hydrogenation of olefins, *J. Am. Chem. Soc.*, 2017, **139**, 13499.

27 Y. Zhou, S. Raoufmoghaddam, T. Szilvási and M. Driess, A Bis(silylene)–Substituted *ortho*–Carborane as a Superior Ligand in the Nickel–Catalyzed Amination of Arenes, *Angew. Chem., Int. Ed.*, 2016, **55**, 12868.

28 W. Yang, Y. Dong, H. Sun and X. Li, Progress in the preparation and characterization of silylene iron, cobalt and nickel complexes, *Dalton Trans.*, 2021, **50**, 6766.

29 Y. Heider and D. Scheschkewitz, Stable unsaturated silicon clusters (siliconoids), *Dalton Trans.*, 2018, **47**, 7104.

30 Y. Heider and D. Scheschkewitz, Molecular silicon clusters, *Chem. Rev.*, 2021, **121**, 9674.

31 Y. Wang, J. E. McGrady and Z.-M. Sun, Solution-Based Group 14 Zintl Anions: New Frontiers and Discoveries, *Acc. Chem. Res.*, 2021, **54**, 1506.

32 J. M. Goicoechea and S. C. Sevov, Deltahedral germanium clusters: insertion of transition-metal atoms and addition of organometallic fragments, *J. Am. Chem. Soc.*, 2006, **128**, 4155.

33 O. P. E. Townrow, C. Chung, S. A. Macgregor, A. S. Weller and J. M. Goicoechea, A neutral heteroatomic zintl cluster for the catalytic hydrogenation of cyclic alkenes, *J. Am. Chem. Soc.*, 2020, **142**, 18330.

34 S. Joseph, M. Hamberger, F. Mutzbauer, O. Härtl, M. Meier and N. Korber, Chemistry with Bare Silicon Clusters in Solution: A Transition–Metal Complex of a Polysilicide Anion, *Angew. Chem., Int. Ed.*, 2009, **48**, 8770.

35 L. J. Schiegerl, A. J. Karttunen, W. Klein and T. F. Fässler, Anionic Siliconoids from Zintl Phases: $R_3Si_9^-$ with Six and $R_2Si_9^{2-}$ with Seven Unsubstituted Exposed Silicon Cluster Atoms (R=Si(tBu)$_2$H), *Chem. – Eur. J.*, 2018, **24**, 19171.

36 N. E. Poitiers, L. Giarrana, K. I. Leszczyńska, V. Huch, M. Zimmer and D. Scheschkewitz, Indirect and Direct Grafting of Transition Metals to Siliconoids, *Angew. Chem., Int. Ed.*, 2020, **59**, 8532.
37 N. E. Poitiers, L. Giarrana, V. Huch, M. Zimmer and D. Scheschkewitz, Exohedral functionalization vs. core expansion of siliconoids with Group 9 metals: catalytic activity in alkene isomerization, *Chem. Sci.*, 2020, **11**, 7782.
38 N. E. Poitiers, V. Huch, M. Zimmer and D. Scheschkewitz, Nickel-assisted complete cleavage of CO by a silylene/siliconoid hybrid under formation of an Si=C enol ether bridge, *Chem. Commun.*, 2020, **56**, 10898.
39 K. I. Leszczyńska, V. Huch, C. Präsang, J. Schwabedissen, R. J. F. Berger and D. Scheschkewitz, Atomically precise expansion of unsaturated silicon clusters, *Angew. Chem., Int. Ed.*, 2019, **58**, 5124.
40 L. Giarrana, M. Zimmer, B. Morgenstern and D. Scheschkewitz, Tetrylene-Functionalized Si_7−Siliconoids, *Inorg. Chem.*, 2024, **63**, 20083.
41 W. Yang, H. Fu, H. Wang, M. Chen, Y. Ding, H. W. Roesky and A. Jana, A base-stabilized silylene with a tricoordinate silicon atom as a ligand for a metal complex, *Inorg. Chem.*, 2009, **48**, 5058.
42 T. A. Schmedake, M. Haaf, B. J. Paradise, A. J. Millevolte, D. R. Powell and R. West, Electronic and steric properties of stable silylene ligands in metal (0) carbonyl complexes, *J. Organomet. Chem.*, 2001, **636**, 17.
43 N. C. Breit, C. Eisenhut and S. Inoue, Phosphinosilylenes as a novel ligand system for heterobimetallic complexes, *Chem. Commun.*, 2016, **52**, 5523.
44 F. H. Carre and J. J. E. Moreau, Reactivity of μ-Silanediyl Iron Carbonyl Complexes with Alkynes. Molecular Structure of $(CO)_4FeSiPh_2CEt{=}CEtSiPh_2$ and of $(CO)_3FeCMe{=}CMeSiPh_2CMe{=}CMeFe(CO)_3$, *Inorg. Chem.*, 1982, **21**, 3099.
45 R. Dorta, E. D. Stevens, N. M. Scott, C. Costabile, L. Cavallo, C. D. Hoff and S. P. Nolan, Steric and Electronic Properties of N-Heterocyclic Carbenes (NHC): A Detailed Study on Their Interaction with $Ni(CO)_4$, *J. Am. Chem. Soc.*, 2005, **127**, 2485.
46 H. Clavier and S. P. Nolan, Percent buried volume for phosphine and N-heterocyclic carbene ligands: steric properties in organometallic chemistry, *Chem. Commun.*, 2010, **46**, 841.
47 L. Falivene, Z. Cao, A. Petta, L. Serra, A. Poater, R. Oliva, V. Scarano and L. Cavallo, Towards the online computer-aided design of catalytic pockets, *Nat. Chem.*, 2019, **11**, 872.
48 L. Falivene, R. Credendino, A. Poater, A. Petta, L. Serra, R. Oliva, V. Scarano and L. Cavallo, SambVca 2. A web tool for analyzing catalytic pockets with topographic steric maps, *Organometallics*, 2016, **35**, 2286.
49 A. Hinz, Pseudo–one–coordinate tetrylenium salts bearing a bulky carbazolyl substituent, *Chem. – Eur. J.*, 2019, **25**, 3267.
50 T. George, T. Grant, I. S. Munhoz, T. Do and J. D. Masuda, Group 11 complexes of a bulky triazene ligand, *Dalton Trans.*, 2024, **53**, 13107.
51 M. Alkan-Zambada, E. C. Constable and C. E. Housecroft, The role of percent volume buried in the characterization of copper(I) complexes for lighting purposes, *Molecules*, 2020, **25**, 2647.
52 D. Lutters, C. Severin, M. Schmidtmann and T. Müller, Activation of 7-silanorbornadienes by N-heterocyclic carbenes: a selective way to N-heterocyclic-carbene-stabilized silylenes, *J. Am. Chem. Soc.*, 2016, **138**, 6061.
53 R. S. Berry, Correlation of rates of intramolecular tunneling processes, with application to some group V compounds, *J. Chem. Phys.*, 1960, **32**, 933.
54 A. D. Becke, Density–functional thermochemistry. III. The role of exact exchange, *J. Chem. Phys.*, 1993, **98**, 5648.
55 C. Lee, W. Yang and R. G. Parr, Development of the Colle-Salvetti correlation-energy formula into a functional of the electron density, *Phys. Rev. B:Condens. Matter Mater. Phys.*, 1988, **37**, 785.
56 F. Weigend and R. Ahlrichs, Balanced basis sets of split valence, triple zeta valence and quadruple zeta valence quality for H to Rn: Design and assessment of accuracy, *Phys. Chem. Chem. Phys.*, 2005, **7**, 3297.
57 F. Weigend, Accurate Coulomb-fitting basis sets for H to Rn, *Phys. Chem. Chem. Phys.*, 2006, **8**, 1057.
58 W. Wang, S. Inoue, S. Yao and M. Driess, An isolable bis-silylene oxide ("disilylenoxane") and its metal coordination, *J. Am. Chem. Soc.*, 2010, **132**, 15890.
59 M. Haaf, T. A. Schmedake and R. West, Stable silylenes, *Acc. Chem. Res.*, 2000, **33**, 704.
60 M.-P. Lücke, S. Yao and M. Driess, Boosting homogeneous chemoselective hydrogenation of olefins mediated by a bis (silylenyl) terphenyl-nickel (0) pre-catalyst, *Chem. Sci.*, 2021, **12**, 2909.
61 M. Stoelzel, C. Präsang, S. Inoue, S. Enthaler and M. Driess, Hydrosilylation of Alkynes by Ni $(CO)_3$−Stabilized Silicon(II) Hydride, *Angew. Chem., Int. Ed.*, 2012, **51**, 399.
62 S. Grimme, A. Hansen, J. G. Brandenburg and C. Bannwarth, Dispersion-corrected mean-field electronic structure methods, *Chem. Rev.*, 2016, **116**, 5105.
63 V. N. Staroverov, G. E. Scuseria, J. Tao and J. P. Perdew, Comparative assessment of a new nonempirical density functional: Molecules and hydrogen-bonded complexes, *J. Chem. Phys.*, 2003, **119**, 12129.
64 G. Tan, S. Enthaler, S. Inoue, B. Blom and M. Driess, Synthesis of Mixed Silylene–Carbene Chelate Ligands from N–Heterocyclic Silylcarbenes Mediated by Nickel, *Angew. Chem., Int. Ed.*, 2015, **54**, 2214.
65 E. Glok, L. Werner and U. Radius, N-Heterocyclic silylene complexes of nickel (0), *Dalton Trans.*, 2025, **54**, 14846.
66 D. Troegel and J. Stohrer, Recent advances and actual challenges in late transition metal catalyzed hydrosilylation of olefins from an industrial point of view, *Coord. Chem. Rev.*, 2011, **255**, 1440.
67 M. Zaranek and P. Pawluc, Markovnikov hydrosilylation of alkenes: how an oddity becomes the goal, *ACS Catal.*, 2018, **8**, 9865.

68 L. D. de Almeida, H. Wang, K. Junge, X. Cui and M. Beller, Recent advances in catalytic hydrosilylations: developments beyond traditional platinum catalysts, *Angew. Chem., Int. Ed.*, 2021, **60**, 550.
69 Y. Nakajima, K. Sato and S. Shimada, Development of nickel hydrosilylation catalysts, *Chem. Rec.*, 2016, **16**, 2379.
70 X. Wu, G. Ding, W. Lu, L. Yang, J. Wang, Y. Zhang, X. Xie and Z. Zhang, Nickel-catalyzed hydrosilylation of terminal alkenes with primary silanes via electrophilic silicon–hydrogen bond activation, *Org. Lett.*, 2021, **23**, 1434.
71 I. Pappas, S. Treacy and P. J. Chirik, Alkene Hydrosilylation Using Tertiary Silanes with α-Diimine Nickel Catalysts. Redox-Active Ligands Promote a Distinct Mechanistic Pathway from Platinum Catalysts, *ACS Catal.*, 2016, **6**, 4105.
72 X. Du and Z. Huang, Advances in base-metal-catalyzed alkene hydrosilylation, *ACS Catal.*, 2017, **7**, 1227.
73 H. Maciejewski, B. Marciniec and I. Kownacki, Catalysis of hydrosilylation: Part XXXIV. High catalytic efficiency of the nickel equivalent of Karstedt catalyst [{Ni(η-CH_2=CHSiMe_2)$_2$O}$_2${μ-(η-CH_2=CHSiMe_2)$_2$O}], *J. Organomet. Chem.*, 2000, **597**, 175.
74 V. M. Chernyshev, A. V. Astakhov, I. E. Chikunov, R. V. Tyurin, D. B. Eremin, G. S. Ranny, V. N. Khrustalev and V. P. Ananikov, Pd and Pt catalyst poisoning in the study of reaction mechanisms: what does the mercury test mean for catalysis?, *ACS Catal.*, 2019, **9**, 2984.
75 I. C. Chagunda, T. Fisher, M. Schierling and J. S. McIndoe, Poisonous Truth about the Mercury Drop Test: The Effect of Elemental Mercury on Pd (0) and Pd(II) ArX Intermediates, *Organometallics*, 2023, **42**, 2938.
76 A. S. Chang, K. E. Kawamura, H. S. Henness, V. M. Salpino, J. C. Greene, L. N. Zakharov and A. K. Cook, (NHC) Ni (0)-catalyzed branched-selective alkene hydrosilylation with secondary and tertiary silanes, *ACS Catal.*, 2022, **12**, 11002.
77 Z. D. Miller, W. Li, T. R. Belderrain and J. Montgomery, Regioselective Allene Hydrosilylation Catalyzed by *N*-Heterocyclic Carbene Complexes of Nickel and Palladium, *J. Am. Chem. Soc.*, 2013, **135**, 15282.
78 B. Marciniec, H. Maciejewski and I. Kownacki, Dehydrogenative coupling of styrene with trisubstituted silanes catalyzed by nickel complexes, *J. Mol. Catal. A: Chem.*, 1998, **135**, 223.
79 D. Bai, K. Zhong, L. Chang, Y. Qiao, F. Wu, G. Xu and J. Chang, Nickel-catalyzed regiodivergent hydrosilylation of α-(fluoroalkyl) styrenes without defluorination, *Nat. Commun.*, 2024, **15**, 6360.
80 D. P. Spence, *Hydrosilylation of Imines Using a Ni (0) Catalyst*, Master Thesis, UC San Diego, 2016.
81 Y. Wei, S.-X. Liu, H. Mueller-Bunz and M. Albrecht, Synthesis of triazolylidene nickel complexes and their catalytic application in selective aldehyde hydrosilylation, *ACS Catal.*, 2016, **6**, 8192.
82 I. Buslov, S. C. Keller and X. Hu, Alkoxy hydrosilanes as surrogates of gaseous silanes for hydrosilylation of alkenes, *Org. Lett.*, 2016, **18**, 1928.
83 Y. Chen, C. Sui-Seng, S. Boucher and D. Zargarian, Influence of $SiMe_3$ Substituents on Structures and Hydrosilylation Activities of ((SiMe_3)$_{1\ or\ 2}$-Indenyl)Ni(PPh_3)Cl, *Organometallics*, 2005, **24**, 149.
84 J. Yang, V. Postils, M. I. Lipschutz, M. Fasulo, C. Raynaud, E. Clot, O. Eisenstein and T. D. Tilley, Efficient alkene hydrosilation with bis (8-quinolyl) phosphine (NPN) nickel catalysts. The dominant role of silyl-over hydrido-nickel catalytic intermediates, *Chem. Sci.*, 2020, **11**, 5043.
85 I. Buslov, J. Becouse, S. Mazza, M. Montandon-Clerc and X. Hu, Chemoselective alkene hydrosilylation catalyzed by nickel pincer complexes, *Angew. Chem., Int. Ed.*, 2015, **54**, 14523.
86 (*a*) CCDC 2504459: Experimental Crystal Structure Determination, 2026, DOI: **10.5517/ccdc.csd.cc2q230y**; (*b*) CCDC 2504461: Experimental Crystal Structure Determination, 2026, DOI: **10.5517/ccdc.csd.cc2q2320**; (*c*) CCDC 2504467: Experimental Crystal Structure Determination, 2026, DOI: **10.5517/ccdc.csd.cc2q2386**; (*d*) CCDC 2504470: Experimental Crystal Structure Determination, 2026, DOI: **10.5517/ccdc.csd.cc2q23c9**.

4. Summary, Conclusion and Outlook

Siliconoids represent potent model systems for silicon surfaces, bridging the gap between molecular compounds and bulk material. Aiming to explore feasible modification pathways and to gain mechanistic insight into their reactivity, siliconoids have been subjected to increasingly detailed investigations in recent years. To this end, the Scheschkewitz group has examined the functionalization of siliconoids in the context of cluster synthesis, as well as endohedral and exohedral expansion, including the incorporation of heteroatoms. The functionalization of *ligato*-lithiated Si_6 cluster **I-80** by grafting of a dangling tetrylene unit to the cluster core was established, which gave rise to a strongly donating hybrid cluster that acted as a rather ordinary σ-donating ligand for an iron carbonyl fragment (see introduction, Chapter 1.2.3). In this case, the interaction of the transition metal was limited to the tetrylene center, with no detectable interaction of the cluster core. Going down the periodic table to the platinum metals, the involvement of the cluster core under ring opening *via* the formation of **I-87a-c** and **I-88** was observed. As intended, **I-87a** was applied in catalysis with a remarkable catalytic performance in alkene isomerization.[334]

Following these results, a rearrangement and reclosure of the cluster scaffold by reductive elimination of the remaining chloride at the dangling silyl moiety of **I-87a** was anticipated. Indeed, applying lithium/ naphthalene to **I-87a** in a reductive chloride elimination led to the formation of lithiated irida-heterosiliconoid **C-1** (Scheme 23) which was supported by X-ray diffraction analysis on a single crystal of **C-1**. The cluster scaffold could be restored under full incorporation of the previously exohedrally coordinated iridium central atom into the cluster core and the cleavage of the dangling silyl side arm under dimerization to $Tip_2Si{=}SiTip_2$ as systematic by-product. The geometry of **C-1** is reminiscent of the homonuclear Si_7 scaffolds **I-91** and **I-92** (see Chapter 1.2.3, Scheme 17), with a slight deviation from the seesaw coordination of the apical silicon atoms. Notably, the anionic charge in **C-1** is distributed between the unsubstituted silicon vertex and the iridium atom, leading to a significantly elongated Si–Ir interaction as opposed to the precursor **I-87a**. The formally negatively charged iridium atom in close contact to a lithium counter-cation in **C-1** represents a rare case of direct transition metal-lithium interaction.

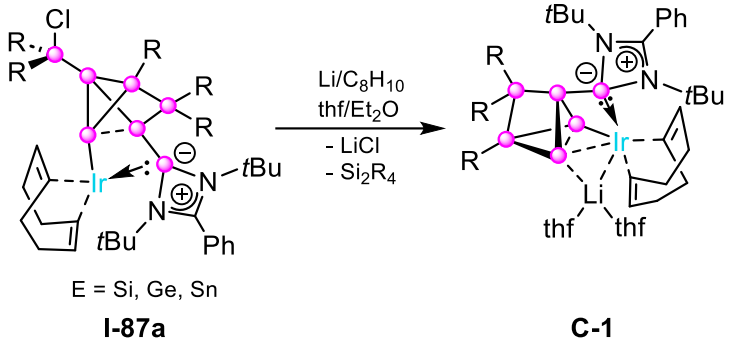

I-87a **C-1**

Scheme 23. Preparation of iridasiliconoid **C-1** (○ = Si, R = 2,4,6-triisopropyphenyl).

Although the reaction of **C-1** toward common electrophiles such as Me_3SiCl or Me_3SnCl did not lead to certainly identifiable products, grafting of Group 4 metallocene chlorides gave rise to the corresponding heterosiliconoids with pending metallocene functionalities **C-2a,b** (Scheme 24). Salt metathesis between the coordinating alkali metal in **C-1** and the chloro metallocene demonstrates that the nucleophilic site is located at the adjacent α–Si rather than the formally negatively charged iridium center. The formation of **C-2a,b** proceeds under retention of the uncompromised iridasiliconoid core. The calculated NMR shifts as well as the UV/Vis bands (TD-DFT) of the optimized structures of **C-1** and **C-2a,b** at the PBE0/def2-TZVPP level of theory were in good agreement with the trends in the experimental spectra.

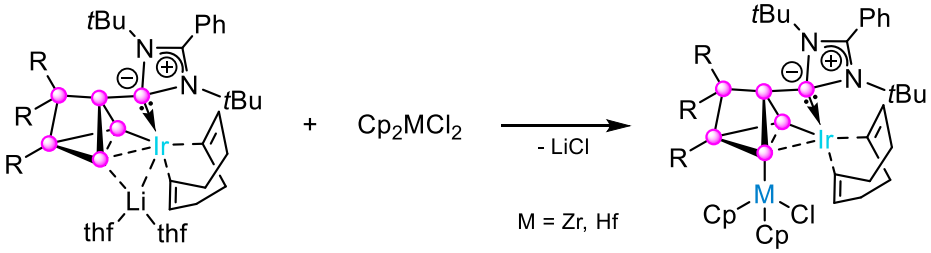

C-1 **C-2a,b**

Scheme 24. Synthesis of heterobimetallic siliconoids **C-2a,b** with exohedrally attached Group 4 metallocenes (○ = Si, M = Zr (**a**), Hf (**b**), R = 2,4,6-triisopropyphenyl).

The isolation of heterobimetallic species **C-2a,b** paves the way for investigations on the catalytic abilities as the geometry suggests the possibility of cooperative behavior of the two transition metal centers with feasible pincer-type interaction with additional support by the α-silicon atom. Moreover, reductive elimination of the chloride in **C-2a,b** could be considered in a similar way to **C-1** for future investigations, regarding the integration of the pending transition metal into the cluster scaffold.

As opposed to the incorporation of an additional silicon vertex into the Si_6 cluster scaffold to obtain Si_7Cp^* **I-91** by the use of decamethylsilicocene **I-1** (see Chapter 1.2.3, Scheme 17),[336] the addition of chloro amidinato tetrylenes **I-7a-c** to **I-81** leads to the exohedral grafting of the tetrylene unit to the cluster core affording **I-85a-c** (Chapter 1.2.3, Scheme 14).[330] This is attributed to the more efficient stabilization arising from electron donation by the nitrogen lone pairs to the tetrel center resulting in a less electrophilic pending tetrylene moiety. The sterical

encumbrance of **I-85a-c** with an almost 1:1 ratio of silicon vertices to Tip substituents restricts access to the reactive, unsubstituted silicon sites, limiting its applicability as a coordinating ligand. As noted earlier, a simple coordination of the tetrylene moiety in **I-85a-c** to the iron center as the only reported 3d transition metal, with no hints for any interaction with the siliconoid cluster core, was reported.[330] With platinum metals of Group 9 (Rh, Ir) a complete rearrangement of the siliconoid/silylene cluster scaffold was observed (Chapter 1.2.3, Scheme 15)[334]. With the aim of preserving the cluster scaffold but rendering it amenable for coordination, an increased accessibility of the unsubstituted silicon cluster vertices was considered essential. This suggested the Si_7 clusters as viable alternatives, as – compared to the *ligato*/*privo*-Si_6 species – they exhibit a less crowded perimeter owing to the increased number of silicon vertices at an identical number of Tip substituents. Hence, in this work, the exohedral grafting of low-valent tetrylene functionalities to the lithiated Si_7 siliconoid **I-92** was performed to afford **C-3a-c** (Scheme 25). The cluster core of **C-3a-c** is best described as [1.1.1]-pentasilapropellane with two of three propeller blades bridged to the third by Tip_2Si moieties resulting in the seesaw-type geometry for the Si_7 siliconoid species. Notably, the central silicon scaffold in **C-3a-c** is largely unaffected regardless of the employed tetrylene (E = Si, Ge, Sn). The molecular structure of **C-3a** was supported by X-ray crystallography, revealing a shortened Si–Si bond distance between the cluster silicon to the silylene central Si atom compared to **I-85a**, which indicates a slightly stronger interaction. In accordance with the decreased sterical bulk, a better solubility of **C-3a-c** in aliphatic and aromatic solvents is observed in contrast to **I-85a-c**.

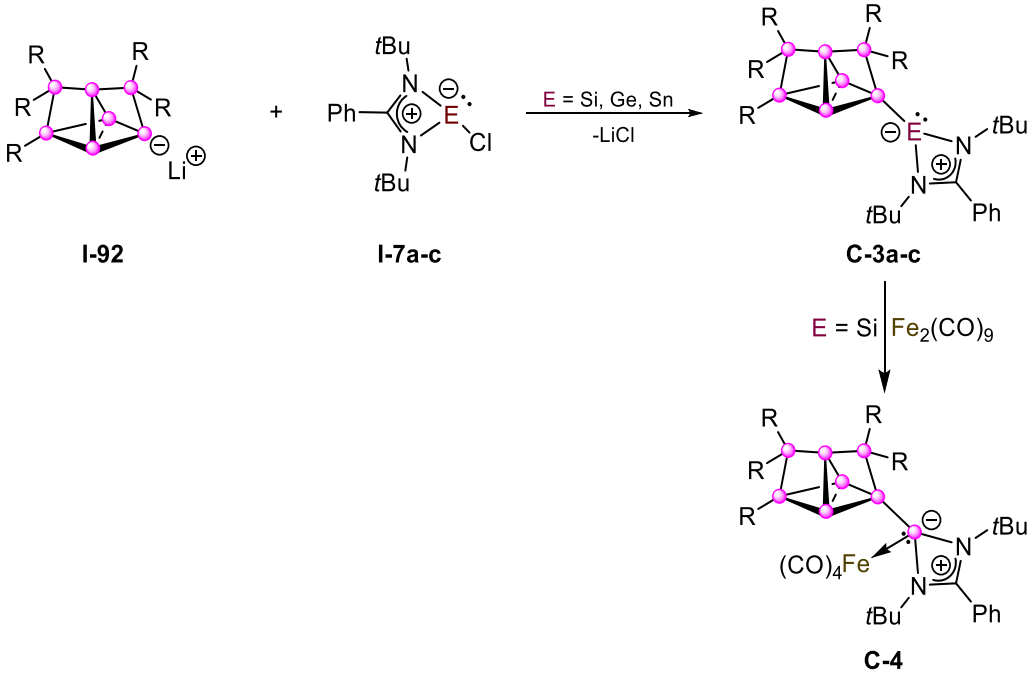

I-92 **I-7a-c** **C-3a-c** **C-4**

Scheme 25. Grafting of tetrylene units to the Si_7 species to obtain siliconoid/tetrylene hybrids **C-3a-c** and follow-up coordination of $Fe(CO)_4$ **C-4** (○ = Si, E = Si (**a**), Ge (**b**), Sn (**c**), R = 2,4,6-triisopropyphenyl).

4. Summary, Conclusion and Outlook

The increase in available space suggested a more facile coordination of 3d transition metals to unsubstituted silicon vertices of **C-3a-c** compared to **I-85a-c**. Initially, **C-3a-c** were tested for the preparation of the corresponding $Fe(CO)_4$ complexes in analogy to the related Si_6 derivatives **I-86a-c**. Only the silylene-functionalized Si_7-siliconoid **C-3a**, however, showed the intended coordination resulting in the isolation of **C-4** (Scheme 25). As previously reported for **I-86a-c**, there is no noticeable interaction between the $Fe(CO)_4$ fragment and the cluster core as to be expected on ground of the 18 electrons at the iron center. The strong σ-donation and π-backbonding interaction between the transition metal center and the CO substituent render the loss of a carbonyl ligand unfeasible. Thus, a 3d transition metal with more labile ligands was anticipated to facilitate ligand elimination and accordingly allow for the complementary interaction of the transition metal center with the unsubstituted silicon vertices of the cluster core. Given that **I-85a** did not show any reactivity at all towards $Ni(cod)_2$, the corresponding reaction employing **C-3a** as a potential ligand system was pursued. This strategy complies with the requirement of a good leaving group at nickel, namely the cyclooctadiene ligand. Indeed, treatment of **C-2a** with $Ni(cod)_2$ in aromatic solvents like toluene or benzene gave rise to the anticipated Ni(cod) siliconoid/silylene complex **C-5a** (Scheme 26). The process involves cleavage of one cod ligand and coordination of the nickel center by both the silylene-Si atom as well as an unsubstituted silicon vertex of the cluster, with additional electron density located between nickel and the Si vertex bridging the unsubstituted and the silylene silicon atom.

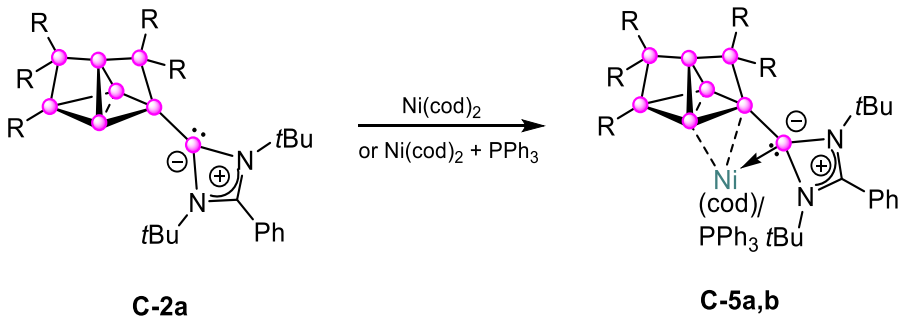

Scheme 26. Complexation of Ni(cod) (**C-5a**) or $Ni(PPh_3)$ (**C-5b**) by siliconoid/silylene hybrid **C-2a** (○ = Si, cod = 1,5-cyclooctadiene, R = 2,4,6-triisopropyphenyl).

The residual cod ligand at the Ni center can be readily replaced by triphenylphosphine to yield **C-5b,** which is also supported by X-ray diffraction analysis. The substitution is achieved either in a simple addition of PPh_3 to **C-5a** or even in a one-pot-route adding one equivalent of $Ni(cod)_2$ and PPh_3 each to siliconoid/silylene hybrid **C-2a** in the aromatic solvent. Concerning the geometry of **C-5a** and **C-5b**, some differences become apparent. Bidentate coordination of the cod ligand gives rise to a tetrahedral geometry around the Ni center by a twofold coordination, whereas coordination by a single phosphine unit leads to a trigonal-planar environment.

As **C-5a,b** comprise the nickel center along with the electron-donating hybrid cluster as a flexible ligand and a readily exchangeable small ligand L (L = cod, PPh_3) on the other hand,

they suggest engagement in the potential activation of small molecules by utilizing a readily generated free coordination site. This approach was investigated by changing the atmosphere from an inert argon one to carbon monoxide at low temperatures, which, however, rather led to a further ligand exchange of cod or PPh_3 of **C-5a,b** forming isolable, dicarbonyl-substituted nickel complex **C-5c** (Scheme 27). This reactivity is in stark contrast to the chemistry reported for the Si_6 siliconoid/tetrylene hybrid. Although no detectable reactivity of **I-85a-c** was observed towards $Ni(cod)_2$ at various reaction conditions under an inert Ar atmosphere, changing to a CO atmosphere led to a rearrangement of the cluster scaffold under reductive cleavage of the carbon monoxide and subsequent incorporation of the CO parts into the siliconoid scaffold to form a silene enol ether bridge **I-90** (Chapter 1.2.3, Scheme 16).[335] The reaction is catalyzed by $Ni(cod)_2$, proposedly leading to a transient $Ni(CO)_3$–cluster complex intermediate. Opposed to that, the molecular solid-state structure of **C-5c** was determined by X-ray diffraction analysis on single crystals and supported by the experimentally as well as theoretically obtained spectroscopical data.

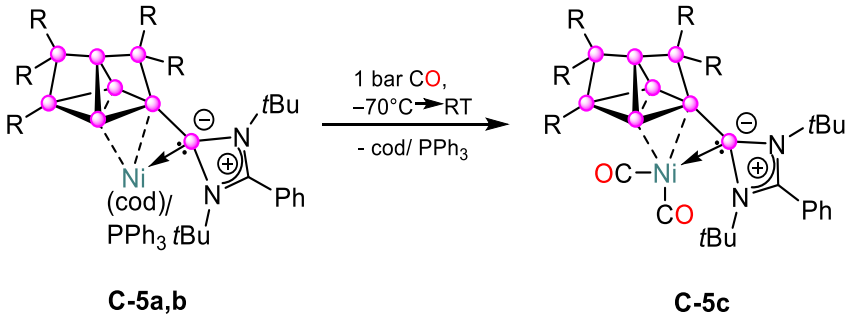

C-5a,b **C-5c**

Scheme 27. Substitution of ligand coordinating nickel by application of CO atmosphere to **C-5a,b** (○ = Si, cod = 1,5-cyclooctadiene, R = 2,4,6-triisopropyphenyl).

The formation of **C-5c** prompted for a deeper look at the catalytic activity of **C-5a,b**. Given that 3d transition metals are frequently employed as catalysts in hydrosilylation reactions, the potential of nickel complexes **C-5a-c** to promote silyl group transfer was evaluated. Preliminary studies included the reactivity of **C-5a** towards primary silane $PhSiH_3$. Since this predominantly resulted in the generation of H_2 and oligosilanes, indicating dehydrocoupling reactions, a sterically more encumbering tertiary silane (Et_3SiH) was employed, which, in contrast, showed no reactivity at all. Hence, utilization of the secondary silane Ph_2SiH_2, with intermediate steric demand, gave rise to the anticipated hydrosilylation reactivity in presence of **C-5a** with only minor formation of oligosilanes as side products (Scheme 28). Notably, terminal alkenes were chosen as suitable substrates since internal alkenes, such as cyclohexene, showed major conversion to the hydrogenated products (cyclohexane). **C-5b** and **C-5c** effected only very slow, almost negligible conversion of the substrates due to their increased ligand stability.

4. Summary, Conclusion and Outlook

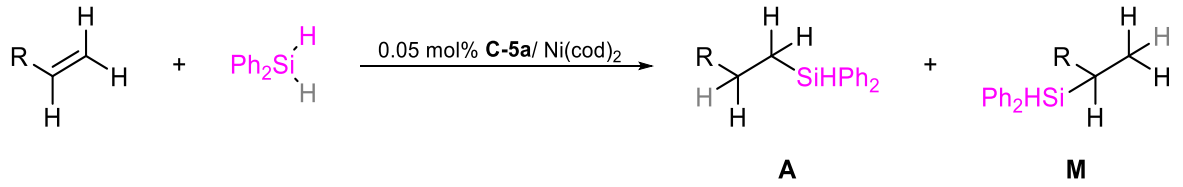

Scheme 28. Catalytic hydrosilylation of terminal alkenes with Ph_2SiH_2 and **C-5a** or $Ni(cod)_2$.

The catalytic investigations revealed a major conversion to the anti-Markovnikov product **A** in the cases employing electron-rich substrates 1-hexene, vinyltrimethylsilane, allyltrimethylsilane, vinyl- and allylcyclohexane with spectroscopic yields up to 59% at catalyst loadings of **C-5a** as low as 0.05 mol%. For the electron-poor substrates styrene and allyl-benzene the formation of the Markovnikov product **M** was observed along with **A** in an approximate ratio of 1:1.

Conclusively, the findings described for the nickel complexes **C-5a-c** confirm the better accessibility and chelating properties of the Si_7/silylene hybrid **C-2a**, exemplary for 3d transition metals, as opposed to the Si_6 derivative. The complexes are obtained under retention of the cluster scaffold and demonstrate considerable potential in catalytic transformations. Given the partial hydrogenation of cyclic alkene substrates observed upon treatment with silanes following dehydrocoupling-side reactions, it may be worth to examine hydrogenation capabilities of **C-5a** using milder hydrogenation agents, such as boranes or tin hydrides, in future experiments.

The investigation of the direct coordination of transition metal centers to the Si_7 cluster core without auxialiary silylene side arm would be the next logical step. The reaction of *ligato*-lithiated Si_6Tip_5 **I-81** and Group 4 metallocene dichlorides (Scheme 14) illustrates the most promising course of action. Such an approach could also be expanded to abundant 3d metals such as the coinage metal copper.

5. Supporting Information

5.1 Heterobimetallic unsaturated silicon clusters (siliconoids) with transition metal-expanded scaffolds

Supplementary Information

Heterobimetallic Unsaturated Silicon Clusters (Siliconoids) with Transition Metal-Expanded Scaffolds

Luisa Giarrana,[a] Nadine E. Poitiers, Alida Stürmer, Michael Zimmer, Volker Huch, Bernd Morgenstern,[b] and David Scheschkewitz*[a]

* Krupp-Chair in Inorganic and General Chemistry, Saarland University, Campus C4.1 Saarbrücken, 66123 Saarbrücken (Germany)

Service Center X-Ray Diffraction, Saarland University Campus Saarbrücken C4.1, 66123 Saarbrücken (Germany)

KEYWORDS: siliconoids • heterobimetallic • low-valent • clusters • anions

Abstract: We report a heterobimetallical unsaturated silicon cluster (siliconoid) with a formally anionic Group 9 metal vertex (Ir) in close contact to the lithium counter-cation, thus constituting a rare example of transition metal-lithium interactions. The anionic cluster is obtained by reductive chloride elimination from the corresponding neutral siliconoid complex of iridium(I) chloride with lithium/naphtalene. The previously exohedral transition metal center is fully incorporated into the siliconoid cluster scaffold giving rise to an irida- heterosiliconoid reminiscent of the corresponding homonuclear Si_7 species. Despite the formal negative charge at the iridium center, the nucleophilic site is on one of the adjacent silicon vertices judging from the reactivity toward Group 4 metallocene dichlorides, Cp_2MCl_2 (M = Zr, Hf). Under elimination of LiCl, the Cp_2MCl moieties in the heterobimetallic products are installed as pending functionalities under retention of the literally uncompromised iridasiliconoid core.

5. Supporting Information

Content

5. Supporting Information

1 Experimental Procedures

All manipulations were carried out under a protective atmosphere of argon, by using a glovebox or standard Schlenk techniques. Solvents were dried and degassed by reflux over sodium/benzophenone under argon. [D_6]-benzene (C_6D_6) was dried over potassium mirror and distilled under argon prior to use. NMR spectra were recorded on a Bruker Avance IV 400 NMR spectrometer (^{1}H = 400.13 MHz, ^{7}Li = 155.51 MHz, ^{13}C = 100.6 MHz, ^{29}Si = 79.5 MHz). The ^{1}H and ^{13}C{1H} NMR spectra were referenced to the residual proton and natural abundance ^{13}C resonances of the deuterated solvent and chemical shifts were reported relative to $SiMe_4$ (C_6D_6: δ^1H = 7.16 ppm and δ^{13}C = 128.06 ppm). Solid State NMR spectra were measured on a Bruker Avance III 400 WB spectrometer (^{7}Li = 155.57 MHz, ^{29}Si =79.53 MHz). UV-Vis spectra were recorded on a Shimadzu UV-2600 spectrometer in quartz cells with a path length of 0.1 cm and Infrared spectra on a Shimadzu IR Affinity-1S spectrometer in a platinum ATR diamond cell. Elemental analyses were performed on an elemental analyzer Leco CHN-900 and/or an elementar vario Micro Cube. Mass spectrometry was measured on a Bruker SolariX 7 Tesla MALDI/ESI/APPI FTICR imaging MS. Melting points were determined under argon in NMR tubes and are uncorrected. The molten samples were examined by NMR spectroscopy to confirm whether decomposition had occurred upon melting. Crystallographic data of the structure reported in this paper has been deposited with the Cambridge Crystallographic Data Centre, CCDC, 12 Union Road, Cambridge CB21EZ, UK. (Fax: +44-1223-336-033; E-Mail: deposit@ccdc.cam.ac.uk, http://www.ccdc.cam.ac.uk). Group 9 transition metal siliconoid hybrid **1** was prepared following the literature protocol.[S1]

2 Preparation, data and spectra (NMR, UV-Vis)

2.1 Preparation of Si_6Ir-Li 2

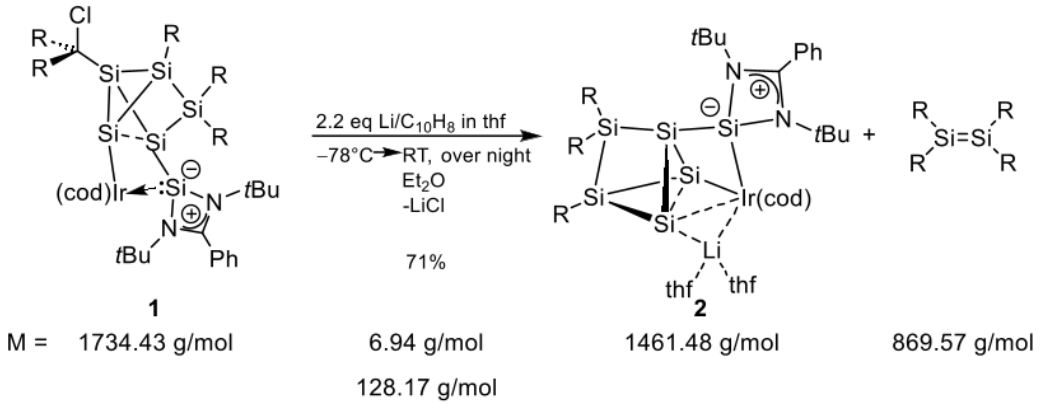

Supplementary Scheme S1: Synthesis of the iridasiliconoid **2** (R = 2,4,6-triisopropylphenyl, cod = cyclooctadienyl).

Iridium siliconoid complex **1**[S1] (720 mg 0.42 mmol, 1.0 eq) is dissolved in 10 mL diethyl ether. After cooling the solution to –78°C, a freshly prepared lithium/naphthalene solution (1.8 mL, 0.93 mmol, 2.21 eq) in thf is added dropwise to the precooled mixture at –78°C. The resulting brown reaction mixture is allowed to warm to ambient temperature under stirring overnight. All volatiles are removed under reduced

pressure. The dark-red-brown residue is filtered from 20 mL of hexane and washed 3x with 3 mL hexane. The solvent of the filtrate is distilled off under reduced pressure and the residue is dried thoroughly. This affords iridasiliconoid **2** as a dark-red-brown crystalline solid in a yield of 71% (627 mg, 0.30 mmol) along with thf (1.9 eq), naphthalene ($C_{10}H_8$, 1.6 eq) and Tip_4-disilene (0.35 eq) according to the ^{1}H NMR. Depending on crystallization conditions different amounts of thf, naphthalene and disilene co-crystallize. Single crystals of **2** were obtained as red blocks from a concentrated solution of **2** in hexane at –26°C.

^{1}H NMR (400.13 MHz, C_6D_6, 300 K) δ = 7.356 (d, $^3J_{HH}$ = 1.56 Hz, 1H, Ar-*H*), 7.270 (d, $^3J_{HH}$ = 1.56 Hz, 1H Ar-*H*), 7.205– 7.184 (m, 1H, Ar-*H*), 7.138 (d, $^3J_{HH}$ = 1.32 Hz, 1H, Ar-*H*), 7.053 (d, $^3J_{HH}$ = 1.32 Hz, 1H, Ar-*H*), 6.981 (d, $^3J_{HH}$ = 1.60 Hz, 1H, Ar-*H*), 6.939 – 6.906 (m, 3H, Ar-*H*), 6.849 – 6.809 (m, 1H, Ar-*H*), 6.535 (sept, $^3J_{HH}$ = 6.69 Hz, 1H, Ar-*H*), 5.257 (sept, $^3J_{HH}$ = 6.69 Hz, 1H, Tip-*i*Pr-C*H*), 5.039 (sept, $^3J_{HH}$ = 6.59 Hz, 1H, Tip-*i*Pr-C*H*), 4.382 – 4.317 (m, 3H, Tip-*i*Pr-C*H*), 3.884 – 3.806 (m, 3H, Tip-*i*Pr-C*H* overlapping with COD-C*H*), 2.591 – 3.558 (m, 8H, thf), 3.239 (sept, $^3J_{HH}$ = 6.56 Hz, 1H, Tip-*i*Pr-C*H*), 2.861 – 2.751 (m, 3H, Tip-*i*Pr-C*H* overlapping with COD-C*H*), 2.317 – 2.267 (m, 6H, COD-CH_2), 2.233 – 2.194 (m, 3H, Tip-*i*Pr-C*H* overlapping with COD-CH_2), 1.937 (d, $^3J_{HH}$ = 6.56 Hz, 3H, Tip-*i*Pr-CH_3), 1.748 – 1.718 (m, 9H, Tip-*i*Pr-CH_3), 1.583 (dd, $^3J_{HH}$ = 6.56 Hz, $^3J_{HH}$ = 4.56 Hz, 6H, Tip-*i*Pr-CH_3), 1.507 (d, $^3J_{HH}$ = 6.57 Hz, 3H, Tip-*i*Pr-CH_3), 1.401 (s, 9H, PhC(N(C(CH_3)$_3$)$_2$Si), 1.373 – 1.340 (m, 7H, Tip-*i*Pr-CH_3), 1.295 (s, 9H, PhC(N(C(CH_3)$_3$)$_2$Si), 1.275 (d, $^3J_{HH}$ = 1.58 Hz, 2H, Tip-*i*Pr-CH_3), 1.258 (d, $^3J_{HH}$ = 1.11 Hz, 2H, Tip-*i*Pr-CH_3), 1.241 (d, $^3J_{HH}$ = 1.34 Hz, 3H, Tip-*i*Pr-CH_3), 1.231 – 1.225 (m, 4H, Tip-*i*Pr-CH_3), 1.211 (d, $^3J_{HH}$ = 2.61 Hz, 3H, Tip-*i*Pr-CH_3), 0.861 (d, $^3J_{HH}$ = 6.72 Hz, 3H, Tip-*i*Pr-CH_3), 0.776 (t, $^3J_{HH}$ = 6.26 Hz, 6H Tip-*i*Pr-CH_3), 0.466 (d, $^3J_{HH}$ = 6.46 Hz, 3H, Tip-*i*Pr-CH_3) ppm.

^{13}C NMR (100.61 MHz, C_6D_6, 300 K) δ = 168.62 (s, 1C, Ph*C*(N(C(CH$_3$)$_3$)$_2$Si), 153.61, 153.50, 153.18, 152.67, 152.10, 151.94, 148.68, 148.24, 147.76, 144.68, 143.51, 141.83, 133.53 (s, 1C, each Ar-*C*), 129.90, 128.35, 128.11, 128.06, 127.87, 125.90 (s, 1C, each Ar-*C*H), 122.48, 122.46 (each s, 2C, COD-*C*H), 122.06, 120.85, 120.60, 119.52 (s, 1C, each Ar-*C*H), 68.51 (s, 2C, thf), 56.40 (s, 1C, PhC(N(*C*(CH$_3$)$_3$)$_2$Si), 54.13 (s, 1C, PhC(N(*C*(CH$_3$)$_3$)$_2$Si), 35.49, 35.19, 34.84, 34.73, 34.64 (each s, 1C, Tip-*i*Pr-*C*H), 33.73 (s, 3C, PhC(N(C(*C*H$_3$)$_3$)$_2$Si), 33.15, 33.03, 32.66, 32.20 (each s, Tip-*i*Pr-*C*H), 31.78 (s, 3C, PhC(N(C(*C*H$_3$)$_3$)$_2$Si), 29.25 (s, 2C, COD-*C*H$_2$), 28.81 (s, 1C, Tip-*i*Pr-*C*H$_3$), 27.62 (s, 2C, COD-*C*H$_2$), 27.38 (each s, 1C, Tip-*i*Pr-*C*H$_3$), 25.47 (s, 2C, thf), 25.36, 25.22, 24.83, 24.63, 24.57, 24.47, 24.41(each s, 1C, Tip-*i*Pr-*C*H$_3$), 24.36 (s, 2C, Tip-*i*Pr-*C*H$_3$), 24.20, 24.22, 24.13, 24.08, 23.72, 23.09, 21.30 (each s, 1C, Tip-*i*Pr-*C*H$_3$) ppm.

^{7}Li NMR (155.51 MHz, C_6D_6, 300 K) δ = 5.99 (s, *Li*), 1.12 (brs, *Li*) ppm.

^{29}Si NMR (79.49 MHz, C_6D_6, 300 K) δ = 152.8 (s, *Si*Tip), 108.2 (s, Ph*C*(N(C(CH$_3$)$_3$)$_2$*Si*), 36.0 (s, *Si*Tip$_2$), –103.2 (s, unsubstituted *Si*), –184.0 (s, unsubstituted *Si*), –226.3 (brs, *Si*Li) ppm.

Elemental analysis: calculated for $C_{76}H_{120}Si_6N_2O_2IrLi$: C:62.46%; H: 8.28%; N: 1.92%. Found: C: 62.48%; H: 7.28%; N: 1.51%. The lower values compared to those calculated are quite common for unsaturated silicon clusters due to incomplete combustion typically attributed to the formation of silicon

carbides and/or nitrides. In addition, elemental analysis has come under scrutiny because of highly variable results of bona fide identical samples.[S2]

UV-Vis (hexane): λ (ε [M^{-1} cm^{-1}]) = 543 (2860), .425 (7660) nm.

Melting Point: Decomposition under color change to a dark-brown/black solid was observed starting from 145°C with subsequent melting of the dark solid from 178°C-186°C.

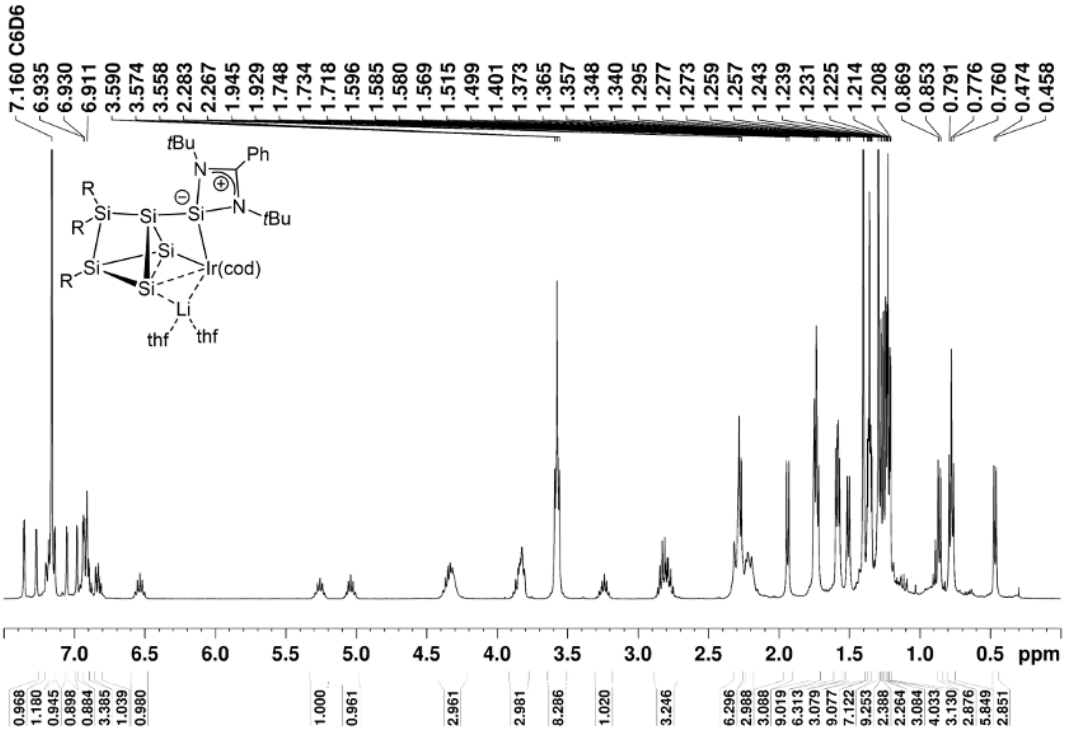

Supplementary Figure S1. ^{1}H NMR spectrum of **2** in C_6D_6 (400.13 MHz, 300 K).

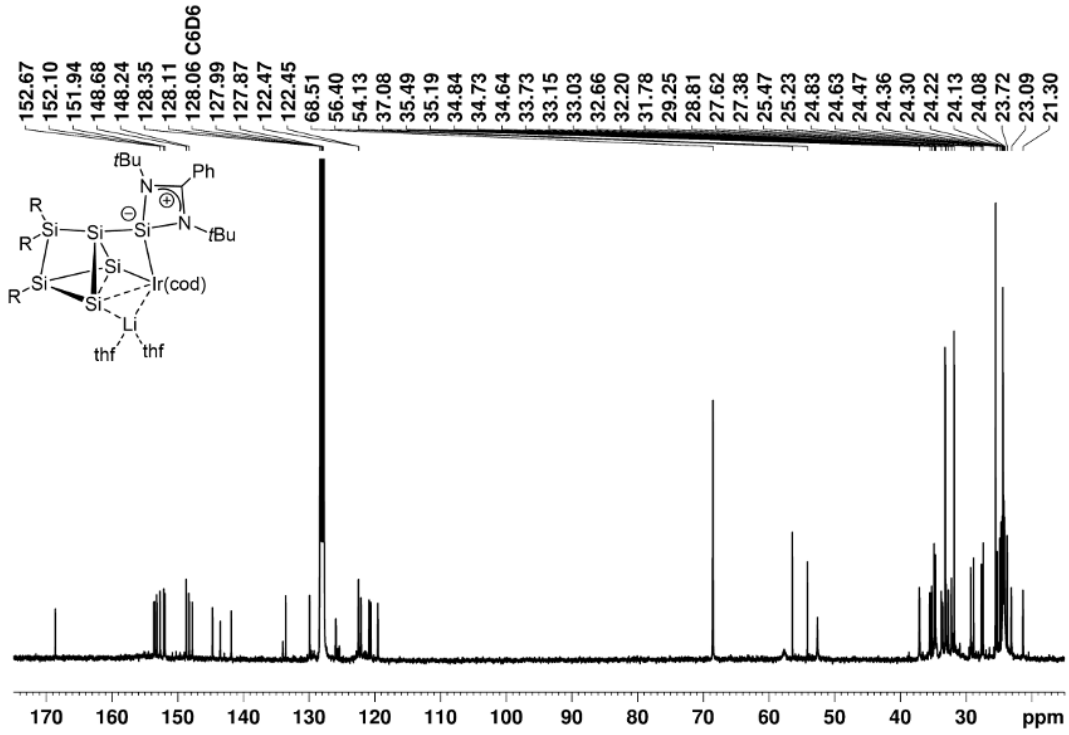

Supplementary Figure S2. ^{13}C NMR spectrum of **2** in C_6D_6 (100.61 MHz, 300 K).

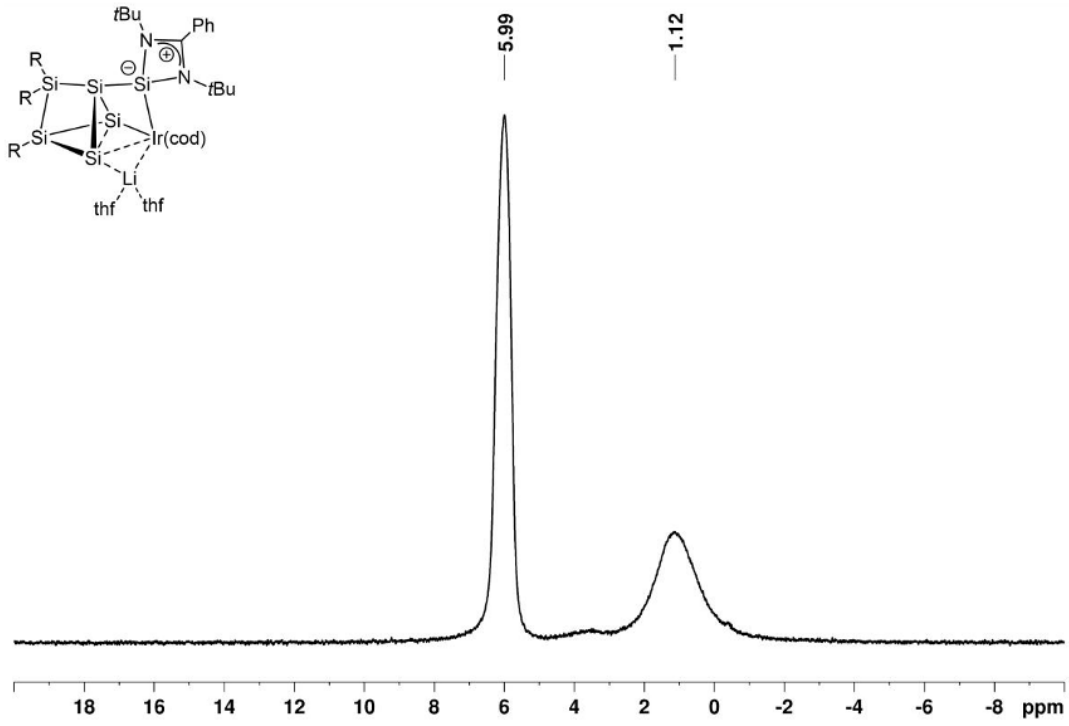

Supplementary Figure S3. ^{7}Li NMR spectrum of **2** in C_6D_6 (155.51 MHz, 300 K).

5. Supporting Information

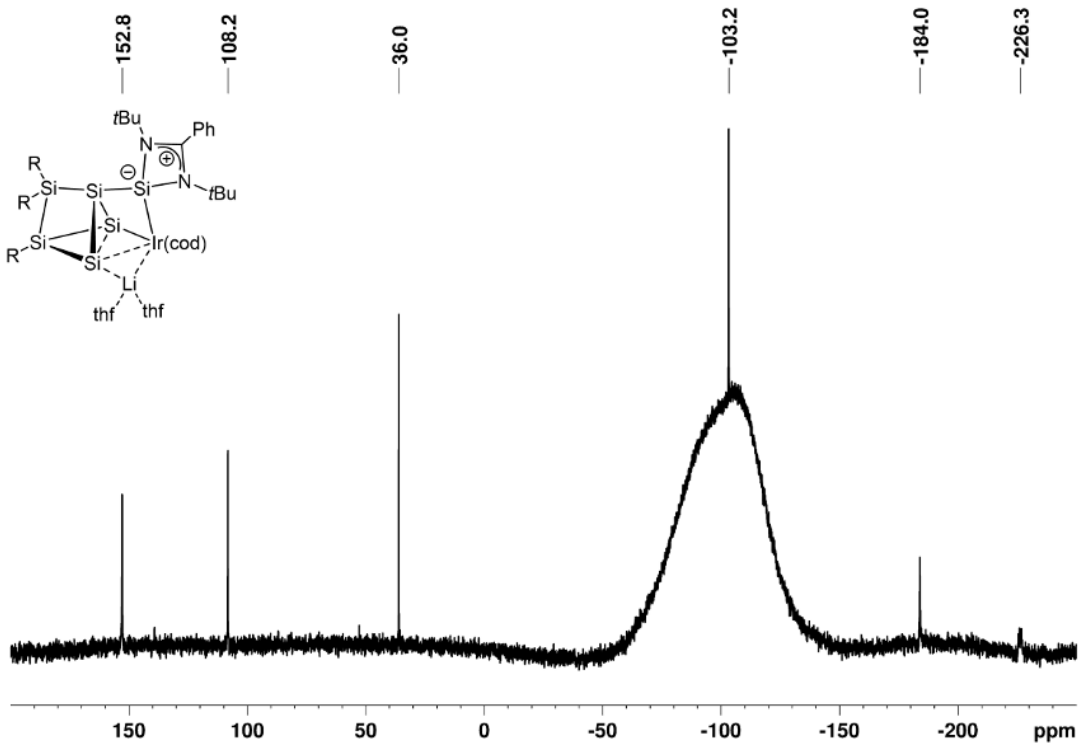

Supplementary Figure S4. ^{29}Si NMR spectrum of **2** in C_6D_6 (79.49 MHz, 300 K).

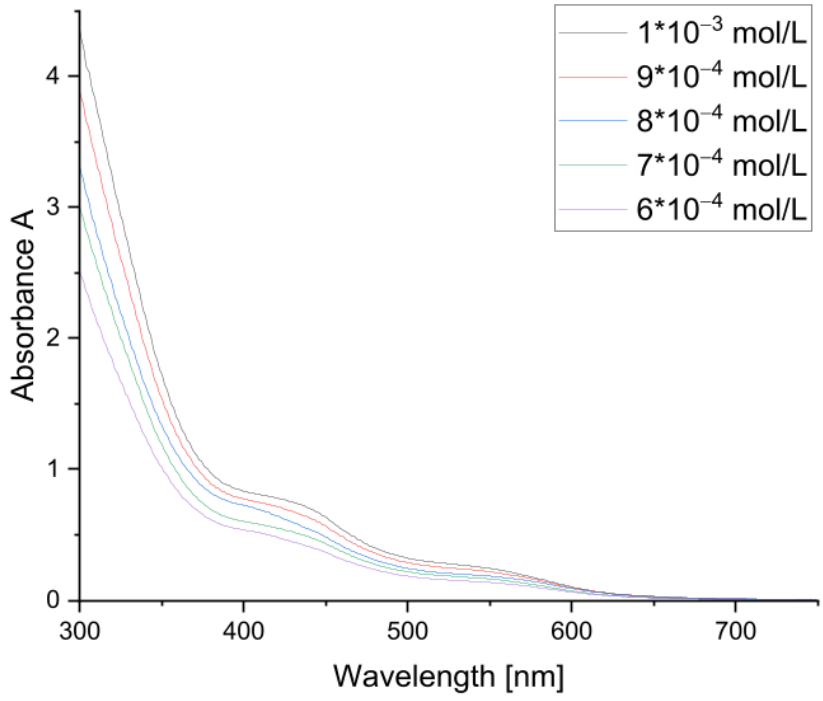

Supplementary Figure S5. UV-Vis spectra of Si_6Ir-Li complex **2** in hexane at different concentrations.

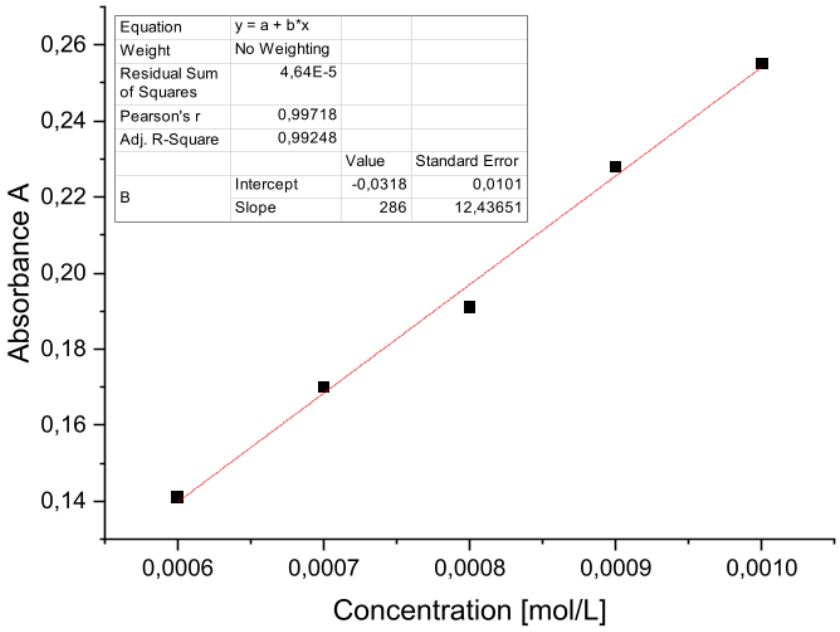

Supplementary Figure S6. Determination of the extinction coefficient $\varepsilon = 2860\ M^{-1}\ cm^{-1}$ of **2** by linear regression at $\lambda_{max} = 543$ nm against the concentration.

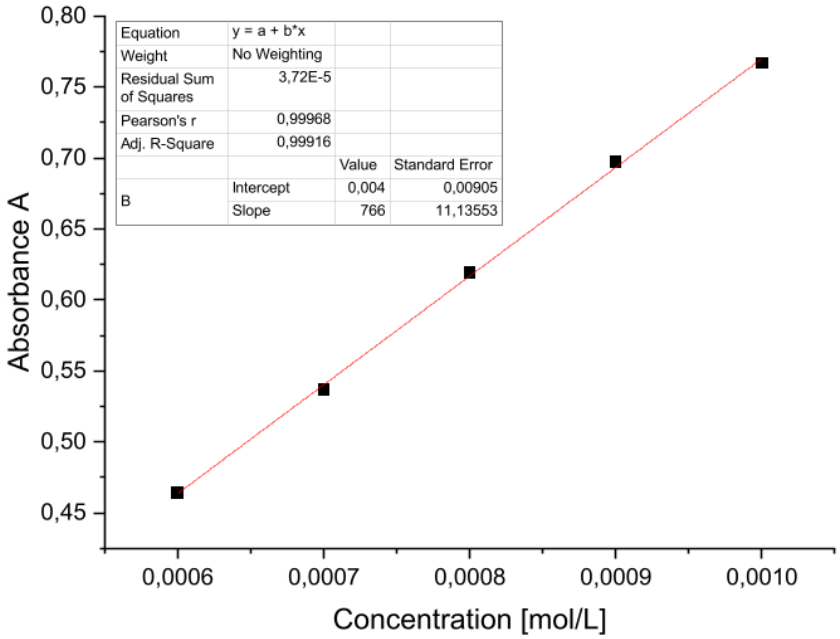

Supplementary Figure S7. Determination of the extinction coefficient $\varepsilon = 7660\ M^{-1}\ cm^{-1}$ of **2** by linear regression at $\lambda_{max} = 425$ nm against the concentration.

2.2 Preparation of Si_6Ir-Zr complex 3a

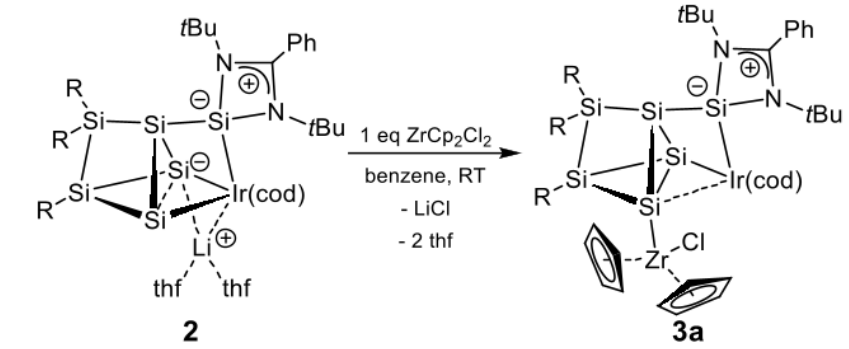

2 **3a**

M = 1461.48 g/mol 292.32 g/mol 1567.12 g/mol

Supplementary Scheme S2. Synthesis of zirconium/iridium siliconoid **3a** (R = 2,4,6-triisopropylphenyl, cod = cyclooctadienyl).

Iridasiliconoid **2** (249 mg, 0.15 mmol, 1.0 eq) is treated with $ZrCp_2Cl_2$ (43.2 mg, 0.15 mmol, 1.0 eq) in 2 mL benzene. After the dark-green solution is stirred 20 minutes at room temperature, all volatiles are removed under reduced pressure and the black-green residue is extracted from 2 mL hexane and washed 3x with 2 mL hexane each. The dark-green-brown filtrate is concentrated and kept overnight, first at –26°C, then at room temperature for crystallization. Removal of the mother liquor and drying of the dark-green-brown crystals yields 32.8 mg (0.021 mmol; 14%) of the zirconium/iridium siliconoid **3a**. The yields are compromised by the competing formation of an unidentified side product, which could be due to the elimination of CpLi according to residual ^{1}H and ^{13}C NMR signals in the spectra of **3a** (5.869/ 114.3 ppm), as well as the co-crystallization of the starting material $ZrCp_2Cl_2$ that cannot be separated completely. Attempts to detect CpLi by ^{7}Li NMR remained unsuccessful.

^{1}H NMR (400.13 MHz, C_6D_6, 300 K) δ = 7.283 (d, $^{4}J_{HH}$ = 1.61 Hz, 1H, Ar-*H*), 7.258 (d, $^{4}J_{HH}$ = 1.46 Hz, 1H, Ar-*H*), 7.1919 – 7.176 (m, 4H, Ar-*H*), 7.101 (d, $^{4}J_{HH}$ = 1.41 Hz,1H, Ar-*H*), 7.056 – 7.033 (m, 1H, Ar-*H*), 6.960 – 6.940 (m, 1H, Ar-*H*), 6.926 (d, $^{4}J_{HH}$ = 1.58 Hz, 1H, Ar-*H*), 6.853 (d, $^{4}J_{HH}$ = 1.43 Hz, 1H, Ar-*H*), 6.297 (s, 5H, Cp-C*H*), 6.230(s, 5H, Cp-C*H*), 6.013 ($ZrCp_2Cl_2$), 5.869 (CpLi?), 5.573 (sept, $^{3}J_{HH}$ = 6.63 Hz, 1H, Tip-*i*Pr-C*H*), 5.487 (sept, $^{3}J_{HH}$ = 6.78 Hz, 1H, Tip-*i*Pr-C*H*), 4.826 (sept, $^{3}J_{HH}$ = 6.50 Hz, 1H, Tip-*i*Pr-C*H*), 4.506 (m, 1H, COD-C*H*), 4.074 (sept, $^{3}J_{HH}$ = 6.59 Hz, 1H, Tip-*i*Pr-C*H*), 3.957 (m, 1H, COD-C*H*), 3.752 (m, 1H, COD-C*H*), 3.648 (sept, 1H, $^{3}J_{HH}$ = 6.65 Hz, Tip-*i*Pr-C*H*), 2.980 (sept, $^{3}J_{HH}$ = 6.47 Hz, 1H, Tip-*i*Pr-C*H*), 2.824 – 2.641 (m, 6H, Tip-*i*Pr-C*H* overlapping with COD-CH_2), 2.422 (m, 1H, COD-C*H*), 2.217 – 2.122 (m, 5H, Tip-*i*Pr-C*H* overlapping with d, $^{3}J_{HH}$ = 6.35 Hz, 3H, Tip-*i*Pr-CH_3), 1.898 – 1.813 (m, 8H, COD-CH_2 overlapping with Tip-*i*Pr-CH_3 (1.890, d, $^{3}J_{HH}$ = 6.47 Hz, 3H; 1.822, d, $^{3}J_{HH}$ = 6.70 Hz, 3H)), 1.773 (d, $^{3}J_{HH}$ = 6.81 Hz, 3H, Tip-*i*Pr-CH_3), 1.694 (d, $^{3}J_{HH}$ = 6.70 Hz, 3H, Tip-*i*Pr-CH_3), 1.449 (dd, $^{3}J_{HH}$ = 10.63, 6.67 Hz, 3H, Tip-*i*Pr-CH_3), 1.366 (d, $^{3}J_{HH}$ = 6.49 Hz, 6H, Tip-*i*Pr-CH_3), 1.257 (s, 9H, PhC(N(C(CH_3)$_3$)$_2$Si), 1.230 (d, $^{4}J_{HH}$ = 1.75 Hz, 3H, Tip-*i*Pr-CH_3), 1.214 – 1.182 (m, 15H, Tip-*i*Pr-CH_3), 1.095 (s, 9H, PhC(N(C(CH_3)$_3$)$_2$Si), 1.028 (d, $^{3}J_{HH}$ = 6.61 Hz, 3H, Tip-*i*Pr-CH_3), 0.925 (d, $^{3}J_{HH}$ = 6.58 Hz,

3H, Tip-*i*Pr-C*H*$_3$), 0.889 (t, 2H, hexane), 0.489 (d, $^3J_{HH}$ = 6.58 Hz, 3H, Tip-*i*Pr-C*H*$_3$), 0.197 (d, $^3J_{HH}$ = 6.30 Hz, 3H, Tip-*i*Pr-C*H*$_3$) ppm.

^{13}C NMR (100.61 MHz, C_6D_6, 300 K) δ = 169.72 (s, 1C, Ph*C*(N(C(*C*H$_3$)$_3$)$_2$Si), 154.11, 154.07, 153.97, 153.64, 153.36, 153.05, 149.80, 149.07, 148.06, 146.79, 141.46, 139.13, 133.03 (each s, 1C, Ar-*C*), 130.12, 128.10, 127.86, 123.74 (each s, Ar-*C*H), 122.67(s, 4C, COD-*C*H), 121.63, 121.10, 120.46 (each s, 1C, Ar-*C*H), 115.65 ($ZrCp_2Cl_2$), 114.32 (CpLi?), 112.07, 110.96 (each s, 10C, Cp-*C*H), 55.67 (s, 1C, PhC(N(*C*(CH$_3$)$_3$)$_2$Si), 54.38 (s, 1C, PhC(N(*C*(CH$_3$)$_3$)$_2$Si), 36.03, 35.55, 34.85 (each s, 1C, Tip-*i*Pr-*C*H), 34.57 – 34.46 (m, 4C, Tip-*i*Pr-*C*H), 33.06, 32.63 (each s, 1C, Tip-*i*Pr-*C*H), 32.37, 32.22(each s, 3C, PhC(N(C(*C*H$_3$)$_3$)$_2$Si), 31.90 (s, hexane), 29.33, 27.96, 27.40, 26.85 (each s, 1C, Tip-*i*Pr-*C*H$_3$), 26.64 (brs, 2C, COD-*C*H$_2$), 25.96, 25.37 (each s, 1C, Tip-*i*Pr-*C*H$_3$), 25.25 (brs, 2C, COD-*C*H$_2$), 25.05, 24.45 (each s, 1C, Tip-*i*Pr-*C*H$_3$), 24.21 – 24.06 (m, 9C, Tip-*i*Pr-*C*H$_3$), 23.82 (s, 1C, Tip-*i*Pr-*C*H$_3$), 22.99 14.30 (s, hexane) ppm.

^{29}Si NMR: (79.49 MHz, C_6D_6, 300 K) δ = 73.8 (brs, *Si*Tip), 73.5 (s, Ph*C*(N(C(CH$_3$)$_3$)$_2$*Si*), 52.8 (Tip$_2$Si=SiTip$_2$) 30.5 (s, *Si*Tip$_2$), −40.9 (s, unsubstituted *Si* (Si3)), −77.9 (s, *Si*Zr), −131.9 (s, unsubstituted *Si*) ppm.

UV-Vis (in hexane)**:** λ (ε [M^{-1} cm^{-1}]) = 601 (3389), 426 (6911), 354 (17431) nm.

Elemental analysis calculated for $C_{78}H_{114}ClIrN_2Si_6Zr$: C: 59.78 %, H: 7.33 %, N: 1.79 %. Found: C: 59.56 %, H: 7.23 %, N: 1.54 %.

Melting point: 310°C.

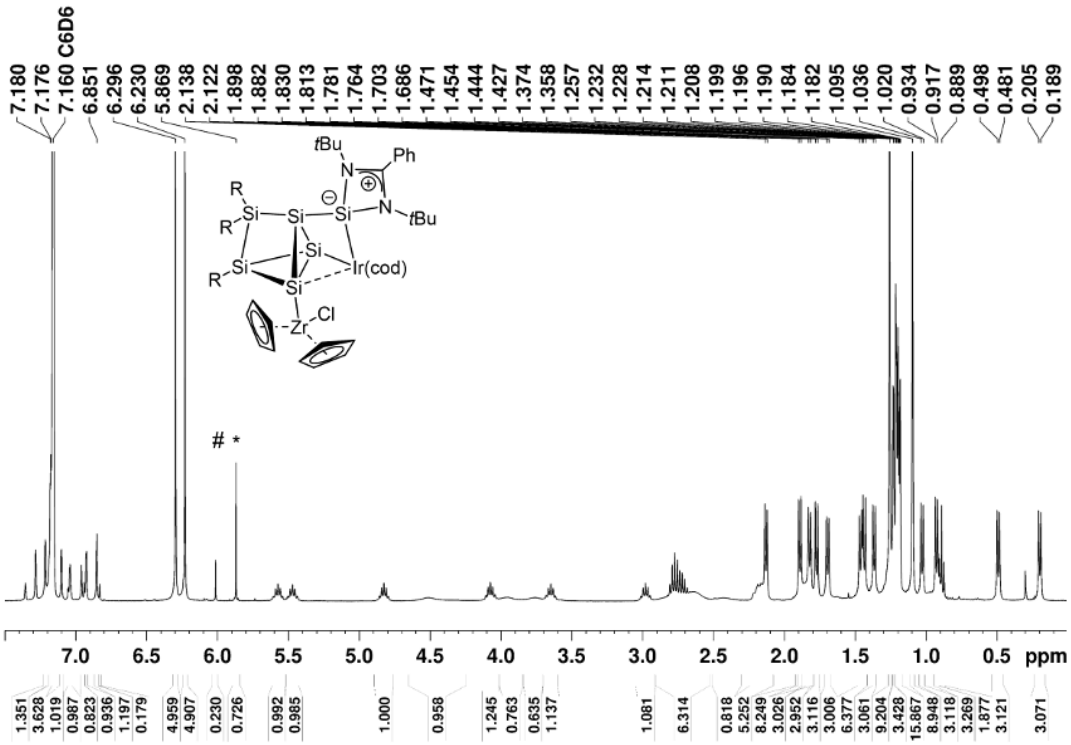

Supplementary Figure S8. ^{1}H NMR spectrum of **3a** in C_6D_6 (400.13 MHz, 300 K), #,* impurities, likely # = Cp_2ZrCl_2, * = CpLi.

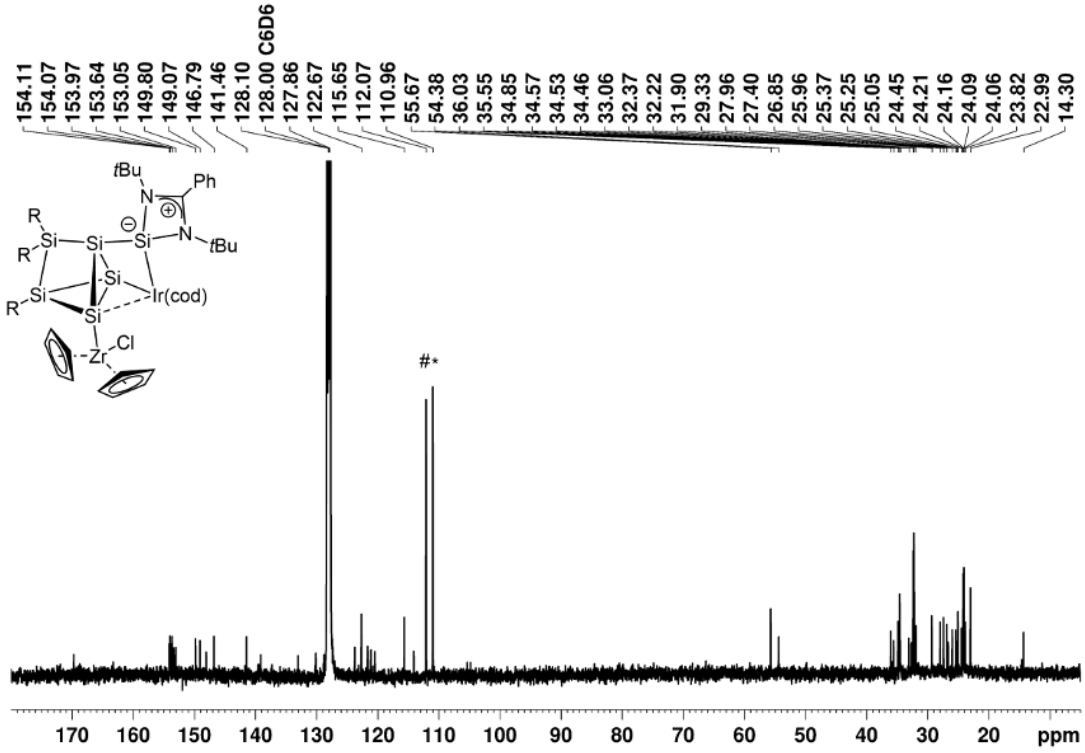

Supplementary Figure S9. ^{13}C NMR spectrum of **3a** in C_6D_6 (100.61 MHz, 300 K), #,* impurities, likely # = Cp_2ZrCl_2, * = CpLi.

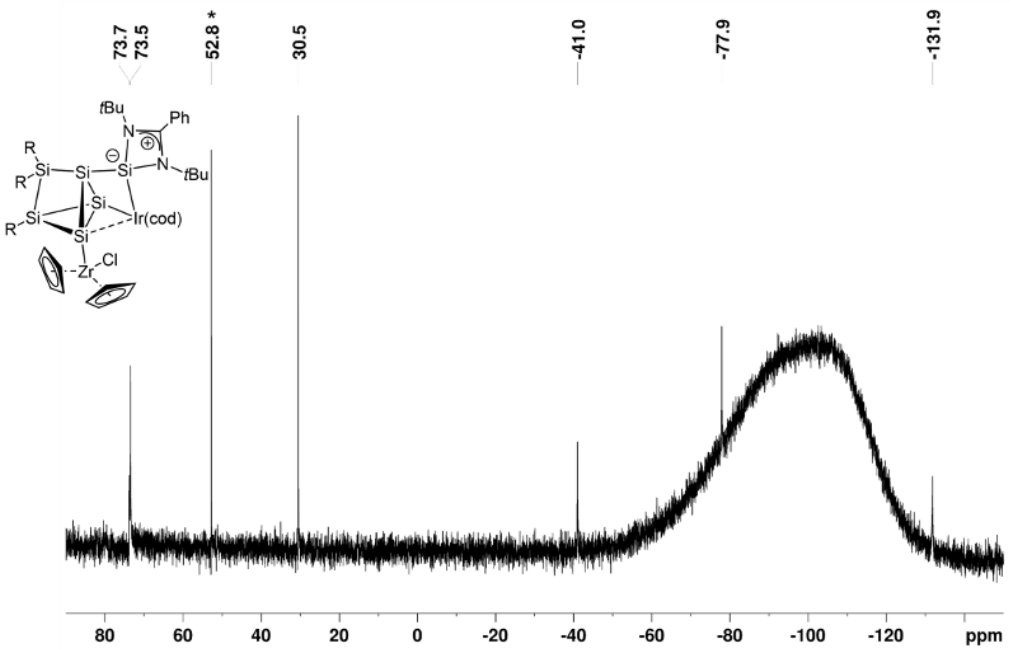

Supplementary Figure S10. ^{29}Si NMR spectrum of **3a** in C_6D_6 (79.49 MHz, 300 K), impurity * = residual $Tip_2Si{=}SiTip_2$.

5. Supporting Information

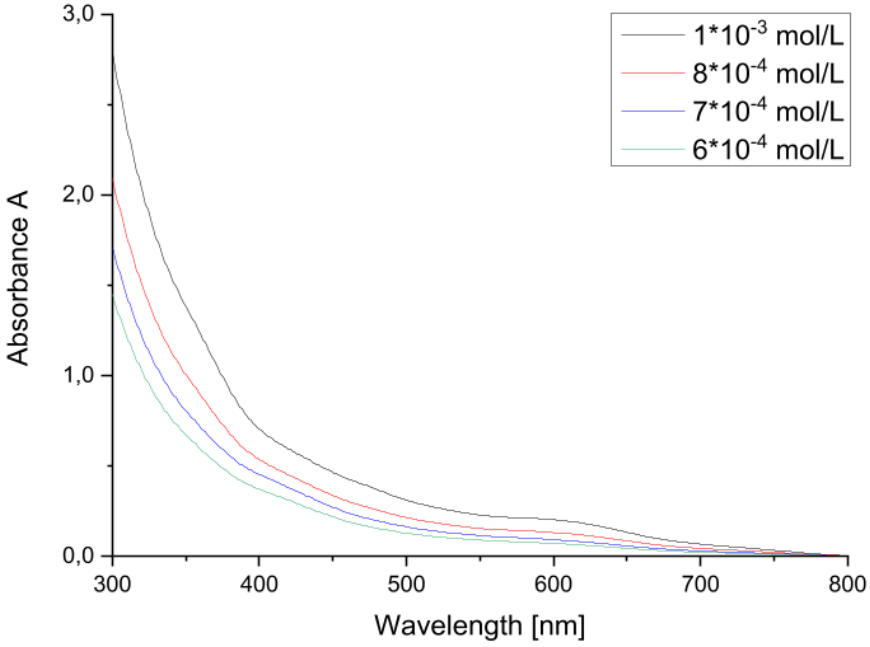

Supplementary Figure S11. UV-Vis spectra of zirconium complex **3a** in hexane at different concentrations.

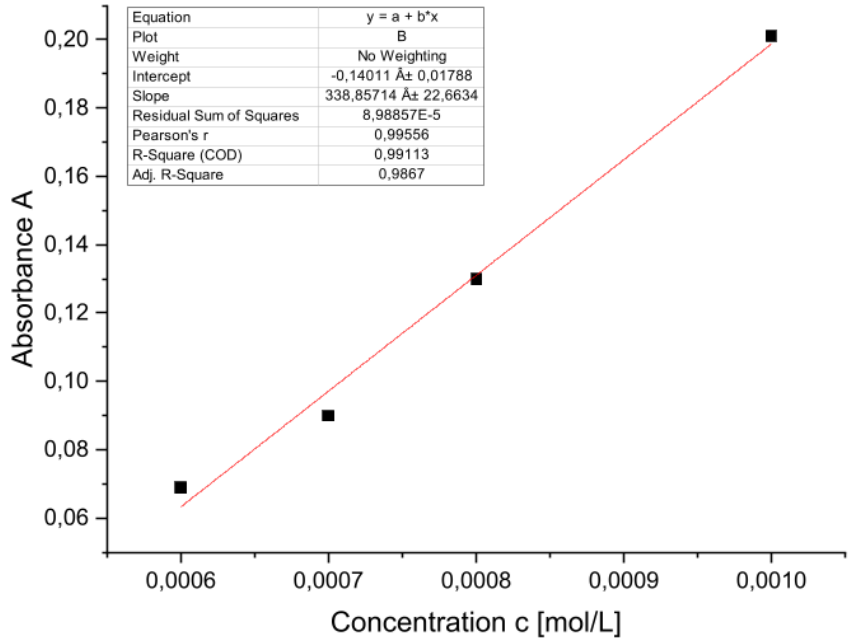

Supplementary Figure S12. Determination of the extinction ε = 3389 M^{-1} cm^{-1} of **3a** by linear regression at λ_{max} = 601 nm.

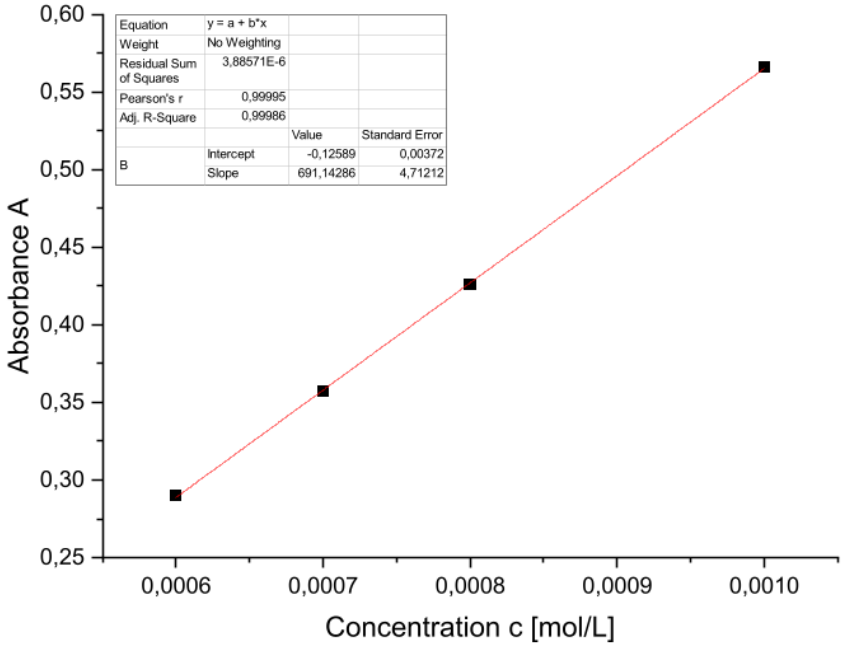

Supplementary Figure S13. Determination of the extinction ε = 6911 M^{-1} cm^{-1} of **3a** by linear regression at λ = 426 nm.

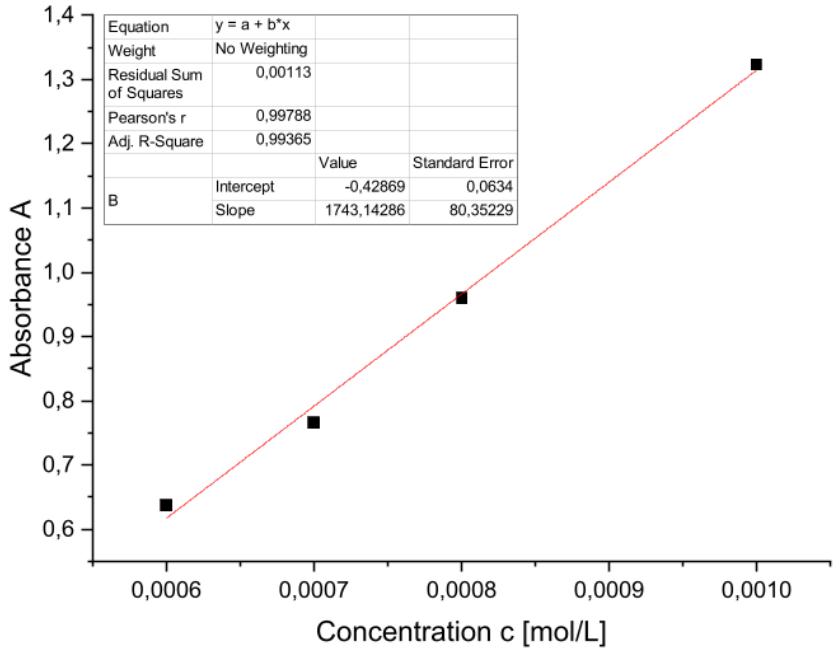

Supplementary Figure S14. Determination of the extinction ε = 17431 M^{-1} cm^{-1} of **3a** by linear regression at λ = 354 nm.

2.3 Preparation of Si_6Ir-Hf complex 3b

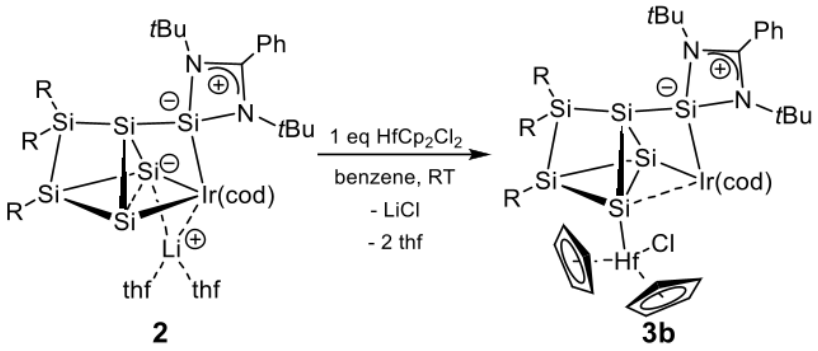

M = 1461.48 g/mol 379.58 g/mol 1654.39g/mol

Supplementary Scheme S3. Synthesis of the hafnium complex **3b** (R = 2,4,6-triisopropylphenyl, cod = cyclooctadienyl).

Hafnocene dichloride (49.6 mg (0.13 mmol, 1.08°eq.) is added to iridasiliconoid **2** (249 mg, 0.15 mmol, 1.0 eq.) in 3 mL benzene. The reaction mixture is stirred for 1.5 hours at room temperature and afterwards the solvent of the brown-orange solution is removed under reduced pressure. The dark-red residue is filtered from 3 mL hexane and washed with 5 mL hexane in total. Afterwards, the red-brown filtrate is concentrated and kept at room temperature for crystallization overnight. The mother liquor is removed *via* cannula and the crystals are dried under reduced pressure to afford 68.4 mg (0.041 mmol; 32%) of hafnium/iridium siliconoid **3b** as dark-violet-brown crystals. The yields are compromised by the competing formation of an unidentified side product, which could be due to the elimination of CpLi according to residual ^{1}H and ^{13}C NMR signals in the spectra of **3b** (5.810 ppm/ 112.85 ppm), as well as the co-crystallization of the starting material $HfCp_2Cl_2$ that cannot be separated completely. Residual naphthalene ($C_{10}H_8$) in the NMR spectra stems from the reduction step with lithium/naphthalene to **2** that could not be completely removed by sublimation and subsequent crystallization.

^{1}H NMR (400.13 MHz, C_6D_6, 300 K) δ = 7.627 (q, 0.2H, $C_{10}H_8$), 7.276 (d, $^{4}J_{HH}$ = 1.65 Hz, 1H, Ar-*H*), 7.251 (q, 0.2H, $C_{10}H_8$), 7.190 (dd, $^{3}J_{HH}$ = 8.05 Hz, $^{4}J_{HH}$ = 1.29 Hz, 3H, Ar-*H*), 7.103 (d, $^{4}J_{HH}$ = 1.50 Hz,1H, Ar-*H*), 7.007 – 7.053 (m, 1H, Ar-*H*), 6.967 – 6.946 (m, 2H, Ar-*H*), 6.917 (d, $^{4}J_{HH}$ = 1.58 Hz, 1H, Ar-*H*), 6.856 (d, $^{4}J_{HH}$ = 1.58 Hz, 2H, Ar-*H*), 6.171 (s, 5H, Cp-C*H*), 6.137 (s, 5H, Cp-C*H*), 5.925 ($HfCp_2Cl_2$), 5.810 (CpLi?), 5.531 (sept, $^{3}J_{HH}$ = 6.60 Hz, 1H, Tip-*i*Pr-C*H*), 5.441 (sept, $^{3}J_{HH}$ = 6.73 Hz, 1H, Tip-*i*Pr-C*H*), 4.847 (sept, $^{3}J_{HH}$ = 6.56 Hz, 1H, Tip-*i*Pr-C*H*), 4.584 – 4.274 (m, 1H, COD-C*H*) 4.068 (sept, $^{3}J_{HH}$ = 6.58 Hz, 1H, Tip-*i*Pr-C*H*), 3.998 – 3.727 (m, 1H, COD-C*H*), 3.633 (sept, $^{3}J_{HH}$ = 6.58 Hz, 1H, Tip-*i*Pr-C*H*), 2.965 (sept, $^{3}J_{HH}$ = 6.48 Hz, 1H, Tip-*i*Pr-C*H*), 2.801 – 2.630 (m, 8H, Tip-*i*Pr-C*H* overlapping with COD-C*H* and COD-CH_2), 2.122 (d, $^{3}J_{HH}$ = 6.39 Hz, 3H, Tip-*i*Pr-CH_3), 1.880 (d, $^{3}J_{HH}$ = 6.39 Hz, 3H, Tip-*i*Pr-CH_3), 1.817 (d, $^{3}J_{HH}$ = 6.70 Hz, 3H, Tip-*i*Pr-CH_3), 1.743 (d, $^{3}J_{HH}$ = 6.70 Hz, 3H, Tip-*i*Pr-CH_3), 1.672 (d, $^{3}J_{HH}$ = 6.70 Hz, 3H, Tip-*i*Pr-CH_3), 1.466 (d, $^{3}J_{HH}$ = 6.68 Hz, 3H, COD-CH_2 overlapping with Tip-*i*Pr-CH_3), 1.421 (t, $^{3}J_{HH}$ = 6.77 Hz, 6H, Tip-*i*Pr-CH_3), 1.254 (s, 9H, PhC(N(C(CH_3)$_3$)$_2$Si), 1.228 – 1.174 (m, 23H, Tip-*i*Pr-CH_3 overlapping with COD-CH_2), 1.106 (s, 9H, PhC(N(C(CH_3)$_3$)$_2$Si), 1.032 (d, $^{3}J_{HH}$ = 6.65 Hz, 3H, Tip-*i*Pr-

C*H*$_3$), 0.937 (d, $^3J_{HH}$ = 6.56 Hz, 3H, Tip-*i*Pr-C*H*$_3$), 0.886 (t, 2H, hexane), 0.481 (d, $^3J_{HH}$ = 6.56 Hz, 3H, Tip-*i*Pr-C*H*$_3$), 0.181 (d, $^3J_{HH}$ = 6.32 Hz, 3H, Tip-*i*Pr-C*H*$_3$) ppm.

^{13}C NMR (100.61 MHz, C_6D_6, 300 K) δ = 169.73 (s, 1C, Ph*C*(N(C(*C*H$_3$)$_3$)$_2$Si), 154.29, 154.13, 154.05, 153.80, 153.41, 153.05, 149.71, 149.04, 148.08, 146.91, 142.03, 138.97, 133.10 (each s, 1C, Ar-*C*), 130.32, 129.83, 128.92, 128.12, 127.88, 127.55, 126.01, 123.75 (each s, 1C, Ar-*C*H), 122.66 (s, 2C, COD-*C*H), 122.62 (s, 2C, COD-*C*H), 121.65, 121.20, 120.41 (each s, 1C, Ar-*C*H), 114.32 ($HfCp_2Cl_2$), 112.85 (CpLi?), 111.11, 110.20 (each s, each 5C, Cp-*C*H), 55.70 (s, 1C, PhC(N(*C*(CH$_3$)$_3$)$_2$Si), 54.33 (s, 1C, PhC(N(*C*(CH$_3$)$_3$)$_2$Si), 36.05, 35.61, 34.84 (each s, 1C, Tip-*i*Pr-*C*H), 34.60 – 34.50 (m, 4C, Tip-*i*Pr-*C*H), 33.22, 32.59 (each s, 1C, Tip-*i*Pr-*C*H), 32.46, 32.30 (each s, 3C, PhC(N(C(*C*H$_3$)$_3$)$_2$Si), 31.90 (s, hexane), 29.36, 28.08 (each s, 1C, Tip-*i*Pr-*C*H$_3$), 27.43 (s, 2C, COD-C*H*$_2$), 27.21, 26.65, 26.06 (each s, 1C, Tip-*i*Pr-*C*H$_3$), 25.59 (s, 2C, COD-C*H*$_2$), 25.53, 25.10, 24.47, 24.24 – 24.10 (m, 9C, Tip-*i*Pr-*C*H$_3$), 23.81 (s, 1C, Tip-*i*Pr-*C*H$_3$), 23.00, 14.32 (each s, hexane) ppm.

^{29}Si NMR (79.49 MHz, C_6D_6, 300 K) δ = 75.9 (s, *Si*Tip), 68.1 (bs, PhC(N(C(CH$_3$)$_3$)$_2$*Si*), 29.9 (s, *Si*Tip$_2$), −36.6 (s, *Si*Hf), −90.4 (s, *Si*Ir), −131.1 (s, unsubstituted *Si*) ppm.

CP-MAS ^{29}Si-NMR (79.53 MHz, 13KHz, 300K) δ = 65.5 (s, *Si*Tip and PhC(N(C(CH$_3$)$_3$)$_2$*Si*), 28.4 (s, *Si*Tip$_2$), −26.3 (s, unsubstituted *Si* (Si3)), −87.0 (s, *Si*Hf), −140.8 (s, unsubstituted *Si*), ppm.

UV-Vis (in hexane)**:** λ (ε [M^{-1} cm^{-1}]) = 647 (1257), 524 (5303), 437 (6871), 340 (20960) nm.

Elemental analysis: calculated for $C_{78}H_{114}ClHfIrN_2Si_6$: C: 56.63 %, H: 6.95 %, N: 1.69 %. Found: C: 55.18 %, H: 6.72 %, N: 1.36 %. The lower values compared to those calculated are quite common for unsaturated silicon clusters due to incomplete combustion typically attributed to the formation of silicon carbides and/or nitrides. In addition, elemental analysis has come under scrutiny because of highly variable results of bona fide identical samples.[S2]

Melting point: 300°C.

C*H*$_3$), 0.937 (d, $^3J_{HH}$ = 6.56 Hz, 3H, Tip-*i*Pr-C*H*$_3$), 0.886 (t, 2H, hexane), 0.481 (d, $^3J_{HH}$ = 6.56 Hz, 3H, Tip-*i*Pr-C*H*$_3$), 0.181 (d, $^3J_{HH}$ = 6.32 Hz, 3H, Tip-*i*Pr-C*H*$_3$) ppm.

^{13}C NMR (100.61 MHz, C_6D_6, 300 K) δ = 169.73 (s, 1C, Ph*C*(N(C(*C*H$_3$)$_3$)$_2$Si), 154.29, 154.13, 154.05, 153.80, 153.41, 153.05, 149.71, 149.04, 148.08, 146.91, 142.03, 138.97, 133.10 (each s, 1C, Ar-*C*), 130.32, 129.83, 128.92, 128.12, 127.88, 127.55, 126.01, 123.75 (each s, 1C, Ar-*C*H), 122.66 (s, 2C, COD-*C*H), 122.62 (s, 2C, COD-*C*H), 121.65, 121.20, 120.41 (each s, 1C, Ar-*C*H), 114.32 ($HfCp_2Cl_2$), 112.85 (CpLi?), 111.11, 110.20 (each s, each 5C, Cp-*C*H), 55.70 (s, 1C, PhC(N(*C*(CH$_3$)$_3$)$_2$Si), 54.33 (s, 1C, PhC(N(*C*(CH$_3$)$_3$)$_2$Si), 36.05, 35.61, 34.84 (each s, 1C, Tip-*i*Pr-*C*H), 34.60 – 34.50 (m, 4C, Tip-*i*Pr-*C*H), 33.22, 32.59 (each s, 1C, Tip-*i*Pr-*C*H), 32.46, 32.30 (each s, 3C, PhC(N(C(*C*H$_3$)$_3$)$_2$Si), 31.90 (s, hexane), 29.36, 28.08 (each s, 1C, Tip-*i*Pr-*C*H$_3$), 27.43 (s, 2C, COD-C*H*$_2$), 27.21, 26.65, 26.06 (each s, 1C, Tip-*i*Pr-*C*H$_3$), 25.59 (s, 2C, COD-C*H*$_2$), 25.53, 25.10, 24.47, 24.24 – 24.10 (m, 9C, Tip-*i*Pr-*C*H$_3$), 23.81 (s, 1C, Tip-*i*Pr-*C*H$_3$), 23.00, 14.32 (each s, hexane) ppm.

^{29}Si NMR (79.49 MHz, C_6D_6, 300 K) δ = 75.9 (s, *Si*Tip), 68.1 (bs, PhC(N(C(CH$_3$)$_3$)$_2$*Si*), 29.9 (s, *Si*Tip$_2$), −36.6 (s, *Si*Hf), −90.4 (s, *Si*Ir), −131.1 (s, unsubstituted *Si*) ppm.

CP-MAS ^{29}Si-NMR (79.53 MHz, 13KHz, 300K) δ = 65.5 (s, *Si*Tip and PhC(N(C(CH$_3$)$_3$)$_2$*Si*), 28.4 (s, *Si*Tip$_2$), −26.3 (s, unsubstituted *Si* (Si3)), −87.0 (s, *Si*Hf), −140.8 (s, unsubstituted *Si*), ppm.

UV-Vis (in hexane)**:** λ (ε [M^{-1} cm^{-1}]) = 647 (1257), 524 (5303), 437 (6871), 340 (20960) nm.

Elemental analysis: calculated for $C_{78}H_{114}ClHfIrN_2Si_6$: C: 56.63 %, H: 6.95 %, N: 1.69 %. Found: C: 55.18 %, H: 6.72 %, N: 1.36 %. The lower values compared to those calculated are quite common for unsaturated silicon clusters due to incomplete combustion typically attributed to the formation of silicon carbides and/or nitrides. In addition, elemental analysis has come under scrutiny because of highly variable results of bona fide identical samples.[S2]

Melting point: 300°C.

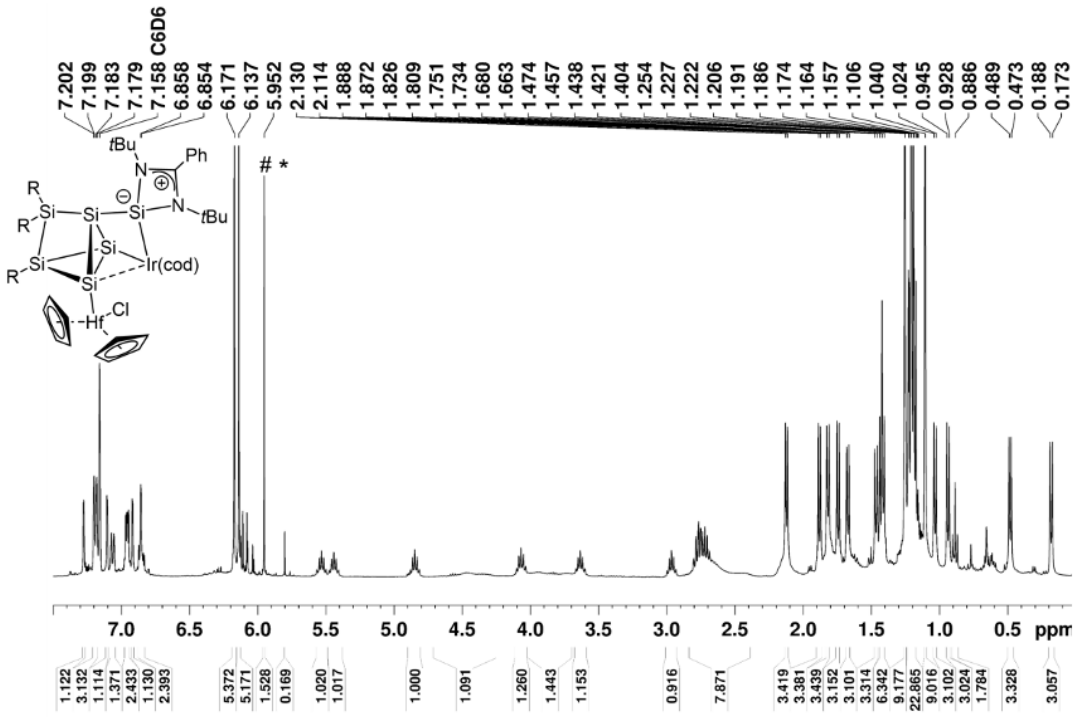

Supplementary Figure S15. ^{1}H NMR spectrum of **3b** in C_6D_6 (400.13 MHz, 300 K), #,* impurities, likely # = Cp_2HfCl_2, * = CpLi.

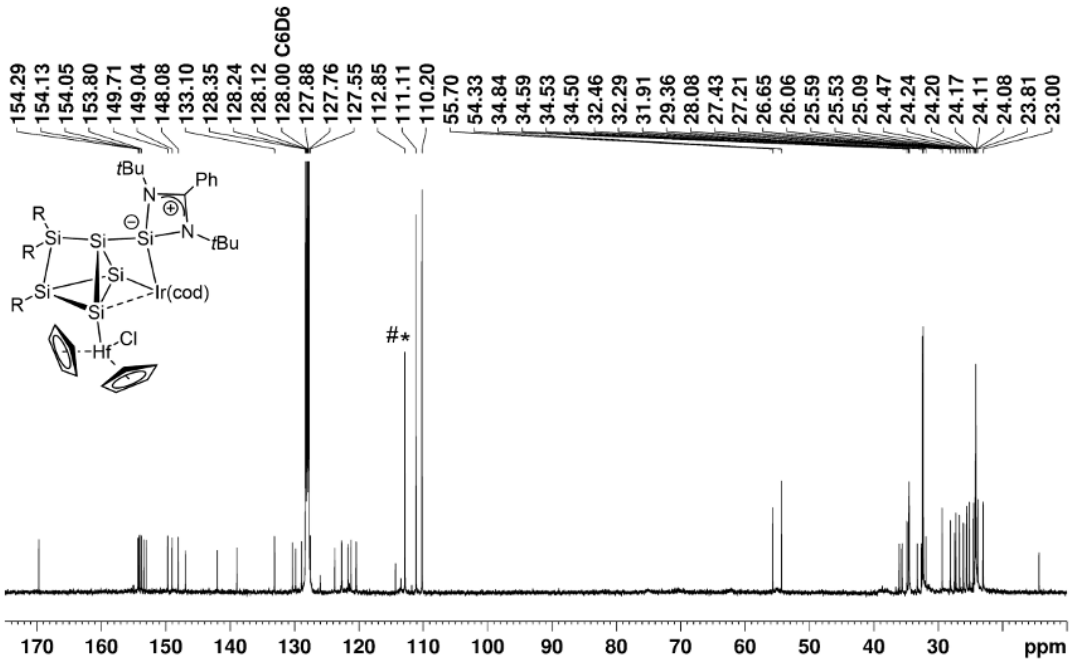

Supplementary Figure S16. ^{13}C NMR spectrum of **3b** in C_6D_6 (100.61 MHz, 300 K), #,* impurities, likely # = Cp_2HfCl_2, * = CpLi.

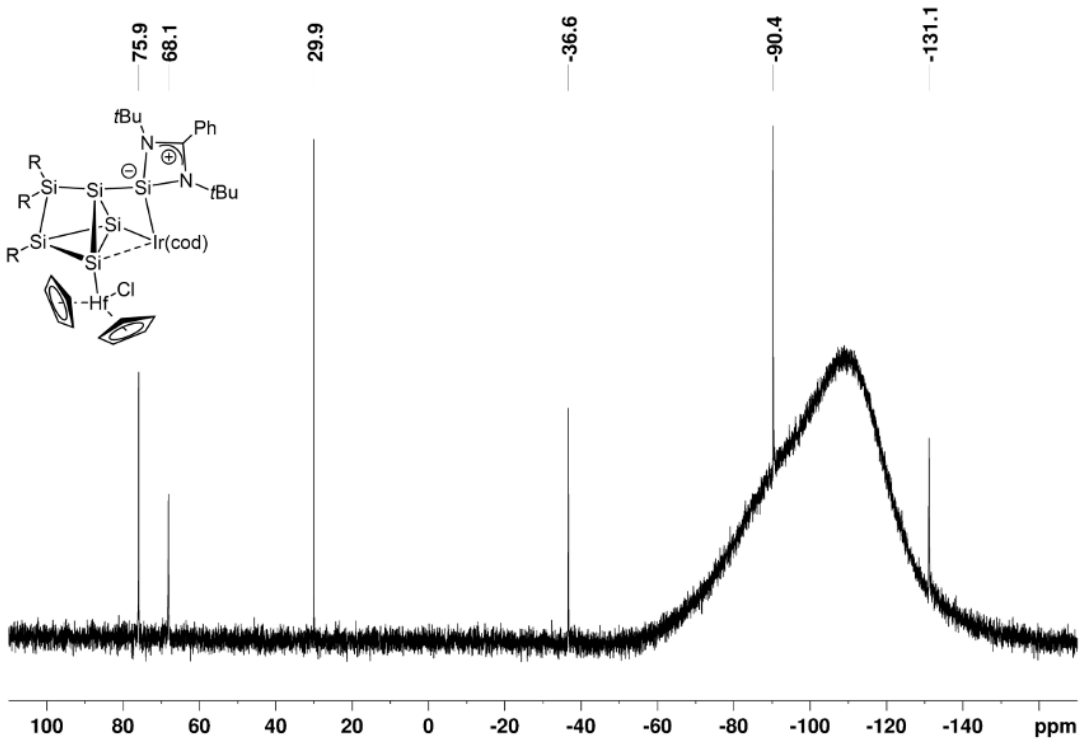

Supplementary Figure S17. ^{29}Si NMR spectrum of **3b** in C_6D_6 (79.49 MHz, 300 K).

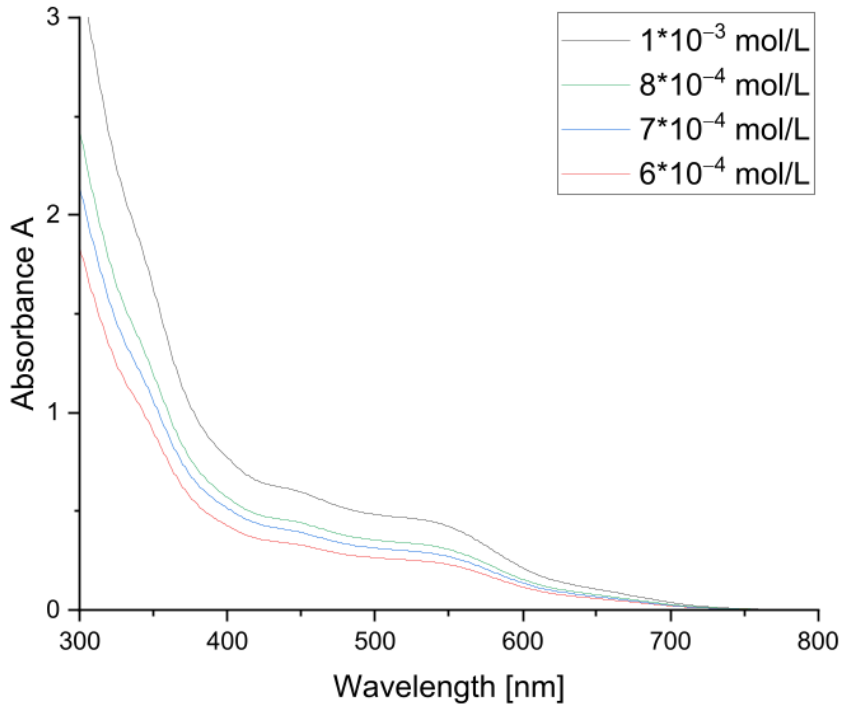

Supplementary Figure S18. UV-Vis spectra of hafnium complex **3b** in hexane at different concentrations.

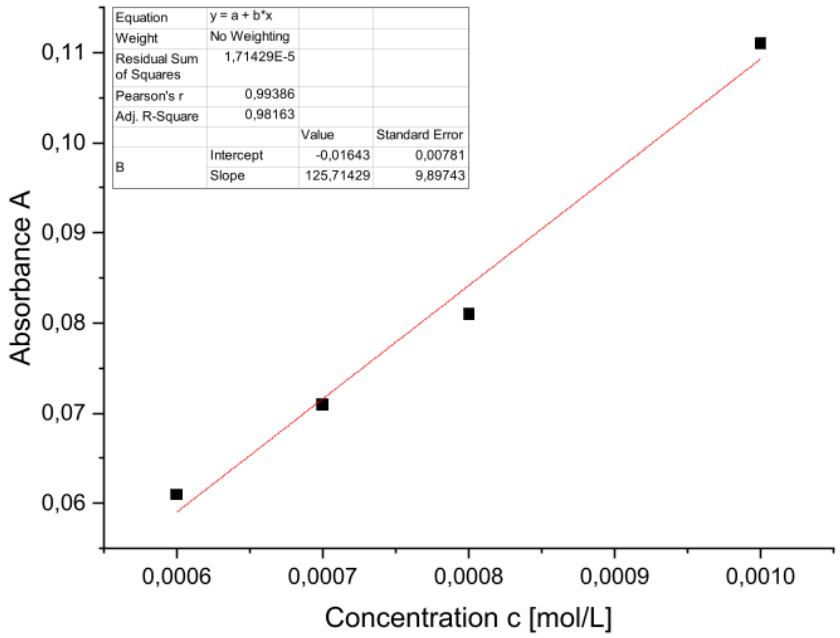

Supplementary Figure S19. Determination of the extinction ε = 1257 M^{-1} cm^{-1} of **3b** by linear regression at λ_{max} = 647 nm.

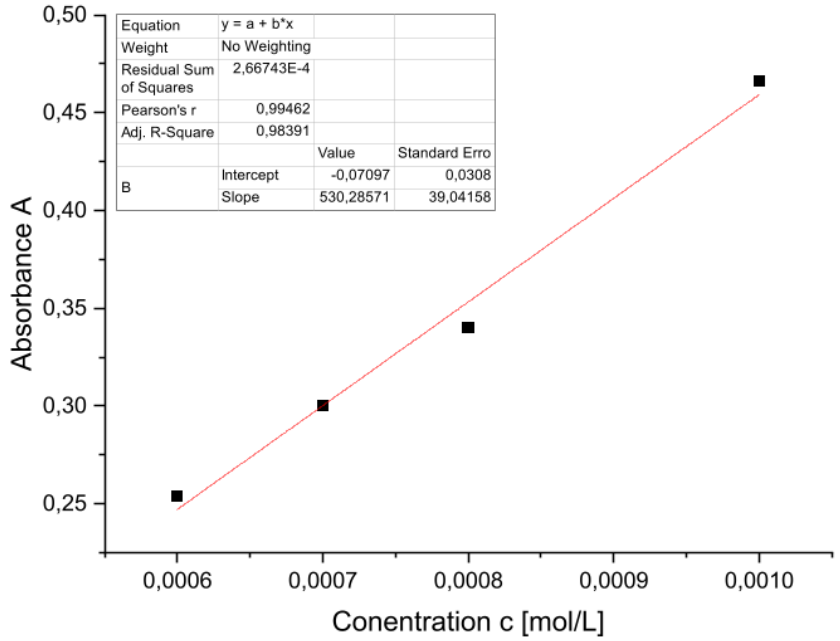

Supplementary Figure S20. of the extinction ε = 5303 M^{-1} cm^{-1} of **3b** by linear regression at λ = 524 nm.

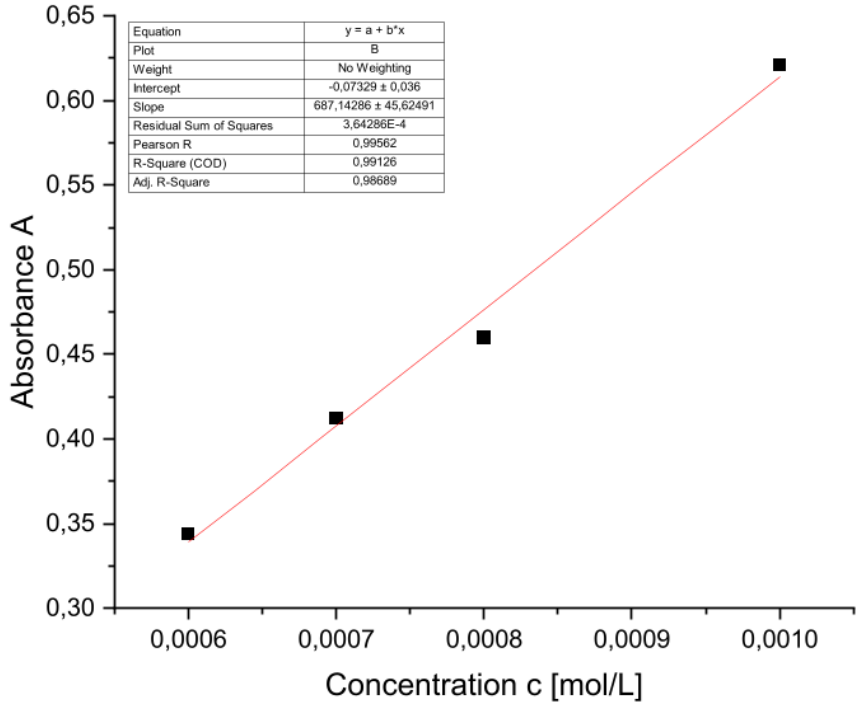

Supplementary Figure S21. Determination of the extinction ε = 6871 M^{-1} cm^{-1} of **3b** by linear regression at λ = 437 nm.

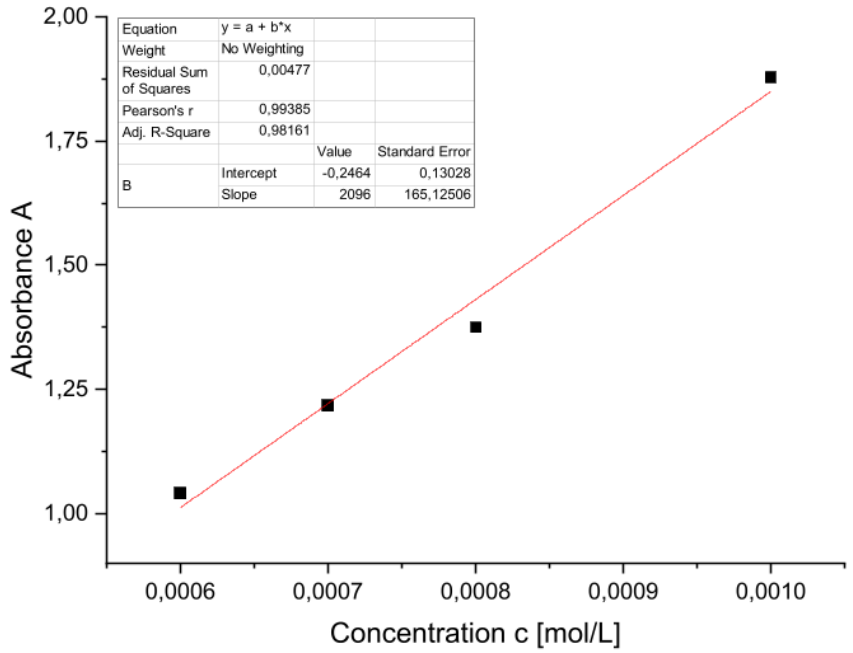

Supplementary Figure S22. Determination of the extinction ε = 20960 M^{-1} cm^{-1} of **3b** by linear regression at λ = 340 nm.

3 Details on X-Ray Diffraction Studies

Crystallographic data

The data set was collected using a Bruker D8 Venture diffractometer with a microfocus sealed tube and a Photon II detector. Graphite-monochromated $Mo_{K\alpha}$ radiation (λ = 0.71073 Å) was used. Data were collected at 122(2) K (**2**) or 133(2) K (**3a,b**) and corrected for absorption effects using the multi-scan method. The structures were solved by direct methods using SHELXS-97 (**2**)[S4a] or SHELXT (**3a,b**)[S4b] and were refined by full matrix least squares calculations on F^2 (SHELXL 2018[S5]) in the graphical user interface Shelxle.[S6] The refinement of the two structures **3a** and **3b** was each extended with the BOND$H command of SHELX to introduce the C-C-H angles and the C-H distances in the cif-file and then refined again. After the refinement, the two structures **3a** and **3b** each show one increased residual electron density peak near a non-heavy atom. This could be an indication of twinning, although neither TwinRotMat (PLATON)[S7] detected a twin law nor was non-merohedral twinning observed in the reciprocal space.

Acknowledgments

Instrumentation and technical assistance for this work were provided by the Service Center X-ray Diffraction, with financial support from Saarland University and German Science Foundation (project number INST 256/506-1).

3.1 Solid State Structure of Si_6Ir-Li 2

Refinement

All non H-atoms were located in the electron density maps and refined anisotropically. C-bound H atoms were placed in positions of optimized geometry and treated as riding atoms. Their isotropic displacement parameters were coupled to the corresponding carrier atoms by a factor of 1.2 (CH, CH2) or 1.5 (CH3). *Disorder*: Two isopropyl-groups (fvar 2: 0.60/0.40; fvar 4: 0.70/0.30), one tert.butyl-group (fvar 5: 0.65/0.35) and a part of the coordinated thf molecule (fvar 3: 0.61/0.39) are split over two positions.

Supplementary Table S1. Crystal data and structure refinement for $Si_5NHSiIrLi$ **2** (CCDC: 2447272).

Empirical formula	C76 H120 Ir Li N2 O2 Si6	
Formula weight	1461.41	
Temperature	122(2) K	
Wavelength	0.71073 Å	
Crystal system	Triclinic	
Space group	P-1	
Unit cell dimensions	a = 14.3574(10) Å	α = 75.099(2)°.
	b = 22.2591(14) Å	β = 88.548(2)°.
	c = 25.9243(17) Å	γ = 77.283(2)°.

Volume	7805.7(9) Å^3
Z	4
Density (calculated)	1.244 Mg/m^3
Absorption coefficient	1.846 mm^{-1}
F(000)	3080
Crystal size	0.510 x 0.144 x 0.060 mm^3
Theta range for data collection	0.971 to 27.986°.
Index ranges	-18<=h<=18, -29<=k<=29, -34<=l<=34
Reflections collected	114921
Independent reflections	37415 [R(int) = 0.0547]
Completeness to theta = 25.242°	99.9 %
Absorption correction	Semi-empirical from equivalents
Max. and min. transmission	0.7456 and 0.5737
Refinement method	Full-matrix least-squares on F^2
Data / restraints / parameters	37415 / 171 / 1715
Goodness-of-fit on F^2	1.025
Final R indices [I>2sigma(I)]	R1 = 0.0442, wR2 = 0.1001
R indices (all data)	R1 = 0.0702, wR2 = 0.1089
Largest diff. peak and hole	1.717 and -2.350 e.Å^{-3}

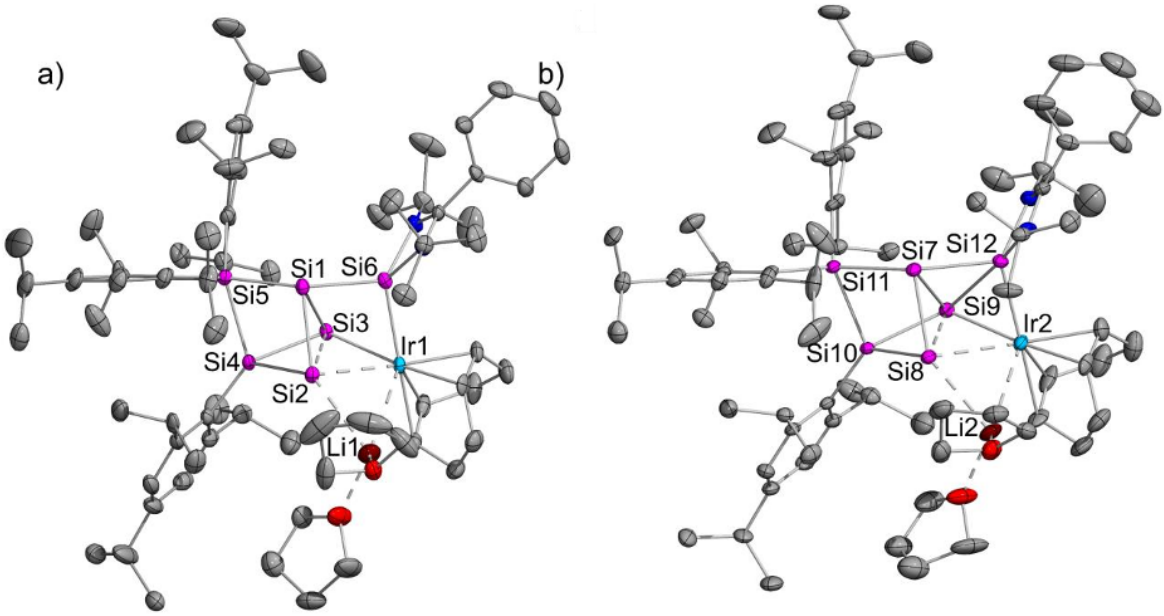

Supplementary Figure S23. Molecular structure of iridasiliconoid **2** in the solid state (a) molecule 1, b) molecule 2). Hydrogen atoms are omitted for clarity. Thermal ellipsoids represent 50% probability.

Supplementary Table S2. Comparison of the bonding parameters in molecule 1 and 2 of iridasiliconoid **2** and averaged arithmetic values.

Molecule 1		Molecule 2		Arithmetic Mean Values
Atoms	**Distance [Å]**	**Atoms**	**Distance [Å]**	**Distance [Å]**
Ir1-Si2	2.658(1)	Ir2-Si8	2.623(1)	2.641(1)
Ir1-Si3	2.404(1)	Ir2-Si9	2.417(1)	2.411(1)
Ir1-Si6	2.343(1)	Ir2-Si12	2.345(1)	2.344(1)
Ir1-Li1	2.880(8)	Ir2-Li2	2.880(8)	2.880(8)
Si1-Si2	2.327(2)	Si7-Si8	2.327(2)	2.327(2)
Si1-Si3	2.438(2)	Si7-Si9	2.408(2)	2.423(2)
Si1-Si5	2.317(2)	Si7-Si11	2.324(2)	2.321(2)
Si1-Si6	2.286(2)	Si7-Si12	2.284(2)	2.285(2)
Si2-Si3	2.466(2)	Si8-Si9	2.484(2)	2.475(2)
Si2-Si4	2.400(2)	Si8-Si10	2.375(2)	2.388(2)
Si2-Li1	2.617(8)	Si8-Li2	2.605(7)	2.611(8)
Si3-Si4	2.321(1)	Si9-Si10	2.341(2)	2.331(2)
Si4-Si5	2.405(2)	Si10-Si11	2.399(1)	2.402(2)
Atoms	**Angle [°]**	**Atoms**	**Angle [°]**	**Angle [°]**
Si5-Si1-Si6	146.2(6)	Si11-Si7-Si12	153.5(7)	149.9(7)
Si6-Ir1-Li1	125.1(2)	Si12-Ir2-Li2	120.3(2)	122.7(2)
Si3-Ir1-Li1	105.8(2)	Si9-Ir2-Li2	108.2(2)	107.1(2)
Si2-Ir1-Li1	56.2(2)	Si8-Ir2-Li2	56.3(2)	56.3(2)
Si3-Si2-Li1	112.4(2)	Si9-Si8-Li2	115.3(2)	113.9(2)
Si6-Ir-Si3	68.4(4)	Si12-Ir2-Si9	69.9(4)	69.2(4)

3.2 Solid State Structure of Si6Ir-Zr 3a

Refinement

All non H-atoms were located on the electron density maps and refined anisotropically. C-bound H atoms were placed in positions of optimized geometry and treated as riding atoms. Their isotropic displacement parameters were coupled to the corresponding carrier atoms by a factor of 1.2 (CH, CH2) or 1.5 (CH3). *Disorder*: One of the isopropyl groups (C28a C30a and C28b C30b) was split over two positions. Its occupancy factors refined to 81.1% for the major component. Some residual electron density (3.11 $Å^3$) was found near (2.28 Å) a isopropyl group (C23) of the Tip substituent due to unmodelled disorder.

Supplementary Table S3. Crystal data and structure refinement for zirconium complex **3a** (CCDC: 2447286).

Empirical formula	C78 H114 Cl Ir N2 Si6 Zr	
Formula weight	1567.12	
Temperature	133(2) K	
Wavelength	0.71073 Å	
Crystal system	Triclinic	
Space group	P-1	
Unit cell dimensions	a = 13.0066(6) Å	α = 85.640(2)°.
	b = 16.0638(8)) Å	β = 73.327(2)°.
	c = 20.4956(10) Å	γ = 70.671(2)°.
Volume	3870.1(3) $Å^3$	

Z	2
Density (calculated)	1.345 Mg/m^3
Absorption coefficient	2.021 mm^{-1}
F(000)	1628
Crystal size	0.176 x 0.109 x 0.064 mm^3
Theta range for data collection	2.075 to 25.681°
Index ranges	-15<=h<=15, -19<=k<=19, -24<=l<=24
Reflections collected	137646
Independent reflections	14647 [R(int) = 0.0688]
Completeness to theta = 25.027°	99.8 %
Absorption correction	Semi-empirical from equivalents
Max. and min. transmission	0.7455 and 0.6989
Refinement method	Full-matrix least-squares on F^2
Data / restraints / parameters	14647 / 87 / 856
Goodness-of-fit on F^2	1.057
Final R indices [I>2sigma(I)]	R1 = 0.0306, wR2 = 0.0629
R indices (all data)	R1 = 0.0383, wR2 = 0.0665
Largest diff. peak and hole	3.312 and –0.598 $e.Å^{-3}$

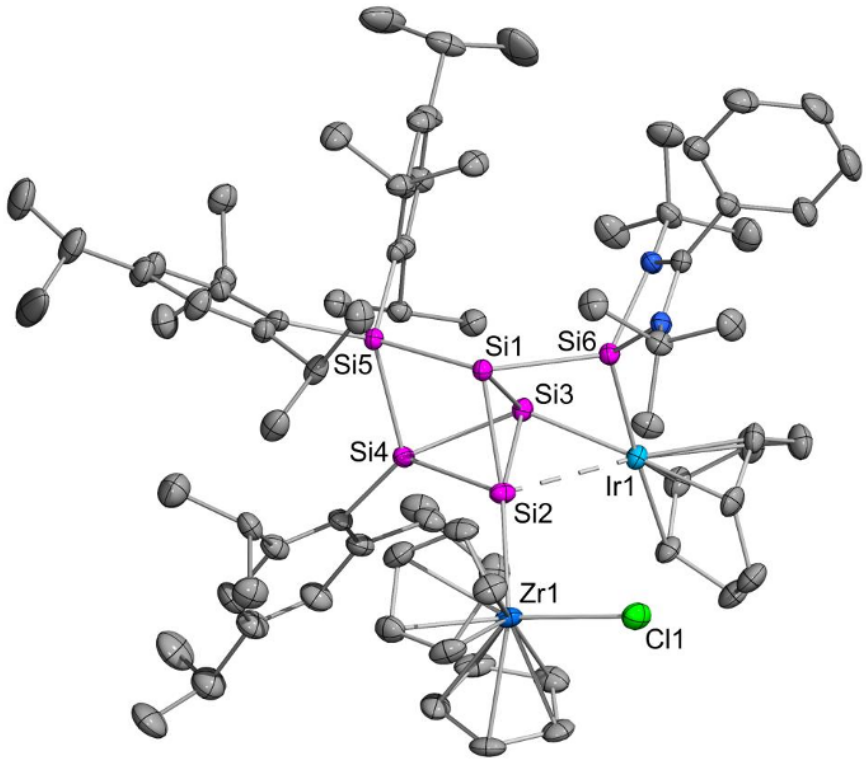

Supplementary Figure S24. Molecular structure of the zirconium complex **3a** in the solid state. Hydrogen atoms are omitte for clarity. Thermal ellipsoids represent 50% probability.

3.3 Solid State Structure of Si6Ir-Hf 3b

Refinement

5. Supporting Information

All non H-atoms were located on the electron density maps and refined anisotropically. C-bound H atoms were placed in positions of optimized geometry and treated as riding atoms. Their isotropic displacement parameters were coupled to the corresponding carrier atoms by a factor of 1.2 (CH, CH2) or 1.5 (CH3). Disorder: One of the isopropyl groups is split over two positions. Its occupancy factors refined to 78 % and 22 %, respectively.

Supplementary Table S4. Crystal data and structure refinement for hafnium complex **3b** (CCDC: 2447266).

Empirical formula	C78 H114 Cl Hf Ir N2 Si6	
Formula weight	1654.39	
Temperature	133(2) K	
Wavelength	0.71073 Å	
Crystal system	Triclinic	
Space group	P-1	
Unit cell dimensions	a = 12.9983(9) Å	α = 85.512(3)°.
	b = 16.0655(12) Å	β = 73.304(3)°.
	c = 20.4888(14) Å	γ = 70.764(3)°.
Volume	3868.7(5) $Å^3$	
Z	2	
Density (calculated)	1.420 Mg/m^3	
Absorption coefficient	3.228 mm^{-1}	
F(000)	1692	
Crystal size	0.172 x 0.138 x 0.074 mm^3	
Theta range for data collection	2.076 to 25.027°	
Index ranges	-15<=h<=15, -19<=k<=19, -24<=l<=24	
Reflections collected	106012	
Independent reflections	13360 [R(int) = 0.0607]	
Completeness to theta = 25.027°	97.7 %	
Absorption correction	Semi-empirical from equivalents	
Max. and min. transmission	0.7455 and 0.6256	
Refinement method	Full-matrix least-squares on F^2	
Data / restraints / parameters	13360 / 87 / 852	
Goodness-of-fit on F^2	1.107	
Final R indices [I>2sigma(I)]	R1 = 0.0331, wR2 = 0.0644	
R indices (all data)	R1 = 0.0469, wR2 = 0.0698	
Largest diff. peak and hole	2.548 and –1.354 $e.Å^{-3}$	

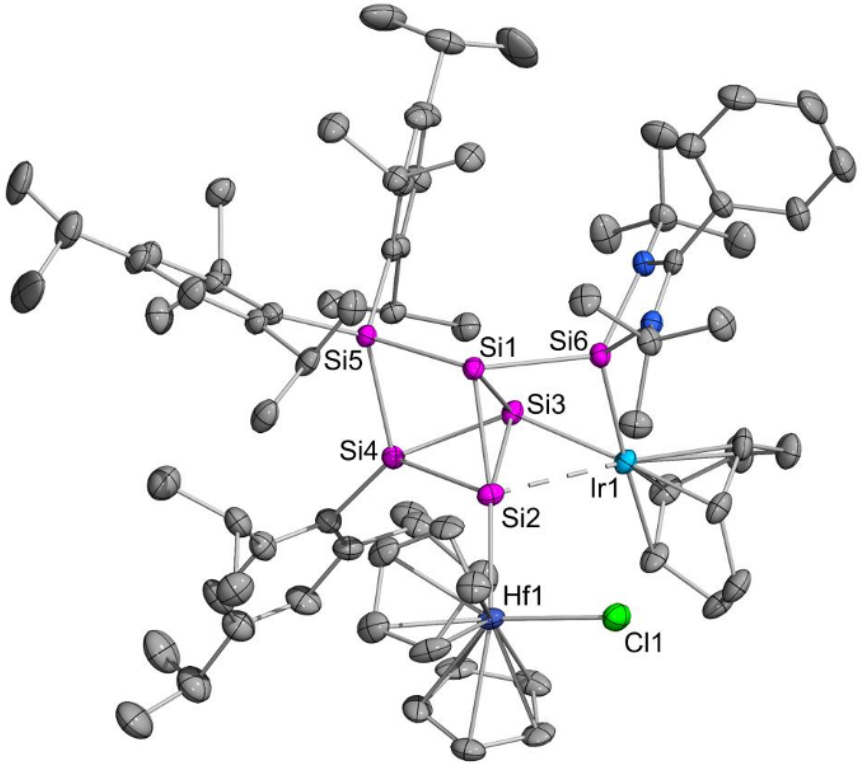

Supplementary Figure S25. Molecular structure of the hafnium complex **3b** in the solid state. Hydrogen atoms are omitted for clarity. Thermal ellipsoids represent 50% probability.

4 DFT Calculations

Computations were carried out with orca 5.0.4/6.0.1[S8] and the Gaussian 16 program package.[S9] Structural optimizations in the gas-phase, frequency analyses and single point calculations were performed at the B3LYP or PBE0/def2TZVPP level of theory [S10,11] for **2** and **3a,b** including the dispersion correction by Grimme.[S12] Tighter than default convergence had to be chosen for the scf (thightscf) in the TD-DFT calculation for **2**. Implicit correction for solvation effects (solvents: hexane or benzene) were investigated with the CPCM model for geometry optimizations for spectroscopy calculations.[S13]
Pictures of Kohn-Sham orbitals were displayed with ChemCraft 1.8.[S14]

4.1 Si_6Ir-Li 2

4.1.1 Optimization and single point

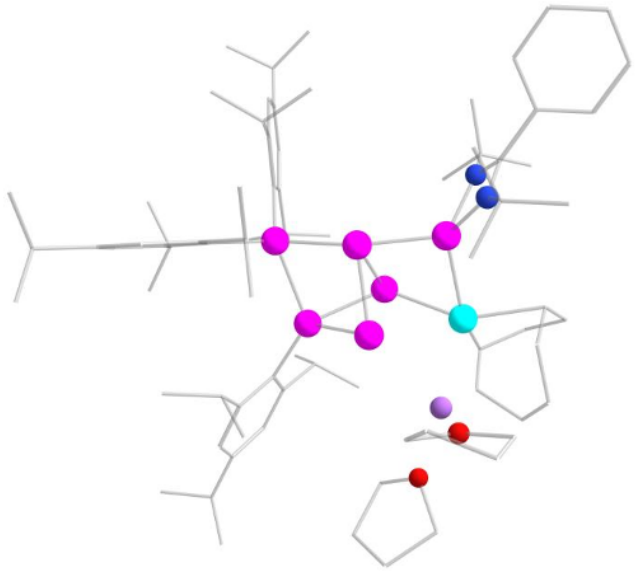

Supplementary Figure S26. Optimized molecular structure of Si_6Ir-Li **2** at the PBE0/def2-TZVPP level of theory.[S10c-e,11] Hydrogen atoms omitted for clarity.

Supplementary Table S5. Coordinates of the optimized geometry of Si_6Ir-Li **2** at the PBE0/def2-TZVPP level of theory.[S10c-e,11]

N	-4.003520	1.429997	-0.641711
N	-4.079205	0.511421	1.304294
Ir	-2.236352	-1.939778	-0.977011
Si	-0.566039	0.799395	0.538374
Si	0.006983	-1.467187	0.607132
Si	-0.486513	-0.353416	-1.564285
Si	1.713660	-0.476850	-0.741557
Si	1.509895	1.829638	0.109458
Si	-2.731759	0.177280	0.001477
C	-4.343464	-2.458043	-1.215834
H	-4.987477	-1.654359	-0.877117
C	-4.715009	-2.994602	-2.597061
H	-5.023935	-4.040604	-2.523957
H	-5.591585	-2.458305	-2.967219
C	-3.565450	-2.841285	-3.607125
H	-3.636641	-3.603863	-4.395877
H	-3.659058	-1.876972	-4.110048
C	-2.192354	-2.884098	-2.967422
H	-1.427516	-2.413509	-3.571432
C	-1.752323	-3.871596	-2.060260
H	-0.688535	-4.068889	-2.057884
C	3.318908	-1.444840	-1.247983
C	3.571022	-1.858713	-2.578651
C	4.659912	-2.687962	-2.857690
H	4.835500	-3.001199	-3.879889

C	5.536577	-3.126850	-1.875282
C	5.294568	-2.706129	-0.571726
H	5.966063	-3.026419	0.215501
C	4.218696	-1.884005	-0.239873
C	2.678465	-1.463832	-3.749296
H	2.032455	-0.652496	-3.413143
C	3.471281	-0.951365	-4.961368
H	2.792101	-0.543380	-5.712404
H	4.040733	-1.748367	-5.442772
H	4.173885	-0.167793	-4.677325
C	1.759910	-2.622866	-4.166178
H	1.149386	-2.962184	-3.329811
H	2.342859	-3.473242	-4.527944
H	1.086358	-2.311663	-4.967733
C	6.717046	-4.016385	-2.226552
H	6.655861	-4.212244	-3.301253
C	8.060032	-3.317165	-1.964810
H	8.121207	-2.370050	-2.502095
H	8.892057	-3.946767	-2.287903
H	8.195571	-3.105905	-0.902363
C	6.657535	-5.374139	-1.510460
H	6.721592	-5.254747	-0.427059
H	7.487539	-6.011801	-1.822513
H	5.726326	-5.897111	-1.733602
C	4.056162	-1.517025	1.233526
H	3.268771	-0.765102	1.305542
C	5.323855	-0.900058	1.842209
H	5.677262	-0.051472	1.260108
H	6.135951	-1.627211	1.906472
H	5.117432	-0.545709	2.853168
C	3.607689	-2.727145	2.068307
H	3.481309	-2.443197	3.115376
H	4.352808	-3.525157	2.028224
H	2.656515	-3.120914	1.709807
C	2.832752	2.244912	1.489651
C	4.102763	2.727161	1.078752
C	5.085887	3.030404	2.022680
H	6.043821	3.404966	1.681350
C	4.889447	2.870155	3.385269
C	3.652450	2.383617	3.788091
H	3.467024	2.241595	4.845629
C	2.632622	2.070607	2.888721
C	4.482022	2.964008	-0.381195
H	3.648764	2.645552	-1.003881
C	5.696713	2.134184	-0.826163
H	5.510654	1.066211	-0.717522
H	6.590766	2.383231	-0.252156

H	5.919306	2.326560	-1.877801
C	4.712060	4.458527	-0.660637
H	4.948112	4.623626	-1.713434
H	5.546354	4.843449	-0.071303
H	3.827160	5.046443	-0.418612
C	5.982148	3.218983	4.380872
H	6.849135	3.543272	3.797505
C	5.576802	4.390708	5.288524
H	5.298376	5.266082	4.700369
H	6.401206	4.671188	5.947926
H	4.723711	4.126635	5.916737
C	6.418734	2.004955	5.215061
H	5.598589	1.633000	5.832341
H	7.240900	2.271581	5.882844
H	6.752095	1.186366	4.576071
C	1.341821	1.544296	3.513522
H	0.604927	1.432399	2.721416
C	0.742682	2.503792	4.554693
H	0.606315	3.505790	4.149079
H	1.372556	2.589512	5.442182
H	-0.232953	2.137375	4.882274
C	1.534259	0.150308	4.130056
H	0.592776	-0.209560	4.552016
H	2.276200	0.168650	4.931554
H	1.856878	-0.569759	3.379421
C	1.209805	3.455553	-0.934243
C	0.687789	4.581180	-0.237459
C	0.416209	5.770517	-0.912013
H	0.027356	6.608719	-0.346858
C	0.623248	5.917724	-2.277436
C	1.114261	4.814699	-2.957336
H	1.274810	4.902136	-4.025285
C	1.411616	3.601909	-2.329211
C	0.370056	4.576868	1.256348
H	0.647356	3.608415	1.663856
C	1.184825	5.628490	2.025092
H	0.941997	6.641615	1.699937
H	2.254645	5.476274	1.882823
H	0.977275	5.569116	3.095393
C	-1.135764	4.743593	1.517418
H	-1.498473	5.714086	1.173319
H	-1.348311	4.669867	2.586672
H	-1.707394	3.968589	1.004432
C	0.346209	7.223095	-3.002746
H	0.493224	7.028041	-4.069307
C	1.343882	8.319557	-2.595685
H	1.174317	9.231378	-3.172817

H	2.372333	7.997182	-2.762909
H	1.242042	8.570286	-1.537764
C	-1.100501	7.704086	-2.819767
H	-1.310300	7.945738	-1.776051
H	-1.813207	6.940803	-3.134923
H	-1.283235	8.604911	-3.409598
C	1.938401	2.500260	-3.244059
H	2.173544	1.634916	-2.623879
C	3.225078	2.910421	-3.981702
H	3.049742	3.751457	-4.654389
H	3.594479	2.080874	-4.585667
H	4.013954	3.200490	-3.289955
C	0.872781	2.060769	-4.260655
H	-0.034256	1.724762	-3.760673
H	1.244285	1.236690	-4.871878
H	0.610011	2.880007	-4.932989
C	-4.712936	1.356685	0.490071
C	-4.326117	2.098154	-1.928969
H	-5.635332	3.726968	-1.238846
C	-3.077760	2.022998	-2.814077
H	-3.284317	2.508679	-3.768393
H	-2.791169	0.991322	-3.006745
H	-2.231596	2.527219	-2.348662
C	-5.478757	1.364936	-2.637046
H	-5.232029	0.312768	-2.776975
H	-5.653702	1.807808	-3.619139
C	-4.680503	3.582760	-1.737329
H	-4.744638	4.060178	-2.716149
H	-3.904777	4.093085	-1.165721
H	-6.407342	1.435048	-2.072192
C	-4.336932	0.143680	2.713194
C	-4.251506	1.369639	3.639919
H	-5.059670	2.074116	3.458057
H	-3.300206	1.884138	3.501557
H	-4.318073	1.049750	4.681387
C	-3.238004	-0.844244	3.124725
H	-3.403068	-1.156122	4.157119
H	-5.782265	-1.398216	2.191408
H	-2.250179	-0.390905	3.051959
C	-5.702070	-0.548062	2.870070
H	-5.813262	-0.915633	3.891932
H	-6.528516	0.130999	2.671872
H	-3.240992	-1.725862	2.486132
C	-8.392187	2.207549	0.790604
C	-8.339940	3.470619	1.368932
C	-7.217820	1.519470	0.506739
H	-9.254256	4.005335	1.589878

H	-7.264950	0.533962	0.063617
C	-7.107176	4.044568	1.661356
C	-5.977847	2.090815	0.795252
H	-7.057761	5.028381	2.109001
C	-5.932958	3.359745	1.375627
H	-4.976779	3.814520	1.595801
H	-9.347189	1.754388	0.559591
C	-3.789520	-3.278426	-0.185321
H	-4.089584	-3.041862	0.831797
C	-3.496066	-4.756421	-0.392533
H	-2.982058	-5.137396	0.496735
H	-4.430003	-5.334497	-0.439442
C	-2.630389	-5.046376	-1.638967
H	-1.992278	-5.909387	-1.438136
H	-3.269206	-5.345221	-2.472905
Li	-1.039881	-3.832940	0.808605
C	-2.288139	-4.987424	4.845261
C	-2.659124	-4.854159	3.370520
C	-0.443321	-4.054753	3.670226
C	-1.175986	-3.943360	4.999800
H	-1.903072	-5.987167	5.055226
H	-3.438518	-4.105328	3.216322
H	-2.984260	-5.792458	2.920604
H	0.022811	-3.130149	3.333614
H	-1.600096	-2.945322	5.116176
H	-0.521824	-4.136250	5.848813
H	-3.140495	-4.811422	5.500074
H	0.310995	-4.846432	3.691884
O	-1.458494	-4.413907	2.696278
C	1.686256	-6.966105	1.151639
C	0.222324	-6.652002	0.851462
C	1.391904	-5.186400	-0.490212
C	2.455561	-6.129296	0.101809
H	1.899911	-8.031996	1.082041
H	-0.433242	-6.685344	1.718558
H	-0.177925	-7.315125	0.075388
H	1.111049	-5.490508	-1.501960
H	3.267584	-5.569190	0.559013
H	2.886655	-6.757607	-0.676268
H	1.937962	-6.638917	2.160328
O	0.235055	-5.304148	0.366895
H	1.681527	-4.138992	-0.502534

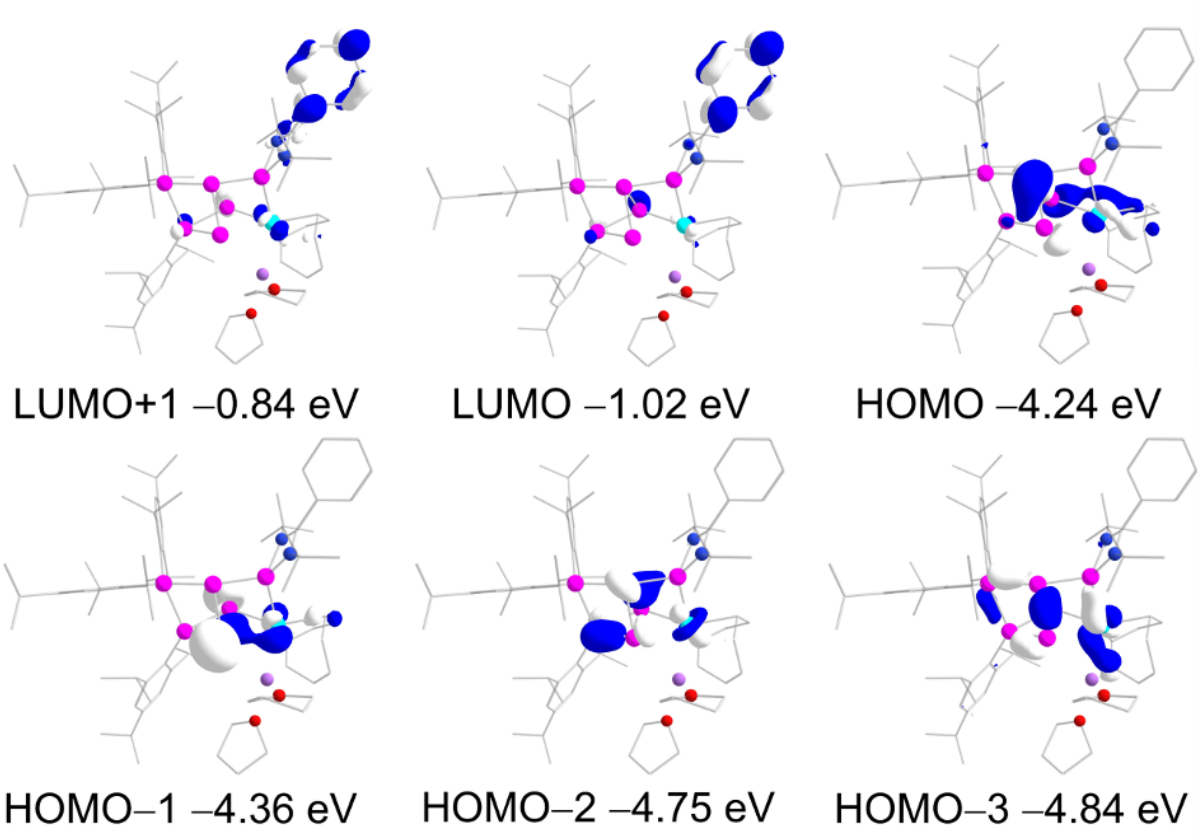

Supplementary Figure S27. Selected molecular orbitals of Si_6Ir-Li **2** at the PBE0/def2-TZVPP level of theory.[S10c-e,11]

4.1.2 Experimental vs. calculated NMR shifts

Supplementary Table S6. Comparison of experimental vs. calculated NMR chemical shifts for compound **2** at the PBE0/def2-TZVPP level of theory.[S10c-e,11]

	Exp. **2** $\delta(^{29}Si)$ [ppm]	Calc. **2** $\delta(^{29}Si)$ [ppm]
Si4 (SiTip)	149.6	163.8
Si6 (NHSi)	109.3	63.8
Si5 (SiTip2)	34.7	56.5
Si3 (unsubstituted)	−104.0	−125.6
Si1 (unsubstituted)	−178.4	−132.4
Si2 (SiLi)	−230.7	−228.1

4.1.3 TD-DFT calculations

Supplementary Table S7. Transition Energy, wavelength, and oscillator strengths of the electronic transition of **2** calculated at the TD-PBE0/def2-TZVPP[S10c-e,11] level of theory (the 354th orbital is the highest occupied orbital (HOMO), the 355th orbital is the lowest unoccupied orbital (LUMO) shown in Supplementary Figure S27).

STATE 1:	E= 0.086317 au	2.349 eV	18944.5 cm**-1	<S**2> = 0.000000
352a -> 355a :	0.025043 (c= -0.15825039)			
353a -> 355a :	0.119009 (c= 0.34497659)			

354a -> 355a : 0.780130 (c= -0.88324964)
354a -> 356a : 0.041454 (c= 0.20360142)

STATE 2: E= 0.096573 au 2.628 eV 21195.3 cm**-1 <S**2> = 0.000000
352a -> 355a : 0.014257 (c= -0.11940426)
353a -> 355a : 0.747358 (c= -0.86449849)
353a -> 356a : 0.045571 (c= 0.21347460)
354a -> 355a : 0.105743 (c= -0.32518084)

STATE 3: E= 0.104750 au 2.850 eV 22990.0 cm**-1 <S**2> = 0.000000
350a -> 355a : 0.016180 (c= -0.12720221)
351a -> 355a : 0.465084 (c= -0.68197088)
351a -> 356a : 0.033331 (c= 0.18256717)
352a -> 355a : 0.252146 (c= 0.50214093)
352a -> 356a : 0.019937 (c= -0.14119824)
354a -> 355a : 0.024805 (c= -0.15749643)
354a -> 358a : 0.126904 (c= -0.35623528)

STATE 4: E= 0.106014 au 2.885 eV 23267.4 cm**-1 <S**2> = 0.000000
350a -> 355a : 0.010256 (c= -0.10127226)
351a -> 355a : 0.054853 (c= -0.23420798)
352a -> 355a : 0.057100 (c= 0.23895615)
353a -> 358a : 0.012092 (c= -0.10996332)
354a -> 356a : 0.015019 (c= -0.12255032)
354a -> 358a : 0.777601 (c= 0.88181668)
354a -> 359a : 0.010213 (c= -0.10105993)
354a -> 360a : 0.011501 (c= -0.10724418)

STATE 5: E= 0.108957 au 2.965 eV 23913.3 cm**-1 <S**2> = 0.000000
350a -> 355a : 0.019609 (c= -0.14003041)
351a -> 355a : 0.351928 (c= 0.59323535)
351a -> 356a : 0.026662 (c= -0.16328523)
351a -> 358a : 0.011981 (c= -0.10945658)
352a -> 355a : 0.392372 (c= 0.62639634)
352a -> 356a : 0.029236 (c= -0.17098616)
353a -> 358a : 0.019052 (c= 0.13802776)
354a -> 355a : 0.025053 (c= -0.15828021)
354a -> 356a : 0.049962 (c= -0.22352213)

STATE 6: E= 0.110015 au 2.994 eV 24145.4 cm**-1 <S**2> = 0.000000
350a -> 355a : 0.037823 (c= -0.19448192)

352a -> 355a : 0.042958 (c= 0.20726424)
354a -> 355a : 0.030581 (c= 0.17487438)
354a -> 356a : 0.824560 (c= 0.90805287)
354a -> 359a : 0.012751 (c= -0.11291919)

STATE 7: E= 0.112359 au 3.057 eV 24659.9 cm**-1 <S**2> = 0.000000
350a -> 355a : 0.015053 (c= 0.12268916)
353a -> 355a : 0.013355 (c= -0.11556420)
353a -> 356a : 0.031876 (c= -0.17853884)
353a -> 358a : 0.842142 (c= 0.91768291)
353a -> 359a : 0.010692 (c= -0.10340175)
353a -> 360a : 0.013885 (c= -0.11783457)
354a -> 358a : 0.017342 (c= 0.13169027)

STATE 8: E= 0.114068 au 3.104 eV 25034.9 cm**-1 <S**2> = 0.000000
350a -> 355a : 0.785383 (c= -0.88621826)
350a -> 356a : 0.049204 (c= 0.22182005)
352a -> 355a : 0.057413 (c= -0.23961054)
353a -> 356a : 0.010010 (c= -0.10004820)
353a -> 358a : 0.013348 (c= 0.11553288)
354a -> 356a : 0.018957 (c= -0.13768535)
354a -> 360a : 0.010756 (c= 0.10371112)

STATE 9: E= 0.115253 au 3.136 eV 25295.2 cm**-1 <S**2> = 0.000000
353a -> 355a : 0.051500 (c= -0.22693617)
353a -> 356a : 0.866596 (c= -0.93091126)
353a -> 358a : 0.029305 (c= -0.17118788)
353a -> 359a : 0.022462 (c= 0.14987372)

STATE 10: E= 0.118964 au 3.237 eV 26109.5 cm**-1 <S**2> = 0.000000
354a -> 357a : 0.981156 (c= -0.99053304)

STATE 11: E= 0.120989 au 3.292 eV 26554.0 cm**-1 <S**2> = 0.000000
354a -> 356a : 0.016082 (c= 0.12681322)
354a -> 357a : 0.013803 (c= -0.11748776)
354a -> 358a : 0.030064 (c= 0.17338990)
354a -> 359a : 0.753038 (c= 0.86777759)
354a -> 360a : 0.129971 (c= 0.36051552)

STATE 12: E= 0.124346 au 3.384 eV 27290.8 cm**-1 <S**2> = 0.000000
353a -> 357a : 0.969806 (c= -0.98478707)

353a -> 359a : 0.019472 (c= -0.13954308)

STATE 13: E= 0.124716 au 3.394 eV 27372.1 cm**-1 <S**2> = 0.000000
351a -> 358a : 0.014575 (c= 0.12072508)
352a -> 358a : 0.445379 (c= 0.66736718)
352a -> 359a : 0.019287 (c= -0.13887882)
353a -> 360a : 0.013934 (c= -0.11804188)
354a -> 359a : 0.067341 (c= -0.25950080)
354a -> 360a : 0.330854 (c= 0.57519917)
354a -> 361a : 0.032958 (c= 0.18154363)
354a -> 366a : 0.010713 (c= -0.10350341)

STATE 14: E= 0.125753 au 3.422 eV 27599.6 cm**-1 <S**2> = 0.000000
349a -> 355a : 0.014350 (c= -0.11979132)
351a -> 358a : 0.020051 (c= 0.14160023)
352a -> 358a : 0.114345 (c= 0.33814949)
353a -> 357a : 0.016480 (c= 0.12837497)
353a -> 359a : 0.565328 (c= -0.75188312)
354a -> 359a : 0.011531 (c= 0.10738452)
354a -> 360a : 0.172566 (c= -0.41541117)

STATE 15: E= 0.126005 au 3.429 eV 27654.9 cm**-1 <S**2> = 0.000000
351a -> 358a : 0.064877 (c= -0.25470905)
352a -> 358a : 0.220097 (c= -0.46914493)
353a -> 358a : 0.023479 (c= -0.15322880)
353a -> 359a : 0.305257 (c= -0.55250083)
353a -> 360a : 0.091149 (c= -0.30190838)
354a -> 359a : 0.071144 (c= -0.26672823)
354a -> 360a : 0.132795 (c= 0.36441020)

STATE 16: E= 0.127564 au 3.471 eV 27997.0 cm**-1 <S**2> = 0.000000
347a -> 355a : 0.039910 (c= 0.19977598)
349a -> 355a : 0.661326 (c= -0.81321924)
349a -> 356a : 0.045193 (c= 0.21258682)
351a -> 358a : 0.071443 (c= -0.26728895)
352a -> 355a : 0.011627 (c= -0.10782631)
352a -> 356a : 0.077182 (c= -0.27781689)

STATE 17: E= 0.128860 au 3.506 eV 28281.5 cm**-1 <S**2> = 0.000000
351a -> 358a : 0.229111 (c= -0.47865547)
352a -> 356a : 0.035456 (c= 0.18829799)

353a -> 360a : 0.547197 (c= 0.73972744)
353a -> 361a : 0.031999 (c= 0.17888132)
353a -> 366a : 0.013761 (c= -0.11730625)
353a -> 367a : 0.018366 (c= 0.13552191)
354a -> 360a : 0.029094 (c= 0.17056934)

STATE 18: E= 0.129402 au 3.521 eV 28400.5 cm**-1 <S**2> = 0.000000
349a -> 355a : 0.092068 (c= -0.30342664)
351a -> 358a : 0.014480 (c= 0.12033186)
352a -> 355a : 0.049633 (c= 0.22278529)
352a -> 356a : 0.749328 (c= 0.86563734)
352a -> 359a : 0.013173 (c= -0.11477157)
353a -> 360a : 0.014373 (c= -0.11988929)

STATE 19: E= 0.130273 au 3.545 eV 28591.6 cm**-1 <S**2> = 0.000000
349a -> 355a : 0.018787 (c= 0.13706747)
350a -> 358a : 0.110574 (c= -0.33252732)
351a -> 358a : 0.383557 (c= -0.61931951)
352a -> 356a : 0.025613 (c= 0.16004060)
352a -> 358a : 0.088379 (c= 0.29728551)
353a -> 359a : 0.013837 (c= 0.11763114)
353a -> 360a : 0.127553 (c= -0.35714528)
353a -> 361a : 0.014923 (c= -0.12215982)
354a -> 360a : 0.052368 (c= -0.22883978)

STATE 20: E= 0.132199 au 3.597 eV 29014.4 cm**-1 <S**2> = 0.000000
351a -> 355a : 0.065982 (c= 0.25686865)
351a -> 356a : 0.877305 (c= 0.93664552)
351a -> 359a : 0.010405 (c= -0.10200492)

STATE 21: E= 0.134330 au 3.655 eV 29482.1 cm**-1 <S**2> = 0.000000
350a -> 358a : 0.026559 (c= -0.16296928)
353a -> 361a : 0.019816 (c= -0.14076905)
354a -> 360a : 0.028544 (c= -0.16894829)
354a -> 361a : 0.845602 (c= 0.91956618)

STATE 22: E= 0.137756 au 3.749 eV 30234.0 cm**-1 <S**2> = 0.000000
350a -> 358a : 0.345112 (c= 0.58746230)
350a -> 359a : 0.018897 (c= -0.13746523)
351a -> 358a : 0.045931 (c= -0.21431531)
352a -> 355a : 0.011729 (c= -0.10830108)

352a -> 357a : 0.064097 (c= -0.25317344)
352a -> 359a : 0.344302 (c= -0.58677228)
354a -> 360a : 0.015036 (c= -0.12262134)
354a -> 361a : 0.029557 (c= 0.17192251)
354a -> 366a : 0.014344 (c= -0.11976806)

STATE 23: E= 0.138378 au 3.765 eV 30370.5 cm**-1 <S**2> = 0.000000
350a -> 356a : 0.010723 (c= 0.10355355)
350a -> 358a : 0.204649 (c= 0.45238107)
350a -> 359a : 0.010135 (c= -0.10067306)
351a -> 358a : 0.023051 (c= -0.15182562)
352a -> 357a : 0.506833 (c= 0.71192205)
352a -> 358a : 0.015600 (c= 0.12489905)
352a -> 359a : 0.116432 (c= 0.34122081)
354a -> 362a : 0.012447 (c= -0.11156446)

STATE 24: E= 0.138701 au 3.774 eV 30441.4 cm**-1 <S**2> = 0.000000
350a -> 356a : 0.011927 (c= 0.10921232)
350a -> 358a : 0.072656 (c= 0.26954714)
352a -> 357a : 0.412662 (c= -0.64238777)
352a -> 359a : 0.362965 (c= 0.60246600)
353a -> 361a : 0.040729 (c= -0.20181333)
354a -> 362a : 0.013586 (c= -0.11656028)

STATE 25: E= 0.139017 au 3.783 eV 30510.7 cm**-1 <S**2> = 0.000000
352a -> 359a : 0.019837 (c= -0.14084325)
353a -> 360a : 0.036589 (c= 0.19128162)
353a -> 361a : 0.764663 (c= -0.87445015)
354a -> 361a : 0.022762 (c= -0.15087061)
354a -> 362a : 0.059779 (c= 0.24449698)
354a -> 363a : 0.013945 (c= -0.11808899)
354a -> 366a : 0.028617 (c= -0.16916633)

STATE 26: E= 0.139187 au 3.787 eV 30548.0 cm**-1 <S**2> = 0.000000
348a -> 355a : 0.028458 (c= -0.16869502)
349a -> 356a : 0.010898 (c= -0.10439428)
350a -> 355a : 0.041592 (c= -0.20394196)
350a -> 356a : 0.651378 (c= -0.80708011)
350a -> 358a : 0.030954 (c= 0.17593842)
351a -> 359a : 0.014616 (c= 0.12089761)
353a -> 361a : 0.019892 (c= -0.14104055)

354a -> 362a : 0.072182 (c= -0.26866640)
354a -> 363a : 0.012642 (c= 0.11243498)
354a -> 366a : 0.040198 (c= 0.20049416)

STATE 27: E= 0.139592 au 3.798 eV 30637.0 cm**-1 <S**2> = 0.000000
350a -> 356a : 0.163182 (c= -0.40395741)
351a -> 358a : 0.021900 (c= -0.14798785)
352a -> 359a : 0.038625 (c= 0.19653250)
353a -> 361a : 0.055918 (c= 0.23646950)
354a -> 362a : 0.366002 (c= 0.60498063)
354a -> 363a : 0.058170 (c= -0.24118380)
354a -> 364a : 0.017157 (c= -0.13098629)
354a -> 366a : 0.174603 (c= -0.41785562)

STATE 28: E= 0.141513 au 3.851 eV 31058.5 cm**-1 <S**2> = 0.000000
351a -> 357a : 0.942699 (c= -0.97092702)
351a -> 359a : 0.010075 (c= -0.10037312)
352a -> 360a : 0.016365 (c= 0.12792736)

STATE 29: E= 0.141879 au 3.861 eV 31138.7 cm**-1 <S**2> = 0.000000
346a -> 355a : 0.027680 (c= 0.16637325)
348a -> 355a : 0.127126 (c= 0.35654793)
348a -> 356a : 0.011794 (c= -0.10859997)
350a -> 356a : 0.031828 (c= -0.17840275)
350a -> 358a : 0.029644 (c= -0.17217409)
351a -> 357a : 0.023325 (c= 0.15272371)
351a -> 359a : 0.034896 (c= -0.18680355)
352a -> 360a : 0.170343 (c= 0.41272682)
352a -> 361a : 0.012851 (c= 0.11336076)
353a -> 362a : 0.016007 (c= 0.12651889)
354a -> 360a : 0.012649 (c= -0.11246591)
354a -> 362a : 0.190834 (c= -0.43684517)
354a -> 363a : 0.049295 (c= -0.22202381)
354a -> 364a : 0.012456 (c= 0.11160587)
354a -> 366a : 0.098772 (c= -0.31428010)
354a -> 367a : 0.050926 (c= 0.22566726)

STATE 30: E= 0.142029 au 3.865 eV 31171.7 cm**-1 <S**2> = 0.000000
351a -> 357a : 0.017573 (c= 0.13256295)
351a -> 359a : 0.060322 (c= -0.24560437)
351a -> 360a : 0.021520 (c= -0.14669851)

352a -> 359a : 0.017418 (c= -0.13197614)
352a -> 360a : 0.358032 (c= 0.59835763)
352a -> 361a : 0.013260 (c= 0.11515231)
353a -> 366a : 0.037428 (c= -0.19346226)
354a -> 362a : 0.055759 (c= 0.23613413)
354a -> 363a : 0.068299 (c= 0.26134051)
354a -> 364a : 0.019393 (c= -0.13925826)
354a -> 366a : 0.142448 (c= 0.37742323)
354a -> 367a : 0.055738 (c= -0.23608940)

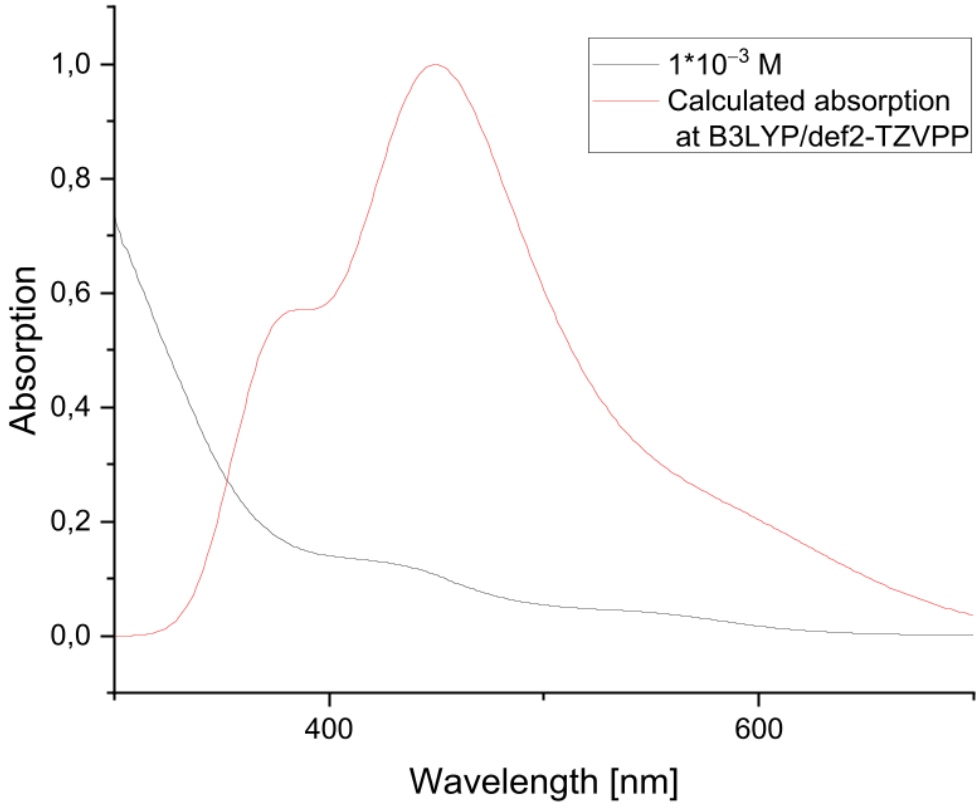

Supplementary Figure S28. Experimental vs. calculated UV-Vis absorption bands of compound **2** at the PBE0/def2-TZVPP[S10c-e,11] level of theory.

4.2 Si_6Ir-Zr 3a

4.2.1 Optimization and single point

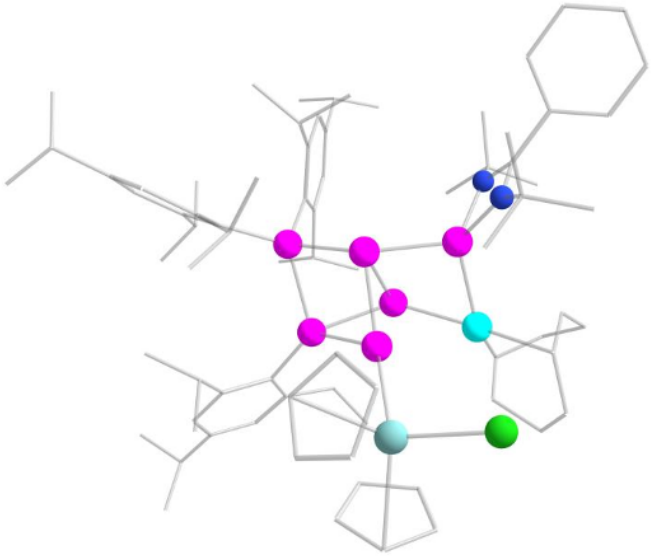

Supplementary Figure S29. Optimized molecular structure of Si_6Ir-Zr **3a** at the PBE0P/def2-TZVPP level of theory.[S10c-e,11] Hydrogen atoms omitted for clarity.

Supplementary Table S8. Coordinates of the optimized geometry of Si_6Ir-Zr **3a** at the PBE0P/def2-TZVPP level of theory.[S10c-e,11]

Ir	-2.772602	-0.703089	-1.303284
Zr	-1.380561	-3.857932	1.770778
Cl	-3.796549	-3.706606	2.033641
Si	1.916248	1.177483	0.366894
Si	-0.324514	0.704357	0.935874
Si	-2.475699	1.131262	0.140038
Si	-0.526737	0.006905	-1.407384
Si	-0.604042	-1.548621	0.403805
Si	1.474809	-0.938050	-0.694749
N	-3.707687	1.747736	1.419813
N	-3.034639	2.870210	-0.277799
C	1.885793	2.837591	-0.636828
C	1.623595	4.006194	0.117407
C	1.601962	5.254805	-0.497965
H	1.403045	6.134523	0.106614
C	1.835448	5.419332	-1.851273
C	2.079227	4.272864	-2.589598
H	2.259466	4.366595	-3.655326
C	2.106474	3.000719	-2.025602
C	2.376890	1.865722	-2.998844
H	2.384682	0.929517	-2.432946
C	1.269624	1.768924	-4.046545
H	1.471259	0.953132	-4.742459
H	1.200703	2.689792	-4.630413
H	0.296214	1.591859	-3.585819

C	3.726713	1.991881	-3.705852
H	4.556800	2.039273	-3.003152
H	3.768097	2.885651	-4.332782
H	3.889059	1.128390	-4.354709
C	1.349396	3.997346	1.609783
H	1.411993	2.966143	1.958172
C	2.387746	4.793308	2.395925
H	2.188691	4.719707	3.467898
H	2.367317	5.852217	2.126808
H	3.394606	4.415755	2.213550
C	-0.064618	4.480111	1.924726
H	-0.260476	4.409498	2.998323
H	-0.808511	3.877808	1.398516
H	-0.202036	5.524238	1.631110
C	1.828744	6.790173	-2.485573
H	1.607055	7.507471	-1.687916
C	0.737346	6.922606	-3.544788
H	-0.246911	6.702018	-3.127762
H	0.909430	6.233557	-4.375198
H	0.716609	7.935757	-3.953491
C	3.195281	7.149502	-3.064457
H	3.975223	7.089754	-2.303418
H	3.188673	8.164356	-3.469469
H	3.469175	6.470019	-3.875103
C	3.383574	1.363773	1.623421
C	3.255831	1.123397	3.011412
C	4.273250	1.506696	3.881996
H	4.141557	1.348551	4.947266
C	5.459844	2.070558	3.448163
C	5.622473	2.212944	2.080131
H	6.558059	2.606914	1.697697
C	4.625602	1.874943	1.171337
C	4.976653	2.068050	-0.292584
H	4.124379	1.739202	-0.888860
C	6.168757	1.209912	-0.717746
H	7.060694	1.442659	-0.132093
H	6.409997	1.393955	-1.767626
H	5.962005	0.145036	-0.608980
C	5.241021	3.537173	-0.616716
H	4.379734	4.159889	-0.373804
H	5.462509	3.666050	-1.678325
H	6.100772	3.909125	-0.054337
C	2.066678	0.421438	3.644558
H	1.475923	-0.021793	2.837780
C	1.155043	1.376811	4.411209
H	0.338233	0.826333	4.885631
H	0.711657	2.127299	3.756427

H	1.708281	1.897015	5.197321
C	2.512396	-0.711360	4.569031
H	3.035464	-0.331859	5.448710
H	3.185426	-1.404136	4.060672
H	1.648523	-1.273590	4.926282
H	8.569489	1.986897	4.972655
H	7.172168	4.291071	3.402997
C	2.831428	-2.045337	-1.482852
C	3.857018	-2.563077	-0.660324
C	4.914133	-3.268791	-1.225226
H	5.691079	-3.656679	-0.574859
C	5.000787	-3.501585	-2.588336
C	3.970458	-3.027132	-3.385984
H	4.016853	-3.221746	-4.451197
C	2.891261	-2.318458	-2.869218
C	1.772040	-1.923186	-3.810716
H	1.348662	-0.985224	-3.439170
C	2.206654	-1.698524	-5.253813
H	3.063859	-1.026412	-5.325561
H	1.383481	-1.261859	-5.823432
H	2.471714	-2.634825	-5.750840
C	0.656018	-2.965207	-3.763127
H	0.239506	-3.045681	-2.758103
H	1.032047	-3.948402	-4.058205
H	-0.157016	-2.693436	-4.440844
C	3.825242	-2.469672	0.854798
H	3.006137	-1.795912	1.135433
C	5.105574	-1.915206	1.469725
H	5.019049	-1.885809	2.558049
H	5.309611	-0.901180	1.132239
H	5.969640	-2.538629	1.229417
C	3.521017	-3.847577	1.442697
H	4.300152	-4.562727	1.168837
H	2.570875	-4.232343	1.070666
H	3.478841	-3.806612	2.534260
C	6.162514	-4.254733	-3.192349
H	5.979403	-4.307487	-4.270818
C	6.247354	-5.685860	-2.666769
H	5.316272	-6.228082	-2.840854
H	6.445230	-5.699253	-1.592245
H	7.057074	-6.229817	-3.158920
C	7.482806	-3.517423	-2.980887
H	7.724712	-3.443097	-1.917994
H	7.439316	-2.503915	-3.383294
H	8.302910	-4.046296	-3.472315
C	-3.866679	2.890431	0.765677
C	-4.797147	3.988097	1.132507

C	-6.127777	3.948079	0.729639
H	-6.487482	3.109680	0.145585
C	-6.992243	4.977237	1.073304
H	-8.025780	4.938922	0.751724
C	-6.535503	6.047833	1.826383
H	-7.211635	6.850028	2.095682
C	-5.209548	6.088539	2.235094
H	-4.847371	6.921653	2.824926
C	-4.342654	5.065579	1.888584
H	-3.306560	5.099951	2.202729
C	-2.989501	3.753227	-1.456580
C	-1.741673	3.383629	-2.245854
H	-0.841677	3.503173	-1.640561
H	-1.655465	4.032340	-3.118855
H	-1.793037	2.348975	-2.585526
C	-2.890714	5.229547	-1.075551
H	-3.798678	5.604894	-0.607696
H	-2.721546	5.812849	-1.982889
H	-2.047954	5.400346	-0.403772
C	-4.221025	3.517240	-2.331644
H	-4.300962	2.460446	-2.588931
H	-4.138876	4.093371	-3.255909
H	-5.137014	3.827390	-1.826240
C	-4.285706	1.269579	2.680936
C	-4.094817	2.277081	3.814636
H	-4.393693	1.816356	4.758389
H	-4.698636	3.172622	3.677516
H	-3.045418	2.567280	3.896003
C	-3.536206	-0.006069	3.042421
H	-3.964953	-0.439844	3.947186
H	-2.482608	0.212703	3.221446
H	-3.598524	-0.748462	2.245427
C	-5.769916	0.946471	2.506983
H	-6.152786	0.474247	3.414049
H	-5.920105	0.255985	1.675509
H	-6.357523	1.846868	2.326086
C	-2.988788	-1.079903	-3.436278
H	-2.069322	-0.786810	-3.932950
C	-2.991967	-2.337905	-2.812996
H	-2.066981	-2.897949	-2.883804
C	-4.254036	-3.152633	-2.621292
H	-4.006160	-4.215990	-2.679943
H	-4.933102	-2.968918	-3.458447
C	-4.949307	-2.870365	-1.285660
H	-6.030968	-3.050797	-1.369192
H	-4.586034	-3.573057	-0.535073
C	-4.690460	-1.482295	-0.755870

H	-4.844221	-1.399477	0.317274
C	-4.869718	-0.304240	-1.535167
H	-5.162994	0.589686	-0.991095
C	-5.367496	-0.345640	-2.970083
H	-5.988632	0.532082	-3.166947
H	-6.024404	-1.208501	-3.106028
C	-4.212815	-0.381791	-3.971244
H	-4.525712	-0.848154	-4.916375
H	-3.922217	0.641749	-4.221250
C	-0.155413	-4.777274	-0.241350
H	0.591539	-4.178605	-0.738900
C	-1.535637	-4.827389	-0.558507
H	-2.030876	-4.229493	-1.305602
C	-2.148090	-5.755906	0.299325
H	-3.198726	-5.994976	0.325815
C	-1.165508	-6.255311	1.180047
H	-1.320665	-6.989669	1.956045
C	0.072650	-5.663602	0.824691
H	1.028316	-5.873372	1.277361
C	-1.207519	-4.495955	4.179735
H	-1.774395	-5.347208	4.525215
C	0.111629	-4.519305	3.672635
H	0.732045	-5.395142	3.570159
C	0.466511	-3.206047	3.319213
H	1.396832	-2.890607	2.877720
C	-0.620317	-2.357175	3.647510
H	-0.652306	-1.292768	3.478538
C	-1.641215	-3.150675	4.189187
H	-2.614561	-2.807415	4.497767
C	6.530897	2.486029	4.428098
C	7.829629	1.711167	4.217419
H	7.663490	0.634222	4.278277
H	8.261213	1.926970	3.237232
C	6.783140	3.991407	4.379100
H	7.517148	4.284628	5.133584
H	5.865034	4.553781	4.558064
H	6.156982	2.242633	5.428480

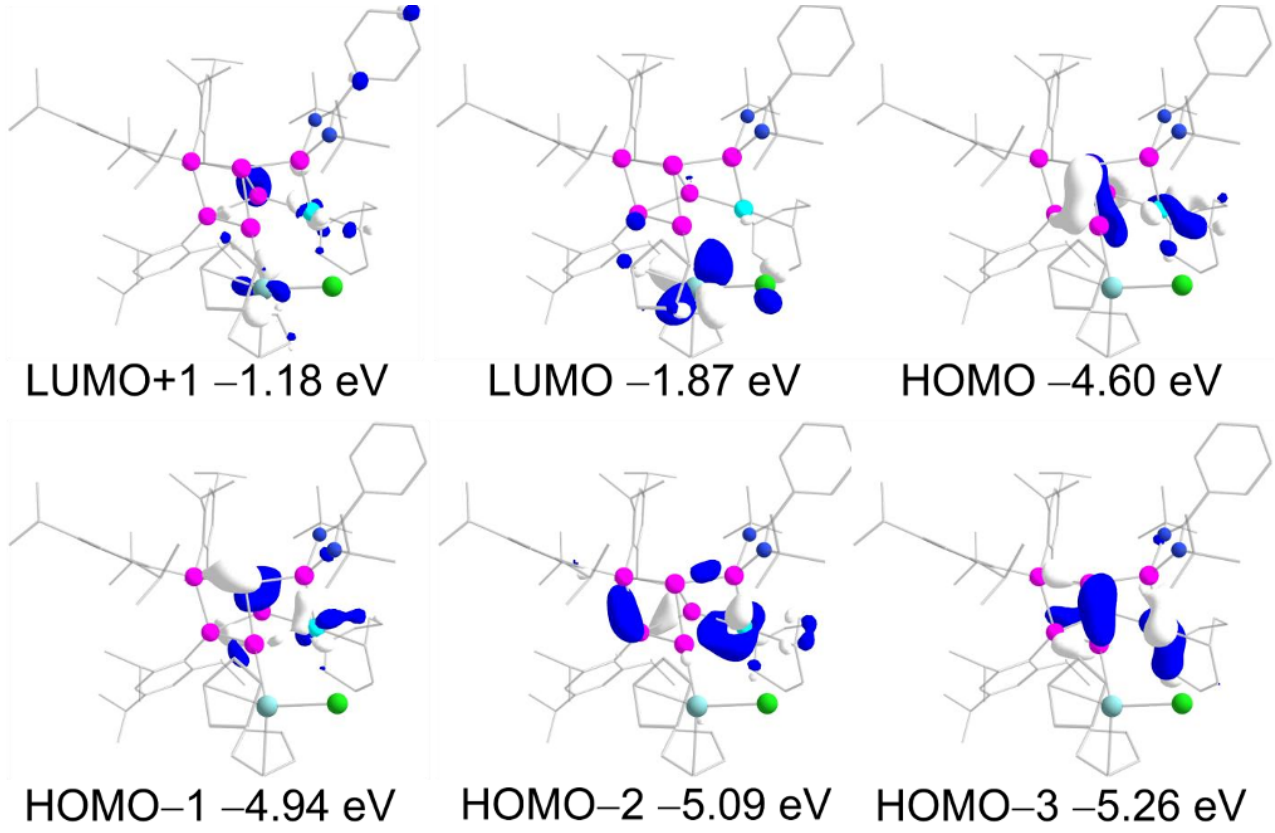

Supplementary Figure S30. Selected molecular orbitals of Si_6Ir-Zr **3a** at the PBE0/def2-TZVPP level of theory.[S10c-e,11]

4.2.2 Experimental vs. calculated NMR shifts

Supplementary Table S9. Comparison of experimental vs. calculated NMR chemical shifts for compound **3a** at the PBE0//def2-TZVPP level of theory.[S10c-e,11]

	Exp. **3a** $\delta(^{29}Si)$ [ppm]	Calc. **3a** $\delta(^{29}Si)$ [ppm]
Si4 (SiTip)	73.7	83.8
Si6 (NHSi)	73.5	61.9
Si5 (SiTip2)	30.5	33.4
Si3 (unsubstituted)	−41.0	−30.1
Si1 (unsubstituted)	−131.9	−168.5
Si2 (SiZr)	−77.9	−67.5

4.2.3 TD-DFT calculations

Supplementary Table S10. Transition Energy, wavelength, and oscillator strengths of the electronic transition of **3a** calculated at the TD-PBE0/def2-TZVPP level of theory [S10c-e,11] (the 362nd orbital is the highest occupied orbital (HOMO), the 363th ortbital is the lowest unoccupied orbital (LUMO) shown in Supplementary Figure S30).

STATE 1: E= 0.071609 au 1.949 eV 15716.3 cm**-1 <S**2> = 0.000000 Mult 1

361a -> 363a : 0.019195 (c= 0.13854517)
362a -> 363a : 0.953738 (c= -0.97659500)

STATE 2: E= 0.084446 au 2.298 eV 18533.8 cm**-1 <S**2> = 0.000000 Mult 1
359a -> 363a : 0.015308 (c= -0.12372531)
360a -> 364a : 0.011827 (c= -0.10875261)
361a -> 363a : 0.904576 (c= 0.95109195)
362a -> 363a : 0.013776 (c= 0.11737081)

STATE 3: E= 0.088659 au 2.413 eV 19458.4 cm**-1 <S**2> = 0.000000 Mult 1
359a -> 363a : 0.015795 (c= -0.12567712)
360a -> 363a : 0.923408 (c= -0.96094111)
362a -> 364a : 0.023071 (c= -0.15189298)

STATE 4: E= 0.094816 au 2.580 eV 20809.7 cm**-1 <S**2> = 0.000000 Mult 1
359a -> 363a : 0.332066 (c= 0.57625152)
360a -> 363a : 0.040628 (c= -0.20156421)
361a -> 364a : 0.033317 (c= -0.18252949)
362a -> 364a : 0.541875 (c= 0.73612148)

STATE 5: E= 0.095664 au 2.603 eV 20995.8 cm**-1 <S**2> = 0.000000 Mult 1
358a -> 363a : 0.017314 (c= 0.13158133)
359a -> 363a : 0.590452 (c= 0.76840856)
361a -> 363a : 0.019978 (c= 0.14134219)
361a -> 364a : 0.076287 (c= 0.27620150)
362a -> 364a : 0.251996 (c= -0.50199221)

STATE 6: E= 0.105162 au 2.862 eV 23080.4 cm**-1 <S**2> = 0.000000 Mult 1
358a -> 363a : 0.259338 (c= 0.50925207)
360a -> 364a : 0.044669 (c= -0.21135063)
361a -> 364a : 0.334792 (c= 0.57861211)
362a -> 364a : 0.057306 (c= 0.23938674)
362a -> 365a : 0.116020 (c= 0.34061647)
362a -> 366a : 0.130542 (c= -0.36130564)

STATE 7: E= 0.105215 au 2.863 eV 23091.9 cm**-1 <S**2> = 0.000000 Mult 1
358a -> 363a : 0.173954 (c= -0.41707775)
360a -> 364a : 0.078194 (c= 0.27963181)
361a -> 364a : 0.010484 (c= -0.10239000)
362a -> 364a : 0.038022 (c= -0.19499212)
362a -> 365a : 0.279291 (c= 0.52848009)

362a -> 366a : 0.359093 (c= -0.59924391)

STATE 8: E= 0.107119 au 2.915 eV 23509.9 cm**-1 <S**2> = 0.000000 Mult 1
358a -> 363a : 0.346484 (c= 0.58862855)
360a -> 364a : 0.029883 (c= -0.17286784)
361a -> 364a : 0.468631 (c= -0.68456661)
362a -> 364a : 0.024569 (c= -0.15674439)
362a -> 365a : 0.017036 (c= 0.13052142)
362a -> 366a : 0.034447 (c= -0.18560011)
362a -> 368a : 0.010478 (c= 0.10236081)

STATE 9: E= 0.109612 au 2.983 eV 24057.0 cm**-1 <S**2> = 0.000000 Mult 1
357a -> 363a : 0.019329 (c= 0.13902718)
358a -> 363a : 0.119060 (c= 0.34505030)
358a -> 364a : 0.035246 (c= -0.18773889)
360a -> 364a : 0.668865 (c= 0.81784182)
360a -> 366a : 0.029476 (c= 0.17168508)
362a -> 365a : 0.015196 (c= -0.12327061)
362a -> 368a : 0.010019 (c= 0.10009392)

STATE 10: E= 0.113326 au 3.084 eV 24872.3 cm**-1 <S**2> = 0.000000 Mult 1
357a -> 363a : 0.888255 (c= 0.94247278)
357a -> 364a : 0.042537 (c= -0.20624501)
358a -> 364a : 0.014451 (c= 0.12021435)
360a -> 364a : 0.013647 (c= -0.11682052)

STATE 11: E= 0.116013 au 3.157 eV 25461.8 cm**-1 <S**2> = 0.000000 Mult 1
359a -> 364a : 0.120074 (c= -0.34651674)
360a -> 364a : 0.010220 (c= 0.10109173)
362a -> 365a : 0.334847 (c= 0.57865945)
362a -> 366a : 0.204107 (c= 0.45178251)
362a -> 368a : 0.276003 (c= -0.52535963)

STATE 12: E= 0.116720 au 3.176 eV 25617.0 cm**-1 <S**2> = 0.000000 Mult 1
359a -> 364a : 0.685810 (c= 0.82813658)
360a -> 364a : 0.014403 (c= -0.12001300)
361a -> 365a : 0.031568 (c= 0.17767272)
361a -> 366a : 0.035763 (c= -0.18911237)
362a -> 365a : 0.057454 (c= 0.23969515)
362a -> 366a : 0.089514 (c= 0.29918825)

STATE 13: E= 0.117557 au 3.199 eV 25800.7 cm**-1 <S**2> = 0.000000 Mult 1
360a -> 366a : 0.016530 (c= 0.12856962)
361a -> 365a : 0.388279 (c= -0.62312062)
361a -> 366a : 0.372863 (c= 0.61062546)
362a -> 365a : 0.026004 (c= 0.16125697)
362a -> 366a : 0.050146 (c= 0.22393192)
362a -> 368a : 0.030489 (c= 0.17460985)
362a -> 369a : 0.015845 (c= -0.12587510)

STATE 14: E= 0.119777 au 3.259 eV 26288.1 cm**-1 <S**2> = 0.000000 Mult 1
357a -> 364a : 0.010857 (c= -0.10419790)
358a -> 364a : 0.014806 (c= -0.12168181)
359a -> 364a : 0.059183 (c= 0.24327639)
359a -> 366a : 0.011810 (c= 0.10867245)
360a -> 366a : 0.010392 (c= 0.10194210)
361a -> 365a : 0.023730 (c= -0.15404677)
361a -> 366a : 0.036683 (c= 0.19152935)
362a -> 365a : 0.080793 (c= -0.28424164)
362a -> 366a : 0.091053 (c= -0.30174989)
362a -> 368a : 0.510997 (c= -0.71484057)
362a -> 369a : 0.050747 (c= 0.22527077)
362a -> 370a : 0.015874 (c= -0.12599083)

STATE 15: E= 0.123975 au 3.374 eV 27209.4 cm**-1 <S**2> = 0.000000 Mult 1
357a -> 363a : 0.014281 (c= -0.11950374)
357a -> 364a : 0.033102 (c= -0.18193987)
358a -> 364a : 0.531155 (c= 0.72880370)
358a -> 368a : 0.012590 (c= 0.11220475)
360a -> 364a : 0.012914 (c= 0.11364015)
360a -> 365a : 0.157312 (c= -0.39662515)
360a -> 366a : 0.154434 (c= 0.39298097)

STATE 16: E= 0.125978 au 3.428 eV 27649.0 cm**-1 <S**2> = 0.000000 Mult 1
357a -> 364a : 0.020745 (c= 0.14403039)
358a -> 363a : 0.010930 (c= -0.10454847)
358a -> 364a : 0.232464 (c= -0.48214473)
359a -> 364a : 0.014518 (c= -0.12049222)
359a -> 365a : 0.034481 (c= -0.18568983)
359a -> 366a : 0.027523 (c= 0.16589911)
360a -> 364a : 0.041689 (c= -0.20417950)
360a -> 365a : 0.160854 (c= -0.40106651)

360a -> 366a : 0.229444 (c= 0.47900302)
361a -> 366a : 0.064162 (c= -0.25330279)
361a -> 368a : 0.056242 (c= 0.23715309)
362a -> 368a : 0.013184 (c= 0.11482094)

STATE 17: E= 0.127872 au 3.480 eV 28064.7 cm**-1 <S**2> = 0.000000 Mult 1
355a -> 363a : 0.033602 (c= 0.18330908)
356a -> 363a : 0.044796 (c= 0.21164997)
359a -> 365a : 0.044949 (c= -0.21201200)
359a -> 366a : 0.038263 (c= 0.19560860)
360a -> 365a : 0.012549 (c= -0.11202091)
360a -> 366a : 0.012131 (c= 0.11014267)
361a -> 365a : 0.277755 (c= 0.52702463)
361a -> 366a : 0.185179 (c= 0.43032458)
361a -> 368a : 0.241633 (c= -0.49156182)
362a -> 371a : 0.016820 (c= 0.12969339)

STATE 18: E= 0.128835 au 3.506 eV 28275.9 cm**-1 <S**2> = 0.000000 Mult 1
355a -> 363a : 0.013379 (c= 0.11566600)
356a -> 363a : 0.032336 (c= 0.17982194)
357a -> 364a : 0.021321 (c= 0.14601704)
361a -> 366a : 0.014654 (c= -0.12105524)
362a -> 365a : 0.026209 (c= -0.16189198)
362a -> 367a : 0.099999 (c= -0.31622581)
362a -> 368a : 0.079433 (c= -0.28183869)
362a -> 369a : 0.598805 (c= -0.77382471)
362a -> 370a : 0.035876 (c= 0.18941038)

STATE 19: E= 0.129461 au 3.523 eV 28413.5 cm**-1 <S**2> = 0.000000 Mult 1
355a -> 363a : 0.088705 (c= 0.29783380)
356a -> 363a : 0.230214 (c= 0.47980612)
357a -> 364a : 0.086785 (c= 0.29459262)
358a -> 364a : 0.022498 (c= 0.14999230)
359a -> 365a : 0.014023 (c= -0.11841778)
359a -> 366a : 0.027982 (c= 0.16727724)
360a -> 365a : 0.013588 (c= 0.11656782)
360a -> 366a : 0.014262 (c= -0.11942491)
361a -> 365a : 0.069564 (c= -0.26375029)
361a -> 366a : 0.050366 (c= -0.22442306)
362a -> 367a : 0.259808 (c= 0.50971361)
362a -> 369a : 0.010713 (c= 0.10350124)

STATE 20: E= 0.129619 au 3.527 eV 28448.1 cm**-1 <S**2> = 0.000000 Mult 1
356a -> 363a : 0.029359 (c= 0.17134389)
357a -> 364a : 0.015318 (c= 0.12376653)
359a -> 366a : 0.013798 (c= 0.11746558)
361a -> 365a : 0.039490 (c= -0.19872087)
361a -> 366a : 0.027613 (c= -0.16617029)
362a -> 367a : 0.607536 (c= -0.77944610)
362a -> 369a : 0.183961 (c= 0.42890679)

STATE 21: E= 0.130541 au 3.552 eV 28650.4 cm**-1 <S**2> = 0.000000 Mult 1
355a -> 363a : 0.113750 (c= -0.33726860)
356a -> 363a : 0.206794 (c= -0.45474568)
357a -> 364a : 0.070694 (c= 0.26588327)
359a -> 365a : 0.030849 (c= -0.17563787)
359a -> 366a : 0.029334 (c= 0.17127041)
361a -> 365a : 0.036397 (c= -0.19077871)
361a -> 366a : 0.042209 (c= -0.20544744)
361a -> 368a : 0.198461 (c= -0.44549007)
361a -> 369a : 0.046418 (c= 0.21544793)
361a -> 370a : 0.010642 (c= -0.10316014)
362a -> 367a : 0.010497 (c= 0.10245602)
362a -> 370a : 0.080357 (c= 0.28347320)
362a -> 372a : 0.013426 (c= -0.11587208)

STATE 22: E= 0.131093 au 3.567 eV 28771.5 cm**-1 <S**2> = 0.000000 Mult 1
355a -> 363a : 0.055922 (c= 0.23647763)
359a -> 365a : 0.189057 (c= 0.43480668)
359a -> 366a : 0.221193 (c= -0.47031159)
359a -> 368a : 0.011474 (c= 0.10711905)
360a -> 365a : 0.069897 (c= -0.26438100)
360a -> 368a : 0.048146 (c= 0.21942301)
361a -> 365a : 0.010054 (c= -0.10026921)
361a -> 366a : 0.020698 (c= -0.14386773)
361a -> 368a : 0.143522 (c= -0.37884299)
361a -> 369a : 0.037140 (c= 0.19271830)
362a -> 370a : 0.076125 (c= -0.27590757)
362a -> 371a : 0.032470 (c= 0.18019504)

STATE 23: E= 0.131685 au 3.583 eV 28901.6 cm**-1 <S**2> = 0.000000 Mult 1
355a -> 364a : 0.011726 (c= -0.10828795)

356a -> 363a : 0.040749 (c= -0.20186450)
357a -> 363a : 0.018122 (c= 0.13461954)
357a -> 364a : 0.524503 (c= 0.72422585)
358a -> 364a : 0.046343 (c= 0.21527406)
361a -> 365a : 0.018749 (c= 0.13692594)
361a -> 366a : 0.061061 (c= 0.24710528)
361a -> 368a : 0.086775 (c= 0.29457585)
361a -> 369a : 0.026039 (c= -0.16136607)
362a -> 370a : 0.040852 (c= -0.20211805)

STATE 24: E= 0.132270 au 3.599 eV 29030.0 cm**-1 <S**2> = 0.000000 Mult 1
352a -> 363a : 0.016358 (c= 0.12789743)
353a -> 363a : 0.038427 (c= -0.19602826)
354a -> 363a : 0.014203 (c= 0.11917750)
355a -> 363a : 0.491048 (c= -0.70074811)
356a -> 363a : 0.210196 (c= 0.45847109)
361a -> 368a : 0.018051 (c= -0.13435408)
362a -> 370a : 0.109300 (c= -0.33060543)
362a -> 372a : 0.013361 (c= 0.11559191)

STATE 25: E= 0.132665 au 3.610 eV 29116.7 cm**-1 <S**2> = 0.000000 Mult 1
355a -> 363a : 0.022992 (c= 0.15163044)
356a -> 363a : 0.093001 (c= -0.30496041)
359a -> 365a : 0.036197 (c= -0.19025423)
359a -> 366a : 0.052828 (c= 0.22984258)
360a -> 365a : 0.047765 (c= 0.21855252)
360a -> 368a : 0.075416 (c= -0.27461981)
361a -> 368a : 0.035151 (c= -0.18748493)
362a -> 369a : 0.046259 (c= -0.21507983)
362a -> 370a : 0.446553 (c= -0.66824648)
362a -> 372a : 0.048099 (c= 0.21931382)

STATE 26: E= 0.134604 au 3.663 eV 29542.2 cm**-1 <S**2> = 0.000000 Mult 1
359a -> 365a : 0.012276 (c= -0.11079660)
359a -> 366a : 0.012239 (c= 0.11063226)
360a -> 365a : 0.169278 (c= -0.41143461)
360a -> 366a : 0.112920 (c= -0.33603535)
360a -> 368a : 0.139520 (c= 0.37352379)
362a -> 371a : 0.426562 (c= -0.65311680)
362a -> 372a : 0.023812 (c= 0.15431006)

STATE 27: E= 0.135317 au 3.682 eV 29698.6 cm**-1 <S**2> = 0.000000 Mult 1
359a -> 366a : 0.040362 (c= -0.20090359)
360a -> 364a : 0.011572 (c= -0.10757237)
360a -> 365a : 0.184478 (c= 0.42950851)
360a -> 366a : 0.299500 (c= 0.54726608)
360a -> 369a : 0.012743 (c= -0.11288299)
360a -> 370a : 0.019103 (c= 0.13821386)
361a -> 368a : 0.020117 (c= -0.14183333)
362a -> 370a : 0.015714 (c= 0.12535417)
362a -> 371a : 0.283599 (c= -0.53254042)

STATE 28: E= 0.138632 au 3.772 eV 30426.3 cm**-1 <S**2> = 0.000000 Mult 1
347a -> 363a : 0.108792 (c= 0.32983692)
348a -> 363a : 0.048221 (c= -0.21959392)
358a -> 364a : 0.011313 (c= -0.10636470)
358a -> 365a : 0.063137 (c= 0.25127120)
358a -> 366a : 0.073189 (c= -0.27053404)
359a -> 368a : 0.019600 (c= -0.14000008)
360a -> 365a : 0.039346 (c= -0.19835907)
360a -> 366a : 0.018359 (c= -0.13549438)
360a -> 368a : 0.252498 (c= -0.50249188)
360a -> 369a : 0.020992 (c= 0.14488661)
361a -> 368a : 0.046436 (c= -0.21548933)
361a -> 369a : 0.015246 (c= -0.12347655)
362a -> 370a : 0.019499 (c= 0.13963758)
362a -> 372a : 0.041327 (c= 0.20328922)
362a -> 373a : 0.038985 (c= -0.19744545)
362a -> 374a : 0.014022 (c= 0.11841650)
362a -> 376a : 0.023298 (c= 0.15263530)

STATE 29: E= 0.139279 au 3.790 eV 30568.1 cm**-1 <S**2> = 0.000000 Mult 1
347a -> 363a : 0.047832 (c= -0.21870447)
348a -> 363a : 0.021815 (c= 0.14769741)
359a -> 365a : 0.063896 (c= 0.25277640)
359a -> 366a : 0.041671 (c= 0.20413393)
359a -> 368a : 0.040201 (c= -0.20050162)
361a -> 365a : 0.026161 (c= -0.16174271)
361a -> 366a : 0.015942 (c= -0.12626203)
361a -> 368a : 0.066317 (c= -0.25752029)
361a -> 369a : 0.536908 (c= -0.73274009)
361a -> 370a : 0.038248 (c= 0.19556970)

STATE 30: E= 0.139477 au 3.795 eV 30611.7 cm**-1 <S**2> = 0.000000 Mult 1

347a -> 363a :	0.194081 (c= -0.44054641)
348a -> 363a :	0.095111 (c= 0.30840027)
358a -> 365a :	0.042766 (c= -0.20679897)
358a -> 366a :	0.046778 (c= 0.21628170)
359a -> 366a :	0.016272 (c= -0.12756212)
360a -> 365a :	0.015330 (c= -0.12381328)
360a -> 366a :	0.018581 (c= -0.13631390)
360a -> 368a :	0.318397 (c= -0.56426701)
360a -> 369a :	0.019070 (c= 0.13809432)
361a -> 371a :	0.012282 (c= 0.11082600)
362a -> 371a :	0.041620 (c= -0.20401069)
362a -> 372a :	0.033998 (c= -0.18438651)

4.3 Si_6Ir-Hf 3b

4.3.1 Optimization and single point

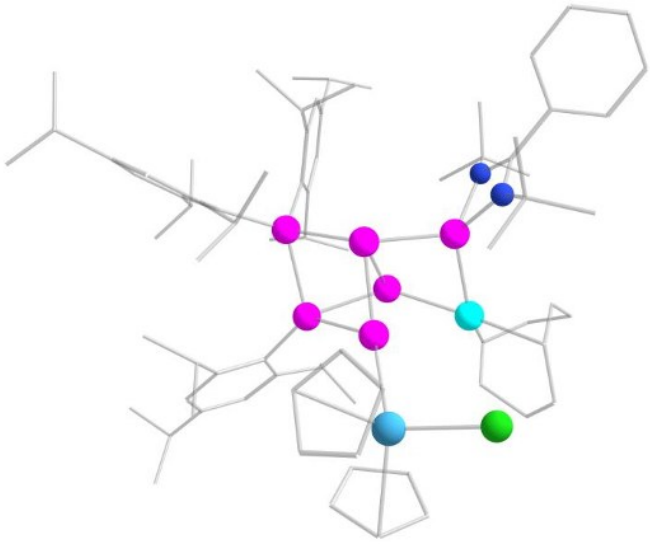

Supplementary Figure S31. Optimized molecular structure of Si_6Ir-Hf **3b** at the PBE0P/def2-TZVPP level of theory.[S10c-e,11] Hydrogen atoms omitted for clarity.

Supplementary Table S11. Coordinates of the optimized geometry of Si_6Ir-Hf **3b** at the PBE0P/def2-TZVPP level of theory.[S10c-e,11]

Ir	-2.781759	-0.693964	-1.311847
Hf	-1.348342	-3.867825	1.766341
Cl	-3.752587	-3.688491	2.003664
Si	1.910778	1.174832	0.369569
Si	-0.331178	0.704093	0.937334
Si	-2.479464	1.135648	0.136028
Si	-0.531039	0.003012	-1.404239

Si	-0.608607	-1.549300	0.409242
Si	1.469558	-0.942879	-0.687385
N	-3.709029	1.753105	1.417949
N	-3.035134	2.876123	-0.278958
C	1.880738	2.833882	-0.636101
C	1.619590	4.003408	0.117070
C	1.599481	5.251507	-0.499384
H	1.401244	6.131978	0.104337
C	1.833421	5.414596	-1.852782
C	2.076020	4.267222	-2.590091
H	2.256424	4.359828	-3.655888
C	2.101802	2.995549	-2.024952
C	2.371597	1.859227	-2.996828
H	2.378183	0.923697	-2.429877
C	1.264691	1.762311	-4.044913
H	1.465725	0.945370	-4.739649
H	1.197159	2.682493	-4.630036
H	0.290893	1.586945	-3.584411
C	3.721855	1.983264	-3.703423
H	4.551722	2.031030	-3.000475
H	3.764228	2.876029	-4.331710
H	3.883782	1.118615	-4.350867
C	1.344394	3.996163	1.609323
H	1.405173	2.965161	1.958590
C	2.383324	4.791215	2.395647
H	2.183115	4.718871	3.467495
H	2.364828	5.849927	2.125607
H	3.389758	4.411906	2.214596
C	-0.069078	4.481268	1.922971
H	-0.265670	4.411900	2.996529
H	-0.813499	3.879590	1.396833
H	-0.204800	5.525338	1.628345
C	1.828679	6.784948	-2.488109
H	1.608069	7.503153	-1.690967
C	0.737410	6.918201	-3.547338
H	-0.247126	6.699464	-3.130015
H	0.908357	6.228195	-4.377184
H	0.718204	7.931049	-3.956871
C	3.195707	7.141829	-3.067344
H	3.975625	7.081500	-2.306324
H	3.190557	8.156385	-3.473128
H	3.468521	6.461322	-3.877490
C	3.378082	1.364595	1.625859
C	3.249912	1.126608	3.014185
C	4.266341	1.512691	3.884676
H	4.134137	1.356607	4.950185
C	5.452746	2.076641	3.450470

C	5.616078	2.216455	2.082269
H	6.551613	2.610362	1.699628
C	4.619885	1.876223	1.173531
C	4.971580	2.067824	-0.290487
H	4.120074	1.737218	-0.886841
C	6.165182	1.211053	-0.714157
H	7.056322	1.445400	-0.127921
H	6.407051	1.395078	-1.763890
H	5.959993	0.145924	-0.605235
C	5.234465	3.536900	-0.616103
H	4.372707	4.159089	-0.373639
H	5.455653	3.664906	-1.677881
H	6.093988	3.910110	-0.054208
C	2.061425	0.424019	3.647877
H	1.471627	-0.021352	2.841520
C	1.148242	1.379220	4.412899
H	0.331814	0.828456	4.887676
H	0.704227	2.128393	3.757042
H	1.700570	1.900968	5.198650
C	2.508957	-0.706496	4.574282
H	3.031953	-0.324680	5.453001
H	3.182837	-1.399141	4.066891
H	1.646201	-1.269284	4.933218
H	8.558780	1.989916	4.981611
H	7.173744	4.291496	3.397449
C	2.826127	-2.050194	-1.476747
C	3.854411	-2.566018	-0.656284
C	4.912162	-3.269155	-1.223325
H	5.691125	-3.655355	-0.574341
C	4.997154	-3.501247	-2.586577
C	3.964235	-3.029072	-3.382198
H	4.008914	-3.223758	-4.447453
C	2.884235	-2.323181	-2.863347
C	1.762362	-1.930927	-3.802962
H	1.338600	-0.992898	-3.432080
C	2.193157	-1.708295	-5.247517
H	3.049638	-1.035631	-5.322645
H	1.368189	-1.273189	-5.815709
H	2.457676	-2.645217	-5.743684
C	0.647923	-2.974402	-3.750880
H	0.233631	-3.053360	-2.744783
H	1.024710	-3.957664	-4.044772
H	-0.166802	-2.705097	-4.427540
C	3.826147	-2.473646	0.859110
H	3.003229	-1.805753	1.142470
C	5.104493	-1.910917	1.470715
H	5.020905	-1.883062	2.559331

H	5.300764	-0.895243	1.133712
H	5.972062	-2.528206	1.227179
C	3.534094	-3.854106	1.447271
H	4.316264	-4.563980	1.168469
H	2.584407	-4.244882	1.080547
H	3.498010	-3.814638	2.539094
C	6.159006	-4.252454	-3.192717
H	5.974484	-4.304626	-4.270968
C	6.246195	-5.683870	-2.668319
H	5.315552	-6.227061	-2.841719
H	6.445304	-5.697795	-1.594028
H	7.055978	-6.226505	-3.161791
C	7.478698	-3.513757	-2.982484
H	7.722024	-3.440023	-1.919876
H	7.433452	-2.499970	-3.383987
H	8.298741	-4.041255	-3.475488
C	-3.866357	2.896817	0.765232
C	-4.794583	3.995778	1.133923
C	-6.125808	3.957972	0.732694
H	-6.487458	3.120385	0.148680
C	-6.988352	4.988163	1.078033
H	-8.022354	4.951501	0.757765
C	-6.529163	6.057570	1.831328
H	-7.203829	6.860497	2.102125
C	-5.202682	6.096024	2.238494
H	-4.838614	6.928155	2.828556
C	-4.337671	5.072038	1.890241
H	-3.301138	5.104786	2.203121
C	-2.990111	3.759156	-1.457724
C	-1.743272	3.387943	-2.247830
H	-0.842653	3.507979	-1.643600
H	-1.657713	4.035389	-3.121828
H	-1.795466	2.352789	-2.585881
C	-2.889584	5.235362	-1.076755
H	-3.796956	5.611648	-0.608473
H	-2.720289	5.818454	-1.984206
H	-2.046346	5.405319	-0.405398
C	-4.222504	3.524540	-2.331915
H	-4.303105	2.468092	-2.590341
H	-4.140896	4.101675	-3.255604
H	-5.137941	3.834521	-1.825401
C	-4.284582	1.275251	2.680238
C	-4.086341	2.280852	3.814404
H	-4.384395	1.820677	4.758703
H	-4.686817	3.178999	3.679539
H	-3.035448	2.566435	3.892808
C	-3.539004	-0.003896	3.037985

H	-3.968041	-0.437721	3.942651
H	-2.484081	0.209733	3.215719
H	-3.605101	-0.744289	2.239488
C	-5.770550	0.957876	2.510599
H	-6.152583	0.486995	3.418733
H	-5.925586	0.268125	1.679391
H	-6.355352	1.860428	2.331434
C	-2.994799	-1.074868	-3.444038
H	-2.073336	-0.785576	-3.939286
C	-3.002334	-2.331046	-2.817000
H	-2.078346	-2.893064	-2.884986
C	-4.265179	-3.144165	-2.624281
H	-4.015814	-4.207609	-2.673300
H	-4.940904	-2.967250	-3.465734
C	-4.967252	-2.852647	-1.293771
H	-6.049670	-3.024989	-1.384681
H	-4.614784	-3.556490	-0.539309
C	-4.702005	-1.464892	-0.766164
H	-4.858430	-1.378357	0.306319
C	-4.875923	-0.288191	-1.549025
H	-5.167287	0.608405	-1.008298
C	-5.371893	-0.333689	-2.984394
H	-5.992333	0.543616	-3.185299
H	-6.028786	-1.196862	-3.118689
C	-4.215376	-0.374079	-3.983072
H	-4.527492	-0.840710	-4.928325
H	-3.921339	0.648389	-4.233499
C	-0.111748	-4.793738	-0.238639
H	0.643673	-4.196229	-0.725185
C	-1.489799	-4.830253	-0.567813
H	-1.973678	-4.226096	-1.317426
C	-2.117262	-5.755824	0.282655
H	-3.169912	-5.986778	0.298990
C	-1.145937	-6.266770	1.170516
H	-1.313387	-7.004384	1.940798
C	0.100673	-5.686292	0.825313
H	1.050872	-5.905753	1.284765
C	-1.193153	-4.520837	4.175019
H	-1.762430	-5.372280	4.516064
C	0.129889	-4.544438	3.677316
H	0.748681	-5.421232	3.574113
C	0.489434	-3.230389	3.331572
H	1.423137	-2.915065	2.897187
C	-0.598144	-2.380226	3.657195
H	-0.627753	-1.314934	3.493015
C	-1.623496	-3.174033	4.189806
H	-2.597400	-2.829778	4.495457

C	6.523148	2.493987	4.430289
C	7.819285	1.712923	4.226459
H	7.648735	0.637002	4.293017
H	8.253616	1.921375	3.245875
C	6.781201	3.998063	4.374034
H	7.514484	4.292373	5.128795
H	5.864786	4.564780	4.547924
H	6.146363	2.257233	5.431188

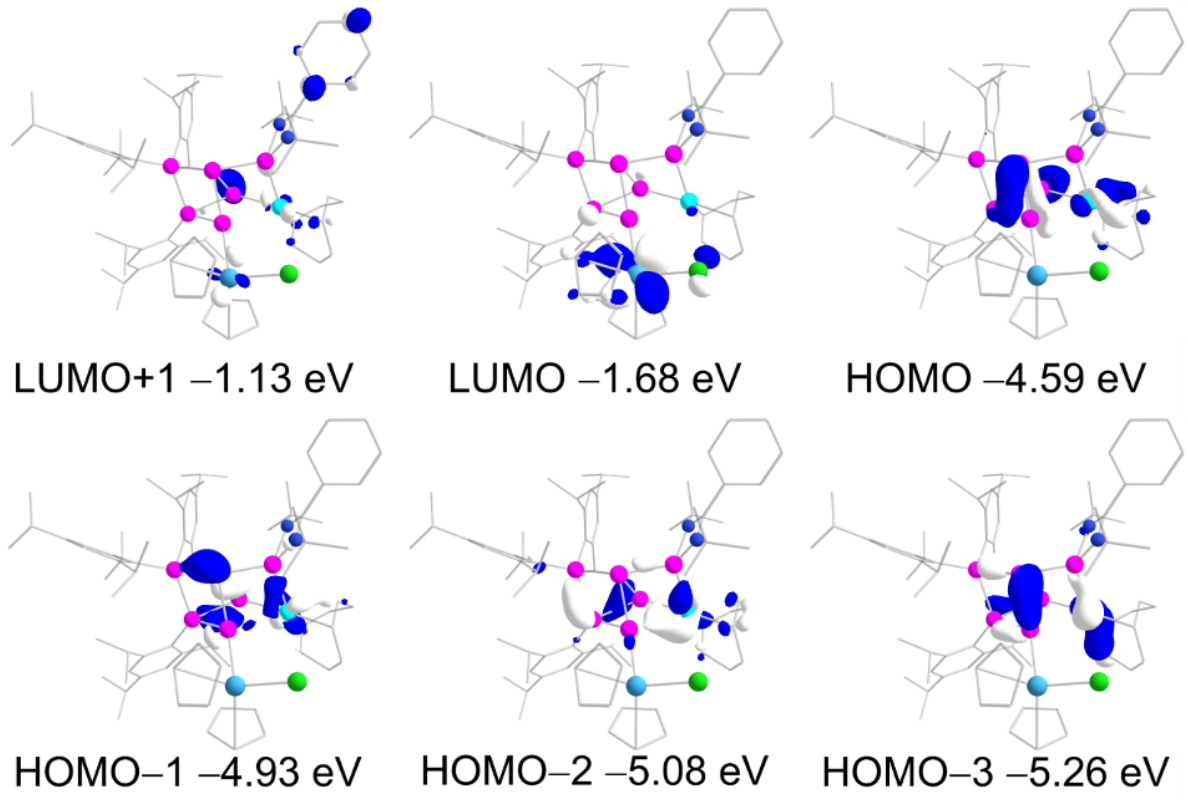

Supplementary Figure S32. Selected molecular orbitals of Si_6Ir-Hf **3b** at the PBE0/def2-TZVPP[S10c-e,11] level of theory.

4.3.2 Experimental vs. calculated NMR shifts

Supplementary Table S12. Comparison of experimental vs. calculated NMR chemical shifts for compound **3b** at the PBE0/def2-TZVPPlevel of theory.[S10c-e,11]

	Exp. **3b** $\delta(^{29}Si)$ [ppm]	Calc. **3b** $\delta(^{29}Si)$ [ppm]
Si4 (SiTip)	75.9	78.6
Si6 (NHSi)	68.2	60.6
Si5 (SiTip2)	29.9	34.3
Si3 (unsubstituted)	−36.7	−46.2
Si1 (unsubstituted)	−131.2	−167.4
Si2 (SiHf)	−90.4	−91.1

4.3.3 TD-DFT calculations

Supplementary Table S13. Transition Energy, wavelength, and oscillator strengths of the electronic transition of **3b** calculated at the TD-B3LYP/def2-TZVPP[S10b-e,11] level of theory (the 362nd orbital is the highest occupied orbital (HOMO), the 363th orbital is the lowest unoccupied orbital (LUMO) shown in Supplementary Figure S32).

STATE 1: E= 0.072633 au 1.976 eV 15941.0 cm**-1 <S**2> = 0.000000 Mult 1
361a -> 363a : 0.022796 (c= -0.15098219)
362a -> 363a : 0.953327 (c= -0.97638481)

STATE 2: E= 0.085082 au 2.315 eV 18673.4 cm**-1 <S**2> = 0.000000 Mult 1
361a -> 363a : 0.911679 (c= -0.95481893)
362a -> 363a : 0.016656 (c= 0.12905775)
362a -> 364a : 0.013836 (c= 0.11762739)

STATE 3: E= 0.089824 au 2.444 eV 19714.0 cm**-1 <S**2> = 0.000000 Mult 1
359a -> 363a : 0.010113 (c= -0.10056234)
360a -> 363a : 0.931440 (c= -0.96511158)
362a -> 364a : 0.036533 (c= 0.19113692)

STATE 4: E= 0.093266 au 2.538 eV 20469.6 cm**-1 <S**2> = 0.000000 Mult 1
359a -> 363a : 0.017545 (c= 0.13245713)
360a -> 363a : 0.037595 (c= -0.19389483)
361a -> 363a : 0.015740 (c= -0.12546017)
361a -> 364a : 0.100259 (c= -0.31663674)
362a -> 364a : 0.755468 (c= -0.86917652)
362a -> 365a : 0.023055 (c= 0.15183871)

STATE 5: E= 0.096377 au 2.623 eV 21152.3 cm**-1 <S**2> = 0.000000 Mult 1
359a -> 363a : 0.907501 (c= 0.95262848)
361a -> 364a : 0.037874 (c= 0.19461188)

STATE 6: E= 0.102248 au 2.782 eV 22440.8 cm**-1 <S**2> = 0.000000 Mult 1
360a -> 364a : 0.016981 (c= -0.13031091)
362a -> 364a : 0.017790 (c= -0.13337916)
362a -> 365a : 0.060375 (c= -0.24571240)
362a -> 366a : 0.863639 (c= -0.92932186)

STATE 7: E= 0.104048 au 2.831 eV 22836.0 cm**-1 <S**2> = 0.000000 Mult 1
358a -> 363a : 0.019159 (c= 0.13841661)
359a -> 363a : 0.019632 (c= 0.14011413)
360a -> 364a : 0.027540 (c= 0.16595298)

360a -> 366a : 0.011882 (c= -0.10900261)
361a -> 364a : 0.722006 (c= -0.84970940)
361a -> 365a : 0.025586 (c= 0.15995525)
362a -> 364a : 0.105698 (c= 0.32511191)

STATE 8: E= 0.106890 au 2.909 eV 23459.7 cm**-1 <S**2> = 0.000000 Mult 1
358a -> 363a : 0.294718 (c= 0.54287933)
360a -> 364a : 0.540311 (c= 0.73505854)
360a -> 365a : 0.018195 (c= -0.13488769)
361a -> 364a : 0.039618 (c= 0.19904151)
362a -> 365a : 0.026307 (c= -0.16219460)

STATE 9: E= 0.107466 au 2.924 eV 23586.1 cm**-1 <S**2> = 0.000000 Mult 1
358a -> 363a : 0.119015 (c= -0.34498586)
362a -> 364a : 0.017819 (c= -0.13348912)
362a -> 365a : 0.733011 (c= -0.85616076)
362a -> 366a : 0.062672 (c= 0.25034372)
362a -> 368a : 0.024334 (c= -0.15599408)

STATE 10: E= 0.108710 au 2.958 eV 23859.0 cm**-1 <S**2> = 0.000000 Mult 1
358a -> 363a : 0.487458 (c= -0.69818198)
358a -> 364a : 0.019696 (c= 0.14034078)
360a -> 364a : 0.256347 (c= 0.50630721)
360a -> 366a : 0.031917 (c= 0.17865299)
361a -> 366a : 0.010269 (c= -0.10133849)
362a -> 365a : 0.108211 (c= 0.32895488)
362a -> 366a : 0.021925 (c= -0.14807115)

STATE 11: E= 0.113122 au 3.078 eV 24827.4 cm**-1 <S**2> = 0.000000 Mult 1
357a -> 363a : 0.903968 (c= 0.95077211)
357a -> 364a : 0.033921 (c= -0.18417538)
358a -> 364a : 0.014626 (c= 0.12093847)
361a -> 366a : 0.014797 (c= 0.12164333)

STATE 12: E= 0.114633 au 3.119 eV 25159.1 cm**-1 <S**2> = 0.000000 Mult 1
357a -> 363a : 0.013049 (c= 0.11423317)
359a -> 364a : 0.322843 (c= 0.56819273)
359a -> 365a : 0.016336 (c= -0.12781345)
360a -> 364a : 0.021359 (c= -0.14614841)
361a -> 365a : 0.084003 (c= -0.28983346)
361a -> 366a : 0.481894 (c= -0.69418618)

STATE 13: E= 0.114928 au 3.127 eV 25223.9 cm**-1 <S**2> = 0.000000 Mult 1
359a -> 364a : 0.398748 (c= -0.63146482)
359a -> 365a : 0.017597 (c= 0.13265343)
360a -> 366a : 0.017024 (c= -0.13047692)
361a -> 365a : 0.041628 (c= -0.20402970)
361a -> 366a : 0.252825 (c= -0.50281741)
362a -> 368a : 0.153477 (c= 0.39176163)
362a -> 369a : 0.040198 (c= -0.20049344)

STATE 14: E= 0.116210 au 3.162 eV 25505.1 cm**-1 <S**2> = 0.000000 Mult 1
359a -> 364a : 0.146265 (c= -0.38244564)
359a -> 366a : 0.011671 (c= -0.10803056)
360a -> 366a : 0.016157 (c= -0.12711159)
361a -> 366a : 0.026413 (c= -0.16252075)
362a -> 368a : 0.683351 (c= -0.82665052)
362a -> 369a : 0.031682 (c= 0.17799465)

STATE 15: E= 0.118243 au 3.218 eV 25951.4 cm**-1 <S**2> = 0.000000 Mult 1
362a -> 367a : 0.992677 (c= -0.99633183)

STATE 16: E= 0.119201 au 3.244 eV 26161.5 cm**-1 <S**2> = 0.000000 Mult 1
361a -> 364a : 0.027480 (c= 0.16577006)
361a -> 365a : 0.770219 (c= 0.87762150)
361a -> 366a : 0.131726 (c= -0.36294085)
361a -> 368a : 0.016095 (c= 0.12686454)
361a -> 369a : 0.010325 (c= 0.10161247)

STATE 17: E= 0.121328 au 3.301 eV 26628.4 cm**-1 <S**2> = 0.000000 Mult 1
357a -> 364a : 0.013106 (c= -0.11448186)
358a -> 364a : 0.106868 (c= 0.32690748)
359a -> 366a : 0.012647 (c= -0.11245702)
360a -> 365a : 0.042496 (c= -0.20614585)
360a -> 366a : 0.235104 (c= -0.48487574)
362a -> 368a : 0.054190 (c= 0.23278830)
362a -> 369a : 0.426362 (c= 0.65296371)
362a -> 370a : 0.029352 (c= -0.17132477)

STATE 18: E= 0.122079 au 3.322 eV 26793.2 cm**-1 <S**2> = 0.000000 Mult 1
357a -> 364a : 0.013163 (c= 0.11473032)
358a -> 364a : 0.345700 (c= -0.58796260)

358a -> 365a : 0.014031 (c= 0.11845193)
360a -> 365a : 0.022241 (c= 0.14913438)
360a -> 366a : 0.130376 (c= 0.36107683)
362a -> 365a : 0.011616 (c= -0.10777852)
362a -> 368a : 0.019489 (c= 0.13960269)
362a -> 369a : 0.346253 (c= 0.58843306)
362a -> 370a : 0.027842 (c= -0.16685976)

STATE 19: E= 0.123831 au 3.370 eV 27177.8 cm**-1 <S**2> = 0.000000 Mult 1
357a -> 364a : 0.021487 (c= -0.14658508)
358a -> 363a : 0.017598 (c= 0.13265714)
358a -> 364a : 0.286501 (c= 0.53525752)
358a -> 365a : 0.012238 (c= -0.11062463)
359a -> 365a : 0.015481 (c= 0.12442104)
359a -> 366a : 0.046150 (c= 0.21482665)
360a -> 364a : 0.026143 (c= -0.16168815)
360a -> 366a : 0.339050 (c= 0.58227959)
361a -> 368a : 0.037004 (c= 0.19236344)
362a -> 369a : 0.049923 (c= 0.22343486)
362a -> 370a : 0.035898 (c= 0.18946723)

STATE 20: E= 0.125766 au 3.422 eV 27602.4 cm**-1 <S**2> = 0.000000 Mult 1
359a -> 365a : 0.019270 (c= 0.13881560)
359a -> 366a : 0.094787 (c= 0.30787490)
360a -> 364a : 0.012889 (c= -0.11352986)
360a -> 365a : 0.335546 (c= -0.57926371)
360a -> 366a : 0.022374 (c= 0.14958047)
362a -> 369a : 0.024698 (c= -0.15715518)
362a -> 370a : 0.413754 (c= -0.64323723)
362a -> 371a : 0.018867 (c= 0.13735569)

STATE 21: E= 0.126208 au 3.434 eV 27699.5 cm**-1 <S**2> = 0.000000 Mult 1
358a -> 364a : 0.041208 (c= 0.20299655)
359a -> 366a : 0.024001 (c= 0.15492184)
360a -> 365a : 0.515165 (c= 0.71775024)
360a -> 366a : 0.018004 (c= -0.13417986)
360a -> 368a : 0.017829 (c= 0.13352583)
361a -> 368a : 0.023339 (c= 0.15277016)
362a -> 370a : 0.296459 (c= -0.54448094)

STATE 22: E= 0.126818 au 3.451 eV 27833.3 cm**-1 <S**2> = 0.000000 Mult 1

356a -> 363a : 0.017324 (c= 0.13162037)
357a -> 364a : 0.095495 (c= 0.30902289)
359a -> 365a : 0.020907 (c= -0.14459179)
359a -> 366a : 0.188392 (c= -0.43404180)
361a -> 368a : 0.508257 (c= 0.71292147)
361a -> 369a : 0.053711 (c= -0.23175711)

STATE 23: E= 0.128463 au 3.496 eV 28194.3 cm**-1 <S**2> = 0.000000 Mult 1
356a -> 363a : 0.018461 (c= -0.13587264)
357a -> 363a : 0.012078 (c= -0.10990179)
357a -> 364a : 0.417862 (c= -0.64642237)
357a -> 365a : 0.016746 (c= 0.12940580)
358a -> 364a : 0.067010 (c= -0.25886241)
359a -> 364a : 0.013090 (c= 0.11441118)
359a -> 366a : 0.054258 (c= 0.23293385)
360a -> 366a : 0.028500 (c= -0.16882027)
360a -> 368a : 0.010802 (c= -0.10393375)
361a -> 368a : 0.219967 (c= 0.46900635)
361a -> 369a : 0.029307 (c= -0.17119315)
362a -> 370a : 0.011870 (c= 0.10895129)

STATE 24: E= 0.129639 au 3.528 eV 28452.5 cm**-1 <S**2> = 0.000000 Mult 1
355a -> 363a : 0.010472 (c= -0.10233326)
356a -> 363a : 0.041724 (c= 0.20426422)
357a -> 364a : 0.230261 (c= -0.47985487)
357a -> 365a : 0.011291 (c= 0.10625894)
359a -> 365a : 0.012425 (c= -0.11146552)
359a -> 366a : 0.290258 (c= -0.53875629)
360a -> 366a : 0.067843 (c= 0.26046690)
360a -> 368a : 0.083167 (c= 0.28838629)
361a -> 367a : 0.010760 (c= -0.10372920)
361a -> 368a : 0.013232 (c= -0.11503168)
361a -> 369a : 0.011943 (c= 0.10928379)
362a -> 369a : 0.012215 (c= -0.11052157)
362a -> 370a : 0.058510 (c= -0.24188854)

STATE 25: E= 0.129824 au 3.533 eV 28493.1 cm**-1 <S**2> = 0.000000 Mult 1
361a -> 367a : 0.976110 (c= 0.98798277)

STATE 26: E= 0.130964 au 3.564 eV 28743.2 cm**-1 <S**2> = 0.000000 Mult 1
355a -> 363a : 0.017358 (c= -0.13175000)

356a -> 363a : 0.252944 (c= 0.50293543)
359a -> 365a : 0.066190 (c= -0.25727480)
359a -> 366a : 0.045194 (c= 0.21258807)
360a -> 368a : 0.037273 (c= -0.19306263)
361a -> 369a : 0.029278 (c= -0.17110721)
362a -> 371a : 0.465348 (c= -0.68216395)

STATE 27: E= 0.131191 au 3.570 eV 28793.1 cm**-1 <S**2> = 0.000000 Mult 1
355a -> 363a : 0.167804 (c= -0.40963887)
356a -> 363a : 0.362585 (c= 0.60215013)
359a -> 365a : 0.131184 (c= 0.36219288)
362a -> 370a : 0.034572 (c= 0.18593598)
362a -> 371a : 0.178961 (c= 0.42303779)
362a -> 374a : 0.014666 (c= 0.12110411)
362a -> 375a : 0.010027 (c= 0.10013609)

STATE 28: E= 0.131716 au 3.584 eV 28908.4 cm**-1 <S**2> = 0.000000 Mult 1
355a -> 363a : 0.085306 (c= -0.29207143)
356a -> 363a : 0.042784 (c= -0.20684408)
359a -> 364a : 0.021106 (c= 0.14528062)
359a -> 365a : 0.354039 (c= 0.59501142)
359a -> 366a : 0.036386 (c= -0.19075225)
361a -> 368a : 0.027478 (c= 0.16576543)
361a -> 369a : 0.139360 (c= 0.37330943)
362a -> 371a : 0.205806 (c= -0.45365849)

STATE 29: E= 0.132057 au 3.593 eV 28983.2 cm**-1 <S**2> = 0.000000 Mult 1
355a -> 363a : 0.093866 (c= 0.30637557)
356a -> 363a : 0.093629 (c= 0.30598904)
359a -> 365a : 0.027220 (c= -0.16498505)
359a -> 366a : 0.026062 (c= 0.16143696)
361a -> 365a : 0.021727 (c= -0.14740207)
361a -> 368a : 0.070883 (c= 0.26623801)
361a -> 369a : 0.566299 (c= 0.75252865)
361a -> 370a : 0.027865 (c= -0.16692690)

STATE 30: E= 0.132558 au 3.607 eV 29093.1 cm**-1 <S**2> = 0.000000 Mult 1
354a -> 363a : 0.032152 (c= 0.17931093)
355a -> 363a : 0.445208 (c= 0.66723936)
356a -> 363a : 0.086140 (c= 0.29349547)
359a -> 365a : 0.240376 (c= 0.49028178)

359a -> 366a : 0.026830 (c= -0.16379813)
360a -> 368a : 0.012655 (c= 0.11249298)
361a -> 369a : 0.058625 (c= -0.24212626)

4.4 Summary of calculated TD-DFT data of 2-3b

Supplementary Table S14. Extended comparison of wavelengths λ_{max}, oscillator strengths f, and excitation energy E from experimental and TD-DFT calculations for iridasiliconoid salt **2** and the bimetallic compounds **3a,b**.

	Experimental		TD-DFT			
	λ_{max} (nm)	Excitation energy E (eV)	λ_{max} (nm)	Excitation energy E (eV)	Oscillator strength f	Transitions (% contribution)
2	543	2.283	528	2.349	0.0388	HOMO−2→LUMO (2.5) HOMO−1→LUMO (11.9) HOMO→LUMO (78.0) HOMO→LUMO+1 (4.1)
	425	2.917	430	2.885	0.0201	HOMO−4→LUMO (1.0) HOMO−3→LUMO (5.5) HOMO−2→LUMO (5.7) HOMO−1→LUMO+3 (1.2) HOMO→LUMO+1 (1.5) HOMO→LUMO+3 (77.8) HOMO→LUMO+4 (1.0) HOMO→LUMO+5 (1.2)
			418	2.965	0.0592	HOMO−4→LUMO (2.0) HOMO−3→LUMO (35.2) HOMO−3→LUMO+1 (2.7) HOMO−3→LUMO+3 (1.2) HOMO−2→LUMO (39.2) HOMO−2→LUMO+1 (2.9) HOMO−1→LUMO+3 (1.9) HOMO→LUMO (2.5) HOMO→LUMO+1 (1.2)
3a	601	2.063	636	1.949	0.0181	HOMO−1→LUMO (1.9) HOMO→LUMO (95.4)
	426	2.910	425	2.915	0.0540	HOMO−4→LUMO (34.6) HOMO−2→LUMO+1 (3.0) HOMO−1→LUMO+1 (46.9)

						HOMO→LUMO+1 (2.5) HOMO→LUMO+2 (1.7) HOMO→LUMO+3 (3.4) HOMO→LUMO+5 (1.0)
	354	3.502	354	3.506	0.002341513	HOMO−7→LUMO (1.3) HOMO−6→LUMO (3.2) HOMO−5→LUMO+1 (2.1) HOMO−1→LUMO+3 (1.5) HOMO→LUMO+2 (2.6) HOMO→LUMO+4 (10.0) HOMO→LUMO+5 (7.9) HOMO→LUMO+6 (59.9) HOMO→LUMO+7 (3.6)
3b	647	1.916	627	1.976	0.0179	HOMO−1→LUMO (2.3) HOMO→LUMO (95.3)
	524	2.366	536	2.315	0.0645	HOMO−1→LUMO (91.2) HOMO→LUMO (1.7) HOMO→LUMO+1 (1.4)
	340	3.647	344	3.607	0.00306	HOMO−8→LUMO (3.2) HOMO−7→LUMO (44.5) HOMO−6→LUMO (8.6) HOMO−3→LUMO+2 (24.0) HOMO−3→LUMO+3 (2.7) HOMO−2→LUMO+5 (1.3) HOMO−1→LUMO+6 (5.9)

5 References

S1 N. E. Poitiers, L. Giarrana, V. Huch, M. Zimmer and D. Scheschkewitz, Exohedral functionalization vs. core expansion of siliconoids with Group 9 metals: catalytic activity in alkene isomerization, *Chem. Sci.*, 2020, **11**, 7782.

S2 R. E. H. Kuveke, L. Barwise, Y. van Ingen, K. Vashisth, N. J. Roberts, S. S. Chitnis, J. L. Dutton, C. D. Martin and R. L. Melen, An International Study Evaluating Elemental Analysis, *ACS Cent. Sci.*, 2022, **8**, 855.

S3 S. Bachmann, B. Gernert and D. Stalke, Solution structures of alkali metal cyclopentadienides in THF estimated by ECC-DOSY NMR-spectroscopy (incl. software), *Chem. Commun.*, 2016, **52**, 12861.

S4 a) G. M. Sheldrick, A short history of SHELX, *Acta Cryst.*, 2008, **A64**, 112; b) G. M. Sheldrick, SHELXT – Integrated space-group and crystal, *Acta Cryst.*, 2015, **A71**, 3.

S5 G. M. Sheldrick, Crystal structure refinement with SHELXL, *Acta Cryst.*, 2015, **C71**, 3.

S6 C. B. Hübschle, G. M. Sheldrick and B. Dittrich, ShelXle: a Qt graphical user interface for SHELXL, *J. Appl. Crystallogr.*, 2011, **44**, 1281.

S7 A. L. Spek, 2003, PLATON: A Multipurpose Crystallographic Tool. Utrecht University, Utrecht, The Netherlands.

S8 F. Neese, The ORCA program system, *Comput. Mol. Sci.*, 2012, **2**, 73.

S9 Gaussian 09, Revision A.02, M. J. Frisch, G. W. Trucks, H. B. Schlegel, G. E. Scuseria, M. A. Robb, J. R. Cheeseman, G. Scalmani, V. Barone, G. A. Petersson, H. Nakatsuji, X. Li, M. Caricato, A. Marenich, J. Bloino, B. G. Janesko, R. Gomperts, B. Mennucci, H. P. Hratchian, J. V. Ortiz, A. F. Izmaylov, J. L. Sonnenberg, D. Williams-Young, F. Ding, F. Lipparini, F. Egidi, J. Goings, B. Peng, A. Petrone, T. Henderson, D. Ranasinghe, V. G. Zakrzewski, J. Gao, N. Rega, G. Zheng, W. Liang, M. Hada, M. Ehara, K. Toyota, R. Fukuda, J. Hasegawa, Ishida, M. T. Nakajima, Y. Honda, O. Kitao, H. Nakai, T. Vreven, K. Throssell, J. A. Montgomery Jr, J. E. Peralta, F. Ogliaro, M. Bearpark, J. J. Heyd, E. Brothers, K. N. Kudin, V. N. Staroverov, T. Keith, R. Kobayashi, J. Normand, K. Raghavachari, A. Rendell, J. C. Burant, S. S. Iyengar, J. Tomasi, M. Cossi, J. M. Millam, M. Klene, C. Adamo, R. Cammi, J. W. Ochterski, R. L. Martin, K. Morokuma, O. Farkas, J. B. Foresman and D. J. Fox, Gaussian, Inc., Wallingford CT, 2016.

S10 a) J. P. Perdew, Density-functional approximation for the correlation energy of the inhomogeneous electron gas, *Phys. Rev. B*, 1986, **33**, 8822; b) A. D. Becke, Density-functional exchange-energy approximation with correct asymptotic behavior, *Phys. Rev. A*, 1988, **38**, 3098; c) C. Adamo V. J. Barone, Toward reliable density functional methods without adjustable parameters: The PBE0 model, *Chem. Phys.*, 1999, **110**, 6158; d) M. Ernzerhof and G. E. Scuseria, Assessment of the Perdew–Burke–Ernzerhof exchange-correlation functional, *J. Chem. Phys.*, 1999, **110**, 5029.

S11 a) A. Schäfer, H. Horn and R. Ahlrichs, Fully optimized contracted Gaussian basis sets for atoms Li to Kr, *J. Chem. Phys.*, 1992, **97**, 2571; b) A. Schäfer, C. Huber and R. Ahlrichs, Fully optimized contracted Gaussian basis sets of triple zeta valence quality for atoms Li to Kr, *J. Chem. Phys.*, 1994, **100**, 5829; c) F. Weigend and R. Ahlrichs, Balanced basis sets of split valence, triple zeta valence and quadruple zeta valence quality for H to Rn: Design and assessment of accuracy, *Phys. Chem. Chem. Phys.*, 2005, **7**, 3297; d) F. Weigend, Accurate Coulomb-fitting basis sets for H to Rn, *Phys. Chem. Chem. Phys.*, 2006, **8**, 1057.

S12 S. Grimme, J. Antony, S. Ehrlich and H. Krieg, A consistent and accurate ab initio parametrization of density functional dispersion correction (DFT-D) for the 94 elements H-Pu, *J. Chem. Phys.*, 2010, **132**, 154104.

S13 V. Barone and M. Cossi, Quantum calculation of molecular energies and energy gradients in solution by a conductor solvent model, *J. Phys. Chem. A*, 1998, **102**, 1995-2001.

S14 Chemcraft - graphical software for visualization of quantum chemistry computations. Version 1.8, https://www.chemcraftprog.com

5.2 Tetrylene-Functionalized Si_7–Siliconoids

Supporting Information

Inorganic Chemistry

Tetrylene-Functionalized Si_7 Siliconoids

Luisa Giarrana, Michael Zimmer, Bernd Morgenstern and David Scheschkewitz*

L. Giarrana, Dr. M. Zimmer, Prof. Dr. D. Scheschkewitz − Krupp-Chair for General and Inorganic Chemistry, Saarland University, 66123 Saarbrücken, Germany
Dr. B. Morgenstern – Service Center X-ray Diffraction, Saarland University, 66123 Saarbrücken, Germany

E-Mail: scheschkewitz@mx.uni-saarland.de

Institute and/or researcher Twitter usernames: @scheschkewitz @LuisaGiarrana

5. Supporting Information

Table of Contents

5. Supporting Information

1. Experimental Procedures

All manipulations were carried out under a protective atmosphere of argon, by using a glovebox or standard Schlenk techniques. Solvents were dried and degassed by reflux over sodium/benzophenone under argon. [D_6]-benzene (C_6D_6) was dried over potassium mirror and distilled under argon prior to use. Si_7Tip_5Li siliconoid **II**[S1] and the chloro amidinato tetrylenes **1a-c**[S2] were prepared following the literature protocols. NMR spectra were recorded on a Bruker Avance IV 400 NMR spectrometer (^1H = 400.13 MHz, ^{13}C = 100.6 MHz, ^{29}Si = 79.6 MHz). The ^1H and $^{13}C\{1H\}$ NMR spectra were referenced to the residual proton and natural abundance ^{13}C resonances of the deuterated solvent and chemical shifts were reported relative to $SiMe_4$ (C_6D_6: δ^1H = 7.16 ppm and $\delta^{13}C$ = 128.06 ppm). UV-Vis spectra were recorded on a Shimadzu UV-2600 spectrometer in quartz cells with a path length of 0.1 cm. Elemental analyses were performed on an elemental analyzer Leco CHN-900. Mass spectrometry was measured on a Bruker SolariX 7 Tesla MALDI/ESI/APPI FTICR imaging MS. Melting points were determined under argon in NMR tubes and are uncorrected. The molten samples were examined by NMR spectroscopy to confirm whether decomposition had occurred upon melting. Crystallographic data of the structure reported in this paper has been deposited with the Cambridge Crystallographic Data Centre, CCDC, 12 Union Road, Cambridge CB21EZ, UK. (Fax: +44-1223-336-033; E-Mail: deposit@ccdc.cam.ac.uk, http://www.ccdc.cam.ac.uk).

2. Preparation, data and spectra

General procedure for the synthesis of the tetrylene-siliconoids

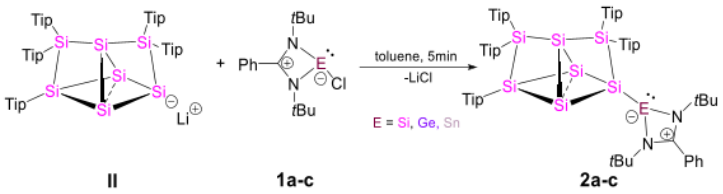

Supplementary Scheme S1. Synthesis of tetrylene-siliconoids **2a-c** (Ph = phenyl, *t*Bu = tert-butyl, Tip = 2,4,6-triisopropylbenzene).

The lithiated Si_7Tip_5 siliconoid **II** is dissolved in toluene and the corresponding chloro tetrylene **1a-c**[S2] is added as a solid. The resulting red-brown reaction mixture is stirred for 5 minutes at room temperature. All volatiles are removed under reduced pressure. The dark red-brown residue is taken up in hexane or pentane and separated from the precipitating LiCl salt by filtration. After washing 3x with 1 mL hexane/ pentane the solvent of the filtrate is removed under reduced pressure and the solid residues are washed 3x with 0.5 mL hexane/ pentane. The solid is dried thoroughly affording the tetrylenes-siliconoids **2a-c** as crude, clean product according to NMR spectroscopy.

5. Supporting Information

2.1 Preparation of NHSilylene-substituted siliconoid 2a

Quantities: II 98.0 mg (0.0622 mmol), chloro silylene 20.4 mg (0.0692 mmol), 1.5 mL toluene, let stay for 5 minutes, filtered from 4 mL pentane. Yield: 58.9 mg (0.040 mmol; 64 %) brown crystals. Single crystals of **2a** were obtained from a concentrated solution of **2a** in hexane at –26°C.

^{1}H NMR (400.13 MHz, C_6D_6, 300 K) δ = 7.625 (C_8H_{10}), 7.446 – 7.432 (bd, $^{3}J_{HH}$ = 5.50 Hz, 1H, Ar-*H*), 7.400 – 7.396 (d, $^{4}J_{HH}$ = 1.73 Hz, 1H, Ar-*H*), 7.299 – 7.296 (d, $^{4}J_{HH}$ = 1.60 Hz, 1H, Ar-*H*), 7.251 (C_8H_{10}), 7.144 – 7.140 (d, $^{4}J_{HH}$ = 1.85 Hz, 1H, Ar-*H*), 7.131 – 7.129 (d, $^{4}J_{HH}$ = 1.02 Hz, 2H, Ar-*H*), 7.107 – 7.103 (d, $^{4}J_{HH}$ = 1.63 Hz, 1H, Ar-*H*), 7.027 – 7.046 (d, $^{4}J_{HH}$ = 1.63 Hz, 1H, Ar-*H*), 6.992 – 6.988 (d, $^{4}J_{HH}$ = 1.63 Hz, 1H, Ar-*H*), 6.972 – 6.968 (m, 1H, Ar-*H*), 6.924 (m, 1H, Ar-*H*), 6.815 – 6.798 (m, 3H, Ar-*H*), 5.733 – 5.701 (m, 1H, Tip-*i*Pr-C*H*Me$_2$), 5. 358 – 5.294 (m, 1H, Tip-*i*Pr-C*H*Me$_2$), 5.040 – 4.963 (m, 1H, Tip-*i*Pr-C*H*Me$_2$), 4.804 – 4.739 (m, 1H, Tip-*i*Pr-C*H*Me$_2$), 4.404 – 4.359 (m, 1H, Tip-*i*Pr-C*H*Me$_2$), 3.953 – 3.888 (m, 1H, Tip-*i*Pr-C*H*Me$_2$), 3.742 – 3.659 (m, 2H, Tip-*i*Pr-C*H*Me$_2$), 3.441 – 3.3761 (m, 1H, Tip-*i*Pr-C*H*Me$_2$), 3.114 – 3.028 (m, 1H, Tip-*i*Pr-C*H*Me$_2$), 2.957 – 2.802 (m, 2H, Tip-*i*Pr-C*H*Me$_2$ overlapping with pentane-CH_2), 2.778 – 2.634 (m, 3H, Tip-*i*Pr-C*H*Me$_2$), 2.209 – 2.193 (d, $^{3}J_{HH}$ = 6.45 Hz, 3H, Tip-*i*Pr-CH_3), 2.108 – 2.092 (d, $^{3}J_{HH}$ = 6.45 Hz, 3H, Tip-*i*Pr-CH_3), 1.829 – 1.787 (dd, $^{3}J_{HH}$ = 10.48 Hz, $^{3}J_{HH}$ = 6.45 Hz, 6H, Tip-*i*Pr-CH_3), 1.727 – 1.667 (dd, $^{3}J_{HH}$ = 17.73 Hz, $^{3}J_{HH}$ = 6.45 Hz, 6H, Tip-*i*Pr-CH_3), 1.636 – 1.620 (d, $^{3}J_{HH}$ = 6.45 Hz, 3H, Tip-*i*Pr-CH_3), 1.582 – 1.535 (m, 12H, Tip-*i*Pr-CH_3), 1.489 – 1.472 (d, $^{3}J_{HH}$ = 6.68 Hz, 3H, Tip-*i*Pr-CH_3), 1.372 – 1.218 (m, 24H, Tip-*i*Pr-CH_3), 1.202 – 1.156 (m, 12H, Tip-*i*Pr-CH_3), 1.116 – 1.098 (d, $^{3}J_{HH}$ = 6.80 Hz, 6H, Tip-*i*Pr-CH_3), 0.996 – 0.989 (d, $^{4}J_{HH}$ = = 2.80 Hz, 18H, *t*BuC(CH_3)$_3$), 0.905 – 0.850 (t, 3H, pentane-CH_3), 0.702 – 0.663 (dd, $^{3}J_{HH}$ = 8.73 Hz, $^{3}J_{HH}$ = 6.80 Hz, 6H, Tip-*i*Pr-CH_3), 0.623 – 0.567 (dd, $^{3}J_{HH}$ = 17.40 Hz, $^{3}J_{HH}$ = 6.40 Hz, 6H, Tip-*i*Pr-CH_3), 0.424– 0.399 (dd, $^{3}J_{HH}$ = 6.40 Hz, $^{4}J_{HH}$ = 3.80 Hz, 6H, Tip-*i*Pr-CH_3) ppm.

^{13}C NMR (100.61 MHz, C_6D_6, 300 K) δ = 155.65 (s, 1C, Ar-*C*), 154.99, 154.19, 153.88, 153.25, 153.16, 152.97, 152.54, 152.30, 151.77 (s, each 1C, Ar-*C*), 150.35, 149.10, 148.95, (s, each 1C, Ar-*C*), 141.03, 139.79, 137.62, 137.46, 137.35, 133.96, 129.59, 129.29, (s, each 1C, Ar-*C*), 123.23, 122.84, 122.57, 122.45, 121.80, 121.45, 121.26, 120.91, 119.83 (s, each 1C, Ar-*C*H), 53.48 (s, 1C, *C*(CH$_3$)$_3$), 53.24 (s, 1C, *C*(CH$_3$)$_3$), 36.26, 35.14, 35.10, 35.05, 35.00, 34.35, 34.28, 34.24, 34.19, 34.08 (bs, each 1C, Tip-*i*Pr-CH), 33.07 (bs, each 1C, Tip-*i*Pr-*C*H), 32.65 (s, 1C Tip-*i*Pr-*C*H), 31.49, 31.52, 30.62 (s, each 3C, Tip-*i*Pr-CH), 28.80, 27.41, 27.29, 27.22, 26.92, 26.82, 26.60, 26.06, 25.25, (bs, each 2C, Tip-*i*Pr-*C*H$_3$), 24.90, 24.71, 24.50, 24.28, 24.06, 23.91, 23.78, 23.66, 23.57, 22.38 (s, 2C, Tip-*i*Pr-*C*H$_3$), 21.32 (s, 6C, C(*C*H$_3$)$_3$), 13.94 ppm.

^{29}Si NMR (79.49 MHz, C_6D_6, 300 K) δ = –219.0 (s, *Si*), –211.6 (s, *Si*), –101.2 (s, *Si*), 0.3 (s, *Si*Tip$_2$), 24.1 (s, *Si*(N*t*Bu)$_2$CPh), 32.4 (s, *Si*Tip$_2$), 159.6 (s, *Si*Tip), 211.7 (s, *Si*(Si(N*t*Bu)$_2$CPh)) ppm.

CP-MAS ^{29}Si-NMR (79.53 MHz, 13 KHz, 300 K) δ = 221.4 (s, *Si*(Si(N*t*Bu)$_2$CPh)), 155.6 (s, *Si*Tip), 29.3 (s, *Si*Tip$_2$), 17.3 (s, *Si*(N*t*Bu)$_2$CPh), –3.0 (s, *Si*Tip$_2$), –106.6 (s, *Si*), –210.7 (s, *Si*), –224.2 (s, *Si*) ppm.

5. Supporting Information

Elemental analysis: calculated for $C_{90}H_{138}Si_8N_2$: C: 73.40%; H: 9.44%; N: 1.90%. Found: C: 71.90 %; H: 8,64%; N: 1.49%. The lower values compared to those calculated are quite common for unsaturated silicon clusters due to incomplete combustion typically attributed to the formation of silicon carbides and/or nitrides. In addition, elemental analysis has come under scrutiny because of highly variable results of bona fide identical samples.[S3]

UV-Vis (hexane): λ_{max} (ε) = 336 (26647 M^{-1} cm^{-1}), 371 (12940 M^{-1} cm^{-1}), 532 (704 M^{-1} cm^{-1}) nm.

Melting Point: 290°C (decomp.).

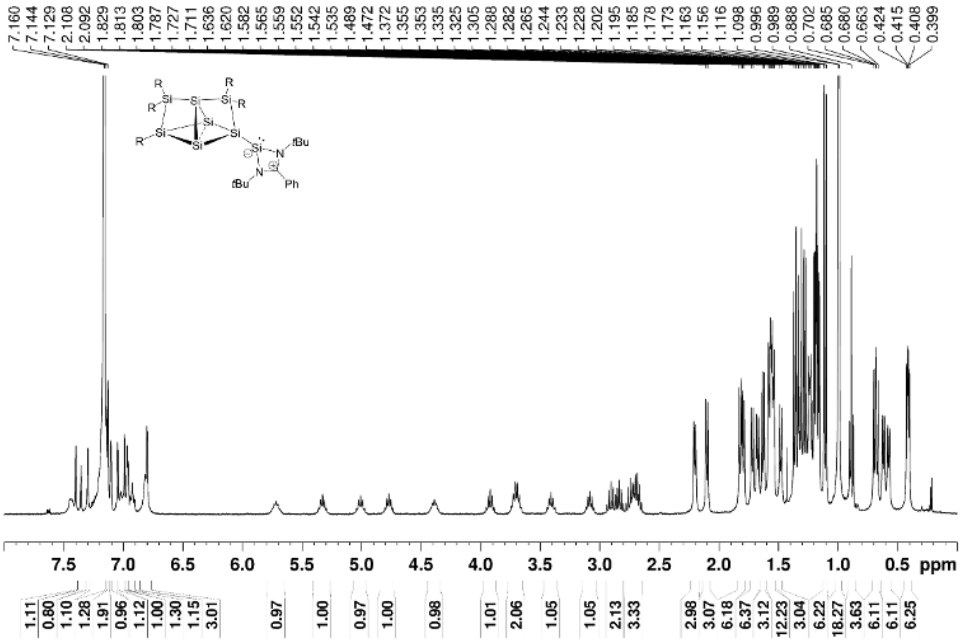

Supplementary Figure S1. ^{1}H NMR of **2a** in C_6D_6 (400.13 MHz, 300 K).

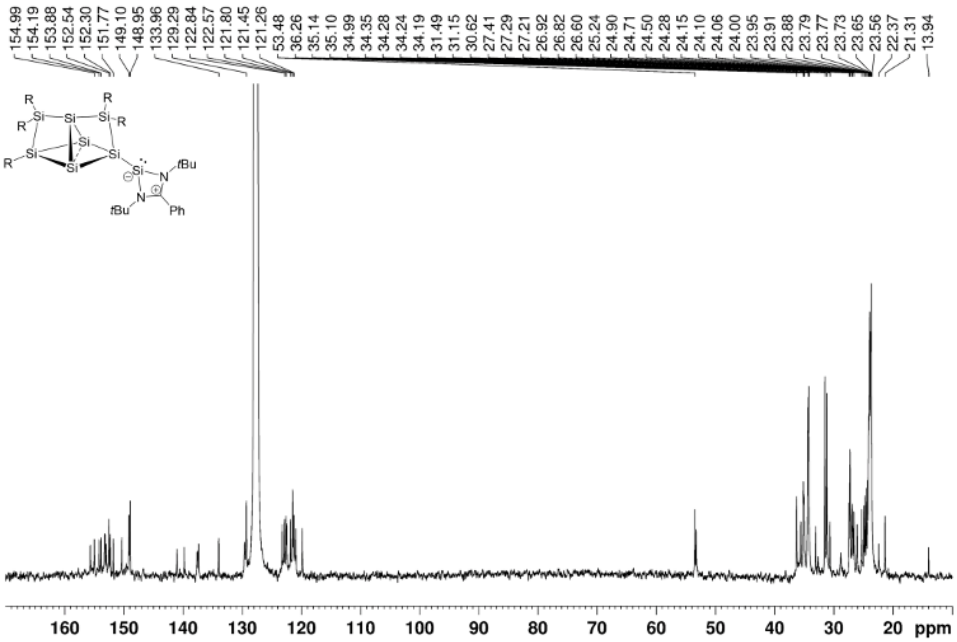

5. Supporting Information

Supplementary Figure S2. ^{13}C NMR of **2a** in C_6D_6 (100.61 MHz, 300 K).

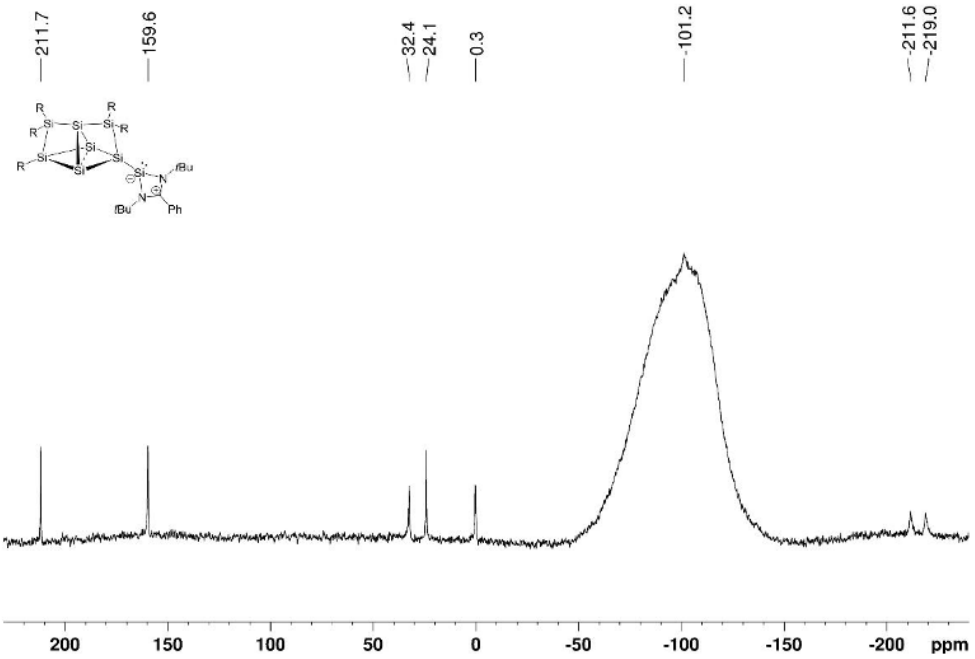

Supplementary Figure S3. ^{29}Si NMR of **2a** in C_6D_6 (79.49 MHz, 300 K).

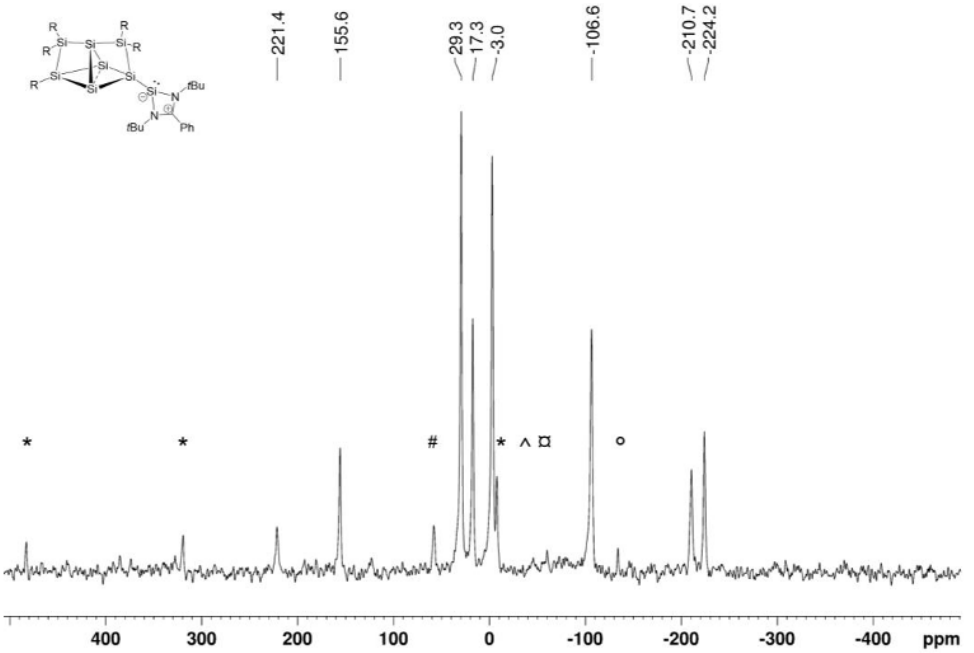

Supplementary Figure S4. CP-MAS ^{29}Si NMR of **2a** (79.53 MHz, 13 KHz, 300 K), side spinning bands: #221.4, *155.6, °29.3 , ^–210.7, ¤–224.2 ppm.

5. Supporting Information

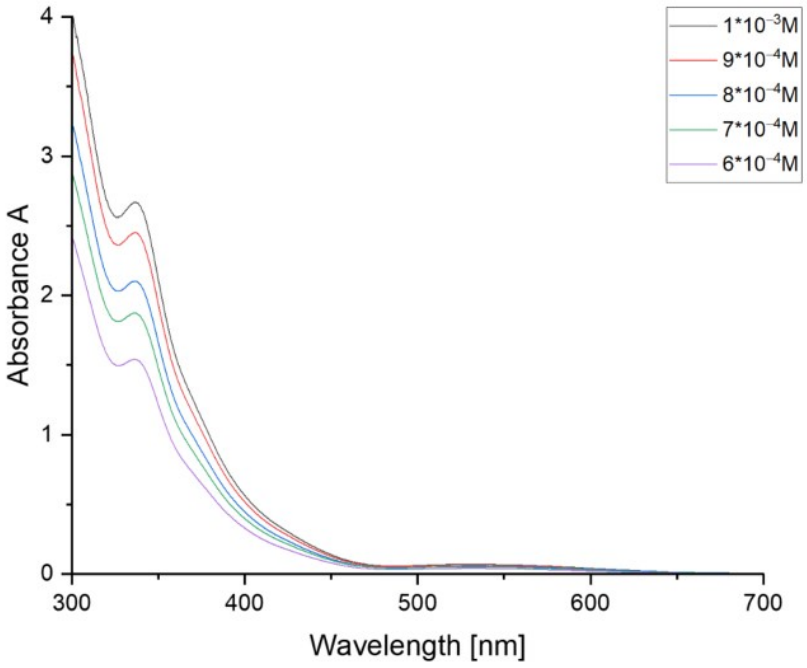

Supplementary Figure S5. UV-Vis spectra of the NHSilylene-substituted siliconoid **2a** in hexane at different concentrations.

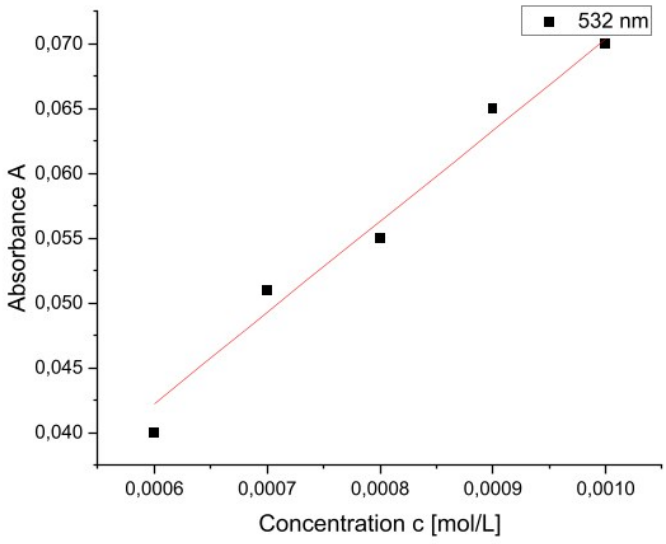

Supplementary Figure S6. Determination of the extinction ε = 704 $M^{-1} \cdot cm^{-1}$ of **2a** by linear regression at λ_{max} = 532 nm.

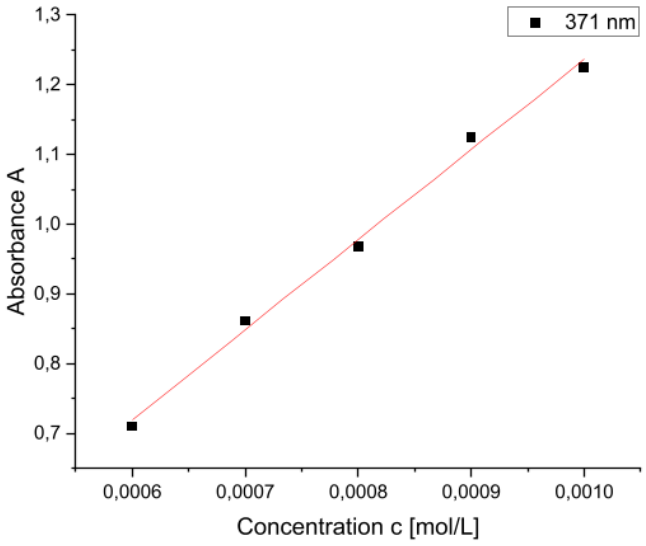

Supplementary Figure S7. Determination of the extinction ε = 12940 $M^{-1}{\cdot}cm^{-1}$ of **2a** by linear regression at λ = 371 nm.

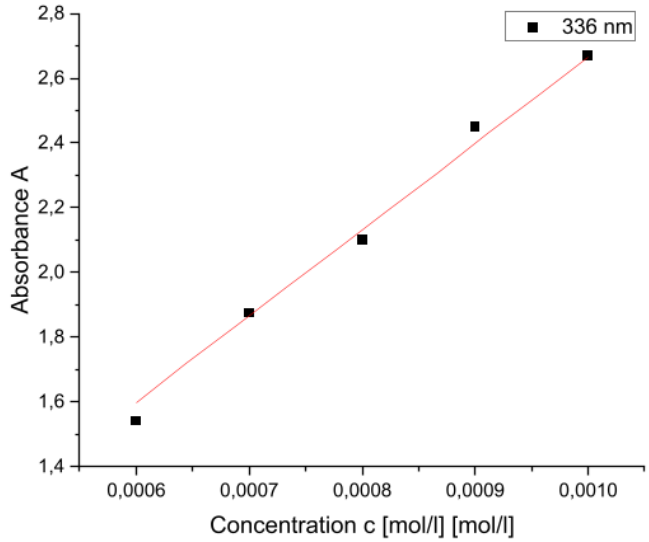

Supplementary Figure S8. Determination of the extinction ε = 26647 $M^{-1}{\cdot}cm^{-1}$ of **2a** by linear regression at λ = 336 nm.

2.1.2 Preparation of 2b

Quantities: II 100.7 mg (0.0642 mmol), chloro germylene 23.8 mg (0.0701 mmol), 1.5 mL toluene, let stay for 5 minutes, filtered from 4 mL hexane. Yield: 65.0 mg (0.0428 mmol; 67 %) red-brown solid.

^{1}H NMR (400.13 MHz, C_6D_6, 300 K) δ = 7.627 (C_8H_{10}), 7.402 – 7.383 (bd, $^3J_{HH}$ = 7.58 Hz, 1H, Ar-*H*), 7.368 – 7.364(d, $^4J_{HH}$ = 1.54 Hz, 1H, Ar-*H*), 7.291 – 7.288 (d, $^4J_{HH}$ = 1.54 Hz, 1H, Ar-*H*), 7.251 (C_8H_{10}), 7.133 – 7.118 (m, 3H, Ar-*H*), 7.093 – 7.089 (d, $^4J_{HH}$ = 1.47 Hz, 1H, Ar-*H*), 7.045 – 7.030 (m, 2H, Ar-*H*),

6.975 – 6.971 (d, $^4J_{HH}$ = 1.31 Hz, 1H, Ar-*H*), 6.956 – 6.903 (m, 3H, Ar-*H*), 6.870 – 6.852 (m, 1H, Ar-*H*), 6.795 – 6.792 (d, $^4J_{HH}$ = 1.47 Hz, 1H, Ar-*H*), 5.656 – 5.592 (m ,1H, Tip-*i*Pr-C*H*Me$_2$), 5.411 – 5.312 (sept, $^3J_{HH}$ = 6.53 Hz, 1H, Tip-*i*Pr-C*H*Me$_2$), 5.024 – 4.927 (sept, $^3J_{HH}$ = 6.47 Hz, 1H, Tip-*i*Pr-C*H*Me$_2$), 4.790 – 4.692 (sept, $^3J_{HH}$ = 6.47 Hz, 1H, Tip-*i*Pr-C*H*Me$_2$), 4.423 – 4.322 (sept, $^3J_{HH}$ = 6.51 Hz, 1H, Tip-*i*Pr-C*H*Me$_2$), 3.944 – 3.848 (sept, $^3J_{HH}$ = 6.43 Hz, 1H, Tip-*i*Pr-C*H*Me$_2$), 3.704 – 3.627 (m, 2H, Tip-*i*Pr-C*H*Me$_2$), 3.454 – 3.359 (sept, $^3J_{HH}$ = 6.50 Hz, 1H, Tip-*i*Pr-C*H*Me$_2$), 3.140 – 3.045 (sept, $^3J_{HH}$ = 6.50 Hz, 1H, Tip-*i*Pr-C*H*Me$_2$), 2.923– 2.805 (m, 2H, Tip-*i*Pr-C*H*Me$_2$), 2.763 -2.629 (m, 4H, Tip-*i*Pr-C*H*Me$_2$ C*H*Me$_2$ overlapping with hexane-C*H*$_2$), 2.210 – 2.194 (d, $^3J_{HH}$ = 6.32 Hz, 3H, Tip-*i*Pr-C*H*$_3$), 2.067 – 2.052 (d, $^3J_{HH}$ = 6.32 Hz, 3H, Tip-*i*Pr-C*H*$_3$), 1.802 – 1.768 (m, 6H, Tip-*i*Pr-C*H*$_3$), 1.714 – 1.698 (d, $^3J_{HH}$ = 6.42 Hz, 3H, Tip-*i*Pr-C*H*$_3$), 1.628 – 1.573 (m, 6H, Tip-*i*Pr-C*H*$_3$), 1.1573 – 1.530 (m, 12H, Tip-*i*Pr-C*H*$_3$) 1.485 – 1.469 (d, $^3J_{HH}$ = 6.62 Hz, 3H, Tip-*i*Pr-C*H*$_3$), 1.351 – 1.286 (m, 16H, Tip-*i*Pr-C*H*$_3$), 1.268 (bs, 2H, Tip-*i*Pr-C*H*$_3$), 1.227 – 1.211 (m, 4H, Tip-*i*Pr-C*H*$_3$), 1.189 (bs, 1H, Tip-*i*Pr-C*H*$_3$), 1.179 – 1.149 (m, 12H, Tip-*i*Pr-C*H*$_3$, overlapping with hexane-C*H*$_3$), 1.109 – 1-092 (d, $^3J_{HH}$ = 6.94 Hz, 6H, Tip-*i*Pr-C*H*$_3$), 0.917 – 0.915 (d, $^4J_{HH}$ = = 0.85 Hz, 18H, *t*BuC(C*H*$_3$)$_3$), 0.684 – 0.668 (d, $^3J_{HH}$ = 6.60 Hz, 6H, Tip-*i*Pr-C*H*$_3$), 0.596 – 0.545 (dd, $^3J_{HH}$ = 12.86 Hz, $^3J_{HH}$ = 6.29 Hz, 6H, Tip-*i*Pr-C*H*$_3$), 0.424 – 0.404 (dd, $^3J_{HH}$ = 6.29 Hz, $^4J_{HH}$ = 1.60 Hz, 6H, Tip-*i*Pr-C*H*$_3$) ppm.

^{13}C NMR (100.61 MHz, C_6D_6, 300 K) δ = 162.52 (s, 1C, Ar-*C*), 155.34, 154.79, 154.41, 153.52, 153.16, 152.95 – 152.91 (d, *J* = 2.98 Hz, 1C, Ar-*C*), 152.74, 152.15, 150.72 (s, each 1C, Ar-*C*), 149.51, 149.35 (s, each 1C, Ar-*C*), 141.18, 140.08, 138.16, 137.85, 137.73, 136.11, 134.07 (s, each 1C, Ar-*C*), 129.75, 129.34, 128.47, 128.17, 127.93, 127.52, 127.49, 126.05 (s, each 1C, Ar-*C*), 123.42, 123.23, 122.99 - 122.92 (d, 1C, *J* = 6.70 Hz, Ar-*C*H), 122.20, 121.84, 121.71, 121.15, 120.25 (s, each 1C, Ar-*C*H), 53.78 (s, 1C, *C*(CH$_3$)$_3$), 53.64 (s, 1C, *C*(CH$_3$)$_3$), 36.65, 35.95, 35.64, 36.54, 35.46, 35.42, 34.73, 34.68, 34.63, 34.54, 33.52, 32.23, 31.93, 31.62, 30.84 (s, each 1C, Tip-*i*Pr-*C*H), 27.88, 27.70, 27.60, 27.28, 27.05, 26.82, 26.28, 25.55, 25.19, 25.00, 24.91, 24.61, 24.52, 24.36, 24.28, 24.21, 24.10, 24.01 21.89, (s, each 2C, Tip-*i*Pr-*C*H$_3$), 14.34 (s, 6C, C(*C*H$_3$)$_3$)) ppm.

^{29}Si NMR (79.49 MHz, C_6D_6, 300 K) δ = 220.2 (s, *Si*(Ge(N*t*Bu)$_2$CPh), 160.4 (s, *Si*Tip), 32.4 (s, *Si*Tip$_2$), −0.1 (s, *Si*Tip$_2$), –100.7 (s, *Si*), –209.6 (s, *Si*), –217.6 (s, *Si*) ppm.

CP-MAS ^{29}Si-NMR (79.53 MHz, 13 KHz, 300 K) δ = 218.3 (s, *Si*(Ge(N*t*Bu)$_2$CPh), 161.2 (s, *Si*Tip), 30.7 (s, *Si*Tip$_2$), −1.8 (s, SiTip$_2$), –59.4 (s, *Si*H?), –101.9 (s, *Si*), –216.9 (s, *Si*), –220.9 (s, *Si*) ppm.

Elemental analysis: calculated for $C_{90}H_{138}GeN_2Si_7$: C: 71.24%; H: 9.17%; N: 1.85%. Found: C: 71.67%; H: 8.75%; N: 1.64%. The lower values compared to those calculated are quite common for unsaturated silicon clusters due to incomplete combustion typically attributed to the formation of silicon carbides and/or nitrides. In addition, elemental analysis has come under scrutiny because of highly variable results of bona fide identical samples.[S3]

UV-Vis (hexane): λ_{max} (ε) = 345 (18200 M^{-1} cm^{-1}), 407 (3190 M^{-1} cm^{-1}), 514 (580 M^{-1} cm^{-1}) nm.

Melting Point: 161°C.

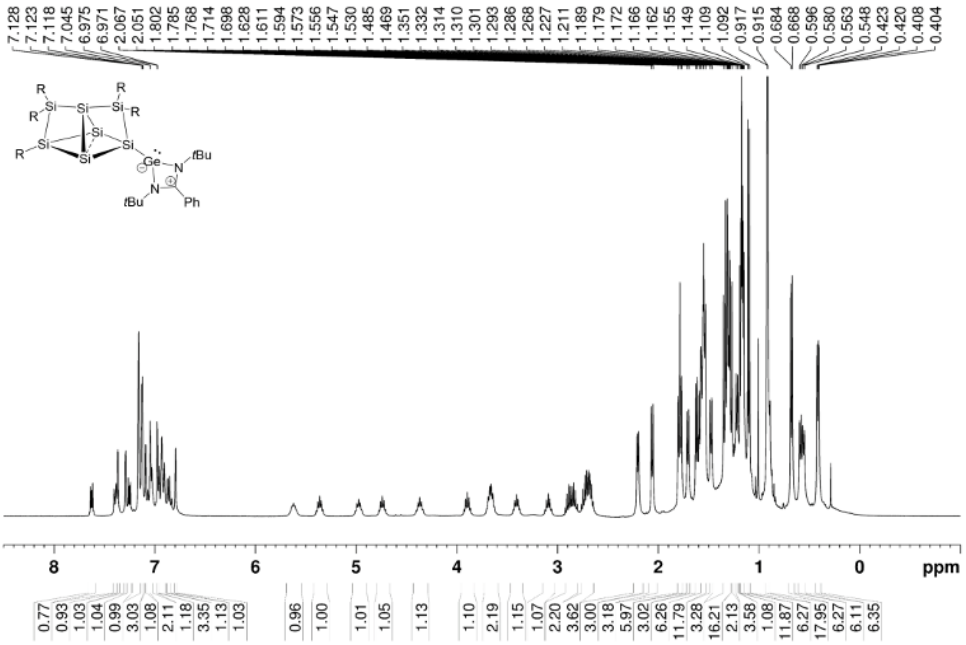

Supplementary Figure S9. ^{1}H NMR of **2b** in C_6D_6 (400.13 MHz, 300 K).

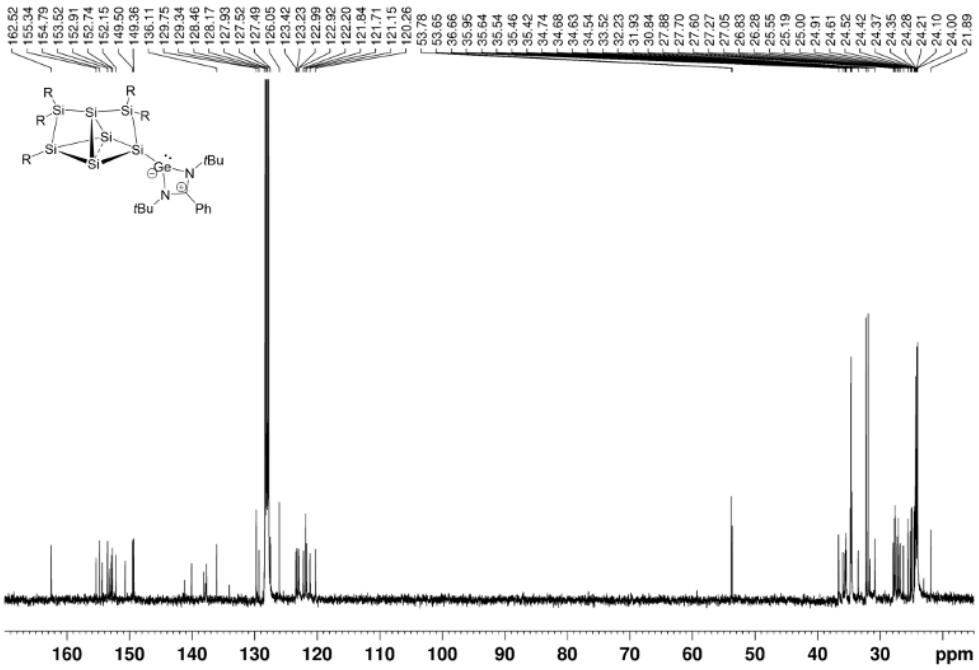

Supplementary Figure S10. ^{13}C NMR of **2b** in C_6D_6 (100.61 MHz, 300 K).

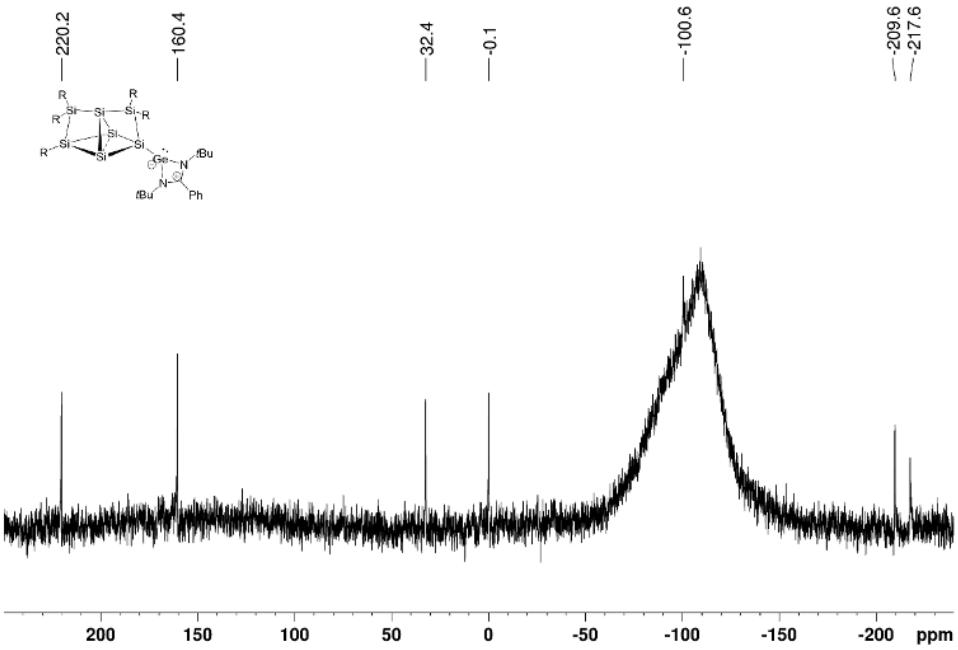

Supplementary Figure S11. ^{29}Si NMR of **2b** in C_6D_6 (79.49 MHz, 300 K).

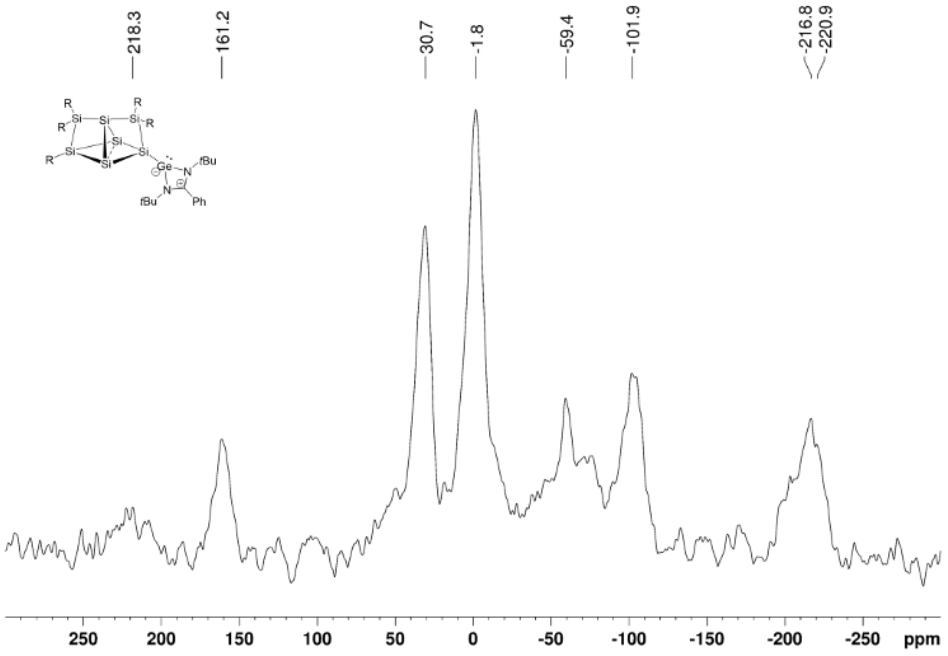

Supplementary Figure S12. CP-MAS ^{29}Si NMR of **2b** (79.53 MHz, 13 KHz, 300 K).

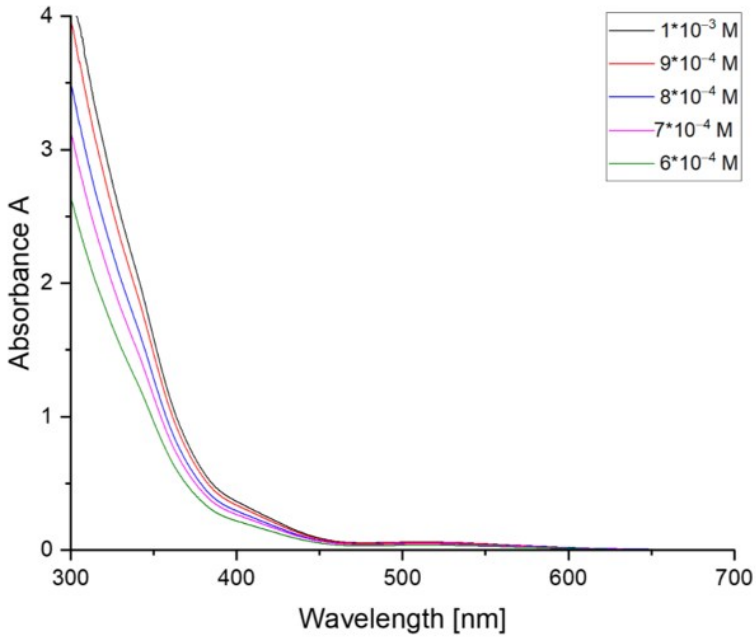

Supplementary Figure S13. UV-Vis spectra of the NHGermylene-substituted siliconoid **2b** in hexane at differ concentrations.

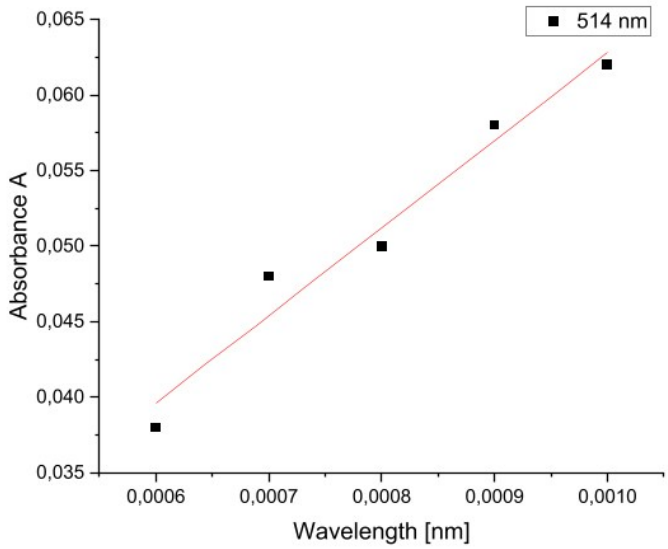

Supplementary Figure S14. Determination of the extinction ε = 580 $M^{-1} \cdot cm^{-1}$ of **2b** by linear regression at λ_{max} = 514 nm.

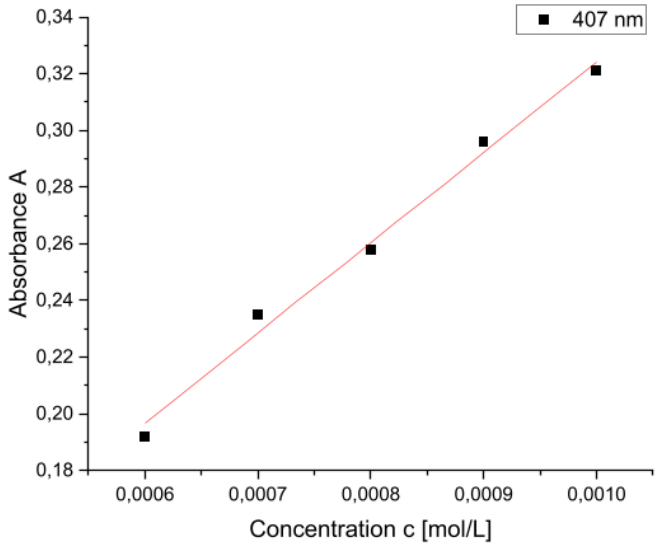

Supplementary Figure S15. Determination of the extinction ε = 3190 $M^{-1} \cdot cm^{-1}$ of **2b** by linear regression at λ = 407 nm.

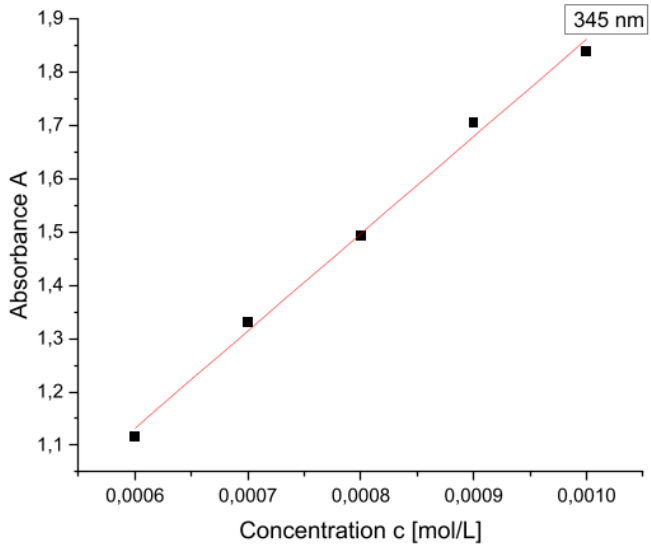

Supplementary Figure S16. Determination of the extinction ε = 18200 $M^{-1} \cdot cm^{-1}$ of **2b** by linear regression at λ = 345 nm.

2.1.3 Preparation of 2c

Quantities: II 100.1 mg (0.0638 mmol), chloro stannylene 27.0 mg (0.0700 mmol), 1.5 mL toluene, let stay for 5 minutes, filtered from 4 mL hexane. Yield: 70.4 mg (0.0450 mmol; 71 %) brown solid.

^{1}H NMR (400.13 MHz, C_6D_6, 300 K) δ = 7.627 (C_8H_{10}), 7.351 – 7.347 (bd, $^4J_{HH}$ = 1.38 Hz, 1H, Ar-*H*), 7.324 – 7.305 (bd, $^3J_{HH}$ = 7.64 Hz, 1H, Ar-*H*), 7.293 – 7.289 (d, $^4J_{HH}$ = 1.57 Hz, 1H, Ar-*H*), 7.248 (C_8H_{10}),

7.1423 – 7.139 (d, $^4J_{HH}$ = 1.49 Hz, 1H, Ar-*H*), 7.127 – 7.123 – 7.109 (dd, $^3J_{HH}$ = 5.61 Hz, $^4J_{HH}$ = 1.63 Hz, 2H, Ar-*H*), 7.092 – 7.088 (d, $^4J_{HH}$ = 1.34 Hz, 1H, Ar-*H*), 7.047 – 7.043 (d, $^4J_{HH}$ = 1.65 Hz, 1H, Ar-*H*), 7.035 – 7.015 (m, 1H, Ar-*H*), 6.967 – 6.946 (m, 2H, Ar-*H*), 6.921 – 6.904 (m, 2H, Ar-*H*), 6.891 – 6.874 (m, 1H, Ar-*H*), 6.806 – 6.802 (d, $^4J_{HH}$ = 1.54 Hz, 1H, Ar-*H*), 5.464 – 5.397 (m, 2H, Tip-*i*Pr-C*H*Me$_2$), 5.098 – 5.033 (m, 1H, Tip-*i*Pr-C*H*Me$_2$), 4.757 – 4.659 (m, 1H, Tip-*i*Pr-C*H*Me$_2$), 4.509 – 4.412 (sept, $^3J_{HH}$ = 6.60 Hz, 1H, Tip-*i*Pr-C*H*Me$_2$), 3.880 – 3.720 (m, 2H, Tip-*i*Pr-C*H*Me$_2$), 3.638 – 3.541 (sept, $^3J_{HH}$ = 6.60 Hz, 1H, Tip-*i*Pr-C*H*Me$_2$), 3.466– 3.369 (sept, $^3J_{HH}$ = 6.60 Hz, 1H, Tip-*i*Pr-C*H*Me$_2$), 3.167 – 3.068 (sept, $^3J_{HH}$ = 6.60 Hz, 1H, Tip-*i*Pr-C*H*Me$_2$), 2.913 – 2.796 (m, 2H, Tip-*i*Pr-C*H*Me$_2$), 2.760 – 2.635 (m, 4H, Tip-*i*Pr-C*H*Me$_2$ overlapping with hexane-CH_2), 2.231 – 2.215 (d, $^3J_{HH}$ = 6.42 Hz, 3H, Tip-*i*Pr-CH_3), 2.035 – 2.019 (d, $^3J_{HH}$ = 6.42 Hz, 3H, Tip-*i*Pr-CH_3), 1.810 – 1.757 (dd, $^3J_{HH}$ = 14.49 Hz, $^3J_{HH}$ = 6.79 Hz, 6H, Tip-*i*Pr-CH_3), 1.709 – 1.693 (d, $^3J_{HH}$ = 6.61 Hz, 3H, Tip-*i*Pr-CH_3), 1.630– 1.614 (d, $^3J_{HH}$ = 6.45 Hz, 3H, Tip-*i*Pr-CH_3), 1.546 – 1.520 (dd, $^3J_{HH}$ = 6.50 Hz, $^4J_{HH}$ = 3.84 Hz, 6H, Tip-*i*Pr-CH_3), 1.546 – 1.520 (dd, $^3J_{HH}$ = 14.09 Hz, $^3J_{HH}$ = 6.60 Hz, 6H, Tip-*i*Pr-CH_3), 1.327 – 1.310 (m, 8H, Tip-*i*Pr-CH_3), 1.300 (bs, 6H, Tip-*i*Pr-CH_3), 1.283 – 1.281 (d, $^4J_{HH}$ = 0.74Hz, 3H, Tip-*i*Pr-CH_3), 1.231 – 1.215 (m, 4H, Tip-*i*Pr-CH_3), 1.176 – 1.141 (m, 16H, Tip-*i*Pr-CH_3), 1.118 – 1.100 (d, $^3J_{HH}$ = 6.95 Hz, 6H, Tip-*i*Pr-CH_3), 0.906 – 0.872 (t, 2H, hexane-CH_3), 0.848 – 0.831 (d, $^3J_{HH}$ = 6.87 Hz, 3H, Tip-*i*Pr-CH_3), 0.740 – 0.724(d, $^3J_{HH}$ = 6.73 Hz, 3H, Tip-*i*Pr-CH_3), 0.678 – 0.662 (d, $^3J_{HH}$ = 6.52 Hz, 3H, Tip-*i*Pr-CH_3), 0.606 – 0.590 (d, $^3J_{HH}$ = 6.30 Hz, 3H, Tip-*i*Pr-CH_3), 0.551 – 0.535 (d, $^3J_{HH}$ = 6.30 Hz, 3H, Tip-*i*Pr-CH_3), 0.455 – 0.416 (dd, $^3J_{HH}$ = 9.25 Hz, $^3J_{HH}$ = 6.46Hz, 6H, Tip-*i*Pr-CH_3) ppm.

^{13}C NMR (100.61 MHz, C_6D_6, 300 K) δ = 167.52 (s, 1C, Ar-*C*), 155.18, 154.51, 153.59, 153.26 (s, each 1C, Ar-*C*), 153.08 – 153.01 (d, *J* = 2.98 Hz, 1C, Ar-*C*), 152.67, 152.13, 150.73, 149.54, 149.44, 149.41, 149.38 (s, each 1C, Ar-*C*), 140.94, 140.59. 139.88, 138.90, 138.15, 138.08, 137.76, 134.07, 129.94, 129.51, 128.47, 128.17, 127.93, 127.35 (s, each 1C, Ar-*C*), 127.26, 126.05, 123.21, 123.16, 122.25, 121.91, 121.88, 121.81, 121.04, 120.41 (s, each 1C, Ar-*C*H), 53.16 (s, 1C, *C*(CH$_3$)$_3$), 52.71 (s, 1C, *C*(CH$_3$)$_3$), 36.73, 36.32, 36.06, 35.73, 35.51, 35.42, 34.76, 34.61, 34.51, 33.66, 32.78, 32.46, 31.96, 30.87, 28.54, (s, 1C, Tip-*i*Pr-*C*H), 27.83, 27.51, 27.32, 27.18, 26.92, 26.52, 25.94, 25.30, 24.97, 24.59, 24.52, 24.44, 24.33, 24.28, 24.20, 24.13 (s, each 2C Tip-*i*Pr-*C*H$_3$), 24.07 – 24.05 (d, *J* = 2.84 Hz, 2C Tip-*i*Pr-*C*H$_3$), 23.04, 22.12 (s, 2C Tip-*i*Pr-*C*H$_3$), 14.35 (s, 6C, C(*C*H$_3$)$_3$) ppm.

^{29}Si NMR (79.49 MHz, C_6D_6, 300 K) δ = 237.8 (s, (s, *Si*(Sn(N*t*Bu)$_2$CPh)), 163.3 (s, *Si*Tip), 37.9 (s, *Si*Tip$_2$), 5.7 (s, *Si*Tip$_2$), –85.8 (s, *Si*), –198.3 (s, *Si*), –210.9 (s, *Si*) ppm.

^{119}Sn NMR (149.21 MHz, C6D6, 300 K) δ = 196.6 ppm.

CP-MAS ^{29}Si-NMR (79.53 MHz, 13 KHz, 300 K) δ = 238.9 (s, *Si*(Sn(N*t*Bu)$_2$CPh)), 160.9 – 165.5 (d, *J* = 371.05 Hz, *Si*Tip), 34.4 (s, *Si*Tip$_2$), 1.6 (s, SiTip$_2$), –60.1 (m, *Si*H?) –83.0 (m, *Si*), –198.9 – –195.3 (m, *Si*), –205.6 (s, *Si*?), –215.8 – –211.3 (m, *Si*), ppm.

Elemental analysis: calculated for $C_{90}H_{138}N_2Si_7Sn$: C: 69.14%; H: 8.90%; N: 1.79%. Found: C: 67.11 %; H: 8.06%; N: 1.88%. The lower values compared to those calculated are quite common for unsaturated silicon clusters due to incomplete combustion typically attributed to the formation of silicon carbides and/or nitrides. In addition, elemental analysis has come under scrutiny because of highly variable results of bona fide identical samples.[S3]

UV-Vis (hexane): λ_{max} (ε) = 324 (31580 M^{-1} cm^{-1}), 417 (3910 M^{-1} cm^{-1}), 520 (870 M^{-1} cm^{-1}) nm.

Melting Point: 177°C.

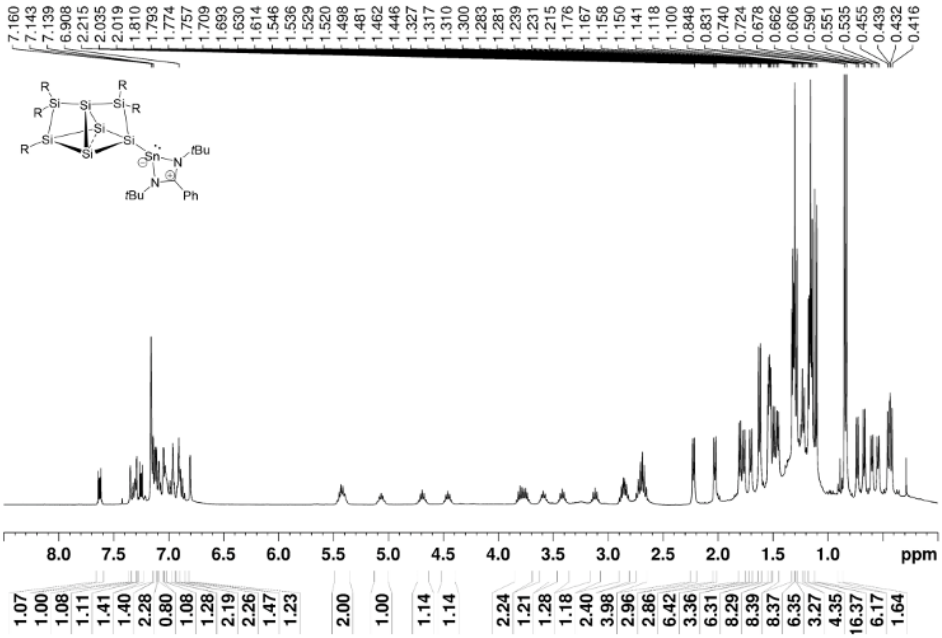

Supplementary Figure S17. ^{1}H NMR of **2c** in C_6D_6 (400.13 MHz, 300 K).

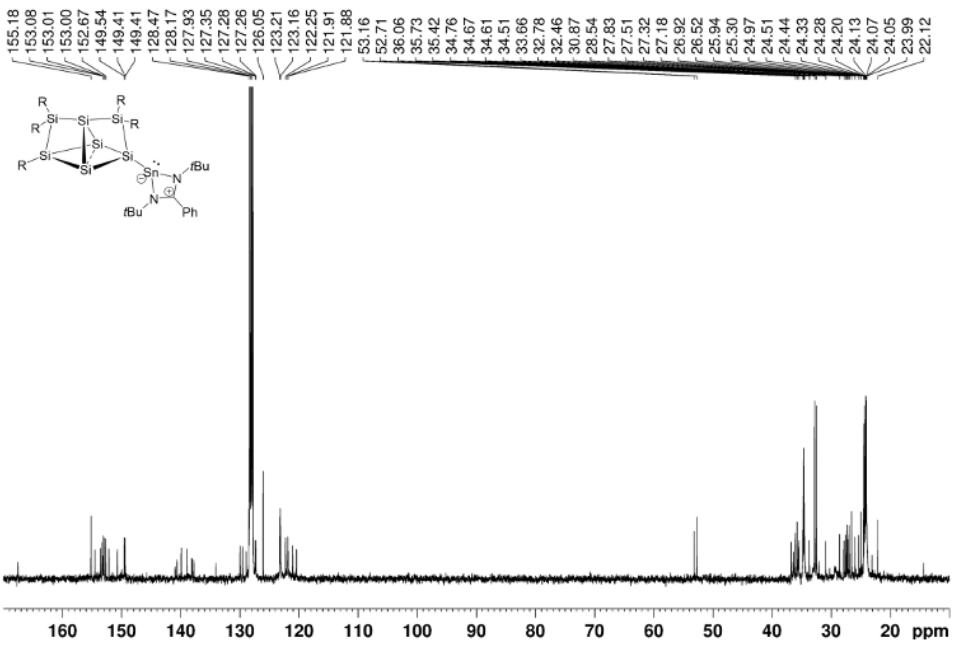

Supplementary Figure S18. ^{13}C NMR of **2c** in C_6D_6 (100.61 MHz, 300 K).

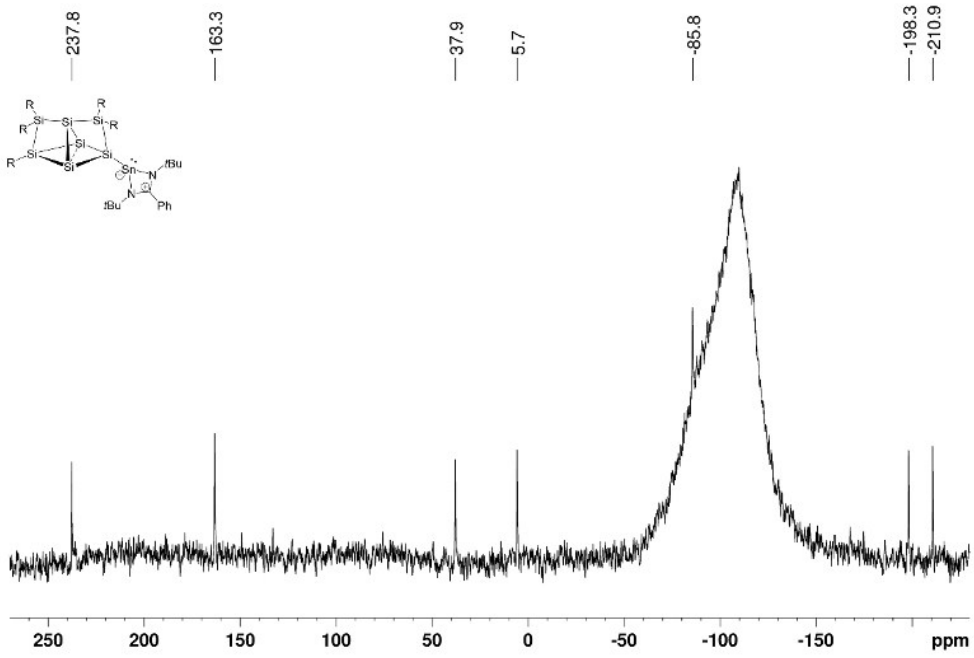

Supplementary Figure S19. ^{29}Si NMR of **2c** in C_6D_6 (79.49 MHz, 300 K).

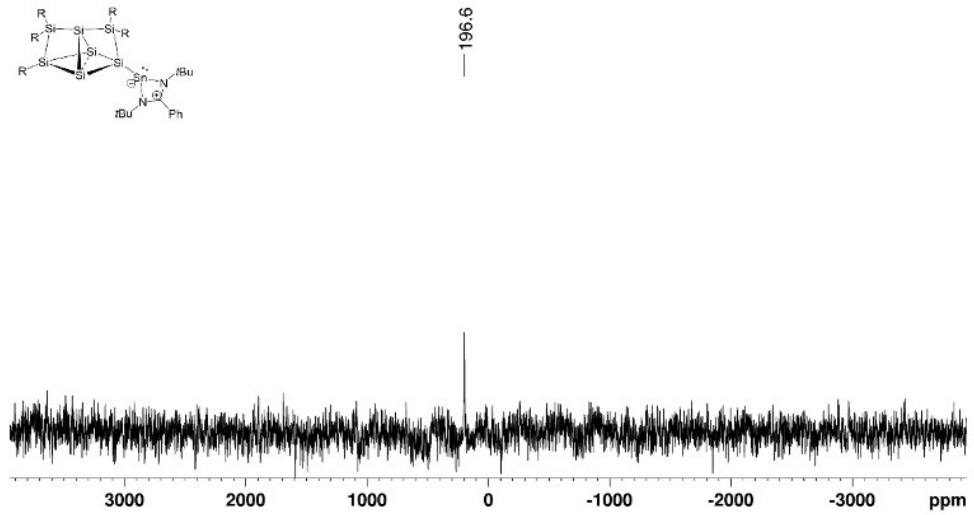

Supplementary Figure S20. ^{119}Sn NMR of **2c** in C_6D_6 (79.49 MHz, 300 K).

5. Supporting Information

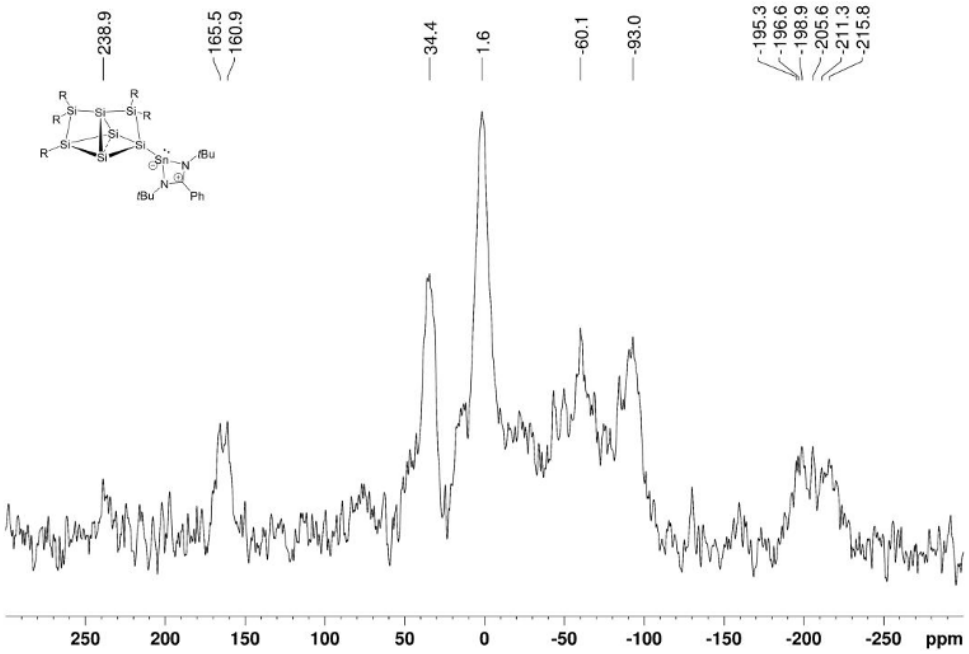

Supplementary Figure S21. CP-MAS ^{29}Si NMR of **2b** (79.53 MHz, 13 KHz, 300 K).

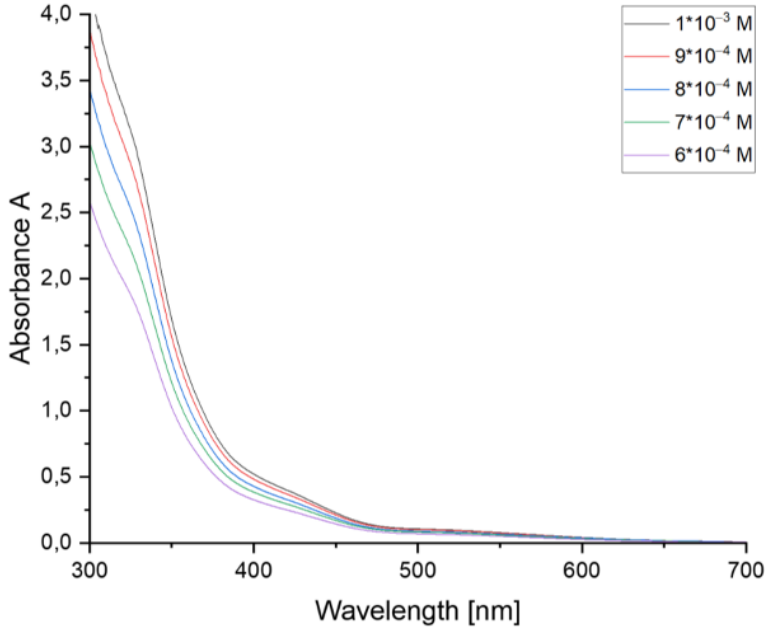

Supplementary Figure S22. UV-Vis spectra of the new NHStannylene-substituted siliconoid **2c** in hexane at different concentrations.

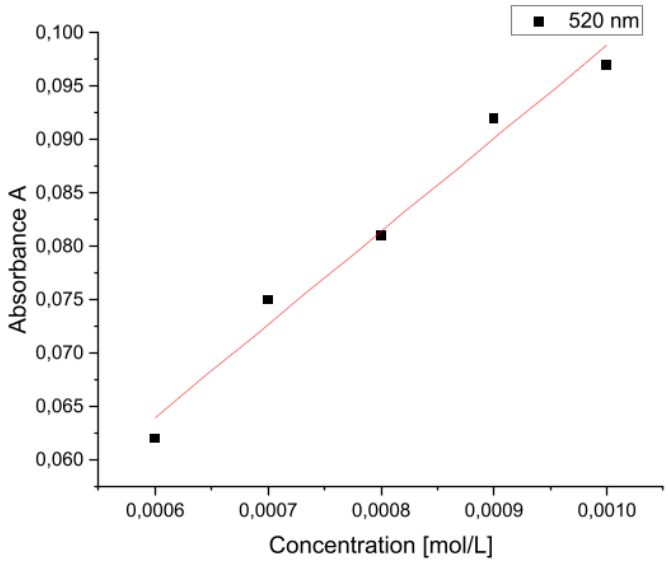

Supplementary Figure S23. Determination of the extinction ε = 870 $M^{-1} \cdot cm^{-1}$ of **2c** by linear regression at λ_{max} = 520 nm.

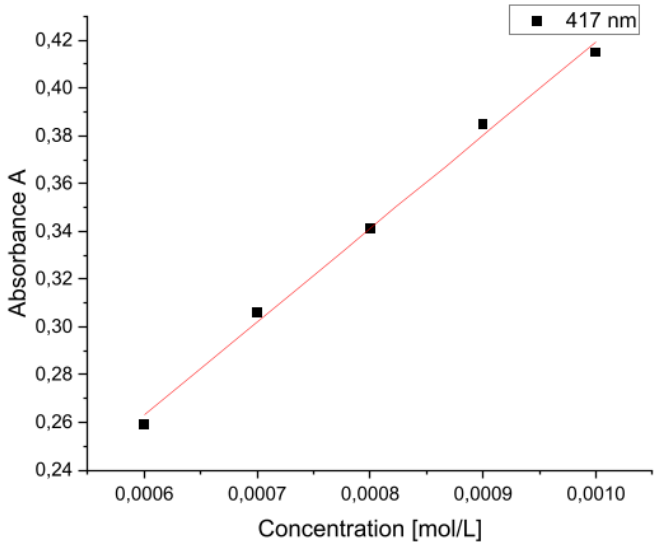

Supplementary Figure S24. Determination of the extinction ε = 3910 $M^{-1} \cdot cm^{-1}$ of **2c** by linear regression at λ = 417 nm.

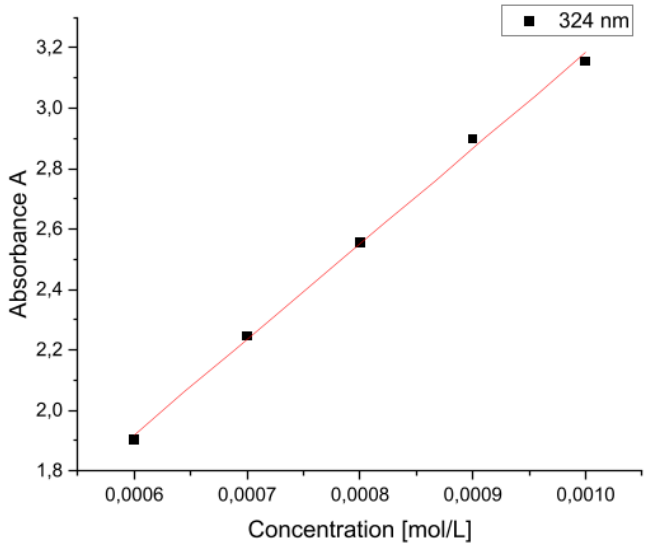

Supplementary Figure S25. Determination of the extinction ε = 31580 $M^{-1}\cdot cm^{-1}$ of **2c** by linear regression at λ = 324 nm.

3. Details on X-Ray Diffraction Studies

The crystallographic data set was collected using a Bruker D8 Venture diffractometer with a microfocus sealed tube and a Photon II detector. Monochromated $Mo_{K\alpha}$ radiation (λ = 0.71073 Å) was used. Data were collected at 143(2) K and corrected for absorption effects using the multi-scan method. The structure was solved by direct methods using SHELXT[S4] and was refined by full matrix least squares calculations on F^2 (SHELXL2018[S5]) in the graphical user interface Shelxle[S6]. All non-H atoms were located in the electron density maps and refined anisotropically. C-bound H atoms were placed in positions of optimized geometry and treated as riding atoms. Their isotropic displacement parameters were coupled to the corresponding carrier atoms by a factor of 1.2 (CH) or 1.5 (CH_3). *Disorder*: An isopropyl-residue of one tip-group and a larger part of another tip-group were split over two positions. For the isopropyl-residue of the latter tip group an EADP constraint was used in the refinement. The occupancy factors refined to 0.58 and 0.71 for the major components. *SQUEEZE*: One pentane solvent molecule has been treated as a diffuse contribution of the overall scattering without specific atom positions with the SQUEEZE tool[S7] implemented in PLATON[S8]. The number of squeezed electrons and their calculated volume (64e, V = 419Å3 / cell) correspond to approximately one pentane solvent in the asymmetric unit.

Acknowledgement:
Instrumentation and technical assistance for this work were provided by the Service Center X-ray Diffraction, with financial support from Saarland University and German Science Foundation (project number INST 256/506-1).

5. Supporting Information

Supplementary Table S1. Crysta data and structure refinement for NHSilylene-substituted siliconoid **2a** (CCDC: 2308133).

Empirical formula	C95 H150 N2 Si8	
Formula weight	1544.88	
Temperature	143(2) K	
Wavelength	0.71073 Å	
Crystal system	Triclinic	
Space group	*P*–1	
Unit cell dimensions	a = 15.0497(7) Å	α = 93.6620(10)°.
	b = 15.2633(6) Å	β = 101.1000(10)°.
	c = 21.4987(10) Å	γ = 90.410(2)°.
Volume	4835.2(4) $Å^3$	
Z	2	
Density (calculated)	1.061 mg/m^3	
Absorption coefficient	0.153 mm^{-1}	
F(000)	1692	
Crystal size	0.060 x 0.026 x 0.020 mm^3	
Theta range for data collection	1.940 to 27.207°.	
Index ranges	-19<=h<=19, -17<=k<=19, -27<=l<=27	
Reflections collected	174462	
Independent reflections	21396 [R(int) = 0.0802]	
Completeness to theta = 25.242°	99.7 %	
Absorption correction	Semi-empirical from equivalents	
Max. and min. transmission	0.7455 and 0.6751	
Refinement method	Full-matrix least-squares on F^2	
Data / restraints / parameters	21396 / 455 / 1013	
Goodness-of-fit on F^2	1.021	
Final R indices [I>2sigma(I)]	R1 = 0.0513, wR2 = 0.1189	
R indices (all data)	R1 = 0.0812, wR2 = 0.1370	
Largest diff. peak and hole	0.429 and –0.516 $e.Å^{-3}$	

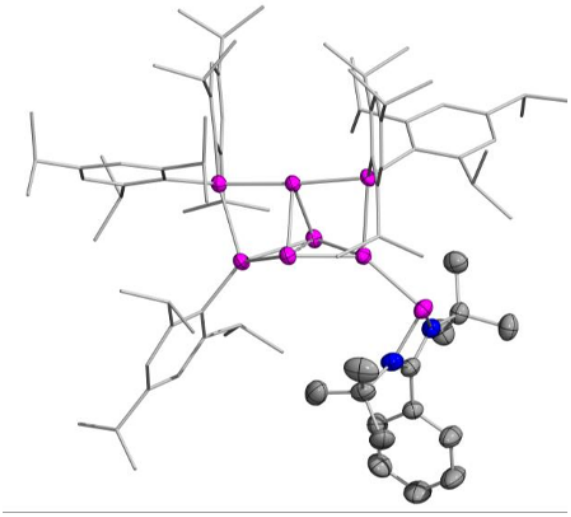

Supplementary Figure S26. Molecular structure NHSilylene-substituted siliconoid **2a** in the solid state. Hydrogen atoms are omitted for clarity. Thermal ellipsoids represent 50% probability.

4. Computational Details

The structure of **2a-c** was optimized at the density functional theory (DFT) level using Becke's three-parameter functional in combination with the Lee-Yang-Parr exchange-correlation functional (B3LYP).[S9,10] Triple-ζ quality basis sets augmented with polarization functions (def2-TZVP) and the m5 grid with scfconf = 8 and deconv = 0.1d-06 were employed.[S10] Single point PCM/TDB3LYP/def2-TZVP[S10] calculations were performed for 20 excited states to estimate the change in the UV-Vis spectrum of optimized structures of **2a-c** in the presence of hexane solvent (Supplementary Table S5-7). The nuclear magnetic shieldings were calculated at the OLYP/def2-TZVP[S9] level with GIAO as implemented into the Gaussian09 program package.[S11] All chemical shifts were referenced to the value calculated for $Si(CH_3)_4$ at the same level of theory. Pictures of Kohn-Sham orbitals were displayed with ChemCraft.[S12]

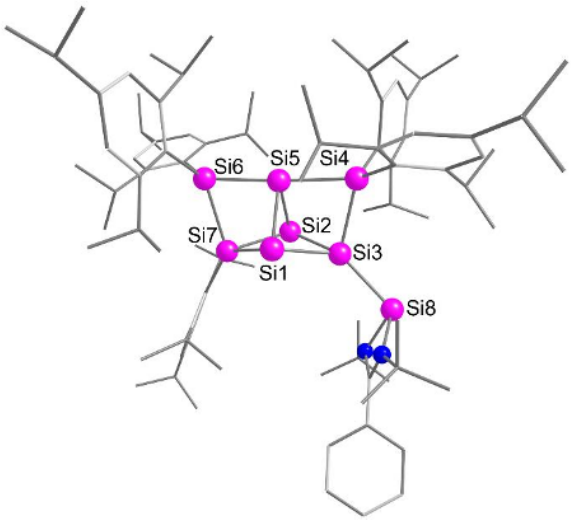

Supplementary Figure S27. Calculated structure of Tip_5Si_7NHSi **2a**. Hydrogen atoms are omitted for clarity.

Supplementary Table S2. Coordinates of Tip_5Si_7NHSi **2a**.

Si	–0.351029000	0.891249000	1.110925000
Si	0.055515000	0.638846000	-1.463655000
Si	-2.092185000	0.760534000	-0.483736000
Si	-2.094865000	-1.690295000	-0.355148000
Si	0.237694000	-1.123716000	0.054993000
Si	2.594136000	-0.715410000	0.491593000
Si	1.638932000	1.528456000	0.016976000
Si	-4.110380000	2.094770000	-0.958426000
N	-3.446315000	3.823779000	-1.284115000
N	-4.263196000	3.168120000	0.581849000
C	-3.907434000	4.262880000	-0.102029000
C	-4.128775000	5.681200000	0.304452000
C	-3.102222000	6.432538000	0.876800000
H	-2.131999000	5.981475000	1.030189000
C	-3.323758000	7.749368000	1.261186000
H	-2.519055000	8.319209000	1.708100000
C	-4.572138000	8.331842000	1.075195000
H	-4.743819000	9.357807000	1.374936000
C	-5.599642000	7.590925000	0.502288000
H	-6.573914000	8.038103000	0.350827000
C	-5.380178000	6.273268000	0.120051000
H	-6.181745000	5.703517000	-0.331640000

C	-3.056023000	4.551414000	-2.510855000
C	-2.647683000	3.482970000	-3.532329000
H	-2.346321000	3.956492000	-4.467449000
H	-3.482038000	2.812565000	-3.748456000
H	-1.811086000	2.888717000	-3.164119000
C	-1.849462000	5.464390000	-2.247182000
H	-1.504153000	5.897056000	-3.188134000
H	-1.025871000	4.897367000	-1.811968000
H	-2.100398000	6.284832000	-1.577305000
C	-4.227590000	5.363340000	-3.088528000
H	-3.942249000	5.792184000	-4.051357000
H	-4.515639000	6.183006000	-2.432352000
H	-5.095719000	4.720905000	-3.246445000
C	-4.878357000	2.993913000	1.914436000
C	-4.688195000	1.519839000	2.291588000
H	-5.134998000	0.858668000	1.547781000
H	-5.170880000	1.312223000	3.247215000
H	-3.630744000	1.272374000	2.379578000
C	-4.187614000	3.858557000	2.979004000
H	-3.110598000	3.685299000	2.974803000
H	-4.570473000	3.586874000	3.964412000
H	-4.371131000	4.921025000	2.833735000
C	-6.383421000	3.309523000	1.866003000
H	-6.562685000	4.362559000	1.651789000
H	-6.845848000	3.080653000	2.828376000
H	-6.876007000	2.709978000	1.099084000
C	-3.343180000	-2.333981000	0.996402000
C	-4.720779000	-2.441216000	0.647208000
C	-5.647000000	-2.917806000	1.572767000
H	-6.683324000	-3.000058000	1.269770000
C	-5.294457000	-3.289477000	2.863311000
C	-3.959427000	-3.160910000	3.207725000
H	-3.660251000	-3.435779000	4.212582000
C	-2.984486000	-2.699861000	2.319728000
C	-1.570499000	-2.627025000	2.886466000
H	-0.902659000	-2.297830000	2.093340000
C	-1.054517000	-3.989194000	3.376651000

H	-1.108210000	-4.746010000	2.593421000
H	-1.629136000	-4.356770000	4.229384000
H	-0.013274000	-3.902967000	3.694297000
C	-1.468840000	-1.588115000	4.013169000
H	-0.438032000	-1.509713000	4.363753000
H	-2.092149000	-1.865055000	4.866529000
H	-1.786618000	-0.601902000	3.672375000
C	-5.287485000	-2.074327000	-0.724135000
H	-4.506033000	-1.574400000	-1.295891000
C	-5.716060000	-3.321737000	-1.514055000
H	-6.099592000	-3.039239000	-2.496920000
H	-6.511552000	-3.855256000	-0.988708000
H	-4.887120000	-4.011041000	-1.663434000
C	-6.464354000	-1.089773000	-0.639525000
H	-6.203074000	-0.192206000	-0.080871000
H	-7.337135000	-1.542857000	-0.165715000
H	-6.761552000	-0.773824000	-1.641318000
C	-6.314511000	-3.808937000	3.860335000
H	-5.768850000	-4.030080000	4.783216000
C	-6.967078000	-5.116713000	3.388694000
H	-7.546097000	-4.963920000	2.475175000
H	-7.646663000	-5.504547000	4.151335000
H	-6.215452000	-5.880480000	3.182405000
C	-7.378768000	-2.754477000	4.198552000
H	-6.919921000	-1.836733000	4.570570000
H	-8.061652000	-3.128695000	4.965067000
H	-7.974600000	-2.496952000	3.320019000
C	-2.258989000	-2.826206000	-1.929069000
C	-2.591668000	-2.370482000	-3.231496000
C	-2.704150000	-3.282610000	-4.283559000
H	-2.957135000	-2.911504000	-5.269884000
C	-2.515571000	-4.645655000	-4.126555000
C	-2.187239000	-5.089098000	-2.852919000
H	-2.031590000	-6.148567000	-2.691649000
C	-2.047509000	-4.223920000	-1.769467000
C	-1.667327000	-4.880046000	-0.444904000
H	-1.474157000	-4.094527000	0.285545000

C	-0.375018000	-5.699674000	-0.561396000
H	-0.496309000	-6.550214000	-1.234440000
H	-0.089291000	-6.095308000	0.414347000
H	0.448480000	-5.092586000	-0.936617000
C	-2.800508000	-5.755944000	0.112134000
H	-3.031758000	-6.575501000	-0.572050000
H	-3.711303000	-5.181211000	0.272703000
H	-2.508082000	-6.195640000	1.068362000
C	-2.853051000	-0.915391000	-3.609234000
H	-2.792039000	-0.315235000	-2.702166000
C	-4.255845000	-0.694644000	-4.198223000
H	-4.429808000	0.370237000	-4.365604000
H	-5.036627000	-1.056480000	-3.530500000
H	-4.373774000	-1.203450000	-5.157017000
C	-1.786283000	-0.385575000	-4.578284000
H	-1.813910000	-0.925657000	-5.527181000
H	-0.784221000	-0.490133000	-4.162628000
H	-1.953938000	0.671956000	-4.792530000
C	-2.660163000	-5.596782000	-5.300693000
H	-2.929281000	-4.986891000	-6.169015000
C	-1.339264000	-6.307389000	-5.631158000
H	-0.541184000	-5.587868000	-5.821823000
H	-1.018769000	-6.950264000	-4.808278000
H	-1.451315000	-6.934873000	-6.518600000
C	-3.791958000	-6.612080000	-5.084784000
H	-4.740093000	-6.109845000	-4.885600000
H	-3.918468000	-7.240622000	-5.969505000
H	-3.579067000	-7.269479000	-4.238827000
C	4.065342000	-1.060576000	-0.732926000
C	5.344690000	-0.544674000	-0.393991000
C	6.441561000	-0.789347000	-1.221012000
H	7.410849000	-0.396853000	-0.935469000
C	6.346094000	-1.514804000	-2.398341000
C	5.089051000	-1.994566000	-2.740568000
H	4.977008000	-2.557282000	-3.659298000
C	3.959645000	-1.789788000	-1.948159000
C	2.660352000	-2.387421000	-2.480569000

H	1.879631000	-2.215460000	-1.741435000
C	2.747629000	-3.905430000	-2.704014000
H	1.772680000	-4.295875000	-3.002830000
H	3.060386000	-4.430186000	-1.801093000
H	3.457411000	-4.157765000	-3.494479000
C	2.208415000	-1.694106000	-3.774655000
H	2.930059000	-1.849397000	-4.580157000
H	2.092272000	-0.619662000	-3.630667000
H	1.247633000	-2.094920000	-4.103685000
C	5.627452000	0.277697000	0.862054000
H	4.684526000	0.444614000	1.380500000
C	6.552279000	-0.474273000	1.832570000
H	6.125048000	-1.430869000	2.131284000
H	6.722053000	0.114889000	2.736269000
H	7.525861000	-0.665046000	1.376131000
C	6.200650000	1.668180000	0.546671000
H	7.168038000	1.602067000	0.044967000
H	6.350339000	2.230093000	1.471501000
H	5.528783000	2.246034000	-0.086834000
C	7.568336000	-1.765945000	-3.263341000
H	8.410015000	-1.267756000	-2.771667000
C	7.909301000	-3.260909000	-3.353208000
H	7.113303000	-3.819021000	-3.851231000
H	8.049217000	-3.694109000	-2.361427000
H	8.828625000	-3.412172000	-3.923999000
C	7.425138000	-1.150091000	-4.662753000
H	8.342108000	-1.290936000	-5.239875000
H	7.221255000	-0.079686000	-4.604465000
H	6.608772000	-1.615626000	-5.219499000
C	3.098267000	-1.402017000	2.247034000
C	3.429584000	-2.783257000	2.342040000
C	3.795693000	-3.339876000	3.565975000
H	4.056407000	-4.390326000	3.597488000
C	3.833337000	-2.604699000	4.742547000
C	3.497658000	-1.264720000	4.649974000
H	3.519752000	-0.668523000	5.554647000
C	3.146726000	-0.648334000	3.446432000

C	2.856972000	0.844722000	3.545472000
H	2.660000000	1.214844000	2.538976000
C	1.607721000	1.124518000	4.393355000
H	1.395753000	2.195184000	4.427330000
H	1.746650000	0.783743000	5.421478000
H	0.731365000	0.620141000	3.988179000
C	4.057065000	1.631913000	4.097876000
H	4.955813000	1.466852000	3.505022000
H	4.282712000	1.345539000	5.126566000
H	3.842844000	2.700863000	4.096710000
C	3.422793000	-3.746595000	1.158259000
H	2.994032000	-3.233528000	0.297921000
C	2.540673000	-4.975121000	1.419596000
H	2.482785000	-5.595700000	0.524090000
H	1.528044000	-4.685313000	1.698444000
H	2.942151000	-5.597987000	2.220725000
C	4.843186000	-4.187238000	0.770997000
H	4.814437000	-4.860946000	-0.088228000
H	5.321760000	-4.721461000	1.594876000
H	5.470414000	-3.336562000	0.508741000
C	4.223730000	-3.225651000	6.071426000
H	4.168936000	-2.428741000	6.820001000
C	3.245115000	-4.327987000	6.502535000
H	2.221588000	-3.952050000	6.547031000
H	3.509860000	-4.712484000	7.490391000
H	3.261508000	-5.167806000	5.804319000
C	5.668567000	-3.746291000	6.060551000
H	5.790978000	-4.560297000	5.342549000
H	5.947248000	-4.128127000	7.045586000
H	6.370949000	-2.955908000	5.790590000
C	3.290159000	2.355941000	-2.619694000
H	2.971263000	1.399441000	-2.201203000
C	2.313310000	2.714268000	-3.751162000
H	2.595150000	3.661238000	-4.217675000
H	1.292537000	2.810696000	-3.380440000
H	2.321136000	1.942789000	-4.524606000
C	4.698246000	2.136996000	-3.190081000

H	4.683879000	1.301271000	-3.891738000
H	5.418776000	1.900719000	-2.408756000
H	5.058690000	3.012911000	-3.733346000
C	1.664461000	4.214937000	1.916910000
H	1.573599000	3.164890000	2.197705000
C	2.309210000	4.952412000	3.098503000
H	3.359815000	4.687268000	3.218324000
H	1.786884000	4.702716000	4.024309000
H	2.250537000	6.036652000	2.983567000
C	0.239958000	4.743095000	1.690407000
H	0.270986000	5.795640000	1.396624000
H	-0.351984000	4.659643000	2.605388000
H	-0.270264000	4.184058000	0.905666000
C	2.528893000	3.203860000	-0.293231000
C	2.468560000	4.284302000	0.624491000
C	3.102879000	5.487009000	0.322201000
H	3.047437000	6.298878000	1.035520000
C	3.802827000	5.683664000	-0.863243000
C	3.842046000	4.628662000	-1.762451000
H	4.372117000	4.768209000	-2.696967000
C	3.226186000	3.401937000	-1.511481000
C	4.497563000	6.997280000	-1.174211000
H	4.958245000	6.884292000	-2.160590000
C	5.622858000	7.302543000	-0.174518000
H	6.347880000	6.487901000	-0.136091000
H	6.151314000	8.215874000	-0.457771000
H	5.228815000	7.445890000	0.834113000
C	3.507020000	8.167687000	-1.262657000
H	2.725335000	7.968649000	-1.997814000
H	3.022258000	8.350747000	-0.301020000
H	4.022471000	9.085884000	-1.553925000

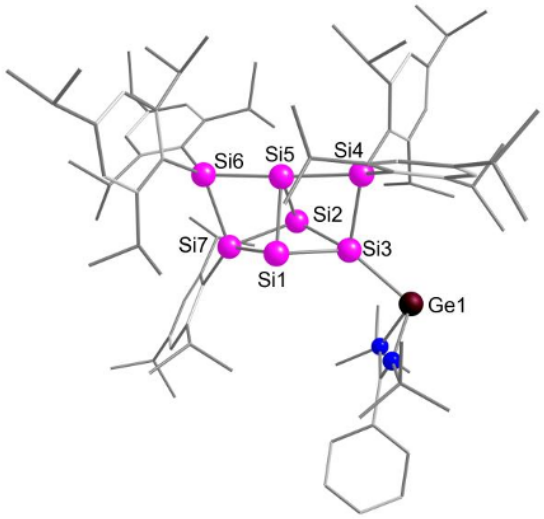

Supplementary Figure S 28. Calculated structure of Tip_5Si_7NHGe **2b**. Hydrogen atoms are omitted for clarity.

Supplementary Table S3. Coordinates of Tip_5Si_7NHGe **2b**.

Si	-0.352762000	0.738098000	1.164562000
Si	0.034521000	0.599444000	-1.423547000
Si	-2.089008000	0.400916000	-0.400457000
Si	-1.746099000	-2.029368000	-0.313173000
Si	0.493409000	-1.150412000	0.048680000
Si	2.778140000	-0.423426000	0.454267000
Si	1.505154000	1.672865000	0.053316000
N	-3.866460000	3.421050000	-1.193888000
N	-4.580296000	2.696332000	0.723268000
C	-4.357580000	3.788910000	-0.006738000
C	-4.690691000	5.188316000	0.403257000
C	-3.719334000	6.025988000	0.951136000
H	-2.710460000	5.660347000	1.080299000
C	-4.042790000	7.320096000	1.339781000
H	-3.279170000	7.957337000	1.767483000
C	-5.339969000	7.794656000	1.181973000
H	-5.591209000	8.803175000	1.484812000
C	-6.313074000	6.967666000	0.632719000
H	-7.325075000	7.329891000	0.503005000
C	-5.990921000	5.672019000	0.246890000
H	-6.751918000	5.034793000	-0.184409000
C	-3.610876000	4.193205000	-2.426715000

C	-3.063621000	3.186585000	-3.447486000
H	-2.842333000	3.687722000	-4.390661000
H	-3.796046000	2.401896000	-3.650913000
H	-2.148054000	2.720121000	-3.082680000
C	-2.547845000	5.280567000	-2.202608000
H	-2.280542000	5.734454000	-3.159034000
H	-1.644938000	4.851243000	-1.766942000
H	-2.907390000	6.072747000	-1.549069000
C	-4.899607000	4.815041000	-2.992630000
H	-4.698963000	5.270010000	-3.965022000
H	-5.295144000	5.590427000	-2.338573000
H	-5.666075000	4.049585000	-3.128072000
C	-5.142748000	2.506441000	2.074286000
C	-4.803589000	1.065737000	2.479212000
H	-5.222571000	0.348584000	1.771084000
H	-5.222567000	0.840343000	3.460713000
H	-3.724901000	0.915768000	2.521829000
C	-4.515022000	3.454757000	3.108064000
H	-3.426497000	3.392252000	3.074814000
H	-4.840922000	3.162234000	4.108076000
H	-4.809551000	4.490362000	2.953605000
C	-6.672856000	2.672570000	2.062512000
H	-6.960422000	3.697642000	1.831703000
H	-7.086923000	2.421402000	3.041418000
H	-7.124597000	2.010312000	1.322049000
C	-2.847776000	-2.862283000	1.062513000
C	-4.210076000	-3.142860000	0.755181000
C	-5.030897000	-3.768685000	1.691163000
H	-6.057626000	-3.979293000	1.418552000
C	-4.585052000	-4.129557000	2.955579000
C	-3.268089000	-3.830628000	3.262087000
H	-2.899389000	-4.090993000	4.247488000
C	-2.396588000	-3.214038000	2.361065000
C	-0.989326000	-2.957161000	2.888795000
H	-0.398648000	-2.523289000	2.084892000
C	-0.273306000	-4.241721000	3.334528000
H	-0.245839000	-4.985249000	2.537304000

H	-0.763042000	-4.700728000	4.195864000
H	0.755366000	-4.015782000	3.623059000
C	-1.000972000	-1.933782000	4.034063000
H	0.018300000	-1.717511000	4.359281000
H	-1.554994000	-2.310141000	4.897119000
H	-1.463809000	-0.996793000	3.721467000
C	-4.871297000	-2.802934000	-0.579358000
H	-4.175371000	-2.200468000	-1.162823000
C	-5.189870000	-4.064165000	-1.397999000
H	-5.646400000	-3.796458000	-2.353476000
H	-5.894521000	-4.704053000	-0.862091000
H	-4.293812000	-4.646414000	-1.605850000
C	-6.144455000	-1.959846000	-0.406582000
H	-5.961631000	-1.073629000	0.200382000
H	-6.944509000	-2.530616000	0.068331000
H	-6.511897000	-1.624712000	-1.378451000
C	-5.489321000	-4.812029000	3.965888000
H	-4.886319000	-4.983343000	4.863312000
C	-5.975223000	-6.182380000	3.471307000
H	-6.601491000	-6.083695000	2.581801000
H	-6.568778000	-6.681041000	4.241304000
H	-5.134972000	-6.830346000	3.216432000
C	-6.673599000	-3.922531000	4.372321000
H	-6.330057000	-2.962110000	4.760533000
H	-7.272239000	-4.408488000	5.146510000
H	-7.329365000	-3.722971000	3.521832000
C	-1.812783000	-3.149900000	-1.906215000
C	-2.246874000	-2.719506000	-3.187510000
C	-2.282118000	-3.621660000	-4.253466000
H	-2.615113000	-3.269943000	-5.223020000
C	-1.918897000	-4.952518000	-4.130512000
C	-1.489342000	-5.370311000	-2.878533000
H	-1.194756000	-6.403675000	-2.744218000
C	-1.418581000	-4.511178000	-1.783590000
C	-0.903213000	-5.132799000	-0.488588000
H	-0.787202000	-4.340608000	0.251086000
C	0.481198000	-5.769956000	-0.671991000

H	0.446559000	-6.618535000	-1.357427000
H	0.857567000	-6.138613000	0.283385000
H	1.199969000	-5.052097000	-1.066697000
C	-1.887639000	-6.161084000	0.090044000
H	-2.032380000	-6.994016000	-0.601675000
H	-2.860524000	-5.715897000	0.292913000
H	-1.504244000	-6.571725000	1.026807000
C	-2.701210000	-1.302900000	-3.527389000
H	-2.680528000	-0.714468000	-2.610840000
C	-4.141220000	-1.250575000	-4.063541000
H	-4.452474000	-0.213659000	-4.207347000
H	-4.846651000	-1.717423000	-3.377111000
H	-4.229802000	-1.756648000	-5.026796000
C	-1.745429000	-0.626476000	-4.520723000
H	-1.741259000	-1.148355000	-5.480174000
H	-0.723442000	-0.612237000	-4.142647000
H	-2.050899000	0.405801000	-4.704388000
C	-1.988773000	-5.896658000	-5.317089000
H	-2.363420000	-5.312117000	-6.163461000
C	-0.603952000	-6.433731000	-5.707940000
H	0.091816000	-5.618593000	-5.913945000
H	-0.175689000	-7.043637000	-4.909358000
H	-0.671693000	-7.057699000	-6.602310000
C	-2.978173000	-7.047087000	-5.080255000
H	-3.972846000	-6.668774000	-4.838590000
H	-3.059210000	-7.674142000	-5.971334000
H	-2.654531000	-7.684588000	-4.254470000
C	4.253790000	-0.525482000	-0.808775000
C	5.455796000	0.155420000	-0.478441000
C	6.557542000	0.087974000	-1.332071000
H	7.468665000	0.604910000	-1.053384000
C	6.538409000	-0.613700000	-2.527352000
C	5.353075000	-1.255143000	-2.860639000
H	5.300498000	-1.803913000	-3.793079000
C	4.223702000	-1.230177000	-2.042550000
C	3.008125000	-1.988184000	-2.568358000
H	2.226764000	-1.942575000	-1.811539000

C	3.297812000	-3.474174000	-2.832814000
H	2.379102000	-3.988329000	-3.122703000
H	3.700018000	-3.971518000	-1.950074000
H	4.017333000	-3.608111000	-3.643171000
C	2.439122000	-1.333240000	-3.835974000
H	3.159384000	-1.367112000	-4.656774000
H	2.177757000	-0.289171000	-3.661752000
H	1.537113000	-1.855973000	-4.160388000
C	5.649054000	0.977102000	0.794901000
H	4.705068000	0.994688000	1.337540000
C	6.694836000	0.339904000	1.723983000
H	6.415953000	-0.675811000	2.002375000
H	6.800542000	0.922827000	2.641369000
H	7.674546000	0.302968000	1.242987000
C	6.011148000	2.442736000	0.507507000
H	6.964716000	2.527607000	-0.017327000
H	6.103768000	2.996376000	1.444722000
H	5.247922000	2.935052000	-0.094090000
C	7.765278000	-0.670927000	-3.419880000
H	8.540179000	-0.073576000	-2.928899000
C	8.307305000	-2.101550000	-3.556926000
H	7.585849000	-2.751820000	-4.056704000
H	8.525857000	-2.535973000	-2.579992000
H	9.226822000	-2.109714000	-4.147055000
C	7.509757000	-0.045548000	-4.798945000
H	8.425578000	-0.042578000	-5.394771000
H	7.160546000	0.984237000	-4.707330000
H	6.754861000	-0.605846000	-5.355120000
C	3.413578000	-1.081142000	2.177599000
C	3.929607000	-2.407090000	2.224499000
C	4.386787000	-2.945579000	3.425604000
H	4.786167000	-3.951963000	3.420673000
C	4.345235000	-2.246958000	4.624186000
C	3.833644000	-0.961258000	4.577713000
H	3.792007000	-0.393986000	5.500106000
C	3.383264000	-0.362413000	3.398604000
C	2.900630000	1.075720000	3.546619000

H	2.643803000	1.446628000	2.553832000
C	1.636932000	1.162611000	4.414436000
H	1.288782000	2.194894000	4.488272000
H	1.832304000	0.807770000	5.428514000
H	0.828031000	0.562957000	3.999013000
C	3.994157000	1.997410000	4.112319000
H	4.899554000	1.968206000	3.507384000
H	4.267717000	1.714006000	5.130150000
H	3.642070000	3.028635000	4.144875000
C	4.036664000	-3.324476000	1.009598000
H	3.527488000	-2.848822000	0.172125000
C	3.337688000	-4.671557000	1.238277000
H	3.351158000	-5.264187000	0.322225000
H	2.299514000	-4.534405000	1.539027000
H	3.834666000	-5.259014000	2.012164000
C	5.498082000	-3.549559000	0.591070000
H	5.549484000	-4.192544000	-0.290364000
H	6.060036000	-4.037591000	1.390609000
H	5.995792000	-2.611266000	0.350620000
C	4.835410000	-2.849524000	5.928294000
H	4.689048000	-2.088723000	6.701724000
C	4.016464000	-4.082733000	6.337137000
H	2.953450000	-3.845747000	6.406073000
H	4.345416000	-4.457831000	7.309188000
H	4.131004000	-4.892382000	5.612982000
C	6.335575000	-3.175518000	5.883729000
H	6.552003000	-3.945249000	5.139548000
H	6.677532000	-3.545928000	6.853072000
H	6.924125000	-2.292257000	5.629946000
C	2.955985000	2.790998000	-2.598223000
H	2.782640000	1.788971000	-2.201452000
C	1.915308000	3.036931000	-3.702309000
H	2.052099000	4.025205000	-4.147678000
H	0.899098000	2.980213000	-3.311339000
H	2.014475000	2.293523000	-4.496674000
C	4.369265000	2.786860000	-3.197259000
H	4.457953000	1.977132000	-3.923546000

H	5.130823000	2.632390000	-2.434515000
H	4.593399000	3.719429000	-3.719145000
C	1.222328000	4.279936000	2.034985000
H	1.288277000	3.219490000	2.281611000
C	1.804388000	5.064312000	3.218993000
H	2.885250000	4.943340000	3.293910000
H	1.356669000	4.718287000	4.152820000
H	1.593477000	6.132918000	3.143023000
C	-0.268760000	4.611629000	1.875243000
H	-0.393148000	5.666921000	1.618755000
H	-0.808748000	4.420340000	2.805861000
H	-0.727600000	4.011292000	1.089152000
C	2.145585000	3.462514000	-0.230394000
C	1.961428000	4.498909000	0.720850000
C	2.406701000	5.787819000	0.437072000
H	2.258965000	6.564493000	1.175993000
C	3.033298000	6.113486000	-0.760900000
C	3.195938000	5.098044000	-1.691269000
H	3.671619000	5.336039000	-2.635151000
C	2.770905000	3.789193000	-1.459931000
C	3.525915000	7.520095000	-1.050166000
H	3.948718000	7.504615000	-2.059605000
C	4.647673000	7.941977000	-0.089323000
H	5.478166000	7.234693000	-0.117987000
H	5.031675000	8.929396000	-0.356274000
H	4.288110000	7.992096000	0.940927000
C	2.383886000	8.546759000	-1.047535000
H	1.600124000	8.267568000	-1.753807000
H	1.927806000	8.631216000	-0.058550000
H	2.756214000	9.535498000	-1.325636000
Ge	-4.358352000	1.474212000	-0.885663000

5. Supporting Information

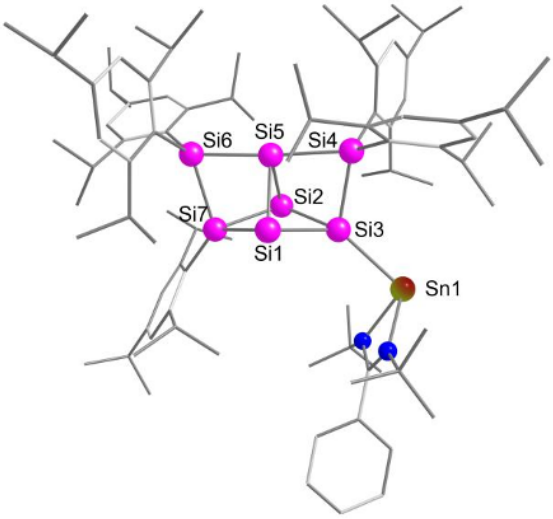

Supplementary Figure S29. Calculated structure of Tip_5Si_7NHSn **2c**. Hydrogen atoms are omitted for clarity.

Supplementary Table S4. Coordinates of Tip_5Si_7NHSn **2c**.

Si	-0.393286000	0.562424000	1.185109000
Si	-0.014500000	0.527756000	-1.403672000
Si	-2.031064000	-0.153914000	-0.360511000
Si	-1.128386000	-2.441390000	-0.284551000
Si	0.851505000	-1.077202000	0.048312000
Si	2.917217000	0.142405000	0.442417000
Si	1.195438000	1.899263000	0.062767000
N	-4.519282000	2.734727000	-1.118071000
N	-5.193449000	1.794979000	0.762096000
C	-5.098098000	2.928672000	0.067965000
C	-5.644326000	4.245389000	0.536582000
C	-4.851837000	5.144819000	1.248465000
H	-3.820528000	4.898816000	1.457964000
C	-5.374996000	6.357893000	1.681491000
H	-4.746357000	7.045288000	2.233348000
C	-6.696309000	6.688486000	1.405577000
H	-7.103041000	7.633675000	1.741937000
C	-7.493495000	5.797568000	0.695355000
H	-8.524793000	6.045001000	0.477460000
C	-6.971579000	4.584008000	0.265820000
H	-7.601281000	3.890265000	-0.276027000
C	-4.346070000	3.637150000	-2.274054000
C	-3.534178000	2.836481000	-3.303501000

H	-3.346814000	3.437664000	-4.194171000
H	-4.079053000	1.942369000	-3.618849000
H	-2.573815000	2.528392000	-2.888465000
C	-3.544796000	4.899410000	-1.914073000
H	-3.305845000	5.453430000	-2.824198000
H	-2.607317000	4.632288000	-1.424830000
H	-4.102015000	5.564637000	-1.258235000
C	-5.690955000	4.025730000	-2.913998000
H	-5.519836000	4.569905000	-3.845519000
H	-6.279089000	4.666164000	-2.259207000
H	-6.277073000	3.134214000	-3.146073000
C	-5.629338000	1.535528000	2.148045000
C	-5.564054000	0.012233000	2.328877000
H	-6.253845000	-0.489142000	1.646605000
H	-5.842931000	-0.264502000	3.346248000
H	-4.553921000	-0.359746000	2.147355000
C	-4.665401000	2.183490000	3.157042000
H	-3.638628000	1.877694000	2.952065000
H	-4.920375000	1.872207000	4.172472000
H	-4.718939000	3.270297000	3.119671000
C	-7.074285000	1.985594000	2.427140000
H	-7.175326000	3.068404000	2.429237000
H	-7.389096000	1.620471000	3.407114000
H	-7.755525000	1.575122000	1.679262000
C	-1.980197000	-3.504312000	1.109549000
C	-3.251575000	-4.080230000	0.829899000
C	-3.887195000	-4.885592000	1.772606000
H	-4.847525000	-5.317846000	1.519655000
C	-3.339527000	-5.150134000	3.020654000
C	-2.116905000	-4.563918000	3.302677000
H	-1.675124000	-4.743776000	4.275865000
C	-1.429090000	-3.757580000	2.392589000
C	-0.104727000	-3.193094000	2.895012000
H	0.357378000	-2.634902000	2.083530000
C	0.890598000	-4.284662000	3.318356000
H	1.068952000	-5.001376000	2.516055000
H	0.534445000	-4.843857000	4.185996000

H	1.847387000	-3.833360000	3.588842000
C	-0.323981000	-2.202541000	4.048241000
H	0.626658000	-1.763124000	4.355748000
H	-0.761258000	-2.697912000	4.918251000
H	-0.992778000	-1.393307000	3.752237000
C	-4.010991000	-3.870278000	-0.478079000
H	-3.470151000	-3.134972000	-1.073707000
C	-4.099073000	-5.159554000	-1.309296000
H	-4.635953000	-4.978841000	-2.243225000
H	-4.638211000	-5.936685000	-0.763090000
H	-3.111353000	-5.543901000	-1.559080000
C	-5.417811000	-3.298586000	-0.242272000
H	-5.387481000	-2.412590000	0.392442000
H	-6.071635000	-4.026224000	0.242028000
H	-5.881697000	-3.021794000	-1.191148000
C	-4.041097000	-6.028714000	4.040506000
H	-3.389723000	-6.073233000	4.919154000
C	-4.226136000	-7.466385000	3.533334000
H	-4.884078000	-7.498087000	2.661957000
H	-4.672461000	-8.093408000	4.308865000
H	-3.271166000	-7.909137000	3.245521000
C	-5.380470000	-5.428332000	4.492888000
H	-5.246762000	-4.420138000	4.888824000
H	-5.834084000	-6.043609000	5.273614000
H	-6.088488000	-5.369552000	3.663150000
C	-0.975060000	-3.549529000	-1.882076000
C	-1.513565000	-3.224024000	-3.154945000
C	-1.368308000	-4.111087000	-4.224151000
H	-1.785487000	-3.839601000	-5.186921000
C	-0.720661000	-5.330269000	-4.112931000
C	-0.188554000	-5.644103000	-2.870067000
H	0.329056000	-6.587098000	-2.745410000
C	-0.288510000	-4.790654000	-1.772881000
C	0.379479000	-5.281996000	-0.491875000
H	0.328934000	-4.485284000	0.250047000
C	1.868226000	-5.589161000	-0.705991000
H	2.012725000	-6.421674000	-1.396755000

H	2.337250000	-5.865639000	0.239497000
H	2.398033000	-4.726088000	-1.108825000
C	-0.335884000	-6.506628000	0.099392000
H	-0.301516000	-7.350352000	-0.593540000
H	-1.380331000	-6.292815000	0.321734000
H	0.147689000	-6.820513000	1.027118000
C	-2.271028000	-1.940432000	-3.481979000
H	-2.364025000	-1.363439000	-2.562785000
C	-3.695426000	-2.203796000	-3.997175000
H	-4.226447000	-1.259919000	-4.139898000
H	-4.273362000	-2.809648000	-3.299835000
H	-3.686138000	-2.722223000	-4.957799000
C	-1.502594000	-1.066897000	-4.484031000
H	-1.401956000	-1.569111000	-5.448691000
H	-0.502097000	-0.832099000	-4.121598000
H	-2.028336000	-0.124203000	-4.652375000
C	-0.599914000	-6.264874000	-5.302876000
H	-1.109135000	-5.776839000	-6.140079000
C	0.862812000	-6.480492000	-5.718623000
H	1.356689000	-5.530812000	-5.931120000
H	1.428903000	-6.981390000	-4.930118000
H	0.920349000	-7.102394000	-6.615123000
C	-1.305140000	-7.606620000	-5.056163000
H	-2.354621000	-7.459063000	-4.795903000
H	-1.260587000	-8.234290000	-5.949355000
H	-0.833732000	-8.158102000	-4.239619000
C	4.362947000	0.382184000	-0.836696000
C	5.384509000	1.314407000	-0.513148000
C	6.464559000	1.499813000	-1.376978000
H	7.239043000	2.207128000	-1.103193000
C	6.591388000	0.816503000	-2.576295000
C	5.576717000	-0.073003000	-2.903075000
H	5.639159000	-0.615599000	-3.838514000
C	4.478628000	-0.305377000	-2.075106000
C	3.458214000	-1.313290000	-2.596291000
H	2.692251000	-1.445986000	-1.833979000
C	4.069842000	-2.696068000	-2.871464000

H	3.286652000	-3.401247000	-3.157413000
H	4.580517000	-3.094581000	-1.994700000
H	4.794052000	-2.662797000	-3.687994000
C	2.746608000	-0.796502000	-3.855717000
H	3.449084000	-0.663929000	-4.681878000
H	2.259133000	0.161350000	-3.672609000
H	1.982201000	-1.506677000	-4.177316000
C	5.400430000	2.153660000	0.763289000
H	4.482862000	1.954539000	1.315047000
C	6.573096000	1.766759000	1.678620000
H	6.531127000	0.714621000	1.958252000
H	6.556851000	2.359123000	2.595878000
H	7.530521000	1.949205000	1.186160000
C	5.417558000	3.664100000	0.480607000
H	6.321975000	3.964947000	-0.051792000
H	5.390641000	4.221435000	1.419806000
H	4.556964000	3.971860000	-0.112172000
C	7.790671000	1.039287000	-3.480291000
H	8.414996000	1.796143000	-2.994758000
C	8.640917000	-0.231579000	-3.626258000
H	8.080518000	-1.027729000	-4.121465000
H	8.961070000	-0.606097000	-2.652545000
H	9.532985000	-0.031216000	-4.224509000
C	7.386993000	1.591451000	-4.855146000
H	8.272603000	1.801785000	-5.459443000
H	6.814884000	2.515508000	-4.757422000
H	6.772994000	0.875303000	-5.405866000
C	3.702032000	-0.364452000	2.154742000
C	4.504332000	-1.540185000	2.186635000
C	5.080546000	-1.970270000	3.380186000
H	5.697255000	-2.860113000	3.363955000
C	4.891435000	-1.307850000	4.585196000
C	4.102970000	-0.170222000	4.553148000
H	3.942373000	0.366871000	5.480566000
C	3.520528000	0.320576000	3.381947000
C	2.732096000	1.614928000	3.544114000
H	2.388035000	1.923292000	2.556288000

C	1.490718000	1.418750000	4.426227000
H	0.925860000	2.349404000	4.510133000
H	1.771274000	1.112030000	5.436003000
H	0.827495000	0.658067000	4.016670000
C	3.601791000	2.753154000	4.104129000
H	4.483915000	2.927353000	3.489413000
H	3.943511000	2.532276000	5.116830000
H	3.031154000	3.680922000	4.147832000
C	4.807247000	-2.399657000	0.962304000
H	4.196429000	-2.045226000	0.132836000
C	4.435759000	-3.872556000	1.181222000
H	4.575835000	-4.438198000	0.258669000
H	3.396569000	-3.978844000	1.490423000
H	5.060613000	-4.338243000	1.945240000
C	6.277961000	-2.282450000	0.532284000
H	6.466684000	-2.889168000	-0.356143000
H	6.942915000	-2.636793000	1.323182000
H	6.547166000	-1.253501000	0.298456000
C	5.516456000	-1.792690000	5.880647000
H	5.205911000	-1.091813000	6.662153000
C	5.005219000	-3.183971000	6.282673000
H	3.916810000	-3.197426000	6.360868000
H	5.419635000	-3.481457000	7.248866000
H	5.295979000	-3.940067000	5.549965000
C	7.051013000	-1.765802000	5.823833000
H	7.431884000	-2.459792000	5.071206000
H	7.476700000	-2.055216000	6.787566000
H	7.419328000	-0.769270000	5.574422000
C	2.320581000	3.316974000	-2.605917000
H	2.372789000	2.299825000	-2.213573000
C	1.241496000	3.334569000	-3.700326000
H	1.156142000	4.330341000	-4.141773000
H	0.265206000	3.057181000	-3.302050000
H	1.492975000	2.633233000	-4.499318000
C	3.695542000	3.623289000	-3.215663000
H	3.950430000	2.857904000	-3.950707000
H	4.479510000	3.630821000	-2.460065000

H	3.707831000	4.586634000	-3.729563000
C	0.379735000	4.375261000	2.063901000
H	0.682924000	3.354814000	2.301915000
C	0.798599000	5.266228000	3.241527000
H	1.880796000	5.386690000	3.294730000
H	0.457048000	4.828341000	4.181633000
H	0.355734000	6.262103000	3.176198000
C	-1.150482000	4.370695000	1.935143000
H	-1.508988000	5.373323000	1.688339000
H	-1.615712000	4.060997000	2.874169000
H	-1.482635000	3.687529000	1.153122000
C	1.418213000	3.787062000	-0.222174000
C	1.025839000	4.755193000	0.737698000
C	1.167091000	6.111306000	0.452970000
H	0.862826000	6.834569000	1.198205000
C	1.683123000	6.569948000	-0.754148000
C	2.052695000	5.617353000	-1.691712000
H	2.447214000	5.956465000	-2.642114000
C	1.934209000	4.246399000	-1.460042000
C	1.840730000	8.051342000	-1.046361000
H	2.244543000	8.131231000	-2.060529000
C	2.847757000	8.718591000	-0.097732000
H	3.816703000	8.218088000	-0.135791000
H	2.994814000	9.766797000	-0.368555000
H	2.497413000	8.688304000	0.936440000
C	0.494925000	8.790915000	-1.029542000
H	-0.212741000	8.338964000	-1.726643000
H	0.042981000	8.770814000	-0.035276000
H	0.628876000	9.837980000	-1.311158000
Sn	-4.646990000	0.503820000	-0.977724000

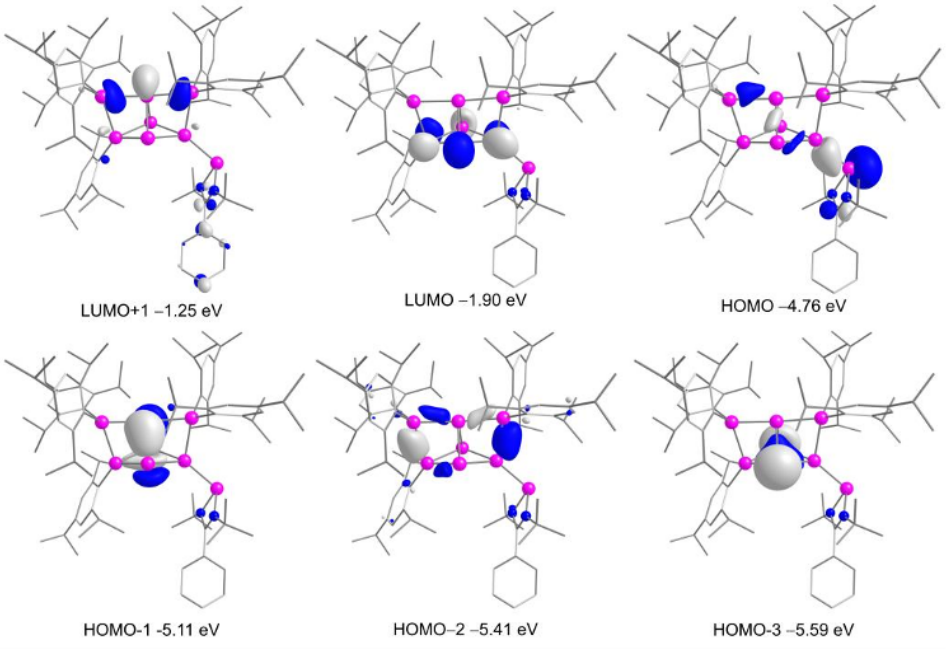

Supplementary Figure S*30*. Calculated MOs of Tip_5Si_7NHSi **2a** at B3LYP/def2-TZVP level of theory. Hydrogen atoms are omitted for clarity.

Supplementary Table S5. Transition Energy, wavelength, and oscillator strengths of the electronic transition of **2a** calculated at the TD-B3LYP/def2-TZVP level of theory (the 402th orbital is the highest occupied orbital, shown in Supplementary Fig. S25).

Excited State 1: Singlet-A 2.1138 eV 586.54 nm f=0.0124 <S**2>=0.000
402 -> 403 0.70244
This state for optimization and/or second-order correction.
Total Energy, E(CIS/TDA) = -5939.68032520
Copying the excited state density for this state as the 1-particle RhoCI density.

Excited State 2: Singlet-A 2.4115 eV 514.13 nm f=0.0052 <S**2>=0.000
401 -> 403 0.70011

Excited State 3: Singlet-A 2.7471 eV 451.33 nm f=0.0012 <S**2>=0.000
400 -> 403 0.70062

Excited State 4: Singlet-A 2.9232 eV 424.14 nm f=0.0568 <S**2>=0.000
402 -> 404 0.69169

Excited State 5: Singlet-A 3.0232 eV 410.12 nm f=0.0112 <S**2>=0.000
398 -> 403 0.13090
401 -> 404 0.66714

Excited State 6: Singlet-A 3.0924 eV 400.94 nm f=0.0002 <S**2>=0.000
398 -> 403 0.61936
401 -> 404 -0.12116
402 -> 405 -0.27888

Excited State 7: Singlet-A 3.1475 eV 393.91 nm f=0.0130 <S**2>=0.000
398 -> 403 0.28448
402 -> 405 0.63758

Excited State 8: Singlet-A 3.2449 eV 382.08 nm f=0.0052 <S**2>=0.000
399 -> 403 0.62156
401 -> 404 -0.11405
401 -> 407 -0.11520

Excited State 9: Singlet-A 3.3404 eV 371.16 nm f=0.0011 <S**2>=0.000
397 -> 403 0.45496
399 -> 403 -0.12344
400 -> 404 0.39874
402 -> 406 0.12574
402 -> 407 -0.25055

Excited State 10: Singlet-A 3.4003 eV 364.62 nm f=0.0377 <S**2>=0.000
397 -> 403 0.18127
400 -> 404 0.23201
402 -> 406 -0.29631
402 -> 407 0.54367

Excited State 11: Singlet-A 3.4624 eV 358.09 nm f=0.0001 <S**2>=0.000
402 -> 406 0.62153
402 -> 407 0.33211

Excited State 12: Singlet-A 3.5734 eV 346.97 nm f=0.1019 <S**2>=0.000
397 -> 403 -0.33134
399 -> 404 -0.26994
400 -> 404 0.37345
401 -> 406 0.14622

401 -> 407 -0.28423

Excited State 13: Singlet-A 3.5975 eV 344.64 nm f=0.0445 <S**2>=0.000
397 -> 403 -0.20140
399 -> 404 0.46884
400 -> 404 0.20865
401 -> 405 -0.31122
401 -> 406 -0.10310
401 -> 407 0.22066

Excited State 14: Singlet-A 3.6279 eV 341.75 nm f=0.0281 <S**2>=0.000
399 -> 404 0.33144
400 -> 404 0.12472
401 -> 405 0.53712
401 -> 407 -0.14643

Excited State 15: Singlet-A 3.6434 eV 340.30 nm f=0.0383 <S**2>=0.000
393 -> 403 -0.12882
397 -> 403 -0.12577
399 -> 403 0.10273
399 -> 404 -0.23835
401 -> 405 0.22771
401 -> 406 -0.22156
401 -> 407 0.42995
402 -> 408 -0.18930
402 -> 410 0.11422

Excited State 16: Singlet-A 3.6915 eV 335.86 nm f=0.3352 <S**2>=0.000
397 -> 403 -0.11856
400 -> 404 0.13324
401 -> 405 0.12673
401 -> 407 0.15719
402 -> 408 0.52525
402 -> 409 -0.13014
402 -> 410 -0.21242
402 -> 411 -0.11599
402 -> 412 0.10603

Excited State 17: Singlet-A 3.7064 eV 334.51 nm f=0.0316 <S**2>=0.000

395 -> 403	-0.11691
402 -> 408	0.38022
402 -> 409	0.32255
402 -> 410	0.33416
402 -> 411	0.24141
402 -> 412	-0.13242

Excited State 18: Singlet-A 3.7559 eV 330.11 nm f=0.0170 <S**2>=0.000

392 -> 403	0.11820
393 -> 403	0.38397
394 -> 403	-0.16383
395 -> 403	0.45419
402 -> 409	0.12376
402 -> 410	0.12262

Excited State 19: Singlet-A 3.8305 eV 323.67 nm f=0.0223 <S**2>=0.000

392 -> 403	-0.12067
393 -> 403	0.49595
394 -> 403	0.26150
395 -> 403	-0.26104
401 -> 408	0.11423
402 -> 409	-0.19009
402 -> 410	0.13030

Excited State 20: Singlet-A 3.8495 eV 322.08 nm f=0.0023 <S**2>=0.000

396 -> 403	0.69589

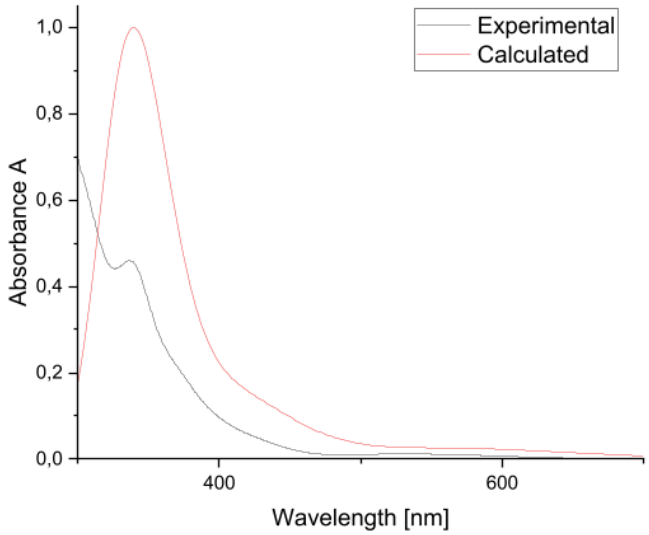

Supplementary Figure S31. Normalized experimental (c = $1 \cdot 10^{-3}$ mol/L) and TD-DFT simulated UV-Vis spectra of **2a** in hexane at RT.

Supplementary Table S6. Transition Energy, wavelength, and oscillator strengths of the electronic transition of **2b** calculated at the TD-B3LYP/def2-TZVP level of theory (the 411th orbital is the highest occupied orbital).

Excited State 1: Singlet-A 2.2286 eV 556.33 nm f=0.0085 <S**2>=0.000
411 -> 412 0.70267
This state for optimization and/or second-order correction.
Total Energy, E(CIS/TDA) = -7727.22098238
Copying the excited state density for this state as the 1-particle RhoCI density.

Excited State 2: Singlet-A 2.4150 eV 513.40 nm f=0.0056 <S**2>=0.000
410 -> 412 0.69951

Excited State 3: Singlet-A 2.7688 eV 447.79 nm f=0.0014 <S**2>=0.000
409 -> 412 0.69990

Excited State 4: Singlet-A 3.0215 eV 410.34 nm f=0.0272 <S**2>=0.000
410 -> 413 0.61924
411 -> 413 -0.28244

Excited State 5: Singlet-A 3.0415 eV 407.64 nm f=0.0605 <S**2>=0.000
410 -> 413 0.27898

411 -> 413 0.62003

Excited State 6: Singlet-A 3.1411 eV 394.72 nm f=0.0010 <S**2>=0.000
407 -> 412 0.67205
411 -> 414 -0.11069

Excited State 7: Singlet-A 3.2381 eV 382.89 nm f=0.0083 <S**2>=0.000
408 -> 412 0.63006
410 -> 413 -0.12834
410 -> 415 -0.12471

Excited State 8: Singlet-A 3.3051 eV 375.13 nm f=0.0088 <S**2>=0.000
406 -> 412 -0.18344
407 -> 412 0.13395
409 -> 413 -0.10547
411 -> 414 0.63232
411 -> 418 0.13034

Excited State 9: Singlet-A 3.3692 eV 367.99 nm f=0.0151 <S**2>=0.000
406 -> 412 0.47490
409 -> 413 0.40481
411 -> 414 0.21814
411 -> 415 -0.13790

Excited State 10: Singlet-A 3.5258 eV 351.64 nm f=0.0204 <S**2>=0.000
406 -> 412 0.10684
408 -> 413 -0.10319
409 -> 413 0.10459
411 -> 415 0.65458

Excited State 11: Singlet-A 3.5755 eV 346.76 nm f=0.0863 <S**2>=0.000
405 -> 412 -0.11745
406 -> 412 -0.30206
408 -> 413 -0.18396
409 -> 413 0.39467
410 -> 414 -0.26544
410 -> 415 -0.28558

Excited State 12: Singlet-A 3.6039 eV 344.03 nm f=0.0452 <S**2>=0.000
405 -> 412 -0.12078
406 -> 412 -0.15914
408 -> 413 0.55829
409 -> 413 0.22482
410 -> 415 0.23924

Excited State 13: Singlet-A 3.6211 eV 342.39 nm f=0.0226 <S**2>=0.000
403 -> 412 -0.11601
405 -> 412 -0.26133
406 -> 412 -0.11917
408 -> 413 -0.17023
409 -> 413 0.11157
410 -> 414 0.54972
410 -> 418 0.13498
411 -> 415 -0.10838

Excited State 14: Singlet-A 3.6542 eV 339.29 nm f=0.0063 <S**2>=0.000
405 -> 412 -0.11489
408 -> 412 0.13298
408 -> 413 -0.28663
410 -> 414 -0.18812
410 -> 415 0.55325

Excited State 15: Singlet-A 3.6918 eV 335.84 nm f=0.0650 <S**2>=0.000
405 -> 412 0.58330
406 -> 412 -0.15676
409 -> 413 0.19812
410 -> 414 0.17589

Excited State 16: Singlet-A 3.7198 eV 333.31 nm f=0.0003 <S**2>=0.000
411 -> 416 0.70229

Excited State 17: Singlet-A 3.7714 eV 328.75 nm f=0.0931 <S**2>=0.000
399 -> 412 -0.10026
401 -> 412 -0.12034

402 -> 412 0.10821
403 -> 412 -0.24813
411 -> 414 -0.13848
411 -> 417 0.21439
411 -> 418 0.50351

Excited State 18: Singlet-A 3.8100 eV 325.42 nm f=0.0259 <S**2>=0.000
399 -> 412 0.10529
401 -> 412 0.21361
402 -> 412 -0.19047
403 -> 412 0.46258
405 -> 412 -0.12978
411 -> 417 0.12317
411 -> 418 0.31818

Excited State 19: Singlet-A 3.8476 eV 322.24 nm f=0.0017 <S**2>=0.000
404 -> 412 0.69313

Excited State 20: Singlet-A 3.8538 eV 321.72 nm f=0.2151 <S**2>=0.000
411 -> 417 0.61697
411 -> 418 -0.26995

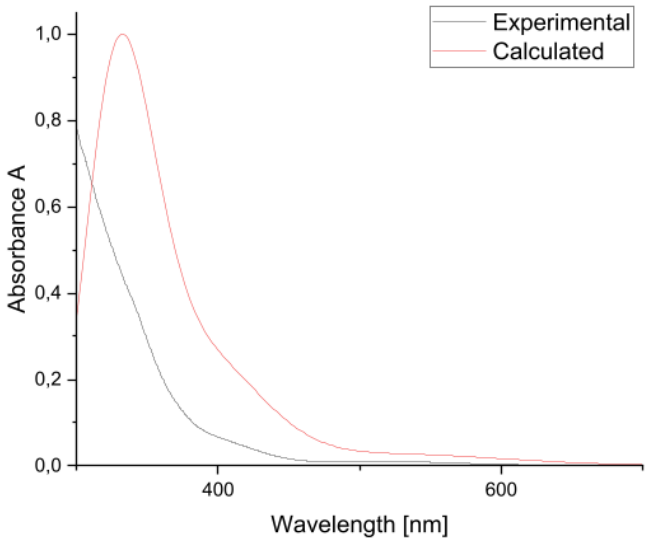

Supplementary Figure S32. Normalized experimental (c = $1 \cdot 10^{-3}$ mol/L) and TD-DFT simulated UV-Vis spectra of **2b** in hexane at RT.

Supplementary Table S7. Transition Energy, wavelength, and oscillator strengths of the electronic transition of **2c** calculated at the TD-B3LYP/def2-TZVP level of theory (the 406th orbital is the highest occupied orbital, shown in Supplementary Fig. S25).

Excited State 1: Singlet-A 2.2077 eV 561.59 nm f=0.0088 <S**2>=0.000
406 -> 407 0.70215
This state for optimization and/or second-order correction.
Total Energy, E(CIS/TDA) = -5864.56275847
Copying the excited state density for this state as the 1-particle RhoCI density.

Excited State 2: Singlet-A 2.4055 eV 515.42 nm f=0.0067 <S**2>=0.000
405 -> 407 0.69714

Excited State 3: Singlet-A 2.7690 eV 447.77 nm f=0.0013 <S**2>=0.000
404 -> 407 0.69721

Excited State 4: Singlet-A 3.0002 eV 413.26 nm f=0.0596 <S**2>=0.000
402 -> 407 0.13377
405 -> 408 0.36512
406 -> 408 0.54761
406 -> 409 0.14666

Excited State 5: Singlet-A 3.0279 eV 409.48 nm f=0.0130 <S**2>=0.000
403 -> 407 0.15576
405 -> 408 0.56153
406 -> 408 -0.33134
406 -> 409 -0.16544

Excited State 6: Singlet-A 3.1115 eV 398.47 nm f=0.0300 <S**2>=0.000
401 -> 407 0.14688
402 -> 407 0.43010
403 -> 407 0.12280
406 -> 408 -0.21437
406 -> 409 0.45016

Excited State 7: Singlet-A 3.1735 eV 390.68 nm f=0.0194 <S**2>=0.000
402 -> 407 0.49256
403 -> 407 0.10757
405 -> 408 -0.10586
406 -> 409 -0.45297

Excited State 8: Singlet-A 3.1867 eV 389.06 nm f=0.0066 <S**2>=0.000
402 -> 407 -0.18523
403 -> 407 0.60791
403 -> 408 0.10402
405 -> 408 -0.15136
405 -> 410 -0.12886

Excited State 9: Singlet-A 3.3479 eV 370.34 nm f=0.0458 <S**2>=0.000
401 -> 407 0.56214
404 -> 408 0.32050
406 -> 408 0.10746
406 -> 410 0.15552

Excited State 10: Singlet-A 3.4159 eV 362.97 nm f=0.0011 <S**2>=0.000
400 -> 407 0.28941
405 -> 409 0.60439
405 -> 413 0.12291

Excited State 11: Singlet-A 3.4333 eV 361.12 nm f=0.0018 <S**2>=0.000
400 -> 407 0.53863
401 -> 407 -0.13625
404 -> 408 0.26671
405 -> 409 -0.25632
406 -> 410 0.14520

Excited State 12: Singlet-A 3.5134 eV 352.89 nm f=0.0457 <S**2>=0.000
401 -> 407 -0.10265
403 -> 408 0.13192
404 -> 408 -0.10967
405 -> 409 0.10720
406 -> 410 0.63222

Excited State 13: Singlet-A 3.5890 eV 345.46 nm f=0.0044 <S**2>=0.000
403 -> 408 0.55228
405 -> 410 0.38395
406 -> 410 -0.12972

Excited State 14: Singlet-A 3.6118 eV 343.27 nm f=0.1733 <S**2>=0.000
400 -> 407 -0.26508
401 -> 407 -0.26416
403 -> 408 0.10228
404 -> 408 0.48896
405 -> 410 -0.13833

Excited State 15: Singlet-A 3.6356 eV 341.03 nm f=0.0113 <S**2>=0.000
401 -> 407 -0.10991
403 -> 407 0.11882
403 -> 408 -0.34892
403 -> 409 0.16575
404 -> 408 0.12749
405 -> 410 0.51789

Excited State 16: Singlet-A 3.7550 eV 330.19 nm f=0.0696 <S**2>=0.000
396 -> 407 0.13343
398 -> 407 0.24651

399 -> 407 0.14102
404 -> 409 -0.25816
405 -> 412 0.16446
406 -> 412 0.22610
406 -> 413 0.44774

Excited State 17: Singlet-A 3.7708 eV 328.80 nm f=0.0548 <S**2>=0.000
398 -> 407 -0.17287
404 -> 409 0.21828
406 -> 409 -0.10740
406 -> 412 -0.33655
406 -> 413 0.49353

Excited State 18: Singlet-A 3.7861 eV 327.47 nm f=0.1598 <S**2>=0.000
396 -> 407 0.18317
398 -> 407 0.41902
399 -> 407 0.20042
404 -> 409 0.11605
406 -> 412 -0.40221

Excited State 19: Singlet-A 3.8146 eV 325.02 nm f=0.0014 <S**2>=0.000
406 -> 411 0.69088

Excited State 20: Singlet-A 3.8197 eV 324.59 nm f=0.2315 <S**2>=0.000
394 -> 407 0.13247
398 -> 407 0.18837
399 -> 407 -0.14344
402 -> 408 0.11276
404 -> 409 0.50862
405 -> 412 0.11765
406 -> 412 0.29745

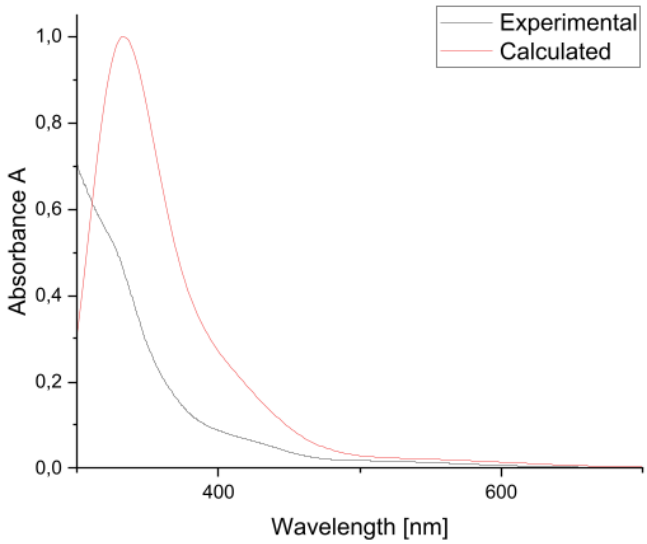

Supplementary Figure S33. Normalized experimental (c = $1 \cdot 10^{-3}$ mol/L) and TD-DFT simulated UV-Vis spectra of **2c** in hexane at RT.

Supplementary Table S8. Extended comparison of wavelengths λ_{max}, oscillator strengths f, and excitation energy E from experimental and TD-DFT[S11] calculations for siliconoid-tetrylene hybrids **2a-c**.

	Experimental		DFT			
	λ_{max} (nm)	Excitation energy E (eV)	λ_{max} (nm)	Excitation energy E (eV)	Oscillator strength f	Transitions (% contribution)
2a	532	2.3308	589	2.1138	0.0124	HOMO→LUMO (99)
			514	2.4115	0.0052	HOMO–1→LUMO (98)
	371	3.3418	424	2.9232	0.0568	HOMO→LUMO+1 (96)
	336	3.9000	336	3.6920	0.3352	HOMO–5→LUMO (3) HOMO–2→LUMO+1 (4) HOMO–1→LUMO+2 (3) HOMO–1→LUMO+4 (5) HOMO→LUMO+5 (55) HOMO→LUMO+6 (3) HOMO→LUMO+7 (9) HOMO→LUMO+8 (3) HOMO→LUMO+9 (2)
2b	514	2.4125	556	2.2286	0.0085	HOMO→LUMO (99)
			513	2.4150	0.0056	HOMO–1→LUMO (98)
	407	3.0463	408	3.0415	0.0605	HOMO→LUMO+1 (76)

						HOMO–1→LUMO+1 (16)
	345	3.5937	322	3.8538	0.2151	HOMO→LUMO+5 (76) HOMO–1→LUMO+6 (15)
2c	520	2.3843	562	2.2077	0.0088	HOMO→LUMO (99)
			515	2.4055	0.0067	HOMO–1→LUMO (97)
	417	2.9732	413	3.0002	0.0596	HOMO–3→LUMO (4) HOMO–1→LUMO+1 (3) HOMO→LUMO+1 (60) HOMO→LUMO+2 (4)
	324	3.8266	325	3.8197	0.2315	HOMO–12→LUMO (4) HOMO–8→LUMO (7) HOMO–7→LUMO (4) HOMO–4→LUMO+1 (7) HOMO–2→LUMO+2 (52) HOMO–1→LUMO+5 (3) HOMO→LUMO+5 (18)

5. References

S1 Leszczyńska, K. I.; Huch, V.; Präsang, C.; Schwabedissen, J.; Berger, R. J. F.; Scheschkewitz, D.; Erweiterung ungesättigter Siliciumcluster mit atomarer Genauigkeit. *Angew. Chem*. **2019**, *131*, 5178–5182 DOI: 10.1002/ange.201811331; Atomically Precise Expansion of Unsaturated Silicon Clusters. *Angew. Chem. Int. Ed.* 2019, *58*, 5124–5128. DOI: 10.1002/anie.201811331

S2 a) So, C.-W.; Roesky, H. W.; Magull, J.; Oswald, R. B.; Synthesis and Characterization of [PhC(N*t*Bu)$_2$]SiCl: A Stable Monomeric Chlorosilylene. *Angew. Chem.* **2006**, *118*, 4052–4054. DOI: 10.1002/anie.200600647; *Angew. Chem. Int. Ed.* **2006**, *45*, 3948–3950. DOI: 10.1002/anie.200600647; b) Sen, S. S.; Roesky, H. W.; Stern, D.; Henn, J.; Stalke, D.; High Yield Access to Silylene RSiCl (R = PhC(N*t*Bu)$_2$) and Its Reactivity toward Alkyne: Synthesis of Stable Disilacyclobutene. *J. Am. Chem. Soc.* **2010**, *132*, 1123–1126. DOI: 10.1021/ja9091374; c) Nagendran, S.; Sen, S. S.; Roesky, H. W.; Koley, D.; Grubmüller, H.; Pal, A.; Herbst-Irmer, R.; RGe(I)Ge(I)R Compound (R = PhC(N*t*Bu)$_2$) with a Ge−Ge Single Bond and a Comparison with the Gauche Conformation of Hydrazine. *Organometallics* **2008**, *27*, 5459–5463. DOI: 10.1021/om800714f; d) Sen, S. S.; Kritzler-Kosch, M. P.; Nagendran, S.; Roesky, H. W.; Beck, T.; Pal, A.; Herbst-Irmer, R.; Synthesis of Monomeric Divalent Tin(II) Compounds with Terminal Chloride, Amide, and Triflate Substituents. *Eur. J. Inorg. Chem.* **2010**, *33*, 5304–5311. DOI: 10.1002/ejic.201000803.

S3 Kuveke, R. E. H.; Barwise, L.; van Ingen, Y.; Vashisth, K.; Roberts, N. J.; Chitnis, S. S.; Dutton, J. L.; Martin, C. D.; Melen, R. L.; An International Study Evaluating Elemental Analysis. *ACS Cent. Sci.* **2022**, *8*, 855−863. DOI: 10.1021/acscentsci.2c00325.

S4 Sheldrick, G. M.; *SHELXT* – Integrated space-group and crystal-structure determination. *Acta Cryst.* **2015**, *A71*, 3–8. DOI: 10.1107/S2053273314026370.

S5 Sheldrick, G. M.; Crystal structure refinement with *SHELXL*. *Acta Cryst.* **2015**, *C71*, 3–8. DOI: 10.1107/S2053229614024218.

S6 Hübschle, C. B.; Sheldrick, G. M.; Dittrich, B.; ShelXle: a Qt graphical user interface for SHELXL. *J. Appl. Crystallogr.* **2011**, *44*, 1281–1284. DOI: 10.1107/S0021889811043202.

S7 Spek, A. L.; *PLATON* SQUEEZE: a tool for the calculation of the disordered solvent contribution to the calculated structure factors. *Acta Cryst.* **2015**, *C71*, 9–18. DOI: 10.1107/S2053229614024929.

S8 Spek, A. L.; Structure validation in chemical crystallography. *Acta Cryst.* **2009**, *D65*, 148–155. DOI: 10.1107/S090744490804362X.

S9 a) Schäfer, A.; Horn, H.; Ahlrichs, R.; Fully optimized contracted Gaussian basis sets for atoms Li to Kr. *J. Chem. Phys.* **1992**, *97*, 2571–2577. DOI: 10.1063/1.463096; b) Schäfer, A.; Huber, C.; Ahlrichs, R.; Fully optimized contracted Gaussian basis sets of triple zeta valence quality for atoms Li to Kr. *J. Chem. Phys.* **1994**, *100*, 5829–5835. DOI: 10.1063/1.467146; c) Weigend, F.; Ahlrichs, R.; Balanced basis sets of split valence, triple zeta valence and quadruple zeta valence quality for H to Rn: Design and assessment of accuracy. *Phys. Chem. Chem. Phys.* **2005**, *7*, 3297–3305. DOI: 10.1039/B508541A; d) Weigend, F.; Accurate Coulomb-fitting basis sets for H to Rn. *Phys. Chem. Chem. Phys.* **2006**, *8*, 1057–1065. DOI: 10.1039/B515623H.

S10 a) Perdew, J. P.; Density-functional approximation for the correlation energy of the inhomogeneous electron gas. *Phys. Rev. B* **1986**, *33*, 8822–8824. DOI: 10.1103/PhysRevB.33.8822; b) Becke, A. D.; Density-functional exchange-energy approximation with correct asymptotic behavior. *Phys. Rev. A* **1988**, *38*, 3098 –3100. DOI: 10.1103/PhysRevA.38.3098; c) Lee, C.; Parr, R. G.; Development of the Colle-Salvetti correlation-energy formula into a functional of the electron density. *Phys. Rev. B* **1988**, *37*, 785-789. DOI: 10.1103/PhysRevB.37.785.

S11 Gaussian 16, Revision C.01, Frisch, M. J.; Trucks, G. W.; Schlegel, H. B.; Scuseria, G. E.; Robb, M. A.; Cheeseman, J. R.; Scalmani, G.; Barone, V.; Petersson, G. A.; Nakatsuji, H.; Li, X.; Caricato, M.; Marenich, A. V.; Bloino, J.; Janesko, B. G.; Gomperts, R.; Mennucci, B.; Hratchian, H. P.; Ortiz, J. V.; Izmaylov, A. F.; Sonnenberg, J. L.; Williams-Young, D.; Ding, F.; Lipparini, F.; Egidi, F.; Goings, J.; Peng, B.; Petrone, A.; Henderson, T.; Ranasinghe, D.; Zakrzewski, V. G.; Gao, J.; Rega, N.; Zheng, G.; Liang, W.; Hada, M.; Ehara, M.; Toyota, K.; Fukuda, R.; Hasegawa, J.; Ishida, M.; Nakajima, T.; Honda, Y.; Kitao, O.; Nakai, H.; Vreven, T.; Throssell, K.; Montgomery, J. A., Jr.; Peralta, J. E.; Ogliaro, F.; Bearpark, M. J.; Heyd, J. J.; Brothers, E. N.; Kudin, K. N.;

Staroverov, V. N.; Keith, T. A.; Kobayashi, R.; Normand, J.; Raghavachari, K.; Rendell, A. P.; Burant, J. C.; Iyengar, S. S.; Tomasi, J.; Cossi, M.; Millam, J. M.; Klene, M.; Adamo, C.; Cammi, R.; Ochterski, J. W.; Martin, R. L.; Morokuma, K.; Farkas, O.; Foresman, J. B.; Fox, D. J. Gaussian, Inc., Wallingford CT, **2016**.

S12 Chemcraft - graphical software for visualization of quantum chemistry computations. https://www.chemcraftprog.com

6. Author Contributions

L. Giarrana. performed the synthetic work and data analysis, L. Giarrana. and D. Scheschkewitz designed the study, D. Scheschkewitz acquired the funding; B. Morgenstern performed the X-ray diffraction studies, M. Zimmer performed the solid state NMR measurements, L. Giarrana performed the DFT calculations, L. Giarrana and D. Scheschkewitz wrote the manuscript.

5.3 Stable Nickel Complexes of a Siliconoid/Silylene Hybrid Ligand: Competent Hydrosilylation Catalysts for Terminal Olefins

Supplementary Information

Stable Nickel complexes of a Siliconoid/Silylene Hybrid Ligand: Competent Hydrosilylation Catalysts for Terminal Alkenes

Luisa Giarrana,[a] Dennis Welterlich,[a] Michael Zimmer,[a] Bernd Morgenstern[b] and David Scheschkewitz*[a]

M. Sc. L. Giarrana, M. Sc. D. Welterlich, Dr. M. Zimmer, Prof. Dr. D. Scheschkewitz − Krupp-Chair for General and Inorganic Chemistry, Saarland University, 66123 Saarbrücken, Germany
Dr. B. Morgenstern – Service Center X-ray Diffraction, Saarland University, 66123 Saarbrücken, Germany

E-Mail: david.scheschkewitz@uni-saarland.de

Institute and/or researcher X usernames: @scheschkewitz @LuisaGiarrana

5. Supporting Information

Table of Contents

5. Supporting Information

1 Experimental Procedures

All manipulations were carried out under a protective atmosphere of argon, by using a glovebox or standard Schlenk techniques. Solvents were dried and degassed by reflux over sodium/benzophenone under argon. [D_6]-benzene (C_6D_6) was dried over potassium mirror and distilled under argon prior to use. Si_7Li siliconoid,[1] chloro silylene[2,3] and siliconoid hybrid Si_7NHSi **1**[4] were prepared following the literature protocols while transition metal precursors, triphenyl phosphine and diphenyl silane were used as commercially purchased (under inert gas) and stored in a glove box. NMR spectra were recorded on a Bruker Avance III 300 and a Bruker Avance IV 400 NMR spectrometer (^{1}H = 300.13/ 400.13 MHz, ^{13}C = 75.47/ 100.61 MHz, ^{29}Si = 59.63/ 79.49 MHz). The ^{1}H and ^{13}C{1H} NMR spectra were referenced to the residual proton and natural abundance ^{13}C resonances of the deuterated solvent and chemical shifts were reported relative to $SiMe_4$ (C_6D_6: δ^1H = 7.16 ppm and δ^{13}C = 128.06 ppm, toluene-d_8 δ^1H = 7.09, 7.01, 6.97, 2.08 ppm and δ^{13}C = 137.48, 128.87, 127.96, 125.13, 20.43 ppm). Solid-state NMR data were collected from a Bruker Avance III 400 WB. UV-Vis spectra were recorded on a Shimadzu UV-2600 spectrometer in quartz cells with a path length of 0.1 cm. Elemental analyses were performed on an elemental analyzer Leco CHN-900. Mass spectrometry was measured on a Bruker SolariX 7 Tesla MALDI/ESI/APPI FTICR imaging MS. Melting points were determined under argon in NMR tubes and are uncorrected. The molten samples were examined by NMR spectroscopy to confirm whether decomposition had occurred upon melting. Crystallographic data of the structures reported in this paper has been deposited with the Cambridge Crystallographic Data Centre, CCDC, 12 Union Road, Cambridge CB21EZ, UK. (Fax: +44-1223-336-033; E-Mail: deposit@ccdc.cam.ac.uk, http://www.ccdc.cam.ac.uk).

2 Preparation, data and spectra

2.1 Preparation of $Fe(CO)_4$ siliconoid/silylene complex 2

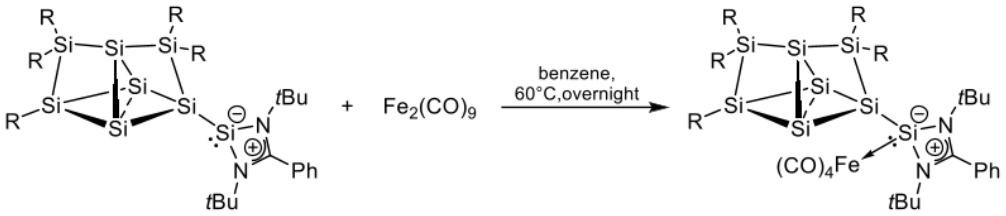

1 **2**

M [g/mol] = 1472.79 1640.67

To Si_7 siliconoid/silylene **1**[4] (100 mg, 0.0679 mmol, 1.0 eq.) added diiron (0) nonacarbonyl $Fe_2(CO)_9$ (27.7 mg, 0.0747 mmol, 1.1 eq.) and 1.0 mL benzene. The brown solution was heated to 60°C and stirred overnight. After cooling to ambient temperature, all volatiles were removed under reduced pressure, and the compound was dried thoroughly. The resulting solid was extracted from 3.0 mL pentane, washed

two times with approximately 0.5 mL pentane. Afterwards the solution was concentrated under reduced pressure and at room temperature for crystallization. The title compound **2** was isolated in 46% yield (51.5 mg, 0.0314 mmol).

^{1}H NMR (400.13 MHz, C_6D_6, 300 K) δ = 7.640 – 7.616 (m, $C_{10}H_8$), 7.503 (d, $^{3}J_{HH}$ = 7.53 Hz, 1H, ArC-*H*), 7.406 (s, 1H, ArC-*H*), 7.334 (s, 1H, ArC-*H*), 7.264 – 7.240 (m, $C_{10}H_8$), 7.089 – 7.035 (m, 5H, ArC-*H*), 7.012 – 6.995 (m, 2H, ArC-*H*), 6.940 – 6.904 (m, 2H, ArC-*H*), 6.891 (s, 1H, ArC-*H*), 6.816 (m, 1H, ArC-*H*), 6.733 (m, 1H, ArC-*H*), 5.810 (sept, $^{3}J_{HH}$ = 6.62 Hz, 1H, Tip-C*H*(CH_3)$_2$), 4.839 (sept, $^{3}J_{HH}$ = 6.48 Hz, 1H, Tip-C*H*(CH_3)$_2$), 4.668 (sept, $^{3}J_{HH}$ = 6.46 Hz, 1H, Tip-C*H*(CH_3)$_2$), 4.521 (sept, $^{3}J_{HH}$ = 6.46 Hz, 1H, Tip-C*H*(CH_3)$_2$), 3.989 (sept, $^{3}J_{HH}$ = 6.58 Hz, 1H, Tip-C*H*(CH_3)$_2$), 3.881 (sept, $^{3}J_{HH}$ = 6.46 Hz, 1H, Ar-C*H*(CH_3)$_2$), 3.500 (sept, $^{3}J_{HH}$ = 6.49 Hz, 2H, Tip-C*H*(CH_3)$_2$), 3.114 (sept, $^{3}J_{HH}$ = 6.58 Hz, 2H, Tip-C*H*(CH_3)$_2$), 2.907 (sept, $^{3}J_{HH}$ = 6.82 Hz, 1H, Tip-C*H*(CH_3)$_2$), 2.810 (sept, $^{3}J_{HH}$ = 6.82 Hz, 1H, Tip-C*H*(CH_3)$_2$), 2.693 – 2.615 (m, 3H, Tip-C*H*(CH_3)$_2$), 2.225 (t, $^{3}J_{HH}$ = 5.64 Hz, 6H, Tip-CH(C*H*$_3$)$_2$), 2.080 (d, $^{3}J_{HH}$ = 6.64 Hz, 3H, Tip-CH(C*H*$_3$)$_2$), 1.7202 (d, $^{3}J_{HH}$ = 6.53 Hz, 3H, Tip-CH(C*H*$_3$)$_2$), 1.648 (d, $^{3}J_{HH}$ = 6.36 Hz, 3H, Tip-CH(C*H*$_3$)$_2$), 1.590 (d, $^{3}J_{HH}$ = 6.53 Hz, 3H, Tip-CH(C*H*$_3$)$_2$), 1.554 (d, $^{3}J_{HH}$ = 6.38Hz, 3H, Tip-CH(C*H*$_3$)$_2$), 1.512 (d, $^{3}J_{HH}$ = 6.53 Hz, 3H, Tip-CH(C*H*$_3$)$_2$), 1.4678 (d, $^{3}J_{HH}$ = 6.69 Hz, 3H, Tip-CH(C*H*$_3$)$_2$), 1.4255 (d, $^{3}J_{HH}$ = 6.68 Hz, 3H, Tip-CH(C*H*$_3$)$_2$), 1.388 (t, $^{3}J_{HH}$ = 7.40 Hz, 8H, Tip-CH(C*H*$_3$)$_2$), 1.319 (t, $^{3}J_{HH}$ = 6.27 Hz, 8H, Tip-CH(C*H*$_3$)$_2$), 1.269 – 1.233 (m, hexane), 1.186 (d, $^{3}J_{HH}$ = 6.62 Hz, 6H, Tip-CH(C*H*$_3$)$_2$), 1.150 (s, 12H, Si(N(C(C*H*$_3$)$_3$))$_2$CPh overlapping with Tip-CH(C*H*$_3$)$_2$), 1.129 (s, 5H, Tip-CH(C*H*$_3$)$_2$), 1.101 (s, 3H, Tip-CH(C*H*$_3$)$_2$), 1.084 (s, 3H, Tip-CH(C*H*$_3$)$_2$), 1.067 (t, $^{3}J_{HH}$ = 6.27 Hz, 6H, Tip-CH(C*H*$_3$)$_2$), 0.890 (t, hexane), 0.855 (s, 9H, Si(N(C(C*H*$_3$)$_3$))$_2$CPh), 0.637 (d, $^{3}J_{HH}$ = 6.62 Hz, 3H, Tip-CH(C*H*$_3$)$_2$), 0.578 (dd, $^{3}J_{HH}$ = 9.50 Hz, 6.62 Hz, 6H, Tip-CH(C*H*$_3$)$_2$), 0.507 (d, 3H, $^{3}J_{HH}$ = 6.33 Hz, Tip-CH(C*H*$_3$)$_2$), 0.3903 (d, 3H, $^{3}J_{HH}$ = 6.33 Hz, Tip-CH(C*H*$_3$)$_2$), 0.265 (d, 3H, $^{3}J_{HH}$ = 6.33 Hz, Tip-CH(C*H*$_3$)$_2$) ppm.

^{13}C{^{1}H} NMR (100.61 MHz, C_6D_6, 300 K) δ = 216.79 (s, 4C, *C*O), 167.35 (s, Si(N(C(CH$_3$)$_3$))$_2$*C*Ph), 155.18, 154.84, 154.75, 153.38, 153.04, 152.61, 151.74, 151.11, 150.20, 149.90, 149.61, 149.40, 141.75, 138.70, 138.11, 137.43, 137.00, 134.01, 131.40 (s, each 1C, Ar-*C*), 130.59, 129.32, 128.89, 128.54, 128.35, (s, each 1C, Ar-C*H*), 128.12, 127.88 (s, each 1C, Ar-*C*), 127.53, 126.02, 124.30 (s, each 1C, Ar-*C*H), 123.30 (d, ^{4}J = 4.83 Hz, Ar-*C*H), 122.68, 122.37, 122.29 (s, each 1C, Ar-*C*H), 122.15 (d, ^{4}J = 4.83 Hz, Ar-*C*H), 121.97, 121.37 (s, each 1C, Ar-*C*H), 55.91, 55.25 (s, Si(N(*C*(CH$_3$)$_3$))$_2$CPh), 37.53, 37.21, 36.58, 36.37, 35.79, 35.42, 35.34, 34.93, 34.84, 34.77, 34.67, 34.61, 34.52, 34.42, 32.92 (s, each 1C, Tip-CH(*C*H$_3$)$_2$), 31.92 (s, hexane), 31.80, 31.71 (s, each 3C, Si(N(C(*C*H$_3$)$_3$))$_2$CPh), 29.15, 28.67, 27.89, 27.84, 27.48, 27.42, 27.16, 26.63, 26.35, 26.27, 25.99, 25.58, 24.87, 24.82, 24.52, 24.45, 24.42, 24.22, 24.15, 24.11, 24.08, 23.99, 23.95, 23.87, 23.80, 23.14 (s, each 1C, Tip-CH(*C*H$_3$)$_2$), 23.01, 14.32 (s, hexane) ppm.

^{29}Si{^{1}H} NMR (79.49 MHz, C_6D_6, 300 K) δ = 172.7 (s, *Si*(Si(N(C(CH$_3$)$_3$))$_2$CPh)), 157.1 (s, *Si*Tip), 100.5 (s, Fe*Si*(N(C(CH$_3$)$_3$))$_2$CPh), 33.6 (s, *Si*Tip$_2$), 5.9 (s, *Si*Tip$_2$), −98.2 (s, *Si* unsubstituted), −198.5 (s, *Si* unsubstituted), −209.0 (s, *Si* unsubstituted) ppm.

5. Supporting Information

CP-MAS $^{29}Si\{^1H\}$ NMR (79.53 MHz, 13 KHz, 300 K) δ = 170.6 (s, *Si*(Si(N(C(CH$_3$)$_3$))$_2$CPh)), 164.0 (s, *Si*Tip), 101.1 (s, Fe*Si*(N(C(CH$_3$)$_3$))$_2$CPh), 39.1 (s, *Si*Tip$_2$), 9.9 (s, *Si*Tip$_2$), −88.8 (s, *Si* unsubstituted), −206.9 (s, *Si* unsubstituted), −212.5 (s, *Si* unsubstituted) ppm.

Elemental analysis: calculated for $C_{94}H_{138}N_2FeO_4Si_8$: C 68.82 %, H 8.48 %, N 1.71%; Found: C 68.08 %, H 7.43 %, N 1.31 %. The lower values compared to those calculated are quite common for unsaturated silicon clusters due to incomplete combustion typically attributed to the formation of silicon carbides and/or nitrides. In addition, elemental analysis has come under scrutiny because of highly variable results of bona fide identical samples.[5]

UV-Vis (hexane): λ (ε) = 525 (380 M^{-1} cm^{-1}), 342 nm (1200 M^{-1} cm^{-1}) nm.

Solid State FT-IR $\tilde{\nu}_{CO}$ = 1907 (w), 1923 (w), 1953 (w), 2026 (w) cm^{-1}.

Melting Point: 251 – 267°C (decomposition).

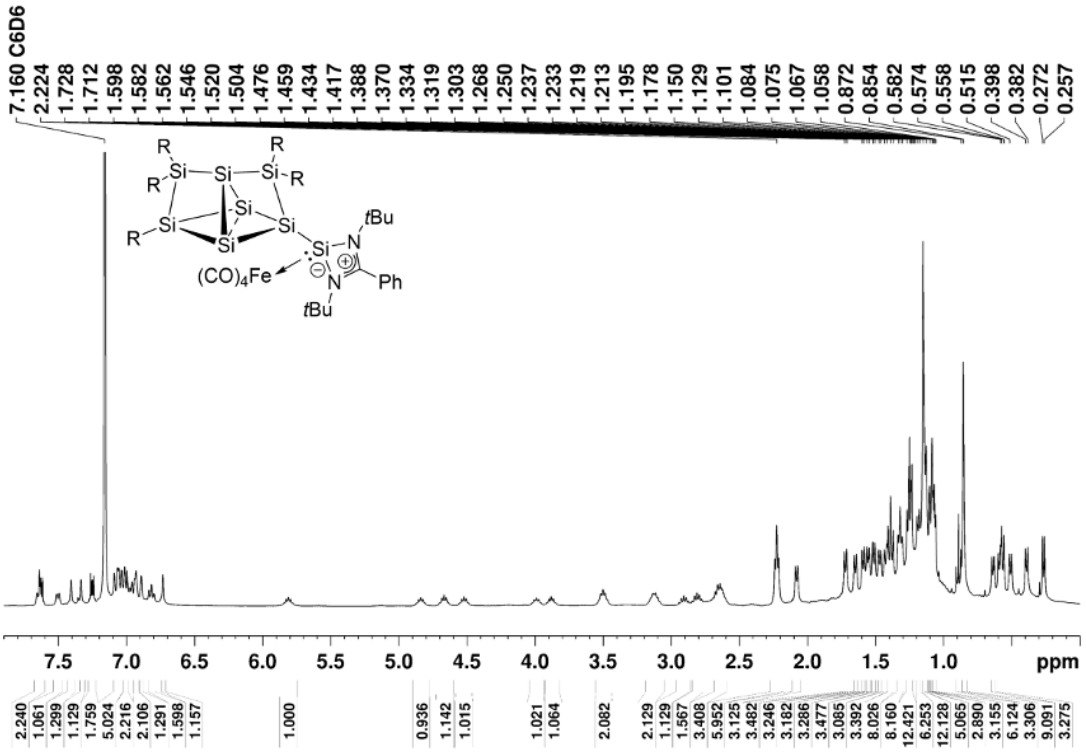

Supplementary Figure S1. ^1H NMR spectrum of $Fe(CO)_4$ siliconoid/silylene complex **2** in C_6D_6 (400.13 MHz, 300 K).

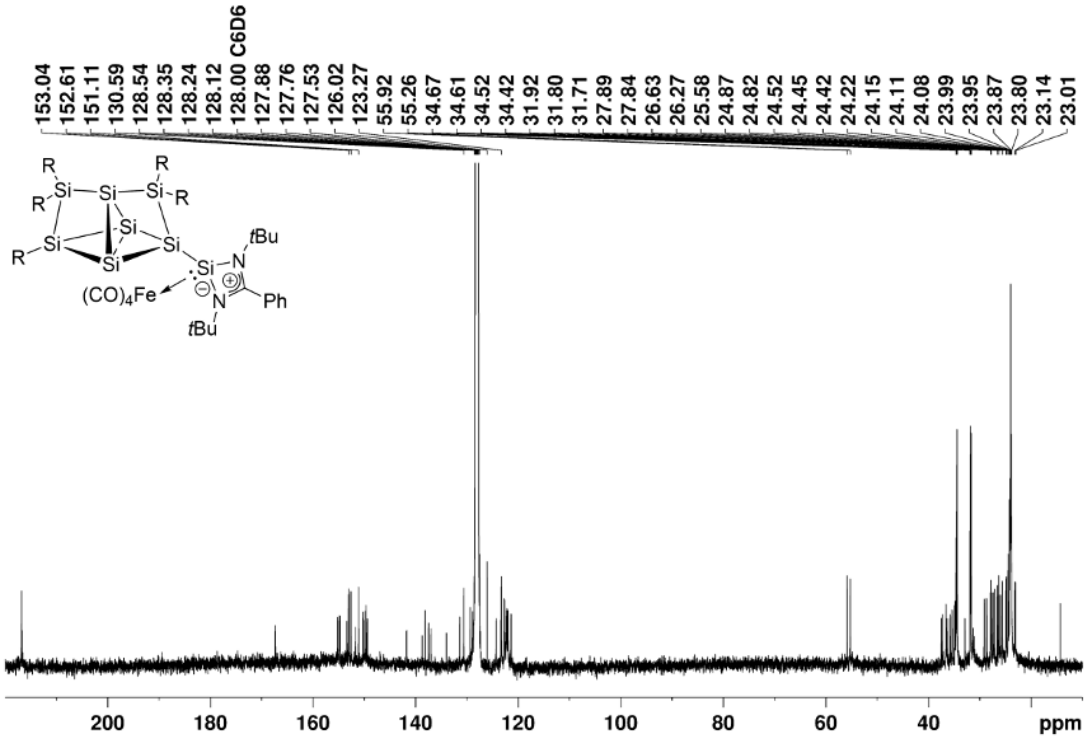

Supplementary Figure S2. $^{13}C\{^1H\}$ NMR spectrum of $Fe(CO)_4$ siliconoid/silylene complex **2** in C_6D_6 (100.61 MHz, 300 K).

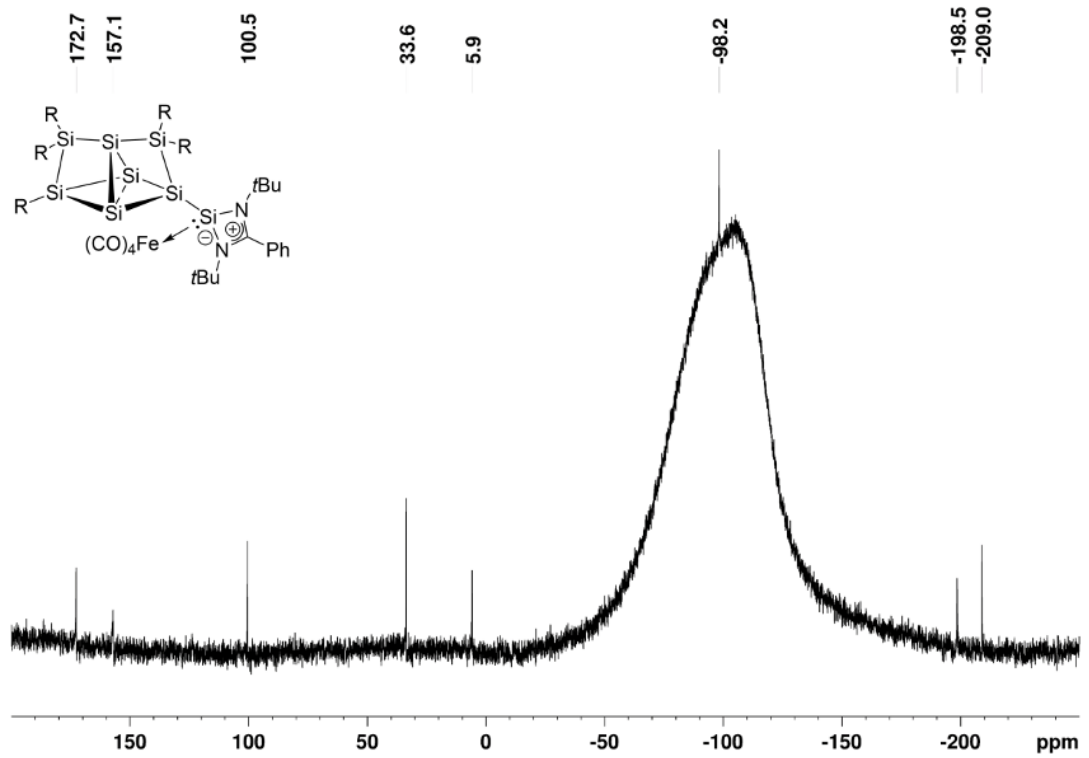

Supplementary Figure S3. $^{29}Si\{^1H\}$ NMR spectrum of $Fe(CO)_4$ siliconoid/silylene complex **2** in C_6D_6 (79.49 MHz, 300 K).

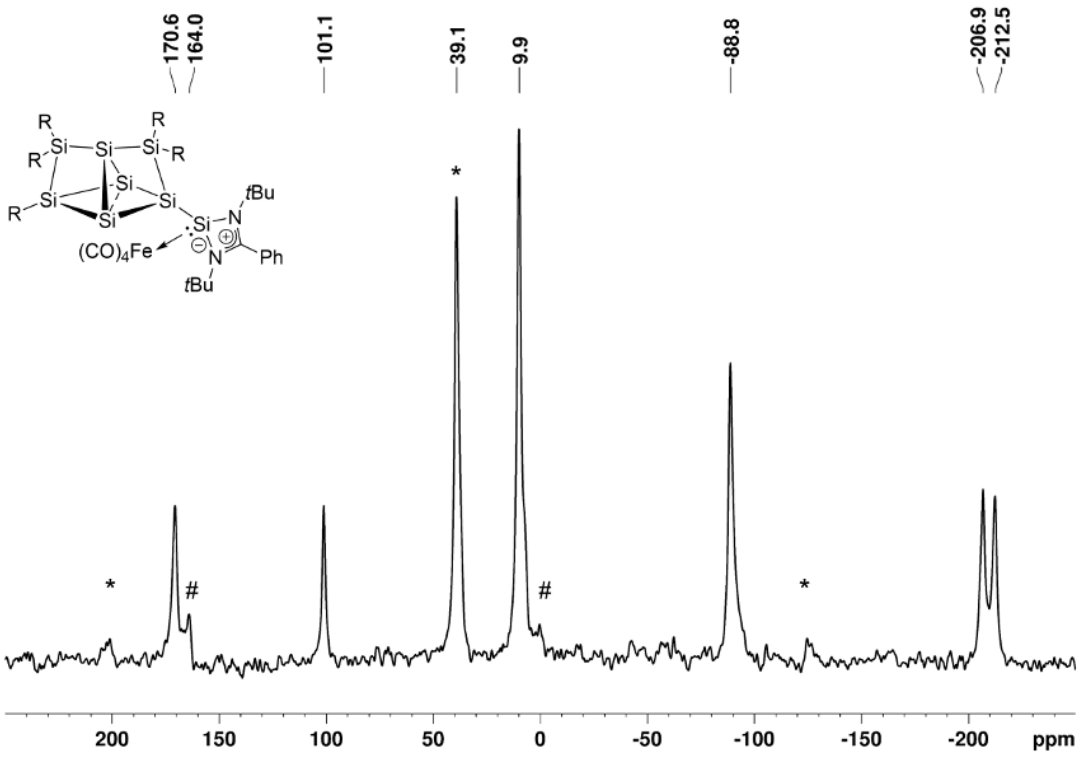

Supplementary Figure S 4. CP-MAS $^{29}Si\{^{1}H\}$ NMR spectrum of $Fe(CO)_4$ siliconoid/silylene complex **2** (79.53 MHz, 13 KHz, 300 K).

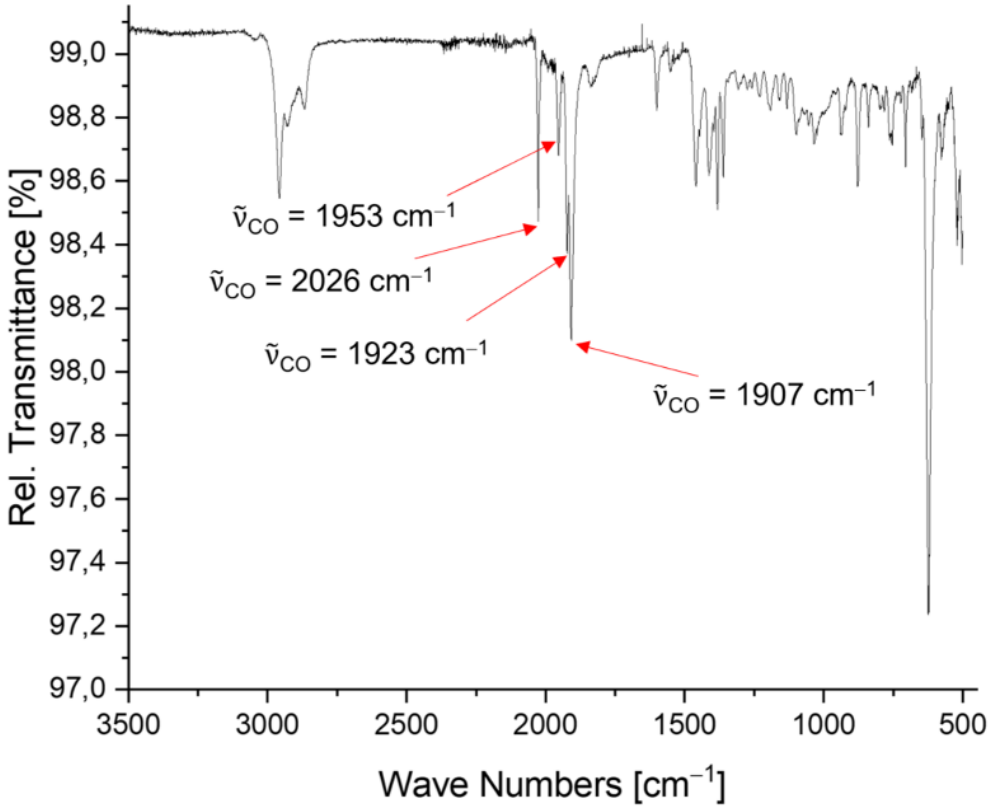

Supplementary Figure S5. FT-IR spectrum of $Fe(CO)_4$ siliconoid/silylene complex **2** in the solid state.

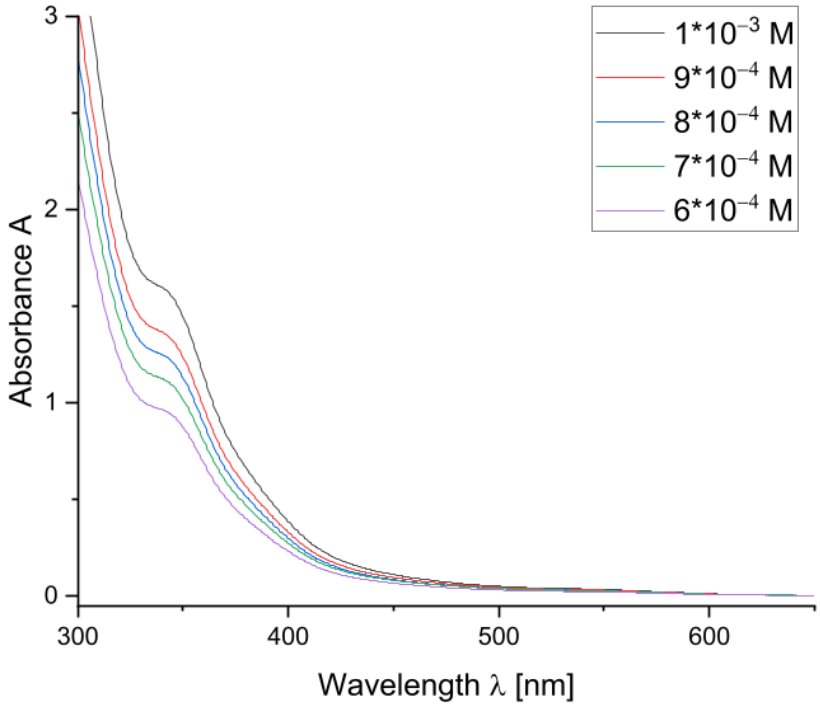

Supplementary Figure S6. UV-Vis spectra of $Fe(CO)_4$ siliconoid/silylene complex **2** in hexane at different concentrations.

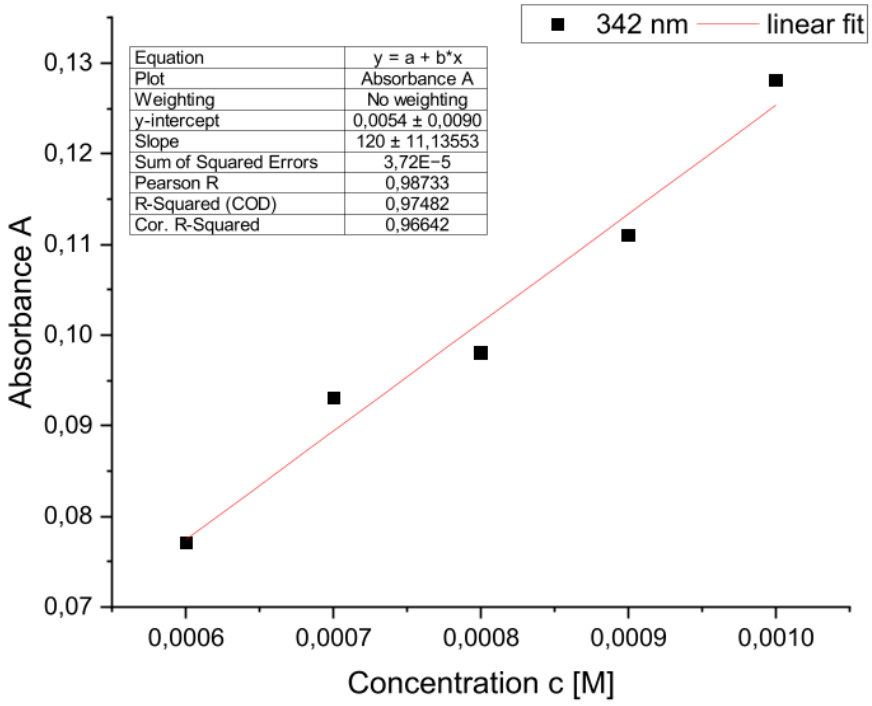

Supplementary Figure S7. Determination of the extinction ε = 1200 M^{-1} cm^{-1} of **2** by linear regression at λ = 342 nm.

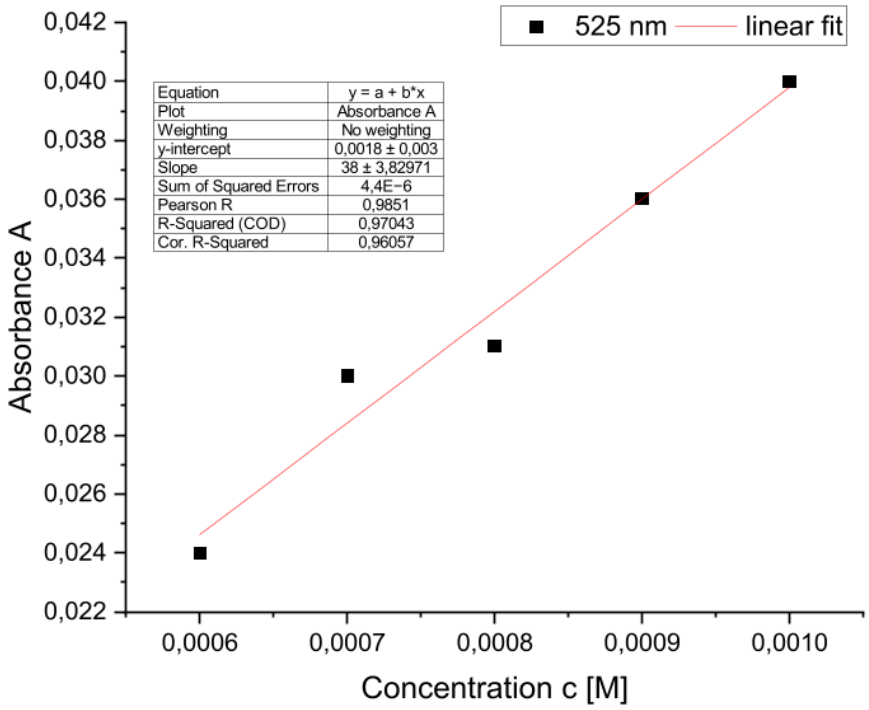

Supplementary Figure S8. Determination of the extinction ε = 380 M^{-1} cm^{-1} of **2** by linear regression at λ_{max} = 525 nm.

2.2 Preparation of nickel siliconoid/silylene complexes 3a,b

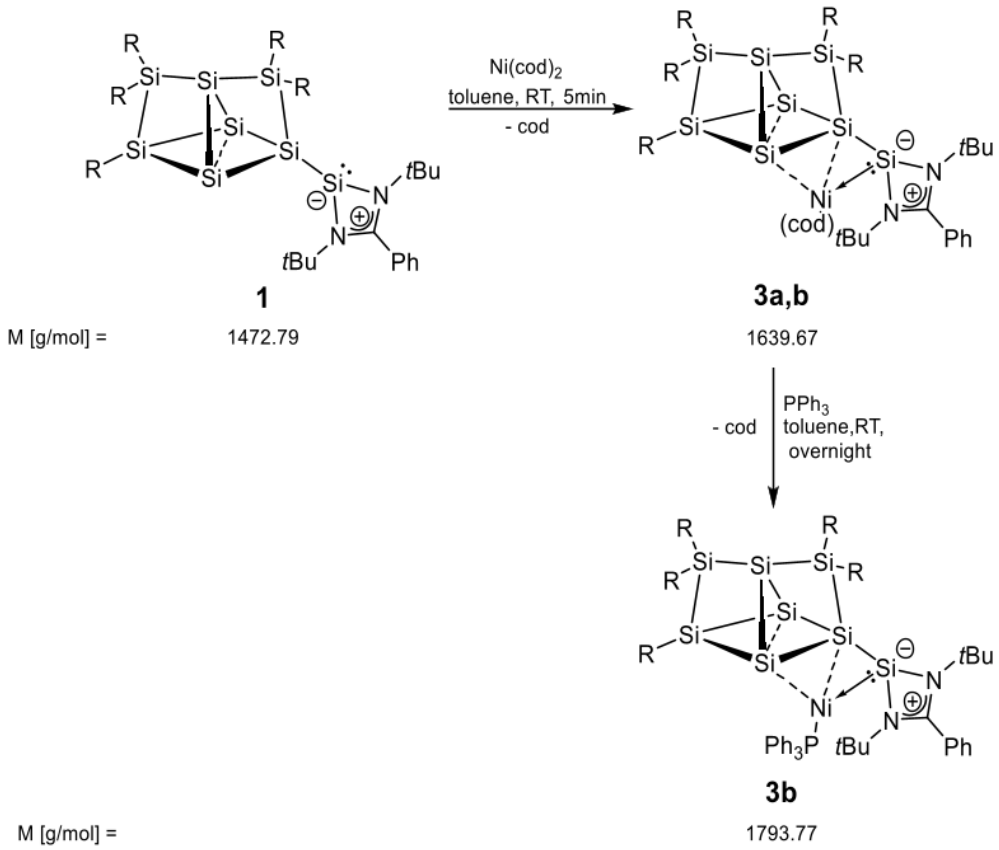

Siliconoid/silylene hybrid **1**[4] is dissolved in toluene and the transition metal precursor is added either without (1) or with additional triphenylphosphine (2). All volatiles are removed under reduced pressure. The dark purple residue is taken up in pentane and separated from the precipitating LiCl salt by filtration. After washing 3x with 1 mL pentane, the desired product crystallizes from the concentrated mother liquor at −26°C.

2.2.1 Ni(cod) siliconoid/silylene complex 3a

Quantities: 1[4] 256.0 mg (0.174 mmol, 1.0 eq.), 2.5 mL toluene, bis(cycloocta-1,5-diene) nickel 55.0 mg (0.200 mmol, 1.1 eq.) let stir for 30min at ambient temperature, filtered from 5 mL pentane, washed residue with 3x 1mL pentane, removed solvent in vacuo, dissolved in 0.15 mL toluene and 0.4 mL pentane, stored at −30°C. Yield: 131.9 mg (0.174 mmol; 46 %) blackberry-red crystals of **3a** from pentane at −26°C.

^{1}H NMR (300.13 MHz, C_6D_6, 300 K) δ = 7.472 (d, $^4J_{HH}$ = 1.18 Hz, 1H, ArC-*H*), 7.420 (d, $^4J_{HH}$ = 1.27 Hz, 1H, ArC-*H*), 7.304 – 7.279 (m, 1H, ArC-*H*), 7.221 (d, $^4J_{HH}$ = 1.27 Hz, 1H, ArC-*H*), 7.135 (m, 2H, ArC-*H* overlapping with toluene), 7.115 (m, 1H, ArC-*H*), 7.069 – 7.00 (m, 2H, ArC-*H*, overlapping with toluene), 6.922 – 6.901 (m, 2H, ArC-*H*), 6. 857 (d, $^4J_{HH}$ = 1.27 Hz, 1H, ArC-*H*), 6.830 – 6.818 (m, 3H, ArC-*H*), 5.835 – 5.799 (bm, 1H, Tip-C*H*(CH_3)$_2$), 5.539 (dsept, $^2J_{HH}$ = 20.55 Hz, $^3J_{HH}$ = 6.58 Hz, 2H, Tip-C*H*(CH_3)$_2$),

5.229 (sept, $^3J_{HH}$ = 6.63 Hz, 1H, Tip-C*H*(CH_3)$_2$), 4.929 (sept, $^3J_{HH}$ = 6.46 Hz, 1H, Tip-C*H*(CH_3)$_2$), 4.683 – 4.643 (bm, 1H, Tip-C*H*(CH_3)$_2$), 4.460 (sept, $^3J_{HH}$ = 6.43 Hz, 1H, Tip-C*H*(CH_3)$_2$), 4.142 – 4.112 (bm, 1H, Tip-C*H*(CH_3)$_2$), 3.934 (sept, $^3J_{HH}$ = 6.43 Hz, 1H, Tip-C*H*(CH_3)$_2$), 3-615 – 3.515 (m, 3H, Tip-CH(C*H*$_3$)$_2$), 3.3987 (sept, $^3J_{HH}$ = 6.28 Hz, 1H, Tip-C*H*(CH_3)$_2$), 3.217 (sept, $^3J_{HH}$ = 6.28 Hz, 1H, Tip-C*H*(CH_3)$_2$), 2.947 (qd, $^3J_{HH}$ = 6.98 Hz, 3.07 Hz, 3H, cod(C*H*) overlapping with Tip-C*H*(CH_3)$_2$), 2.768 – 2.700 (m, 3H, Tip-CH(C*H*$_3$)$_2$), 2.660 (d, $^3J_{HH}$ = 6.41 Hz, 4H, Tip-CH(C*H*$_3$)$_2$), 2.619 – 2.551 (m, 3H, Tip-CH(C*H*$_3$)$_2$), 2.409 (d, $^3J_{HH}$ = 6.48 Hz, 3H, Tip-CH(C*H*$_3$)$_2$), 2.113 (s, 2H, Tip-CH(C*H*$_3$)$_2$ overlapping with toluene), 2.066 – 1.969 (m, 2H, cod(C*H*)), 1.783 (d, $^3J_{HH}$ = 6.42 Hz, 3H, Tip-CH(C*H*$_3$)$_2$), 1.623 (d, $^3J_{HH}$ = 6.61 Hz, 6H, Tip-CH(C*H*$_3$)$_2$), 1.574 (d, $^3J_{HH}$ = 6.61 Hz, 9H, Tip-CH(C*H*$_3$)$_2$), 1.477 (d, $^3J_{HH}$ = 6.62 Hz, 6H, Tip-CH(C*H*$_3$)$_2$), 1.435 – 1.395 (m, 12H, Tip-CH(C*H*$_3$)$_2$ overlapping with cod(C*H*$_2$)), 1.328 (d, $^4J_{HH}$ = 1.94Hz, 6H, Tip-CH(C*H*$_3$)$_2$), 1.269 (s, 9H, Si(N(C(C*H*$_3$)$_3$))$_2$CPh), 1.224 (d, $^4J_{HH}$ = 2.43 Hz, 3H, Tip-CH(C*H*$_3$)$_2$), 1.200 (d, $^4J_{HH}$ = 2.43 Hz, 3H, Tip-CH(C*H*$_3$)$_2$), 1.772 (d, $^4J_{HH}$ = 2.52 Hz, 3H, Tip-CH(C*H*$_3$)$_2$), 1.154 (d, $^4J_{HH}$ = 6.94 Hz, 3H, Tip-CH(C*H*$_3$)$_2$), 1.394 (dd, $^3J_{HH}$ = 6.90 Hz, 1.08 Hz, 6H, Tip-CH(C*H*$_3$)$_2$), 0.792 (d, $^4J_{HH}$ = 6.58 Hz, 3H, Tip-CH(C*H*$_3$)$_2$), 0.646 (t, $^3J_{HH}$ = 7.33 Hz, 9H, Tip-CH(C*H*$_3$)$_2$), 0.570 – 0.549 (m, 3H, Tip-CH(C*H*$_3$)$_2$), 0.538 (s, 9H, Si(N(C(C*H*$_3$)$_3$))$_2$CPh), 0.393 (d, $^3J_{HH}$ = 6.18 Hz, 3H, Tip-CH(C*H*$_3$)$_2$) ppm.

^{13}C{^{1}H} NMR (75.47 MHz, C_6D_6, 300 K) δ = 162.22 (s, 1C, Ar-*C*), 156.09, 155.60, 155.20, 154.09, 153.29, 153.15, 153.07, 152.99, 152.83, 149.56, 149.28, 148.88, 148.74, 148.69, 140.93, 139.62, 138.77, 138.32, 137.69, 132.97 (s, each 1C, Ar-*C*), 129.99, 129.85, 129.31, 129.27, 128.50, 128.41, 126.00 (s, each 1C, Ar-*C*H), 125.63 (s, 1C, Ar-*C*), 123.67 (s, each 1C, Ar-*C*H), 123.32 (m, 1C, Ar-*C*H), 122.80, 122.34, 122.21, 121.68, 121.38, 120.53, (s, each 1C, Ar-*C*H), 89.64, 86.65 (s, each 2C, COD-*C*H), 54.70, 53.64 (s, each 1C, Si(N(*C*(CH_3)$_3$))$_2$CPh), 36.39, 36.15, 35.81, 35.47, 35.08, 35.01, 34.71, 34.67, 34.62, 34.58, 34.40, 34.01, 33.15 (s, each 1C, Tip-*i*Pr-*C*H), 32.85, 32.22 (s, each 3C, Si(N(*C*(CH_3)$_3$))$_2$CPh), 30.81 (s, 4C, COD-*C*H$_2$), 29.39, 28.65 (s, each 1C, Tip-*i*Pr-*C*H), 28.10, 28.03, 27.55, 27.51, 27.39, 27.06, 27.03, 26.86, 26.82, 26.75, 26.69, 26.58, 26.45, 26.40, 26.33, 26.02, 25.97, 25.26, 25.13, 25.00, 24.40, 24.38, 24.36, 24.17, 24.11, 24.08, 24.04, 24.01, 23.98, 23.78 (s, each 1C, Tip-*i*Pr-*C*H_3) ppm.

^{29}Si{^{1}H} NMR (59.63 MHz, C_6D_6, 300 K) δ = 89.1 (s, Ni*Si*(N(C(CH_3)$_3$))$_2$CPh), 50.0 (s, *Si*Tip), 39.0 (s, *Si*Tip$_2$), −10.2 (s, *Si*(Si(N*t*Bu)$_2$CPh)), −13.3 (s, *Si*Tip$_2$), −83.1 (s, *Si* unsubstituted), −154.0 (s, *Si*Ni), −340.7 (s, *Si* unsubstituted) ppm.

CP-MAS ^{29}Si{^{1}H} NMR (79.53 MHz, 10 KHz, 300 K) δ = 86.4 (s, Ni*Si*(N(C(CH_3)$_3$))$_2$CPh), 55.3 (s, *Si*Tip), 37.5 (s, *Si*Tip$_2$), 0.4 (s, *Si*(Si(N*t*Bu)$_2$CPh)), −16.2 (s, *Si*Tip$_2$), −85.1 (s, *Si* unsubstituted), −159.1 (s, *Si*Ni), −332.9 (s, *Si* unsubstituted) ppm.

Elemental analysis: calculated for $C_{98}H_{150}N_2NiSi_8$: C: 71.79%; H: 9.22%; N: 1.71%. Found: C: 71.67%; H: 8.75%; N: 1.64%. The lower values compared to those calculated are quite common for unsaturated silicon clusters due to incomplete combustion typically attributed to the formation of silicon carbides and/or nitrides. In addition, elemental analysis has come under scrutiny because of highly variable results of bona fide identical samples.[5]

5. Supporting Information

UV-Vis (hexane): λ_{max} (ε) = 538 (8190 M^{-1} cm^{-1}), 392 (9590 M^{-1} cm^{-1}) nm.

Melting Point: 185°C decomposition, 193 – 206°C melting.

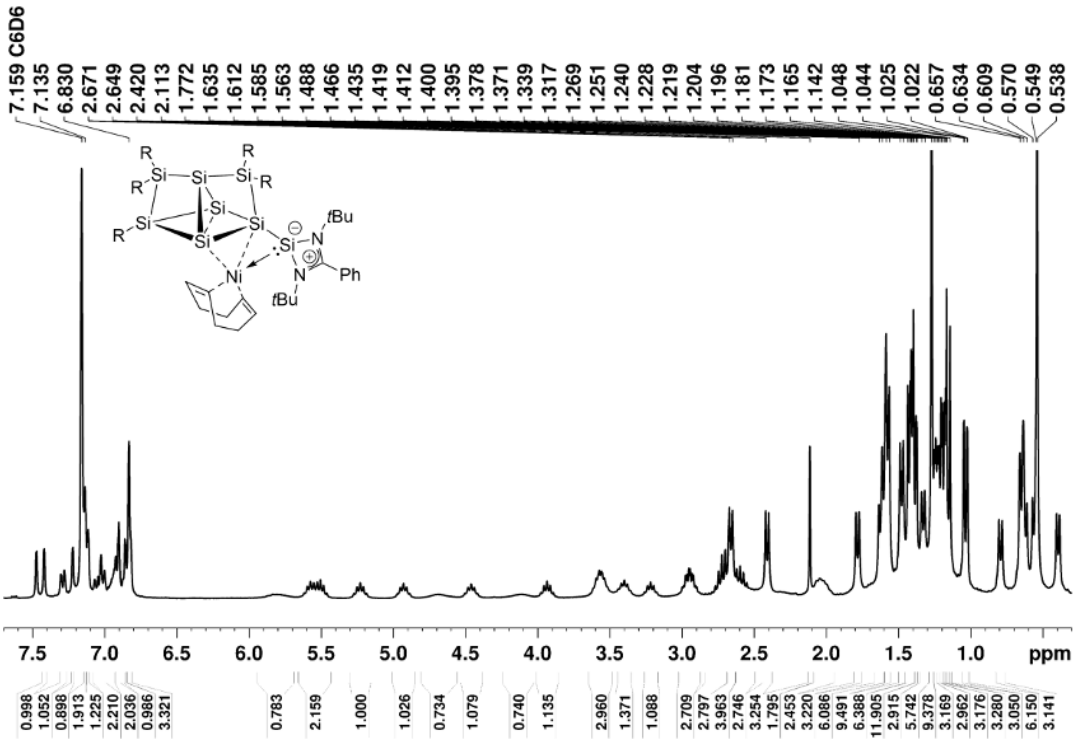

Supplementary Figure S9. ^{1}H NMR spectrum of Ni(cod) siliconoid/silylene complex **3a** in C_6D_6 (300.13 MHz, 300 K).

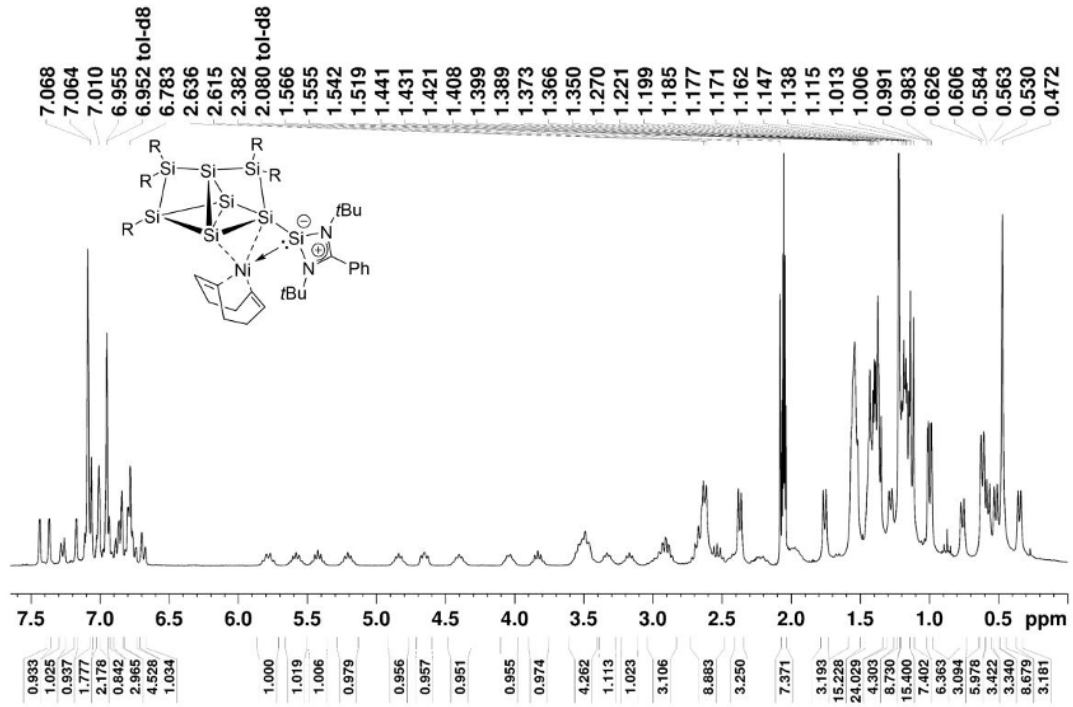

Supplementary Figure S10. ^{1}H NMR spectrum of Ni(cod) siliconoid/silylene complex **3a** in toluene-d_8 (300.13 MHz, 253 K).

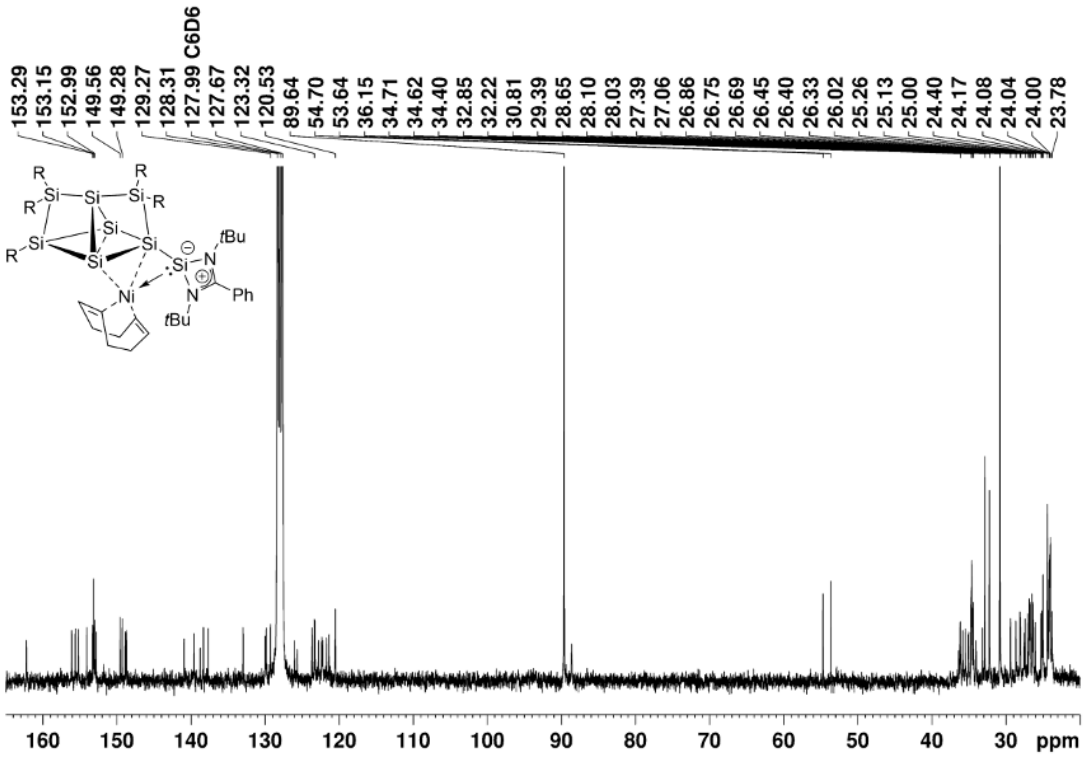

Supplementary Figure S11. $^{13}C\{^{1}H\}$ NMR spectrum of Ni(cod) siliconoid/silylene complex **3a** in C_6D_6 (75.47 MHz, 300 K).

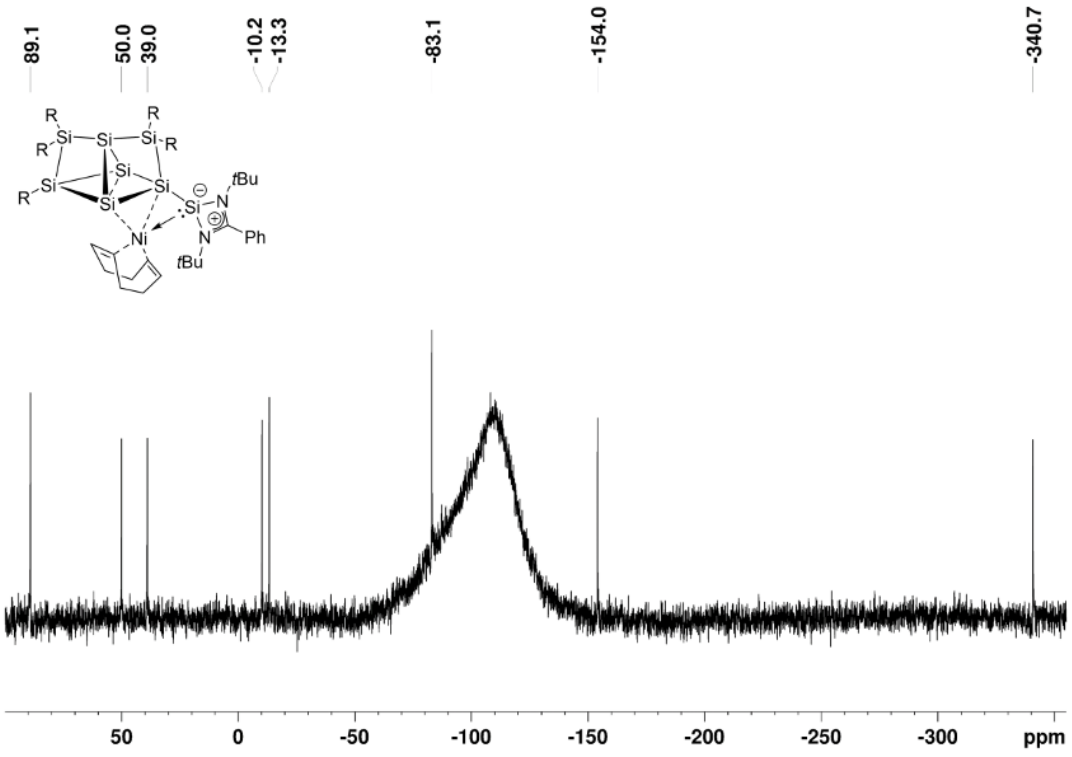

Supplementary Figure S12. $^{29}Si\{^{1}H\}$ NMR spectrum of Ni(cod) siliconoid/silylene complex **3a** in C_6D_6 (59.63 MHz, 300 K).

5. Supporting Information

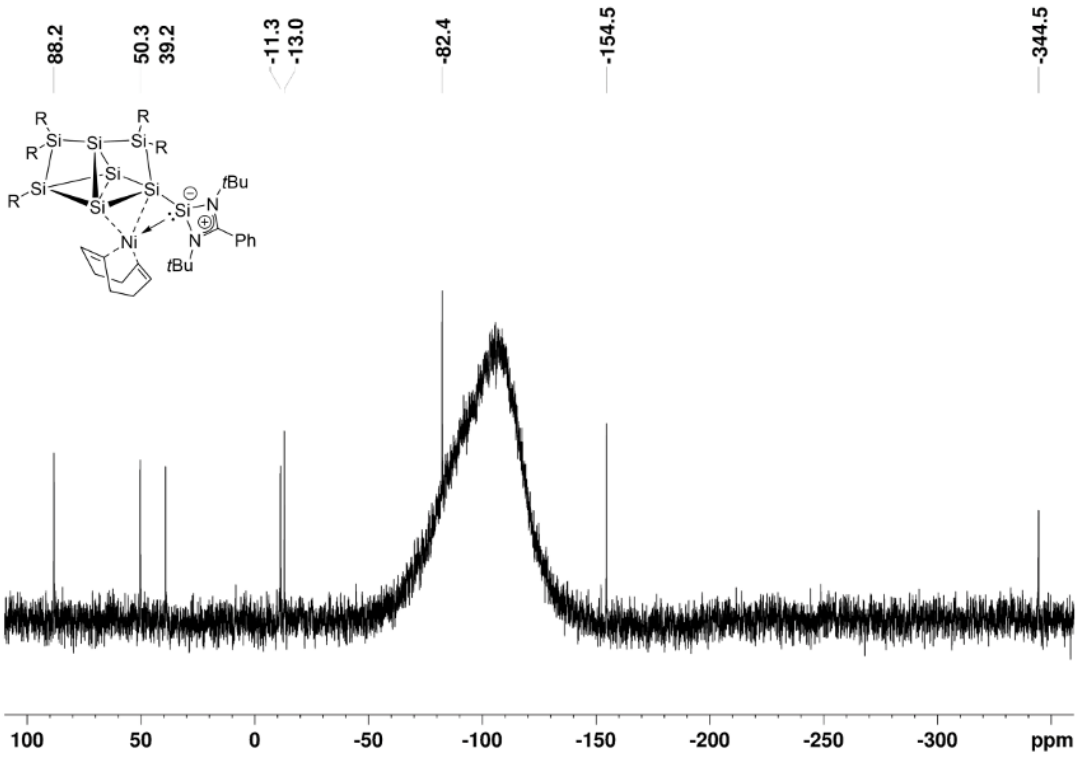

Supplementary Figure S13. $^{29}Si\{^{1}H\}$ NMR spectrum of Ni(cod) siliconoid/silylene complex **3a** in toluene-d_8 (59.63 MHz, 223 K).

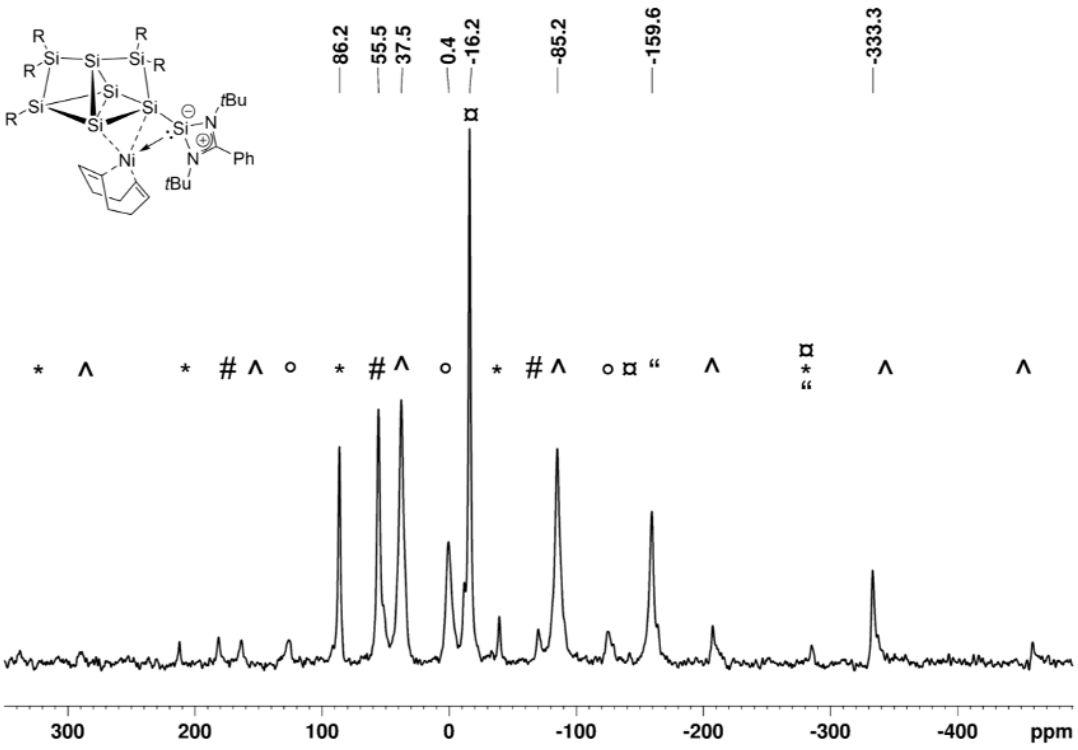

Supplementary Figure S14. CP-MAS $^{29}Si\{^{1}H\}$ NMR spectrum of Ni(cod) siliconoid/silylene complex (79.53 MHz, 10 KHz, 300 K), side spinning bands: *86.2, 55.5, ^ 37.5/ −85.2/ −333.3, ° 0.4, ¤ −16.2, “ −159.6 ppm.

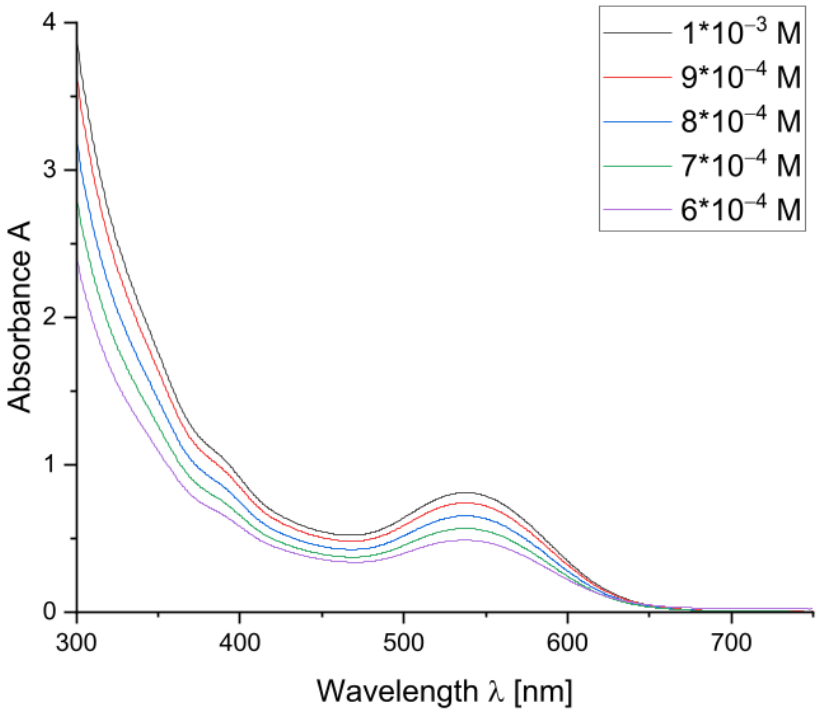

Supplementary Figure S15. UV-Vis spectra of Ni(cod) siliconoid/silylene complex **3a** in hexane at different concentrations.

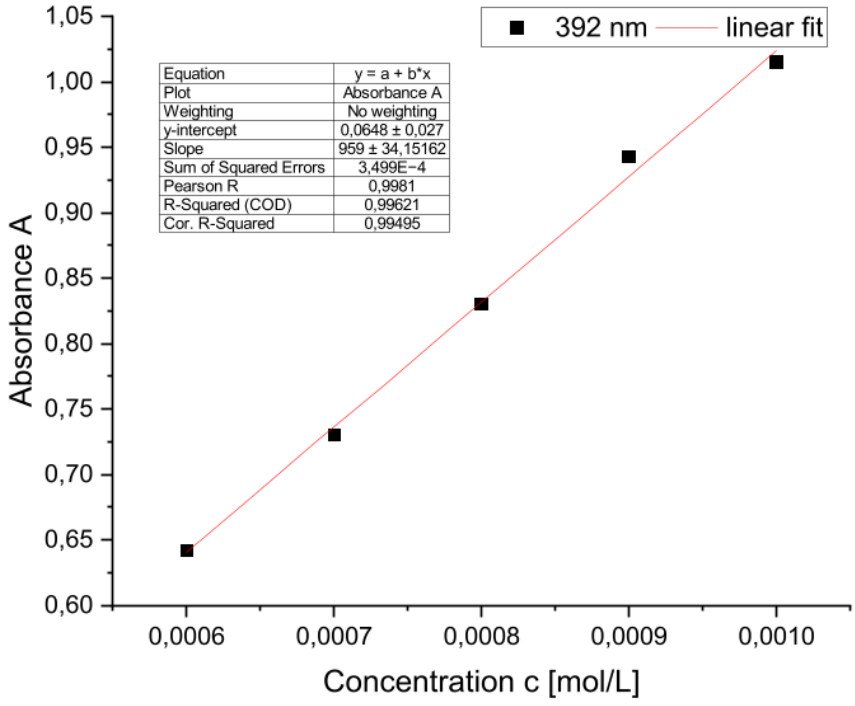

Supplementary Figure S16. Determination of the extinction ε = 9590 M^{-1} cm^{-1} of **3a** by linear regression at λ = 392 nm.

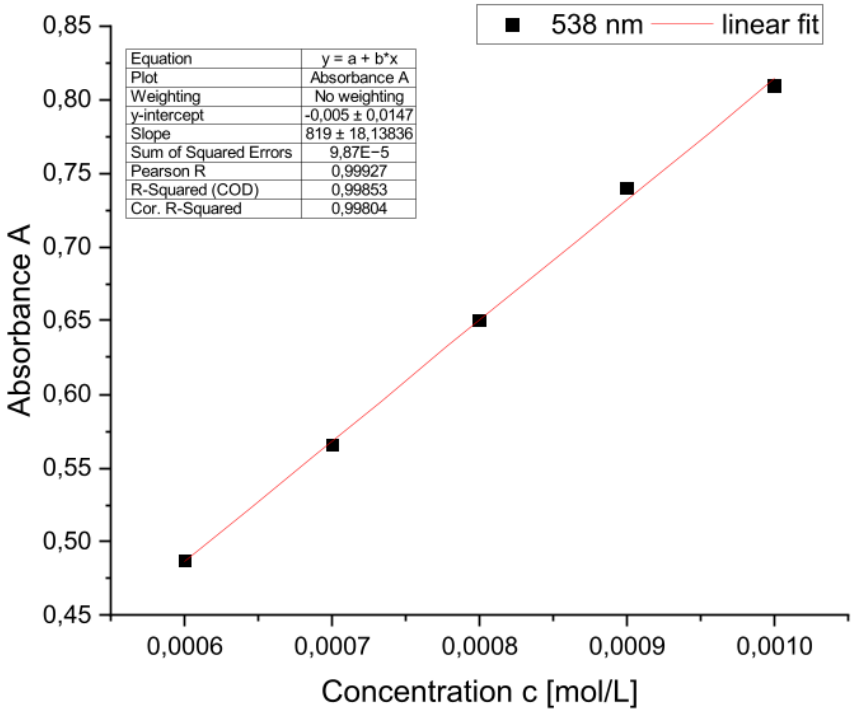

Supplementary Figure S17. Determination of the extinction ε = 8190 M^{-1} cm^{-1} of **3a** by linear regression at λ_{max} = 538 nm.

2.2.2 Preparation of Ni(PPh$_3$) siliconoid/silylene complex 3b

Quantities: 1[4] 150.0 mg (0.0928 mmol, 1.0 eq.), 2.0 mL toluene, 29.3 mg bis(cycloocta-1,5-diene) nickel (0.107 mmol, 1.2 eq), triphenylphosphine 36.4 mg (0.103 mmol, 1.1 eq), let stir overnight at RT, filtered from 4 mL pentane, washed residue with 3x 0.5mL pentane. Yield: 82.1 mg (0.0458 mmol, 49 %) brown crystals of **3b** from pentane at −26°C.

^{1}H NMR (300.13 MHz, C_6D_6, 300 K) δ = 7.830 (t, $^3J_{HH}$ = 8.81 Hz, 6H, P(ArC-*H*)), 7.424 (dd, $^3J_{HH}$ = 4.41 Hz, 1.54 Hz, 2H, P(ArC-*H*)), 7.230 – 7.198 (m, 2H, ArC-*H*), 7.100 – 7.083 (m, 4H, ArC-*H*), 7.057 – 7.018 (m, 4H, ArC-*H*), 6.992 (d, $^4J_{HH}$ = 1.74 Hz, 2H, ArC-*H*), 6.966 – 6.927 (m, 6H, ArC-*H*), 6.903 – 6.868 (m, 3H, ArC-*H*), 6. 851 (d, $^4J_{HH}$ = 1.45 Hz, 1H, ArC-*H*), 6.652 (sept, 1H, Tip-C*H*(CH$_3$)$_2$), 5.576 – 5.500 (m, 2H, Tip-C*H*(CH$_3$)$_2$), 5.144 (sept, d, $^3J_{HH}$ = 6.51 Hz, 1H, Tip-C*H*(CH$_3$)$_2$), 4.350 (sept, d, $^3J_{HH}$ = 6.60 Hz, 1H, Tip-C*H*(CH$_3$)$_2$), 3.547 (sept, $^3J_{HH}$ = 6.41 Hz, 1H, Tip-C*H*(CH$_3$)$_2$), 3.481 – 3.366 (m, 3H, Tip-C*H*(CH$_3$)$_2$), 3.162 (sept, $^3J_{HH}$ = 6.41 Hz, 1H, Tip-C*H*(CH$_3$)$_2$), 2.924 (dsept, $^2J_{HH}$ = 21.54 Hz, $^3J_{HH}$ = 6.93 Hz, 2H, Tip-C*H*(CH$_3$)$_2$), 2.819 – 2.693 (m, 2H, Tip-C*H*(CH$_3$)$_2$), 2.623 (sept, $^3J_{HH}$ = 6.88 Hz, 1H, Tip-C*H*(CH$_3$)$_2$), 2.502 (d, $^3J_{HH}$ = 6.47 Hz, 3H, Tip-CH(C*H*$_3$)$_2$), 2.5240 (d, $^3J_{HH}$ = 6.47 Hz, 3H, Tip-CH(C*H*$_3$)$_2$), 1.718 (d, $^3J_{HH}$ = 6.31 Hz, 3H, Tip-CH(C*H*$_3$)$_2$), 1.680 (d, $^3J_{HH}$ = 6.58 Hz, 3H, Tip-CH(C*H*$_3$)$_2$), 1.620 – 1.576 (m, 9H, Tip-CH(C*H*$_3$)$_2$), 1.509 (d, $^3J_{HH}$ = 6.61 Hz, 3H, Tip-CH(C*H*$_3$)$_2$), 1.452 – 1.400 (m, 15H, Tip-CH(C*H*$_3$)$_2$), 1.315 (t, $^3J_{HH}$ = 6.59 Hz, 7H, Tip-CH(C*H*$_3$)$_2$), 1.257 (d, $^4J_{HH}$ = 2.66 Hz, 3H, Tip-CH(C*H*$_3$)$_2$), 1.234 (d, $^4J_{HH}$ = 2.53

Hz, 3H, Tip-CH(CH_3)$_2$), 1.218 (d, $^4J_{HH}$ = 2.15 Hz, 3H, Tip-CH(CH_3)$_2$), 1.195 (d, $^4J_{HH}$ = 2.10 Hz, 3H, Tip-CH(CH_3)$_2$), 1.123 – 1.057 (m, 12H, Tip-CH(CH_3)$_2$), 0.907 – 0.876 (m, 2H, Tip-CH(CH_3)$_2$), 0.849 (s, 9H, Si(N(C(CH_3)$_3$))$_2$CPh), 0.801 (d, $^4J_{HH}$ = 6.77 Hz, 3H, Tip-CH(CH_3)$_2$), 0.775 (s, 9H, Si(N(C(CH_3)$_3$))$_2$CPh), 0.715 (d, $^4J_{HH}$ = 6.51 Hz, 3H, Tip-CH(CH_3)$_2$), 0.551 (d, $^3J_{HH}$ = 6.26 Hz, 3H, Tip-CH(CH_3)$_2$), 0.518 (d, $^3J_{HH}$ = 6.50 Hz, 3H, Tip-CH(CH_3)$_2$), 0.476 (d, $^3J_{HH}$ = 6.36 Hz, 3H, Tip-CH(CH_3)$_2$), 0.403 (d, $^3J_{HH}$ = 6.22 Hz, 3H, Tip-CH(CH_3)$_2$) ppm.

^{13}C{^{1}H} NMR (100.61 MHz, C_6D_6, 300 K) δ = 161.13 (s, Si(N(C(CH$_3$)$_3$))$_2$*C*Ph), 156.46, 155.47, 153.95, 153.90, 153.58, 153.48, 153.38, 153.24, 153.11, 152.92, 149.42, 149.23, 149.06, 148.66, 148.50, 141.11, 140.38, 139.38, 138.53, 138.04 (s, each 1C, Ar-*C*), 134.35 (d, $^2J_{C-P}$ = 13.9 Hz, 15C, P(Ar-*C*H)), 134.07 (d, $^2J_{C-P}$ = 14.6 Hz, 3C, P(Ar-*C*)), 133.01 (s, each 1C, Ar-*C*), 130 .06, 129.66, 129.25, 129.03, 128.38, 128.30 (s, each 1C, Ar-C*H*), 128.11, 127.87 (s, each 1C, Ar-*C*), 127.60, 126.01, 123.52 (s, each 1C, Ar-*C*H), 123.05 (s, 5C, P(Ar-*C*H)), 122.40 (d, ^4J = 5.09 Hz, Ar-*C*H), 121.86, 121.66, 121.52, 120.61 (s, each 1C, Ar-*C*H), 54.90, 53.43 (s, each 1C, Si(N(*C*(CH$_3$)$_3$))$_2$CPh), 35.95, 35.80 (s, each 1C, Tip-*C*H(CH$_3$)$_2$, 35.68 (s, 2C, Tip-*C*H(CH$_3$)$_2$), 35.53, 35.40, 35.29, 35.14, 34.77, 34.67 (s, each 1C, Tip-*C*H(CH$_3$)$_2$), 34.60 (s, 2C, Tip-*C*H(CH$_3$)$_2$, 34.54 (s, each 1C, Tip-*C*H(CH$_3$)$_2$), 34.39 (s, pentane), 34.31, 32.81 (s, each 1C, Tip-*C*H(CH$_3$)$_2$), 32.56, 32.20 (s, each 3C, Si(N(C(*C*H$_3$)$_3$))$_2$CPh), 32.11, 31.62, 31.41, 30.53, 29.12, 28.93, 28.45, 28.42, 27.88, 27.69, 27.55, 26.38, 25.92, 25.75 (s, each 1C, Tip-CH(*C*H$_3$)$_2$), 25.04 (s, 2C, Tip-CH(*C*H$_3$)$_2$), 24.87, 24.72, 24.54 (s, each 1C, Tip-CH(*C*H$_3$)$_2$), 24.48, 24.29, 24.24 (s, each 2C, Tip-CH(*C*H$_3$)$_2$), 24.14, 24.06, 24.03, 23.69, 23.33 (s, each 1C, Tip-CH(*C*H$_3$)$_2$), 22.68, 14.25 (s, pentane) ppm.
^{31}P{^{1}H} NMR (126.98 MHz, C_6D_6, 300 K) δ = 26.4 (s, 1P, Ni*P*(Ph)$_3$) ppm.

^{29}Si{^{1}H} NMR (79.49 MHz, C_6D_6, 300 K) δ = 73.6 (d, $^3J_{Si-P}$ = 4.67 Hz, *Si*(N*t*Bu)$_2$CPh), 63.9 (d, $^3J_{Si-P}$ = 9.06 Hz, *Si*Tip), 39.7 (s, *Si*Tip$_2$), 0.4 (d, $^3J_{Si-P}$ = 3.45 Hz, *Si*(Si(N*t*Bu)$_2$CPh), −41.4 (d, $^3J_{Si-P}$ = 11.84 Hz, *Si*Tip$_2$), −60.0 (d, $^3J_{Si-P}$ = 5.64 Hz, *Si*), −87.3 (d, $^3J_{Si-P}$ = 8.77 Hz, *Si*Ni), −287.6 (d, $^2J_{Si-P}$ = 27.84 Hz, *Si*) ppm.

CP-MAS ^{29}Si{^{1}H}-NMR (79.53 MHz, 13 KHz, 300 K) δ = 72.7 (s, Ni*Si*(N(C(CH$_3$)$_3$))$_2$CPh), 69.0 (s, *Si*Tip), 37.6 (s, *Si*Tip$_2$), −5.9 (s, $^3J_{Si-P}$ = 3.45 Hz, *Si*(Si(N(C(CH$_3$)$_3$))$_2$CPh)), −44.7 (s, *Si*Tip$_2$), −68.0 (s, *Si* unsubstituted), −82.8 (s, *Si*Ni), −279.6 (s, *Si* unsubstituted) ppm.

Elemental analysis: calculated for $C_{108}H_{153}N_2NiPSi_7$: C: 72.32%; H: 8.60%; N: 1.56%. Found: C: 67.11 %; H: 8.06%; N: 1.88%. The lower values compared to those calculated are quite common for unsaturated silicon clusters due to incomplete combustion typically attributed to the formation of silicon carbides and/or nitrides. In addition, elemental analysis has come under scrutiny because of highly variable results of bona fide identical samples.[5]

UV-Vis (hexane): λ_{max} (ε) = 365 (1879 M^{-1} cm^{-1}), 519 (1127 M^{-1} cm^{-1}), 596 (624 M^{-1} cm^{-1}) nm.

Melting Point: 187 – 191°C (melting, decomposition).

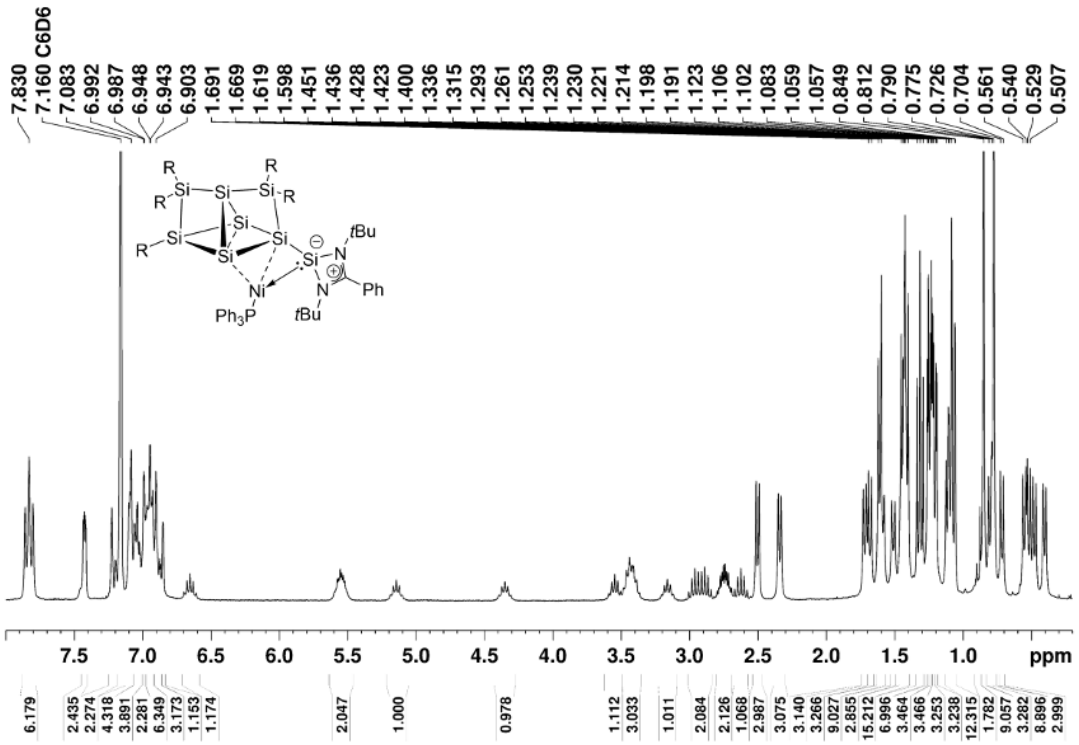

Supplementary Figure S18. ^{1}H NMR spectrum of Ni(PPh_3) siliconoid/silylene complex **3b** in C_6D_6 (300.13 MHz, 300 K).

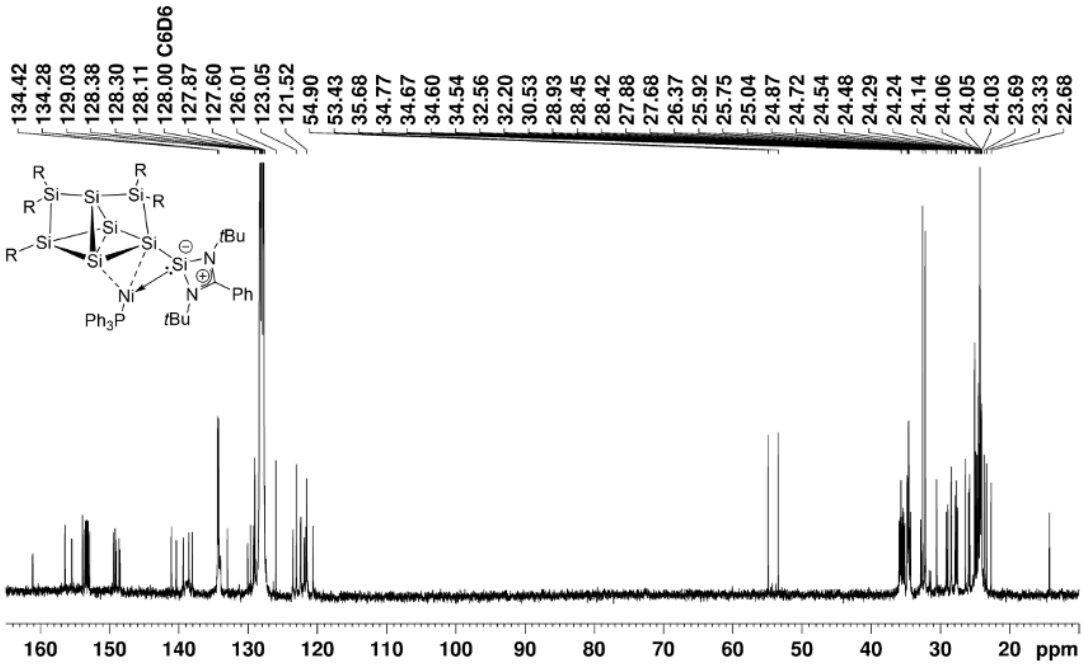

Supplementary Figure S19. $^{13}C\{^{1}H\}$ NMR spectrum of Ni(PPh_3) siliconoid/silylene complex **3b** in C_6D_6 (100.61 MHz, 300 K).

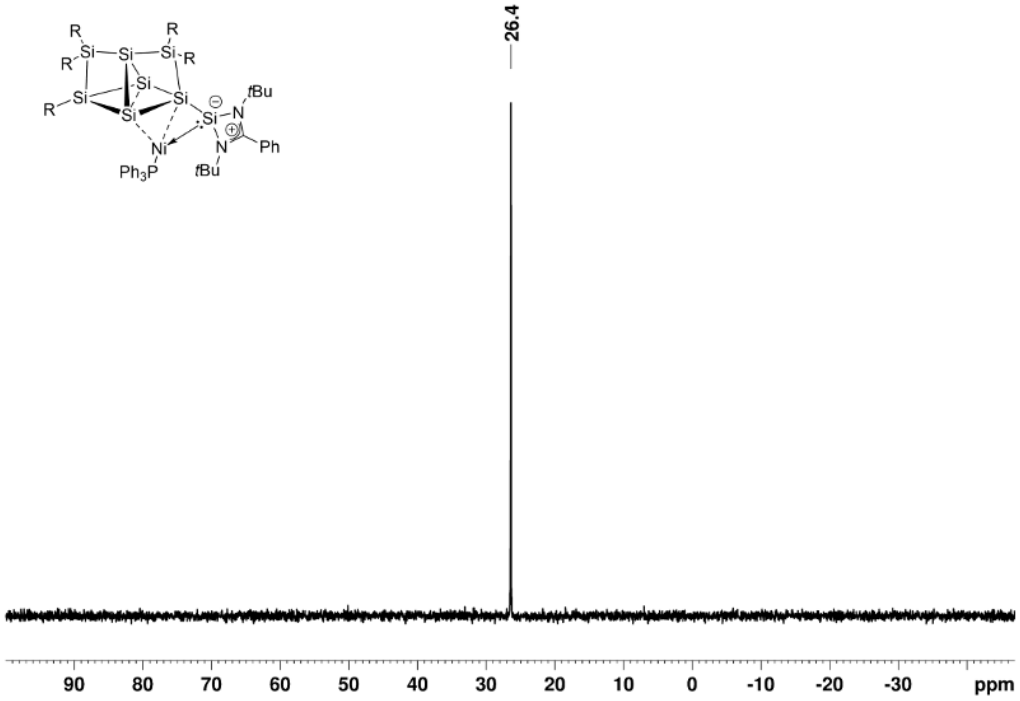

Supplementary Figure S20.$^{31}P\{^{1}H\}$ NMR spectrum of Ni(PPh_3) siliconoid/silylene complex **3b** in C_6D_6 (161.98 MHz, 300 K).

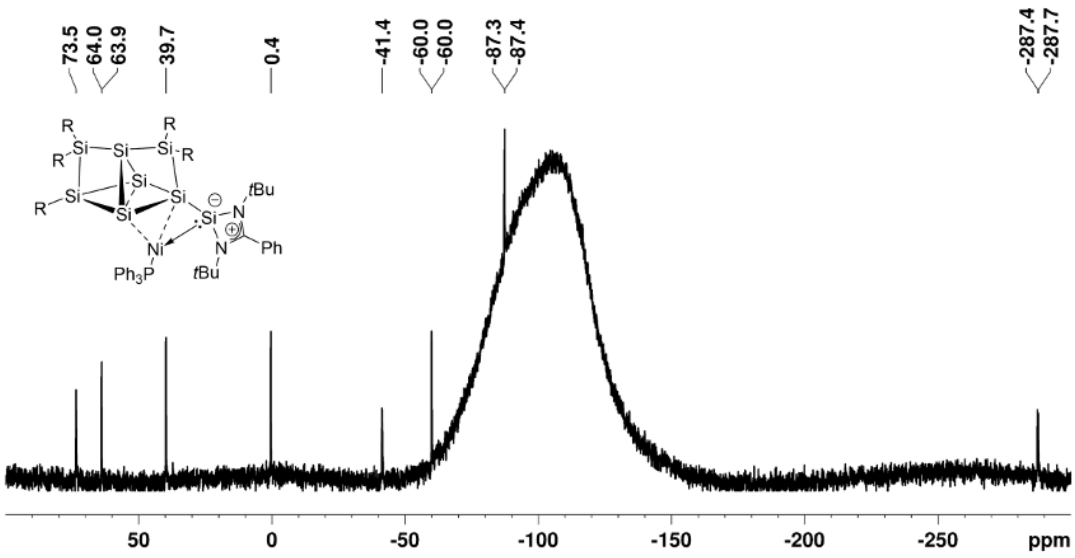

Supplementary Figure S21. $^{29}Si\{^{1}H\}$ NMR spectrum of Ni(PPh_3) siliconoid/silylene complex **3b** in C_6D_6 (79.49 MHz, 300 K).

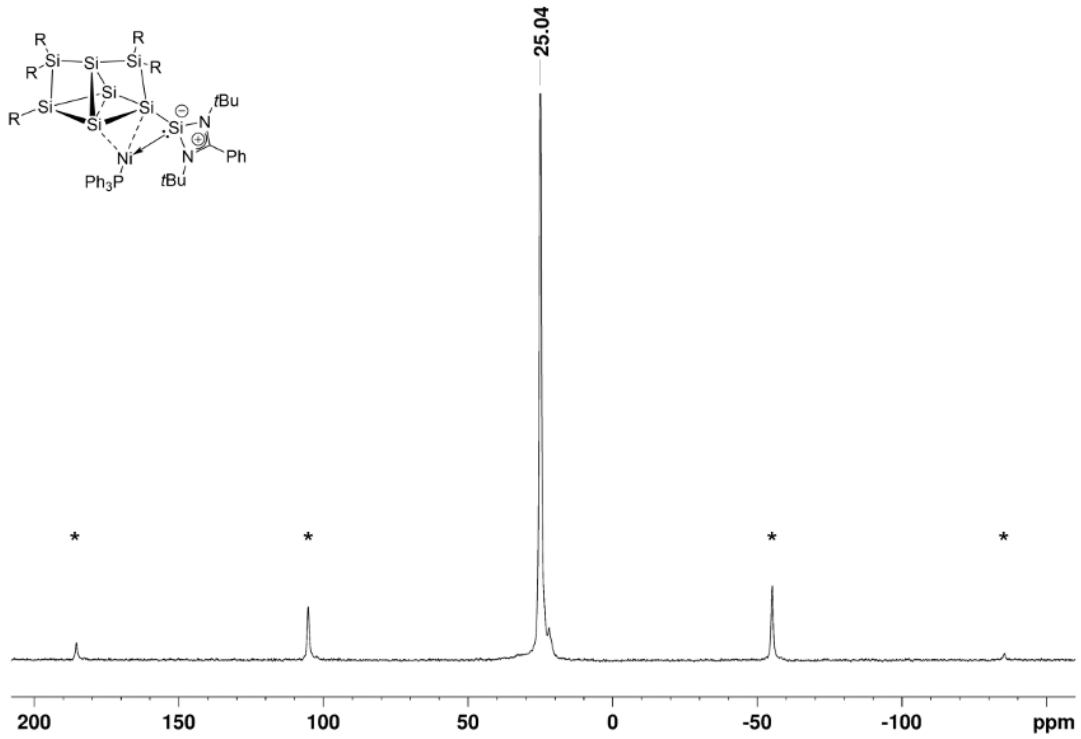

Supplementary Figure S22. CP-MAS $^{31}P\{^{1}H\}$ NMR spectrum of Ni(PPh_3) siliconoid/silylene complex **3b** (162.04 MHz, 13 KHz, 300 K), * side spinning bands.

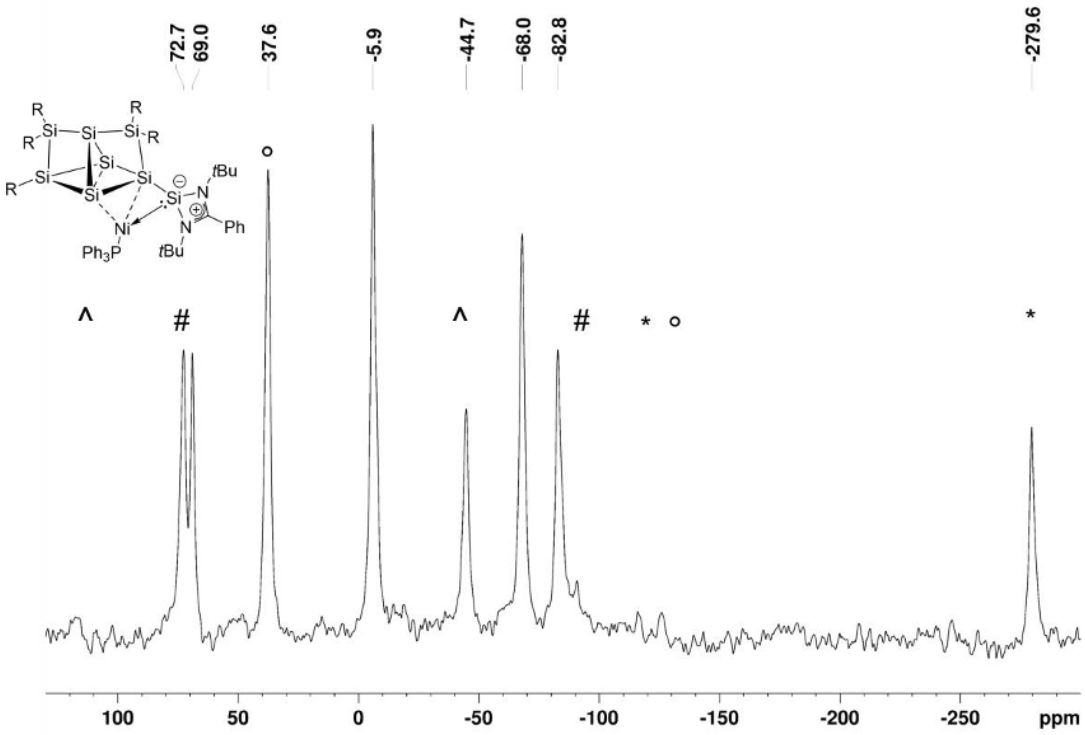

Supplementary Figure S23. CP-MAS $^{29}Si\{^{1}H\}$ NMR spectrum of Ni(PPh_3) siliconoid/silylene complex **3b** (79.53 MHz, 13 KHz, 300 K), side spinning bands # 72.7, ° 37.6, ^ −44.7, * −279.6 ppm.

5. Supporting Information

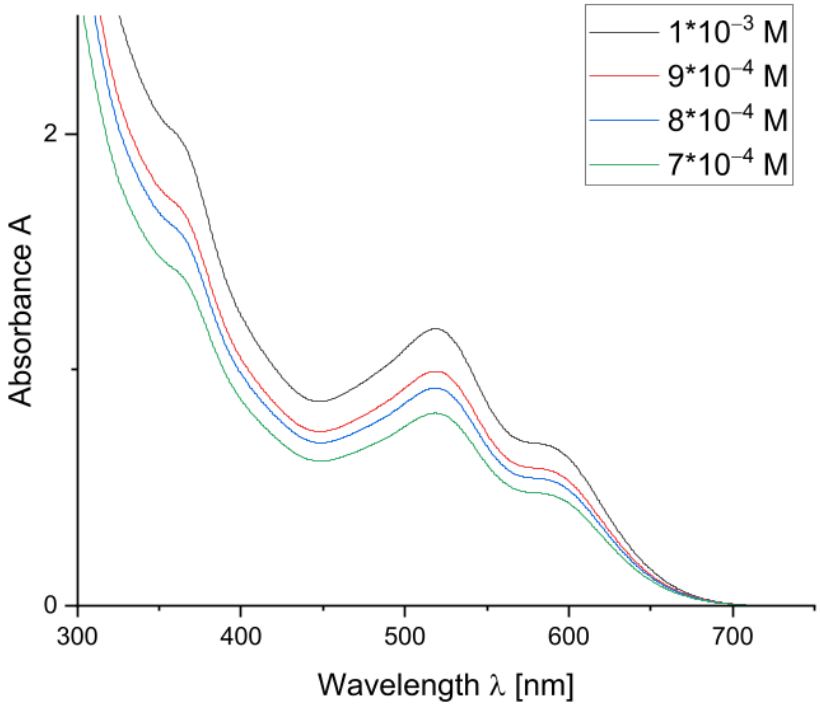

Supplementary Figure S24. UV-Vis spectra of Ni(PPh_3) siliconoid/silylene complex **3b** in hexane at different concentrations.

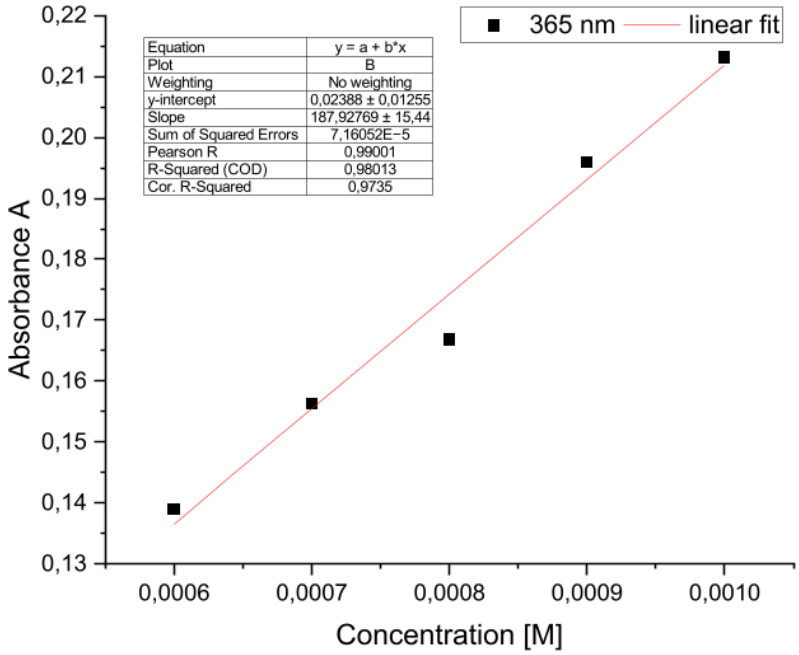

Supplementary Figure S25. Determination of the extinction ε = 1879 M^{-1} cm^{-1} of **3b** by linear regression at λ = 365 nm.

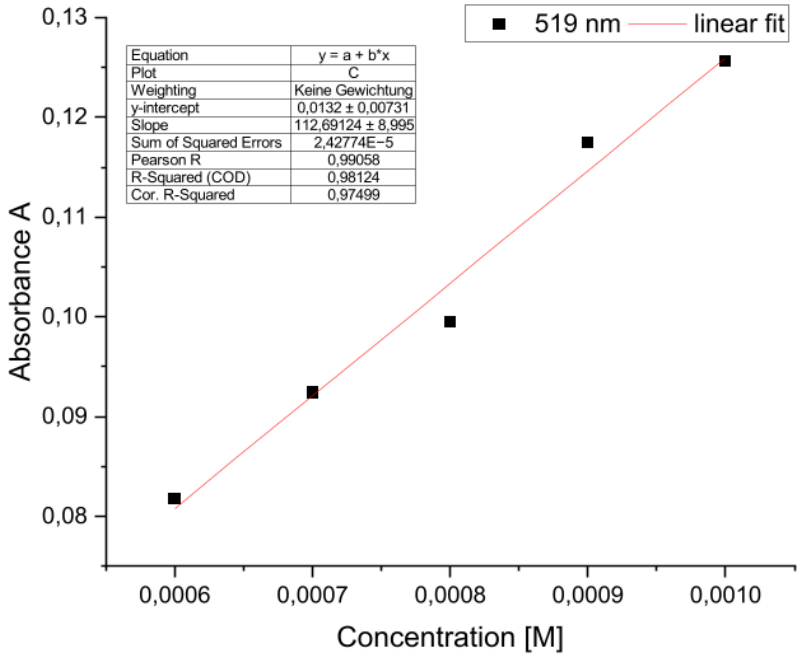

Supplementary Figure S26. Determination of the extinction ε = 1127 M^{-1} cm^{-1} of **3b** by linear regression at λ = 519 nm.

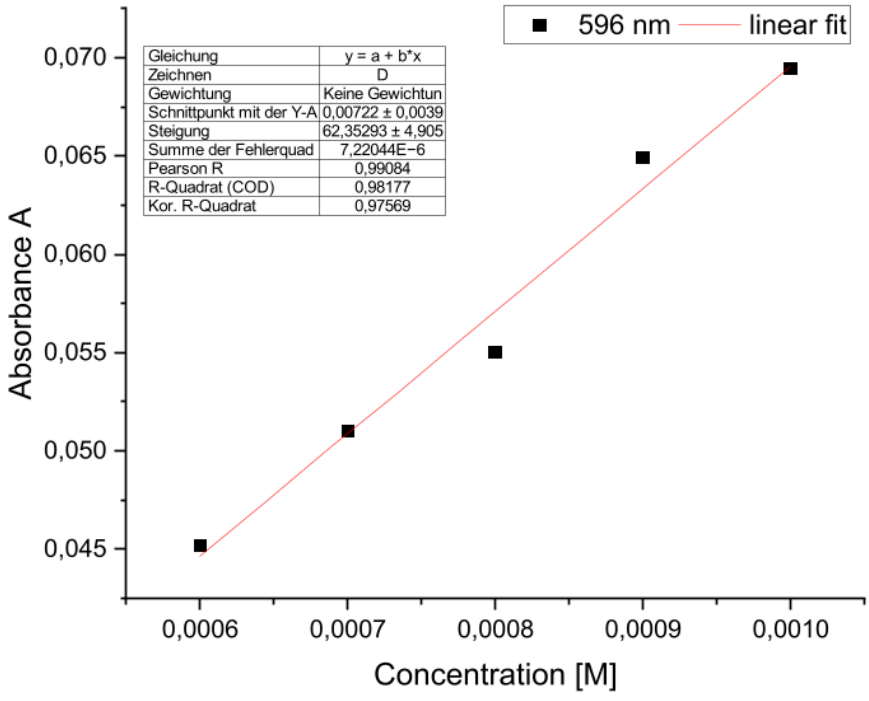

Supplementary Figure S27. Determination of the extinction ε = 624 M^{-1} cm^{-1} of **3b** by linear regression at λ_{max} = 596 nm.

2.3 Preparation of $Ni(CO)_2$ siliconoid/silylene complex 3c

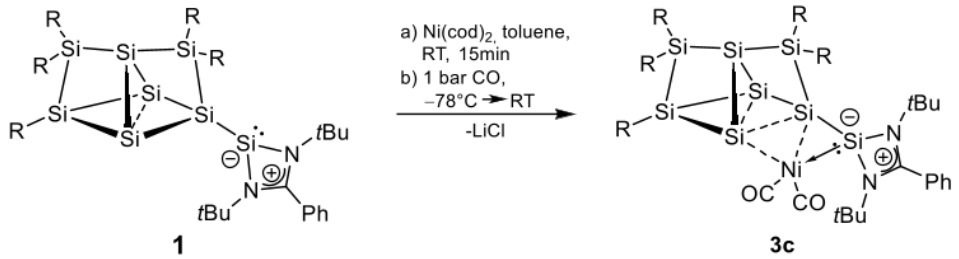

M [g/mol] = 1472.79 1587.50

1[4] (100 mg, 0.0638 mmol, 1.0 eq) was dissolved in 1.4 mL toluene and solid bis(cycloocta-1,5-diene) nickel (19.7 mg, 0.0701mmol, 1.1 eq) was added. The reaction mixture was stirred for 15 minutes at ambient temperature, then cooled to −80°C for 5 minutes and 1 bar CO gas was bubbled through under maintained Argon gas flow until the colour change to "blood red" was completed (no traces of blackberry red visible). The solvent and all volatiles were removed in vacuo and the product was extracted from 0.6 mL pentane. The residue was washed with 3 x 0.5 mL pentane. Red crystals of **3c** (121.5 mg, 0.1261 mmol, 44 %) were obtained from a concentrated solution in pentane at −70°C after five days.

^{1}H NMR (400.13 MHz, C_6D_6, 300 K) δ = 7.629 (q, C_8H_{10}), 7.7.450 (d, $^4J_{HH}$ = 1.58 Hz, 1H, Ar-*H*), 7.398 (d, $^4J_{HH}$ = 1.58 Hz, 1H, Ar-*H*), 7.251 (q, C_8H_{10}), 7.197 (d, $^4J_{HH}$ = 1.69 Hz, 1H, Ar-*H*), 7.190 – 7.171 (m, 2H, Ar-*H*), 7.137 (d, $^4J_{HH}$ = 1.67 Hz, 1H, Ar-*H*), 7.092 – 7.080 (m, 2H, Ar-*H*), 6.994 (d, $^4J_{HH}$ = 1.67 Hz, 1H, Ar-*H*), 6.898 (d, $^4J_{HH}$ = 1.74 Hz, 1H, Ar-*H*), 6.888 (d, $^4J_{HH}$ = 1.52 Hz, 1H, Ar-*H*), 6.872 (d, $^4J_{HH}$ = 1.52 Hz, 1H, Ar-*H*), 6.818 (d, $^4J_{HH}$ = 1.49 Hz, 1H, Ar-*H*), 6.772 – 6.695 (m, 2H, Ar-*H*), 5.672 (sept, $^3J_{HH}$ = 6.51 Hz, 1H, Tip-C*H*$(CH_3)_2$), 5.597 (sept, $^3J_{HH}$ = 6.60 Hz, 1H, Tip-C*H*$(CH_3)_2$), 5.407 (sept, $^3J_{HH}$ = 6.51 Hz, 1H, Tip-C*H*$(CH_3)_2$), 4.928 (sept, $^3J_{HH}$ = 6.60 Hz, 1H, Tip-C*H*$(CH_3)_2$), 4.346 (sept, $^3J_{HH}$ = 6.60 Hz, 1H, Tip-C*H*$(CH_3)_2$), 4.002 (sept, $^3J_{HH}$ = 6.50 Hz, 1H, Tip-C*H*$(CH_3)_2$), 3.439 (sept, $^3J_{HH}$ = 6.26 Hz, 2H, Tip-C*H*$(CH_3)_2$), 3.336 (sept, $^3J_{HH}$ = 6.42 Hz, 1H, Tip-C*H*$(CH_3)_2$), 3.217 (sept, $^3J_{HH}$ = 6.50 Hz, 1H, Tip-C*H*$(CH_3)_2$), 2.906 (sept, $^3J_{HH}$ = 6.71 Hz, 2H, Tip-C*H*$(CH_3)_2$), 2.738 – 2.655 (m, 3H, Tip-C*H*$(CH_3)_2$), 2.760 – 2.635 (sept, 1H, Tip-C*H*$(CH_3)_2$ overlapping with d, $^3J_{HH}$ = 6.58 Hz, 3H, Tip-CH(C*H*$_3)_2$), 2.381 (d, $^3J_{HH}$ = 6.49 Hz, 3H, Tip-CH(C*H*$_3)_2$), 1.743 (d, $^3J_{HH}$ = 6.63 Hz, 3H, Tip-CH(C*H*$_3)_2$), 1.676 (d, $^3J_{HH}$ = 6.63 Hz, 3H, Tip-CH(C*H*$_3)_2$), 1.632 – 1.599 (m, 14H, Tip-CH(C*H*$_3)_2$), 1.565 (d, $^3J_{HH}$ = 6.49 Hz, 3H, Tip-CH(C*H*$_3)_2$, 1.526 (d, $^3J_{HH}$ = 6.63 Hz, 3H, Tip-CH(C*H*$_3)_2$), 1.420 (d, $^3J_{HH}$ = 6.63 Hz, 3H, Tip-CH(C*H*$_3)_2$), 1.396 (d, $^3J_{HH}$ = 7.04 Hz, 6H, Tip-CH(C*H*$_3)_2$), 1.378 – 1.360 (m, 10H, Tip-CH(C*H*$_3)_2$), 1.339 (d, $^3J_{HH}$ = 3.04 Hz, 3H, Tip-CH(C*H*$_3)_2$), 1.318 – 1.3296 (m, 6H, Tip-CH(C*H*$_3)_2$), 1.182 (d, $^3J_{HH}$ = 2.21 Hz, 3H, Tip-CH(C*H*$_3)_2$), 1,165 (d, $^3J_{HH}$ = 2.21 Hz, 3H, Tip-CH(C*H*$_3)_2$), 1.150 (d, $^3J_{HH}$ = 2.21 Hz, 3H, Tip-CH(C*H*$_3)_2$), 1.133 (d, $^3J_{HH}$ = 2.21 Hz, 3H, Tip-CH(C*H*$_3)_2$), 1.124 (s, 9H, Si(N(C(C*H*$_3)_3))_2$CPh), 1.082 – 1.048 (m, 10H impurity), 0.724 (d, $^3J_{HH}$ = 6.63 Hz, 3H, Tip-CH(C*H*$_3)_2$), 0.651 (s, 9H, Si(N(C(C*H*$_3)_3))_2$CPh), 0.580 (d, $^3J_{HH}$ = 6.49 Hz, 6H, Tip-CH(C*H*$_3)_2$), 0.526 (dd, $^3J_{HH}$ = 9.53 Hz, 6.63 Hz, 6H, Tip-CH(C*H*$_3)_2$),) 0.391 (d, $^3J_{HH}$ = 6.21 Hz, 3H, Tip-CH(C*H*$_3)_2$) ppm.

$^{13}C\{^1H\}$ NMR (75.47 MHz, C_6D_6, 300 K) δ = 204.95 (s, Ni(*C*O)$_2$), 196.31 (s, Ni(*C*O)$_2$), 164.39 (s, Si(N(C(CH$_3$)$_3$))$_2$*C*Ph), 156.20, 156.09, 154.98, 153.95, 153.30, 153.13, 153.07, 152.97, 152.94, 150.03, 149.77, 149.26, 149.17, 139.88, 138.89, 138.71 (s, each 1C, Ar-*C*), 137.85 (s, toluene), 137.22, 137.10, 136.97, 134.88, 132.13 (s, each 1C, Ar-*C*), 130.40 (s, 1C, Ar-*C*H), 129.39 (s, toluene), 129.27, 128.88, 128.85, 128.75, 128.60 (s, each 1C, Ar-*C*H), 128.50, 125.63 (s, toluene), 123.35, 123.27, 123.18, 123.09, 122.27, 122.05 (s, each 1C, Ar-*C*H), 121.74 (d, ^4J-= 1.84 Hz, 1C, Ar-*C*), 121.33, 120.77 (s, each 1C, Ar-*C*H), 55.32, 54.70 (s, each 1C, Si(N(*C*(CH$_3$)$_3$))$_2$CPh), 37.42, 37.24, 26.46, 36.25, 35.67, 35.56, 35.48, 35.33, 34.69, 34.62, 34.59, 34.53 (s, each 1C, Tip-*C*H(CH$_3$)$_2$), 34.46 (s, pentane), 34.38, 34.28, 32.73 (s, each 1C, Tip-*C*H(CH$_3$)$_2$), 32.20, 31.74 (s, each 3C, Si(N(C(*C*H$_3$)$_3$))$_2$CPh), 31.38, 31.20, 29.30, 28.32, 28.23, 27.90, 27.43, 27.01, 26.78, 26.57, 26.32, 26.02, 25.69, 25.57, 25.34, 25.10, 24.78, 24.76, 24.75, 24.57, 24.39, 24.35, 24.21, 24.22, 24.18, 24.08, 24.01, 23.91, 23.82, 23.18 (s, each 1C, Tip-CH(*C*H$_3$)$_2$), 22.67 (s, pentane), 21.37 (s, toluene), 14.21 (s, pentane) ppm.

$^{29}Si\{^1H\}$ NMR (59.63 MHz, C_6D_6, 300 K) δ = 96.6 (s, Ni*Si*(N(C(CH$_3$)$_3$))$_2$CPh), 70.9 (s, *Si*Tip), 44.6 (s, *Si*Tip$_2$), −3.9 (s, *Si*Tip$_2$), −10.0 (s, *Si*(Si(N(C(CH$_3$)$_3$))$_2$CPh)), −81.9 (s, *Si* unsubstituted), −160.4 (s, *Si*Ni), −342.0 (s, *Si* unsubstituted) ppm.

Elemental analysis: calculated for $C_{94}H_{138}N_2NiO_2Si_8$: C: 69.61; H: 8.76; N: 1.76%. Found: C: 68.56 %; H: 7.96%; N: 1.29%. The lower values compared to those calculated are quite common for unsaturated silicon clusters due to incomplete combustion typically attributed to the formation of silicon carbides and/or nitrides. In addition, elemental analysis has come under scrutiny because of highly variable results of bona fide identical samples.[5]

UV-Vis (hexane): λ_{max} (ε) = 363 (12350 M^{-1} cm^{-1}), 472 (7860 M^{-1} cm^{-1}), 523 (9630 M^{-1} cm^{-1}) nm.

Solid State FT-IR $\tilde{\nu}_{CO}$ = 2015 (s), 1976 (s) cm^{-1}.

Melting Point: 107°C (decomposition), 205 – 245°C (melting).

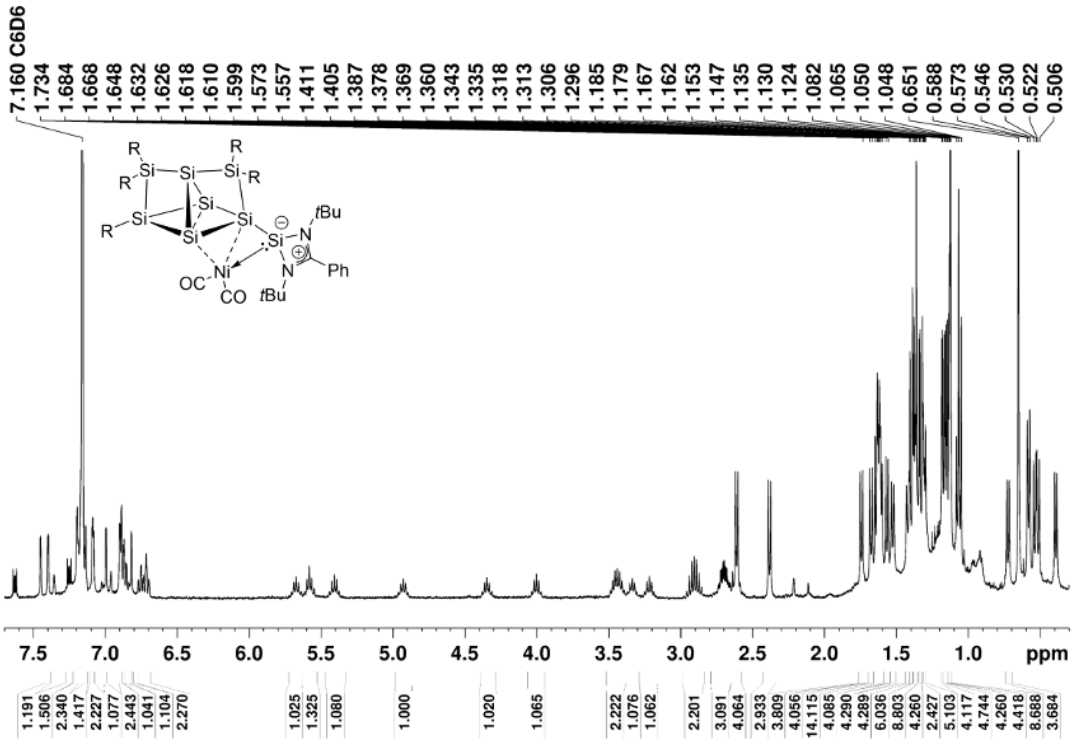

Supplementary Figure S28. ^{1}H NMR spectrum of $NiCO)_2$ siliconoid/silylene complex **3c** in C_6D_6 (400.13 MHz, 300 K).

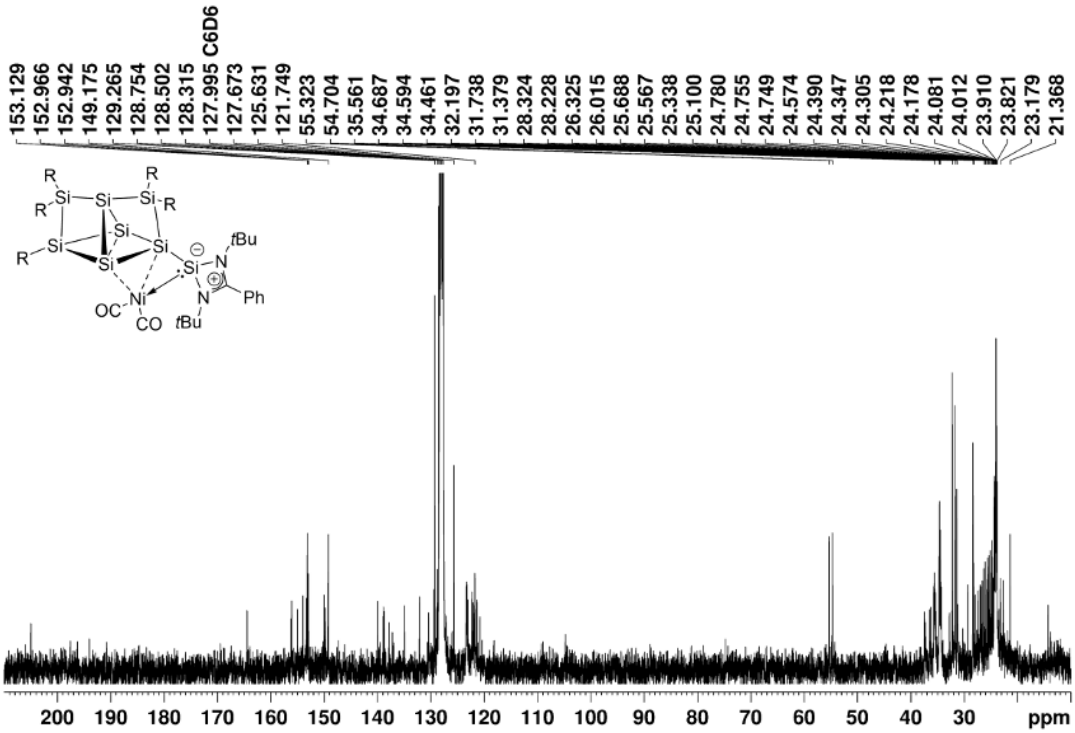

Supplementary Figure S29. ^{13}C NMR spectrum of $NiCO)_2$ siliconoid/silylene complex **3c** in C_6D_6 (75.47 MHz, 300 K).

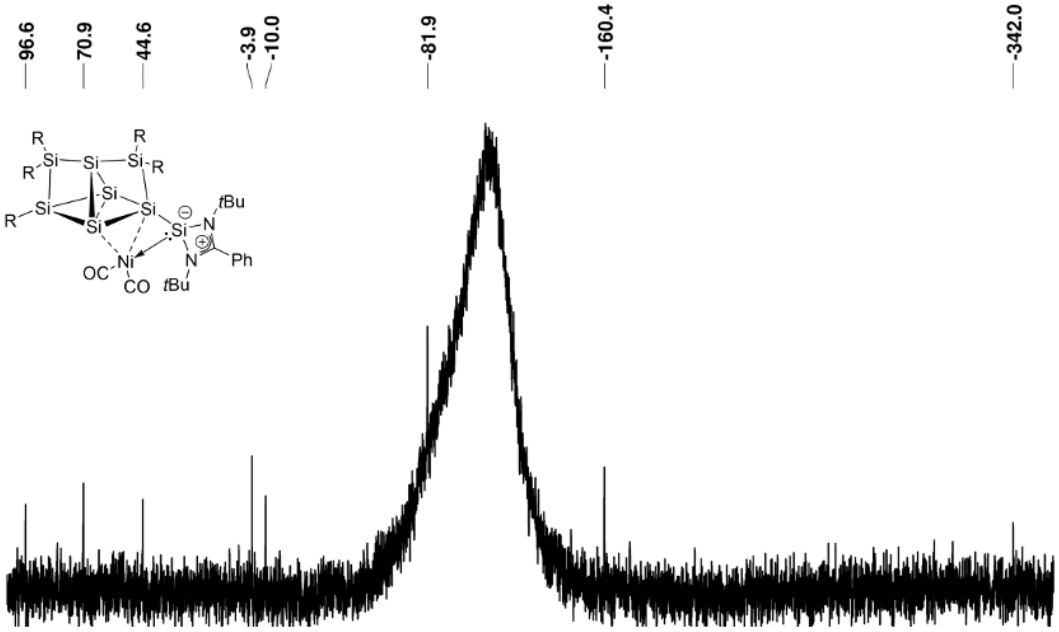

Supplementary Figure S30. ^{29}Si NMR spectrum of $NiCO)_2$ siliconoid/silylene complex **3c** in C_6D_6 (59.63 MHz, 300 K).

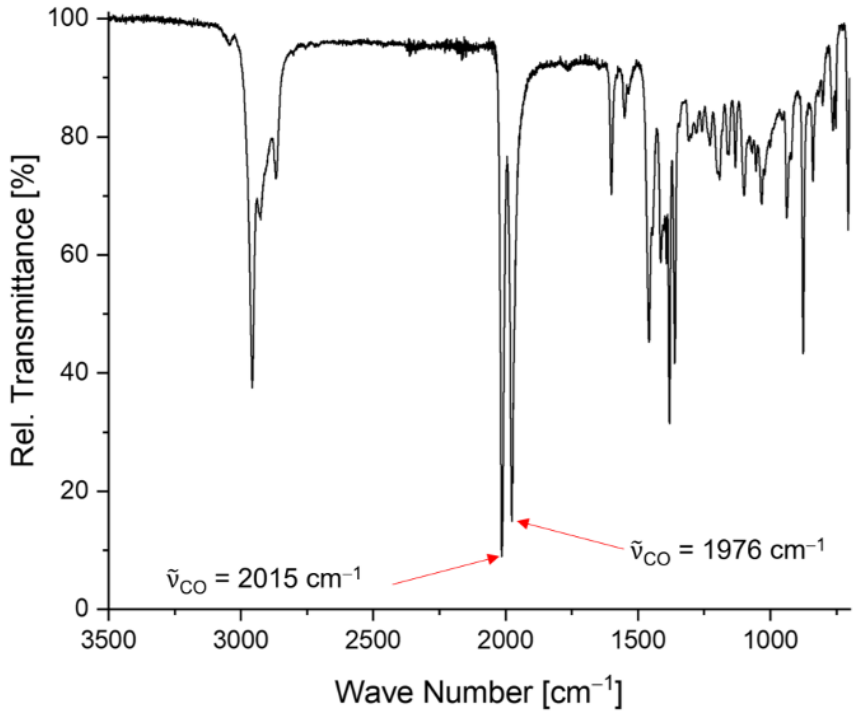

Supplementary Figure S31: FT-IR spectrum of $NiCO)_2$ siliconoid/silylene complex **3c** in the solid state.

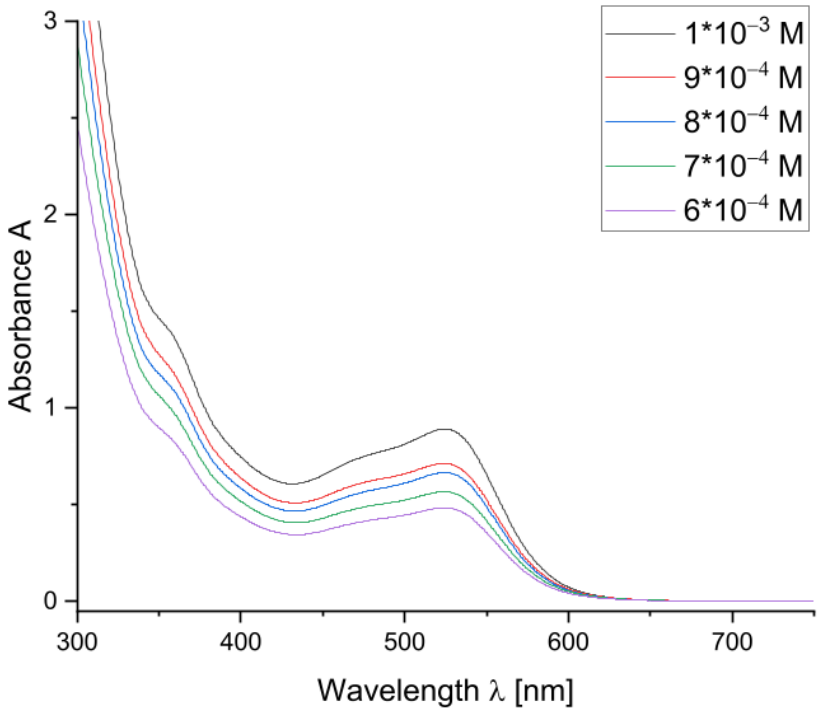

Supplementary Figure S32. UV-Vis spectra of $NiCO)_2$ siliconoid/silylene complex **3c** in hexane at different concentration

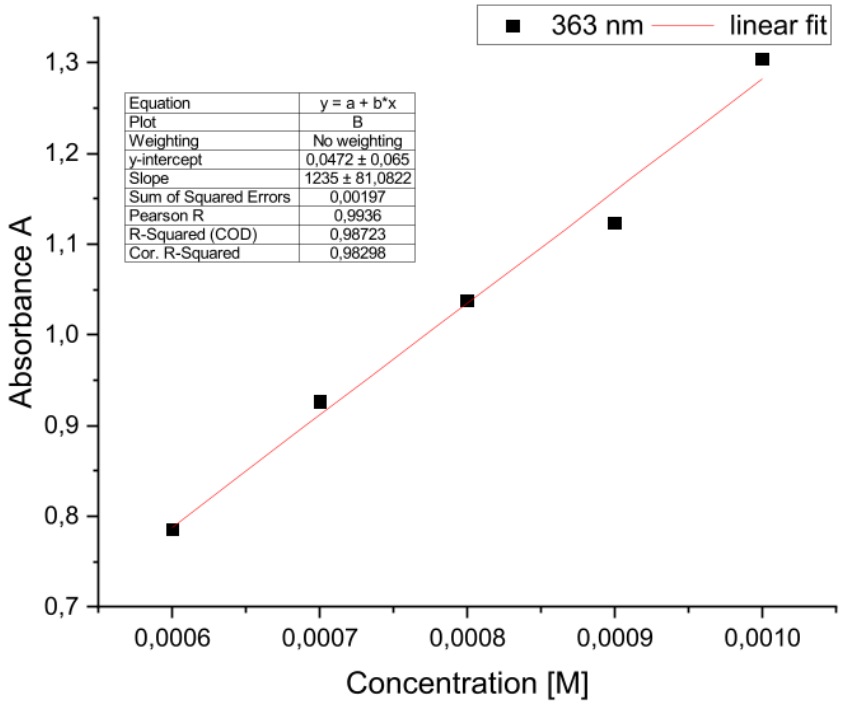

Supplementary Figure S33. Determination of the extinction ε = 12350 M^{-1} cm^{-1} of **3c** by linear regression at λ = 363 nm.

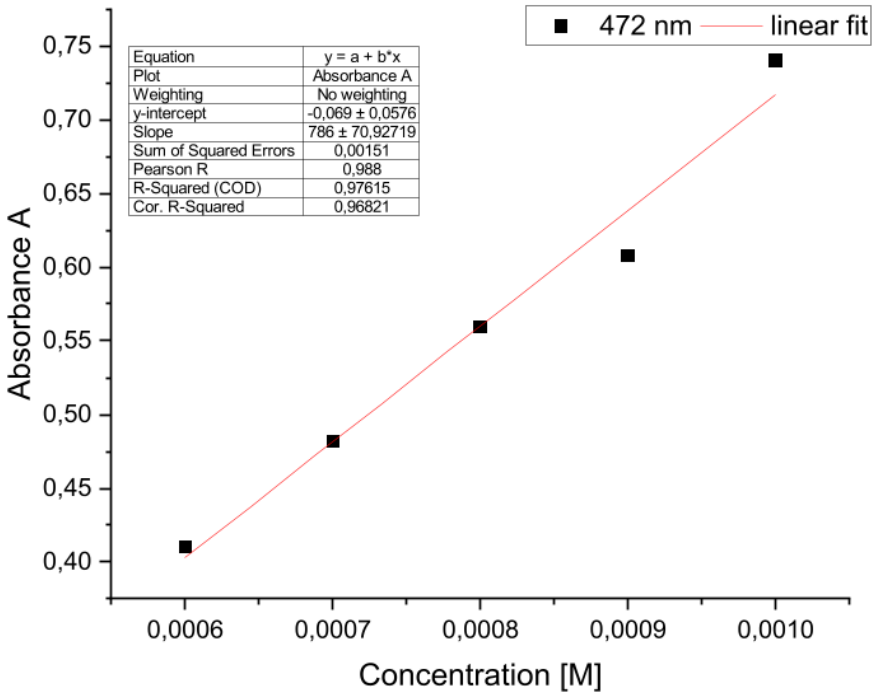

Supplementary Figure S34. Determination of the extinction ε = 7860 M^{-1} cm^{-1} of **3c** by linear regression at λ = 472 nm.

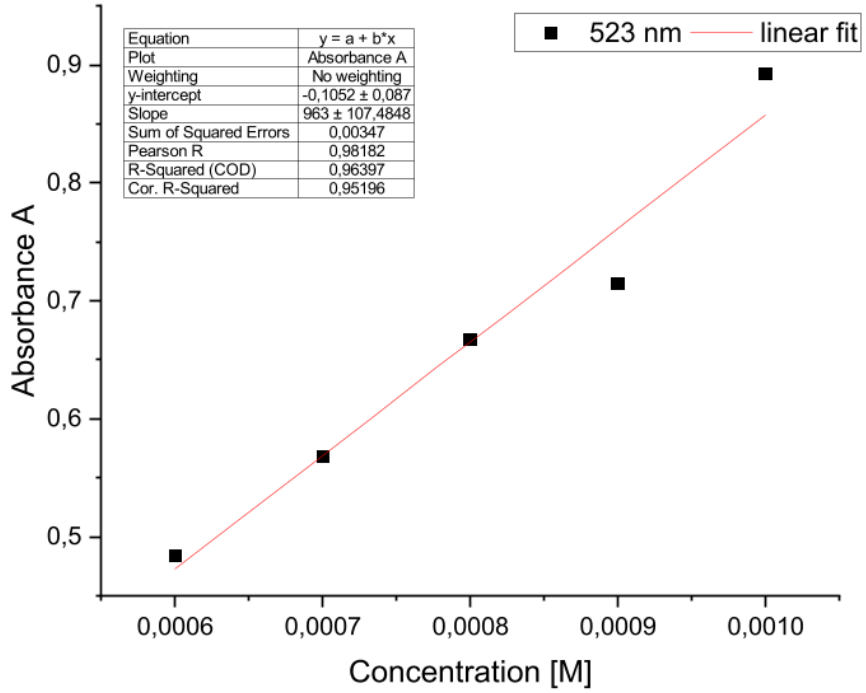

Supplementary Figure S35. Determination of the extinction ε = 9630 M^{-1} cm^{-1} of **3c** by linear regression at λ_{max} = 523 nm.

2.4 Hydrosilylation of terminal alkenes with diphenylsilane

General procedure

The substrate was dissolved in 0.1 mL C_6D_6. Diphenylsilane and mesitylene, as the internal standard, were added to the solution at ambient temperature. A reference ^{1}H NMR spectrum was recorded. A solution of the catalyst, **3a/b/c** or $Ni(cod)_2$ respectively, in 0.1 mL C_6D_6 was added to the reaction mixture. The reaction progress was monitored by ^{1}H NMR spectra until full conversion of the substrate. The conversion was determined by integration against the internal standard. The use of a slight excess of diphenylsilane (1.1 eq.) was chosen based on the complete consumption before the complete conversion of the substrate observed in preliminary, stoichiometric studies due to the dehydro-coupling side-reactions. To explore the substrate scope, stock solutions of **3a** and $Ni(cod)_2$ were prepared accordingly.

Quantities:

a) 0.5 mol%: substrate (0.6 mmol, 1.0 eq.), diphenylsilane (0.66 mmol, 1.1 eq.), mesitylene (0.30 mmol, 0.5 eq.), catalyst (0.008 mmol, 0.05 eq.)

b) 0.05 mol%: substrate (1.6 mmol, 1.0 eq.), diphenylsilane (1.76 mmol, 1.1 eq.), mesitylene (0.80 mmol, 0.5 eq.), catalyst (0.0008 mmol, 0.005 eq.)

Mercury drop test

In a glove box, a 50 mL Schlenk flask containing a stirring bar was charged with vinyltrimethylsilane (0.24 mL, 1.60 mmol, 1.0 eq.), C_6D_6 (0.1 mL), diphenylsilane (0.34 mL, 1.76 mmol, 1.1 eq.) and mesitylene (0.11 mL, 0.80 mmol, 0.5 eq.). Elemental mercury (1.68 g, 8.0 mmol, 5.0 eq) was added *via* disposable glass pipette. The addition of 0.1 mL of the corresponding stock solution of **3a** or $Ni(cod)_2$ in C_6D_6 was added with a syringe and the conversion was monitored with ^{1}H NMR spectroscopy. The mercury drop test revealed a slower reaction to **A** with an overall lower spectroscopic yield, however exhibiting a higher ratio of **A** compared to the twofold-substituted silylation product (23:6) than in the reaction without the presence of Hg (9:5), indicating that the catalyst is partially decomposed to nickel particles in the course of the reaction, which are known to be highly active but unselective in heterogenous catalysis.[6,7] In the case of $Ni(cod)_2$, the mercury drop test revealed a similar reactivity to the one without mercury (>99% conversion within 5.5 h).

Assignment

In addition to the ^{1}H NMR spectra reproduced in this present Supporting Information, the products obtained from the catalytic hydrosilylation were assigned according to the corresponding hetero nuclei and correlation NMR spectra as well as the results found in the literature.[8–13] A blank spectrum of diphenylsilane was recorded in C_6D_6 at ambient temperature.

5. Supporting Information

Ph_2SiH_2 reference spectrum:

^{1}H NMR (400.13, MHz, C_6D_6, 293 K) δ = 7.485 (m, 4H, H_{Ar}), 7.115 (m, 6H, H_{Ar} overlapping with C_6D_6), 5.068 (brs, 2H, Si-*H*) ppm.

^{13}C{^{1}H} NMR (100.61 MHz, C_6D_6, 293 K): δ = 136.00 (4C, $C_{Ar}H$), 131.62 (2C, C_{quart}), 130.11 (2C, $C_{Ar}H$), 128.44 (4C, $C_{Ar}H$) ppm.

^{29}Si{^{1}H} NMR (79.49 MHz, C_6D_6, 293 K): δ = −33.5 ppm.

^{29}Si NMR (79.49 MHz, C_6D_6, 293 K): δ = −33.5 (t, $^2J_{Si-H}$ = 21.6 Hz) ppm.

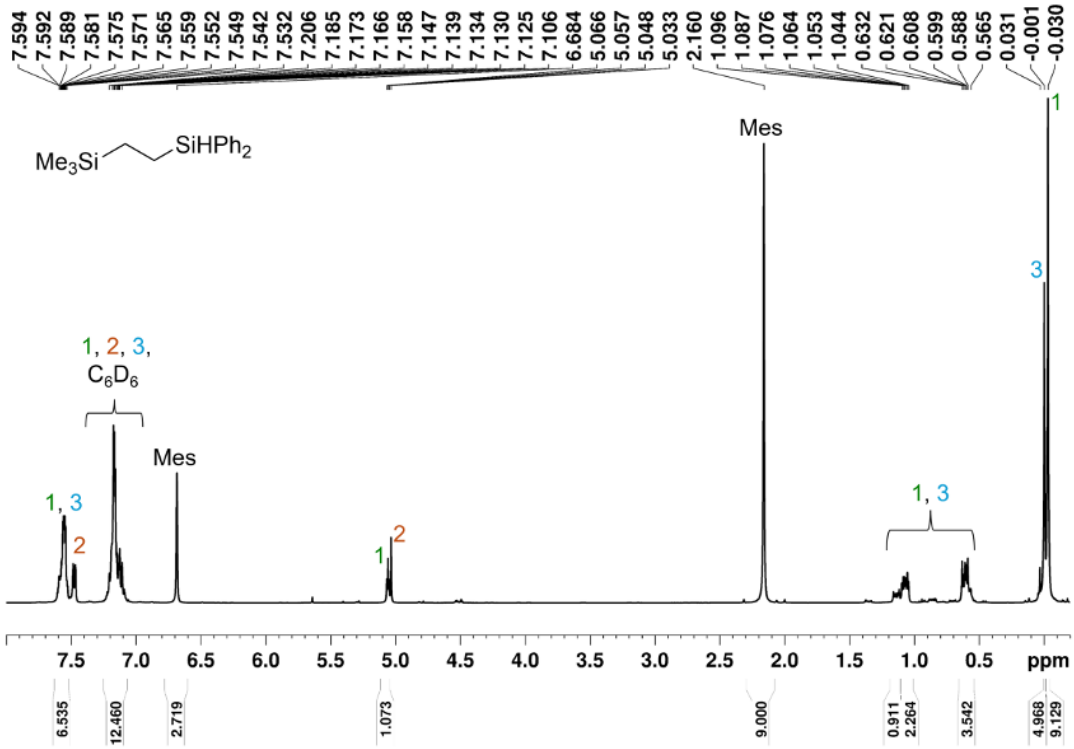

Supplementary Figure S36. ^{1}H NMR spectrum of the crude reaction mixture of the hydrosilylation of vinyltrimethylsilane and Ph_2SiH_2 catalyzed by 0.05 mol% **3a** in C_6D_6 after 8 h at 293 K. Internal standard mesitylene (Mes), 1 anti-Markovnikov product, 2 Ph_2SiH_2, 3 disubstituted product.

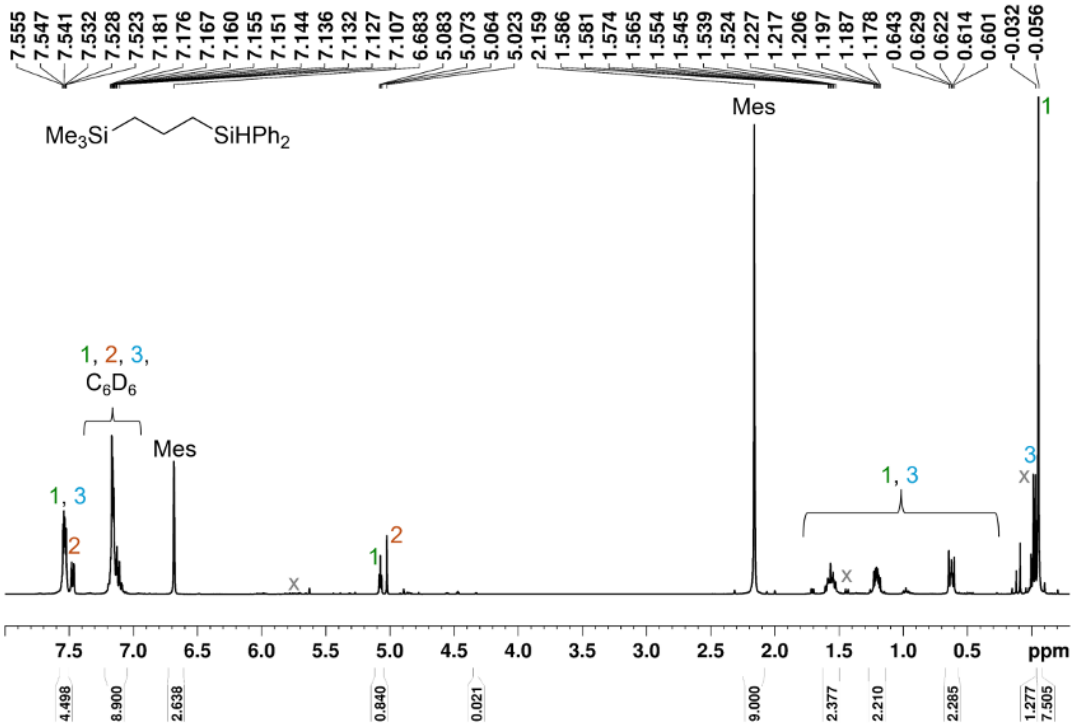

Supplementary Figure S37. ^{1}H NMR spectrum of the crude reaction mixture of the hydrosilylation of allyltrimethylsilane and Ph_2SiH_2 catalyzed by 0.05 mol% **3a** in C_6D_6 after 408 h at 293 K. Internal standard mesitylene (Mes), 1 anti-Markovnikov product, 2 Ph_2SiH_2, 3 disubstituted product, x allyltrimehtylsilane.

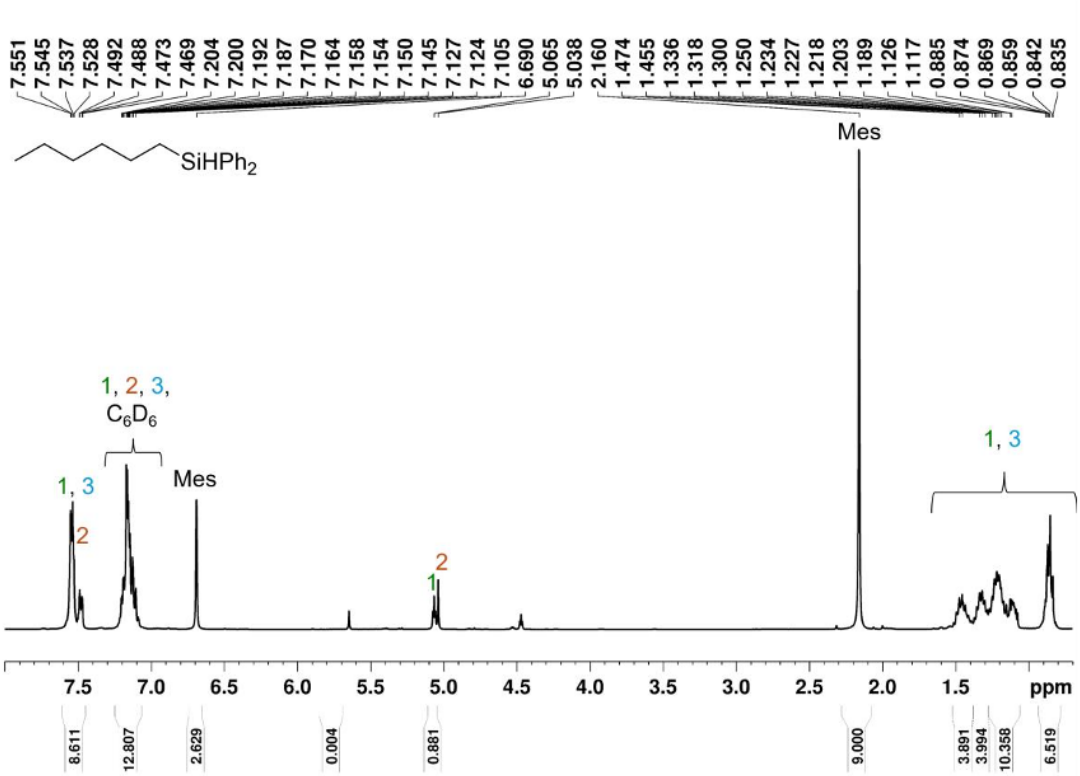

Supplementary Figure S 38. ^{1}H NMR spectrum of the crude reaction mixture of the hydrosilylation of 1-hexene and Ph_2SiH_2 catalyzed by 0.05 mol% **3a** in C_6D_6 after 15 min at 293 K. Internal standard mesitylene (Mes), 1 anti-Markovnikov product, 2 Ph_2SiH_2, 3 disubstituted product.

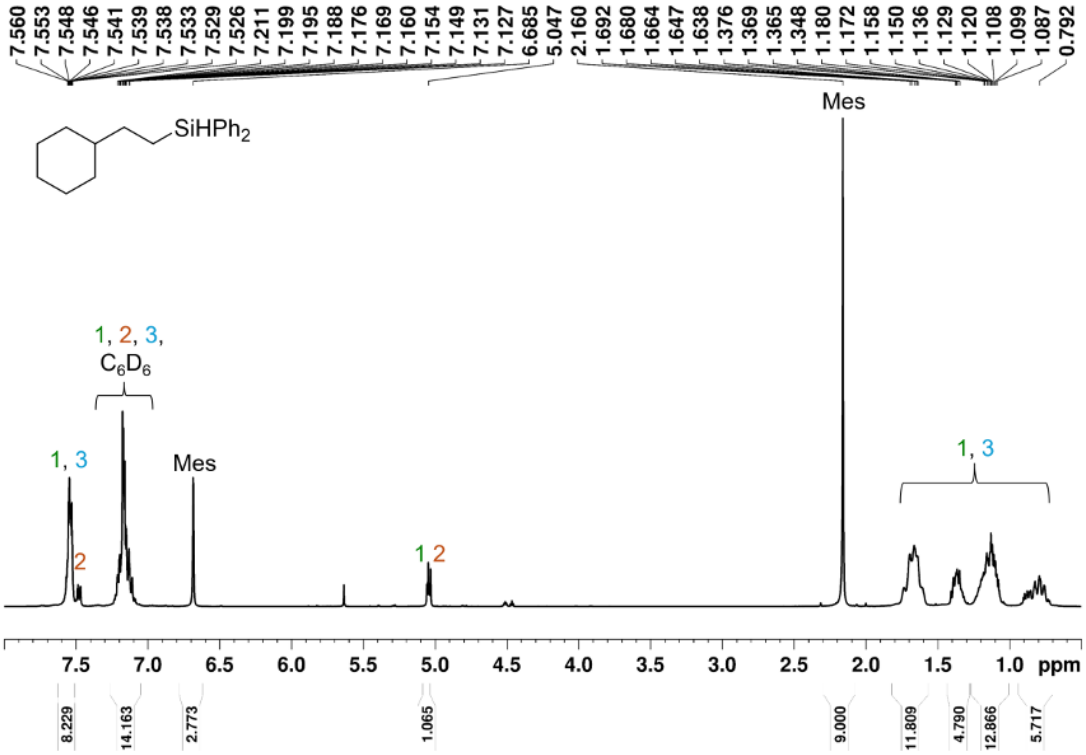

Supplementary Figure S39. ^{1}H NMR spectrum of the crude reaction mixture of the hydrosilylation of vinylcyclohexane and Ph_2SiH_2 catalyzed by 0.05 mol% **3a** in C_6D_6 after 168 h at 293 K. Internal standard mesitylene (Mes), 1 anti-Markovnikov product, 2 Ph_2SiH_2, 3 disubstituted product.

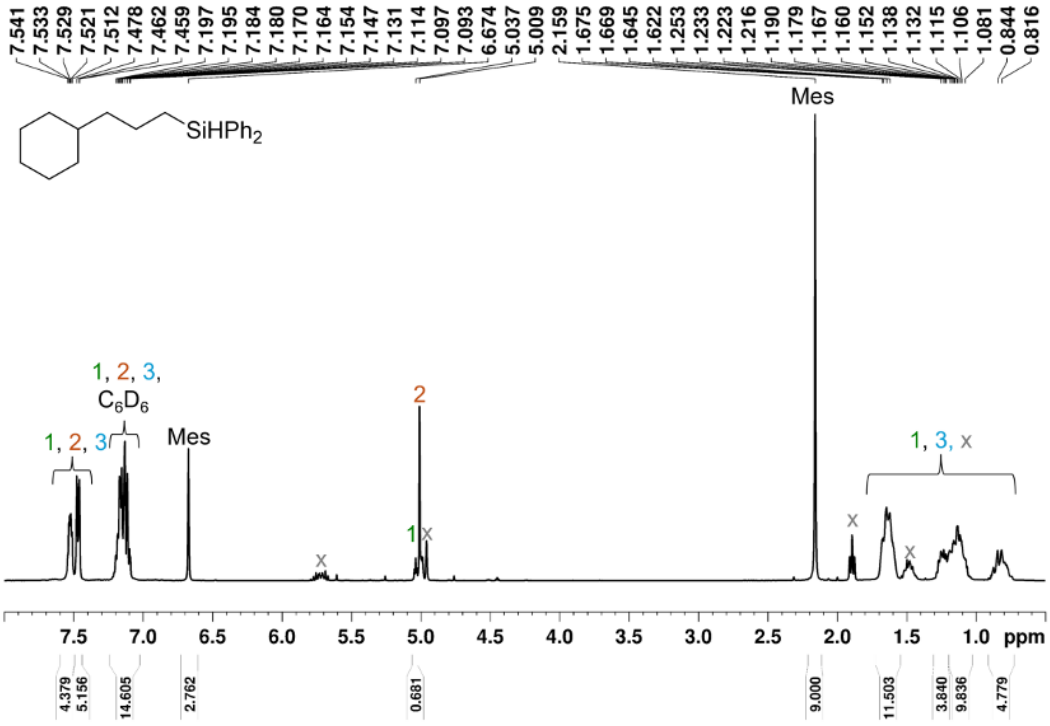

Supplementary Figure S40. ^{1}H NMR spectrum of the crude reaction mixture of the hydrosilylation of allylcyclohexane and Ph_2SiH_2 catalyzed by 0.05 mol% **3a** in C_6D_6 after 408 h at 293 K. Internal standard mesitylene (Mes), 1 anti-Markovnikov product, 2 Ph_2SiH_2, 3 disubstituted product, x allyltrimehtylsilane.

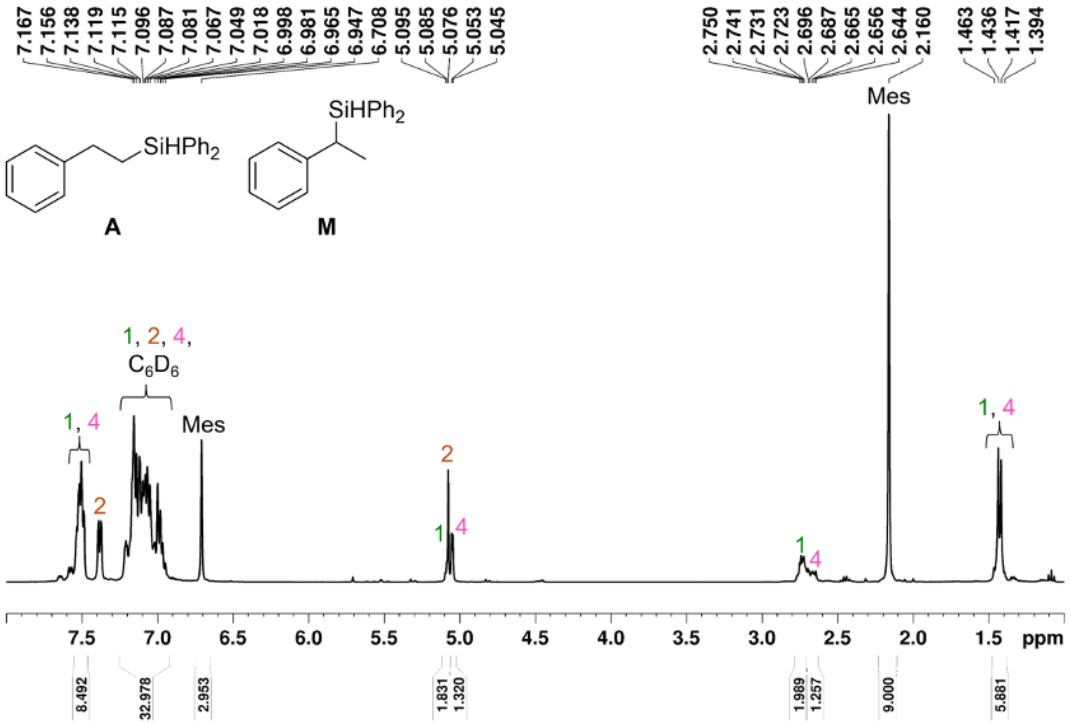

Supplementary Figure S41. ^{1}H NMR spectrum of the crude reaction mixture of the hydrosilylation of styrene and Ph_2SiH_2 catalyzed by 0.05 mol% **3a** in C_6D_6 after 54 h at 293 K. Internal standard mesitylene (Mes), 1 anti-Markovnikov product, 2 Ph_2SiH_2, 4 Markovnikov product.

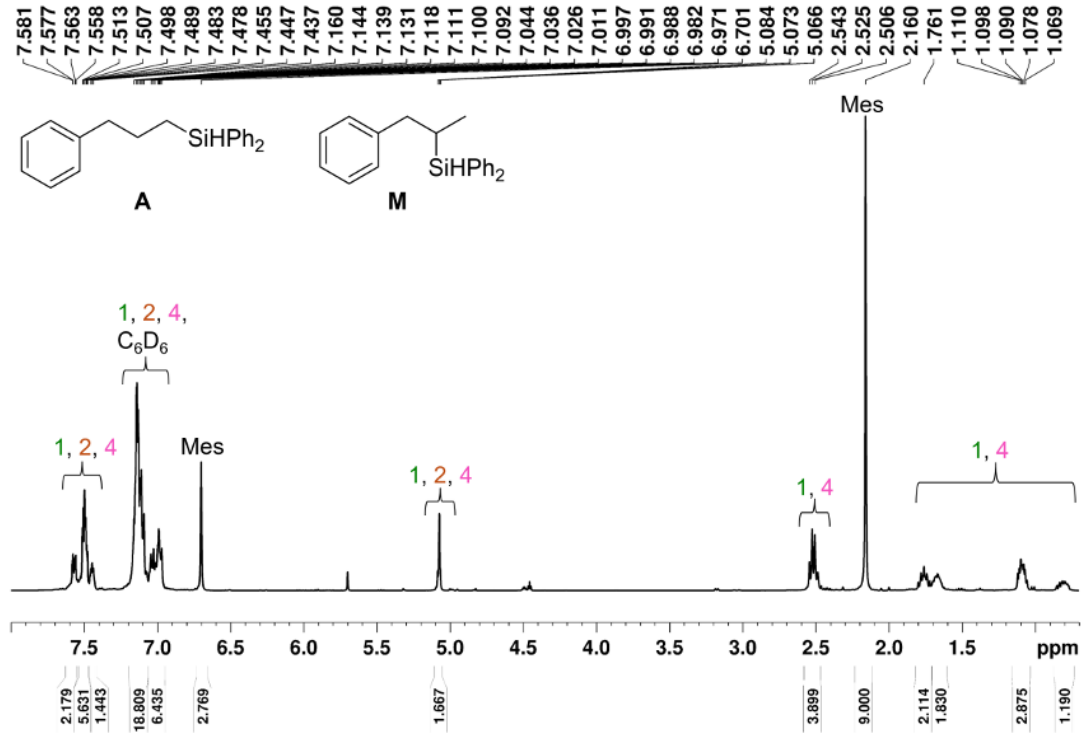

Supplementary Figure S42. ^{1}H NMR spectrum of the crude reaction mixture of the hydrosilylation of allylbenzene and Ph_2SiH_2 catalyzed by 0.05 mol% **3a** in C_6D_6 after 54 h at 293 K. Internal standard mesitylene (Mes), 1 anti-Markovnikov product, 2 Ph_2SiH_2, 4 Markovnikov product.

5. Supporting Information

Supplementary Table S1. Catalytic hydrosilylation of terminal olefins with Ph_2SiH_2 using nickel complex $Ni(cod)_2$ as a catalyst.

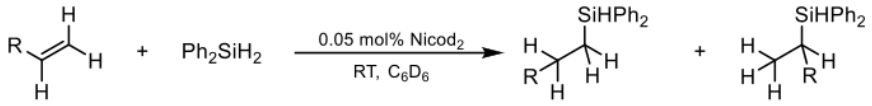

Entry	Substrate	Time [h]	Conversion [%]	Product	Spectr. Yield [%]	TOF [h^{-1}]
1		0.083	>99	**A**	36	24000
2A		0.5	32	**A**	23	1272
2B		2	72	**A**	35	716
2C		5.5	>99	**A**	44	637
3A		0.083	24	**A**	18	5832
3B	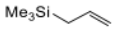	0.5	69	**A**	35	2744
3C		3	93	**A**	41	620
4A		0.083	58	**A**	10	13848
4B		24	94	**A**	32	78
4C		216	>99	**A**	37	9
5A		4	12	**A**	7	62
5B		120	65	**A**	23	11
5C		336	78	**A**	29	5
6A		0.083	25	**A : M**	8 : 19	6096
6B		0.5	75	**A : M**	22 : 40	3008
6C		3	>99	**A : M**	30 : 43	500
7A		2	18	**A : M**	8 : 10	184
7B		120	72	**A : M**	31 : 31	12
7C		312	>99	**A : M**	41 : 35	6

3 Details on X-Ray Diffraction Studies

The data set was collected using a Rigaku XtaLAB Synergy-S diffractometer with a microfocus sealed tube and a HyPix-6000HE Hybrid Photon Counting (HPC) detector (**2**, **3c**), a Bruker D8 Venture diffractometer with a microfocus sealed tube and a Photon II detector (**3a**) and a Bruker X8 Apex diffractometer (**3b**). Graphite-monochromated $Mo_{K\alpha}$ radiation (λ = 0.71073 Å) was used. Data were collected at 133(2) K (**2**, **3a**, **3c**)/ 154(2) K (**3b**) and corrected for absorption effects using the multi-scan method. The structure was solved by direct methods using SHELXT[14] and was refined by full matrix

least squares calculations on F^2 (SHELXL2019 (**2**, **3c**), SHELXL2018 (**3a,b**))[15] in the graphical user interface Shelxle.[16]

Acknowledgments

Instrumentation and technical assistance for this work were provided by the Service Center X-ray Diffraction, with financial support from Saarland University and German Science Foundation (project number INST 256/506-1 (D8 Venture) and 256/582-1 (Synergy-S)).

3.1 Solid State Structure of $Fe(CO)_4$ siliconoid/silylene 2

Refinement Details

All non-H-atoms were located in the electron density maps and refined anisotropically. C-bound H atoms were placed in positions of optimized geometry and treated as riding atoms. Their isotropic displacement parameters were coupled to the corresponding carrier atoms by a factor of 1.2 (CH, CH_2) or 1.5 (CH_3). *Disorder:* One tert-butyl group is split over two positions (fvar 2: 0.57/0.43).

Supplementary Table S2. Crystal data and structure refinement for $Fe(CO)_4$ siliconoid/silylene **2** (CCDC: 2504459).

Empirical formula	C_{99} H_{150} Fe N_2 O_4 Si_8	
Formula weight	1712.77	
Temperature	133(2) K	
Wavelength	0.71073 Å	
Crystal system	Triclinic	
Space group	P-1	
Unit cell dimensions	a = 14.9881(3) Å	α = 104.518(2)°.
	b = 17.1703(3) Å	β = 100.700(2)°.
	c = 20.6186(4) Å	γ = 97.1940(10)°.
Volume	4964.47(17) $Å^3$	
Z	2	
Density (calculated)	1.146 Mg/m^3	
Absorption coefficient	0.297 mm^{-1}	
F(000)	1856	
Crystal size	0.220 x 0.200 x 0.100 mm^3	
Theta range for data collection	2.015 to 27.125°.	
Index ranges	-19<=h<=18, -21<=k<=22, -26<=l<=26	
Reflections collected	70038	
Independent reflections	21884 [R(int) = 0.0480]	
Completeness to theta = 25.242°	99.9 %	
Absorption correction	Semi-empirical from equivalents	

Max. and min. transmission	1.0000 and 0.8232
Refinement method	Full-matrix least-squares on F^2
Data / restraints / parameters	21884 / 36 / 1090
Goodness-of-fit on F^2	1.035
Final R indices [I>2sigma(I)]	R_1 = 0.0480, wR_2 = 0.1268
R indices (all data)	R_1 = 0.0665, wR_2 = 0.1357
Largest diff. peak and hole	0.673 and -0.486 e.Å^{-3}

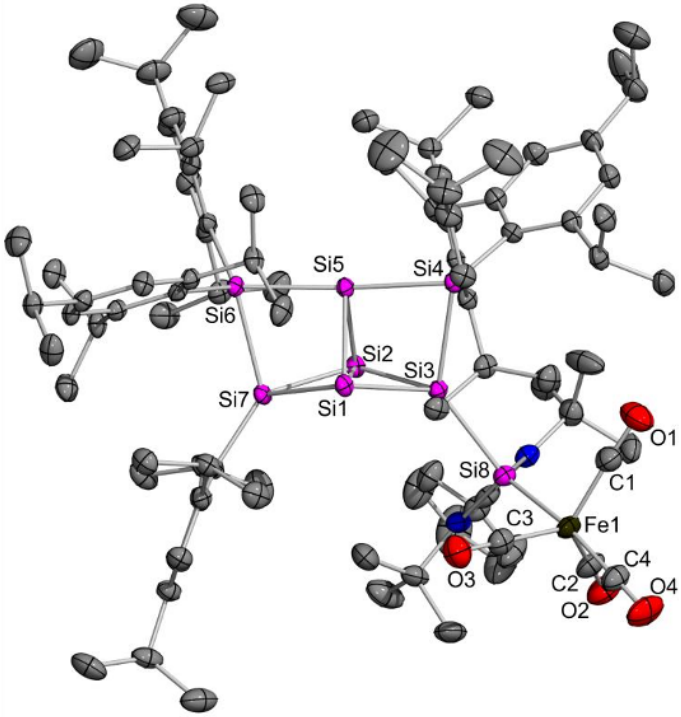

Supplementary Figure S43. Molecular structure $Fe(CO)_4$ siliconoid/silylene **2** in the solid state. Hydrogen atoms are omitted for clarity. Thermal ellipsoids represent 50% probability.

3.2 Solid State Structure of Ni(cod) siliconoid/silylene 3a

Refinement Details

All non-H-atoms were located in the electron density maps and refined anisotropically. C-bound H atoms were placed in positions of optimized geometry and treated as riding atoms. Their isotropic displacement parameters were coupled to the corresponding carrier atoms by a factor of 1.2 (CH, CH_2) or 1.5 (CH_3). *Disorder:* Three isopropyl-groups and one tert-butyl group are split over two positions. One of the solvent n-pentane molecules is split over two positions. Its occupancy factors refined to 0.58 for the major component.

Supplementary Table S3. Crystal data and structure refinement for Ni(cod) siliconoid/silylene **3a** (CCDC: 2504461).

Empirical formula	C108 H174 N2 Ni Si8
Formula weight	1783.91
Temperature	133(2) K

5. Supporting Information

Wavelength	0.71073 Å	
Crystal system	Triclinic	
Space group	P-1	
Unit cell dimensions	a = 14.6865(6) Å	α = 87.707(2)°.
	b = 18.5075(7) Å	β = 73.3410(10)°.
	c = 22.7349(8) Å	γ = 67.462(2)°.
Volume	5451.0(4) $Å^3$	
Z	2	
Density (calculated)	1.087 Mg/m^3	
Absorption coefficient	0.310 mm^{-1}	
F(000)	1952	
Crystal size	0.360 x 0.240 x 0.080 mm^3	
Theta range for data collection	1.876 to 27.912°.	
Index ranges	-19<=h<=19, -24<=k<=24, -29<=l<=29	
Reflections collected	151157	
Independent reflections	26031 [R(int) = 0.0651]	
Completeness to theta = 25.242°	100.0 %	
Absorption correction	Semi-empirical from equivalents	
Max. and min. transmission	0.7367 and 0.7072	
Refinement method	Full-matrix least-squares on F^2	
Data / restraints / parameters	26031 / 509 / 1281	
Goodness-of-fit on F^2	1.025	
Final R indices [I>2sigma(I)]	R1 = 0.0409, wR2 = 0.1054	
R indices (all data)	R1 = 0.0545, wR2 = 0.1154	
Largest diff. peak and hole	0.513 and -0.448 $e.Å^{-3}$	

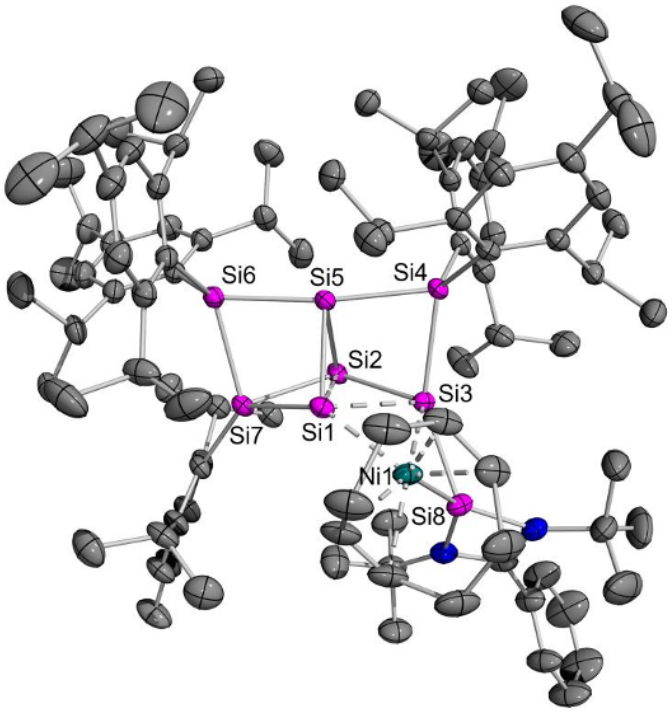

Supplementary Figure S44. Molecular structure Ni(cod) siliconoid/silylene **3a** in the solid state. Hydrogen atoms are omitted for clarity. Thermal ellipsoids represent 50% probability.

3.3 Solid State Structure of Ni(PPh$_3$) siliconoid/silylene 3b

Refinement Details

All non-H-atoms were located in the electron density maps and refined anisotropically. C-bound H atoms were placed in positions of optimized geometry and treated as riding atoms. Their isotropic displacement parameters were coupled to the corresponding carrier atoms by a factor of 1.2 (CH) or 1.5 (CH_3). *Disorder:* Five isopropyl-groups and one tert-butyl-group were split over two positions. Their occupancy factors of the major components refined to 0.70, 0.67, 0.88, 0.76, 0.48 and 0.86, respectively. SQUEEZE: The scattering contribution of eight pentane solvent molecules in the unit cell has been treated with the SQUEEZE tool[17] in PLATON.[18] BerSQUEEZE found 250 electrons in the solvent accessible volume of 1839 Å^3.

Supplementary Table S4. Crystal data and structure refinement for Ni(PPh$_3$) siliconoid/silylene **3b** (CCDC: 2504467).

Empirical formula	C_{113} H_{165} N_2 Ni P Si_8	
Formula weight	1865.86	
Temperature	154(2) K	
Wavelength	0.71073 Å	
Crystal system	Monoclinic	
Space group	I2/a	
Unit cell dimensions	a = 38.3683(15) Å	α = 90°.

	b = 14.2013(5) Å	β = 92.947(2)°.
	c = 40.6910(14) Å	γ = 90°.
Volume	22142.4(14) Å^3	
Z	8	
Density (calculated)	1.119 Mg/m^3	
Absorption coefficient	0.322 mm^{-1}	
F(000)	8096	
Crystal size	0.200 x 0.200 x 0.080 mm^3	
Theta range for data collection	1.063 to 27.163°.	
Index ranges	-49<=h<=39, -18<=k<=18, -52<=l<=50	
Reflections collected	164785	
Independent reflections	24510 [R(int) = 0.1094]	
Completeness to theta = 25.242°	100.0 %	
Absorption correction	Semi-empirical from equivalents	
Max. and min. transmission	0.7455 and 0.7117	
Refinement method	Full-matrix least-squares on F^2	
Data / restraints / parameters	24510 / 484 / 1281	
Goodness-of-fit on F^2	1.004	
Final R indices [I>2sigma(I)]	R_1 = 0.0494, wR_2 = 0.0955	
R indices (all data)	R_1 = 0.1078, wR_2 = 0.1171	
Largest diff. peak and hole	0.371 and -0.370 e.Å^{-3}	

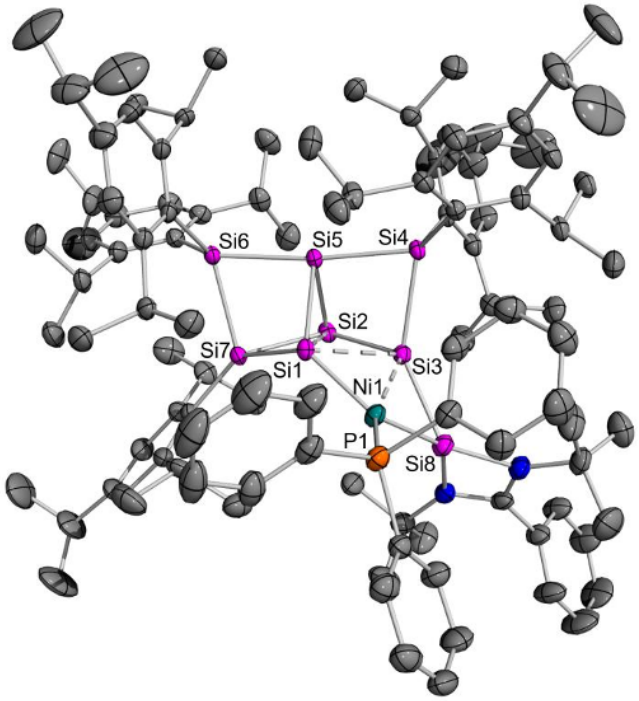

Supplementary Figure S45. Molecular structure Ni(PPh$_3$) siliconoid/silylene **3b** in the solid state. Hydrogen atoms are omitted for clarity. Thermal ellipsoids represent 50% probability.

3.4 Solid State Structure of $Ni(CO)_2$ siliconoid/silylene 3c

Refinement Details

All non H-atoms were located in the electron density maps and refined anisotropically. C-bound H atoms were placed in positions of optimized geometry and treated as riding atoms. Their isotropic displacement parameters were coupled to the corresponding carrier atoms by a factor of 1.2 (CH, CH_2) or 1.5 (CH_3). *Disorder:* three isopropyl-residues (fvar 2: 0.62/0.38; fvar 3: 0.68/0.32 and fvar 4: 0.80/0.20) and one n-pentane solvent (fvar 5: 0.59/0.41) are split over two positions. Three n-pentane solvent molecules are located over a crystallographic twofold axis and hence, they are handled using the PART-1 instruction of SHELX (sof: 0.5).

Supplementary Table S5. Crystal data and structure refinement for $Ni(CO)_2$ siliconoid/silylene **3c** (CCDC: 2504470).

Empirical formula	$C_{209}H_{336}N_4Ni_2O_4Si_{16}$	
Formula weight	3535.66	
Temperature	133(2) K	
Wavelength	0.71073 Å	
Crystal system	Monoclinic	
Space group	I2/a	
Unit cell dimensions	a = 20.6821(5) Å	α = 90°.
	b = 34.0729(8) Å	β = 92.710(2)°.
	c = 31.1785(6) Å	γ = 90°.
Volume	21946.9(9) $Å^3$	
Z	4	
Density (calculated)	1.070 Mg/m^3	
Absorption coefficient	0.308 mm^{-1}	
F(000)	7720	
Crystal size	0.300 x 0.080 x 0.040 mm^3	
Theta range for data collection	1.972 to 26.372°.	
Index ranges	-25<=h<=25, -42<=k<=42, -35<=l<=38	
Reflections collected	151269	
Independent reflections	22428 [R(int) = 0.1233]	
Completeness to theta = 25.242°	99.9 %	
Absorption correction	Semi-empirical from equivalents	
Max. and min. transmission	1.00000 and 0.69666	
Refinement method	Full-matrix least-squares on F^2	
Data / restraints / parameters	22428 / 640 / 1294	
Goodness-of-fit on F^2	1.050	
Final R indices [I>2sigma(I)]	R_1 = 0.0696, wR_2 = 0.1455	
R indices (all data)	R_1 = 0.1066, wR_2 = 0.1609	

Largest diff. peak and hole	0.855 and -0.337 e.Å^{-3}

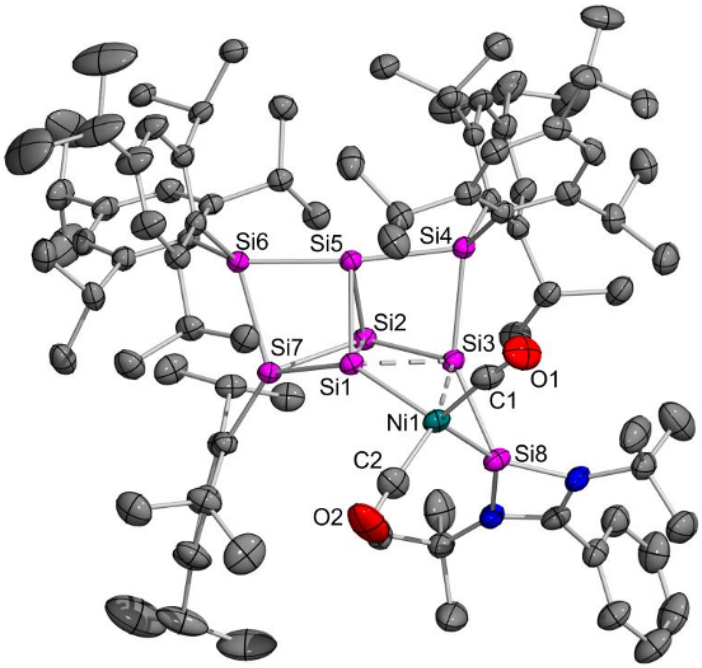

Supplementary Figure S46. Molecular structure Ni(CO)$_2$ siliconoid/silylene **3c** in the solid state. Hydrogen atoms are omitted for clarity. Thermal ellipsoids represent 50% probability.

3.5 Calculation of Percent Buried Volume

The percent buried volume %V_{bur} of **X**-Fe(CO)$_4$, **2** and **3b** was determined with the Sambvca open-source application on the corresponding crystallographic data, applying the common parameters of 3.50 Å sphere radius, 0.00 Å or 2.28 Å distance metal-ligand bond, with the hydrogen atoms included and the scaled bond radii used as recommended by Cavallo).[19]

%V_{bur} of **X**-Fe(CO)$_4$[20]

Parameters:
center of sphere: Fe1
z-axis: C4 (CO linear to Fe-Si7)
xz plane: C1, C2, C3 (remaining CO ligands)
deleted atoms: C1, C2, C3, C4, O1, O2, O3, O4
atomic radii: Bondi radii scaled by 1.17
Sphere radius: 3.5
Distance coordination point to center of sphere: 0.0
Mesh spacing for numerical integration: 0.10
H atoms: included

Supplementary Table S6. Distribution of ligand volume in **X**.[19]

%V Free	%V Buried	% V Tot/V Ex
35.3	64.7	99.9

Quadrant	V f	V b	V t	%V f	%V b
SW	10.1	34.7	44.9	22.6	77.4
NW	15.7	29.2	44.9	35.0	65.0
NE	18.4	26.4	44.9	41.1	58.9
SE	19.1	25.8	44.9	42.5	57.5

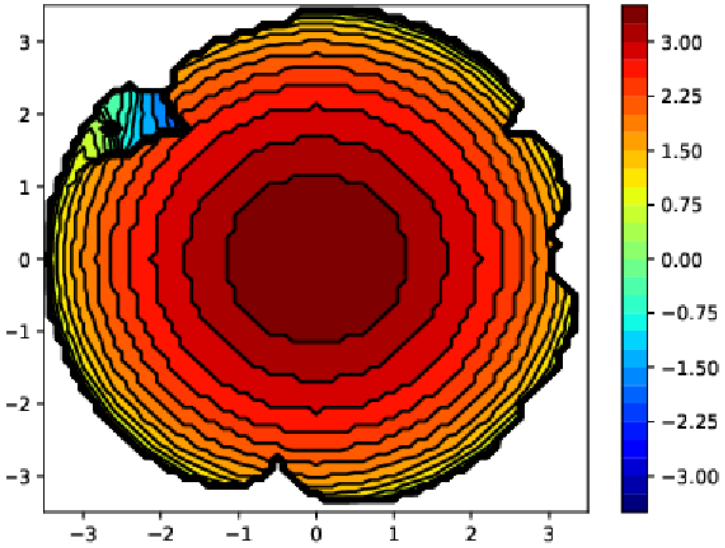

Supplementary Figure S47. Steric map of **X** produced by SambVca.[19]

$\%V_{bur}$ of **2**

Parameters:

center of sphere: Fe1

z-axis: C4 (CO linear to Fe-Si8)

xz plane: C1, C2, C3 (remaining CO ligands)

deleted atoms: C1, C2, C3, C4, O1, O2, O3, O4

atomic radii: Bondi radii scaled by 1.17

Sphere radius: 3.5

Distance coordination point to center of sphere: 0.0

Mesh spacing for numerical integration: 0.10

H atoms: included

Supplementary Table S7. Distribution of ligand volume in **2**.[19]

%V Free	%V Buried	% V Tot/V Ex
44.7	55.3	99.9

Quadrant	V f	V b	V t	%V f	%V b
SW	20.0	24.9	44.9	44.5	55.5
NW	18.3	26.6	44.9	40.7	59.3
NE	19.0	25.9	44.9	42.3	57.7
SE	22.9	21.9	44.9	51.1	48.9

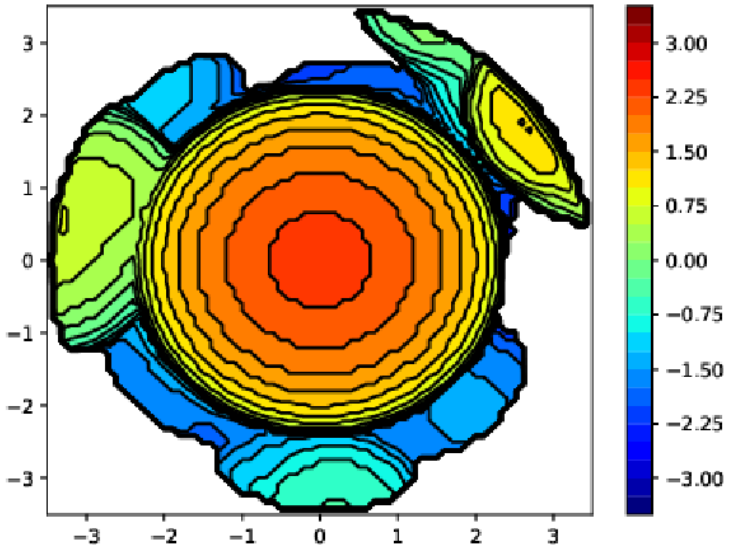

Supplementary Figure S48. Steric map of **2** produced by SambVca.[19]

3b

Parameters: **center of sphere:** Ni1
z-axis: P1
xz plane: C91, C97, C103 (*ipso*-Cs of phenyl ligands)
deleted atoms: P1, C91-C108, H92-108
atomic radii: Bondi radii scaled by 1.17
Sphere radius: 3.5
Distance coordination point to center of sphere: 0.0
Mesh spacing for numerical integration: 0.10
H atoms: included

Supplementary Table S8. Distribution of ligand volume in **3b**.[19]

%V Free	%V Buried	% V Tot/V Ex
30.1	69.9	99.9

Quadrant	V f	V b	V t	%V f	%V b
SW	10.8	34.1	44.9	24.1	75.9
NW	14.3	30.5	44.9	31.9	68.1
NE	10.6	34.3	44.9	23.6	76.4
SE	18.4	26.5	44.9	41.0	59.0

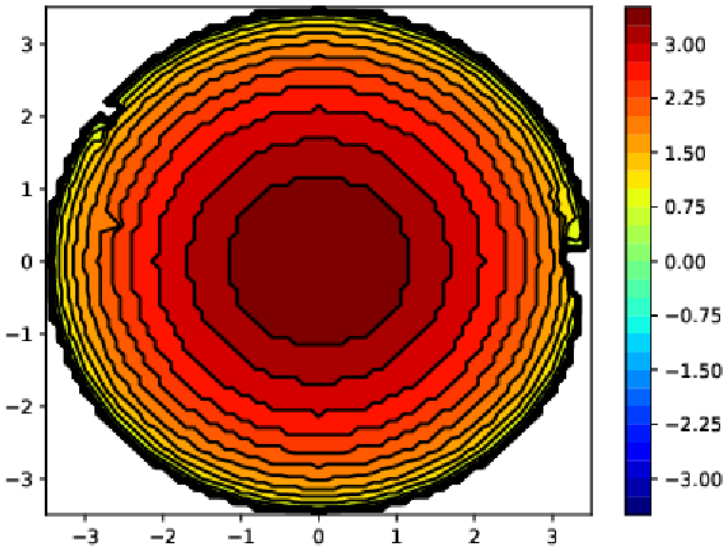

Supplementary Figure S49. Steric map of **3b** produced by SambVca.[19]

4 Computational Details

Computations were carried out with orca 5.0.4/6.0.1.[21,22] Structural optimizations in the gas-phase, frequency analyses and single point calculations for **2** and **3a-c** were performed at the B3LYP/def2-TZVP level of theory[23–29] including the dispersion correction by Grimme (D3BJ).[30] Tighter than default convergence had to be chosen for the optimization (tightopt) and scf (thightscf). Implicit correction for solvation effects (solvents: hexane or benzene) were investigated with the CPCM model[31] for spectroscopic calculations. NMR chemical shifts (GIAO)[32] for **2-3a-c** were calculated using TPSSh/def2-TZVP.[26–29,33] UV-Vis data was received using time-dependent calculations (TD-DFT).[34] FT-IR spectra were corrected according to literature procedures by multiplying the harmonic frequencies with 1.0044.[35] Moreover, a constant offset value of $\Delta\tilde{\nu}_{CO}$ = 100 cm^{-1} was subtracted, determined by comparison of the calculated CO stretching frequency (2243 cm^{-1} at the B3LYP/def2-TZVP level of theory) with the experimental value reported in the literature (2143 cm^{-1}).[36] Pictures of Kohn-Sham orbitals were displayed with ChemCraft 1.8.[37]

5. Supporting Information

4.1 $Fe(CO)_4$ siliconoid/silylene 2

4.1.1 Optimization and molecular orbitals

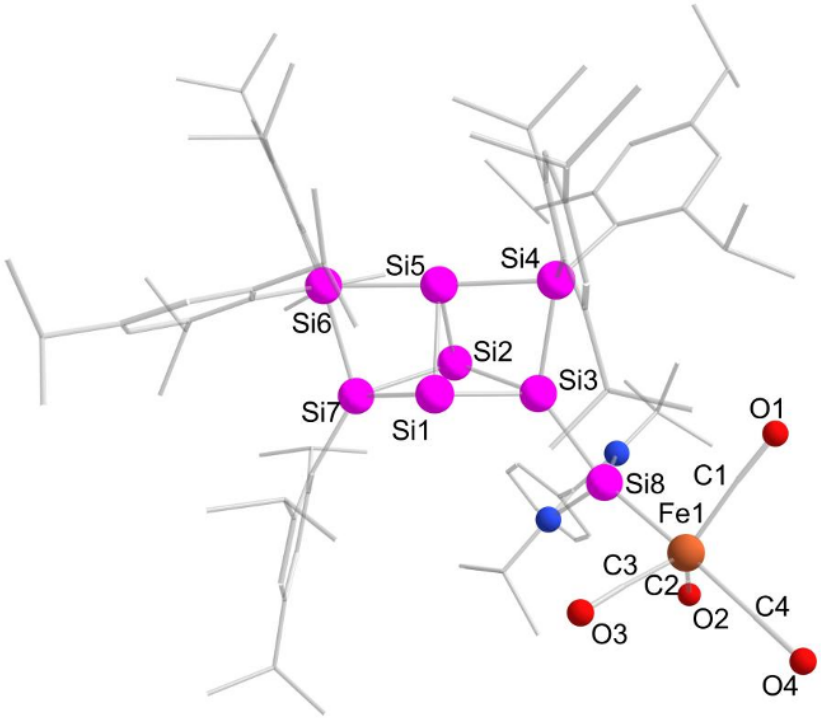

Supplementary Figure S 50. Optimized molecular structure of $Fe(CO)_4$ siliconoid/silylene **2** at B3LYP/def2-TZVP.[23–29] Hydrogen atoms are omitted for clarity.

Supplementary Table S9. Coordinates of $Fe(CO)_4$ siliconoid/silylene **2** at B3LYP/def2-TZVP.[23–29]

Fe	-5.066573	5.160465	17.213219
Si	-3.08786	6.274186	17.162991
C	-5.921721	6.70898	17.325657
C	-4.400704	4.463731	18.701501
C	-4.680145	4.484404	15.615365
C	-6.579618	4.207269	17.333629
Si	-2.20004	7.933712	15.721009
N	-1.578527	5.276905	17.52376
N	-2.35152	6.856205	18.746616
C	-1.404553	5.919456	18.680009
O	-6.523026	7.683711	17.435108
O	-3.964407	4.0198	19.673265
O	-4.463839	4.004459	14.590218
O	-7.541785	3.594582	17.416102
Si	-1.198581	7.677349	13.660494
Si	0.120575	8.404824	15.811979
Si	-2.78731	10.174186	15.054281
C	-0.958228	4.063619	16.947838
C	-2.665524	7.883257	19.755149
C	-0.379185	5.633856	19.703783

Si	-0.603881	9.881335	14.125511
Si	1.095821	7.454585	13.889628
C	-3.208425	11.515113	16.356629
C	-3.932925	10.409296	13.551816
C	-1.03906	4.225861	15.429661
C	-1.741454	2.822993	17.392956
C	0.510623	3.909789	17.337751
C	-3.450061	8.977987	19.027591
C	-1.404758	8.510875	20.357389
C	-3.533082	7.260697	20.855236
C	-0.66815	4.743489	20.73342
C	0.869124	6.243961	19.631451
Si	1.356412	9.618702	12.814598
C	1.856751	5.741767	13.626753
C	-2.207692	12.320103	16.952745
C	-4.556874	11.876959	16.580353
C	-3.828142	11.652641	12.881088
C	-4.828491	9.451505	13.036466
H	-0.630387	3.346611	14.934469
H	-0.462901	5.090662	15.108643
H	-2.066054	4.349639	15.093549
H	-1.295922	1.931559	16.948127
H	-2.781627	2.882007	17.079592
H	-1.715588	2.715986	18.47755
H	0.940621	3.103845	16.743509
H	0.642449	3.663542	18.388762
H	1.068107	4.813346	17.113315
H	-3.779576	9.735973	19.738132
H	-2.834265	9.472128	18.277292
H	-4.33674	8.576872	18.53808
H	-1.693458	9.383379	20.945095
H	-0.875735	7.825955	21.015196
H	-0.724291	8.838898	19.571052
H	-3.79778	8.018491	21.594723
H	-4.451046	6.849504	20.436376
H	-2.99856	6.457579	21.362608
H	-1.64185	4.274638	20.778924
C	0.301822	4.459956	21.687111
C	1.833563	5.956649	20.584058
H	1.076132	6.940369	18.830904
C	2.647072	11.006978	13.111512
C	1.427425	9.102548	10.984975
C	2.802575	5.224008	14.531783
C	1.272559	4.867907	12.681466
C	-2.555019	13.494276	17.609386
C	-0.731742	11.97064	16.920983
C	-4.853361	13.062063	17.251073

C	-5.745987	11.019639	16.175857
C	-4.569577	11.891789	11.731911
C	-2.950961	12.789988	13.378536
C	-5.556374	9.743502	11.882932
C	-5.083817	8.087334	13.655459
H	0.079751	3.765813	22.487008
C	1.551693	5.062929	21.612515
H	2.805323	6.428905	20.523925
C	3.567341	10.999877	14.179449
C	2.689807	12.112249	12.221543
C	0.366281	9.188421	10.058898
C	2.660615	8.566988	10.546152
C	3.003588	3.848984	14.600652
C	3.683048	6.132386	15.371745
C	1.527142	3.504764	12.769474
C	0.416091	5.355596	11.525161
H	-1.767001	14.107232	18.027292
C	-3.873227	13.90625	17.742119
H	-0.63409	10.959717	16.534482
C	0.054535	12.896163	15.985502
C	-0.120403	11.950443	18.327542
H	-5.890306	13.341187	17.390238
H	-5.369968	10.072124	15.787722
C	-6.613831	11.672927	15.092986
C	-6.614867	10.69644	17.39983
H	-4.471525	12.850498	11.238121
C	-5.441264	10.946388	11.208657
H	-2.429009	12.459237	14.271171
C	-1.874912	13.178667	12.370512
C	-3.778367	14.012001	13.794021
H	-6.241559	9.000611	11.493696
H	-4.481683	8.003469	14.56197
C	-6.547092	7.90063	14.075656
C	-4.659741	6.960189	12.70874
H	2.305818	4.838082	22.355599
C	4.481996	12.040937	14.327455
C	3.640289	9.897155	15.21647
C	3.649865	13.103613	12.388307
C	1.723961	12.312414	11.063105
C	0.563017	8.771861	8.746461
C	-1.01019	9.726232	10.410783
C	2.81093	8.179758	9.217805
C	3.876572	8.415609	11.452285
H	3.699354	3.448052	15.3278
C	2.349605	2.967257	13.752446
H	3.534214	7.145866	14.997717
C	5.16386	5.782584	15.170251

C	3.331204	6.144853	16.859149
H	1.063295	2.842294	12.049651
H	0.352846	6.441966	11.585208
C	-1.008623	4.797781	11.577816
C	1.074289	5.037494	10.176474
C	-4.23117	15.219302	18.401984
H	1.109222	12.618946	15.95133
H	-0.012292	13.934435	16.317861
H	-0.330127	12.84737	14.966447
H	0.894821	11.551965	18.291386
H	-0.708423	11.323141	18.998767
H	-0.066431	12.94865	18.765686
H	-7.435398	11.009855	14.816408
H	-6.046959	11.896885	14.194037
H	-7.049655	12.603397	15.463632
H	-7.408361	10.003035	17.127278
H	-7.079165	11.600003	17.797274
H	-6.02983	10.239766	18.196145
C	-6.24639	11.219438	9.957202
H	-1.263457	13.98541	12.774847
H	-2.303789	13.525934	11.429388
H	-1.220806	12.33684	12.14711
H	-3.129266	14.773729	14.230755
H	-4.525991	13.744221	14.536835
H	-4.28929	14.453508	12.935856
H	-6.671235	6.930084	14.556875
H	-7.213656	7.936155	13.212252
H	-6.86575	8.666931	14.78
H	-4.789038	5.988653	13.181964
H	-3.61442	7.059335	12.419882
H	-5.258128	6.973691	11.795665
H	5.169955	12.02373	15.163671
C	4.557787	13.095216	13.436492
H	2.960719	9.105101	14.906746
C	3.1607	10.374312	16.589341
C	5.046903	9.298637	15.309236
H	3.677914	13.921981	11.681524
H	0.890039	11.625264	11.194377
C	1.141572	13.732464	11.047194
C	2.379272	12.015626	9.708211
H	-0.26125	8.849533	8.048822
C	1.779776	8.27855	8.297429
H	-0.985744	10.063541	11.446751
C	-1.418406	10.922852	9.543754
C	-2.077026	8.630549	10.319613
H	3.765232	7.790428	8.884452
H	3.571713	8.615449	12.480452

C	4.972553	9.43151	11.106037
C	4.442292	6.991171	11.436463
C	2.555408	1.473174	13.87647
H	5.802657	6.506988	15.675427
H	5.425506	5.772377	14.11245
H	5.394294	4.79879	15.581272
H	4.01619	6.795557	17.407874
H	3.396313	5.146521	17.295057
H	2.32069	6.52056	17.010288
H	-1.610934	5.214535	10.768213
H	-1.496696	5.041097	12.521574
H	-1.011436	3.711286	11.47087
H	0.49413	5.485104	9.368528
H	1.127969	3.96096	10.001306
H	2.083776	5.442521	10.125029
H	-5.323534	15.281376	18.419796
C	-3.710664	16.40611	17.58085
C	-3.737977	15.289915	19.851649
H	-6.841876	10.323255	9.758114
C	-5.340913	11.455375	8.742551
C	-7.218742	12.38812	10.158929
C	5.583603	14.193787	13.605865
H	3.17248	9.549839	17.305711
H	2.141648	10.750538	16.530867
H	3.798449	11.172034	16.976405
H	5.081013	8.527512	16.07725
H	5.786397	10.054129	15.574981
H	5.352186	8.853357	14.361347
H	0.293559	13.786434	10.362684
H	1.87968	14.459577	10.705739
H	0.804147	14.036898	12.035686
H	1.665323	12.1692	8.896624
H	2.743529	10.994392	9.646479
H	3.222581	12.690674	9.545973
C	1.982428	7.871483	6.853913
H	-2.374709	11.318082	9.886331
H	-1.532426	10.634467	8.497077
H	-0.682529	11.724329	9.588341
H	-3.035421	8.998561	10.686247
H	-1.798885	7.759821	10.913243
H	-2.208495	8.298888	9.286856
H	5.823822	9.314096	11.780128
H	4.613838	10.454714	11.194388
H	5.32836	9.279824	10.084777
H	5.269394	6.910957	12.144496
H	4.83108	6.725984	10.452016
H	3.687793	6.25793	11.714981

H	3.252605	1.31326	14.704659
C	1.245043	0.756595	14.225311
C	3.189035	0.878571	12.613119
H	-4.020309	17.35288	18.029149
H	-4.089644	16.36968	16.558301
H	-2.619487	16.398116	17.53281
H	-4.063316	16.219656	20.323604
H	-2.647408	15.256634	19.900332
H	-4.124107	14.454404	20.43787
H	-5.937888	11.595965	7.838726
H	-4.669309	10.610643	8.582599
H	-4.726475	12.347981	8.878396
H	-7.837409	12.533083	9.270481
H	-6.679552	13.319262	10.346365
H	-7.876435	12.206397	11.010305
H	6.165979	13.952865	14.500591
C	6.552901	14.242909	12.418563
C	4.919038	15.55669	13.834645
H	3.013969	7.51759	6.763144
C	1.815652	9.068387	5.909476
C	1.058209	6.716852	6.450096
H	1.41375	-0.314362	14.356713
H	0.505002	0.884083	13.43258
H	0.814198	1.147597	15.148636
H	3.387016	-0.18713	12.746789
H	4.130772	1.376048	12.37595
H	2.526776	0.989197	11.75203
H	7.325365	14.998017	12.580732
H	6.028345	14.49553	11.494485
H	7.0408	13.278052	12.271005
H	5.670776	16.326973	14.021019
H	4.241685	15.523376	14.689552
H	4.338324	15.860894	12.961217
H	2.026115	8.778588	4.87756
H	2.491095	9.880461	6.183351
H	0.795477	9.456695	5.946449
H	1.245896	6.416721	5.416766
H	0.008464	7.008216	6.527257
H	1.212031	5.848115	7.091257

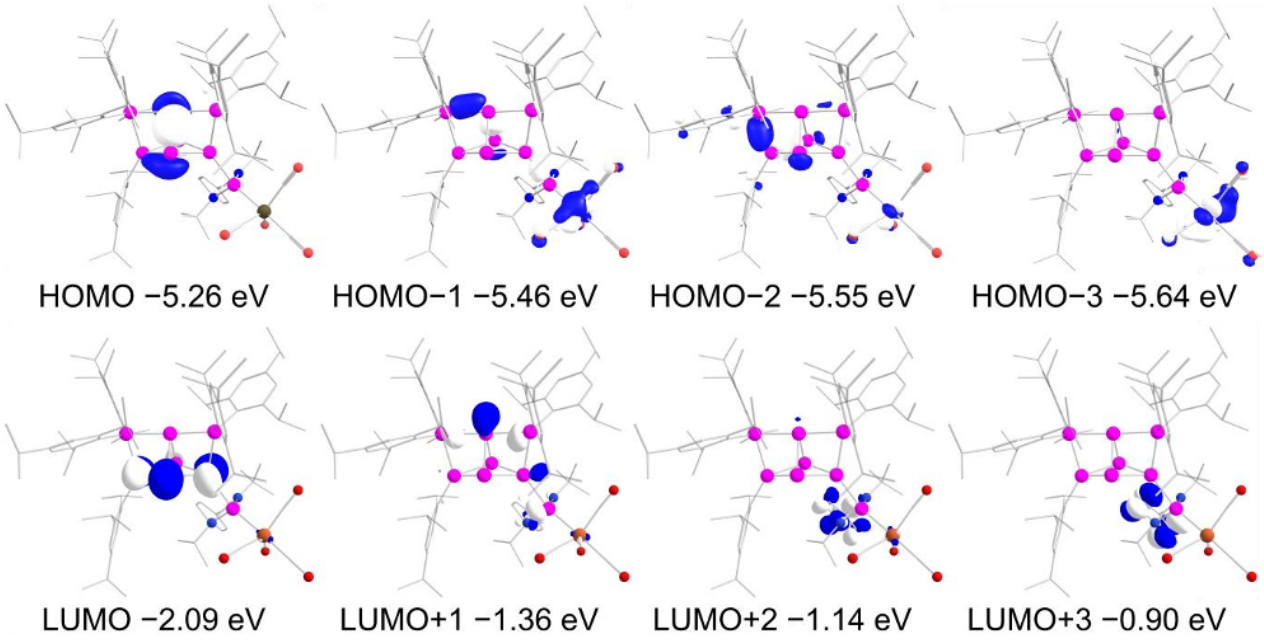

Supplementary Figure S51. Selected frontier orbitals of $Fe(CO)_4$ siliconoid/silylene **2** at B3LYP/def2-TZVP level of theory (contour value 0.05).[23–29] Hydrogen atoms are omitted for clarity.

4.1.2 Experimental vs. calculated NMR shifts

Supplementary Table S10. Comparison of experimental vs. calculated NMR chemical shifts for compound **2** at the TPSSh/def2-TZVP level of theory.[26–29,33]

	Exp. **2** $\delta(^{29}Si)$ [ppm]	Calc. **2** $\delta(^{29}Si)$ [ppm]
Si3 (*Si*NHSi)	172.7	175.4
Si8 (NH*Si*)	157.1	171.3
Si7 (*Si*Tip)	100.5	106.3
Si6 (*Si*Tip$_2$)	33.6	23.4
Si4 (*Si*Tip$_2$)	5.9	−7.3
Si5 (unsubstituted)	−98.2	−96.6
Si1 (unsubstituted)	−198.5	−200.6
Si2 (unsubstituted)	−209.0	−214.2

4.1.3 Experimental vs. calculated FT-IR spectra

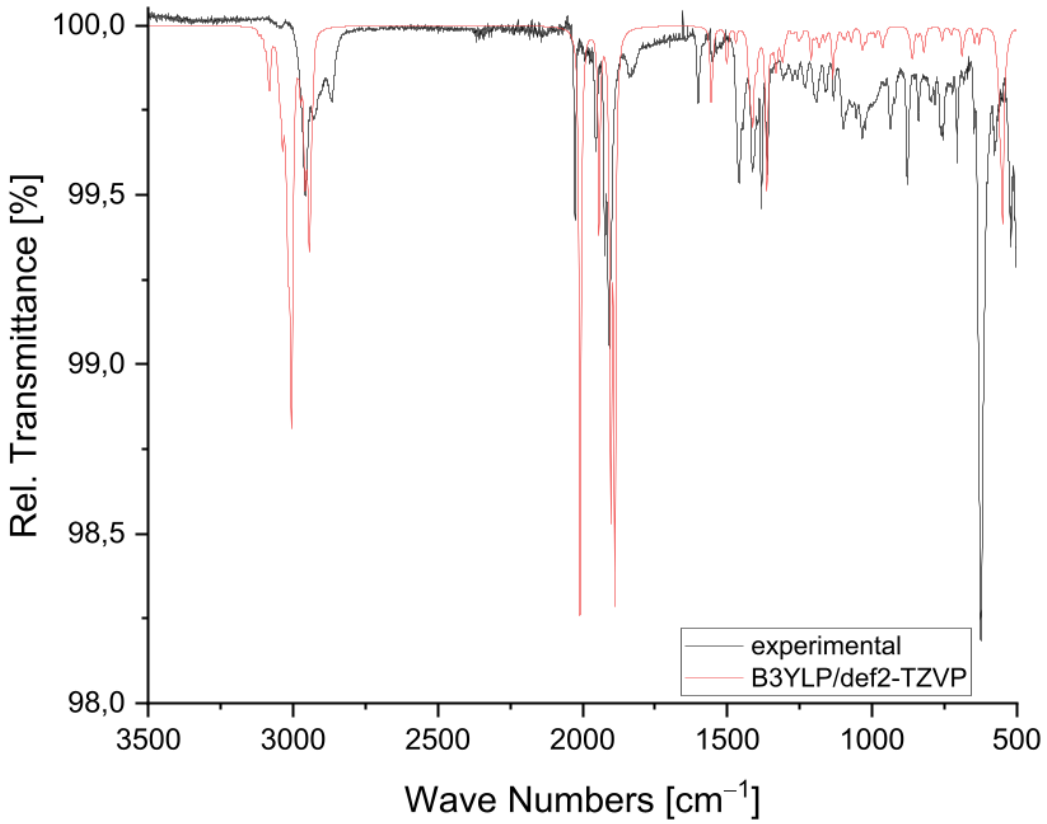

Supplementary Figure S52. Experimental vs. theoretical FT-IR spectrum of $Fe(CO)_4$ siliconoid/silylene **2** at the B3LYP/def2-TZVP level of theory.[23–29]

4.1.4 TD-DFT calculations

Supplementary Table S11. Transition Energy, wavelength, and oscillator strengths of the electronic transition of **2** calculated at the TD-TPSSh/def2-TZVPP.[26–29,33,34] level of theory (the 442nd orbital is the highest occupied orbital (HOMO) and 443rd orbital is the lowest unoccupied molecular orbital (LUMO) shown in Supplementary Figure S51).

```
STATE  1:  E=   0.086311 au      2.349 eV    18943.0 cm**-1 <S**2> =   0.000000 Mult 1
  442a -> 443a  :     0.985982 (c= -0.99296646)

STATE  2:  E=   0.092487 au      2.517 eV    20298.5 cm**-1 <S**2> =   0.000000 Mult 1
  438a -> 443a  :     0.026654 (c= -0.16326156)
  439a -> 443a  :     0.018809 (c= -0.13714414)
  441a -> 443a  :     0.943242 (c=  0.97120660)

STATE  3:  E=   0.096374 au      2.622 eV    21151.6 cm**-1 <S**2> =   0.000000 Mult 1
  437a -> 443a  :     0.048696 (c=  0.22067112)
  440a -> 443a  :     0.924143 (c=  0.96132341)

STATE  4:  E=   0.100662 au      2.739 eV    22092.8 cm**-1 <S**2> =   0.000000 Mult 1
  438a -> 443a  :     0.091020 (c=  0.30169581)
  439a -> 443a  :     0.848619 (c=  0.92120535)
```

```
  440a -> 443a  :     0.018409 (c= -0.13568144)
  441a -> 443a  :     0.031345 (c=  0.17704561)

STATE  5:  E=   0.103636 au      2.820 eV    22745.5 cm**-1 <S**2> =   0.000000 Mult 1
  438a -> 443a  :     0.862558 (c= -0.92874027)
  439a -> 443a  :     0.107539 (c=  0.32793153)
  441a -> 443a  :     0.012856 (c= -0.11338407)

STATE  6:  E=   0.113231 au      3.081 eV    24851.3 cm**-1 <S**2> =   0.000000 Mult 1
  437a -> 443a  :     0.041700 (c=  0.20420462)
  441a -> 444a  :     0.023548 (c= -0.15345247)
  442a -> 444a  :     0.898991 (c= -0.94815137)

STATE  7:  E=   0.114828 au      3.125 eV    25201.8 cm**-1 <S**2> =   0.000000 Mult 1
  434a -> 443a  :     0.016916 (c= -0.13006298)
  435a -> 443a  :     0.062523 (c=  0.25004571)
  436a -> 443a  :     0.749213 (c= -0.86557067)
  437a -> 443a  :     0.128598 (c= -0.35860563)

STATE  8:  E=   0.116576 au      3.172 eV    25585.4 cm**-1 <S**2> =   0.000000 Mult 1
  427a -> 443a  :     0.015335 (c=  0.12383485)
  434a -> 443a  :     0.014288 (c=  0.11953045)
  435a -> 443a  :     0.027960 (c= -0.16721171)
  436a -> 443a  :     0.196865 (c= -0.44369447)
  437a -> 443a  :     0.553990 (c=  0.74430479)
  440a -> 443a  :     0.021423 (c= -0.14636723)
  440a -> 444a  :     0.030601 (c= -0.17493054)
  442a -> 444a  :     0.049721 (c=  0.22298250)

STATE  9:  E=   0.121142 au      3.296 eV    26587.6 cm**-1 <S**2> =   0.000000 Mult 1
  435a -> 443a  :     0.010094 (c= -0.10046657)
  441a -> 444a  :     0.903690 (c= -0.95062586)
  441a -> 445a  :     0.013464 (c= -0.11603370)
  442a -> 444a  :     0.016306 (c=  0.12769514)

STATE 10:  E=   0.122638 au      3.337 eV    26916.0 cm**-1 <S**2> =   0.000000 Mult 1
  433a -> 443a  :     0.028461 (c= -0.16870528)
  434a -> 443a  :     0.349310 (c=  0.59102462)
  435a -> 443a  :     0.459924 (c=  0.67817733)
  437a -> 443a  :     0.010435 (c=  0.10215245)
  440a -> 444a  :     0.114328 (c=  0.33812387)

STATE 11:  E=   0.123817 au      3.369 eV    27174.8 cm**-1 <S**2> =   0.000000 Mult 1
  430a -> 443a  :     0.022494 (c=  0.14998024)
  431a -> 443a  :     0.037893 (c=  0.19466030)
  434a -> 443a  :     0.416581 (c=  0.64543083)
  435a -> 443a  :     0.034600 (c= -0.18601091)
  437a -> 443a  :     0.041571 (c= -0.20388933)
  440a -> 444a  :     0.365009 (c= -0.60415941)

STATE 12:  E=   0.124587 au      3.390 eV    27343.7 cm**-1 <S**2> =   0.000000 Mult 1
  431a -> 443a  :     0.052329 (c=  0.22875540)
  432a -> 443a  :     0.028475 (c=  0.16874499)
  433a -> 443a  :     0.484934 (c= -0.69637186)
  434a -> 443a  :     0.163273 (c= -0.40407087)
  435a -> 443a  :     0.113234 (c=  0.33650316)
  440a -> 444a  :     0.134003 (c= -0.36606448)

STATE 13:  E=   0.125353 au      3.411 eV    27511.9 cm**-1 <S**2> =   0.000000 Mult 1
  430a -> 443a  :     0.022075 (c=  0.14857775)
  431a -> 443a  :     0.094465 (c= -0.30735159)
```

```
  432a -> 443a  :     0.117333 (c= -0.34253954)
  433a -> 443a  :     0.443083 (c= -0.66564485)
  434a -> 443a  :     0.019326 (c=  0.13901727)
  435a -> 443a  :     0.137939 (c= -0.37140193)
  437a -> 443a  :     0.010104 (c= -0.10051752)
  440a -> 444a  :     0.104668 (c=  0.32352502)

STATE 14:  E=   0.126901 au      3.453 eV    27851.5 cm**-1 <S**2> =   0.000000 Mult 1
  430a -> 443a  :     0.026695 (c=  0.16338700)
  431a -> 443a  :     0.163721 (c=  0.40462415)
  432a -> 443a  :     0.735415 (c= -0.85756367)
  435a -> 443a  :     0.020802 (c=  0.14422820)
  440a -> 444a  :     0.010847 (c= -0.10414877)

STATE 15:  E=   0.127299 au      3.464 eV    27938.8 cm**-1 <S**2> =   0.000000 Mult 1
  430a -> 443a  :     0.011124 (c= -0.10547124)
  431a -> 443a  :     0.020476 (c= -0.14309432)
  439a -> 444a  :     0.797963 (c=  0.89328761)
  439a -> 445a  :     0.027952 (c=  0.16718912)
  440a -> 444a  :     0.014305 (c= -0.11960342)
  440a -> 445a  :     0.010192 (c= -0.10095499)
  441a -> 445a  :     0.023446 (c=  0.15312096)
  442a -> 445a  :     0.034360 (c= -0.18536585)

STATE 16:  E=   0.127681 au      3.474 eV    28022.7 cm**-1 <S**2> =   0.000000 Mult 1
  430a -> 443a  :     0.014464 (c= -0.12026623)
  431a -> 443a  :     0.102948 (c= -0.32085443)
  439a -> 444a  :     0.010095 (c=  0.10047461)
  440a -> 444a  :     0.010309 (c= -0.10153557)
  442a -> 445a  :     0.796798 (c=  0.89263567)

STATE 17:  E=   0.127902 au      3.480 eV    28071.2 cm**-1 <S**2> =   0.000000 Mult 1
  428a -> 443a  :     0.014035 (c= -0.11846730)
  429a -> 443a  :     0.011015 (c=  0.10495393)
  430a -> 443a  :     0.814618 (c=  0.90256197)
  431a -> 443a  :     0.067410 (c= -0.25963431)
  432a -> 443a  :     0.017896 (c=  0.13377645)
  435a -> 443a  :     0.013872 (c=  0.11778087)
  442a -> 446a  :     0.011878 (c=  0.10898566)

STATE 18:  E=   0.128353 au      3.493 eV    28170.2 cm**-1 <S**2> =   0.000000 Mult 1
  427a -> 443a  :     0.058954 (c= -0.24280479)
  428a -> 443a  :     0.016131 (c= -0.12700658)
  429a -> 443a  :     0.276604 (c=  0.52593126)
  430a -> 443a  :     0.049850 (c= -0.22327037)
  431a -> 443a  :     0.258018 (c= -0.50795471)
  432a -> 443a  :     0.037089 (c= -0.19258383)
  435a -> 443a  :     0.012652 (c=  0.11248137)
  437a -> 444a  :     0.012087 (c=  0.10994290)
  439a -> 444a  :     0.050787 (c= -0.22536017)
  440a -> 444a  :     0.075138 (c= -0.27411273)
  442a -> 445a  :     0.105861 (c= -0.32536261)

STATE 19:  E=   0.129214 au      3.516 eV    28359.2 cm**-1 <S**2> =   0.000000 Mult 1
  427a -> 443a  :     0.060839 (c=  0.24665619)
  429a -> 443a  :     0.689109 (c=  0.83012566)
  431a -> 443a  :     0.105746 (c=  0.32518675)
  432a -> 443a  :     0.017841 (c=  0.13356924)
  437a -> 444a  :     0.011291 (c= -0.10625947)
  439a -> 444a  :     0.011181 (c=  0.10574092)
  440a -> 444a  :     0.042212 (c=  0.20545666)
```

```
  442a -> 445a  :     0.012537 (c=  0.11196882)

STATE 20:  E=   0.130083 au      3.540 eV    28549.8 cm**-1 <S**2> =   0.000000 Mult 1
  438a -> 444a  :     0.545367 (c=  0.73848953)
  438a -> 445a  :     0.024772 (c=  0.15739141)
  438a -> 450a  :     0.014920 (c=  0.12214769)
  439a -> 444a  :     0.028580 (c= -0.16905487)
  441a -> 444a  :     0.016780 (c= -0.12953777)
  441a -> 445a  :     0.267793 (c=  0.51748701)
  441a -> 450a  :     0.013204 (c=  0.11490956)

STATE 21:  E=   0.131043 au      3.566 eV    28760.6 cm**-1 <S**2> =   0.000000 Mult 1
  427a -> 443a  :     0.011025 (c= -0.10500213)
  428a -> 443a  :     0.862728 (c=  0.92883162)
  437a -> 444a  :     0.016732 (c=  0.12935413)
  442a -> 446a  :     0.057113 (c=  0.23898260)

STATE 22:  E=   0.133049 au      3.620 eV    29200.9 cm**-1 <S**2> =   0.000000 Mult 1
  437a -> 444a  :     0.048931 (c=  0.22120291)
  438a -> 444a  :     0.304674 (c= -0.55197278)
  439a -> 444a  :     0.010730 (c= -0.10358509)
  441a -> 445a  :     0.485937 (c=  0.69709173)
  442a -> 446a  :     0.055723 (c= -0.23605643)

STATE 23:  E=   0.133251 au      3.626 eV    29245.2 cm**-1 <S**2> =   0.000000 Mult 1
  427a -> 443a  :     0.031030 (c= -0.17615209)
  428a -> 443a  :     0.013995 (c= -0.11830000)
  437a -> 444a  :     0.226281 (c= -0.47568999)
  438a -> 444a  :     0.030634 (c= -0.17502598)
  441a -> 445a  :     0.072670 (c=  0.26957290)
  442a -> 446a  :     0.524427 (c=  0.72417331)
  442a -> 447a  :     0.024974 (c= -0.15803014)

STATE 24:  E=   0.134205 au      3.652 eV    29454.6 cm**-1 <S**2> =   0.000000 Mult 1
  426a -> 443a  :     0.076039 (c= -0.27575101)
  427a -> 443a  :     0.416790 (c=  0.64559268)
  437a -> 443a  :     0.012662 (c= -0.11252524)
  437a -> 444a  :     0.220833 (c=  0.46992874)
  442a -> 446a  :     0.126915 (c=  0.35625174)
  442a -> 447a  :     0.051322 (c= -0.22654291)
  442a -> 449a  :     0.020005 (c= -0.14143922)

STATE 25:  E=   0.135469 au      3.686 eV    29732.1 cm**-1 <S**2> =   0.000000 Mult 1
  425a -> 443a  :     0.113565 (c=  0.33699455)
  426a -> 443a  :     0.262143 (c=  0.51199877)
  427a -> 443a  :     0.263370 (c=  0.51319541)
  431a -> 443a  :     0.017651 (c= -0.13285790)
  437a -> 444a  :     0.221825 (c= -0.47098251)
  440a -> 444a  :     0.015002 (c= -0.12248154)
  442a -> 449a  :     0.011073 (c= -0.10523067)

STATE 26:  E=   0.136468 au      3.713 eV    29951.3 cm**-1 <S**2> =   0.000000 Mult 1
  425a -> 443a  :     0.015475 (c=  0.12439897)
  426a -> 443a  :     0.036219 (c=  0.19031310)
  437a -> 444a  :     0.020369 (c=  0.14272083)
  439a -> 444a  :     0.029847 (c=  0.17276404)
  439a -> 445a  :     0.204555 (c= -0.45227726)
  439a -> 449a  :     0.045188 (c= -0.21257470)
  439a -> 450a  :     0.012790 (c= -0.11309207)
  440a -> 445a  :     0.254677 (c=  0.50465515)
  440a -> 447a  :     0.012164 (c= -0.11029255)
```

441a -> 445a : 0.018288 (c= 0.13523387)
441a -> 449a : 0.056572 (c= -0.23784922)
442a -> 447a : 0.190590 (c= -0.43656580)

STATE 27: E= 0.136960 au 3.727 eV 30059.2 cm**-1 <S**2> = 0.000000 Mult 1
426a -> 443a : 0.055783 (c= 0.23618387)
438a -> 444a : 0.012299 (c= 0.11090052)
439a -> 445a : 0.196164 (c= 0.44290432)
439a -> 449a : 0.020610 (c= 0.14356035)
440a -> 445a : 0.036198 (c= -0.19025799)
441a -> 446a : 0.018186 (c= 0.13485690)
442a -> 446a : 0.021457 (c= -0.14648196)
442a -> 447a : 0.538472 (c= -0.73380627)
442a -> 448a : 0.014606 (c= 0.12085502)

STATE 28: E= 0.137671 au 3.746 eV 30215.2 cm**-1 <S**2> = 0.000000 Mult 1
426a -> 443a : 0.260602 (c= 0.51049182)
427a -> 443a : 0.010432 (c= -0.10213913)
428a -> 443a : 0.013968 (c= -0.11818591)
431a -> 443a : 0.010231 (c= 0.10114605)
435a -> 443a : 0.015899 (c= -0.12609179)
437a -> 444a : 0.062231 (c= 0.24946215)
439a -> 445a : 0.028346 (c= 0.16836174)
439a -> 447a : 0.010336 (c= -0.10166494)
439a -> 449a : 0.011427 (c= 0.10689835)
440a -> 445a : 0.120214 (c= 0.34671923)
440a -> 449a : 0.016953 (c= -0.13020444)
441a -> 446a : 0.059609 (c= -0.24414948)
441a -> 447a : 0.043729 (c= -0.20911434)
441a -> 449a : 0.089369 (c= 0.29894640)
442a -> 446a : 0.069216 (c= 0.26308881)
442a -> 447a : 0.027996 (c= 0.16731861)
442a -> 449a : 0.038981 (c= -0.19743676)

STATE 29: E= 0.137828 au 3.750 eV 30249.7 cm**-1 <S**2> = 0.000000 Mult 1
425a -> 443a : 0.553826 (c= 0.74419508)
427a -> 443a : 0.026877 (c= -0.16394163)
435a -> 443a : 0.011033 (c= -0.10503627)
437a -> 444a : 0.043812 (c= 0.20931404)
440a -> 445a : 0.080444 (c= -0.28362651)
441a -> 446a : 0.051803 (c= 0.22760214)
441a -> 447a : 0.021282 (c= 0.14588181)
442a -> 446a : 0.015305 (c= 0.12371223)
442a -> 447a : 0.019503 (c= 0.13965260)
442a -> 449a : 0.071946 (c= 0.26822661)

STATE 30: E= 0.138289 au 3.763 eV 30350.8 cm**-1 <S**2> = 0.000000 Mult 1
425a -> 443a : 0.017588 (c= -0.13262099)
426a -> 443a : 0.064482 (c= 0.25393343)
437a -> 444a : 0.017763 (c= 0.13327859)
439a -> 445a : 0.194793 (c= -0.44135380)
440a -> 445a : 0.380085 (c= -0.61651058)
441a -> 446a : 0.187861 (c= -0.43342928)
441a -> 447a : 0.017321 (c= -0.13161102)
442a -> 447a : 0.020820 (c= -0.14429020)
442a -> 449a : 0.019601 (c= 0.14000441)

4.2 Ni(cod) siliconoid/silylene 3a

4.2.1 Optimization and molecular orbitals

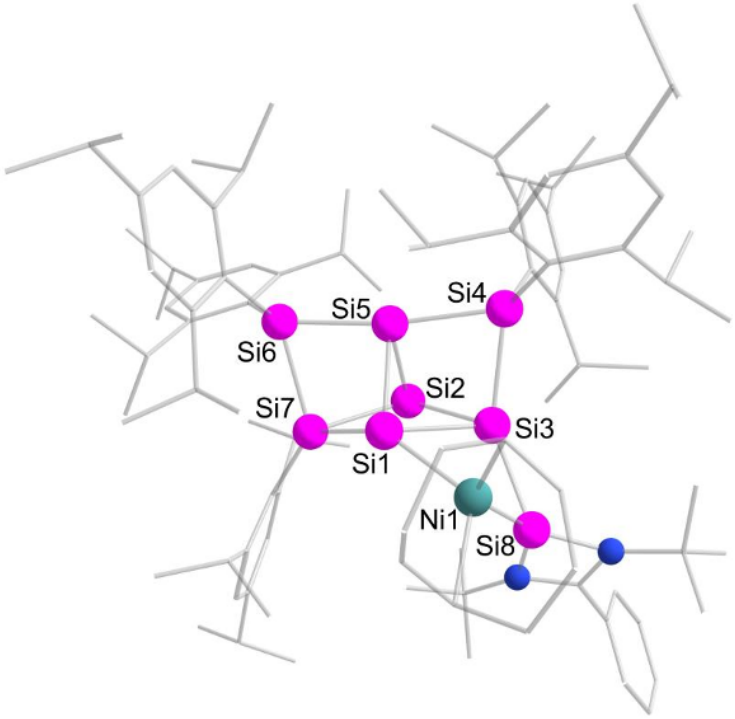

Supplementary Figure S1. Optimized molecular structure of Ni(cod) siliconoid/silylene **3a** at the B3LYP/def2-TZVP level of theory.[23–29] Hydrogen atoms are omitted for clarity. Contour value at 0.05.

Supplementary Table S12. Coordinates of Ni(cod) siliconoid/silylene **3a** at the B3LYP/def2-TZVP level of theory.[23–29]

Ni	18.45466	8.9424	18.70953
Si	17.892297	11.061103	17.954707
Si	17.447081	9.140304	16.54695
Si	16.891888	7.501234	18.036751
C	20.597281	8.955439	18.441452
C	20.211351	7.657259	18.673526
C	18.401899	8.443955	20.833313
C	19.012818	9.66467	20.770055
Si	15.977399	10.957959	16.07106
Si	18.069348	11.930833	15.756746
Si	16.102104	12.524356	17.818329
Si	18.879789	9.942347	14.783437
N	15.084273	7.219591	18.29722
N	16.437562	5.804329	17.441658
C	15.170959	5.96751	17.846058
C	21.183299	9.90199	19.45659
C	20.3207	6.933799	20.001074
C	19.112215	7.117147	20.950513
C	20.506774	9.869458	20.835193
Si	17.339288	14.064386	16.417274

C	14.519107	12.765402	18.850757
C	18.103737	9.777943	13.034334
C	20.762013	9.571394	14.680944
C	13.913021	8.023519	18.688121
C	17.194583	4.587487	17.122169
C	14.095782	4.953465	17.818952
C	18.801242	15.225229	16.869045
C	15.997725	15.109762	15.557673
C	13.264314	12.791888	18.193257
C	14.530245	12.673567	20.254911
C	16.993833	8.962842	12.709449
C	18.609203	10.625843	12.017744
C	21.181003	8.439292	13.950082
C	21.766989	10.479817	15.115353
C	13.137932	8.44273	17.435559
C	12.995875	7.272932	19.660051
C	14.460594	9.262541	19.389851
C	16.390268	3.588939	16.281951
C	17.670144	3.924864	18.422339
C	18.396783	5.052223	16.30549
C	13.262908	4.851845	16.708037
C	13.917363	4.089257	18.896589
C	19.383792	15.284949	18.153796
C	19.389818	16.014755	15.85047
C	15.508614	14.925988	14.248692
C	15.457171	16.16508	16.331777
C	12.099588	12.607731	18.92857
C	13.102488	13.064118	16.70657
C	13.334853	12.497512	20.949786
C	15.799053	12.777429	21.079994
C	16.387854	9.084874	11.459155
C	16.410961	7.887623	13.614659
C	17.975276	10.702915	10.784044
C	19.87603	11.448165	12.180264
C	22.518604	8.287912	13.588287
C	20.244509	7.316699	13.533037
C	23.083902	10.289303	14.714609
C	21.502685	11.688764	16.005802
C	12.260204	3.892399	16.675137
C	12.915432	3.129863	18.86201
C	20.514423	16.063109	18.381068
C	18.829902	14.548908	19.358152
C	20.495634	16.81099	16.138626
C	18.882873	16.062005	14.416164
C	14.530998	15.788733	13.75436
C	15.993796	13.830061	13.312925
C	14.506913	17.015966	15.782439

C	15.894214	16.452911	17.762893
C	12.110662	12.429525	20.306336
C	12.465084	11.888267	15.962012
C	12.28776	14.340017	16.461354
C	15.712644	13.958647	22.054786
C	16.105415	11.480087	21.831728
C	16.841757	9.960146	10.488025
C	16.595254	6.48234	13.026246
C	14.93206	8.119595	13.939533
C	19.661446	12.934376	11.912493
C	21.012475	10.900834	11.307493
C	23.483354	9.216012	13.929613
C	20.719852	5.978733	14.114491
C	20.100993	7.210253	12.009845
C	21.319624	12.979554	15.200679
C	22.609963	11.921772	17.043536
C	12.085592	3.029613	17.750797
C	21.088815	16.841288	17.389659
C	19.776915	13.44775	19.837519
C	18.491463	15.50913	20.503092
C	20.015985	15.989057	13.384427
C	18.045549	17.32069	14.154055
C	14.027874	16.848005	14.491086
C	14.931276	12.744244	13.108222
C	16.438292	14.373659	11.949764
C	14.718562	16.458593	18.747081
C	16.685799	17.763209	17.849846
C	10.836593	12.165911	21.079015
C	16.130467	10.096316	9.160027
C	24.916329	9.062269	13.470809
C	22.3181	17.68255	17.653775
C	12.998897	17.788795	13.902365
C	17.04123	9.728984	7.982902
C	15.542867	11.502878	8.987982
C	25.320412	10.203632	12.528975
C	25.888048	8.949052	14.651054
C	23.528351	16.80596	17.999441
C	22.067148	18.731715	18.743267
C	11.698684	17.800339	14.7149
C	13.56546	19.206276	13.751756
H	13.408713	5.518114	15.86848
H	11.616671	3.817439	15.808339
H	11.304111	2.281433	17.724208
H	12.780607	2.462319	19.703088
H	14.55805	4.178304	19.763706
H	13.804515	8.941282	16.733321
H	12.341191	9.137289	17.704057

H	12.689324	7.580089	16.942545
H	12.245257	7.966896	20.04134
H	13.565715	6.889235	20.508053
H	12.473525	6.444622	19.186725
H	15.161035	9.794695	18.748958
H	14.978334	8.984543	20.307783
H	13.65108	9.945127	19.6406
H	17.063368	2.806482	15.927949
H	15.952905	4.077555	15.411234
H	15.59361	3.113085	16.847913
H	18.301436	3.061294	18.204451
H	16.82141	3.582891	19.01595
H	19.05019	4.211908	16.073457
H	18.976609	5.790249	16.857109
H	18.24626	4.633255	19.018534
H	18.070778	5.508841	15.372915
H	15.525937	8.468671	11.231954
H	18.381411	11.366304	10.031102
H	20.211988	11.363459	13.207658
H	19.30346	13.121313	10.899159
H	20.600079	13.474112	12.034388
H	18.936712	13.356321	12.605907
H	20.764853	10.979329	10.246386
H	21.216112	9.856761	11.533157
H	21.928502	11.467909	11.485946
H	16.952077	7.902298	14.55896
H	16.066663	6.377113	12.07694
H	16.194626	5.735614	13.71551
H	17.643825	6.253059	12.848529
H	14.304675	7.982127	13.056191
H	14.765654	9.123434	14.326969
H	14.602848	7.40765	14.699739
H	15.296835	9.387057	9.168512
H	16.490906	9.774199	7.040305
H	17.443022	8.720938	8.09852
H	17.885705	10.417551	7.907937
H	14.986385	11.578348	8.050884
H	16.332565	12.257042	8.970665
H	14.86886	11.749312	9.809745
H	22.816151	7.422484	13.008743
H	23.829483	11.005967	15.029649
H	24.972723	8.127826	12.903764
H	26.335078	10.054529	12.152589
H	25.293137	11.164963	13.046775
H	24.642593	10.265812	11.676077
H	25.608694	8.125698	15.31053
H	25.893946	9.864878	15.245849

H	26.906742	8.775586	14.296752
H	19.258812	7.519175	13.954813
H	20.001756	5.188651	13.890486
H	20.843439	6.040475	15.195698
H	21.678637	5.683621	13.686223
H	19.636441	8.099412	11.590475
H	19.486527	6.349796	11.73896
H	21.077061	7.077602	11.539601
H	20.580024	11.505622	16.555861
H	22.202555	13.170432	14.585409
H	21.173237	13.829852	15.867243
H	20.457381	12.929507	14.541672
H	23.505542	12.348741	16.587956
H	22.898428	11.002494	17.550316
H	22.263392	12.637886	17.790574
H	20.950484	16.068471	19.371869
H	20.926773	17.418553	15.353499
H	18.248706	15.191766	14.252341
H	19.601682	15.828054	12.388445
H	20.7068	15.178024	13.603119
H	20.585454	16.919002	13.349421
H	18.660416	18.212954	14.2948
H	17.188011	17.389811	14.817106
H	17.675715	17.324951	13.126593
H	17.905623	14.061291	19.053436
H	19.995523	12.750263	19.030136
H	19.324497	12.88413	20.656178
H	20.721868	13.863543	20.19442
H	17.745067	16.242151	20.197727
H	19.373383	16.05494	20.841522
H	18.098033	14.957806	21.354973
H	22.547197	18.215175	16.725599
H	23.722962	16.078104	17.210007
H	24.424147	17.416763	18.133671
H	22.944584	19.368915	18.875329
H	21.852095	18.257192	19.703153
H	21.216819	19.365976	18.487533
H	23.357685	16.253432	18.926126
H	14.156558	15.6383	12.749131
H	14.125778	17.83125	16.384241
H	16.557371	15.652309	18.088193
H	14.007637	17.254218	18.517302
H	15.082815	16.626748	19.763072
H	14.185938	15.509386	18.735839
H	17.578852	17.729161	17.228167
H	16.998342	17.956422	18.877968
H	16.07343	18.606282	17.523275

H	12.76208	17.417393	12.900488
H	10.954728	18.444894	14.241165
H	11.870758	18.177219	15.725343
H	11.279016	16.797569	14.802248
H	14.478173	19.201762	13.153809
H	13.808871	19.63369	14.727024
H	12.839472	19.86478	13.269124
H	16.854447	13.34565	13.776097
H	14.056513	13.149097	12.592431
H	14.604991	12.325917	14.058147
H	15.33747	11.926418	12.509794
H	16.845899	13.56358	11.345418
H	17.201062	15.146384	12.046908
H	15.59858	14.801825	11.399789
H	11.151111	12.608539	18.406607
H	13.357574	12.400294	22.028654
H	16.629586	12.964997	20.396529
H	15.54596	14.895821	21.523561
H	16.63314	14.049224	22.63398
H	14.892818	13.825015	22.762467
H	16.224284	10.649067	21.139557
H	15.30115	11.228285	22.525949
H	17.024981	11.578952	22.412142
H	14.091725	13.233538	16.28263
H	12.353546	12.12667	14.90269
H	11.473388	11.663106	16.360192
H	13.079219	10.994022	16.04491
H	12.287197	14.577117	15.397317
H	12.706627	15.192612	16.990366
H	11.250908	14.2168	16.782129
H	11.104586	12.137528	22.139716
C	10.247711	10.797798	20.710434
C	9.802128	13.280852	20.889743
H	9.356922	10.583674	21.305509
H	10.974005	10.001484	20.8827
H	9.963465	10.768564	19.656273
H	10.218398	14.251556	21.163524
H	8.920908	13.097842	21.508752
H	9.47162	13.340477	19.850785
H	20.753577	9.237948	17.408843
H	20.103777	7.029229	17.80083
H	21.235751	7.250328	20.504422
H	20.444206	5.865898	19.807743
H	18.381196	6.336563	20.738103
H	19.440578	6.9612	21.986955
H	17.343075	8.42477	21.056254
H	18.401606	10.541578	20.908551

H	20.950645	9.090799	21.456394
H	20.710838	10.813512	21.344242
H	21.098158	10.909044	19.056681
H	22.259683	9.711643	19.568597

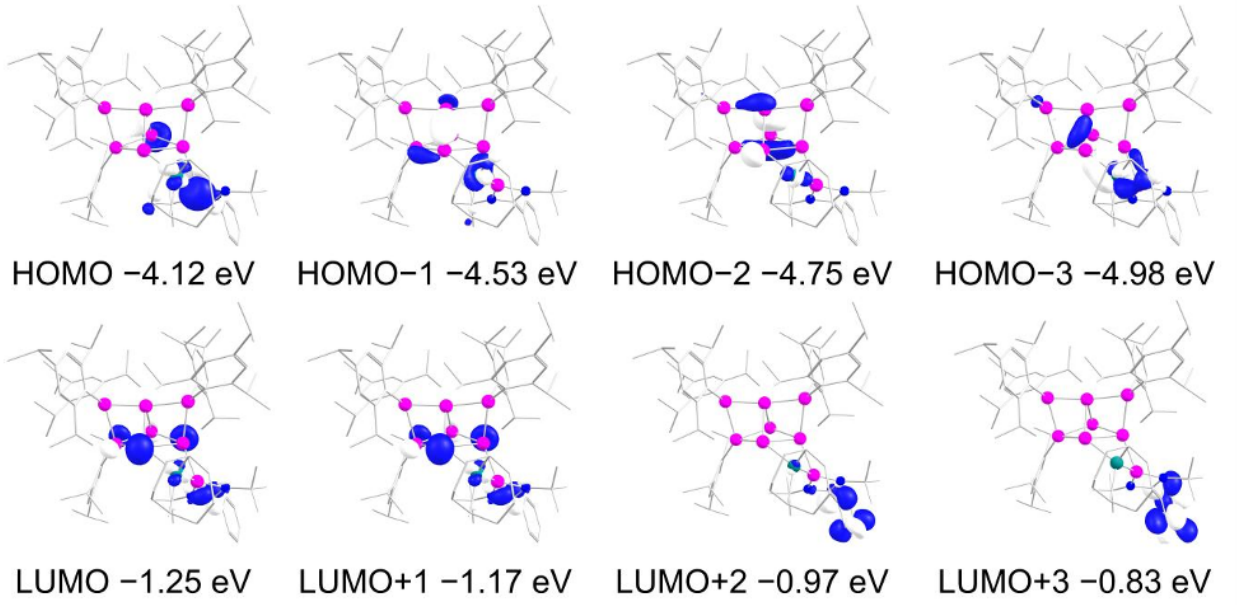

Supplementary Figure S53. Selected frontier orbitals of Ni(cod) siliconoid/silylene **3a** at B3LYP/def2-TZVP level of theory (contour value at 0.05).[23–29] Hydrogen atoms are omitted for clarity.

4.2.2 Experimental vs. calculated NMR shifts

Supplementary Table S13. Comparison of experimental vs. calculated NMR chemical shifts for Ni(cod) siliconoid/silylene **3a** at the TPSSh/def2-TZVP level of theory.[26–29,33]

	Exp. **3a** $\delta(^{29}Si)$ [ppm]	Calc. **3a** $\delta(^{29}Si)$ [ppm]
Si3 (*Si*NHSi)	−10.2	0.7
Si8 (NH*Si*)	89.1	90.5
Si7 (*Si*Tip)	50.0	60.0
Si6 (*Si*Tip$_2$)	39.0	32.9
Si4 (*Si*Tip$_2$)	−13.3	−19.0
Si5 (unsubstituted)	−83.1	−80.8
Si1 (unsubstituted)	−154.0	−151.9
Si2 (unsubstituted)	−340.7	−346.2

4.2.3 TD-DFT calculations

Supplementary Table S14. Transition Energy. wavelength. and oscillator strengths of the electronic transition of Ni(cod) siliconoid/silylene **3a** calculated at the TD-TPSSh/def2-TZVP.[26–29,33,34] level of theory (the 445th orbital is the highest occupied orbital (HOMO) and 446th orbital is the lowest unoccupied molecular orbital (LUMO) shown in Supplementary Figure S53).

STATE 1: E= 0.083385 au 2.269 eV 18300.9 cm**-1 <S**2> = 0.000000 Mult 1
443a -> 446a : 0.011432 (c= -0.10691906)
444a -> 446a : 0.189275 (c= 0.43505786)
445a -> 446a : 0.516370 (c= -0.71858895)
445a -> 447a : 0.190026 (c= 0.43591937)
445a -> 448a : 0.048401 (c= -0.22000263)

STATE 2: E= 0.087666 au 2.386 eV 19240.5 cm**-1 <S**2> = 0.000000 Mult 1
443a -> 446a : 0.034645 (c= 0.18613295)
444a -> 446a : 0.726046 (c= 0.85208323)
445a -> 446a : 0.052594 (c= 0.22933452)
445a -> 447a : 0.135751 (c= -0.36844452)

STATE 3: E= 0.088283 au 2.402 eV 19375.8 cm**-1 <S**2> = 0.000000 Mult 1
443a -> 446a : 0.021628 (c= -0.14706523)
444a -> 446a : 0.022816 (c= -0.15104870)
445a -> 446a : 0.236832 (c= -0.48665352)
445a -> 447a : 0.654462 (c= -0.80898846)
445a -> 448a : 0.029734 (c= -0.17243672)

STATE 4: E= 0.096911 au 2.637 eV 21269.5 cm**-1 <S**2> = 0.000000 Mult 1
443a -> 446a : 0.101779 (c= 0.31902874)
444a -> 447a : 0.046828 (c= -0.21639831)
445a -> 446a : 0.035528 (c= 0.18848842)
445a -> 448a : 0.748071 (c= -0.86491075)
445a -> 451a : 0.012017 (c= -0.10962389)

STATE 5: E= 0.098576 au 2.682 eV 21634.9 cm**-1 <S**2> = 0.000000 Mult 1
442a -> 446a : 0.611813 (c= 0.78218496)
443a -> 446a : 0.061309 (c= -0.24760556)
444a -> 447a : 0.227232 (c= -0.47668854)
444a -> 448a : 0.020730 (c= 0.14398064)
445a -> 448a : 0.010527 (c= 0.10259909)

STATE 6: E= 0.098839 au 2.690 eV 21692.6 cm**-1 <S**2> = 0.000000 Mult 1
445a -> 449a : 0.995456 (c= -0.99772528)

STATE 7: E= 0.099683 au 2.713 eV 21877.9 cm**-1 <S**2> = 0.000000 Mult 1
442a -> 446a : 0.059601 (c= 0.24413405)
443a -> 446a : 0.359974 (c= -0.59997839)
444a -> 447a : 0.387787 (c= 0.62272532)
444a -> 448a : 0.019063 (c= -0.13806779)
445a -> 446a : 0.017034 (c= 0.13051551)
445a -> 448a : 0.103391 (c= -0.32154539)
445a -> 450a : 0.016132 (c= 0.12701138)

STATE 8: E= 0.101674 au 2.767 eV 22314.8 cm**-1 <S**2> = 0.000000 Mult 1
442a -> 446a : 0.157245 (c= -0.39654150)
443a -> 446a : 0.288001 (c= -0.53665721)
444a -> 447a : 0.148598 (c= -0.38548423)
445a -> 446a : 0.059421 (c= 0.24376525)
445a -> 448a : 0.015773 (c= -0.12558895)
445a -> 450a : 0.253762 (c= -0.50374768)

STATE 9: E= 0.104272 au 2.837 eV 22885.1 cm**-1 <S**2> = 0.000000 Mult 1
441a -> 446a : 0.037269 (c= 0.19305180)

```
  442a -> 446a  :     0.053510 (c= -0.23132189)
  443a -> 446a  :     0.045147 (c= -0.21247761)
  444a -> 446a  :     0.015297 (c=  0.12368296)
  444a -> 447a  :     0.115523 (c= -0.33988606)
  444a -> 448a  :     0.016450 (c= -0.12825648)
  445a -> 450a  :     0.627163 (c=  0.79193652)
  445a -> 451a  :     0.028855 (c=  0.16986808)

STATE 10:  E=   0.106830 au      2.907 eV    23446.5 cm**-1 <S**2> =   0.000000 Mult 1
  443a -> 447a  :     0.014203 (c=  0.11917719)
  444a -> 447a  :     0.033465 (c=  0.18293556)
  444a -> 448a  :     0.896608 (c=  0.94689413)
  445a -> 450a  :     0.019291 (c=  0.13889108)

STATE 11:  E=   0.110187 au      2.998 eV    24183.4 cm**-1 <S**2> =   0.000000 Mult 1
  440a -> 446a  :     0.054144 (c= -0.23268882)
  441a -> 446a  :     0.069531 (c=  0.26368663)
  442a -> 447a  :     0.029740 (c=  0.17245290)
  443a -> 447a  :     0.592754 (c= -0.76990544)
  443a -> 448a  :     0.067045 (c=  0.25893073)
  445a -> 451a  :     0.112023 (c=  0.33469904)

STATE 12:  E=   0.110424 au      3.005 eV    24235.2 cm**-1 <S**2> =   0.000000 Mult 1
  440a -> 446a  :     0.040442 (c= -0.20110085)
  441a -> 446a  :     0.346095 (c=  0.58829801)
  445a -> 451a  :     0.546615 (c= -0.73933385)

STATE 13:  E=   0.110698 au      3.012 eV    24295.4 cm**-1 <S**2> =   0.000000 Mult 1
  440a -> 446a  :     0.197356 (c=  0.44424763)
  441a -> 446a  :     0.158476 (c= -0.39809095)
  442a -> 446a  :     0.012104 (c= -0.11001794)
  442a -> 447a  :     0.028935 (c= -0.17010158)
  443a -> 447a  :     0.257880 (c= -0.50781896)
  443a -> 448a  :     0.027391 (c=  0.16550193)
  445a -> 450a  :     0.017013 (c=  0.13043204)
  445a -> 451a  :     0.211001 (c= -0.45934896)

STATE 14:  E=   0.111719 au      3.040 eV    24519.4 cm**-1 <S**2> =   0.000000 Mult 1
  444a -> 449a  :     0.995849 (c=  0.99792252)

STATE 15:  E=   0.113376 au      3.085 eV    24883.2 cm**-1 <S**2> =   0.000000 Mult 1
  440a -> 446a  :     0.020744 (c=  0.14402607)
  441a -> 446a  :     0.055346 (c= -0.23525685)
  442a -> 446a  :     0.012901 (c=  0.11358255)
  442a -> 447a  :     0.745817 (c=  0.86360689)
  442a -> 448a  :     0.066960 (c= -0.25876557)
  442a -> 450a  :     0.014727 (c= -0.12135572)
  444a -> 450a  :     0.028627 (c= -0.16919656)

STATE 16:  E=   0.114091 au      3.105 eV    25040.1 cm**-1 <S**2> =   0.000000 Mult 1
  440a -> 446a  :     0.023437 (c= -0.15309071)
  441a -> 446a  :     0.020166 (c= -0.14200590)
  444a -> 450a  :     0.071302 (c=  0.26702350)
  445a -> 452a  :     0.832679 (c= -0.91251245)
  445a -> 453a  :     0.010213 (c= -0.10105994)

STATE 17:  E=   0.115254 au      3.136 eV    25295.4 cm**-1 <S**2> =   0.000000 Mult 1
  440a -> 446a  :     0.089954 (c=  0.29992256)
  441a -> 446a  :     0.022278 (c=  0.14925664)
  442a -> 447a  :     0.016400 (c=  0.12806330)
  443a -> 448a  :     0.011549 (c=  0.10746703)
```

444a -> 450a : 0.721015 (c= 0.84912615)
444a -> 451a : 0.011720 (c= -0.10825705)
445a -> 452a : 0.041912 (c= 0.20472541)

STATE 18: E= 0.116696 au 3.175 eV 25611.7 cm**-1 <S**2> = 0.000000 Mult 1
440a -> 446a : 0.049909 (c= 0.22340305)
441a -> 446a : 0.037458 (c= 0.19354155)
443a -> 448a : 0.016204 (c= -0.12729434)
445a -> 452a : 0.046768 (c= -0.21625983)
445a -> 453a : 0.760765 (c= 0.87221870)
445a -> 455a : 0.035034 (c= 0.18717384)

STATE 19: E= 0.117873 au 3.207 eV 25870.0 cm**-1 <S**2> = 0.000000 Mult 1
440a -> 446a : 0.047149 (c= 0.21713921)
441a -> 446a : 0.014848 (c= 0.12185056)
443a -> 447a : 0.077355 (c= -0.27812731)
443a -> 448a : 0.652797 (c= -0.80795825)
444a -> 451a : 0.042291 (c= 0.20564669)
445a -> 453a : 0.072490 (c= -0.26923997)
445a -> 454a : 0.012673 (c= 0.11257473)

STATE 20: E= 0.118289 au 3.219 eV 25961.5 cm**-1 <S**2> = 0.000000 Mult 1
438a -> 446a : 0.014644 (c= 0.12101376)
439a -> 446a : 0.013983 (c= 0.11825020)
440a -> 446a : 0.172327 (c= 0.41512300)
440a -> 447a : 0.023075 (c= -0.15190425)
441a -> 446a : 0.120048 (c= 0.34647911)
443a -> 448a : 0.112931 (c= 0.33605167)
443a -> 450a : 0.015749 (c= -0.12549533)
444a -> 450a : 0.032590 (c= -0.18052695)
444a -> 451a : 0.014182 (c= -0.11909007)
445a -> 450a : 0.012019 (c= -0.10963270)
445a -> 451a : 0.023114 (c= 0.15203363)
445a -> 452a : 0.035491 (c= -0.18839031)
445a -> 453a : 0.069434 (c= -0.26350280)
445a -> 454a : 0.209576 (c= 0.45779489)
445a -> 457a : 0.012786 (c= 0.11307668)

STATE 21: E= 0.119303 au 3.246 eV 26183.9 cm**-1 <S**2> = 0.000000 Mult 1
442a -> 447a : 0.015057 (c= -0.12270730)
443a -> 448a : 0.068239 (c= -0.26122572)
444a -> 451a : 0.776575 (c= -0.88123518)
444a -> 452a : 0.037932 (c= 0.19476178)
444a -> 453a : 0.013357 (c= 0.11557234)
445a -> 454a : 0.016957 (c= 0.13022059)

STATE 22: E= 0.120301 au 3.274 eV 26403.0 cm**-1 <S**2> = 0.000000 Mult 1
438a -> 446a : 0.036876 (c= 0.19203215)
439a -> 446a : 0.218163 (c= 0.46707894)
439a -> 447a : 0.010152 (c= -0.10075949)
440a -> 447a : 0.028087 (c= -0.16759120)
441a -> 446a : 0.026184 (c= 0.16181347)
441a -> 447a : 0.019977 (c= 0.14133858)
442a -> 448a : 0.018853 (c= 0.13730728)
444a -> 451a : 0.032581 (c= -0.18050255)
445a -> 453a : 0.010814 (c= -0.10398940)
445a -> 454a : 0.434603 (c= -0.65924411)
445a -> 455a : 0.047286 (c= 0.21745342)

STATE 23: E= 0.120685 au 3.284 eV 26487.2 cm**-1 <S**2> = 0.000000 Mult 1
437a -> 446a : 0.033779 (c= 0.18379159)

```
  439a -> 446a  :     0.443319 (c=  0.66582186)
  440a -> 446a  :     0.077201 (c= -0.27785138)
  444a -> 450a  :     0.013866 (c=  0.11775418)
  445a -> 453a  :     0.016682 (c=  0.12915737)
  445a -> 454a  :     0.113323 (c=  0.33663492)
  445a -> 455a  :     0.176764 (c= -0.42043294)
  445a -> 456a  :     0.014109 (c=  0.11878040)

STATE 24:  E=   0.122088 au      3.322 eV    26795.2 cm**-1 <S**2> =   0.000000 Mult 1
  439a -> 446a  :     0.051154 (c= -0.22617341)
  440a -> 446a  :     0.018114 (c=  0.13458938)
  441a -> 447a  :     0.026078 (c=  0.16148785)
  442a -> 447a  :     0.023590 (c=  0.15359186)
  442a -> 448a  :     0.221448 (c=  0.47058251)
  445a -> 453a  :     0.012558 (c=  0.11206142)
  445a -> 454a  :     0.051346 (c= -0.22659662)
  445a -> 455a  :     0.508078 (c= -0.71279564)
  445a -> 456a  :     0.014414 (c=  0.12005735)

STATE 25:  E=   0.122484 au      3.333 eV    26882.2 cm**-1 <S**2> =   0.000000 Mult 1
  440a -> 446a  :     0.028709 (c= -0.16943706)
  440a -> 447a  :     0.026980 (c=  0.16425725)
  441a -> 447a  :     0.087093 (c=  0.29511576)
  442a -> 447a  :     0.042513 (c=  0.20618563)
  442a -> 448a  :     0.480229 (c=  0.69298571)
  445a -> 454a  :     0.085953 (c=  0.29317692)
  445a -> 455a  :     0.132346 (c=  0.36379332)

STATE 26:  E=   0.123100 au      3.350 eV    27017.4 cm**-1 <S**2> =   0.000000 Mult 1
  440a -> 447a  :     0.014324 (c= -0.11968461)
  441a -> 447a  :     0.517138 (c= -0.71912303)
  441a -> 448a  :     0.049129 (c=  0.22164982)
  442a -> 447a  :     0.011208 (c=  0.10586644)
  442a -> 448a  :     0.129138 (c=  0.35935741)
  444a -> 452a  :     0.022131 (c=  0.14876405)
  445a -> 456a  :     0.097353 (c= -0.31201431)
  445a -> 457a  :     0.041252 (c=  0.20310669)
  445a -> 460a  :     0.014649 (c= -0.12103396)

STATE 27:  E=   0.123466 au      3.360 eV    27097.6 cm**-1 <S**2> =   0.000000 Mult 1
  443a -> 449a  :     0.978057 (c= -0.98896766)

STATE 28:  E=   0.123817 au      3.369 eV    27174.7 cm**-1 <S**2> =   0.000000 Mult 1
  438a -> 446a  :     0.015701 (c=  0.12530530)
  441a -> 447a  :     0.168338 (c= -0.41028996)
  442a -> 448a  :     0.018389 (c=  0.13560468)
  443a -> 449a  :     0.015379 (c= -0.12401042)
  443a -> 450a  :     0.082141 (c= -0.28660221)
  445a -> 455a  :     0.016554 (c=  0.12866265)
  445a -> 456a  :     0.213787 (c=  0.46237113)
  445a -> 457a  :     0.254089 (c= -0.50407223)
  445a -> 458a  :     0.022300 (c=  0.14933092)
  445a -> 460a  :     0.080564 (c=  0.28383878)
  445a -> 461a  :     0.051960 (c= -0.22794664)

STATE 29:  E=   0.124215 au      3.380 eV    27261.9 cm**-1 <S**2> =   0.000000 Mult 1
  440a -> 447a  :     0.017508 (c= -0.13231759)
  441a -> 447a  :     0.016472 (c=  0.12834327)
  444a -> 451a  :     0.070670 (c=  0.26583882)
  444a -> 452a  :     0.701188 (c=  0.83736991)
  444a -> 453a  :     0.080264 (c=  0.28330960)
```

444a -> 454a : 0.015041 (c= 0.12264069)
445a -> 456a : 0.012464 (c= 0.11164087)

STATE 30: E= 0.125447 au 3.414 eV 27532.5 cm**-1 <S**2> = 0.000000 Mult 1
438a -> 446a : 0.030534 (c= 0.17474092)
439a -> 446a : 0.019015 (c= -0.13789490)
440a -> 447a : 0.304872 (c= -0.55215223)
440a -> 448a : 0.023920 (c= 0.15466103)
442a -> 450a : 0.017156 (c= 0.13097958)
443a -> 450a : 0.050936 (c= 0.22568996)
444a -> 452a : 0.082585 (c= -0.28737578)
444a -> 453a : 0.047041 (c= 0.21688900)
444a -> 455a : 0.010708 (c= 0.10348105)
445a -> 454a : 0.012094 (c= 0.10997456)
445a -> 455a : 0.015145 (c= -0.12306418)
445a -> 456a : 0.145021 (c= -0.38081607)
445a -> 457a : 0.068600 (c= -0.26191543)
445a -> 458a : 0.047196 (c= 0.21724677)
445a -> 460a : 0.021540 (c= 0.14676366)
445a -> 461a : 0.017694 (c= -0.13301787)

4.3 Ni(PPh$_3$) siliconoid/silylene 3b

4.3.1 Optimization and molecular orbitals

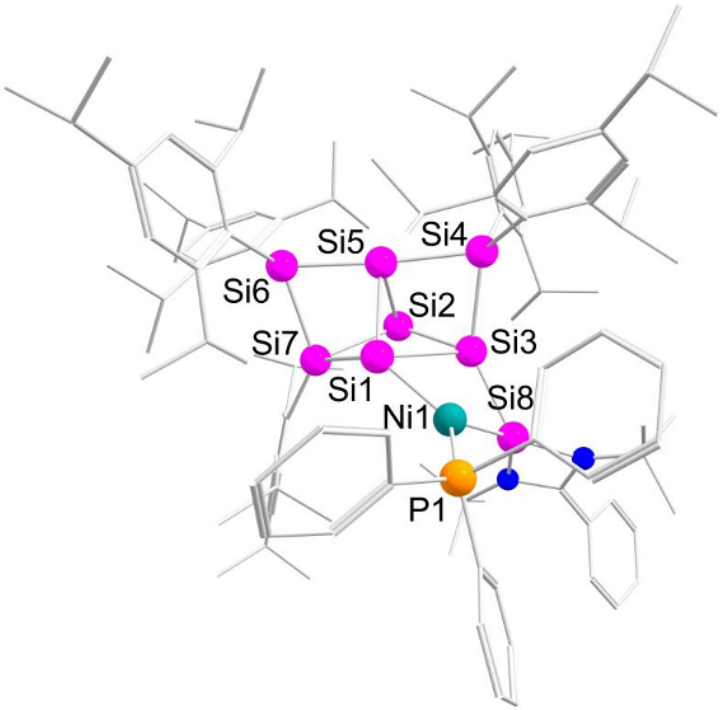

Supplementary Figure S54. Calculated structure of Ni(PPh$_3$) siliconoid/silylene **3b** at the B3LYP/def2-TZVP level of theory.[23–29] Hydrogen atoms are omitted for clarity.

Supplementary Table S15. Coordinates of Ni(PPh_3) siliconoid/silylene **3b** at the B3LYP/def2-TZVP level of theory.[23–29]

Ni	20.167835	10.285606	23.707713
Si	18.620602	9.077116	24.660077
P	19.510486	11.655672	22.122047
Si	22.277925	9.976204	24.259896
Si	20.503717	9.39304	25.900699
N	18.048507	7.348857	24.388392
C	16.811029	7.671676	24.779645
C	18.596592	6.11476	23.79516
N	16.880585	8.947848	25.190527
C	15.853229	9.898658	25.636065
C	18.685256	12.975751	23.089936
C	20.634271	12.588611	21.013947
C	18.224583	11.085347	20.941211
Si	23.622821	8.131859	24.180682
Si	23.375485	10.091814	26.33133
Si	22.391858	7.980396	26.195998
Si	21.476965	10.910637	27.487906
C	21.585508	10.195735	29.263618
C	21.026973	12.772874	27.573194
Si	25.370709	9.339331	25.310132
C	26.551274	8.018355	26.011401
C	26.421009	10.785641	24.611513
C	23.578418	6.625168	23.029363
C	15.602201	6.824742	24.729029
C	14.915795	6.646643	23.529888
C	15.141282	6.200052	25.885428
C	14.008118	5.399401	25.841031
C	13.326843	5.222302	24.642538
C	13.781371	5.848903	23.487535
C	18.045343	4.863062	24.485726
C	20.109405	6.165046	24.00175
C	18.285919	6.081257	22.292827
C	16.497566	11.280867	25.528263
C	15.483457	9.609061	27.095243
C	14.606444	9.860061	24.745018
C	23.829826	5.343251	23.56748
C	23.049014	6.716085	21.724364
C	23.518083	4.211761	22.81859
C	24.390042	5.122063	24.963573
C	22.957449	4.291973	21.552913
C	22.740755	5.556145	21.021853
C	22.573406	3.04079	20.792608
C	22.759767	8.042052	21.041681
C	23.387064	8.119988	19.644843
C	21.255087	8.316484	20.968556
C	23.338153	4.49401	25.88638

C	25.657483	4.260544	24.965522
C	21.049173	2.929941	20.652288
C	23.260388	2.959593	19.425111
C	22.560038	10.759055	30.118328
C	20.867052	9.073136	29.74032
C	21.194818	8.514226	30.972747
C	19.690594	8.432748	29.017737
C	22.187831	9.033744	31.789739
C	22.838773	10.174673	31.35001
C	22.570479	8.37573	33.097531
C	23.323238	12.02526	29.772223
C	24.835063	11.819391	29.770719
C	22.930233	13.194525	30.683279
C	19.918955	6.950483	28.703035
C	18.381616	8.600756	29.801076
C	21.367121	8.156999	34.020209
C	23.320101	7.060804	32.843147
C	20.014147	13.186692	28.468458
C	21.772164	13.779675	26.91162
C	21.566295	15.116767	27.240733
C	22.800239	13.485245	25.830178
C	20.622548	15.521141	28.171887
C	19.838632	14.537125	28.753933
C	20.416727	16.986485	28.486324
C	19.036149	12.222698	29.121937
C	17.588589	12.589578	28.765173
C	19.200988	12.159289	30.644921
C	24.234743	13.476382	26.369632
C	22.705669	14.447621	24.640418
C	20.551347	17.277032	29.984756
C	19.068773	17.48	27.943622
C	26.561168	7.536124	27.335108
C	27.465079	7.456846	25.086513
C	28.367247	6.486838	25.502528
C	27.540851	7.897802	23.630218
C	28.388426	6.011861	26.807148
C	27.468518	6.541184	27.697402
C	29.390614	4.968066	27.251305
C	25.631117	8.050572	28.422221
C	26.393634	8.57969	29.642822
C	24.618848	6.985418	28.856957
C	27.371078	6.741398	22.639855
C	28.834795	8.672815	23.35417
C	29.301567	3.685114	26.417439
C	30.816568	5.534222	27.237984
C	26.306026	11.286015	23.297742
C	27.352168	11.419126	25.472427

C	27.073317	12.377246	22.893213
C	25.373742	10.704873	22.252477
C	27.989344	12.991443	23.727369
C	28.117648	12.484333	25.012183
C	28.805282	14.175712	23.257963
C	27.591829	10.988577	26.912132
C	28.878687	10.162674	27.042073
C	27.651567	12.180006	27.875776
C	24.219143	11.663624	21.953076
C	26.1081	10.316443	20.96493
C	28.44695	15.444964	24.04122
C	30.310651	13.893257	23.323488
C	17.59611	9.863023	21.172058
C	17.849597	11.829254	19.819778
C	16.857796	11.368884	18.964273
C	16.232685	10.150905	19.209918
C	16.607901	9.397277	20.314804
C	19.20881	13.24759	24.356054
C	17.556427	13.673429	22.664035
C	18.629872	14.205827	25.175204
C	17.504444	14.895936	24.741035
C	16.967706	14.626046	23.48736
C	21.095365	12.008098	19.829123
C	21.146177	13.829964	21.388382
C	22.042293	12.649231	19.044694
C	22.553522	13.882573	19.433963
C	22.100086	14.469917	20.607752
H	15.682985	6.329252	26.812694
H	13.659534	4.911237	26.74173
H	12.44337	4.598219	24.608531
H	13.249951	5.71869	22.553794
H	15.262255	7.149284	22.6374
H	20.595022	5.325261	23.505596
H	20.356561	6.135875	25.061689
H	20.53275	7.078202	23.589741
H	18.673638	6.97454	21.804678
H	17.212669	6.019805	22.113439
H	18.756904	5.211221	21.832829
H	16.990845	4.700285	24.274078
H	18.17926	4.933399	25.566072
H	18.598479	3.99218	24.131411
H	14.885092	9.973321	23.696135
H	13.9477	10.687498	25.013641
H	14.046908	8.934275	24.861164
H	16.69888	11.540498	24.490733
H	17.4421	11.306782	26.071227
H	15.841962	12.039757	25.95366

H	14.786565	10.362909	27.465485
H	16.374372	9.625572	27.721939
H	15.008255	8.633104	27.192102
H	23.703092	3.231397	23.241318
H	22.312074	5.643095	20.031518
H	23.203509	8.834618	21.644178
H	22.894527	7.443311	18.94382
H	24.445518	7.859009	19.672223
H	23.290874	9.132169	19.24611
H	21.060241	9.217591	20.388994
H	20.831728	8.472255	21.962502
H	20.727135	7.48738	20.493635
H	24.662992	6.092113	25.38127
H	25.442405	3.23712	24.650703
H	26.071021	4.222746	25.973669
H	26.424166	4.66436	24.309281
H	22.44238	5.110877	25.941598
H	23.736926	4.386646	26.897167
H	23.053748	3.502003	25.527912
H	20.770283	1.99882	20.153418
H	20.651433	3.759471	20.063179
H	20.565139	2.952301	21.630492
H	23.012787	2.021203	18.923643
H	24.345004	3.017825	19.528676
H	22.943416	3.77785	18.775048
H	20.648202	7.640799	31.304076
H	23.593894	10.61989	31.987159
H	23.050825	12.3232	28.764796
H	25.12413	11.063585	29.041737
H	25.207596	11.504498	30.746592
H	25.337261	12.750555	29.510418
H	23.446807	14.103668	30.368129
H	23.199424	12.99387	31.722703
H	21.860077	13.386336	30.639576
H	19.550961	8.944839	28.066597
H	18.154335	9.64837	29.988292
H	18.429521	8.09493	30.767503
H	17.551521	8.166196	29.239195
H	19.110658	6.573641	28.071086
H	19.940011	6.349474	29.614741
H	20.858006	6.801738	28.171895
H	23.259282	9.056528	33.607521
H	23.63968	6.607088	33.784347
H	22.680434	6.345006	32.321861
H	24.202618	7.226925	32.223866
H	21.689115	7.749874	34.981287
H	20.838095	9.093649	34.203992

H	20.656198	7.451694	33.584763
H	22.154603	15.876583	26.742371
H	19.061226	14.825448	29.449764
H	19.222467	11.227029	28.718484
H	20.172525	11.760806	30.926527
H	18.434444	11.52097	31.088127
H	19.095859	13.153388	31.084211
H	17.469973	12.742257	27.694774
H	17.280595	13.507492	29.269123
H	16.905682	11.797717	29.079521
H	22.588915	12.490516	25.44287
H	23.291612	14.059887	23.806494
H	23.099485	15.436793	24.882388
H	21.676245	14.568325	24.307766
H	24.942335	13.235902	25.574627
H	24.363754	12.736774	27.157007
H	24.496109	14.45476	26.780985
H	21.205609	17.539383	27.967304
H	18.991729	17.301082	26.869674
H	18.241019	16.958746	28.43
H	18.944681	18.550301	28.123601
H	20.468637	18.34883	30.178357
H	19.767623	16.775355	30.556399
H	21.513899	16.932273	30.365809
H	29.070935	6.085704	24.78372
H	27.466944	6.172502	28.716366
H	25.059396	8.879709	28.0063
H	24.075071	6.588759	28.000916
H	23.885778	7.416232	29.54148
H	25.117236	6.154746	29.363491
H	26.955839	7.784534	30.136039
H	25.693088	8.993246	30.369457
H	27.099636	9.362934	29.367184
H	26.71363	8.576655	23.433789
H	28.860403	9.022192	22.320159
H	29.708256	8.037165	23.515486
H	28.921019	9.542013	24.003923
H	27.41039	7.120812	21.616241
H	26.411661	6.244259	22.770987
H	28.161802	5.995792	22.744462
H	29.145896	4.709733	28.286281
H	29.551535	3.876861	25.371908
H	28.295766	3.264242	26.445519
H	29.999384	2.933384	26.793314
H	31.117431	5.805559	26.223551
H	31.53032	4.7976	27.614515
H	30.887384	6.430504	27.85636

H	26.957396	12.757298	21.885483
H	28.830852	12.941353	25.68461
H	26.753442	10.365808	27.225923
H	28.845429	9.260822	26.437165
H	29.041306	9.865427	28.080199
H	29.737389	10.75837	26.723741
H	28.570766	12.752301	27.742448
H	27.637603	11.828582	28.90822
H	26.810309	12.85557	27.730479
H	24.940772	9.79392	22.661693
H	24.582001	12.584715	21.49377
H	23.688513	11.932384	22.866199
H	23.498213	11.214146	21.270078
H	25.420949	9.836092	20.269635
H	26.925998	9.625279	21.16812
H	26.527177	11.189537	20.462189
H	28.545122	14.348142	22.208858
H	28.996367	16.307101	23.655659
H	28.696214	15.33385	25.098787
H	27.378934	15.658288	23.972262
H	30.566823	13.000304	22.751021
H	30.635605	13.733244	24.353768
H	30.879662	14.734958	22.921896
H	18.342117	12.768651	19.60777
H	16.575934	11.95927	18.101522
H	15.464573	9.789558	18.537826
H	16.1418	8.437805	20.502284
H	17.896494	9.283002	22.034189
H	20.068607	12.691255	24.706449
H	19.053246	14.402998	26.149103
H	17.044273	15.637569	25.381963
H	16.087092	15.156658	23.147284
H	17.123252	13.465383	21.695977
H	20.702074	11.053506	19.508202
H	22.384349	12.182626	18.129425
H	23.297787	14.380425	18.825896
H	22.488077	15.430935	20.92098
H	20.79781	14.301585	22.295018
H	22.914024	2.18748	21.38697

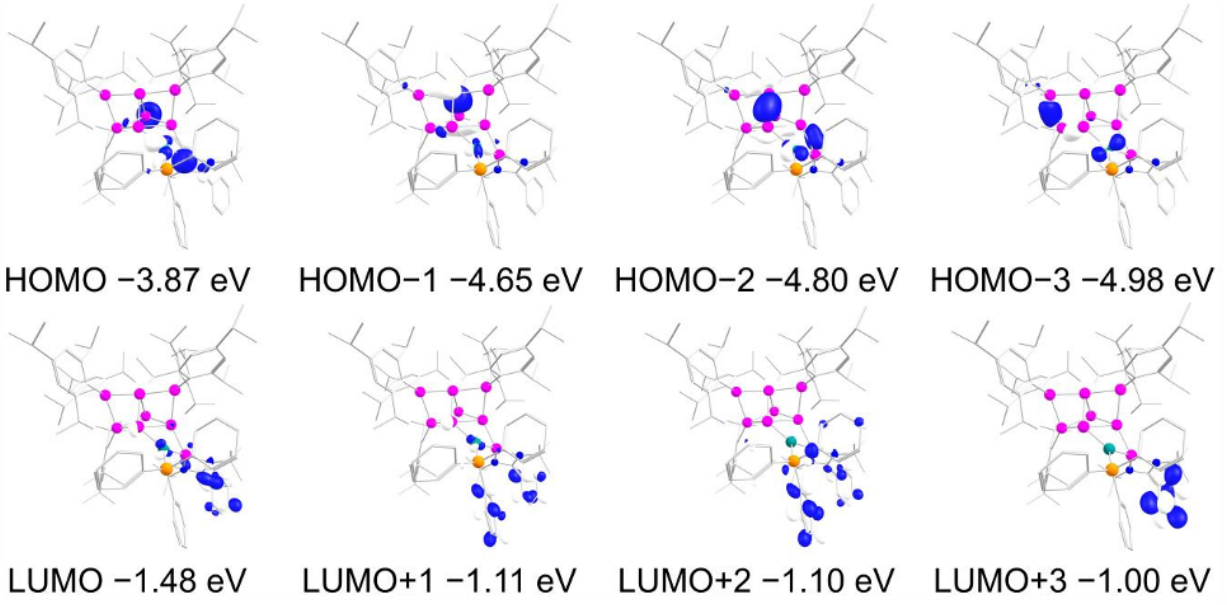

Supplementary Figure S55. Selected frontier orbitals of Ni(PPh_3) siliconoid/silylene **3b** at B3LYP/def2-TZVP level of theory (contour value 0.05).[23–29] Hydrogen atoms are omitted for clarity.

4.3.2 Experimental vs. calculated NMR shifts

Supplementary Table S16. Comparison of experimental vs. calculated NMR chemical shifts for compound Ni(PPh_3) siliconoid/silylene **3b** at the TPSSh/def2-TVZP level of theory.[26–29,33]

	Exp. **3b** $\delta(^{29}Si)$ [ppm]	Calc. **3b** $\delta(^{29}Si)$ [ppm]
Si3 (*Si*NHSi)	0.4	−6.5
Si8 (NH*Si*)	73.5	84.6
Si7 (*Si*Tip)	63.9	65.4
Si6 (*Si*Tip_2)	39.7	30.6
Si4 (*Si*Tip_2)	−41.4	−45.2
Si5 (unsubstituted)	−60.0	−68.2
Si1 (unsubstituted)	−87.3	−68.5
Si2 (unsubstituted)	−287.6	−291.0

4.3.3 TD-DFT calculations

Supplementary Table S17. Transition Energy. wavelength. and oscillator strengths of the electronic transition of **3b** calculated at the TD-TPSSh/def2-TZVP level of theory.[26–29,33,34] (the 485th orbital is the highest occupied orbital (HOMO) and 486th orbital is the lowest unoccupied molecular orbital (LUMO) shown in Supplementary Figure S55).

```
STATE  1:  E=   0.061541 au      1.675 eV    13506.8 cm**-1 <S**2> =   0.000000 Mult 1
   484a -> 485a  :     0.896349 (c= -0.94675721)
   484a -> 486a  :     0.042288 (c= -0.20563982)
   484a -> 488a  :     0.022256 (c= -0.14918536)

STATE  2:  E=   0.079702 au      2.169 eV    17492.6 cm**-1 <S**2> =   0.000000 Mult 1
   482a -> 485a  :     0.026768 (c= -0.16360917)
   483a -> 485a  :     0.024734 (c=  0.15727088)
```

```
  484a -> 486a  :     0.767862 (c=  0.87627710)
  484a -> 487a  :     0.035725 (c=  0.18901015)
  484a -> 488a  :     0.114284 (c= -0.33805947)

STATE  3:  E=   0.082033 au      2.232 eV    18004.1 cm**-1 <S**2> =   0.000000 Mult 1
  484a -> 485a  :     0.017014 (c=  0.13043664)
  484a -> 486a  :     0.030942 (c= -0.17590265)
  484a -> 487a  :     0.922539 (c=  0.96048886)

STATE  4:  E=   0.083644 au      2.276 eV    18357.7 cm**-1 <S**2> =   0.000000 Mult 1
  481a -> 485a  :     0.035895 (c= -0.18946097)
  482a -> 485a  :     0.023219 (c=  0.15237695)
  483a -> 485a  :     0.756897 (c= -0.86999843)
  483a -> 487a  :     0.011471 (c=  0.10710315)
  484a -> 488a  :     0.140011 (c= -0.37418072)

STATE  5:  E=   0.085929 au      2.338 eV    18859.3 cm**-1 <S**2> =   0.000000 Mult 1
  478a -> 485a  :     0.020508 (c=  0.14320531)
  480a -> 485a  :     0.034744 (c= -0.18639676)
  482a -> 485a  :     0.296719 (c=  0.54471964)
  483a -> 485a  :     0.112468 (c=  0.33536190)
  484a -> 486a  :     0.027096 (c= -0.16460868)
  484a -> 488a  :     0.441311 (c= -0.66431249)

STATE  6:  E=   0.087996 au      2.395 eV    19313.0 cm**-1 <S**2> =   0.000000 Mult 1
  479a -> 485a  :     0.065321 (c= -0.25557990)
  480a -> 485a  :     0.029641 (c= -0.17216701)
  481a -> 485a  :     0.819704 (c= -0.90537520)
  481a -> 487a  :     0.013734 (c=  0.11719024)
  482a -> 485a  :     0.010166 (c= -0.10082526)
  483a -> 485a  :     0.026851 (c=  0.16386248)

STATE  7:  E=   0.088564 au      2.410 eV    19437.5 cm**-1 <S**2> =   0.000000 Mult 1
  482a -> 485a  :     0.082596 (c=  0.28739447)
  484a -> 489a  :     0.010216 (c= -0.10107525)
  484a -> 490a  :     0.864804 (c= -0.92994816)

STATE  8:  E=   0.090650 au      2.467 eV    19895.3 cm**-1 <S**2> =   0.000000 Mult 1
  478a -> 485a  :     0.014729 (c=  0.12136355)
  480a -> 485a  :     0.247037 (c= -0.49702867)
  481a -> 485a  :     0.020547 (c=  0.14334352)
  482a -> 485a  :     0.397028 (c= -0.63010125)
  484a -> 486a  :     0.029353 (c= -0.17132719)
  484a -> 488a  :     0.115220 (c= -0.33944006)
  484a -> 489a  :     0.034622 (c= -0.18607082)
  484a -> 490a  :     0.079781 (c= -0.28245543)

STATE  9:  E=   0.091043 au      2.477 eV    19981.5 cm**-1 <S**2> =   0.000000 Mult 1
  484a -> 489a  :     0.953121 (c= -0.97627903)
  484a -> 490a  :     0.023046 (c=  0.15180963)

STATE 10:  E=   0.094246 au      2.565 eV    20684.7 cm**-1 <S**2> =   0.000000 Mult 1
  479a -> 485a  :     0.012736 (c= -0.11285295)
  480a -> 485a  :     0.046337 (c= -0.21525998)
  481a -> 485a  :     0.017704 (c=  0.13305512)
  484a -> 491a  :     0.712125 (c=  0.84387490)
  484a -> 492a  :     0.128624 (c=  0.35864253)
  484a -> 493a  :     0.037360 (c= -0.19328864)

STATE 11:  E=   0.095291 au      2.593 eV    20913.9 cm**-1 <S**2> =   0.000000 Mult 1
  480a -> 485a  :     0.011281 (c= -0.10621051)
```

```
  484a -> 491a  :     0.170377 (c= -0.41276745)
  484a -> 492a  :     0.788219 (c=  0.88781691)

STATE 12:  E=   0.096605 au      2.629 eV    21202.4 cm**-1 <S**2> =   0.000000 Mult 1
  478a -> 485a  :     0.063240 (c=  0.25147517)
  479a -> 485a  :     0.154794 (c= -0.39343855)
  480a -> 485a  :     0.309627 (c= -0.55644161)
  481a -> 485a  :     0.027224 (c=  0.16499697)
  482a -> 485a  :     0.053299 (c=  0.23086666)
  483a -> 485a  :     0.023313 (c= -0.15268491)
  484a -> 485a  :     0.021662 (c= -0.14717936)
  484a -> 486a  :     0.045656 (c=  0.21367187)
  484a -> 488a  :     0.092683 (c=  0.30443820)
  484a -> 491a  :     0.040507 (c= -0.20126353)
  484a -> 492a  :     0.072132 (c= -0.26857319)

STATE 13:  E=   0.100256 au      2.728 eV    22003.7 cm**-1 <S**2> =   0.000000 Mult 1
  483a -> 486a  :     0.022004 (c= -0.14833663)
  484a -> 491a  :     0.032236 (c= -0.17954512)
  484a -> 493a  :     0.895534 (c= -0.94632682)
  484a -> 494a  :     0.016980 (c= -0.13030674)

STATE 14:  E=   0.102011 au      2.776 eV    22388.9 cm**-1 <S**2> =   0.000000 Mult 1
  478a -> 485a  :     0.054471 (c=  0.23339017)
  479a -> 485a  :     0.441583 (c= -0.66451720)
  480a -> 485a  :     0.155701 (c=  0.39458939)
  481a -> 485a  :     0.021192 (c=  0.14557574)
  482a -> 485a  :     0.020186 (c= -0.14207724)
  483a -> 486a  :     0.135157 (c= -0.36763703)
  483a -> 488a  :     0.028736 (c= -0.16951681)
  484a -> 488a  :     0.012814 (c= -0.11320037)
  484a -> 494a  :     0.017451 (c=  0.13210167)

STATE 15:  E=   0.102557 au      2.791 eV    22508.8 cm**-1 <S**2> =   0.000000 Mult 1
  478a -> 485a  :     0.064751 (c=  0.25446269)
  479a -> 485a  :     0.062273 (c= -0.24954605)
  480a -> 485a  :     0.037514 (c=  0.19368416)
  481a -> 486a  :     0.051341 (c=  0.22658620)
  482a -> 485a  :     0.013993 (c= -0.11828998)
  482a -> 486a  :     0.017447 (c= -0.13208626)
  483a -> 486a  :     0.635325 (c=  0.79707305)
  483a -> 488a  :     0.034882 (c=  0.18676817)
  484a -> 493a  :     0.014625 (c= -0.12093437)

STATE 16:  E=   0.104971 au      2.856 eV    23038.5 cm**-1 <S**2> =   0.000000 Mult 1
  478a -> 485a  :     0.038170 (c= -0.19537224)
  484a -> 493a  :     0.015810 (c= -0.12573613)
  484a -> 494a  :     0.881353 (c=  0.93880384)
  484a -> 495a  :     0.011613 (c= -0.10776263)

STATE 17:  E=   0.106147 au      2.888 eV    23296.6 cm**-1 <S**2> =   0.000000 Mult 1
  478a -> 485a  :     0.312606 (c=  0.55911136)
  479a -> 485a  :     0.075988 (c=  0.27565966)
  480a -> 485a  :     0.019857 (c=  0.14091648)
  482a -> 486a  :     0.107478 (c= -0.32783887)
  482a -> 488a  :     0.024156 (c= -0.15542294)
  483a -> 486a  :     0.017746 (c= -0.13321413)
  483a -> 487a  :     0.052044 (c=  0.22813132)
  484a -> 494a  :     0.013418 (c=  0.11583408)
  484a -> 495a  :     0.310525 (c= -0.55724728)
```

STATE 18: E= 0.106212 au 2.890 eV 23310.8 cm**-1 <S**2> = 0.000000 Mult 1
478a -> 485a : 0.022154 (c= 0.14884112)
481a -> 486a : 0.120782 (c= 0.34753773)
482a -> 486a : 0.556643 (c= 0.74608492)
482a -> 488a : 0.070715 (c= 0.26592225)
483a -> 487a : 0.018992 (c= -0.13781036)
484a -> 495a : 0.137826 (c= -0.37124941)

STATE 19: E= 0.106570 au 2.900 eV 23389.4 cm**-1 <S**2> = 0.000000 Mult 1
478a -> 485a : 0.299510 (c= -0.54727532)
479a -> 485a : 0.065466 (c= -0.25586305)
481a -> 486a : 0.149368 (c= 0.38648114)
482a -> 486a : 0.088228 (c= -0.29703227)
483a -> 488a : 0.017704 (c= -0.13305716)
484a -> 494a : 0.032504 (c= -0.18028994)
484a -> 495a : 0.268370 (c= -0.51804444)

STATE 20: E= 0.107243 au 2.918 eV 23537.2 cm**-1 <S**2> = 0.000000 Mult 1
479a -> 486a : 0.010086 (c= -0.10042821)
480a -> 486a : 0.011357 (c= -0.10656860)
481a -> 486a : 0.395923 (c= -0.62922397)
481a -> 488a : 0.024549 (c= -0.15668271)
483a -> 486a : 0.028005 (c= 0.16734597)
483a -> 487a : 0.194709 (c= -0.44125831)
483a -> 488a : 0.022203 (c= 0.14900693)
484a -> 495a : 0.228699 (c= -0.47822450)
484a -> 496a : 0.019854 (c= 0.14090342)

STATE 21: E= 0.108086 au 2.941 eV 23722.2 cm**-1 <S**2> = 0.000000 Mult 1
481a -> 486a : 0.077172 (c= -0.27779811)
481a -> 487a : 0.018955 (c= 0.13767650)
481a -> 488a : 0.026239 (c= -0.16198423)
482a -> 486a : 0.055460 (c= 0.23549933)
483a -> 486a : 0.031088 (c= 0.17631852)
483a -> 487a : 0.462073 (c= 0.67975943)
483a -> 488a : 0.066998 (c= -0.25883956)
484a -> 496a : 0.186298 (c= 0.43162281)

STATE 22: E= 0.108649 au 2.956 eV 23845.7 cm**-1 <S**2> = 0.000000 Mult 1
481a -> 486a : 0.049157 (c= 0.22171333)
481a -> 488a : 0.013290 (c= 0.11528433)
482a -> 486a : 0.012180 (c= -0.11036386)
483a -> 486a : 0.020140 (c= -0.14191567)
483a -> 487a : 0.037711 (c= -0.19419216)
483a -> 488a : 0.049673 (c= 0.22287408)
484a -> 496a : 0.759085 (c= 0.87125474)

STATE 23: E= 0.110141 au 2.997 eV 24173.1 cm**-1 <S**2> = 0.000000 Mult 1
479a -> 485a : 0.013893 (c= 0.11786654)
480a -> 486a : 0.017625 (c= 0.13275733)
481a -> 486a : 0.010046 (c= 0.10022974)
481a -> 488a : 0.024396 (c= -0.15619264)
482a -> 485a : 0.010656 (c= 0.10322907)
482a -> 487a : 0.128707 (c= 0.35875730)
483a -> 486a : 0.056803 (c= 0.23833297)
483a -> 487a : 0.107762 (c= -0.32827055)
483a -> 488a : 0.555472 (c= -0.74529973)
484a -> 496a : 0.010614 (c= 0.10302547)

STATE 24: E= 0.110938 au 3.019 eV 24348.2 cm**-1 <S**2> = 0.000000 Mult 1
482a -> 487a : 0.207041 (c= -0.45501762)

```
  482a -> 488a  :     0.030943 (c=  0.17590490)
  483a -> 487a  :     0.012711 (c= -0.11274365)
  483a -> 488a  :     0.028724 (c= -0.16948244)
  484a -> 497a  :     0.666219 (c= -0.81622263)

STATE 25:  E=   0.111874 au      3.044 eV    24553.5 cm**-1 <S**2> =   0.000000 Mult 1
  480a -> 486a  :     0.025211 (c=  0.15878103)
  482a -> 486a  :     0.044339 (c= -0.21056716)
  482a -> 487a  :     0.383836 (c= -0.61954526)
  482a -> 488a  :     0.143644 (c=  0.37900400)
  483a -> 488a  :     0.048939 (c= -0.22122139)
  484a -> 497a  :     0.268648 (c=  0.51831245)
  484a -> 500a  :     0.018620 (c=  0.13645506)

STATE 26:  E=   0.112775 au      3.069 eV    24751.3 cm**-1 <S**2> =   0.000000 Mult 1
  480a -> 486a  :     0.029997 (c= -0.17319636)
  481a -> 486a  :     0.019467 (c=  0.13952447)
  481a -> 487a  :     0.607177 (c=  0.77921554)
  481a -> 488a  :     0.139599 (c= -0.37362981)
  482a -> 487a  :     0.032997 (c=  0.18165122)
  482a -> 488a  :     0.034254 (c=  0.18507793)
  483a -> 488a  :     0.029174 (c=  0.17080537)
  483a -> 490a  :     0.011364 (c= -0.10660336)

STATE 27:  E=   0.113253 au      3.082 eV    24856.1 cm**-1 <S**2> =   0.000000 Mult 1
  476a -> 485a  :     0.017831 (c=  0.13353163)
  478a -> 486a  :     0.035228 (c=  0.18769188)
  480a -> 486a  :     0.626016 (c= -0.79121191)
  481a -> 487a  :     0.062664 (c= -0.25032736)
  482a -> 488a  :     0.047024 (c=  0.21684936)
  483a -> 490a  :     0.053552 (c=  0.23141219)
  484a -> 498a  :     0.014312 (c=  0.11963187)
  484a -> 499a  :     0.035970 (c= -0.18965629)

STATE 28:  E=   0.113867 au      3.098 eV    24990.9 cm**-1 <S**2> =   0.000000 Mult 1
  476a -> 485a  :     0.010311 (c= -0.10154497)
  481a -> 487a  :     0.024340 (c= -0.15601169)
  481a -> 488a  :     0.032043 (c=  0.17900449)
  482a -> 486a  :     0.050979 (c= -0.22578589)
  482a -> 487a  :     0.143173 (c=  0.37838205)
  482a -> 488a  :     0.549474 (c=  0.74126544)
  483a -> 487a  :     0.013435 (c=  0.11591105)
  483a -> 488a  :     0.010811 (c=  0.10397652)
  483a -> 490a  :     0.020595 (c= -0.14350884)
  484a -> 498a  :     0.068643 (c= -0.26199777)
  484a -> 499a  :     0.011043 (c=  0.10508398)

STATE 29:  E=   0.113988 au      3.102 eV    25017.4 cm**-1 <S**2> =   0.000000 Mult 1
  480a -> 486a  :     0.012348 (c= -0.11112229)
  482a -> 487a  :     0.011483 (c= -0.10715993)
  482a -> 488a  :     0.018875 (c= -0.13738799)
  483a -> 490a  :     0.014875 (c=  0.12196241)
  484a -> 498a  :     0.885651 (c= -0.94109021)

STATE 30:  E=   0.114486 au      3.115 eV    25126.7 cm**-1 <S**2> =   0.000000 Mult 1
  477a -> 485a  :     0.019038 (c=  0.13797865)
  479a -> 488a  :     0.010742 (c= -0.10364192)
  481a -> 486a  :     0.047410 (c=  0.21773753)
  481a -> 487a  :     0.175534 (c= -0.41896768)
  481a -> 488a  :     0.406791 (c= -0.63780194)
  481a -> 490a  :     0.014903 (c= -0.12207693)
```

```
  483a -> 488a  :     0.024067 (c=  0.15513618)
  483a -> 490a  :     0.125329 (c= -0.35401785)
  484a -> 499a  :     0.100853 (c=  0.31757387)
  484a -> 500a  :     0.011222 (c=  0.10593584)

STATE 31:  E=   0.115209 au      3.135 eV    25285.5 cm**-1 <S**2> =   0.000000 Mult 1
  482a -> 488a  :     0.012558 (c= -0.11206414)
  483a -> 490a  :     0.416936 (c= -0.64570581)
  484a -> 499a  :     0.491911 (c= -0.70136393)

STATE 32:  E=   0.115611 au      3.146 eV    25373.7 cm**-1 <S**2> =   0.000000 Mult 1
  477a -> 485a  :     0.018693 (c= -0.13672171)
  478a -> 486a  :     0.015365 (c= -0.12395390)
  480a -> 486a  :     0.079992 (c=  0.28282807)
  481a -> 487a  :     0.025505 (c= -0.15970252)
  481a -> 488a  :     0.193381 (c= -0.43975062)
  482a -> 488a  :     0.019884 (c=  0.14100997)
  483a -> 488a  :     0.020183 (c=  0.14206658)
  483a -> 490a  :     0.220418 (c=  0.46948735)
  484a -> 499a  :     0.281493 (c= -0.53055939)
  484a -> 500a  :     0.034452 (c= -0.18561366)

STATE 33:  E=   0.117439 au      3.196 eV    25774.9 cm**-1 <S**2> =   0.000000 Mult 1
  477a -> 485a  :     0.369714 (c=  0.60804104)
  478a -> 486a  :     0.024279 (c= -0.15581818)
  480a -> 487a  :     0.183186 (c=  0.42800280)
  480a -> 488a  :     0.054160 (c= -0.23272298)
  482a -> 486a  :     0.010341 (c=  0.10169096)
  482a -> 490a  :     0.212275 (c= -0.46073300)
  483a -> 490a  :     0.038222 (c=  0.19550498)

STATE 34:  E=   0.117917 au      3.209 eV    25879.9 cm**-1 <S**2> =   0.000000 Mult 1
  477a -> 485a  :     0.041106 (c= -0.20274635)
  480a -> 487a  :     0.082419 (c=  0.28708627)
  483a -> 491a  :     0.011920 (c=  0.10917860)
  484a -> 500a  :     0.704107 (c=  0.83911096)
  484a -> 501a  :     0.014406 (c=  0.12002599)
  484a -> 502a  :     0.029724 (c= -0.17240747)

STATE 35:  E=   0.118524 au      3.225 eV    26013.0 cm**-1 <S**2> =   0.000000 Mult 1
  477a -> 485a  :     0.017004 (c=  0.13040041)
  479a -> 486a  :     0.011984 (c= -0.10946923)
  480a -> 487a  :     0.124580 (c= -0.35295941)
  480a -> 488a  :     0.014542 (c=  0.12058929)
  483a -> 489a  :     0.704153 (c=  0.83913827)
  483a -> 491a  :     0.011553 (c=  0.10748429)
  484a -> 501a  :     0.046993 (c=  0.21677874)
  484a -> 502a  :     0.013419 (c= -0.11583984)

STATE 36:  E=   0.118572 au      3.226 eV    26023.5 cm**-1 <S**2> =   0.000000 Mult 1
  476a -> 485a  :     0.011479 (c= -0.10713847)
  477a -> 485a  :     0.036471 (c=  0.19097290)
  479a -> 486a  :     0.043200 (c= -0.20784570)
  480a -> 487a  :     0.240251 (c= -0.49015387)
  480a -> 488a  :     0.026106 (c=  0.16157346)
  482a -> 490a  :     0.033951 (c= -0.18425787)
  483a -> 489a  :     0.257326 (c= -0.50727316)
  484a -> 499a  :     0.016384 (c= -0.12799915)
  484a -> 500a  :     0.023161 (c=  0.15218878)
  484a -> 501a  :     0.180962 (c=  0.42539640)
  484a -> 502a  :     0.054691 (c= -0.23386066)
```

STATE 37: E= 0.119102 au 3.241 eV 26139.8 cm**-1 <S**2> = 0.000000 Mult 1
478a -> 486a : 0.032191 (c= -0.17941896)
479a -> 486a : 0.574423 (c= 0.75790707)
479a -> 488a : 0.062411 (c= 0.24982278)
480a -> 486a : 0.022538 (c= -0.15012731)
480a -> 487a : 0.080563 (c= -0.28383552)
480a -> 488a : 0.058791 (c= 0.24246868)
481a -> 486a : 0.013014 (c= -0.11407868)
483a -> 491a : 0.021139 (c= 0.14539269)
484a -> 501a : 0.041034 (c= -0.20256812)

STATE 38: E= 0.119553 au 3.253 eV 26238.9 cm**-1 <S**2> = 0.000000 Mult 1
477a -> 485a : 0.155397 (c= -0.39420472)
479a -> 486a : 0.030434 (c= 0.17445382)
480a -> 486a : 0.013325 (c= -0.11543578)
480a -> 487a : 0.016506 (c= 0.12847449)
480a -> 488a : 0.023272 (c= 0.15255081)
481a -> 491a : 0.013301 (c= -0.11533051)
482a -> 490a : 0.284429 (c= -0.53331926)
482a -> 491a : 0.023940 (c= 0.15472413)
483a -> 491a : 0.306767 (c= -0.55386564)
484a -> 501a : 0.063293 (c= 0.25158181)

STATE 39: E= 0.119719 au 3.258 eV 26275.2 cm**-1 <S**2> = 0.000000 Mult 1
476a -> 485a : 0.018169 (c= 0.13479115)
479a -> 486a : 0.053771 (c= 0.23188614)
480a -> 487a : 0.044750 (c= 0.21154282)
482a -> 490a : 0.123628 (c= 0.35160818)
483a -> 491a : 0.019318 (c= 0.13898909)
484a -> 500a : 0.028793 (c= -0.16968563)
484a -> 501a : 0.577201 (c= 0.75973731)
484a -> 502a : 0.048012 (c= 0.21911527)
484a -> 503a : 0.026335 (c= -0.16227938)

STATE 40: E= 0.119967 au 3.264 eV 26329.7 cm**-1 <S**2> = 0.000000 Mult 1
476a -> 485a : 0.079655 (c= 0.28223203)
477a -> 485a : 0.153660 (c= -0.39199503)
478a -> 486a : 0.019544 (c= 0.13980028)
480a -> 488a : 0.032746 (c= -0.18095938)
481a -> 491a : 0.029467 (c= 0.17165928)
482a -> 490a : 0.178502 (c= -0.42249497)
483a -> 491a : 0.415977 (c= 0.64496315)
484a -> 500a : 0.013819 (c= -0.11755508)

STATE 41: E= 0.120215 au 3.271 eV 26384.1 cm**-1 <S**2> = 0.000000 Mult 1
476a -> 485a : 0.195989 (c= -0.44270610)
479a -> 486a : 0.036036 (c= -0.18983237)
480a -> 486a : 0.028806 (c= -0.16972396)
480a -> 487a : 0.084948 (c= 0.29145877)
480a -> 488a : 0.421777 (c= 0.64944362)
482a -> 490a : 0.015207 (c= -0.12331754)
482a -> 491a : 0.011534 (c= -0.10739518)
483a -> 491a : 0.068055 (c= 0.26087334)
484a -> 502a : 0.015988 (c= 0.12644474)

STATE 42: E= 0.121047 au 3.294 eV 26566.8 cm**-1 <S**2> = 0.000000 Mult 1
481a -> 488a : 0.020188 (c= -0.14208345)
481a -> 490a : 0.651140 (c= 0.80693234)
481a -> 491a : 0.019448 (c= -0.13945661)
482a -> 490a : 0.015436 (c= -0.12424051)

```
  483a -> 492a  :     0.011028 (c=  0.10501197)
  484a -> 502a  :     0.193295 (c=  0.43965330)

STATE 43:  E=   0.121532 au      3.307 eV    26673.1 cm**-1 <S**2> =   0.000000 Mult 1
  476a -> 485a  :     0.132456 (c= -0.36394442)
  478a -> 486a  :     0.021450 (c=  0.14645799)
  480a -> 487a  :     0.033720 (c= -0.18363009)
  480a -> 488a  :     0.060832 (c= -0.24664080)
  481a -> 490a  :     0.180336 (c= -0.42466042)
  483a -> 492a  :     0.031564 (c=  0.17766356)
  484a -> 500a  :     0.027584 (c=  0.16608314)
  484a -> 502a  :     0.367841 (c=  0.60649882)
  484a -> 504a  :     0.014608 (c=  0.12086509)

STATE 44:  E=   0.122244 au      3.326 eV    26829.6 cm**-1 <S**2> =   0.000000 Mult 1
  476a -> 485a  :     0.200331 (c=  0.44758312)
  478a -> 486a  :     0.188309 (c= -0.43394585)
  478a -> 488a  :     0.037582 (c= -0.19386061)
  479a -> 486a  :     0.036941 (c= -0.19220011)
  479a -> 487a  :     0.025989 (c=  0.16121163)
  480a -> 488a  :     0.057162 (c=  0.23908659)
  483a -> 492a  :     0.081162 (c=  0.28488879)
  484a -> 502a  :     0.108077 (c=  0.32875114)
  484a -> 503a  :     0.081795 (c=  0.28599770)
  484a -> 504a  :     0.079613 (c=  0.28215764)

STATE 45:  E=   0.122361 au      3.330 eV    26855.2 cm**-1 <S**2> =   0.000000 Mult 1
  478a -> 486a  :     0.014967 (c=  0.12233885)
  481a -> 492a  :     0.063208 (c=  0.25141173)
  482a -> 492a  :     0.012536 (c= -0.11196440)
  483a -> 491a  :     0.019861 (c= -0.14092921)
  483a -> 492a  :     0.665023 (c=  0.81548950)
  484a -> 502a  :     0.066150 (c= -0.25719578)
  484a -> 504a  :     0.079128 (c= -0.28129630)
  484a -> 506a  :     0.021232 (c= -0.14571312)

STATE 46:  E=   0.122650 au      3.337 eV    26918.5 cm**-1 <S**2> =   0.000000 Mult 1
  482a -> 489a  :     0.959512 (c= -0.97954704)
  482a -> 491a  :     0.014318 (c= -0.11965719)

STATE 47:  E=   0.123148 au      3.351 eV    27027.9 cm**-1 <S**2> =   0.000000 Mult 1
  478a -> 486a  :     0.010364 (c= -0.10180601)
  483a -> 492a  :     0.015776 (c=  0.12560157)
  484a -> 503a  :     0.392305 (c= -0.62634295)
  484a -> 504a  :     0.072464 (c=  0.26919227)
  484a -> 505a  :     0.449760 (c=  0.67064171)

STATE 48:  E=   0.123375 au      3.357 eV    27077.7 cm**-1 <S**2> =   0.000000 Mult 1
  478a -> 486a  :     0.031658 (c= -0.17792642)
  482a -> 491a  :     0.109649 (c=  0.33113333)
  484a -> 502a  :     0.017379 (c= -0.13183049)
  484a -> 503a  :     0.242166 (c= -0.49210350)
  484a -> 504a  :     0.085641 (c=  0.29264415)
  484a -> 505a  :     0.417829 (c= -0.64639681)
  484a -> 506a  :     0.014077 (c=  0.11864838)
  484a -> 507a  :     0.011758 (c= -0.10843491)

STATE 49:  E=   0.123447 au      3.359 eV    27093.4 cm**-1 <S**2> =   0.000000 Mult 1
  479a -> 487a  :     0.015135 (c=  0.12302315)
  481a -> 491a  :     0.033108 (c=  0.18195589)
  482a -> 489a  :     0.011847 (c=  0.10884479)
```

```
  482a -> 490a  :     0.010034 (c= -0.10017069)
  482a -> 491a  :     0.705668 (c= -0.84004067)
  483a -> 491a  :     0.028209 (c= -0.16795465)
  484a -> 503a  :     0.062666 (c= -0.25033105)
  484a -> 504a  :     0.029325 (c=  0.17124398)
  484a -> 505a  :     0.046656 (c= -0.21600026)

STATE 50:  E=   0.123909 au      3.372 eV    27194.8 cm**-1 <S**2> =   0.000000 Mult 1
  476a -> 485a  :     0.021548 (c=  0.14679366)
  479a -> 487a  :     0.049284 (c= -0.22199950)
  479a -> 491a  :     0.013091 (c= -0.11441553)
  481a -> 489a  :     0.079588 (c= -0.28211309)
  481a -> 490a  :     0.041300 (c= -0.20322438)
  481a -> 491a  :     0.429368 (c= -0.65526198)
  481a -> 492a  :     0.032713 (c= -0.18086600)
  482a -> 491a  :     0.042209 (c= -0.20544924)
  483a -> 491a  :     0.019750 (c=  0.14053535)
  484a -> 503a  :     0.019501 (c= -0.13964580)
  484a -> 504a  :     0.149406 (c= -0.38653011)
  484a -> 505a  :     0.014360 (c= -0.11983189)
  484a -> 506a  :     0.010151 (c= -0.10075393)

STATE 51:  E=   0.124431 au      3.386 eV    27309.5 cm**-1 <S**2> =   0.000000 Mult 1
  478a -> 486a  :     0.099187 (c=  0.31493960)
  479a -> 486a  :     0.020437 (c=  0.14295721)
  480a -> 487a  :     0.016926 (c=  0.13010181)
  481a -> 489a  :     0.336210 (c= -0.57983658)
  481a -> 490a  :     0.018743 (c=  0.13690457)
  481a -> 491a  :     0.069777 (c= -0.26415307)
  482a -> 490a  :     0.010184 (c=  0.10091588)
  483a -> 492a  :     0.018119 (c=  0.13460528)
  484a -> 502a  :     0.014298 (c= -0.11957329)
  484a -> 503a  :     0.043971 (c=  0.20969232)
  484a -> 504a  :     0.244002 (c=  0.49396532)

STATE 52:  E=   0.124562 au      3.390 eV    27338.3 cm**-1 <S**2> =   0.000000 Mult 1
  478a -> 486a  :     0.033139 (c= -0.18204083)
  479a -> 487a  :     0.035244 (c=  0.18773277)
  481a -> 489a  :     0.560084 (c= -0.74838751)
  481a -> 491a  :     0.190659 (c=  0.43664537)
  484a -> 503a  :     0.014996 (c= -0.12245856)
  484a -> 504a  :     0.071684 (c= -0.26773816)

STATE 53:  E=   0.124785 au      3.396 eV    27387.1 cm**-1 <S**2> =   0.000000 Mult 1
  476a -> 485a  :     0.015738 (c=  0.12545104)
  478a -> 487a  :     0.027047 (c=  0.16446032)
  478a -> 488a  :     0.010407 (c= -0.10201449)
  479a -> 486a  :     0.016303 (c= -0.12768234)
  479a -> 487a  :     0.606609 (c= -0.77885095)
  479a -> 488a  :     0.077482 (c=  0.27835620)
  480a -> 490a  :     0.048564 (c=  0.22037165)
  481a -> 491a  :     0.057191 (c=  0.23914638)
  481a -> 492a  :     0.018821 (c=  0.13719022)
  482a -> 491a  :     0.015712 (c= -0.12534913)
  484a -> 503a  :     0.011119 (c=  0.10544687)

STATE 54:  E=   0.125776 au      3.423 eV    27604.7 cm**-1 <S**2> =   0.000000 Mult 1
  476a -> 485a  :     0.011845 (c= -0.10883584)
  478a -> 486a  :     0.013736 (c= -0.11720241)
  478a -> 487a  :     0.011239 (c=  0.10601607)
  479a -> 487a  :     0.017324 (c=  0.13162024)
```

480a -> 488a : 0.015865 (c= -0.12595615)
480a -> 490a : 0.152898 (c= 0.39102135)
482a -> 492a : 0.679132 (c= 0.82409486)
482a -> 493a : 0.014459 (c= -0.12024649)
484a -> 504a : 0.014633 (c= -0.12096811)

STATE 55: E= 0.126139 au 3.432 eV 27684.4 cm**-1 <S**2> = 0.000000 Mult 1
476a -> 485a : 0.017151 (c= -0.13096068)
478a -> 486a : 0.075979 (c= -0.27564232)
478a -> 487a : 0.036169 (c= 0.19018249)
479a -> 486a : 0.019801 (c= 0.14071479)
479a -> 488a : 0.190799 (c= -0.43680489)
480a -> 486a : 0.011277 (c= -0.10619410)
480a -> 488a : 0.031848 (c= -0.17845886)
480a -> 490a : 0.255035 (c= 0.50500966)
481a -> 491a : 0.017357 (c= -0.13174477)
481a -> 492a : 0.020202 (c= 0.14213435)
482a -> 492a : 0.153654 (c= -0.39198713)
482a -> 493a : 0.017850 (c= 0.13360426)
484a -> 506a : 0.019417 (c= 0.13934652)

STATE 56: E= 0.126337 au 3.438 eV 27727.7 cm**-1 <S**2> = 0.000000 Mult 1
479a -> 487a : 0.013209 (c= -0.11493180)
479a -> 488a : 0.025968 (c= -0.16114538)
480a -> 490a : 0.012934 (c= -0.11372781)
481a -> 492a : 0.047755 (c= 0.21852810)
481a -> 493a : 0.015792 (c= 0.12566721)
482a -> 492a : 0.010307 (c= 0.10152367)
483a -> 493a : 0.664723 (c= 0.81530527)
484a -> 504a : 0.021292 (c= -0.14591885)
484a -> 506a : 0.118456 (c= 0.34417490)
484a -> 507a : 0.016738 (c= -0.12937686)

STATE 57: E= 0.126576 au 3.444 eV 27780.3 cm**-1 <S**2> = 0.000000 Mult 1
478a -> 486a : 0.012878 (c= -0.11348086)
478a -> 487a : 0.010420 (c= 0.10207793)
479a -> 487a : 0.034615 (c= -0.18605075)
479a -> 488a : 0.034599 (c= -0.18600930)
480a -> 490a : 0.246064 (c= -0.49604845)
481a -> 492a : 0.080164 (c= 0.28313171)
481a -> 493a : 0.019237 (c= -0.13869592)
482a -> 492a : 0.024741 (c= 0.15729428)
483a -> 493a : 0.218855 (c= -0.46781897)
484a -> 504a : 0.029871 (c= -0.17283097)
484a -> 506a : 0.210921 (c= 0.45926118)
484a -> 507a : 0.023494 (c= -0.15327807)

STATE 58: E= 0.126864 au 3.452 eV 27843.4 cm**-1 <S**2> = 0.000000 Mult 1
478a -> 486a : 0.064337 (c= 0.25364740)
478a -> 488a : 0.032196 (c= -0.17943154)
479a -> 486a : 0.015015 (c= -0.12253507)
479a -> 487a : 0.055099 (c= 0.23473206)
479a -> 488a : 0.275387 (c= 0.52477301)
480a -> 490a : 0.080212 (c= 0.28321757)
481a -> 492a : 0.014902 (c= 0.12207192)
482a -> 492a : 0.037576 (c= -0.19384523)
484a -> 504a : 0.025881 (c= -0.16087466)
484a -> 506a : 0.283671 (c= 0.53260815)
484a -> 507a : 0.020322 (c= -0.14255651)

STATE 59: E= 0.126979 au 3.455 eV 27868.8 cm**-1 <S**2> = 0.000000 Mult 1

478a -> 487a : 0.029339 (c= 0.17128772)
479a -> 487a : 0.018317 (c= -0.13534177)
479a -> 488a : 0.019024 (c= -0.13792859)
479a -> 492a : 0.015500 (c= -0.12449912)
481a -> 491a : 0.030330 (c= 0.17415643)
481a -> 492a : 0.633339 (c= -0.79582623)
483a -> 492a : 0.070536 (c= 0.26558585)
484a -> 506a : 0.116209 (c= 0.34089393)

STATE 60: E= 0.127855 au 3.479 eV 28060.9 cm**-1 <S**2> = 0.000000 Mult 1
476a -> 485a : 0.028151 (c= -0.16778264)
478a -> 486a : 0.093655 (c= -0.30603183)
478a -> 487a : 0.487824 (c= -0.69844416)
478a -> 488a : 0.072614 (c= 0.26946983)
479a -> 486a : 0.012500 (c= -0.11180271)
479a -> 488a : 0.048297 (c= 0.21976620)
480a -> 491a : 0.049260 (c= 0.22194649)
483a -> 492a : 0.012200 (c= 0.11045360)
483a -> 494a : 0.015290 (c= 0.12365331)
484a -> 506a : 0.025478 (c= 0.15961977)

4.4 $Ni(CO)_2$ siliconoid/silylene 3c

4.4.1 Optimization and molecular orbitals

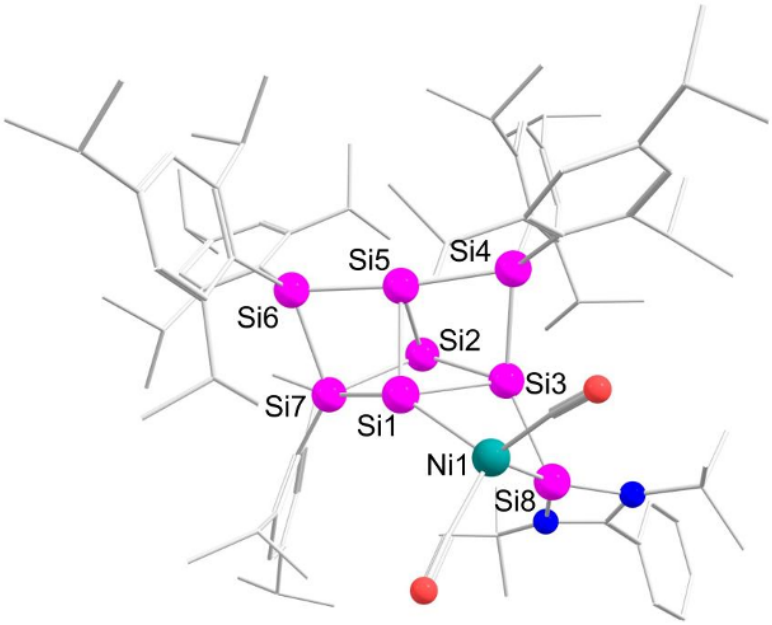

Supplementary Figure S56. Calculated structure of $Ni(CO)_2$ siliconoid/silylene **3c** at the B3LYP/def2-TZVP level of theory.[23–29] Hydrogen atoms are omitted for clarity.

Supplementary Table S18. Coordinates of $Ni(CO)_2$) siliconoid/silylene **3c** at the B3LYP/def2-TZVP level of theory.[23–29]

Ni	9.710638	16.765035	10.0919
Si	8.737086	15.609136	8.302706
Si	7.279631	16.049883	10.225285
Si	8.10697	18.073091	10.948841
C	10.344276	15.785786	11.468736

C	11.038791	17.681304	9.302116
Si	6.065646	15.60913	8.246405
Si	7.389753	13.689203	8.396245
Si	7.47064	15.83611	6.38638
Si	7.146311	13.710909	10.7459
N	6.985322	19.465753	10.500391
N	7.43699	18.816725	12.4863
C	6.728644	19.713221	11.787349
O	10.758063	15.271994	12.401638
O	11.911261	18.288857	8.88341
Si	7.486771	13.43487	6.059948
C	7.091108	17.284233	5.217181
C	8.396826	12.890338	11.930234
C	5.386155	13.042899	11.099703
C	6.360002	19.981936	9.267294
C	7.665697	18.659945	13.930712
C	5.806098	20.731459	12.33464
C	8.938804	12.302838	5.522588
C	5.996822	13.123336	4.91776
C	5.742214	17.599085	4.925428
C	8.090344	18.196448	4.831612
C	9.573819	12.246047	11.480077
C	8.051564	12.759024	13.294148
C	4.247134	13.826385	11.400532
C	5.20057	11.649127	10.952212
C	4.921824	19.464938	9.15627
C	7.191046	19.438697	8.107517
C	6.385311	21.513639	9.219724
C	8.856605	17.70998	14.065549
C	6.428943	18.031249	14.581385
C	8.008098	19.992991	14.603954
C	4.501844	20.363871	12.657741
C	6.220174	22.046911	12.530091
C	8.713027	10.905427	5.421294
C	10.249795	12.766069	5.290182
C	4.722722	12.665288	5.317836
C	6.212386	13.392547	3.547248
C	5.432264	18.837266	4.37596
C	4.590265	16.633766	5.151015
C	7.729983	19.42797	4.289073
C	9.568544	17.89635	4.983858
C	10.272078	11.411928	12.348085
C	10.142939	12.416808	10.07964
C	8.794225	11.929279	14.126619
C	6.908116	13.526628	13.939111
C	2.993153	13.226071	11.471966
C	4.278042	15.317244	11.705409

C	3.927467	11.094873	11.045118
C	6.34772	10.682337	10.718056
H	4.491491	19.771433	8.201985
H	4.295752	19.86372	9.954589
H	4.906438	18.37675	9.203603
H	6.761081	19.746384	7.155567
H	7.213838	18.349976	8.121978
H	8.215035	19.806559	8.161102
H	6.067979	21.843045	8.229262
H	7.395963	21.885931	9.394869
H	5.71504	21.960398	9.950623
H	8.659918	16.7709	13.55122
H	9.042348	17.486929	15.115849
H	9.757686	18.148456	13.636799
H	5.570318	18.698736	14.518969
H	6.621213	17.822274	15.634826
H	6.178377	17.095596	14.085161
H	8.829648	20.48683	14.082419
H	8.320929	19.806896	15.632541
H	7.155263	20.667652	14.631449
H	4.179533	19.343196	12.500912
C	3.618554	21.305255	13.169627
C	5.337809	22.984816	13.045978
H	7.233138	22.331765	12.279612
C	9.76091	10.052009	5.097149
C	7.357658	10.250413	5.643937
C	11.275332	11.864456	5.009292
C	10.638367	14.230511	5.302699
C	3.731229	12.472752	4.360668
C	4.356698	12.353857	6.761034
C	5.19623	13.158938	2.625987
C	7.539913	13.901974	3.000945
H	4.394627	19.070301	4.174413
C	6.406952	19.781454	4.078174
H	4.998967	15.702705	5.543031
C	3.578933	17.172257	6.167235
C	3.883108	16.285031	3.836124
H	8.502872	20.140122	4.026441
H	9.664107	16.846285	5.264128
C	10.203022	18.724296	6.101151
C	10.319349	18.09399	3.661923
H	11.155109	10.899973	11.98723
C	9.890435	11.216472	13.665997
H	9.686792	13.302811	9.644336
C	11.655875	12.670684	10.083662
C	9.81692	11.23075	9.163453
H	8.502621	11.832743	15.164804

H	6.487841	14.200957	13.191525
C	5.781886	12.611377	14.433808
C	7.423044	14.398861	15.09146
H	2.133524	13.848499	11.68407
C	2.802127	11.865772	11.282147
H	5.302319	15.6711	11.589761
C	3.865909	15.605514	13.155474
C	3.401644	16.127506	10.744868
H	3.808445	10.02487	10.9239
H	7.258784	11.256475	10.58241
C	6.166816	9.854849	9.449981
C	6.58633	9.774444	11.930398
H	2.605678	21.013515	13.414331
C	4.035542	22.616005	13.365506
H	5.666533	24.004628	13.197403
H	9.560445	8.993043	5.011378
C	11.058168	10.503646	4.902713
H	6.728602	10.950035	6.194161
C	7.458834	8.975252	6.490408
C	6.659706	9.922751	4.317185
H	12.279706	12.240439	4.857266
H	9.729008	14.812099	5.439779
C	11.56726	14.567432	6.471962
C	11.261329	14.660973	3.97023
H	2.758969	12.122188	4.682593
C	3.94836	12.694241	3.007815
H	5.261731	12.433883	7.363337
C	3.808253	10.932692	6.935835
C	3.358602	13.372015	7.323505
H	5.380846	13.345038	1.574587
H	8.19073	14.139492	3.84199
C	8.251927	12.826027	2.171925
C	7.391489	15.200548	2.199918
C	6.0429	21.151449	3.548514
H	3.113256	18.09157	5.805475
H	4.056168	17.384478	7.122705
H	2.786407	16.441261	6.338521
H	3.400187	17.161851	3.399367
H	3.115755	15.532184	4.019056
H	4.578021	15.877994	3.104771
H	11.260111	18.480256	6.214581
H	9.709352	18.529739	7.050538
H	10.12336	19.792853	5.888629
H	9.899025	17.471321	2.871169
H	11.373137	17.837351	3.779629
H	10.274777	19.132671	3.331493
C	10.658062	10.275104	14.567919

H	12.218535	11.779962	10.369911
H	11.925565	13.473339	10.768585
H	11.982952	12.951032	9.081528
H	10.205696	11.403443	8.158235
H	8.743282	11.070863	9.076747
H	10.261318	10.310695	9.551015
H	5.326454	12.057789	13.616289
H	4.998861	13.195697	14.921105
H	6.161077	11.894638	15.165095
H	8.266191	15.011306	14.777593
H	7.755293	13.785338	15.93051
H	6.631745	15.056429	15.456548
C	1.42288	11.244592	11.310981
H	3.900993	16.678837	13.35335
H	4.522465	15.108538	13.867348
H	2.847644	15.263774	13.349353
H	3.655246	15.915743	9.707285
H	3.54188	17.197201	10.915064
H	2.342965	15.904132	10.891413
H	6.093555	10.495176	8.572579
H	5.269791	9.234829	9.487748
H	7.020574	9.19191	9.315698
H	5.726838	9.124954	12.111436
H	7.459437	9.142548	11.755829
H	3.347753	23.349384	13.765804
C	12.190283	9.54979	4.591694
H	7.8894	8.151798	5.918724
H	6.466421	8.658706	6.813234
H	8.075475	9.130392	7.373696
H	6.513658	10.806524	3.703164
H	5.680408	9.476307	4.501422
H	7.256716	9.205032	3.749409
H	12.523639	14.048319	6.377941
H	11.119714	14.277893	7.422388
H	11.767496	15.640302	6.509513
H	10.573551	14.499599	3.139876
H	12.174372	14.103518	3.756438
H	11.52136	15.717337	3.995735
C	2.865826	12.439224	1.981107
H	2.861682	10.803486	6.408121
H	3.628805	10.731891	7.992805
H	4.503395	10.182607	6.55895
H	3.738517	14.387913	7.227954
H	3.178133	13.182691	8.382975
H	2.403243	13.31504	6.795519
H	7.643411	12.533463	1.313538
H	8.453007	11.936259	2.766113

H	9.20519	13.200927	1.794041
H	8.375303	15.561552	1.892033
H	6.920408	15.982727	2.79248
H	6.798373	15.049327	1.296294
H	6.980572	21.66282	3.310252
C	5.322206	21.97712	4.623036
C	5.213158	21.076514	2.262054
H	11.475282	9.857505	13.971979
C	11.280865	11.009647	15.761094
C	9.77684	9.109922	15.035118
H	1.558761	10.161921	11.226921
C	0.689389	11.520425	12.627929
C	0.589969	11.704152	10.106938
H	13.099	10.151946	4.494765
C	12.412602	8.550304	5.733748
C	11.966599	8.824767	3.259281
H	3.299647	12.655943	1.000036
C	2.426033	10.970228	1.980079
C	1.66671	13.37499	2.174029
H	5.104995	22.984148	4.259629
H	5.932512	22.062559	5.523945
H	4.376169	21.508218	4.902796
H	5.024702	22.077293	1.867154
H	4.245814	20.603598	2.443037
H	5.730112	20.496709	1.49586
H	11.878821	10.324203	16.366065
H	11.924274	11.825068	15.426975
H	10.509001	11.43611	16.405529
H	9.354354	8.572104	14.184851
H	10.354759	8.404244	15.636332
H	8.946679	9.469999	15.646785
H	0.496913	12.587678	12.756826
H	1.276809	11.181292	13.482756
H	-0.273832	11.005673	12.646781
H	1.099048	11.479102	9.168648
H	0.419577	12.782583	10.141363
H	-0.383955	11.209251	10.098114
H	11.540273	7.906475	5.864848
H	12.589316	9.067751	6.678037
H	13.272844	7.910166	5.525061
H	11.833253	9.536865	2.44326
H	11.075124	8.195204	3.301654
H	1.698851	10.78494	1.186205
H	1.959727	10.699436	2.929829
H	3.279132	10.307235	1.827531
H	1.973254	14.420597	2.126177
H	1.191819	13.210393	3.144003

H	0.914379	13.20248	1.400872
H	12.817618	8.182814	3.02044
H	6.771224	10.356192	12.830232

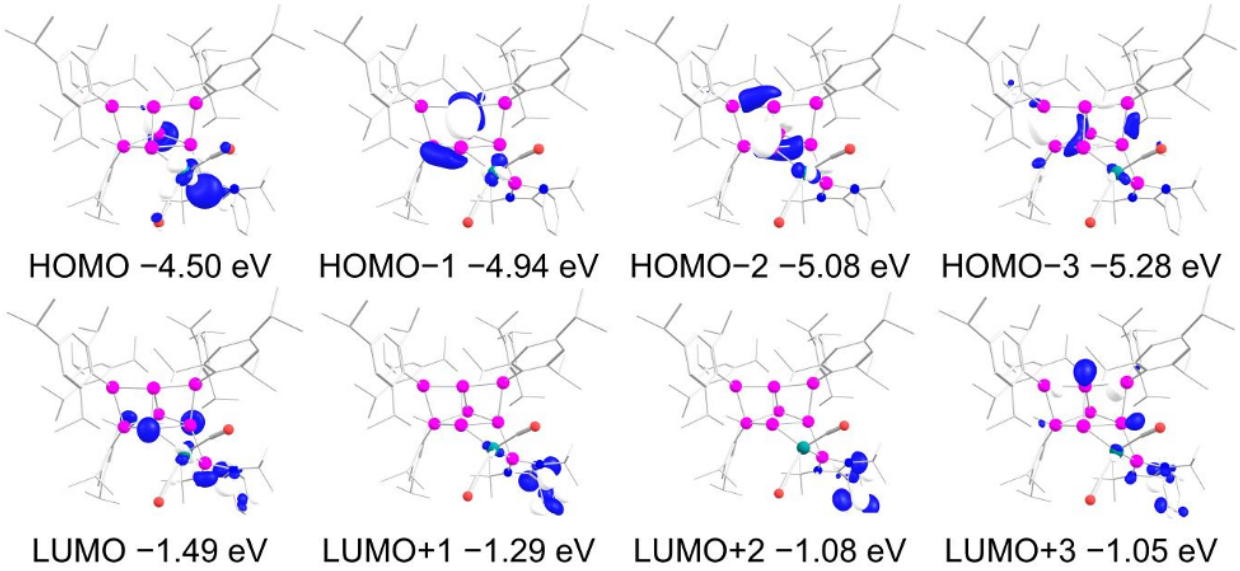

Supplementary Figure S57. Selected frontier orbitals of $Ni(CO)_2$ siliconoid/silylene **3c** at B3LYP/def2-TZVP level of theory (contour value 0.05).[23–29] Hydrogen atoms are omitted for clarity.

4.4.2 Experimental vs. calculated NMR shifts

Supplementary Table S19. Comparison of experimental vs. calculated NMR chemical shifts for compound $Ni(CO)_2$ siliconoid/silylene **3c** at the TPSSh/def2-TZVP level of theory.[26–29,33]

	Exp. **3c** $\delta(^{29}Si)$ [ppm]	Calc. **3c** $\delta(^{29}Si)$ [ppm]
Si3 (*Si*NHSi)	−4.0	−7.0
Si8 (NH*Si*)	96.5	93.1
Si7 (*Si*Tip)	70.9	80.1
Si6 (*Si*Tip_2)	44.6	37.1
Si4 (*Si*Tip_2)	−10.1	−11.6
Si5 (unsubstituted)	−81.9	−78.5
Si1 (*Si*Ni)	−160.5	−160.9
Si2 (unsubstituted)	−342.2	−354.4

4.4.3 Experimental vs. calculated FT-IR shifts

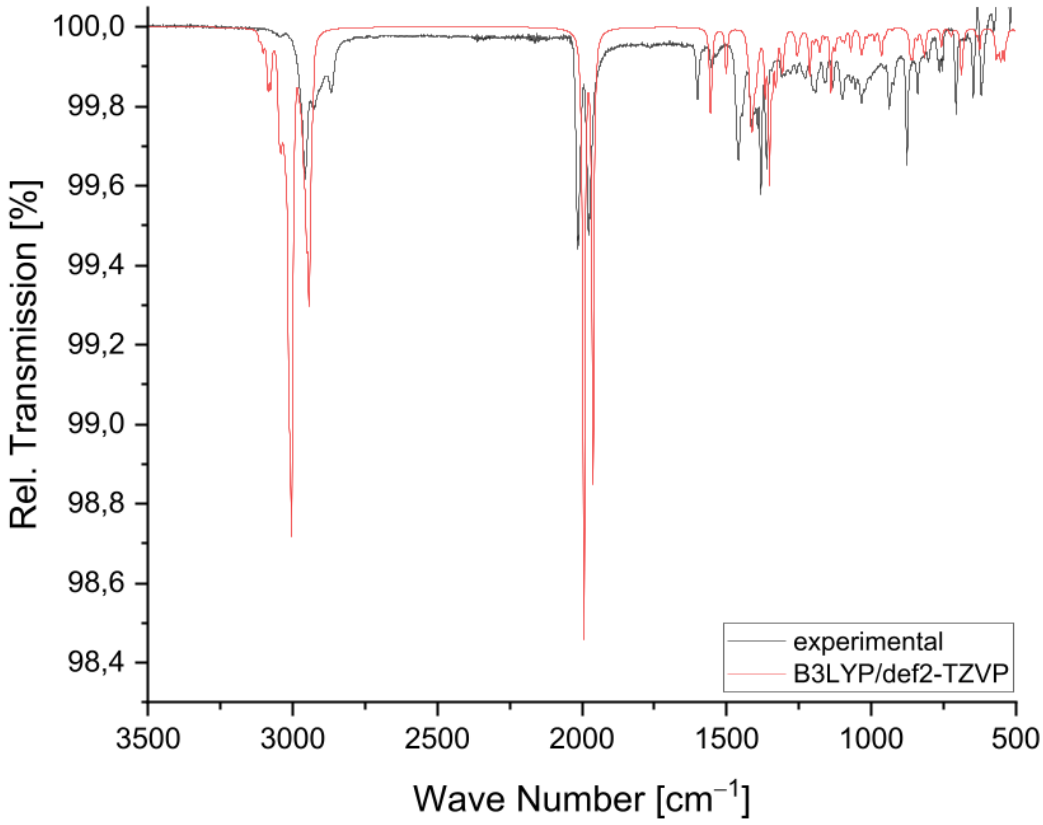

Supplementary Figure S58. Experimental vs. theoretical FT-IR spectrum of $Ni(CO)_2$ siliconoid/silylene **3c** at the B3LYP/def2-TZVP level of theory.[23–29]

4.4.4 TD-DFT calculations

Supplementary Table S20. Transition Energy. wavelength. and oscillator strengths of the electronic transition of $Ni(CO)_2$ siliconoid/silylene **3c** calculated at the TD-TPSSh/def2-TZVP level of theory.[26–29,33,34] (the 429th orbital is the highest occupied orbital (HOMO). the 430th orbital is the lowest unoccupied orbital (LUMO) shown in Supplementary Figure S57).

```
STATE  1:  E=   0.090101 au      2.452 eV    19775.0 cm**-1 <S**2> =   0.000000 Mult 1
   427a -> 430a  :     0.015750 (c=  0.12549942)
   428a -> 430a  :     0.048770 (c=  0.22083919)
   429a -> 430a  :     0.784327 (c= -0.88562242)
   429a -> 431a  :     0.031754 (c=  0.17819762)
   429a -> 432a  :     0.078200 (c=  0.27964340)

STATE  2:  E=   0.097680 au      2.658 eV    21438.2 cm**-1 <S**2> =   0.000000 Mult 1
   428a -> 430a  :     0.237174 (c= -0.48700512)
   429a -> 430a  :     0.012157 (c=  0.11025795)
   429a -> 431a  :     0.639359 (c=  0.79959910)
   429a -> 432a  :     0.079818 (c=  0.28252063)
   429a -> 435a  :     0.013073 (c=  0.11433638)

STATE  3:  E=   0.100007 au      2.721 eV    21949.1 cm**-1 <S**2> =   0.000000 Mult 1
```

```
  427a -> 430a  :     0.209767 (c=  0.45800339)
  428a -> 430a  :     0.360491 (c= -0.60040866)
  429a -> 431a  :     0.239800 (c= -0.48969426)
  429a -> 432a  :     0.154545 (c=  0.39312152)

STATE  4:  E=   0.100737 au      2.741 eV    22109.3 cm**-1 <S**2> =   0.000000 Mult 1
  427a -> 430a  :     0.110944 (c=  0.33308251)
  428a -> 430a  :     0.110421 (c= -0.33229665)
  429a -> 430a  :     0.058475 (c= -0.24181590)
  429a -> 431a  :     0.019977 (c=  0.14134001)
  429a -> 432a  :     0.639126 (c= -0.79945385)

STATE  5:  E=   0.104423 au      2.841 eV    22918.2 cm**-1 <S**2> =   0.000000 Mult 1
  426a -> 430a  :     0.030007 (c=  0.17322640)
  427a -> 430a  :     0.593019 (c=  0.77007731)
  428a -> 430a  :     0.198124 (c=  0.44511165)
  429a -> 430a  :     0.064628 (c=  0.25421991)
  429a -> 431a  :     0.041119 (c=  0.20277862)

STATE  6:  E=   0.110528 au      3.008 eV    24258.1 cm**-1 <S**2> =   0.000000 Mult 1
  425a -> 430a  :     0.023527 (c=  0.15338594)
  426a -> 430a  :     0.012842 (c= -0.11332107)
  429a -> 434a  :     0.057400 (c=  0.23958281)
  429a -> 435a  :     0.814421 (c= -0.90245267)
  429a -> 436a  :     0.017847 (c= -0.13359448)
  429a -> 437a  :     0.021769 (c= -0.14754476)

STATE  7:  E=   0.111102 au      3.023 eV    24384.2 cm**-1 <S**2> =   0.000000 Mult 1
  429a -> 433a  :     0.990609 (c=  0.99529333)

STATE  8:  E=   0.111538 au      3.035 eV    24479.9 cm**-1 <S**2> =   0.000000 Mult 1
  426a -> 430a  :     0.809643 (c= -0.89980186)
  427a -> 430a  :     0.018324 (c=  0.13536519)
  429a -> 434a  :     0.125937 (c= -0.35487659)

STATE  9:  E=   0.113061 au      3.077 eV    24814.0 cm**-1 <S**2> =   0.000000 Mult 1
  426a -> 430a  :     0.024360 (c= -0.15607536)
  427a -> 432a  :     0.012657 (c=  0.11250199)
  428a -> 431a  :     0.257348 (c=  0.50729493)
  428a -> 432a  :     0.542571 (c=  0.73659407)
  429a -> 434a  :     0.117140 (c=  0.34225763)

STATE 10:  E=   0.114297 au      3.110 eV    25085.3 cm**-1 <S**2> =   0.000000 Mult 1
  424a -> 430a  :     0.046676 (c=  0.21604598)
  426a -> 430a  :     0.057089 (c= -0.23893230)
  427a -> 432a  :     0.020347 (c= -0.14264149)
  428a -> 431a  :     0.248398 (c= -0.49839585)
  429a -> 434a  :     0.495817 (c=  0.70414242)
  429a -> 435a  :     0.027301 (c=  0.16523091)
  429a -> 436a  :     0.029102 (c=  0.17059327)
  429a -> 437a  :     0.010409 (c=  0.10202426)

STATE 11:  E=   0.116308 au      3.165 eV    25526.6 cm**-1 <S**2> =   0.000000 Mult 1
  424a -> 430a  :     0.021189 (c=  0.14556355)
  427a -> 431a  :     0.046627 (c= -0.21593401)
  427a -> 432a  :     0.049408 (c= -0.22228000)
  428a -> 431a  :     0.440742 (c=  0.66388367)
  428a -> 432a  :     0.309610 (c= -0.55642642)
  429a -> 434a  :     0.058994 (c=  0.24288693)
  429a -> 436a  :     0.024573 (c=  0.15675750)
```

STATE 12: E= 0.117162 au 3.188 eV 25714.0 cm**-1 <S**2> = 0.000000 Mult 1
424a -> 430a : 0.076921 (c= -0.27734714)
425a -> 430a : 0.780892 (c= -0.88368084)
426a -> 431a : 0.010011 (c= -0.10005595)
426a -> 432a : 0.024497 (c= -0.15651419)
429a -> 435a : 0.029589 (c= -0.17201533)

STATE 13: E= 0.118507 au 3.225 eV 26009.2 cm**-1 <S**2> = 0.000000 Mult 1
424a -> 430a : 0.041103 (c= 0.20273775)
427a -> 431a : 0.452221 (c= 0.67247391)
427a -> 432a : 0.211764 (c= 0.46017772)
427a -> 435a : 0.010976 (c= 0.10476627)
428a -> 431a : 0.011080 (c= 0.10526066)
428a -> 432a : 0.089000 (c= -0.29832934)
429a -> 434a : 0.020882 (c= 0.14450678)
429a -> 436a : 0.101090 (c= -0.31794588)

STATE 14: E= 0.118821 au 3.233 eV 26078.1 cm**-1 <S**2> = 0.000000 Mult 1
424a -> 430a : 0.018531 (c= -0.13612786)
425a -> 430a : 0.010808 (c= 0.10396080)
427a -> 431a : 0.044881 (c= 0.21185192)
427a -> 432a : 0.173892 (c= 0.41700420)
429a -> 435a : 0.022736 (c= -0.15078509)
429a -> 436a : 0.596047 (c= 0.77204060)
429a -> 437a : 0.084618 (c= 0.29089141)

STATE 15: E= 0.121014 au 3.293 eV 26559.6 cm**-1 <S**2> = 0.000000 Mult 1
426a -> 432a : 0.012976 (c= 0.11391224)
427a -> 431a : 0.387397 (c= -0.62241239)
427a -> 432a : 0.490025 (c= 0.70001779)
429a -> 434a : 0.014348 (c= 0.11978235)
429a -> 436a : 0.020824 (c= -0.14430524)

STATE 16: E= 0.123391 au 3.358 eV 27081.1 cm**-1 <S**2> = 0.000000 Mult 1
429a -> 435a : 0.010434 (c= 0.10214465)
429a -> 436a : 0.144017 (c= 0.37949551)
429a -> 437a : 0.800862 (c= -0.89490893)
429a -> 438a : 0.010854 (c= 0.10418214)

STATE 17: E= 0.124565 au 3.390 eV 27338.8 cm**-1 <S**2> = 0.000000 Mult 1
423a -> 430a : 0.032007 (c= -0.17890541)
424a -> 430a : 0.556050 (c= -0.74568792)
425a -> 430a : 0.058778 (c= 0.24244124)
426a -> 430a : 0.019458 (c= -0.13949257)
426a -> 431a : 0.015709 (c= 0.12533439)
428a -> 434a : 0.084428 (c= -0.29056576)
428a -> 435a : 0.015547 (c= 0.12468617)
429a -> 434a : 0.027014 (c= 0.16435838)
429a -> 437a : 0.013650 (c= -0.11683214)
429a -> 438a : 0.024323 (c= -0.15595771)
429a -> 439a : 0.023165 (c= 0.15220190)
429a -> 441a : 0.019387 (c= 0.13923822)

STATE 18: E= 0.126712 au 3.448 eV 27810.1 cm**-1 <S**2> = 0.000000 Mult 1
423a -> 430a : 0.016516 (c= -0.12851385)
424a -> 430a : 0.032402 (c= -0.18000692)
425a -> 430a : 0.011033 (c= 0.10503780)
426a -> 431a : 0.029344 (c= -0.17130213)
426a -> 432a : 0.235891 (c= -0.48568611)
428a -> 435a : 0.276639 (c= -0.52596457)
428a -> 436a : 0.014692 (c= -0.12121170)

```
  429a -> 435a  :     0.010011 (c=  0.10005726)
  429a -> 436a  :     0.012309 (c= -0.11094489)
  429a -> 438a  :     0.198402 (c=  0.44542338)
  429a -> 439a  :     0.039682 (c= -0.19920437)
  429a -> 440a  :     0.055004 (c= -0.23452950)

STATE 19:  E=   0.127172 au      3.461 eV    27911.0 cm**-1 <S**2> =   0.000000 Mult 1
  426a -> 431a  :     0.080139 (c= -0.28308875)
  426a -> 432a  :     0.019770 (c= -0.14060567)
  428a -> 434a  :     0.096677 (c=  0.31092931)
  428a -> 435a  :     0.189089 (c= -0.43484398)
  429a -> 438a  :     0.186244 (c= -0.43155946)
  429a -> 439a  :     0.206047 (c=  0.45392391)
  429a -> 440a  :     0.152454 (c=  0.39045380)

STATE 20:  E=   0.127376 au      3.466 eV    27955.8 cm**-1 <S**2> =   0.000000 Mult 1
  425a -> 430a  :     0.013633 (c=  0.11676056)
  425a -> 432a  :     0.018016 (c=  0.13422186)
  426a -> 431a  :     0.133527 (c= -0.36541279)
  426a -> 432a  :     0.308418 (c= -0.55535366)
  428a -> 434a  :     0.036249 (c=  0.19039189)
  428a -> 435a  :     0.335390 (c=  0.57912853)
  429a -> 438a  :     0.054961 (c= -0.23443781)
  429a -> 439a  :     0.030222 (c= -0.17384456)

STATE 21:  E=   0.128235 au      3.489 eV    28144.2 cm**-1 <S**2> =   0.000000 Mult 1
  426a -> 431a  :     0.541675 (c= -0.73598580)
  426a -> 432a  :     0.094653 (c=  0.30765714)
  428a -> 434a  :     0.080061 (c= -0.28294998)
  428a -> 435a  :     0.013374 (c=  0.11564496)
  429a -> 438a  :     0.155080 (c=  0.39380201)
  429a -> 439a  :     0.023225 (c=  0.15239795)
  429a -> 440a  :     0.030784 (c=  0.17545397)

STATE 22:  E=   0.128614 au      3.500 eV    28227.6 cm**-1 <S**2> =   0.000000 Mult 1
  423a -> 430a  :     0.044680 (c= -0.21137712)
  424a -> 430a  :     0.030112 (c= -0.17352876)
  425a -> 432a  :     0.024803 (c= -0.15748834)
  426a -> 431a  :     0.055839 (c= -0.23630204)
  426a -> 432a  :     0.160569 (c=  0.40071084)
  428a -> 433a  :     0.283647 (c=  0.53258507)
  428a -> 434a  :     0.226242 (c=  0.47564949)
  429a -> 438a  :     0.010470 (c= -0.10232263)
  429a -> 439a  :     0.028887 (c= -0.16996264)
  429a -> 440a  :     0.073557 (c= -0.27121319)

STATE 23:  E=   0.128715 au      3.503 eV    28249.7 cm**-1 <S**2> =   0.000000 Mult 1
  423a -> 430a  :     0.010419 (c= -0.10207255)
  426a -> 431a  :     0.043884 (c= -0.20948513)
  426a -> 432a  :     0.060152 (c=  0.24525883)
  428a -> 433a  :     0.554358 (c= -0.74455231)
  428a -> 435a  :     0.016784 (c= -0.12955263)
  429a -> 438a  :     0.121766 (c= -0.34894962)
  429a -> 439a  :     0.064028 (c= -0.25303664)
  429a -> 440a  :     0.079944 (c= -0.28274450)

STATE 24:  E=   0.128866 au      3.507 eV    28282.8 cm**-1 <S**2> =   0.000000 Mult 1
  423a -> 430a  :     0.012124 (c= -0.11010981)
  425a -> 432a  :     0.011593 (c= -0.10767066)
  426a -> 431a  :     0.035505 (c=  0.18842748)
  428a -> 433a  :     0.153020 (c= -0.39117738)
```

```
  428a -> 434a  :     0.351863 (c=  0.59318080)
  428a -> 435a  :     0.066762 (c=  0.25838391)
  429a -> 438a  :     0.198847 (c=  0.44592315)
  429a -> 439a  :     0.065849 (c=  0.25661154)
  429a -> 440a  :     0.023374 (c=  0.15288541)
  429a -> 441a  :     0.016692 (c=  0.12919858)

STATE 25:  E=   0.131415 au      3.576 eV    28842.2 cm**-1 <S**2> =   0.000000 Mult 1
  423a -> 430a  :     0.070095 (c= -0.26475510)
  427a -> 434a  :     0.158507 (c=  0.39812962)
  429a -> 439a  :     0.323882 (c= -0.56910619)
  429a -> 440a  :     0.355148 (c=  0.59594265)
  429a -> 441a  :     0.018214 (c=  0.13495777)

STATE 26:  E=   0.131733 au      3.585 eV    28912.0 cm**-1 <S**2> =   0.000000 Mult 1
  423a -> 430a  :     0.102057 (c= -0.31946304)
  425a -> 431a  :     0.340653 (c=  0.58365460)
  425a -> 432a  :     0.372997 (c=  0.61073484)
  427a -> 434a  :     0.010326 (c=  0.10161763)
  427a -> 435a  :     0.049020 (c=  0.22140487)
  429a -> 439a  :     0.024424 (c=  0.15628094)
  429a -> 440a  :     0.024360 (c= -0.15607833)

STATE 27:  E=   0.132096 au      3.595 eV    28991.6 cm**-1 <S**2> =   0.000000 Mult 1
  425a -> 431a  :     0.014395 (c= -0.11997896)
  427a -> 434a  :     0.131445 (c= -0.36255368)
  427a -> 435a  :     0.588147 (c=  0.76690734)
  429a -> 439a  :     0.014598 (c= -0.12082119)
  429a -> 440a  :     0.052391 (c=  0.22889003)
  429a -> 441a  :     0.116552 (c= -0.34139646)
  429a -> 442a  :     0.011698 (c=  0.10815822)

STATE 28:  E=   0.132420 au      3.603 eV    29062.8 cm**-1 <S**2> =   0.000000 Mult 1
  423a -> 430a  :     0.163145 (c=  0.40391183)
  425a -> 431a  :     0.013986 (c= -0.11826160)
  427a -> 433a  :     0.035675 (c=  0.18887794)
  427a -> 434a  :     0.373712 (c=  0.61132017)
  427a -> 435a  :     0.190185 (c=  0.43610186)
  428a -> 436a  :     0.032681 (c=  0.18077885)
  429a -> 440a  :     0.063246 (c= -0.25148792)
  429a -> 441a  :     0.042638 (c=  0.20648881)
  429a -> 443a  :     0.014796 (c=  0.12163722)

STATE 29:  E=   0.132787 au      3.613 eV    29143.4 cm**-1 <S**2> =   0.000000 Mult 1
  423a -> 430a  :     0.023922 (c= -0.15466785)
  427a -> 433a  :     0.893869 (c=  0.94544637)
  429a -> 441a  :     0.036091 (c= -0.18997575)

STATE 30:  E=   0.132922 au      3.617 eV    29173.1 cm**-1 <S**2> =   0.000000 Mult 1
  423a -> 430a  :     0.166163 (c= -0.40763113)
  425a -> 431a  :     0.016251 (c= -0.12748081)
  425a -> 432a  :     0.067881 (c= -0.26053947)
  427a -> 433a  :     0.063076 (c= -0.25115003)
  427a -> 434a  :     0.225408 (c=  0.47477108)
  428a -> 434a  :     0.014606 (c= -0.12085605)
  428a -> 436a  :     0.021298 (c= -0.14593800)
  429a -> 439a  :     0.098759 (c=  0.31425897)
  429a -> 441a  :     0.196369 (c= -0.44313530)
  429a -> 442a  :     0.030553 (c=  0.17479293)
  429a -> 443a  :     0.012506 (c= -0.11182809)
```

4.5 TD-DFT Overview

Supplementary Table S21. Extended comparison of wavelengths λ_{max}, oscillator strengths f, and excitation energy E from experimental and TD-DFT calculations at TD-TPSSh/def2-TZVP[26–29,33,34] for transition metal complexes **2**-**3c**.

	Experimental		Calculated			
	λ_{max} (nm)	Excitation energy E (eV)	λ_{max} (nm)	Excitation energy E (eV)	Oscillator strength f	Transitions (% contribution)
2	525	2.362	528	2.349	0.00277	HOMO→LUMO (98.6)
	342	3.625	355	3.493	0.0365	HOMO−15→LUMO (5.9) HOMO−14→LUMO (1.6) HOMO−13→LUMO (27.7) HOMO−12→LUMO (5.0) HOMO−11→LUMO (25.8) HOMO−10→LUMO (3.7) HOMO−7→LUMO (1.3) HOMO−5→LUMO+1 (1.2) HOMO−3→LUMO+1 (5.1) HOMO−2→LUMO+1 (7.5) HOMO→LUMO+2 (10.6)
			353	3.516	0.0282	HOMO−15→LUMO (6.1) HOMO−13→LUMO (68.9) HOMO−11→LUMO (10.6) HOMO−10→LUMO (1.8) HOMO−5→LUMO+1 (1.1) HOMO−3→LUMO+1 (1.1) HOMO−2→LUMO+1 (4.2) HOMO→LUMO+2 (1.3)

			350	3.516	0.0054	HOMO−4→LUMO+1 (54.5) HOMO−4→LUMO+2 (2.5) HOMO−4→LUMO+7 (1.5) HOMO−3→LUMO+1 (2.9) HOMO−1→LUMO+1 (1.7) HOMO−1→LUMO+2 (26.8) HOMO−1→LUMO+7 (1.3)
3a	538	2.305	546	2.269	0.0416	HOMO−2→LUMO (1.1) HOMO−1→LUMO (18.9) HOMO→LUMO (52.6) HOMO→LUMO+1 (19.0) HOMO→LUMO+2 (4.8)
			520	2.386	0.0145	HOMO−2→LUMO (3.5) HOMO−1→LUMO (72.6) HOMO→LUMO (5.3) HOMO→LUMO+1 (13.6)
			516	2.402	0.0822	HOMO−2→LUMO (2.2) HOMO−1→LUMO (2.3) HOMO→LUMO (23.7) HOMO→LUMO+1 (65.4) HOMO→LUMO+2 (3.0)
			402	3.085	0.0108	HOMO−5→LUMO (2.1) HOMO−4→LUMO (5.5) HOMO−3→LUMO (1.3) HOMO−3→LUMO+1 (74.6) HOMO−3→LUMO+2 (6.7) HOMO−3→LUMO+4 (1.5) HOMO−1→LUMO+4 (2.9)

	392	3.163	399	3.105	0.0111	HOMO−5→LUMO (2.3) HOMO−4→LUMO (2.0) HOMO−1→LUMO+4 (7.1) HOMO→LUMO+6 (83.3) HOMO→LUMO+7 (1.0)
			395	3.136	0.0145	HOMO−5→LUMO (9.0) HOMO−4→LUMO (2.2) HOMO−3→LUMO+1 (1.6) HOMO−2→LUMO+2 (1.2) HOMO−1→LUMO+4 (72.1) HOMO−1→LUMO+5 (1.2) HOMO→LUMO+6 (4.2)
3b	596	2.080	740	1.675	0.0179	HOMO→LUMO (89.6) HOMO→LUMO+1 (4.2) HOMO→LUMO+3 (2.2)
			572	2.169	0.0439	HOMO−2→LUMO (2.7) HOMO−1→LUMO (2.5) HOMO→LUMO+1 (76.8) HOMO→LUMO+2 (3.6) HOMO→LUMO+3 (11.4)
			555	2.232/	0.0517	HOMO→LUMO (1.7) HOMO→LUMO+1 (3.1) HOMO→LUMO+2 (92.3)
	519	2.389	472	2.629	0.167	HOMO−6→LUMO (6.3) HOMO−5→LUMO (15.5) HOMO−4→LUMO (31.0) HOMO−3→LUMO (2.7) HOMO−2→LUMO (5.3)

					HOMO−1→LUMO (2.3) HOMO→LUMO (2.2) HOMO→LUMO+1 (4.6) HOMO→LUMO+3 (9.3) HOMO→LUMO+6 (4.1) HOMO→LUMO+7 (7.2)
	365	3.397	361	3.432	0.0115	HOMO−8→LUMO (1.7) HOMO−6→LUMO+1 (7.6) HOMO−6→LUMO+2 (3.6) HOMO−5→LUMO+1 (2.0) HOMO−5→LUMO+3 (19.1) HOMO−4→LUMO+1 (1.1) HOMO−4→LUMO+3 (3.1) HOMO−4→LUMO+5 (25.5) HOMO−3→LUMO+6 (1.7) HOMO−3→LUMO+7 (2.0) HOMO−2→LUMO+7 (15.4) HOMO−2→LUMO+8 (1.8) HOMO→LUMO+21 (1.9)
	523	2.371	506	2.45	0.0930	HOMO−2→LUMO (1.6) HOMO−1→LUMO (4.9) HOMO→LUMO (99.6) HOMO→LUMO+1 (3.2) HOMO→LUMO+2 (7.8)
	472	2.627	456	2.721	0.00234	HOMO−2→LUMO (21.0) HOMO−1→LUMO (36.0) HOMO→LUMO+1 (8.0) HOMO→LUMO+2 (1.3)

			452	2.741	0.1091	HOMO−2→LUMO (11.1) HOMO−1→LUMO (11.0) HOMO→LUMO (5.8) HOMO→LUMO+1 (2.0) HOMO→LUMO+2 (63.9)
3c	363	3.416	360	3.358	0.0061	HOMO−6→LUMO (1.7) HOMO−5→LUMO (3.2) HOMO−4→LUMO (1.1) HOMO−3→LUMO+1 (2.9) HOMO−3→LUMO+2 (23.6) HOMO−1→LUMO+5 (27.7) HOMO−1→LUMO+6 (1.5) HOMO→LUMO+5 (1.0) HOMO→LUMO+6 (1.2) HOMO→LUMO+8 (19.8) HOMO→LUMO+9 (4.0) HOMO→LUMO+10 (5.5)
			358	3.461	0.0086	HOMO−3→LUMO+1 (8.0) HOMO−3→LUMO+2 (2.0) HOMO−1→LUMO+4 (9.7) HOMO−1→LUMO+5 (18.9) HOMO→LUMO+8 (18.6) HOMO→LUMO+9 (20.6) HOMO→LUMO+10 (15.2)
			358	3.466	0.0689	HOMO−4→LUMO (1.3) HOMO−4→LUMO+2 (1.8) HOMO−3→LUMO+1 (13.4)

			HOMO−3→LUMO+2 (30.8) HOMO−1→LUMO+4 (3.6) HOMO−1→LUMO+5 (33.5) HOMO→LUMO+8 (5.5) HOMO→LUMO+9 (3.0)

5 References

[1] K. I. Leszczyńska, V. Huch, C. Präsang, J. Schwabedissen, R. J. F. Berger and D. Scheschkewitz, *Angew. Chem. Int. Ed.*, 2019, **58**, 5124.

[2] C. W. So, H. W. Roesky, J. Magull and R. B. Oswald, *Angew. Chem. Int. Ed.*, 2006, **46**, 3948.

[3] S. S. Sen, H. W. Roesky, D. Stern, J. Henn and D. Stalke, *J. Am. Chem. Soc.*, 2010, **132**, 1123.

[4] L. Giarrana, M. Zimmer, B. Morgenstern and D. Scheschkewitz, *Inorg. Chem.*, 2024, **63**, 20083.

[5] R. E. H. Kuveke, L. Barwise, Y. van Ingen, K. Vashisth, N. Roberts, S. S. Chitnis, J. L. Dutton, C. D. Martin and R. L. Melen. *ACS Cent. Sci.*, 2022, **8**, 855.

[6] T. K. Mukhopadhyay, M. Flores, T. L. Groy and R. J. Trovitch, *Chem. Sci.*, 2018, **9**, 7673.

[7] C. L. Rock and R. J. Trovitch, *Dalton Trans.*, 2019, **48**, 461.

[8] T. K. Mukhopadhyay, M. Flores, T. L. Groy and R. J. Trovitch, *Chem. Sci.*, 2018, **9**, 7673.

[9] C. L. Rock and R. J. Trovitch, *Dalton Trans.*, 2019, **48**, 461.

[10] J. Wang, Y. Gurevich, M. Botoshansky and M. S. Eisen, *Organometallics,* 2008, **27**, 4494.

[11] P. M. Keil and T. J. Hadlington, *Angew. Chem. Int. Ed.*, 2022, **61**, e202114143.

[12] C. Zarate, H. Yang, M. J. Bezdek, D. Hesk and P. J. Chirik, *J. Am. Chem. Soc.*, 2019, **141**, 5034.

[13] L. Garcia, C. Dinoi, M. F. Mahon, L. Maron and M. S. Hill, *Chem. Sci.*, 2019, **10**, 8108.

[14] G. M. Sheldrick, *Acta Cryst. A,* 2015, **71**, 3.

[15] G. M. Sheldrick, *Acta Cryst. C, Struct. Chem.*, 2015, **71**, 3.

[16] C. B. Hübschle, G. M. Sheldrick and B, Dittrich, *J. Appl. Cryst.*, 2011, **44**, 1281.

[17] A. L. Spek, *Acta Cryst., C, Struct. Chem.*, 2015, **71**, 9.

[18] A. L. Spek, *Acta Cryst., D, Biol. Cryst.*, 2009, **65**, 148.

[19] L. Falivene, Z. Cao, A. Petta, L. Serra, A. Poater, R. Oliva, V. Scarano and L. Cavallo, *Nat. Chem.*, 2019. **11**. 872.

[20] N. E. Poitiers, L. Giarrana, K. I. Leszczyńska, V. Huch, M. Zimmer and D. Scheschkewitz, *Angew. Chem. Int. Ed.*, 2020, **59**, 8532.

[21] F. Neese, F. Wennmohs, U. Becker and C. Riplinger, *J. Chem. Phys.*, 2020, **152**, 224108.

[22] F. Neese, *WIREs Comput. Mol. Sci.*, 2022, **12**, e1606.

[23] J. P. Perdew, *Phys. Rev. B*, 1986, **33**, 8822.

[24] A. D. Becke, *Phys. Rev. A*, 1988. **38**, 3098.

[25] C. Lee, W. Yang and R. G. Parr, *Phys. Rev. B*, 1988, **37**. 785.

[26] F. Weigend and R. Ahlrichs, *Phys. Chem. Chem. Phys.*, 2005, **7**, 3297.

[27] A. Schäfer, H. Horn and R. Ahlrichs, *J. Chem. Phys.*, 1992. **97**. 2571.

[28] A. Schäfer, C. Huber and R. Ahlrichs, *J. Chem. Phys.,* 1994, **100**, 5829.

[29] F. Weigend, *Phys. Chem. Chem. Phys.*, 2006, **8**, 1057.

[30] S. Grimme, S. Ehrlich and L. Goerigk, *J. Comput. Chem.,* 2011, **32**, 1456.

[31] V. Barone and M. Cossi, *J. Phys. Chem. A*, 1998, **102**, 1995.

[32] G. L. Stoychev, A. A. Auer, R. Izsák and F. Neese, *J. Chem. Theory Comput.*, 2018, **14**, 619.

[33] V. N. Staroverov, G. E. Scuseria, J. Tao, J. P. Perdew, *J. Chem. Phys.*, 2003, **119**, 12129.

[34] E. Runge and E. K. U. Gross, *Phys. Rev. Lett,* 1984, **52**, 997.

[35] M. K. Kesharwani, B. Brauer, J. M. L. Martin, *J. Phys. Chem. A*, 2015, **119**, 1701.

[36] L. Zamirri, Silvia Casassa, A. Rimola, M. Segado-Centellas, C. Ceccarelli, P. Ugliengo, *Mon. Not. R. Astron. Soc.*, 2018, **480**, 1427.

[37] Chemcraft - graphical software for visualization of quantum chemistry computations. https://www.chemcraftprog.com

6 Author Contributions

L. Giarrana performed the synthetic work and data analysis with partial support by D. Welterlich; L. Giarrana. and D. Scheschkewitz designed the study. D. Scheschkewitz acquired the funding; B. Morgenstern performed the X-ray diffraction studies. M. Zimmer performed the solid state and variable temperature NMR measurements. L. Giarrana performed the DFT calculations. L. Giarrana wrote the initial manuscript draft. L. Giarrana and D. Scheschkewitz reviewed and edited the manuscript.

6. References

[1] K. Y. Kamal, *J. Eng. Sci. Technol. Rev.* **2022**, *15*, 110–115.

[2] T. Thomson, in *A system of chemistry in four volumes*, London, Baldwin, Craddock And Joy, **1817**.

[3] Sir H. Davy, *Philos. Trans. R. Soc. Lond.* **1808**, *98*, 333–370.

[4] Sir H. Davy, *Ann. Phys.* **1809**, *32*, 365–368.

[5] Sir H. Davy, *Philos. Trans. R. Soc. Lond.* **1810**, *100*, 16–74.

[6] A. L. de Lavoisier, *Elements of Chemistry: In a New Systematic Order Containing All the Modern Discoveries*, William Creech, Edinburgh, **1799**.

[7] A. L. de Lavoisier, *Traité Élémentaire de Chimie*, Chez Cuchet, **1789**.

[8] J. J. Berzelius, *Ann. Phys.* **1825**, *80*, 117–156.

[9] H. S.-C. Deville, *J. prakt. Chem.***1854**, *63*, 113–120.

[10] D. Yan, in *Handbook of Photovoltaic Silicon*, Springer Berlin Heidelberg, Berlin, Heidelberg, **2019**, pp. 37–68.

[11] M. Tilli, M. Paulasto-Kröckel, M. Petzold, H. Theuss, T. Motooka, V. Lindroos, in *Handbook of Silicon Based MEMS Materials and Technologies*, Elsevier, **2010**, pp. 3–17.

[12] J. Czochralski, *Z. Phys. Chem.* **1918**, *92U*, 219–221.

[13] E. Wiberg, in *Lehrbuch der anorganischen Chemie*, Walter De Gruyter, Berlin, **2007**.

[14] M. A. Brook, in *Silicon in Organic, Organometallic, and Polymer Chemistry*, John Wiley & Sons, **2000**.

[15] E. Riedel, C. Janiak, in *Anorganische Chemie*, Berlin, Boston: De Gruyter, **2007**.

[16] A. Brown, *J. D. Bernal : the sage of science*, Oxford University Press, **2005**.

[17] W. G. Pfann, *JOM* **1952**, *4*, 747–753.

[18] V. Y. Lee, *Org. Chem. Curr. Res.* **2012**, *1*, e112.

[19] P. Siffert, E. Krimmel, in *Silicon: Evolution and future of a technology*, Science & Business Media, Springer, **2004**.

[20] W. Roger Cannon, E. Gugel, G. Leimer, G. Woetting, R. B. Heimann, in *Ullmann's Encyclopedia of Industrial Chemistry*, Wiley-VCH Verlag GmbH & Co. KGaA, Weinheim, Germany, **2011**.

[21] L. R. Pinckney, in *Ullmann's Encyclopedia of Industrial Chemistry*, Wiley-VCH Verlag GmbH & Co. KGaA, Weinheim, Germany, **2013**, pp. 1–15.

[22] C. B. Carter, M. G. Norton, *Ceramic materials: science and engineering*, Springer, **2013**.

[23] J. Kropp, in *Ullmann's Encyclopedia of Industrial Chemistry*, Wiley-VCH Verlag GmbH & Co. KGaA, Weinheim, Germany, **2008**.

[24] P. C. Hewlett M. Liska, in *Lea's chemistry of cement and concrete*, fourth edition, Butterworth-Heinemann, **2019**.

[25] E. Frieden, *Sci. Am.* **1972**, *227*, 52–60.

[26] S. Ghosh, G. Mugesh, *Curr. Sci.* **2019**, *117*, 1971–1985.

[27] R. M. Hazen, R. J. Hemley, A. J. Mangum, *Eos, Trans. Am. Geophys. Union* **2012**, *93*, 17–18.

[28] J. Y. Corey, in *The Chemistry of Organic Silicon Compounds* (Ed.: S. Patai, Z. Rappoport), Volume 2, John Wiley & Sons Ltd, Chichester, UK, **1989**, Chapter 1, pp. 1–56.

[29] C. A. Reed, *Acc. Chem. Res.* **1998**, *31*, 325–332.

[30] L. Pauling, *J. Am. Chem. Soc.* **1932**, *54*, 3570–3582.

[31] P. W. Atkins, J. De Paula, J. Keeler, in *Atkins' Physical Chemistry*, Eighth Edition, Oxford University Press, **2006**.

[32] R. Corriu, *J. Organomet. Chem.* **2003**, *686*, 32–41.

[33] R. Corriu, *J. Organomet. Chem.* **2003**, *686*, 1.

[34] V. Ya. Lee, A. Sekiguchi, in *Organometallic compounds of low-coordinate Si, Ge, Sn, and Pb : from phantom species to stable compounds*, First Edition, John Wiley & Sons Ltd, Chichester, UK, **2010**.

[35] V. Ya Lee, *Organic Chem. Curr. Res.* **2012**, *1*, e112.

[36] D. Seyferth, *Organometallics* **2001**, *20*, 4978–4992.

[37] F. S. Kipping, *Proc. R. Soc. Lond. A Math. Phys. Sci.* **1937**, *159*, 139–148.

[38] H. Moretto, M. Schulze, G. Wagner, in *Ullmann's Encyclopedia of Industrial Chemistry*, Wiley-VCH Verlag GmbH & Co. KGaA, Weinheim, Germany, **2000**.

[39] M. Andriot, J. V. DeGroot, Jr. and R. Meeks, E. Gerlach, M. Jungk, A.T. Wolf, S. Cray, T. Easton, A. Mountney, S. Leadley, S.H. Chao, A. Colas, F. de Buyl, A. Dupont, J. L. Garaud, F. Gubbels, J. P. Lecomte, B. Lenoble, S. Stassen, C. Stevens, X. Thomas, G. Shearer, *Inorg. Polym.* **2007**, 61–161.

[40] E. G. Rochow, *J. Am. Chem. Soc.* **1945**, *67*, 963–965.

[41] R. Müller, G. Seitz, *Chem. Ber.* **1958**, *91*, 22–27.

[42] R. Müller, *Verfahren Zur Herstellung von Kohlenstoff-Silicium-Halogenverbindungen*, **1942**, DD 5348.

[43] E. G. Rochow, *Preparation of Organosilicon Halides*, **1945**, 412, 459, 1–4.

[44] R. Müller, *Z. Angew., Chem. Silicone (Synth.). Chem. Tech.* **1950**, *2*, 41–50.

[45] A. G. Brook, F. Abdesaken, B. Gutekunst, G. Gutekunst, R. K. Kallury, *J. Chem. Soc. Chem. Commun.* **1981**, 191–192.

[46] R. West, M. J. Fink, J. Michl, *Science* **1981**, *214*, 1343–1344.

[47] P. Jutzi, D. Kanne, C. Krüger, *Angew. Chem. Int. Ed.* **1986**, *25*, 164.

[48] B.-X. Leong, J. Lee, Y. Li, M.-C. Yang, C.-K. Siu, M.-D. Su, C.-W. So, *J. Am. Chem. Soc.* **2019**, *141*, 17629–17636.

6. References

[49] Y. Xiong, S. Yao, T. Szilvási, A. Ruzicka, M. Driess, *Chem. Commun.* **2020**, *56*, 747–750.

[50] E. Fritz-Langhals, *Org. Process Res. Dev.* **2019**, *23*, 2369–2377.

[51] E. Fritz-Langhals, R. Weidner, P. Jutzi, *Precious Metal-Free Hydrosilylation of Unsaturated Compounds Catalyzed by Cationic Si(II) Complexes*, **2017**, WO 2017/174290 A1.

[52] M. Majumdar, I. Bejan, V. Huch, A. J. P. White, G. R. Whittell, A. Schäfer, I. Manners, D. Scheschkewitz, *Chem. Eur. J.* **2014**, *20*, 9225–9229.

[53] I. M. T. Davidson, *J. Organomet. Chem.* **1970**, *24*, 97–100.

[54] H. Murakami, T. Kanayama, *Appl. Phys. Lett.* **1995**, *67*, 2341–2343.

[55] M. O. Watanabe, H. Murakami, T. Miyazaki, T. Kanayama, *Appl. Phys. Lett.* **1997**, *71*, 1207–1209.

[56] W. M. M. Kessels, M. C. M. van de Sanden, D. C. Schram, *Appl. Phys. Lett.* **1998**, *72*, 2397–2399.

[57] H. Yorimitsu, M. Kotora, N. T. Patil, *Chem. Rec.* **2021**, *21*, 3335–3337.

[58] P. P. Power, *Nature* **2010**, *463*, 171–177.

[59] S. Yadav, S. Saha, S. S. Sen, *ChemCatChem* **2016**, *8*, 486–501.

[60] P. Sabatier, in *La catalyse en chimie organique*, Nouveau Monde, **1913**.

[61] Z. Hendi, M. K. Pandey, S. K. Kushvaha, H. W. Roesky, *Chem. Commun.* **2024**, *60*, 9483–9512.

[62] Z. Benedek, T. Szilvási, *RSC Adv.* **2015**, *5*, 5077–5086.

[63] T. J. Hadlington, in *On the Catalytic Efficacy of Low-Oxidation State Group 14 Complexes*, Springer International Publishing, Cham, **2017**.

[64] D. Scheschkewitz, in *Functional molecular silicon compounds. II, Low oxidation states*, Springer, **2014**.

[65] C. Weetman, in *Encyclopedia of Inorganic and Bioinorganic Chemistry*, Wiley, **2021**, 1–27.

[66] M. Haaf, T. A. Schmedake, R. West, *Acc. Chem. Res.* **2000**, 704–714.

[67] K. Krogh-Jespersen, *J. Am. Chem. Soc.* **1985**, *107*, 537–543.

[68] H. Tomioka, in *Reactive Intermediate Chemistry*, Wiley, **2003**, Chapter 9, pp. 375–461.

[69] D. Bourissou, O. Guerret, F. P. Gabbaï, G. Bertrand, *Chem. Rev.* **2000**, *100*, 39–92.

[70] F. Hanusch, L. Groll, S. Inoue, *Chem. Sci.* **2021**, *12*, 2001–2015.

[71] Y. Mizuhata, T. Sasamori, N. Tokitoh, *Chem. Rev.* **2009**, *109*, 3479–3511.

[72] C. F. Bender, H. F. Schaefer, *J. Am. Chem. Soc.* **1970**, *92*, 4984–4985.

[73] I. Shavitt, *Tetrahedron* **1985**, *41*, 1531–1542.

[74] P. Pyykko, *Chem. Rev.* **1988**, *88*, 563–594.

[75] P. P. Gaspar, M. Xiao, D. H. Pae, D. J. Berger, T. Haile, T. Chen, D. Lei, W. R. Winchester, P. Jiang, *J. Organomet. Chem.* **2002**, *646*, 68–79.

[76] J. C. Stephens, Y. Yamaguchi, C. David Sherrill, H. F. Schaefer, *J. Phys. Chem. A* **1998**, 3999–4006.

[77] T. J. Van Huis, Y. Yamaguchi, C. D. Sherrill, H. F. Schaefer, *J. Phys. Chem. A* **1997**, 6955–6963.

[78] Y. Apeloig, R. Pauncz, M. Karni, R. West, W. Steiner, D. Chapman, *Organometallics* **2003**, *16*, 3250–3256.

[79] F. Hanusch, L. Groll, S. Inoue, *Chem. Sci.* **2021**, *12*, 2001–2015.

[80] J. Goubeau, *Angew. Chem.* **1957**, *69*, 77–82.

[81] P. Jutzi, *Angew. Chem. Int. Ed.* **1975**, *14*, 232–245.

[82] H. Jacobsen, T. Ziegler, *J. Am. Chem. Soc.* **1994**, *116*, 3667–3679.

[83] P. J. Davidson, D. H. Harris, M. F. Lappert, *J. Chem. Soc., Dalton Trans.* **1976**, 2268–2274.

[84] J. D. Cotton, P. J. Davidson, M. F. Lappert, *J. Chem. Soc., Dalton Trans.* **1976**, 2275–2286.

[85] D. E. Goldberg, D. H. Harris, M. F. Lappert, K. M. Thomas, *J. Chem. Soc., Chem. Commun.* **1976**, 261–262.

[86] P. B. Hitchcock, M. F. Lappert, S. J. Miles, A. J. Thorne, *J. Chem. Soc., Chem. Commun.* **1984**, *347*, 480–482.

[87] P. P. Power, *Chem. Rev.* **1999**, *99*, 3463–3504.

[88] E. A. Carter, W. A. Goddard, *J. Phys. Chem.* **1986**, *90*, 998–1001.

[89] J. P. Malrieu, G. Trinquier, *J. Am. Chem. Soc.* **1989**, *111*, 5916–5921.

[90] R. C. Fischer, P. P. Power, *Chem. Rev.* **2010**, 3877–3923.

[91] M. Karni, Y. Apeloig, *J. Am. Chem. Soc.* **1990**, *112*, 8589–8590.

[92] M. Wind, D. R. Powell, R. West, *Organometallics* **1996**, 5772–5773.

[93] M. J. Fink, M. J. Michalczyk, K. J. Haller, J. Michl, R. West, *Organometallics* **1984**, *3*, 793–800.

[94] B. D. Shepherd, C. F. Campana, R. West, *Heteroat. Chem.* **1990**, *1*, 1–7.

[95] V. Ya. Lee, *Molecules* **2023**, *28*, 1558.

[96] P. J. Thorsten Kühler, *Adv. Organomet. Chem.* **2003**, *49*, 1–34.

[97] A. Igau, A. Baceiredo, G. Trinquier, G. Bertrand, *Angew. Chem. Int. Ed.* **1989**, *28*, 621–622.

[98] A. J. Arduengo, R. L. Harlow, M. Kline, *J. Am. Chem. Soc.* **1991**, *113*, 361–363.

[99] M. Denk, R. Lennon, R. Hayashi, R. West, A. V Belyakov, H. P. Verne, A. Haaland, M. Wagner, N. Metzler, *J. Am. Chem. Soc.* **1994**, *116*, 2691–2692.

[100] P. S. Skell, E. J. Goldstein, *J. Am. Chem. Soc.* **1964**, *86*, 1442–1443.

6. References

[101] W. H. Atwell, D. R. Weyenberg, *Angew. Chem. Int. Ed.* **1969**, *8*, 469–477.

[102] M. Haaf, A. Schmiedl, T. A. Schmedake, D. R. Powell, A. J. Millevolte, M. Denk, R. West, *J. Am. Chem. Soc.* **1998**, *120*, 12714–12719.

[103] B. Gehrhus, P. B. Hitchcock, M. F. Lappert, J. Heinicke, R. Boese, D. Bläser, *J. Organomet. Chem.* **1996**, *521*, 211–220.

[104] M. Kira, S. Ishida, T. Iwamoto, C. Kabuto, *J. Am. Chem. Soc.* **1999**, *121*, 9722–9723.

[105] N. J. Hill, R. West, *J. Organomet. Chem.* **2004**, *689*, 4165–4183.

[106] M. Driess, S. Yao, M. Brym, C. Van Wüllen, D. Lentz, *J. Am. Chem. Soc.* **2006**, *128*, 9628–9629.

[107] C. W. So, H. W. Roesky, J. Magull, R. B. Oswald, *Angew. Chem. Int. Ed.* **2006**, *45*, 3948–3950.

[108] D. Gau, T. Kato, N. Saffon-Merceron, A. De Cózar, F. P. Cossío, A. Baceiredo, *Angew. Chem. Int. Ed.* **2010**, *49*, 6585–6588.

[109] A. Rosas-Sánchez, I. Alvarado-Beltran, A. Baceiredo, N. Saffon-Mer-Ceron, S. Massou, V. Branchadell, T. Kato, *Angew. Chem. Int. Ed.* **2017**, *56*, 10481–10485.

[110] T. Troadec, T. Wasano, R. Lenk, A. Baceiredo, N. Saffon-Merceron, D. Hashizume, Y. Saito, N. Nakata, V. Branchadell, T. Kato, *Angew. Chem. Int. Ed.* **2017**, *56*, 6891–6895.

[111] T. Kosai, S. Ishida, T. Iwamoto, *Angew. Chem. Int. Ed.* **2016**, *55*, 15554–15558.

[112] N. Weyer, M. Heinz, J. I. Schweizer, C. Bruhn, M. C. Holthausen, U. Siemeling, *Angew. Chem. Int. Ed.* **2021**, *60*, 2624–2628.

[113] C. Shan, S. Yao, M. Driess, *Chem. Soc. Rev.* **2020**, *49*, 6733–6754.

[114] L. Wang, Y. Li, Z. Li, M. Kira, *Coord. Chem. Rev.* **2022**, *457*, 214413–214442.

[115] S. S. Sen, H. W. Roesky, D. Stern, J. Henn, D. Stalke, *J. Am. Chem. Soc.* **2010**, *132*, 1123–1126.

[116] A. Rosas-Sánchez, I. Alvarado-Beltran, A. Baceiredo, N. Saffon-Merceron, S. Massou, D. Hashizume, V. Branchadell, T. Kato, *Angew. Chem. Int. Ed.* **2017**, *56*, 15916–15920.

[117] G. H. Lee, R. West, T. Müller, *J. Am. Chem. Soc.* **2003**, *125*, 8114–8115.

[118] A. C. Filippou, O. Chernov, G. Schnakenburg, *Angew. Chem. Int. Ed.* **2009**, *48*, 5687–5690.

[119] R. S. Ghadwal, H. W. Roesky, S. Merkel, J. Henn, D. Stalke, *Angew. Chem. Int. Ed.* **2009**, *48*, 5683–5686.

[120] A. V. Protchenko, K. H. Birjkumar, D. Dange, A. D. Schwarz, D. Vidovic, C. Jones, N. Kaltsoyannis, P. Mountford, S. Aldridge, *J. Am. Chem. Soc.* **2012**, *134*, 6500–6503.

[121] B. D. Rekken, T. M. Brown, J. C. Fettinger, H. M. Tuononen, P. P. Power, *J. Am. Chem. Soc.* **2012**, *134*, 6504–6507.

[122] A. V. Protchenko, A. D. Schwarz, M. P. Blake, C. Jones, N. Kaltsoyannis, P. Mountford, S. Aldridge, *Angew. Chem. Int. Ed.* **2013**, *52*, 568–571.

[123] B. D. Rekken, T. M. Brown, J. C. Fettinger, F. Lips, H. M. Tuononen, R. H. Herber, P. P. Power, *J. Am. Chem. Soc.* **2013**, *135*, 10134–10148.

[124] F. Lips, J. C. Fettinger, A. Mansikkamäki, H. M. Tuononen, P. P. Power, *J. Am. Chem. Soc.* **2014**, *136*, 634–637.

[125] Y. Zhou, M. Driess, *Angew. Chem. Int. Ed.* **2019**, *58*, 3715–3728.

[126] P. P. Gaspar, M. Xiao, D. H. Pae, D. J. Berger, T. Haile, T. Chen, D. Lei, W. R. Winchester, P. Jiang, *J. Organomet. Chem.* **2002**, *646*, 68–79.

[127] A. C. Filippou, Y. N. Lebedev, O. Chernov, M. Straßmann, G. Schnakenburg, *Angew. Chem. Int. Ed.* **2013**, *52*, 6974–6978.

[128] M. Driess, *Nat. Chem.* **2012**, *4*, 525–526.

[129] S. Fujimori, S. Inoue, *Eur. J. Inorg. Chem.* **2020**, *2020*, 3131–3142.

[130] C. Ganesamoorthy, J. Schoening, C. Wölper, L. Song, P. R. Schreiner, S. Schulz, *Nat. Chem.* **2020**, *12*, 608–614.

[131] Z. Mo, T. Szilvási, Y. Zhou, S. Yao, M. Driess, *Angew. Chem. Int. Ed.* **2017**, *56*, 3699–3702.

[132] Y. P. Zhou, M. Driess, *Angew. Chem. Int. Ed.* **2019**, *58*, 3715–3728.

[133] B. Gehrhus, P. B. Hitchcock, M. F. Lappert, *Z. Anorg. Allg. Chem.* **2005**, *631*, 1383–1386.

[134] S. S. Sen, S. Khan, S. Nagendran, H. W. Roesky, *Acc. Chem. Res.* **2012**, *45*, 578–587.

[135] D. Gau, R. Rodriguez, T. Kato, N. Saffon-Merceron, A. de Cózar, F. P. Cossío, A. Baceiredo, *Angew. Chem. Int. Ed.* **2011**, *50*, 1092–1096.

[136] S. Raoufmoghaddam, Y. P. Zhou, Y. Wang, M. Driess, *J. Organomet. Chem.* **2017**, *829*, 2–10.

[137] A. Saddington, S. Yao, M. Driess, *Adv. Inorg. Chem.* **2023**, *82*, 119–156.

[138] R. Waterman, P. G. Hayes, T. D. Tilley, *Acc. Chem. Res.* **2007**, *40*, 712–719.

[139] B. Blom, D. Gallego, M. Driess, *Inorg. Chem. Front.* **2014**, *1*, 134–148.

[140] B. Blom, M. Stoelzel, M. Driess, *Chem. Eur. J.* **2013**, *19*, 40–62.

[141] M. Stoelzel, C. Präsang, B. Blom, M. Driess, *Aust. J. Chem.* **2013**, *66*, 1163–1170.

[142] S. Yao, A. Saddington, Y. Xiong, M. Driess, *Acc. Chem. Res.* **2023**, *56*, 475–488.

[143] A. Fürstner, H. Krause, C. W. Lehmann, *Chem. Commun.* **2001**, 2372–2373.

[144] C. Watanabe, Y. Inagawa, T. Iwamoto, M. Kira, *Dalton Trans.* **2010**, *39*, 9414–9420.

[145] A. Brück, D. Gallego, W. Wang, E. Irran, M. Driess, J. F. Hartwig, *Angew. Chem. Int. Ed.* **2012**, *51*, 11478–11482.

[146] J. A. Cabeza, P. García-Álvarez, L. González-Álvarez, *Chem. Commun.* **2017**, *53*, 10275–10278.

[147] M. Schmidt, B. Blom, T. Szilvási, R. Schomäcker, M. Driess, *Eur. J. Inorg. Chem.* **2017**, *2017*, 1284–1291.

6. References

[148] S. Kalra, D. Pividori, D. Fehn, C. Dai, S. Dong, S. Yao, J. Zhu, K. Meyer, M. Driess, *Chem. Sci.* **2022**, *13*, 8634–8641.

[149] W. Wang, S. Inoue, S. Enthaler, M. Driess, *Angew. Chem. Int. Ed.* **2012**, *51*, 6167–6171.

[150] Z. He, L. Liu, F. J. De Zwart, X. Xue, A. W. Ehlers, K. Yan, S. Demeshko, J. I. Van Der Vlugt, B. De Bruin, J. Krogman, *Inorg. Chem.* **2022**, *61*, 11725–11733.

[151] W. Wang, S. Inoue, S. Yao, M. Driess, *J. Am. Chem. Soc.* **2010**, *132*, 15890–15892.

[152] Y. Wang, A. Kostenko, S. Yao, M. Driess, *J. Am. Chem. Soc.* **2017**, *139*, 13499–13506.

[153] M.-P. Lücke, S. Yao, M. Driess, *Chem. Sci.* **2021**, *12*, 2909–2915.

[154] W. Yang, Y. Dong, H. Sun, X. Li, *Dalton Trans.* **2021**, *50*, 6766–6772.

[155] X. Wu, G. Ding, W. Lu, L. Yang, J. Wang, Y. Zhang, X. Xie, Z. Zhang, *Org. Lett.* **2021**, *23*, 1434–1439.

[156] L. E. Gusel'nikov, M. C. Flowers, *Chem. Commun.* **1967**, 864–865.

[157] L. E. Gusel'nikov, N. S. Nametkin, V. M. Vdovin, *Acc. Chem. Res.* **1975**, *8*, 18–25.

[158] A. G. Brook, S. C. Nyburg, F. Abdesaken, B. Gutekunst, G. Gutekunst, R. Krishna, M. R. Kallury, Y. C. Poon, Y. M. Chang, W. Wong-Ng, *J. Am. Chem. Soc.* **1982**, *104*, 5667–5672.

[159] Y. Apeloig, M. Bendikov, M. Yuzefovich, M. Nakash, D. Bravo-Zhivotovskii, D. Bläser, R. Boese, *J. Am. Chem. Soc.* **1996**, *118*, 12228–12229.

[160] C. Couret, J. Escudié, J. Satge, M. Lazraq, *J. Am. Chem. Soc.* **1982**, *109*, 4411–4412.

[161] Y. Apeloig, D. Bravo-Zhivotovskii, I. Zharov, V. Panov, W. J. Leigh, G. W. Sluggett, *J. Am. Chem. Soc.* **1998**, *120*, 1398–1404.

[162] N. Wiberg, C. M. M. Finger, K. Polborn, *Angew. Chem. Int. Ed.* **1993**, *32*, 1054–1056.

[163] V. Y. Lee, A. Sekiguchi, *Organometallics* **2004**, *23*, 2822–2834.

[164] D. N. Roark, G. J. D. Peddle, *J. Am. Chem. Soc.* **1972**, *94*, 5837–5841.

[165] F. S. Kipping, J. E. Sands, *J. Chem. Soc., Trans.* **1921**, *119*, 830–847.

[166] R. West, *Angew. Chem. Int. Ed.* **1987**, *26*, 1201–1211.

[167] R. West, R. Okazaki, in *Chemistry of Stable Disilenes*, Volume 39, Academic Press Limited, LondonChem, **1996**.

[168] M. Kira, T. Iwamoto, *Adv. Organomet. Chem.* **2006**, *54*, 73–148.

[169] H. Watanabe, K. Takeuchi, K. Nakajima, Y. Nagai, M. Goto, *Chem. Lett.* **1988**, *17*, 1343–1346.

[170] S. Masamune, Y. Eriyama, T. Kawase, *Angew. Chem. Int. Ed.* **1987**, *26*, 584–585.

[171] M. Ichinohe, R. Kinjo, A. Sekiguchi, *Organometallics* **2003**, *22*, 4621–4623.

[172] T. Sasamori, K. Hironaka, Y. Sugiyama, N. Takagi, S. Nagase, Y. Hosoi, Y. Furukawa, N. Tokitoh, *J. Am. Chem. Soc.* **2008**, *130*, 13856–13857.

[173] K. Suzuki, T. Matsuo, D. Hashizume, K. Tamao, *J. Am. Chem. Soc.* **2011**, *133*, 19710–19713.

[174] D. Reiter, R. Holzner, A. Porzelt, P. J. Altmann, P. Frisch, S. Inoue, *J. Am. Chem. Soc.* **2019**, *141*, 13536–13546.

[175] M. Weidenbruch, S. Willms, W. Saak, G. Henkel, *Angew. Chem. Int. Ed.* **1997**, *36*, 2503–2504.

[176] D. Scheschkewitz, *Angew. Chem. Int. Ed* **2004**, *43*, 2965–2967.

[177] S. Inoue, M. Ichinohe, A. Sekiguchi, *Chem. Lett.* **2005**, *34*, 1564–1565.

[178] A. Rammo, D. Scheschkewitz, *Chem. Eur. J.* **2018**, *24*, 6866–6885.

[179] R. West, D. J. De Young, K. J. Haller, *J. Am. Chem. Soc.* **1985**, *107*, 4942–4946.

[180] R. P. Koon. Tan, G. R. Gillette, D. R. Powell, Robert. West, *Organometallics* **1991**, *10*, 546–551.

[181] T. Iwamoto, S. Ishida, in *Functional Molecular Silicon Compounds II Low Oxidation Sates (Ed.: D. Scheschkewitz)*, Cham Springer, **2015**.

[182] D. C. Silva Costa, *Arab. J. Chem.* **2020**, *13*, 799–834.

[183] G. Bary, M. I. Jamil, M. Arslan, L. Ghani, W. Ahmed, H. Ahmad, G. Zaman, K. Ayub, M. Sajid, R. Ahmad, D. Huang, F. Liu, Y. Wang, *J. S. Chem. Soc.* **2021**, *25*, 101260–101291.

[184] M. Zhang, T. Liu, X.-Q. Chen, H. Jin, J.-J. Lv, S. Wang, X. Yu, C. Yang, Z.-J. Wang, *Org. Biomol. Chem.* **2025**, *23*, 2323–2357.

[185] D. Scheschkewitz, *Chem. Eur. J.* **2009**, *15*, 2476–2485.

[186] D. Scheschkewitz, *Chem. Lett.* **2011**, *40*, 2–11.

[187] A. Meltzer, M. Majumdar, A. J. P. White, V. Huch, D. Scheschkewitz, *Organometallics* **2013**, *32*, 6844–6850.

[188] C. Präsang, D. Scheschkewitz, *Chem. Soc. Rev.* **2016**, *45*, 900–921.

[189] R. Kinjo, M. Ichinohe, A. Sekiguchi, *J. Am. Chem. Soc.* **2007**, *129*, 26–27.

[190] K. Abersfelder, D. Güclü, D. Scheschkewitz, *Angew. Chem. Int. Ed.* **2006**, *45*, 1643–1645.

[191] J. Jeck, I. Bejan, A. J. P. White, D. Nied, F. Breher, D. Scheschkewitz, *J. Am. Chem. Soc.* **2010**, *132*, 17306–17315.

[192] I. Bejan, D. Scheschkewitz, *Angew. Chem. Int. Ed.* **2007**, *46*, 5783–5786.

[193] M. Majumdar, I. Bejan, V. Huch, A. J. P. White, G. R. Whittell, A. Schäfer, I. Manners, D. Scheschkewitz, *Chem. Eur. J.* **2014**, *20*, 9225–9229.

[194] K. Abersfelder, A. J. P. White, H. S. Rzepa, D. Scheschkewitz, *Science* **2010**, *327*, 564–566.

[195] M. J. Cowley, K. Abersfelder, A. J. P. White, M. Majumdar, D. Scheschkewitz, *Chem. Commun.* **2012**, *48*, 6595–6597.

6. References

[196] T. L. Nguyen, D. Scheschkewitz, *J. Am. Chem. Soc.* **2005**, *127*, 10174–10175.

[197] S. Ishida, T. Iwamoto, *Coord. Chem. Rev.* **2016**, *314*, 34–63.

[198] M. Mizutori, R. Yamada, in *Semiconductors*, *Ullmann's Encyclopedia of Industrial Chemistry*, Wiley-VCH Verlag GmbH & Co. KGaA, Weinheim, Germany, **2000**.

[199] W. Zulehner, B. Neuer, G. Rau, in *Silicon*, *Ullmann's Encyclopedia of Industrial Chemistry*, Wiley-VCH Verlag GmbH & Co. KGaA, Weinheim, Germany, **2000**.

[200] J. K. Rath, B. Stannowski, P. A. T. T. van Veenendaal, M. K. van Veen, R. E. I. Schropp, *Thin Solid Films* **2001**, *395*, 320–329.

[201] B. K. Teo, X. H. Sun, *Chem. Rev.* **2007**, *107*, 1454–1532.

[202] W. Lu, C. M. Lieber, *Nat. Mater.* **2007**, *6*, 841–850.

[203] L. Venema, *Nature* **2011**, *479*, 309–309.

[204] M. L. Snedaker, Y. Zhang, C. S. Birkel, H. Wang, T. Day, Y. Shi, X. Ji, S. Kraemer, C. E. Mills, A. Moosazadeh, M. Moskovits, G. J. Snyder, G. D. Stucky, *Chem. Mater.* **2013**, *25*, 4867–4873.

[205] T. Miyazaki, T. Uda, I. Štich, K. Terakura, *Chem. Phys. Lett.* **1996**, *261*, 346–352.

[206] G. Belomoin, J. Therrien, A. Smith, S. Rao, R. Twesten, S. Chaieb, M. H. Nayfeh, L. Wagner, L. Mitas, *Appl. Phys. Lett.* **2002**, *80*, 841–843.

[207] D. K. Yu, R. Q. Zhang, S. T. Lee, *J. Appl. Phys.* **2002**, *92*, 7453–7458.

[208] T. V. Torchynska, *Superlattices Microstruct.* **2009**, *45*, 267–270.

[209] H. S. Akira Sekiguchi, *Adv. Organomet. Chem.* **1995**, *37*, 1–38.

[210] S. Kyushin, in *Organosilicon Compounds* (Ed.: V. Y. Lee), Academic Press An Imprint Of Elsevier, London and San Diego and Cambridge and Oxford, **2017**, Chapter 3, pp. 69–144.

[211] K. E. Wentz, A. F. Gittens, R. S. Klausen, *J. Am. Chem. Soc.* **2025**, *147*, 2938–2959.

[212] J. D. Corbett, *Chem. Rev.* **1985**, *85*, 383–397.

[213] J. D. Corbett, in *Structural and Electronic Paradigms in Cluster Chemistry* (Ed.: D. M. P. Mingos), Springer Berlin, Heidelberg, **1997**, 157–193.

[214] S. Scharfe, F. Kraus, S. Stegmaier, A. Schier, T. F. Fässler, *Angew. Chem. Int. Ed.* **2011**, *50*, 3630–3670.

[215] T. F. Fässler, in *Zintl Ions: Principles and Recent Developments*, Structure and Bonding, Volume 139, Springer Heidelberg, Berlin, **2011**, pp. 91–131.

[216] S. Gärtner, M. Witzmann, C. Lorenz-Fuchs, R. M. Gschwind, N. Korber, *Inorg. Chem.* **2024**, *63*, 20240–20249.

[217] R. J. Wilson, B. Weinert, S. Dehnen, *Dalton Trans.* **2018**, *47*, 14861–14869.

[218] T. F. Fässler, *Coord. Chem. Rev.* **2001**, *215*, 347–377.

[219] S. Scharfe, T. F. Fässler, *Philos. Trans. A Math. Phys. Eng. Sci.* **2010**, 368, 1265–1284.

[220] Y. Heider, D. Scheschkewitz, *Dalton Trans.* **2018**, *47*, 7104–7112.

[221] Y. Heider, D. Scheschkewitz, *Chem. Rev.* **2021**, *121*, 9674–9718.

[222] T. Iwamoto, S. Ishida, *Chem. Lett.* **2014**, *43*, 164–170.

[223] A. Indriksons, R. West, *J. Am. Chem. Soc.* **1970**, *92*, 6704–6705.

[224] R. West, A. Indriksons, *J. Am. Chem. Soc.* **1972**, *94*, 6110–6115.

[225] Y. Kabe, T. Kawase, J. Okada, O. Yamashita, M. Goto, S. Masamune, *Angew. Chem. Int. Ed.* **1990**, *29*, 794–796.

[226] T. Iwamoto, D. Tsushima, E. Kwon, S. Ishida, H. Isobe, *Angew. Chem. Int. Ed.* **2012**, *51*, 2340–2344.

[227] E. Hengge, P. K. Jenkner, *Z. Anorg. Allg. Chem.* **1991**, *606*, 97–104.

[228] W. Setaka, N. Hamada, M. Kira, *Chem. Lett.* **2004**, *33*, 626–627.

[229] M. Ishikawa, M. Watanabe, J. Iyoda, H. Ikeda, M. Kumada, *Organometallics* **1982**, *1*, 317–322.

[230] J. Fischer, J. Baumgartner, C. Marschner, *Science* **2005**, *310*, 825–825.

[231] V. Ya. Lee, T. Yokoyama, K. Takanashi, A. Sekiguchi, *Chem. Eur. J.* **2009**, *15*, 8401–8404.

[232] K. Abersfelder, A. Russell, H. S. Rzepa, A. J. P. White, P. R. Haycock, D. Scheschkewitz, *J. Am. Chem. Soc.* **2012**, *134*, 16008–16016.

[233] Y. Kabe, M. Kuroda, Y. Honda, O. Yamashita, T. Kawase, S. Masamune, *Angew. Chem. Int. Ed.* **1988**, *27*, 1725–1727.

[234] T. Iwamoto, K. Uchiyama, C. Kabuto, M. Kira, *Chem. Lett.* **2007**, *36*, 368–369.

[235] F. Meyer-Wegner, S. Scholz, I. Sänger, F. Schödel, M. Bolte, M. Wagner, H.-W. Lerner, *Organometallics* **2009**, *28*, 6835–6837.

[236] A. Sekiguchi, T. Yatabe, C. Kabuto, H. Sakurai, *J. Am. Chem. Soc.* **1993**, *115*, 5853–5854.

[237] H. Matsumoto, K. Higuchi, Y. Hoshino, H. Koike, Y. Naoi, Y. Nagai, *J. Chem. Soc., Chem. Commun.* **1988**, 1083–1084.

[238] H. Matsumoto, K. Higuchi, S. Kyushin, M. Goto, *Angew. Chem. Int. Ed.* **1992**, *31*, 1354–1356.

[239] A. Sekiguchi, T. Yatabe, H. Kamatani, C. Kabuto, H. Sakurai, *J. Am. Chem. Soc.* **1992**, *114*, 6260–6262.

[240] K. Furukawa, M. Fujino, N. Matsumoto, *Appl. Phys. Lett.* **1992**, *60*, 2744–2745.

[241] M. Quest, A. Hepp, M. Hebenbrock, C. G. Daniliuc, J. Bresien, F. Lips, *Chem. Eur. J.* **2024**, *30*, e202400368.

[242] J. Tillmann, L. Meyer, J. I. Schweizer, M. Bolte, H. Lerner, M. Wagner, M. C. Holthausen, *Chem. Eur. J.* **2014**, *20*, 9234–9239.

[243] R. D. Miller, J. Michl, *Chem. Rev.* **1989**, *89*, 1359–1410.

[244] H. A. Fogarty, D. L. Casher, R. Imhof, T. Schepers, D. W. Rooklin, J. Michl, *Pure Appl. Chem.* **2003**, *75*, 999–1020.

[245] A. F. Akihiko Fujii, K. Y. Kenji Yoshimoto, M. Y. Masayoshi Yoshida, Y. O. Yutaka Ohmori, K. Y. Katsumi Yoshino, *Jpn. J. Appl. Phys.* **1995**, *34*, L1365.

[246] S. Hayase, *Prog. Polym. Sci.* **2003**, *28*, 359–381.

[247] M. Unno, K. Higuchi, M. Ida, H. Shioyama, S. Kyushin, H. Matsumoto, M. Goto, *Organometallics* **1994**, *13*, 4633–4640.

[248] M. Unno, H. Shioyama, M. Ida, H. Matsumoto, *Organometallics* **1995**, *14*, 4004–4009.

[249] Y. Li, J. Li, J. Zhang, H. Song, C. Cui, *J. Am. Chem. Soc.* **2018**, *140*, 1219–1222.

[250] Y. Wang, J. E. McGrady, Z.-M. Sun, *Acc. Chem. Res.* **2021**, *54*, 1506–1516.

[251] A. C. Joannis, *C. R. Hebd. Seances Acad. Sci.* **1891**, *113*, 795–798.

[252] E. Zintl, J. Goubean, W. Dullenkopf, *Z. Phys. Chem.* **1931**, *154A*, 1–46.

[253] F. Laves, in *Eduard Zintls Arbeiten über die Chemie und Struktur von Legierungen, Die Naturwissenschaften* (Ed.: F. Süffert), Springer, Berlin, Heidelberg, **1941**, *29*, 244–255.

[254] S. Joseph, C. Suchentrunk, N. Korber, *Z. Naturforsch. B* **2010**, *65*, 1059–1065.

[255] J. M. Goicoechea, S. C. Sevov, *J. Am. Chem. Soc.* **2004**, *126*, 6860–6861.

[256] S. Bobev, S. C. Sevov, *Angew. Chem. Int. Ed.* **2000**, *39*, 4108–4110.

[257] F. Zürcher, R. Nesper, *Angew. Chem. Int. Ed.* **1998**, *37*, 3314–3318.

[258] U. Aydemir, A. Ormeci, H. Borrmann, B. Böhme, F. Zürcher, B. Uslu, T. Goebel, W. Schnelle, P. Simon, W. Carrillo-Cabrera, F. Haarmann, M. Baitinger, R. Nesper, H. G. von Schnering, Y. Grin, *Z. Anorg. Allg. Chem.* **2008**, *634*, 1651–1661.

[259] R. Nesper, H. G. von Schnering, J. Curda, *Chem. Ber.* **1986**, *119*, 3576–3590.

[260] T. K. -J. Köster, E. Salager, A. J. Morris, B. Key, V. Seznec, M. Morcrette, C. J. Pickard, C. P. Grey, *Angew. Chem. Int. Ed.* **2011**, *50*, 12591–12594.

[261] U. Frank, W. Müller, *Z. Naturforsch. B* **1975**, *30*, 313–315.

[262] R. Nesper, J. Curda, H. G. Von Schnering, *J. Solid State Chem.* **1986**, *62*, 199–206.

[263] I. Todorov, S. C. Sevov, *Inorg. Chem.* **2004**, *43*, 6490–6494.

[264] I. Todorov, S. C. Sevov, *Inorg. Chem.* **2005**, *44*, 5361–5369.

[265] H. G. von Schnering, U. Bolle, J. Curda, K. Peters, W. Carrillo-Cabrera, M. Somer, M. Schultheiss, U. Wedig, *Angew. Chem. Int. Ed.* **1996**, *35*, 984–986.

[266] U. Bolle, W. Carrillo-Cabrera, K. Peters, H. G. von Schnering, *Z. Kristallogr. N. Cryst. Struct.* **1998**, *213*, 729.

[267] S. Gärtner, N. Korber, in *1.09 - Zintl Ions* (Ed.: J. Reedjik, K. Poeppelmeier), Comprehensive Inorganic Chemistry II, Second Edition, Elsevier, Amsterdam, **2013**, pp. 251–267.

[268] S. Gärtner, M. Witzmann, C. Lorenz-Fuchs, R. M. Gschwind, N. Korber, *Inorg. Chem.* **2024**, *63*, 20240–20249.

[269] J. D. Corbett, D. G. Adolphson, D. J. Merryman, P. A. Edwards, F. J. Armatis, *J. Am. Chem. Soc.* **1975**, *97*, 6267–6268.

[270] J. D. Corbett, P. A. Edwards, *J. Chem. Soc., Chem. Commun.* **1975**, 984–985.

[271] T. F. Fässler, R. Hoffmann, *Angew. Chem. Int. Ed.* **1999**, *38*, 543–546.

[272] A. Nienhaus, S. D. Hoffmann, T. F. Fässler, *Z. Anorg. Allg. Chem.* **2006**, *632*, 1752–1758.

[273] C. H. E. Belin, J. D. Corbett, A. Cisar, *J. Am. Chem. Soc.* **1977**, *99*, 7163–7169.

[274] D. Kummer, L. Diehl, *Angew. Chem. Int. Ed.* **1970**, *9*, 895–895.

[275] S. Joseph, C. Suchentrunk, F. Kraus, N. Korber, *Eur. J. Inorg. Chem.* **2009**, *2009*, 4641–4647.

[276] K. M. Frankiewicz, N. S. Willeit, V. Hlukhyy, T. F. Fässler, *Nature Commun.* **2024**, *15*, 1–10.

[277] C. B. Benda, T. Henneberger, W. Klein, T. F. Fässler, *Z. Anorg. Allg. Chem.* **2017**, *643*, 146–148.

[278] C. Lorenz, S. Gärtner, N. Korber, *Z. Anorg. Allg. Chem.* **2017**, *643*, 141–145.

[279] L. J. Schiegerl, A. J. Karttunen, W. Klein, T. F. Fässler, *Chem. Sci.* **2019**, *10*, 9130–9139.

[280] M. Waibel, F. Kraus, S. Scharfe, B. Wahl, T. F. Fässler, *Angew. Chem. Int. Ed.* **2010**, *49*, 6611–6615.

[281] J. M. Goicoechea, S. C. Sevov, *Organometallics* **2006**, *25*, 4530–4536.

[282] F. S. Geitner, T. F. Fässler, *Chem. Commun.* **2017**, *53*, 12974–12977.

[283] V. Streitferdt, S. M. Tiefenthaler, I. G. Shenderovich, S. Gärtner, N. Korber, R. M. Gschwind, *Eur. J. Inorg. Chem.* **2021**, *2021*, 3684–3690.

[284] P. A. Braun, F. F. Westermair, R. M. Gschwind, N. Korber, *Z. Anorg. Allg. Chem.* **2023**, *649*, e202300117.

[285] S. Joseph, M. Hamberger, F. Mutzbauer, O. Härtl, M. Meier, N. Korber, *Angew. Chem. Int. Ed.* **2009**, *48*, 8770–8772.

[286] T. Shimoda, Y. Matsuki, M. Furusawa, T. Aoki, I. Yudasaka, H. Tanaka, H. Iwasawa, D. Wang, M. Miyasaka, Y. Takeuchi, *Nature* **2006**, *440*, 783–786.

[287] Z. Shen, T. Masuda, H. Takagishi, K. Ohdaira, T. Shimoda, *Chem. Commun.* **2015**, *51*, 4417–4420.

[288] A. Purath, R. Köppe, H. Schnöckel, *Angew. Chem. Int. Ed.* **1999**, *38*, 2926–2928.

[289] A. Schnepf, G. Stösser, H. Schnöckel, *J. Am. Chem. Soc.* **2000**, *122*, 9178–9181.

[290] A. Schnepf, H. Schnöckel, *Angew. Chem. Int. Ed.* **2002**, *41*, 3532–3554.

[291] A. Schnepf, *Chem. Soc. Rev.* **2007**, *36*, 745–758.

[292] M. K. Bisai, T. Das, K. Vanka, R. G. Gonnade, S. S. Sen, *Angew. Chem. Int. Ed.* **2021**, *60*, 20706–20710.

[293] Y. Li, S. Dong, J. Guo, Y. Ding, J. Zhang, J. Zhu, C. Cui, *J. Am. Chem. Soc.* **2023**, *145*, 21159–21164.

[294] S. Yao, M. S. Budde, X. Yang, Y. Xiong, L. Zhao, M. Driess, *Angew. Chem. Int. Ed.* **2025**, *64*, e202414696.

[295] D. Scheschkewitz, *Angew. Chem. Int. Ed.* **2005**, *44*, 2954–2956.

[296] T. Iwamoto, N. Akasaka, S. Ishida, *Nat. Commun.* **2014**, *5*, 5353.

[297] T. Iwamoto, M. Kobayashi, K. Uchiyama, S. Sasaki, S. Nagendran, H. Isobe, M. Kira, *J. Am. Chem. Soc.* **2009**, *131*, 3156–3157.

[298] D. Nied, R. Köppe, W. Klopper, H. Schnöckel, F. Breher, *J. Am. Chem. Soc.* **2010**, *132*, 10264–10265.

[299] T. Tsumuraya, S. A. Batcheller, S. Masamune, *Angew. Chem. Int. Ed.* **1991**, *30*, 902–930.

[300] R. J. F. Berger, H. S. Rzepa, D. Scheschkewitz, *Angew. Chem. Int. Ed.* **2010**, *49*, 10006–10009.

[301] K. Abersfelder, A. J. P. White, R. J. F. Berger, H. S. Rzepa, D. Scheschkewitz, *Angew. Chem. Int. Ed.* **2011**, *50*, 7936–7939.

[302] K. Leszczyńska, K. Abersfelder, M. Majumdar, B. Neumann, H.-G. Stammler, H. S. Rzepa, P. Jutzi, D. Scheschkewitz, *Chem. Commun.* **2012**, *48*, 7820–7822.

[303] D. Kratzert, D. Leusser, J. J. Holstein, B. Dittrich, K. Abersfelder, D. Scheschkewitz, D. Stalke, *Angew. Chem. Int. Ed.* **2013**, *52*, 4478–4482.

[304] D. Mayeri, B. L. Phillips, M. P. Augustine, S. M. Kauzlarich, *Chem. Mater.* **2001**, *13*, 765–770.

[305] J. He, D. D. Klug, K. Uehara, K. F. Preston, C. I. Ratcliffe, J. S. Tse, *J. Phys. Chem. B* **2001**, *105*, 3475–3485.

[306] T. Goebel, Y. Prots, A. Ormeci, O. Pecher, F. Haarmann, *Z. Anorg. Allg. Chem.* **2011**, *637*, 1982–1991.

[307] T. Goebel, A. Ormeci, O. Pecher, F. Haarmann, *Z. Anorg. Allg. Chem.* **2012**, *638*, 1437–1445.

[308] L. M. Scherf, O. Pecher, K. J. Griffith, F. Haarmann, C. P. Grey, T. F. Fässler, *Eur. J. Inorg. Chem.* **2016**, *2016*, 4674–4682.

[309] L. J. Schiegerl, A. J. Karttunen, J. Tillmann, S. Geier, G. Raudaschl-Sieber, M. Waibel, T. F. Fässler, *Angew. Chem. Int. Ed.* **2018**, *57*, 12950–12955.

[310] M. Neumeier, F. Fendt, S. Gärtner, C. Koch, T. Gärtner, N. Korber, R. M. Gschwind, *Angew. Chem. Int. Ed.* **2013**, *52*, 4483–4486.

[311] F. Hastreiter, C. Lorenz, J. Hioe, S. Gärtner, N. Lokesh, N. Korber, R. M. Gschwind, *Angew. Chem. Int. Ed.* **2019**, *58*, 3133–3137.

[312] J. B. Lambert, S. Zhang, S. M. Ciro, *Organometallics* **1994**, *13*, 2430–2443.

[313] J. B. Lambert, L. Kania, S. Zhang, *Chem. Rev.* **1995**, *95*, 1191–1201.

[314] V. H. G. Rohde, P. Pommerening, H. F. T. Klare, M. Oestreich, *Organometallics* **2014**, *33*, 3618–3628.

[315] A. Simonneau, T. Biberger, M. Oestreich, *Organometallics* **2015**, *34*, 3927–3929.

[316] B. M. Cossairt, C. C. Cummins, A. R. Head, D. L. Lichtenberger, R. J. F. Berger, S. A. Hayes, N. W. Mitzel, G. Wu, *J. Am. Chem. Soc.* **2010**, *132*, 8459–8465.

[317] Y. Heider, N. E. Poitiers, P. Willmes, K. I. Leszczyńska, V. Huch, D. Scheschkewitz, *Chem. Sci.* **2019**, *10*, 4523–4530.

[318] J. Keuter, C. Schwermann, A. Hepp, K. Bergander, J. Droste, M. R. Hansen, N. L. Doltsinis, C. Mück-Lichtenfeld, F. Lips, *Chem. Sci.* **2020**, *11*, 5895–5901.

[319] N. Akasaka, S. Ishida, T. Iwamoto, *Inorganics* **2018**, *6*, 107–119.

[320] R. F. W. Bader, *Atoms in Molecules*, Oxford University Press, **1990**.

[321] G. Knizia, *J. Chem. Theory Comput.* **2013**, *9*, 4834–4843.

[322] G. Knizia, J. E. M. N. Klein, *Angew. Chem. Int. Ed.* **2015**, *54*, 5518–5522.

[323] D. L. Cooper, P. B. Karadakov, B. J. Duke, *J. Phys. Chem. A* **2015**, *119*, 2169–2175.

[324] J. Helmer, A. Hepp, F. Lips, *Dalton Trans.* **2022**, *51*, 3254–3262.

[325] J. Helmer, A. Hepp, R. J. F. Berger, F. Lips, *Dalton Trans.* **2023**, *52*, 14949–14955.

[326] L. J. Schiegerl, A. J. Karttunen, W. Klein, T. F. Fässler, *Chem. Eur. J.* **2018**, *24*, 19171–19174.

[327] P. Willmes, K. Leszczyńska, Y. Heider, K. Abersfelder, M. Zimmer, V. Huch, D. Scheschkewitz, *Angew. Chem. Int. Ed.* **2016**, *55*, 2907–2910.

[328] Y. Heider, N. E. Poitiers, P. Willmes, K. I. Leszczyńska, V. Huch, D. Scheschkewitz, *Chem. Sci.* **2019**, *10*, 4523–4530.

[329] Y. Heider, P. Willmes, V. Huch, M. Zimmer, D. Scheschkewitz, *J. Am. Chem. Soc.* **2019**, *141*, 19498–19504.

[330] N. E. Poitiers, L. Giarrana, K. I. Leszczyńska, V. Huch, M. Zimmer, D. Scheschkewitz, *Angew. Chem. Int. Ed.* **2020**, *59*, 8532–8536.

[331] M. Hunsicker, N. E. Poitiers, V. Huch, B. Morgenstern, M. Zimmer, D. Scheschkewitz, *Z. Anorg. Allg. Chem.* **2022**, *648*, e202200239.

[332] S. Nagendran, S. S. Sen, H. W. Roesky, D. Koley, H. Grubmüller, A. Pal, R. Herbst-Irmer, *Organometallics* **2008**, *27*, 5459–5463.

[333] S. S. Sen, M. P. Kritzler-Kosch, S. Nagendran, H. W. Roesky, T. Beck, A. Pal, R. Herbst-Irmer, *Eur. J. Inorg. Chem.* **2010**, *2010*, 5304–5311.

[334] N. E. Poitiers, L. Giarrana, V. Huch, M. Zimmer, D. Scheschkewitz, *Chem. Sci.* **2020**, *11*, 7782–7788.

[335] N. E. Poitiers, V. Huch, M. Zimmer, D. Scheschkewitz, *Chem. Commun.* **2020**, *56*, 10898–10901.

6. References

[336] K. I. Leszczyńska, V. Huch, C. Präsang, J. Schwabedissen, R. J. F. Berger, D. Scheschkewitz, *Angew. Chem. Int. Ed.* **2019**, *58*, 5124–5128.

[337] M. Tang, C. Z. Wang, W. C. Lu, K. M. Ho, *Phys. Rev. B* **2006**, *74*, 195413.

[338] N. E. Poitiers, V. Huch, B. Morgenstern, M. Zimmer, D. Scheschkewitz, *Angew. Chem. Int. Ed.* **2022**, *61*, e202205399.

[339] N. E. Poitiers, V. Huch, M. Zimmer, D. Scheschkewitz, *Chem. Eur. J.* **2020**, *26*, 16599–16602.

[340] D. Nieder, C. B. Yildiz, A. Jana, M. Zimmer, V. Huch, D. Scheschkewitz, *Chem. Commun.* **2016**, *52*, 2799–2802.

[341] L. Klemmer, V. Huch, A. Jana, D. Scheschkewitz, *Chem. Commun.* **2019**, *55*, 10100–10103.

[342] A. Jana, V. Huch, M. Repisky, R. J. F. Berger, D. Scheschkewitz, *Angew. Chem. Int. Ed.* **2014**, *53*, 3514–3518.

[343] D. Nied, P. Oña-Burgos, W. Klopper, F. Breher, *Organometallics* **2011**, *30*, 1419–1428.

[344] J. Helmer, J. Droste, M. R. Hansen, A. Hepp, F. Lips, *Dalton Trans.* **2022**, *51*, 10535–10542.

[345] J. Keuter, M. Dimitrova, O. Janka, A. Hepp, R. J. F. Berger, F. Lips, *Chem. Eur. J.* **2022**, *28*, e202201473.

[346] J. Keuter, A. Hepp, A. Massolle, J. Neugebauer, C. Mück-Lichtenfeld, F. Lips, *Angew. Chem. Int. Ed.* **2022**, *61*, e202114485.

[347] R. Brimblecombe, G. F. Swiegers, G. C. Dismukes, L. Spiccia, *Angew. Chem. Int. Ed.* **2008**, *47*, 7335–7338.

[348] E. Antolini, *J. Power Sources* **2007**, *170*, 1–12.

[349] S. Song, W. Zhou, Z. Liang, R. Cai, G. Sun, Q. Xin, V. Stergiopoulos, P. Tsiakaras, *Appl. Catal. B* **2005**, *55*, 65–72.

[350] M. Rakowski DuBois, D. L. DuBois, *Chem. Soc. Rev.* **2009**, *38*, 62–72.

[351] P. Buchwalter, J. Rosé, P. Braunstein, *Chem. Rev.* **2015**, *115*, 28–126.

[352] W. Xu, M. Li, L. Qiao, J. Xie, *Chem. Commun.* **2020**, *56*, 8524–8536.

[353] R. Govindarajan, S. Deolka, J. R. Khusnutdinova, *Chem. Sci.* **2022**, *13*, 14008–14031.

Marketplace

Order Date	13-Apr-2026	Type of Use	Republish in a thesis/dissertation
Order License ID	1718876-1		
ISSN	1520-510X	Publisher	AMERICAN CHEMICAL SOCIETY
		Portion	Chapter/article

LICENSED CONTENT

Publication Title	Inorganic chemistry	Publication Type	e-Journal
Article Title	Tetrylene-Functionalized Si 7 –Siliconoids	Start Page	20083
		End Page	20087
Author / Editor	American Chemical Society.	Issue	43
		Volume	63
Date	01/01/1962	URL	http://pubs.acs.org/journals/inocaj/index.html
Language	English		
Country	United States of America		
Rightsholder	American Chemical Society		

REQUEST DETAILS

Portion Type	Chapter/article	Rights Requested	Main product
Page Range(s)	20083–20087	Distribution	Worldwide
Total Number of Pages	5	Translation	Original language of publication
Format (select all that apply)	Print, Electronic	Copies for the Disabled?	No
Who Will Republish the Content?	Academic institution	Minor Editing Privileges?	No
Duration of Use	Life of current edition	Incidental Promotional Use?	No
Lifetime Unit Quantity	Up to 499	Currency	EUR

NEW WORK DETAILS

Title	Tetrylene-Functionalized Si7–Siliconoids	Institution Name	Universität des Saarlandes
		Expected Presentation Date	2026-04-15
Instructor Name	Luisa Giarrana		

ADDITIONAL DETAILS

The Requesting Person / Organization to Appear on the License	Luisa Giarrana

REQUESTED CONTENT DETAILS

Title, Description or Numeric Reference of the Portion(s)	Siliconoids with Pending Silylenes as Platform for Mono– and Bimetallic Homogeneous Catalysts	**Title of the Article / Chapter the Portion Is From**	Tetrylene-Functionalized Si 7 –Siliconoids
Editor of Portion(s)	Giarrana, Luisa; Zimmer, Michael; Morgenstern, Bernd; Scheschkewitz, David	**Author of Portion(s)**	Giarrana, Luisa; Zimmer, Michael; Morgenstern, Bernd; Scheschkewitz, David
Volume / Edition	63	**Publication Date of Portion**	2024-10-28
Page or Page Range of Portion	20083-20087		

Marketplace Permissions General Terms and Conditions

The following terms and conditions ("General Terms"), together with any applicable Publisher Terms and Conditions, govern User's use of Works pursuant to the Licenses granted by Copyright Clearance Center, Inc. ("CCC") on behalf of the applicable Rightsholders of such Works through CCC's applicable Marketplace transactional licensing services (each, a "Service").

1) **Definitions.** For purposes of these General Terms, the following definitions apply:

"License" is the licensed use the User obtains via the Marketplace platform in a particular licensing transaction, as set forth in the Order Confirmation.

"Order Confirmation" is the confirmation CCC provides to the User at the conclusion of each Marketplace transaction. "Order Confirmation Terms" are additional terms set forth on specific Order Confirmations not set forth in the General Terms that can include terms applicable to a particular CCC transactional licensing service and/or any Rightsholder-specific terms.

"Rightsholder(s)" are the holders of copyright rights in the Works for which a User obtains licenses via the Marketplace platform, which are displayed on specific Order Confirmations.

"Terms" means the terms and conditions set forth in these General Terms and any additional Order Confirmation Terms collectively.

"User" or "you" is the person or entity making the use granted under the relevant License. Where the person accepting the Terms on behalf of a User is a freelancer or other third party who the User authorized to accept the General Terms on the User's behalf, such person shall be deemed jointly a User for purposes of such Terms.

"Work(s)" are the copyright protected works described in relevant Order Confirmations.

2) **Description of Service.** CCC's Marketplace enables Users to obtain Licenses to use one or more Works in accordance with all relevant Terms. CCC grants Licenses as an agent on behalf of the copyright rightsholder identified in the relevant Order Confirmation.

3) **Applicability of Terms.** The Terms govern User's use of Works in connection with the relevant License. In the event of any conflict between General Terms and Order Confirmation Terms, the latter shall govern. User acknowledges that Rightsholders have complete discretion whether to grant any permission, and whether to place any limitations on any grant, and that CCC has no right to supersede or to modify any such discretionary act by a Rightsholder.

4) **Representations; Acceptance.** By using the Service, User represents and warrants that User has been duly authorized by the User to accept, and hereby does accept, all Terms.

5) **Scope of License; Limitations and Obligations.** All Works and all rights therein, including copyright rights, remain the sole and exclusive property of the Rightsholder. The License provides only those rights expressly set forth in the terms and conveys no other rights in any Works

6) **General Payment Terms.** User may pay at time of checkout by credit card or choose to be invoiced. If the User chooses to be invoiced, the User shall: (i) remit payments in the manner identified on specific invoices, (ii) unless otherwise specifically stated in an Order Confirmation or separate written agreement, Users shall remit payments upon receipt of the relevant invoice from CCC, either by delivery or notification of availability of the invoice via the Marketplace platform, and (iii) if the User does not pay the invoice within 30 days of receipt, the User may incur a service charge of 1.5% per month or the maximum rate allowed by applicable law, whichever is less. While User may exercise the rights in the License immediately upon receiving the Order Confirmation, the License is automatically revoked and is null and void, as if it had never been issued, if CCC does not receive complete payment on a timely basis.

7) **General Limits on Use.** Unless otherwise provided in the Order Confirmation, any grant of rights to User (i) involves only the rights set forth in the Terms and does not include subsequent or additional uses, (ii) is non-exclusive and non-transferable, and (iii) is subject to any and all limitations and restrictions (such as, but not limited to, limitations on duration of use or circulation) included in the Terms. Upon completion of the licensed use as set forth in the Order Confirmation, User shall either secure a new permission for further use of the Work(s) or immediately cease any new use of the Work(s) and shall render inaccessible (such as by deleting or by removing or severing links or other locators) any further copies of the Work. User may only make alterations to the Work if and as expressly set forth in the Order Confirmation. No Work may be used in any way that is unlawful, including without limitation if such use would violate applicable sanctions laws or regulations, would be defamatory, violate the rights of third parties (including such third parties' rights of copyright, privacy, publicity, or other tangible or intangible property), or is otherwise illegal, sexually explicit, or obscene. In addition, User may not conjoin a Work with any other material that may result in damage to the reputation of the Rightsholder. Any unlawful use will render any licenses hereunder null and void. User agrees to inform CCC if it becomes aware of any infringement of any rights in a Work and to cooperate with any reasonable request of CCC or the Rightsholder in connection therewith.

8) **Third Party Materials.** In the event that the material for which a License is sought includes third party materials (such as photographs, illustrations, graphs, inserts and similar materials) that are identified in such material as having been used by permission (or a similar indicator), User is responsible for identifying, and seeking separate licenses (under this Service, if available, or otherwise) for any of such third party materials; without a separate license, User may not use such third party materials via the License.

9) **Copyright Notice.** Use of proper copyright notice for a Work is required as a condition of any License granted under the Service. Unless otherwise provided in the Order Confirmation, a proper copyright notice will read substantially as follows: "Used with permission of [Rightsholder's name], from [Work's title, author, volume, edition number and year of copyright]; permission conveyed through Copyright Clearance Center, Inc." Such notice must be provided in a reasonably legible font size and must be placed either on a cover page or in another location that any person, upon gaining access to the material which is the subject of a permission, shall see, or in the case of republication Licenses, immediately adjacent to the Work as used (for example, as part of a by-line or footnote) or in the place where substantially all other credits or notices for the new work containing the republished Work are located. Failure to include the required notice results in loss to the Rightsholder and CCC, and the User shall be liable to pay liquidated damages for each such failure equal to twice the use fee specified in the Order Confirmation, in addition to the use fee itself and any other fees and charges specified.

10) **Indemnity.** User hereby indemnifies and agrees to defend the Rightsholder and CCC, and their respective employees and directors, against all claims, liability, damages, costs, and expenses, including legal fees and expenses, arising out of any use of a Work beyond the scope of the rights granted herein and in the Order Confirmation, or any use of a Work which has been altered in any unauthorized way by User, including claims of defamation or infringement of rights of copyright, publicity, privacy, or other tangible or intangible property.

11) **Limitation of Liability.** UNDER NO CIRCUMSTANCES WILL CCC OR THE RIGHTSHOLDER BE LIABLE FOR ANY DIRECT, INDIRECT, CONSEQUENTIAL, OR INCIDENTAL DAMAGES (INCLUDING WITHOUT LIMITATION DAMAGES FOR LOSS OF BUSINESS PROFITS OR INFORMATION, OR FOR BUSINESS INTERRUPTION) ARISING OUT OF THE USE OR INABILITY TO USE A WORK, EVEN IF ONE OR BOTH OF THEM HAS BEEN ADVISED OF THE POSSIBILITY OF SUCH DAMAGES. In any event, the total liability of the Rightsholder and CCC (including their respective employees and directors) shall not exceed the total amount actually paid by User for the relevant License. User assumes full liability for the actions and omissions of its principals, employees, agents, affiliates, successors, and assigns.

12) **Limited Warranties.** THE WORK(S) AND RIGHT(S) ARE PROVIDED "AS IS." CCC HAS THE RIGHT TO GRANT TO USER THE RIGHTS GRANTED IN THE ORDER CONFIRMATION DOCUMENT. CCC AND THE RIGHTSHOLDER DISCLAIM ALL OTHER WARRANTIES RELATING TO THE WORK(S) AND RIGHT(S), EITHER EXPRESS OR IMPLIED, INCLUDING WITHOUT LIMITATION IMPLIED WARRANTIES OF MERCHANTABILITY OR FITNESS FOR A PARTICULAR PURPOSE. ADDITIONAL RIGHTS MAY BE REQUIRED TO USE ILLUSTRATIONS, GRAPHS, PHOTOGRAPHS, ABSTRACTS, INSERTS, OR OTHER PORTIONS OF THE WORK (AS OPPOSED TO THE ENTIRE WORK) IN A MANNER CONTEMPLATED BY USER; USER UNDERSTANDS AND AGREES THAT NEITHER CCC NOR THE RIGHTSHOLDER MAY HAVE SUCH ADDITIONAL RIGHTS TO GRANT.

13) **Effect of Breach.** Any failure by User to pay any amount when due, or any use by User of a Work beyond the scope of the License set forth in the Order Confirmation and/or the Terms, shall be a material breach of such License. Any breach not cured within 10 days of written notice thereof shall result in immediate termination of such License without further notice. Any unauthorized (but licensable) use of a Work that is terminated immediately upon notice thereof may be liquidated by payment of the Rightsholder's ordinary license price therefor; any unauthorized (and unlicensable) use that is not terminated immediately for any reason (including, for example, because materials containing the Work cannot reasonably be recalled) will be subject to all remedies available at law or in equity, but in no event to a payment of less than three times the Rightsholder's ordinary license price for the most closely analogous licensable use plus Rightsholder's and/or CCC's costs and expenses incurred in collecting such payment.

14) **Additional Terms for Specific Products and Services.** If a User is making one of the uses described in this Section 14, the additional terms and conditions apply:

a) ***Print Uses of Academic Course Content and Materials (photocopies for academic coursepacks or classroom handouts).*** For photocopies for academic coursepacks or classroom handouts the following additional terms apply:

i) The copies and anthologies created under this License may be made and assembled by faculty members individually or at their request by on-campus bookstores or copy centers, or by off-campus copy shops and other similar entities.

ii) No License granted shall in any way: (i) include any right by User to create a substantively non-identical copy of the Work or to edit or in any other way modify the Work (except by means of deleting material immediately preceding or following the entire portion of the Work copied) (ii) permit "publishing ventures" where any particular anthology would be systematically marketed at multiple institutions.

iii) Subject to any Publisher Terms (and notwithstanding any apparent contradiction in the Order Confirmation arising from data provided by User), any use authorized under the academic pay-per-use service is limited as follows:

A) any License granted shall apply to only one class (bearing a unique identifier as assigned by the institution, and thereby including all sections or other subparts of the class) at one institution;

B) use is limited to not more than 25% of the text of a book or of the items in a published collection of essays, poems or articles;

C) use is limited to no more than the greater of (a) 25% of the text of an issue of a journal or other periodical or (b) two articles from such an issue;

D) no User may sell or distribute any particular anthology, whether photocopied or electronic, at more than one institution of learning;

E) in the case of a photocopy permission, no materials may be entered into electronic memory by User except in order to produce an identical copy of a Work before or during the academic term (or analogous period) as to which any particular permission is granted. In the event that User shall choose to retain materials that are the subject of a photocopy permission in electronic memory for purposes of producing identical copies more than one day after such retention (but still within the scope of any permission granted), User must notify CCC of such fact in the applicable permission request and such retention shall constitute one copy actually sold for purposes of calculating permission fees due; and

F) any permission granted shall expire at the end of the class. No permission granted shall in any way include any right by User to create a substantively non-identical copy of the Work or to edit or in any other way modify the Work (except by means of deleting material immediately preceding or following the entire portion of the Work copied).

iv) Books and Records; Right to Audit. As to each permission granted under the academic pay-per-use Service, User shall maintain for at least four full calendar years books and records sufficient for CCC to determine the numbers of copies made by User under such permission. CCC and any representatives it may designate shall have the right to audit such books and records at any time during User's ordinary business hours, upon two days' prior notice. If any such audit shall determine that User shall have underpaid for, or underreported, any photocopies sold or by three percent (3%) or more, then User shall bear all the costs of any such audit; otherwise, CCC shall bear the costs of any such audit. Any amount determined by such audit to have been underpaid by User shall immediately be paid to CCC by User, together with interest thereon at the rate of 10% per annum from the date such amount was originally due. The provisions of this paragraph shall survive the termination of this License for any reason.

b) ***Digital Pay-Per-Uses of Academic Course Content and Materials (e-coursepacks, electronic reserves, learning management systems, academic institution intranets).*** For uses in e-coursepacks, posts in electronic reserves, posts in learning management systems, or posts on academic institution intranets, the following additional terms apply:

i) The pay-per-uses subject to this Section 14(b) include:

A) **Posting e-reserves, course management systems, e-coursepacks for text-based content,** which grants authorizations to import requested material in electronic format, and allows electronic access to this material to members of a designated college or university class, under the direction of an instructor designated by the college or university, accessible only under appropriate electronic controls (e.g., password);

B) **Posting e-reserves, course management systems, e-coursepacks for material consisting of photographs or other still images not embedded in text,** which grants not only the authorizations described in Section 14(b)(i)(A) above, but also the following authorization: to include the requested material in course materials

for use consistent with Section 14(b)(i)(A) above, including any necessary resizing, reformatting or modification of the resolution of such requested material (provided that such modification does not alter the underlying editorial content or meaning of the requested material, and provided that the resulting modified content is used solely within the scope of, and in a manner consistent with, the particular authorization described in the Order Confirmation and the Terms), but not including any other form of manipulation, alteration or editing of the requested material;

C) **Posting e-reserves, course management systems, e-coursepacks or other academic distribution for audiovisual content,** which grants not only the authorizations described in Section 14(b)(i)(A) above, but also the following authorizations: (i) to include the requested material in course materials for use consistent with Section 14(b)(i)(A) above; (ii) to display and perform the requested material to such members of such class in the physical classroom or remotely by means of streaming media or other video formats; and (iii) to "clip" or reformat the requested material for purposes of time or content management or ease of delivery, provided that such "clipping" or reformatting does not alter the underlying editorial content or meaning of the requested material and that the resulting material is used solely within the scope of, and in a manner consistent with, the particular authorization described in the Order Confirmation and the Terms. Unless expressly set forth in the relevant Order Conformation, the License does not authorize any other form of manipulation, alteration or editing of the requested material.

ii) Unless expressly set forth in the relevant Order Confirmation, no License granted shall in any way: (i) include any right by User to create a substantively non-identical copy of the Work or to edit or in any other way modify the Work (except by means of deleting material immediately preceding or following the entire portion of the Work copied or, in the case of Works subject to Sections 14(b)(1)(B) or (C) above, as described in such Sections) (ii) permit "publishing ventures" where any particular course materials would be systematically marketed at multiple institutions.

iii) Subject to any further limitations determined in the Rightsholder Terms (and notwithstanding any apparent contradiction in the Order Confirmation arising from data provided by User), any use authorized under the electronic course content pay-per-use service is limited as follows:

A) any License granted shall apply to only one class (bearing a unique identifier as assigned by the institution, and thereby including all sections or other subparts of the class) at one institution;

B) use is limited to not more than 25% of the text of a book or of the items in a published collection of essays, poems or articles;

C) use is limited to not more than the greater of (a) 25% of the text of an issue of a journal or other periodical or (b) two articles from such an issue;

D) no User may sell or distribute any particular materials, whether photocopied or electronic, at more than one institution of learning;

E) electronic access to material which is the subject of an electronic-use permission must be limited by means of electronic password, student identification or other control permitting access solely to students and instructors in the class;

F) User must ensure (through use of an electronic cover page or other appropriate means) that any person, upon gaining electronic access to the material, which is the subject of a permission, shall see:

- a proper copyright notice, identifying the Rightsholder in whose name CCC has granted permission,
- a statement to the effect that such copy was made pursuant to permission,
- a statement identifying the class to which the material applies and notifying the reader that the material has been made available electronically solely for use in the class, and
- a statement to the effect that the material may not be further distributed to any person outside the class, whether by copying or by transmission and whether electronically or in paper form, and User must also ensure that such cover page or other means will print out in the event that the person accessing the material chooses to print out the material or any part thereof.

G) any permission granted shall expire at the end of the class and, absent some other form of authorization, User is thereupon required to delete the applicable material from any electronic storage or to block electronic access to the applicable material.

iv) Uses of separate portions of a Work, even if they are to be included in the same course material or the same university or college class, require separate permissions under the electronic course content pay-per-use Service.

Unless otherwise provided in the Order Confirmation, any grant of rights to User is limited to use completed no later than the end of the academic term (or analogous period) as to which any particular permission is granted.

v) Books and Records; Right to Audit. As to each permission granted under the electronic course content Service, User shall maintain for at least four full calendar years books and records sufficient for CCC to determine the numbers of copies made by User under such permission. CCC and any representatives it may designate shall have the right to audit such books and records at any time during User's ordinary business hours, upon two days' prior notice. If any such audit shall determine that User shall have underpaid for, or underreported, any electronic copies used by three percent (3%) or more, then User shall bear all the costs of any such audit; otherwise, CCC shall bear the costs of any such audit. Any amount determined by such audit to have been underpaid by User shall immediately be paid to CCC by User, together with interest thereon at the rate of 10% per annum from the date such amount was originally due. The provisions of this paragraph shall survive the termination of this license for any reason.

c) ***Pay-Per-Use Permissions for Certain Reproductions (Academic photocopies for library reserves and interlibrary loan reporting) (Non-academic internal/external business uses and commercial document delivery).*** The License expressly excludes the uses listed in Section (c)(i)-(v) below (which must be subject to separate license from the applicable Rightsholder) for: academic photocopies for library reserves and interlibrary loan reporting; and non-academic internal/external business uses and commercial document delivery.

i) electronic storage of any reproduction (whether in plain-text, PDF, or any other format) other than on a transitory basis;

ii) the input of Works or reproductions thereof into any computerized database;

iii) reproduction of an entire Work (cover-to-cover copying) except where the Work is a single article;

iv) reproduction for resale to anyone other than a specific customer of User;

v) republication in any different form. Please obtain authorizations for these uses through other CCC services or directly from the rightsholder.

Any license granted is further limited as set forth in any restrictions included in the Order Confirmation and/or in these Terms.

d) ***Electronic Reproductions in Online Environments (Non-Academic-email, intranet, internet and extranet).*** For "electronic reproductions", which generally includes e-mail use (including instant messaging or other electronic transmission to a defined group of recipients) or posting on an intranet, extranet or Intranet site (including any display or performance incidental thereto), the following additional terms apply:

i) Unless otherwise set forth in the Order Confirmation, the License is limited to use completed within 30 days for any use on the Internet, 60 days for any use on an intranet or extranet and one year for any other use, all as measured from the "republication date" as identified in the Order Confirmation, if any, and otherwise from the date of the Order Confirmation.

ii) User may not make or permit any alterations to the Work, unless expressly set forth in the Order Confirmation (after request by User and approval by Rightsholder); provided, however, that a Work consisting of photographs or other still images not embedded in text may, if necessary, be resized, reformatted or have its resolution modified without additional express permission, and a Work consisting of audiovisual content may, if necessary, be "clipped" or reformatted for purposes of time or content management or ease of delivery (provided that any such resizing, reformatting, resolution modification or "clipping" does not alter the underlying editorial content or meaning of the Work used, and that the resulting material is used solely within the scope of, and in a manner consistent with, the particular License described in the Order Confirmation and the Terms.

15) **Miscellaneous.**

a) User acknowledges that CCC may, from time to time, make changes or additions to the Service or to the Terms, and that Rightsholder may make changes or additions to the Rightsholder Terms. Such updated Terms will replace the prior terms and conditions in the order workflow and shall be effective as to any subsequent Licenses but shall not apply to Licenses already granted and paid for under a prior set of terms.

b) Use of User-related information collected through the Service is governed by CCC's privacy policy, available online at www.copyright.com/about/privacy-policy/.

c) The License is personal to User. Therefore, User may not assign or transfer to any other person (whether a natural person or an organization of any kind) the License or any rights granted thereunder; provided, however, that, where applicable, User may assign such License in its entirety on written notice to CCC in the event of a transfer of all or substantially all of User's rights in any new material which includes the Work(s) licensed under this Service.

d) No amendment or waiver of any Terms is binding unless set forth in writing and signed by the appropriate parties, including, where applicable, the Rightsholder. The Rightsholder and CCC hereby object to any terms contained in any writing prepared by or on behalf of the User or its principals, employees, agents or affiliates and purporting to govern or otherwise relate to the License described in the Order Confirmation, which terms are in any way inconsistent with any Terms set forth in the Order Confirmation, and/or in CCC's standard operating procedures, whether such writing is prepared prior to, simultaneously with or subsequent to the Order Confirmation, and whether such writing appears on a copy of the Order Confirmation or in a separate instrument.

e) The License described in the Order Confirmation shall be governed by and construed under the law of the State of New York, USA, without regard to the principles thereof of conflicts of law. Any case, controversy, suit, action, or proceeding arising out of, in connection with, or related to such License shall be brought, at CCC's sole discretion, in any federal or state court located in the County of New York, State of New York, USA, or in any federal or state court whose geographical jurisdiction covers the location of the Rightsholder set forth in the Order Confirmation. The parties expressly submit to the personal jurisdiction and venue of each such federal or state court.

Last updated October 2022